DATA-DRIVEN SMART CITY OPERATIONS: BRIDGING SHARED MOBILITY AND ELECTRICAL POWER GRID

ZILIANG JIN

PhD

The Hong Kong Polytechnic University

2024

The Hong Kong Polytechnic University
Department of Logistics and Maritime Studies

Data-driven Smart City Operations: Bridging Shared Mobility and Electrical Power Grid

Ziliang Jin

A thesis submitted in partial fulfillment of the requirements for
the degree of Doctor of Philosophy
January 2024

CERTIFICATE OF ORIGINALITY

I hereby declare that this thesis is my own work and that, to the best of my knowledge and belief, it reproduces no material previously published or written, nor material that has been accepted for the award of any other degree or diploma, except where due acknowledgment has been made in the text.

Signature: _____

Name of Student: Ziliang Jin

Abstract

Smart city operations focus on integrating modern technologies and collected data to enhance the quality, efficiency, and sustainability of life for inhabitants in cities. In this thesis, we present three recent studies on the shared mobility and electrical power grid, which are at the crux of smart city operations. Through these studies, we hope to address some challenges in transportation and sustainability in urban areas.

In the first study, we consider two shared micromobility firms competing in the same service area, each providing micromobility vehicles (e.g., bikes and scooters) to satisfy uncertain demands. Each firm solves an integrated vehicle allocation and relocation problem, in which the total number of vehicles allocated by the two firms together in each service region is restricted by the city regulator, and provides a Nash equilibrium. Each firm's decision-making problem is formulated as a two-stage stochastic program on a spatial-temporal network, with the objective of maximizing her expected profit. To improve firms' operations with the limited number of allocated vehicles, we propose an innovative capacity-sharing agreement, under which a firm can share spare capacity for a fee with her opponent. Extensive numerical experiments based on real data reveal that regulator restrictions impact firms' profitability and service level. Capacity sharing can reduce the number of relocated vehicles and also improve firms' profitability. To promote the capacity-sharing agreement, the regulator should provide incentives to the firms.

In the second study, we focus on a shared mobility system with electrical vehicles (EVs). Unlike micromobility vehicles, EVs face additional challenges in managing their battery levels. They must charge adequately to meet trip demands and can discharge electricity to the power grid through vehicle-to-grid (V2G) technology to earn revenue. We frame the operator's EV planning and operation under correlated uncertainties as a two-stage distributionally robust optimization (DRO) problem. To increase computational efficiency, we propose inner and outer approximations for the DRO problem and develop

an algorithmic approach incorporating time-based decomposition techniques. Numerical results based on real data suggest that EVs majorly charge electricity during the early hours when electricity prices and consumer trips are low. Conversely, they discharge electricity when prices are high. Faster charging decreases the number of allocated vehicles, improves the vehicle utilization rate, and reduces total costs. Comparing two pricing schemes for charging EVs, electricity-based and time-based, we observe more frequent charging and discharging under the time-based scheme than the electricity-based scheme.

In the third study, we explore a grid-vehicle integration (GVI) system employing V2G while managing uncertainties in renewable generation, power load, and EV trip demand. We formulate the problem of operating a GVI system as a two-stage robust mixed-integer program. In the first stage, the grid operator, aiming to minimize the worst-case total cost, decides whether to start up a generator. In the second stage, the grid decides power generation levels and charging/discharging interactions with EVs to satisfy the power load. Meanwhile, the mobility operator utilizes the EV fleet to fulfill the interactions and satisfy EV trip demands. To address a significant computational challenge, we propose a machine learning-driven optimization approach. Our approach outperforms a commercial solver in both computational time and solution quality for large-scale instances based on real data. Out-of-sample tests reveal that V2G can reduce the number of required generators and stabilize power generation by "filling" the low power load and "shaving" the peak power load. Moreover, V2G helps achieve a substantial reduction in carbon emissions compared to the case without V2G. The impact of V2G is more pronounced under a bimodal power load pattern than a unimodal pattern. We also find that achieving carbon neutrality in this integration system is feasible yet challenging.

Acknowledgments

I wish to express my deepest gratitude and appreciation to my supervisor Dr. Kai Pan for his constant guidance, support, inspiration, and encouragement throughout my life at PolyU. He guides me into research and helps me shape my academic career. It has been a great opportunity and honor for me to learn from him. He has been an amazing mentor and role model for me not only scientifically but also personally. I cannot thank him enough.

I also wish to express my sincere gratitude to Dr. Jianqiang Cheng, Prof. Yun Fong Lim, Prof. Zuo-Jun Max Shen, Prof. Yulan Wang, and Dr. Wenxin Xu whom I have the pleasure to collaborate with. Their tremendous help contributes to my development as a better researcher. I am honored to have Dr. Daniel Zhuoyu Long, Prof. Miao Song, and Dr. Xuan Wang in my thesis committee. I am very grateful to them for their valuable comments and remarkable advice to improve this thesis.

It is my honor to be a member of the Department of Logistics and Maritime Studies at PolyU, and I would like to thank the entire community for their help during my PhD study. I must thank Dr. Shuli Liu and Dr. Ding Zou for their scientific and emotional support. They are always there when I need help. I would like to extend my gratitude to my friends in offices MN037 and MN038 at PolyU. Our friendships make my life at Hong Kong one of the memorable experiences. I also thank the department, PolyU, and Research Grants Council of Hong Kong for providing me with financial support throughout my PhD study.

Finally, I wish to express my warmest feelings to my parents and Ms. Wenjun Shu for their priceless love, devotion, and understanding. It is their love and support that make me who I am today.

Table of Contents

List of Figures

List of Tables

Chapter 1

Introduction

1.1 Background

The twenty-first century witnesses an unprecedented wave of urbanization, marked by rapid growth and an ever-expanding urban landscape. Recent trends indicate that this urbanization is accelerating globally (Zhang et al. 2022b). According to data from the World Bank (The World Bank 2023), more than half of the world's population resides in urban areas, contributing over 80% of the global GDP. Data also indicates that by 2050, the urban population will double. However, the remarkable speed and scale of urbanization come with societal and environmental challenges. Issues like transportation congestion and pollution have become increasingly prevalent, perplexing both citizens and city regulators. As a result, citizens and regulators all have growing expectations towards cities to address these challenges and enhance the quality, efficiency, and sustainability of modern urban life. The recent popularity of "smart city" is an obvious evidence reflecting the urge for the development of cities. Wikipedia (2023) introduces that smart cities integrate modern technologies and collected data to enhance the quality, efficiency, and sustainability of life for inhabitants in cities. In pursuit of such a vision, cities across the world have emerged construction of smart cities. According to a report by Deloitte (2018), there are over 1000 smart city projects have been initialized worldwide. Within the framework of a smart city, two critical components are shared mobility and electrical power grid, which focus on addressing challenges in transportation and sustainability in urban areas (Qi and Shen 2019).

Shared mobility is a transportation system where firms provide shared vehicles for

rentals and consumers can rent available shared vehicles around the city by paying a rental fee, which is much lower than the costs associated with ownership and maintenance. Popular shared vehicles include bicycles, scooters (classified as micromobility vehicles), and electrical vehicles (EVs). To efficiently serve consumer trips, shared mobility firms need to optimize their allocation capacity, such as micromobility vehicles and EVs, and subsequent fleet operations. Despite some similarities between micromobility vehicles and EVs, the operations of systems running these two vehicle types are fundamentally different. For example, (i) Micromobility vehicles should stay ready for the coming consumers, so their services are not provided on-demand like shared EVs; (ii) Rental prices for shared micromobility are much lower than those for shared EVs, so the shared micromobility firm often bears high investment and operational costs with low rental prices; (iii) Unlike micromobility vehicles, EVs encounter challenges in managing their battery levels during operations. Therefore, our study delves into the shared micromobility system (Chapter 2) and EV-sharing system (Chapter 3) separately to address their distinct operational challenges.

Electrical power grid focuses on planning unit commitments status (start-up/shut-down of generators), power generations, and transmissions intelligently to satisfy consumer's load (i.e., power demand), with the aim of minimizing costs (Fang et al. 2011). The growing popularity of EVs highlights the interactions between shared mobility and the power grid, signaling the potential for bridging these two systems, which supports smart city operations. Specifically, EVs should charge electricity from the power grid adequately to ensure sufficient battery capacity to meet trip demands. Conversely, they can also discharge electricity to the power grid through vehicle-to-grid (V2G) technology to earn revenue. Simultaneously, the activities of EVs, including both charging and discharging, may contribute to the power grid in its power generation. Consequently, this forms a grid-vehicle integration system. In this thesis, we investigate this integration system from the perspectives of shared mobility and power grid, respectively. Specifically, Chapter 3 focuses on shared mobility operations in this system, while Chapter 4 focuses on power grid operations in this system.

1.2 Thesis Outline

In Chapter 2, we consider two shared micromobility firms competing in the same service area, each providing micromobility vehicles to satisfy uncertain demands. These two firms own vehicles and bear high investment and operational costs with low rental prices. They also experience competition among themselves and are subject to vehicle allocation restrictions imposed by city regulators. These factors require the firms to efficiently perform initial allocation and subsequent relocation of vehicles to ensure commercial sustainability. The work in this chapter aims to understand the shared micromobility firms' operations under competition and provide managerial guidance to the firms and the regulator. To enhance the firms' operational efficiency with allocation restrictions, we propose an innovative capacity-sharing agreement between the firms, where a firm can share its spare capacity for a fee with the other firm. Each firm solves an integrated vehicle allocation and relocation problem, where the total number of vehicles allocated by the firms in each region is constrained by the city regulator, and reaches a Nash equilibrium. Each firm's decision-making problem is modeled as a two-stage stochastic program on a spatial-temporal network, where the firm initially allocates vehicles for service regions in the first stage and subsequently relocates vehicles as recourse in the second stage observing realized demands. We explore the optimality condition of each firm's decision-making and seek a Nash equilibrium by optimizing certain objectives (i.e., criteria for selecting an equilibrium) over the joint optimality conditions of both firms. We prove that capacity sharing helps reduce the total demand loss in the entire system. Extensive numerical experiments based on real data suggest that regulator restrictions impact firms' profitability and service level. After introducing capacity sharing, one firm may act like a free rider that relies on the vehicles transferred from her opponent. Meanwhile, many vehicles are shared in periods and regions with high trip demands. Capacity sharing can reduce the number of relocated vehicles by serving as a substitution for relocation and also improves the firms' profitability. To promote the capacity-sharing agreement, the regulator should provide incentives to the firms.

In Chapter 3, we focus on an EV-sharing mobility system incorporating V2G technology. In this system, an operator provides a fleet of EVs to satisfy consumer trips in a service area over an operational horizon, meanwhile, it needs to manage the charging/discharging of EVs during operations. The consumer trips across regions in all periods

are uncertain and correlated. We jointly optimize vehicle initial allocation and subsequent operation, including charging and discharging, under uncertainties. To make a reliable solution under uncertainty with a limited amount of available data, we construct a two-stage distributionally robust optimization (DRO) model. To increase the computational efficiency, we first introduce outer and inner approximations for the DRO problem and then develop an algorithmic approach that incorporates time-based decomposition techniques. Through numerical experiments using real-world data, we show that our proposed approaches can obtain high-quality solutions in significantly short computational time. Our out-of-sample results reveal that most EVs charge electricity during the early hours of the day when electricity prices and trip demands are low. Conversely, EVs discharge electricity during periods of high electricity prices. Additionally, an increased charging speed contributes to a reduction in the number of allocated vehicles, an enhancement in the vehicle utilization rate, and a drop in total costs. We further compare two different pricing schemes for charging EVs: electricity-based and time-based pricing schemes. We find that EVs process charging and discharging more frequently under the time-based pricing scheme than the electricity-based pricing scheme.

In Chapter 4, we consider a grid-vehicle integration (GVI) system employing V2G while managing uncertainties in renewable generation, power load, and EV trip demand. We formulate the problem of operating a GVI system as a two-stage robust mixed-integer program. In the first stage, the grid operator, aiming to minimize the worst-case total cost, decides whether to start up a generator. In the second stage, the grid decides power generation levels and charging/discharging interactions with EVs to satisfy the power load. Meanwhile, the mobility operator utilizes the EV fleet to fulfill the interactions and satisfy EV trip demands. The inherent complexity arising from discrete decisions, uncertainties, and robustness requirements poses a significant computational challenge, prompting the proposal of a machine learning-driven optimization approach. Our approach outperforms a commercial solver in both computational time and solution quality for large-scale instances based on real data. Conducting out-of-sample tests with data from New York City, we reveal that V2G can reduce the number of required generators and stabilize power generation by "filling" the low power load and "shaving" the peak power load. Moreover, the V2G helps achieve a substantial 21.66% average reduction in carbon emissions compared to the case without V2G. The impact of V2G is more

pronounced under a bimodal power load pattern than a unimodal pattern. We also find that achieving carbon neutrality in this integration system is feasible yet challenging.

In Chapter 5, we provide concluding remarks for this thesis.

Chapter 2

Integrated Vehicle Allocation and Relocation for Shared Micromobility under Competition and Demand Uncertainty

2.1 Introduction

A *shared micromobility system* consists of lightweight vehicles (e.g., bikes, e-bikes, e-scooters) and well supports urban short-distance travel (e.g., last-mile transportation), alleviating city congestion because of its eco-friendliness and sustainability (McKinsey 2021). Note that 60% of today's total passenger miles traveled in China, Europe, and the U.S. are less than 8 kilometers (McKinsey 2019), and the energy prices and public interest in social distancing are growing. Thus, the shared micromobility system becomes a significant transportation solution for society.

The shared micromobility system allows consumers to conveniently pick up and drop off vehicles in any service region at any time, offering short-term self-service rental programs (Fishman et al. 2013). A consumer can rent a micromobility vehicle by paying a low rental cost (much lower than the ownership and maintenance costs) for a short-distance trip. Motivated by such convenience, over 1,000 cities worldwide have established similar programs (Wang and Lindsey 2019). For example, nearly seventy bike-sharing companies were operating in China as of July 2017 (Sago 2020); six e-scooter companies (i.e., Lime,

Bird, Tier Mobility, Wind Mobility, Flash, and Hive) are competing in Vienna, and five companies (i.e., Lime, Bird, Lyft, Skip by Helbiz, and Spin) in Washington, DC (Schellong et al. 2019).

A shared micromobility system differs from other shared mobility systems (e.g., car-sharing and ride-hailing) mainly because of the following three features. First, shared micromobility services are not provided on-demand like ride-hailing due to the lack of self-regulated owners for each vehicle. Each micromobility vehicle should stay ready for the coming consumers, significantly challenging the operators to allocate and relocate vehicles efficiently for high service quality and profitability. Second, the convenience of free pick-up and drop-off often creates vehicle supply and demand imbalance in different regions (Jin et al. 2023). For instance, consumers often drop off micromobility vehicles near subway stations, leading to an oversupply of vehicles, while there may be insufficient vehicles in regions far away from central business regions. This can significantly mitigate the firm's operational efficiency, service quality, and profitability. Thus, a shared micromobility firm (referred to as "she") must relocate her vehicles across the service regions efficiently. Third, the shared micromobility firm often owns the vehicles and bears high investment and operational costs with low rental prices (Hasija et al. 2020), and is further responsible for carefully operating the system to match supply with demand. The firm cannot simply raise rental prices to cover these high costs because consumers can easily switch to other mobility services. For example, Indego, a bicycle-sharing system serving Philadelphia, has maintained the price of its annual pass at $156 since April 2018, despite adding approximately 1,000 new bicycles to its system since then (City of Philadelphia 2018, Indego 2023). Thus, efficient vehicle allocation and relocation across regions to ensure profitability and service quality are significantly important for a shared micromobility firm.

Currently, multiple shared micromobility firms operate in a city. The fierce competition among firms brings additional challenges to both the firms and the regulator. On the one hand, such a competition, along with the aforementioned three features of the shared micromobility system, requires the firms to efficiently perform initial allocation and subsequent relocation of vehicles to ensure commercial sustainability. On the other hand, the regulator faces the challenge of regulating the shared micromobility industry to avoid too many vehicles blocking traffic and causing safety issues while maintaining the

benefits of the shared micromobility services to city residents. In many cities worldwide, e.g., Barcelona (Valdivia 2020), San Diego (Hargrove and Ahn 2022), Chicago (City of Chicago 2022), and Boston (American Legal Publishing 2019), regulators limit the number of shared micromobility vehicles allocated in the city via licenses issued to the firms. Each firm should apply for a portion of these licenses. In addition, the City of Chicago requires that the licensed vehicles be allocated relatively fairly in the service regions based on consumer demands to ensure that vehicles can be available to all city residents. They further periodically adjust the number of licensed vehicles by reviewing the utilization rate (City of Chicago 2022). Furthermore, they divide the service area into different types of areas (e.g., equity priority and core areas), each with sub-areas. The regulator sets a specific allocation limit for each sub-area.

With a limited number of vehicles due to the regulator's restriction on vehicle allocation, shared micromobility firms are challenged to provide consumers with high-quality services. To address this challenge, we suggest an innovative *capacity-sharing* agreement between the firms, under which a firm can share spare capacity (i.e., micromobility vehicles) for a fee with her opponent when both of them are competing in the same market. To the best of our knowledge, we are among the first to integrate the initial allocation and subsequent relocation of shared micromobility vehicles under firm competition, regulator restrictions, and demand uncertainty. For such a case, we are interested in the following research questions: How should a shared micromobility operator integrate vehicle allocation and relocation? How do the firm competition and regulator restrictions affect the firms' performance? How does capacity sharing affect the firm's profitability and operations? Should the regulator intervene in the shared micromobility industry to balance social welfare and the industry's economic viability, and if so, what are possible approaches?

To answer these questions, we consider two shared micromobility firms competing in the same service area that is divided into multiple regions (He et al. 2017, Qi and Shen 2019). Each firm provides a fleet of micromobility vehicles to satisfy consumer demands in the service area over an operational horizon with multiple periods. Motivated by the practices in the shared micromobility industry, we consider uncertain consumer demands, and the market consists of two types of consumers (hereafter, we refer to a consumer as "he"): *loyal consumers* and *disloyal consumers*. A loyal consumer of a firm always chooses

that firm when renting micromobility vehicles, whereas a disloyal consumer may choose either firm. The reasons for a loyal consumer's preference vary. For instance, he may prefer the firm's vehicles if the two firms offer different ones, or he may be ineligible to rent the other firm's vehicles if he has not paid a deposit fee yet.

We formulate a two-stage model. In the first stage, each firm builds her capacity by initially allocating micromobility vehicles across service regions without knowing the actual demands in each period. The regulator limits the number of vehicles allocated in each service region by the two firms together. We call this stage *the capacity-development stage*. In the second stage, after the demands are realized, each firm operates her vehicles by subsequently relocating vehicles across service regions in each period to rebalance the vehicles toward satisfying the demands. We call this stage *the operation stage*. Moreover, following the study by Kabra et al. (2020) that examines the impact of bike accessibility and availability upon bike-share ridership, we consider that the consumer demands partially depend on the vehicle capacity (i.e., the number of allocated vehicles). The mismatch between vehicle supply and demand may cause parking costs for idle vehicles and lost-sale penalties. Each firm maximizes her total expected profit over the entire operational horizon, including the revenue from serving consumers and the costs incurred in the two stages. We make the following contributions:

(i) Each shared micromobility firm solves an integrated vehicle allocation and relocation problem and provides a Nash equilibrium. Each firm's decision-making problem is formulated as a two-stage stochastic program on a spatial-temporal network (Fan 2014, Mahmoudi and Zhou 2016, Lu et al. 2017). In the capacity-development stage (1st stage), the firm decides initial vehicle allocation for service regions. In the operation stage (2nd stage), the firms make subsequent vehicle relocation as recourse across service regions to match supply with demand after the demands are realized in each period. We also consider transferred micromobility vehicles when both firms share their capacities (i.e., vehicles). To the best of our knowledge, our formulated spatial-temporal network is the first that incorporates the flows between the two firms.

(ii) We explore the optimality condition of each firm's decision-making and seek the Nash equilibrium by optimizing certain objectives (i.e., criteria for selecting an equilibrium) over the joint optimality conditions of both firms. Specifically, we consider two criteria preferred by the regulator and the firms, respectively: minimizing the total demand loss

and minimizing the total number of allocated vehicles.

(iii) We propose an innovative *capacity-sharing* agreement between the shared micromobility firms. Under this agreement, each firm can share abundant vehicles with her opponent for a fee. We demonstrate the feasibility and effectiveness of the capacity-sharing agreement.

(iv) We perform numerical experiments based on real data collected from Citi Bike (2022) and obtain the following managerial insights for the regulator and the firms. The regulator restrictions impact firms' profitability and service level. The competition benefits the firm with fewer loyal consumers by increasing her profit. After introducing capacity sharing, one firm may act like a free rider that allocates fewer vehicles and asks for vehicles transferred from her opponent if needed. Meanwhile, many vehicles are shared in periods and regions with high trip demands. Capacity sharing can reduce the number of relocated vehicles by serving as a substitution for relocation and also improves the firms' profitability.

The remainder of the chapter is organized as follows. Section 2.2 reviews related studies. Section 2.3 introduces the problem formulation. We conduct numerical experiments in Section 2.4 based on real data from Citi Bike (2022). Section 2.5 concludes the chapter.

2.2 Literature Review

Our work builds on the prior Operations Management (OM) studies on shared mobility. With the advanced development of disruptive technologies and data analytics, the smart city paradigm is shifting from new technology adoption to decision optimization, focusing on improving operational efficiency (Qi and Shen 2019, Mak 2022). In line with this shift, a growing body of OM literature studies smart city problems.

Shared mobility, a component of smart cities, proliferates in industry and has also received attention in recent literature. Most studies on shared mobility focus on car sharing, with which people rent cars from individual car owners (often also drivers) for trips (e.g., see He et al. 2017, Chang et al. 2017, Lu et al. 2017, Qi et al. 2018, Yu and Shen 2020, and Benjaafar et al. 2022a). Shared micromobility, complementary to car sharing, also brings challenges and opportunities to OM researchers (Hasija et al. 2020). Shared micromobility is fundamentally different from car sharing in the ownership of as-

sets. Shared micromobility firms are asset-based, having the ownership of micromobility vehicles (e.g., bikes or scooters), whereas car-sharing firms are often two-sided platforms that provide services to match supply with demand. Recently, Kabra et al. (2020) and He et al. (2021b) study how the bike supply impacts end-user behavior. Kabra et al. (2020) empirically investigate the impact of bike accessibility and availability upon bike-share ridership and find that higher bike availability and a more condensed bike station network would help increase the ridership. Following this study, He et al. (2021b) further take bike stations' geographic locations into account and provide the designing guidance for a bike-share network by examining the relationship between ridership and station density. Our work is more related to Shu et al. (2013), and they formulate two linear programming models to optimize the number of bikes in each dock and the fleet operation, respectively. However, the initial allocation and fleet operations are not independent, especially for the new entrants of the shared micromobility market. In this chapter, each shared micromobility firm integrates the capacity development (i.e., initial vehicle allocation) and fleet operations (i.e., subsequent vehicle relocation) in a two-stage stochastic programming model. Different from another relevant study by Jin et al. (2023), we consider such an integration under firm competition and consumer demands depend on capacity development decisions.

This chapter extends the literature on fleet operation in shared mobility. There is a strand of studies that analyze fleet operation in car sharing. For example, Lu et al. (2017) study the car allocation problem under demand uncertainty. Nair and Miller-Hooks (2011) address the least-cost car redistribution problem to neutralize the imbalance demand at various stations. The fleet operation in shared micromobility, however, depends on capacity decisions (e.g., the number of allocated bikes) due to the difference in asset ownership. Bearing high capacity-development and maintenance costs of the physical assets (i.e., bikes), shared micromobility firms must carefully determine capacity development and operation together to achieve economic viability and sustainability as mentioned in Section 2.1. In addition, it is feasible to consider capacity decisions and study sharing capacities in shared micromobility because the firms can easily decide and adjust the capacity as they often own the assets. In contrast, car-sharing firms have to use incentive instruments to affect the capacity, e.g., motivating more drivers to provide service by increasing their salaries. Several works dedicate to the fleet operation in shared

micromobility (e.g., see Zhang et al. 2017, Lu 2016, and Schuijbroek et al. 2017). For instance, He et al. (2021c) formulate a model wherein a two-sided matching platform (e.g., a free-float bike-sharing company) determines the spatial allocation of parking spaces and the design of incentive instruments that can affect the supply (e.g., price and rewards to users). However, to the best of our knowledge, none of these studies explicitly considers a firm's capacity decision (e.g., bike allocation), which is more critical in shared micromobility than in other shared mobility (e.g., car sharing). Motivated by the necessity and feasibility, our work contributes to this stream of literature by integrating the capacity decision and fleet operation for shared micromobility.

Our study contributes to the steam of literature on competition in shared mobility. Most of the prior works focus on the competition in ride-sharing (e.g., see Nikzad 2017 and Zhang et al. 2022a. The competition in shared micromobility is vastly observed in practice while receiving limited attention in the literature. Most of the related studies on competition in shared micromobility mainly focus on the demand side. Cao et al. (2021) use staggered entry of two deckles bike-sharing firms and observe a positive network effect in demand between the firms. Reck et al. (2022) analyze the impact of competition on demand between different mode choices (i.e., dockless e-scooters and e-bikes and docked e-bikes and bikes). Martin et al. (2021) address a car-sharing relocation problem where multiple operators compete for the deterministic demand while collaborating in relocating their fleets. Our work contributes to this stream of literature by considering the supply side—the capacity decisions. While there is extensive literature on capacity investment under competition and uncertainty (see Van Mieghem 2003 and Chevalier-Roignant et al. 2011 for a detailed literature review), to the best of our knowledge, we are the first to consider competitive capacity investment and operational decisions of shared micromobility firms under demand uncertainty.

2.3 Model

We consider two competing shared micromobility firms (indexed as $k \in \mathcal{K} = \{A, B\}$) that just expand their business into a city. Each firm provides shared micromobility service for a set of regions $\mathcal{M} = \{1, 2, \ldots, M\}$ in each period $t \in \mathcal{T} = \{0, 1, \ldots, T\}$.

2.3.1 Sequence of Events

We formulate a two-stage model, in which we call the first stage the *capacity-development stage* and the second stage the *operation stage*. We introduce the sequence of events and the firms' decisions below.

(a) Capacity-development stage: Each firm $k \in \mathcal{K}$ simultaneously decides the number of micromobility vehicles to be allocated in each region $i \in \mathcal{M}$, denoted by x_i^k. We assume that each firm k is endowed with a budget that can afford at most $\hat{x}^k$ vehicles. In addition, based on approximated trip demands in each region, the regulator (e.g., the city government) restricts the numbers of micromobility vehicle licensing plates and available parking spaces to avoid traffic chaos. Thus, both firms together allocate at most $\bar{x}_i$ vehicles in each region $i \in \mathcal{M}$.

(b) Operation stage: In each period $t \in \mathcal{T}$, consumers arrive to rent micromobility vehicles. Each firm simultaneously decides (i) the number of vehicles that fulfill the consumers' rental requests; (ii) the number of vehicles that are relocated across regions to balance the vehicle inventories with the demands in each period; and (iii) the number of vehicles that stay idle in each region.

2.3.2 Vehicle Movement: A Spatial-temporal Network

We model the vehicle movements among regions and across periods at the operation stage as *flows* in a spatial-temporal network $\mathcal{G} = (\mathcal{N}, \mathcal{E})$, where $\mathcal{N}$ is the set of nodes and $\mathcal{E}$ is the set of directed arcs on the network (see Figure 2.1). A node $n_{i,t}^k \in \mathcal{N}$ represents service region $i \in \mathcal{M}$ in period $t \in \mathcal{T}$ for firm $k \in \mathcal{K}$. For each firm k, the *flow* on the directed arc $(n_{i,t}^k, n_{i',t'}^k) \in \mathcal{E}$ represents the number of micromobility vehicles moving from region i in period t (i.e., node $n_{i,t}^k$) to region i' in period t' (i.e., node $n_{i',t'}^k$).

Based on how vehicles are moved between two nodes, we define three types of arcs in $\mathcal{E}$ for each firm $k \in \mathcal{K}$: (i) *Rental arcs*: The flow on each rental arc $(n_{i,t}^k, n_{i',t'}^k) \in \mathcal{E}_{\mathrm{R}}^k$ represents the number of rental trips from region i in period t to region $i' \neq i$ in period $t' = t + \ell_{i,i'}$, where $\ell_{i,i'}$ represents the number of periods that a micromobility vehicle rider needs to move from region i to region i' and $(i, i', t, t') \in \mathcal{Z}_{\mathrm{R}} = \{\mathcal{M} \times \mathcal{M} \times \mathcal{T} \times \mathcal{T} \mid i \neq i',\ t' = t + \ell_{i,i'}\}$. (ii) *Idle arcs*: The flow of each idle arc $(n_{i,t}^k, n_{i,t+1}^k) \in \mathcal{E}_{\mathrm{I}}^k$ represents the number of idling vehicles in region i from period t to period $t+1$, where

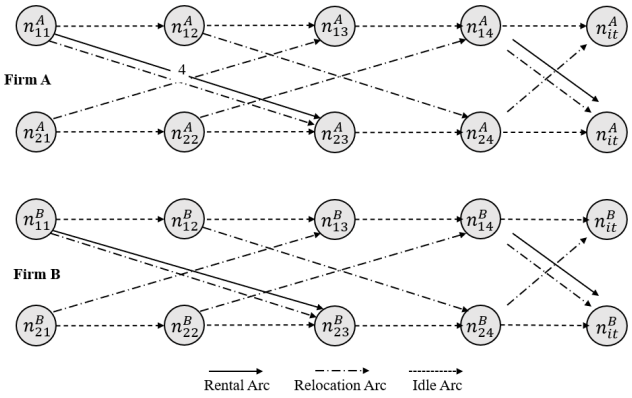

Figure 2.1. Spatial-Temporal Network $\mathcal{G}$

$(i,t) \in \mathcal{Z}_{\mathrm{I}} = \{\mathcal{M} \times \mathcal{T} \mid t \in \mathcal{T} \setminus \{T\}\}$. (iii) *Relocation arcs*: The flow of each relocation arc $(n^k_{i,t}, n^k_{i',t'}) \in \mathcal{E}^k_{\mathrm{L}}$ represents the number of vehicles relocated by the firm from region i in period t to region $i' \neq i$ in period $t' = t + r_{i,i'}$, where $r_{i,i'}$ represents the number of periods that a vehicle needs to be relocated from region i to region i' and $(i,i',t,t') \in \mathcal{Z}_{\mathrm{L}} = \{\mathcal{M} \times \mathcal{M} \times \mathcal{T} \times \mathcal{T} \mid i \neq i',\ t' = t + r_{i,i'}\}$. Let $\mathcal{A} = \{\mathrm{R}, \mathrm{I}, \mathrm{L}\}$. We have $\mathcal{E}^k = \cup_{\forall\, a \in \mathcal{A}} \mathcal{E}^k_a$, $\mathcal{E}^k_{a_1} \cap \mathcal{E}^k_{a_2} = \emptyset$ for given $k \in \mathcal{K}$, $a_1 \neq a_2$, $a_1, a_2 \in \mathcal{A}$, and $\mathcal{E}^A_a \cap \mathcal{E}^B_a = \emptyset$ for given $a \in \mathcal{A}$. Note that both Firm A and Firm B use similar micromobility vehicles and relocation methods and share the geographic regions in $\mathcal{M}$, the values of $\ell_{i,i'}$ and $r_{i,i'}$ are firm-independent for any $i, i' \in \mathcal{M}$. Thus, for any arc $(n^A_{i,t}, n^A_{i',t'}) \in \mathcal{E}^A$, we have a corresponding arc $(n^B_{i,t}, n^B_{i',t'}) \in \mathcal{E}^B$, and these two arcs represent two flows from region i in period t to region i' in period t' for Firm A and Firm B, respectively.

2.3.3 Consumer Types

We consider two types of consumers: *loyal consumers* and *disloyal consumers*. A loyal consumer of a firm always chooses that firm to rent micromobility vehicles from, regardless of the rental prices. The reasons for such a preference are various. For instance, the consumer may prefer the firm's vehicles if the two firms offer different ones, or the consumer is ineligible to rent the other firm's vehicles if he has not paid a deposit fee yet. Let $\alpha_k \in [0,1]$ and $\alpha_{-k} \in [0,1]$ denote the percentage of consumers who are loyal to firm k and firm $-k$, respectively. We assume that the remaining consumers (i.e., a percentage of $1 - \alpha_A - \alpha_B \geq 0$ of all the consumers) are disloyal to both firms, and they choose the firm with more available vehicles. The assumption comes from the phenomenon that many consumers are more likely to choose a shared micromobility firm due to easier access to

the vehicles (Kabra et al. 2020) instead of lower rental prices because the price difference is usually insignificant across firms.

2.3.4 Mathematical Formulation

We formulate the decision-making model of each firm $k \in \mathcal{K}$ as a two-stage stochastic program. In the *capacity-development stage*, each firm $k \in \mathcal{K}$ makes the vehicle allocation decision $\mathbf{x}^k = [x_1^k, x_2^k, \ldots, x_M^k]^\top$ such that the following constraints are satisfied:

$$\sum_{i \in \mathcal{M}} x_i^k \leq \hat{x}^k; \quad x_i^k + x_i^{-k} \leq \bar{x}_i, \ \forall\, i \in \mathcal{M}; \quad x_i^k \geq 0, \ \forall\, i \in \mathcal{M}. \tag{2.1}$$

Given firm $-k$'s decision $\mathbf{x}^{-k}$, we let $\mathcal{X}^k(\mathbf{x}^{-k}) = \left\{\mathbf{x}^k \in \mathbb{R}_+^M \;\middle|\; (2.1)\right\}$. Thus, the vehicle allocation decision of one firm depends on that of the other.

In the *operation stage*, time-dependent demands arrive at each region $i \in \mathcal{M}$ at the start of each period $t \in \mathcal{T} \setminus \{0, T\}$. For each rental arc $e = (n_{i,t}^k, n_{i',t+\ell_{i,i'}}^k) \in \mathcal{E}_{\mathrm{R}}^k$, let $\overline{w}_e^k$ denote the demand (i.e., the number of consumers) from region i in period t to region i' in period $t + \ell_{i,i'}$. The firm receives a revenue $h_{\mathrm{R}}^k \geq 0$ whenever it completes serving a consumer. If the number of micromobility vehicles available in region i cannot satisfy the demands of the region in period t, the unsatisfied demand for $e = (n_{i,t}^k, n_{i',t+\ell_{i,i'}}^k) \in \mathcal{E}_{\mathrm{R}}^k$ is lost and the firm k bears a penalty cost $h_{\mathrm{P}}^k \geq 0$ per consumer lost. The penalty cost accounts for the side effects of demand loss, which cannot be captured solely by revenue loss. For instance, unfulfilled consumers may feel disappointed about their loss, negatively affecting a firm's reputation. In addition, the penalty cost motivates shared micromobility firms to actively serve consumers. If the number of consumers is fewer than the number of vehicles in region i in period t, an idle cost $h_{\mathrm{I}}^k \geq 0$ (e.g., the maintenance cost of idle vehicles) is incurred for each idling vehicle on the arc $e = (n_{i,t}^k, n_{i,t+1}^k) \in \mathcal{E}_{\mathrm{I}}^k$. When each firm $k \in \mathcal{K}$ relocates a vehicle, it pays a cost $h_{\mathrm{L}}^k \geq 0$, including labor and trucking costs.

Anticipating demand uncertainty in the operation stage, each firm $k \in \mathcal{K}$ makes her initial vehicle allocation decision $\mathbf{x}^k$ and subsequent relocation decisions to maximize her expected profit. The profit equals the total revenue minus the total cost. The total cost includes the initial vehicle allocation cost $\mathbf{c}^\top \mathbf{x}^k$ in the capacity-development stage (where $\mathbf{c}^k = [c_1^k, c_2^k, \ldots, c_M^k]^\top$) and demand-loss penalty, idle, and vehicle relocation costs in the operation stage. Given the initial vehicle allocation $\mathbf{x}^k$, let $\varphi^k(\mathbf{x}^k)$ denote the optimal

expected net cost of the operation stage (i.e., the total cost minus the total revenue of the operation stage). Thus, maximizing the firm k's total expected profit is equivalent to minimizing the summation of $\mathbf{c}^\top \mathbf{x}^k$ and $\varphi^k(\mathbf{x}^k)$. Each firm $k \in \mathcal{K}$ optimizes her vehicle allocation decisions by solving the following problem:

$$-\Psi^k = \min_{\mathbf{x}^k} \left\{ {\mathbf{c}^k}^\top \mathbf{x}^k + \varphi^k(\mathbf{x}^k) \;\middle|\; \mathbf{x}^k \in \mathcal{X}^k(\mathbf{x}^{-k}) \right\}, \qquad (\mathcal{D}^k(\mathbf{x}^{-k}))$$

where $\Psi^k \geq 0$ represents the total expected profit of each firm $k \in \mathcal{K}$ and $\varphi^k(\mathbf{x}^k)$ is realized in the operation stage when each firm $k \in \mathcal{K}$ relocates her micromobility vehicles across regions. Problem $(\mathcal{D}^k(\mathbf{x}^{-k}))$ is an integrated vehicle allocation and relocation problem. Solving problem $(\mathcal{D}^k(\mathbf{x}^{-k}))$ for each firm $k \in \mathcal{K}$ simultaneously gives us a Nash equilibrium. We now describe the details of $\varphi^k(\mathbf{x}^k)$ below.

First, we discuss the rental demand of each firm $k \in \mathcal{K}$. For any given time-space range $(i, i', t, t') \in \mathcal{Z}_{\mathrm{R}}$, (i) we have $e_A = (n^A_{i,t}, n^A_{i',t'}) \in \mathcal{E}^A_{\mathrm{R}}$ and $e_B = (n^B_{i,t}, n^B_{i',t'}) \in \mathcal{E}^B_{\mathrm{R}}$ sharing the same time-space range; (ii) we let $Y^k_{i,i',t,t'}$ denote the number of loyal consumers of firm $k \in \mathcal{K}$ on each rental arc $e = (n^k_{i,t}, n^k_{i',t'}) \in \mathcal{E}^k_{\mathrm{R}}$; (iii) we let $Y^0_{i,i',t,t'}$ denote the total number of disloyal consumers on the arcs e_A and e_B together. Thus, the total market demand (i.e., the total number of consumers) for any $(i, i', t, t') \in \mathcal{Z}_{\mathrm{R}}$ (i.e., on the arcs $e_A = (n^A_{i,t}, n^A_{i',t'})$ and $e_B = (n^B_{i,t}, n^B_{i',t'})$ together) is $Y^A_{i,i',t,t'} + Y^B_{i,i',t,t'} + Y^0_{i,i',t,t'}$. Recall that $\sum_{i\in\mathcal{M}} \bar{x}_i$ is the maximum number of micromobility vehicles allowed in the service area by the regulator's restriction, and it approximates the size of trip demands in the area (City of Chicago 2022). We thus assume that firm $k \in \mathcal{K}$ wins the share $(\sum_{i\in\mathcal{M}} x^k_i)/(\sum_{i\in\mathcal{M}} \bar{x}_i)$ of the total number of disloyal consumers over any given time-space range $(i, i', t, t') \in \mathcal{Z}_{\mathrm{R}}$, while firm $-k$ wins the remaining disloyal consumers. [1] Thus, the more capacity a firm has, the more disloyal consumers she wins. Then we can describe the rental demand for each firm $k \in \mathcal{K}$ as follows:

$$\overline{w}_e = Y^0_{i,i',t,t'} \frac{\sum_{i\in\mathcal{M}} x^k_i}{\sum_{i\in\mathcal{M}} \bar{x}_i} + Y^k_{i,i',t,t'}, \;\; \forall\, e = (n^k_{i,t}, n^k_{i',t'}) \in \mathcal{E}^k_{\mathrm{R}}, \;\; k \in \mathcal{K}. \qquad (2.2)$$

Equations (2.2) reflect the impact of vehicle accessibility and availability on consumer demands, as examined by Kabra et al. (2020).

[1] It would be interesting to consider the location proximity that the number of disloyal consumers originating from region $i \in \mathcal{M}$ and choosing vehicles from firm k depends on the number of firm k's available vehicles in this region divided by the number of both firms' available vehicles in i (i.e., $x^k_i/(x^A_i + x^B_i)$). However, it will break down the linear programming-based formulation, creating significant computational difficulty.

Second, for each arc $e \in \mathcal{E}$, we let w_e denote its realized flow. Given any nonnegative integers a and b, we let $[a,b]_{\mathbb{Z}}$ denote the set of all integers between a and b; that is, $[a,b]_{\mathbb{Z}} = \{a, a+1, \ldots, b\}$ if $a \leq b$, and $[a,b]_{\mathbb{Z}} = \emptyset$ if $a > b$. Thus, given any node $n_{i,t}^k \in \mathcal{N}$, the number of micromobility vehicles flowing into this node should be the same as the number of vehicles flowing out from this node:

$$\sum_{e \in f^+(n_{i,0}^k)} w_e - x_i^k = 0, \ \forall\, i \in \mathcal{M}, \ k \in \mathcal{K}, \tag{2.3}$$

$$\sum_{e \in f^+(n_{i,t}^k)} w_e - \sum_{e \in f^-(n_{i,t}^k)} w_e = 0, \ \forall\, t \in [1, T-1]_{\mathbb{Z}}, \ i \in \mathcal{M}, \ k \in \mathcal{K}, \tag{2.4}$$

$$- \sum_{e \in f^-(n_{i,T}^k)} w_e + x_i^k = 0, \ \forall\, i \in \mathcal{M}, \ k \in \mathcal{K}, \tag{2.5}$$

where $f^+(n_{i,t}^k)$ and $f^-(n_{i,t}^k)$ denote the sets of arcs that originate and terminate at node $n_{i,t}^k$, respectively. Constraints (2.3) state that in period $t = 0$, the *outflow* of node $n_{i,0}^k$ equals the number of vehicles initially allocated in region $i \in \mathcal{M}$ by firm $k \in \mathcal{K}$. Constraints (2.5) state that the number of vehicles of firm $k \in \mathcal{K}$ in region $i \in \mathcal{M}$ and period T (i.e., the end of the operational horizon) returns back to the original status in period 0.

Finally, we have the following three constraints:

$$w_e \leq \overline{w}_e, \ \forall\, e \in \mathcal{E}_{\mathrm{R}}^k, \ k \in \mathcal{K}, \tag{2.6}$$

$$w_e \leq x_i^k, \ \forall\, e \in \mathcal{E}_{\mathrm{I}}^k, \ k \in \mathcal{K}, \tag{2.7}$$

$$w_e \geq 0, \ \forall\, e \in \mathcal{E}^k, \ k \in \mathcal{K}. \tag{2.8}$$

Constraints (2.6) ensure that the number of vehicles used to fulfill the demand on each rental arc is no larger than the number of rental requests. Constraints (2.7) ensure that the number of idling vehicles on each arc is no larger than the number of vehicles allocated in region $i \in \mathcal{M}$. That is, each firm is not allowed to park too many vehicles in each region during the operational horizon, thereby avoiding traffic congestion. Constraints (2.8) ensure that the realized flow on each arc is non-negative.

In the operation stage, we consider that both loyal and disloyal consumer trips across regions and periods are uncertain. We model the uncertainty by stochastic optimization, because we have substantial historical data to estimate the true probability distribution

of the uncertainty. Specifically, with the widespread adoption of shared micromobility, we have sufficient data to estimate the true distribution of the uncertain consumer trips with sample-average approximation (SAA). The SAA approach has significant performance, as it guarantees convergence to the optimal solution when the amount of samples is large enough (Shapiro et al. 2021). In this stochastic problem, we take into account a finite number of discrete scenarios of these uncertain trips, all of which are contained in the sample set $\mathcal{S}$. Each scenario $s \in \mathcal{S}$ denotes a possible realization of the uncertain loyal and disloyal consumer trips, with a probability $\theta_s = 1/|\mathcal{S}|$. We do not consider realizations of uncertain loyal and disloyal consumer trips independently, because we assume these two types of consumers have the same trip pattern. This is supported by the fact that loyal and disloyal consumers are in the same system, and thus, their demands are affected by the same broad set of factors (e.g., road conditions and weather).

In the operation stage, each firm $k \in \mathcal{K}$ relocates micromobility vehicles with respect to any possible scenario to maximize her expected profit subject to uncertain demands $\overline{w}_e$ for each rental arc $e \in \mathcal{E}^k_{\mathrm{R}}$. We approximate the joint distribution of random variables $(Y^A_{i,i',t,t'}, Y^B_{i,i',t,t'}, Y^0_{i,i',t,t'})$ over any given time-space range $(i, i', t, t') \in \mathcal{Z}_{\mathrm{R}}$ using a set of finite scenarios $\mathcal{S}$. Each scenario $s \in \mathcal{S}$ has a probability $\theta_s \geq 0$ with $\sum_{s\in\mathcal{S}} \theta_s = 1$. For each scenario $s \in \mathcal{S}$, each firm $k \in \mathcal{K}$ makes recourse decisions (e.g., vehicle relocation) for all the periods in $\mathcal{T}$. We reuse the aforementioned notation and add a superscript s to each decision variable in the operation stage for each scenario. For each $s \in \mathcal{S}$ and $k \in \mathcal{K}$, we let $\mathbf{w}^{k,s} = [w^s_e,\ \forall\, e \in \mathcal{E}^k]^\top$ and $W^{k,s}(\mathbf{x}^k) = \{\mathbf{w}^{k,s} \in \mathbb{R}^{|\mathcal{E}^k_{\mathrm{R}}|+|\mathcal{E}^k_{\mathrm{L}}|+|\mathcal{E}^k_{\mathrm{I}}|} \mid (2.2)-(2.8)\}$, where $|\mathcal{E}^k_{\mathrm{R}}| = \sum_{i\in\mathcal{M}} \sum_{j\in\mathcal{M}\setminus\{i\}} \max\{0, T - \ell_{i,j}\}$, $|\mathcal{E}^k_{\mathrm{L}}| = \sum_{i\in\mathcal{M}} \sum_{j\in\mathcal{M}\setminus\{i\}} \max\{0, T - r_{i,j}\}$, and $|\mathcal{E}^k_{\mathrm{I}}| = M(T-1)$. Given the initial vehicle allocation $\mathbf{x}^k$ for each firm $k \in \mathcal{K}$, the expected net cost $\varphi^k(\mathbf{x}^k)$ in the operation stage can be determined by solving the following network flow optimization problem:

$$\varphi^k(\mathbf{x}^k) = \min_{\substack{\mathbf{w}^{k,s}\in W^{k,s}(\mathbf{x}^k),\\ \forall\, s\in\mathcal{S}}} \sum_{s\in\mathcal{S}} \theta_s \left(\sum_{e\in\mathcal{E}^k_{\mathrm{R}}} \left(h^k_{\mathrm{P}}(\overline{w}^s_e - w^s_e) - h^k_{\mathrm{R}} w^s_e \right) + \sum_{e\in\mathcal{E}^k_{\mathrm{I}}} h^k_{\mathrm{I}} w^s_e + \sum_{e\in\mathcal{E}^k_{\mathrm{L}}} h^k_{\mathrm{L}} w^s_e \right). \qquad (\mathcal{O}^k)$$

2.3.5 Equivalent Reformulation

Each firm $k \in \mathcal{K}$ simultaneously solves her decision-making model ($\mathcal{D}^k(\mathbf{x}^{-k})$) to the optimality, and eventually, both firms reach a Nash equilibrium between them. To examine such an equilibrium, we first represent the optimality condition of problem ($\mathcal{D}^k(\mathbf{x}^{-k})$) for each firm $k \in \mathcal{K}$ and then integrate the optimality conditions of both firms to seek

a feasible solution $(\mathbf{x}^A, \mathbf{x}^B)$ from the integrated model that satisfies both conditions. It follows that firm k's vehicle allocation strategy $\mathbf{x}^k$ must be the best response to the other firm's strategy $\mathbf{x}^{-k}$. Note that problem $(\mathcal{D}^k(\mathbf{x}^{-k}))$ is a linear program for each firm $k \in \mathcal{K}$. Thus, we represent its optimality condition using the Karush-Kuhn-Tucker (KKT) conditions and use $\mathcal{W}_0$ to denote the feasible region defined by the KKT conditions of model $(\mathcal{D}^k(\mathbf{x}^{-k}))$ for any $k \in \mathcal{K}$ (see Appendix A.2 for details).

As many equilibria may exist, we can adopt a certain criterion to choose an equilibrium that satisfies such a criterion. In this chapter, we consider two criteria. First, both the regulator and the firms care about the demand loss. On the one hand, the regulator hopes to see more residents use shared micromobility services, thereby supporting a highly convenient and sustainable society. On the other hand, shared micromobility firms hope to satisfy more consumers, thereby generating higher revenues. Thus, while minimizing the net cost (i.e., maximizing the profit) in Problem $(\mathcal{D}^k(\mathbf{x}^{-k}))$, each firm $k \in \mathcal{K}$ would prefer an equilibrium strategy that minimizes the expected total demand loss in the market.That is, we solve the following optimization problem:

$$\Gamma_0^{\mathrm{DL}} = \min_{\mathbf{\Lambda}_0 \in \mathcal{W}_0} \sum_{k \in \mathcal{K}} \sum_{s \in \mathcal{S}} \theta_s \sum_{e \in \mathcal{E}_{\mathrm{R}}^k} (\overline{w}_e^s - w_e^s), \tag{2.9}$$

where $\mathbf{\Lambda}_0$ denotes the vector of all variables associated with both firms in $\mathcal{K}$ (see Appendix A.3).

Second, both the regulator and the firms care about the number of allocated micromobility vehicles. On the one hand, the regulator would not prefer too many vehicles that may cause traffic chaos. On the other hand, some shared micromobility firms, including non-profit organizations, may concern about both surviving in the industry and balancing between reducing the traffic and serving the public. Thus, each firm $k \in \mathcal{K}$ would prefer an equilibrium strategy that minimizes the total number of allocated vehicles in the city while maintaining a certain service level. Specifically, we consider the following optimization problem:

$$\Gamma_0^{\mathrm{TA}} = \min_{\mathbf{\Lambda}_0 \in \mathcal{W}_0} \left\{ \sum_{k \in \mathcal{K}} \sum_{i \in \mathcal{M}} x_i^k \;\middle|\; \sum_{e \in \mathcal{E}_{\mathrm{R}}^k} w_e^s \geq \epsilon \sum_{e \in \mathcal{E}_{\mathrm{R}}^k} \overline{w}_e^s, \ \forall\, k \in \mathcal{K}, \ s \in \mathcal{S} \right\}, \tag{2.10}$$

by which we eventually choose an equilibrium such that the total number of allocated vehicles is minimized and each firm $k \in \mathcal{K}$ guarantees a minimum service level $\epsilon \in [0, 1]$.

2.3.6 Capacity Sharing

We further extend the model ($\mathcal{D}^k(\mathbf{x}^{-k})$) for each firm $k \in \mathcal{K}$ by considering capacity sharing between the two firms in $\mathcal{K}$. Under a capacity-sharing agreement, each firm $k \in \mathcal{K}$ can share her spare vehicles with firm $-k$ if the latter is in shortage of vehicles to satisfy her demands. To prevent the abuse of this agreement (e.g., a firm does not build any capacity), the firms are required to return the borrowed vehicles within a period of $\Delta = \max\{\ell_{ij} \mid \forall, i, j \in \mathcal{M},\ i \neq j\}$. Thus, in addition to the operational decisions of each firm $k \in \mathcal{K}$ in the problem ($\mathcal{O}^k$), the firm k makes two more decisions in each period and service region: (i) the number of vehicles that the firm shares with her opponent (i.e., firm k sends her own vehicles to firm $-k$); (ii) the number of vehicles that the firm returns to her opponent (i.e., firm k returns firm $-k$'s vehicles back).

We expand the spatial-temporal network $\mathcal{G}$ by adding two more types of arcs in the set $\mathcal{E}$ (see Figure 2.2): (i) *Transfer arcs*: The flow on each transfer arc $e = (n^k_{i,t}, n^{-k}_{i,t}) \in \mathcal{E}^k_{\mathrm{T}}$ represents the number of vehicles transferred from firm $k \in \mathcal{K}$ to firm $-k$ in region $i \in \mathcal{M}$ in period $t \in \mathcal{T}$ to satisfy the consumer demands of firm $-k$, by which firm $-k$ pays firm k a compensation $h_{\mathrm{T}} \geq 0$ for each vehicle. (ii) *Return arcs*: The flow on each return arc $e = (n^k_{i,t}, n^{-k}_{i,t}) \in \mathcal{E}^k_{\mathrm{N}_\delta}$ for any $\delta \in \{1, 2, \ldots, \Delta\}$ represents the number of vehicles that firm k receives in period $t \in [1, T-1]_{\mathbb{Z}}$ and returns back to region $i \in \mathcal{M}$ in period $t + \delta \leq T$. No cost is incurred in the return arcs. Thus, the set $\mathcal{A}$ in Section 2.3.2 is expanded to $\{\mathrm{R}, \mathrm{I}, \mathrm{L}, \mathrm{T}, \mathrm{N}_\delta,\ \forall\, \delta = 1, 2, \ldots, \Delta\}$, by which $\mathcal{E}^k = \cup_{\forall\, a \in \mathcal{A}} \mathcal{E}^k_a$ is also updated.

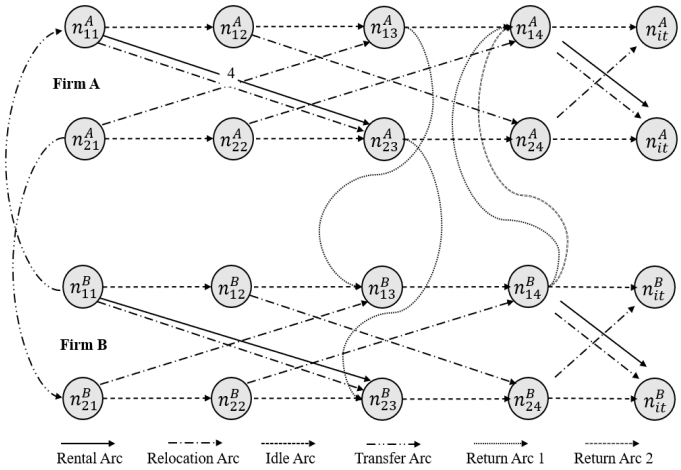

Figure 2.2. Expanded Spatial-Temporal Network $\mathcal{G}$

With the expanded network $\mathcal{G}$ and settings above, the two-stage stochastic program-

ming model for each firm $k \in \mathcal{K}$ is updated as follows:

$$-\Psi^k = \min \ \mathbf{c}^\top \mathbf{x}^k + \sum_{s\in\mathcal{S}} \theta_s \left(\sum_{e\in\mathcal{E}^k_{\mathrm{R}}} \left(h^k_{\mathrm{P}}(\overline{w}^s_e - w^s_e) - h^k_{\mathrm{R}} w^s_e \right) \right. \tag{$\mathcal{C}^k$}$$

$$\left. + \sum_{e\in\mathcal{E}^k_{\mathrm{I}}} h^k_{\mathrm{I}} w^s_e + \sum_{e\in\mathcal{E}^k_{\mathrm{L}}} h^k_{\mathrm{L}} w^s_e - \sum_{e\in\mathcal{E}^k_{\mathrm{T}}} h_{\mathrm{T}} w^s_e + \sum_{e\in\mathcal{E}^{-k}_{\mathrm{T}}} h_{\mathrm{T}} w^s_e \right)$$

$$\text{s.t.} \ \ (2.1);\ (2.2)-(2.4),\ (2.6)-(2.8),\ \forall\, s\in\mathcal{S},$$

$$\sum_{e\in f^+(n^k_{i,T})} w^s_e - \sum_{e\in f^-(n^k_{i,T})} w^s_e + x^k_i = 0,\ \forall\, k\in\mathcal{K},\ i\in\mathcal{M},\ s\in\mathcal{S}, \tag{2.11}$$

$$\sum_{i\in\mathcal{M}} \sum_{e\in\mathcal{E}^{-k}_{\mathrm{T}}(t)} w^s_e - \sum_{i\in\mathcal{M}} \sum_{\delta=1}^{\min\{\Delta, T-t\}} \sum_{e\in\mathcal{E}^k_{\mathrm{N}_\delta}(t)} w^s_e = 0,$$

$$\forall\, k\in\mathcal{K},\ t\in[1,T-1]_{\mathbb{Z}},\ s\in\mathcal{S}, \tag{2.12}$$

where $\mathcal{E}^k_{\mathrm{T}}(t) = \{(n^k_{i,t}, n^{-k}_{i,t}) \in \mathcal{E}^k_{\mathrm{T}} \mid \forall\, i\in\mathcal{M}\}$ and $\mathcal{E}^k_{\mathrm{N}_\delta}(t) = \{(n^k_{i,t}, n^{-k}_{i,t}) \in \mathcal{E}^k_{\mathrm{N}_\delta} \mid \forall\, i\in\mathcal{M}\}$ for any $t\in\mathcal{T}$, $k\in\mathcal{K}$, and $\delta\in[1,\min\{\Delta, T-t\}]$, constraints (2.11) are updated from (2.5) because of the inclusion of return arcs in the network $\mathcal{G}$, and constraints (2.12) ensure that all the vehicles that firm $k\in\mathcal{K}$ borrows from firm $-k$ should be returned back to firm $-k$. Note that it is easy for both firms to comply with the proposed capacity-sharing agreement because each firm can easily receive idling vehicles from her opponent and return them to the opponent in any service region. For instance, if a given firm $k\in\mathcal{K}$ receives 10 and 20 vehicles from two regions in a period, respectively, she can return all of these vehicles to firm $-k$ in any region in $\mathcal{M}$, giving firms the flexibility to use the received vehicles. Indeed, a firm can repeatedly use the received vehicles to fulfill multiple rental requests if the requested trips are short enough. Thus, this capacity-sharing agreement is practically feasible.

We can then examine the Nash equilibrium of the game between Firm A and Firm B under the capacity-sharing agreement by formulating the KKT conditions of model ($\mathcal{C}^k$) for any $k\in\mathcal{K}$, where the feasible region defined by the KKT conditions is denoted by $\mathcal{W}_1$ (see Appendix A.4 for details). We also use the two criteria in Section 2.3.5 (i.e., the expected total demand loss and the total number of allocated micromobility vehicles) to select the corresponding Nash equilibria, respectively. For the first criterion concerning

the expected total demand loss, we solve the following optimization problem:

$$\Gamma_1^{\mathrm{DL}} = \min_{\mathbf{\Lambda}_1 \in \mathcal{W}_1} \sum_{k \in \mathcal{K}} \sum_{s \in \mathcal{S}} \theta_s \sum_{e \in \mathcal{E}_{\mathrm{R}}^k} (\overline{w}_e^s - w_e^s), \tag{2.13}$$

where $\mathbf{\Lambda}_1$ denotes the vector of all variables associated with both firms in $\mathcal{K}$ (see Appendix A.5 for details). For the second criterion concerning the total number of allocated micromobility vehicles, we solve the following optimization problem:

$$\Gamma_1^{\mathrm{TA}} = \min_{\mathbf{\Lambda}_1 \in \mathcal{W}_1} \left\{ \sum_{k \in \mathcal{K}} \sum_{i \in \mathcal{M}} x_i^k \;\middle|\; \sum_{e \in \mathcal{E}_{\mathrm{R}}^k} w_e^s \geq \epsilon \sum_{e \in \mathcal{E}_{\mathrm{R}}^k} \overline{w}_e^s, \; \forall\, k \in \mathcal{K}, \; s \in \mathcal{S} \right\}. \tag{2.14}$$

The following proposition shows that the capacity-sharing agreement between both firms in $\mathcal{K}$ benefits the entire system by reducing the expected total demand loss.

Proposition 1. *When Γ_0^{DL} exists, we have $\Gamma_1^{\mathrm{DL}} - \Gamma_0^{\mathrm{DL}} \leq 0$.*

In addition to Proposition 1, which discusses the impact of capacity sharing on the total demand loss of the two firms, we further investigate its impact on each individual firm in the subsequent section. Specifically, in Section 2.4.5, we analyze the impact of capacity sharing on the relocation of each firm (see Figure 2.15) and its impact on the cost of each firm (see Figure 2.17).

2.4 Numerical Experiments: A Case Study

We conduct numerical experiments based on real operational data from Citi Bike (2022). We first discuss the parameter settings and then obtain managerial insights from various experiments based on the settings. All the numerical experiments are performed on a computing node with 24 2.3-GHz Intel Xeon E5-2670 processors and 32 GB of memory in a high-performance computing cluster. IBM ILOG CPLEX 12.10, under its default setting, is used as the mixed-integer programming (MIP) solver.

2.4.1 Parameter Settings

We collect data from Citi Bike (2022) in New York City (NYC) from January 1 to December 31 in 2019. We focus on Midtown Manhattan in a rectangular area formed by four intersecting streets in NYC: First Avenue, Eleventh Avenue, Twenty-third Street,

and Fifty-seventh Street (see Figure 2.3), and obtain 2,320,205 trips in this area. We specify the geographical locations of all bike docking stations in Figure 2.3 and divide the area into six service regions (i.e., $M = 6$) using k-means clustering based on the Euclidean distance between any two stations. Two stations that are close to each other can be clustered together. The dots of different sizes indicate the station locations and their demand levels, i.e., a larger dot indicates a higher demand level. Note that considering six service regions helps us retain practical features in our models while not leading to a large-scale and expanded spatial-temporal network $\mathcal{G}$, under which the models are difficult to solve.

Based on the trip data, we find that the average trip duration from one region to a neighboring region is 9.77 minutes. For simplicity, we assume the traveling speed between any two neighboring regions is the same and set each period as 10 minutes (leading to 144 periods per day). Table 2.1 summarizes the trip duration in terms of the number of periods (i.e., ℓ_{ij}) between any two service regions $i, j \in \mathcal{M}$ and $i \neq j$.

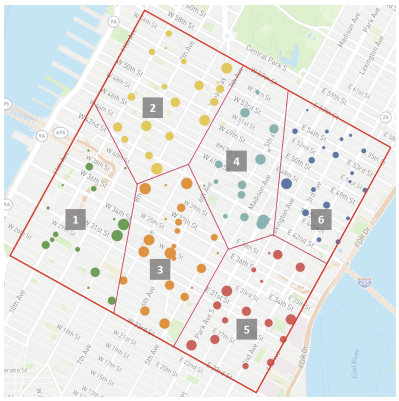

Figure 2.3. Service Regions in Midtown Manhattan

Regions	1	2	3	4	5	6
1	—	1	1	2	1	2
2	1	—	1	1	2	1
3	1	1	—	1	1	1
4	2	1	1	—	1	1
5	1	2	1	1	—	1
6	2	1	1	1	1	—

Table 2.1. Trip Duration Across Service Regions

Figure 2.4 shows the average number of consumer trips in the entire area in a day, with the consumer trips between any starting and destination regions summarized in Figure A.1 (see Appendix A.7). We note that most trip demands occur during the daytime, especially from early morning (approximately 06:00) until night (approximately 22:00), while the demand from 22:00–6:00 is almost negligible. We also note that the demand pattern in the late afternoon exhibits similarity with that in the early morning in most of the regions. Hence, hereafter we assume that the operational horizon for each firm $k \in \mathcal{K}$ is 8 hours, from 6:00 to 14:00 (i.e., the shaded area in Figure 2.4), leading to $T = 48$ periods in our models. It is worth noting that there is at least one peak in

one day, i.e., high volumes of trip demands, regardless of the starting and destination regions. Because the range from 6:00–14:00 covers at least one peak for any starting and destination regions, this operational horizon is appropriate enough to capture both the demand trend and traffic peak.

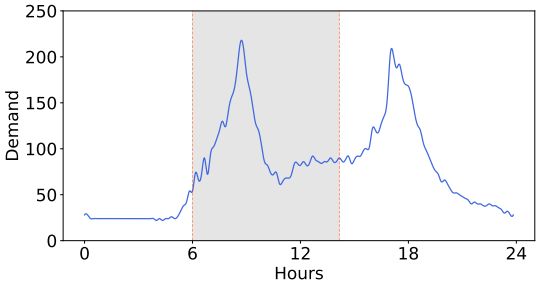

Figure 2.4. Average Number of Consumer Trips in a Day in Midtown Manhattan

For any given 3-tuple (*starting region*, *destination region*, *starting period*), we use the data to obtain the average number of trips (i.e., demands) over all the given data samples between the given starting and destination regions in the given starting period. We let $\overline{D}_{i,j,t}$ denote the average demands from region $i \in \mathcal{M}$ to region $j \in \mathcal{M} \setminus \{i\}$ in period $t \in \mathcal{T}$ (see Figure A.1 for a summary of all these average demands). We let $\hat{D}_{i,t} = \sum_{j \in \mathcal{M} \setminus \{i\}} \overline{D}_{i,j,t}$ for any $i \in \mathcal{M}$ and $t \in \mathcal{T}$, representing the total number of trips originating from region i in period t. Figure 2.5 illustrates the total number of trips originating from each region in three periods: $t = 6$ (low demand level), $t = 18$ (high demand level), and $t = 36$ (low demand level). Clearly, the demands in $t = 18$ represent a peak, and regions 2 and 3 are the busiest regions. We further let $\phi_{i,t,j} = \overline{D}_{i,j,t} / \hat{D}_{i,t}$ for any $i \in \mathcal{M}$, $j \in \mathcal{M} \setminus \{i\}$, and $t \in \mathcal{T}$, representing the percentage of all the trips originating from region i in period t that eventually go to region j. Figure 2.6 illustrates the values of $\phi_{i,t,j}$ for any $i \in \mathcal{M}$ and $j \in \mathcal{M} \setminus \{i\}$ when $t \in \{6, 18, 36\}$.

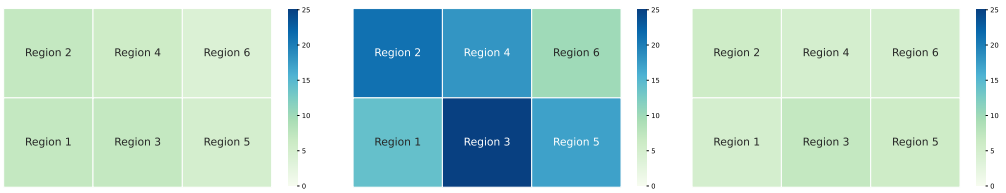

(a) $t = 6$ (7:00–7:10) **(b)** $t = 18$ (9:00–9:10) **(c)** $t = 36$ (12:00–12:10)

Figure 2.5. The Number of Trips Originating From Each Region

For each firm $k \in \mathcal{K}$, we estimate her cost parameters in USD as follows: The micro-

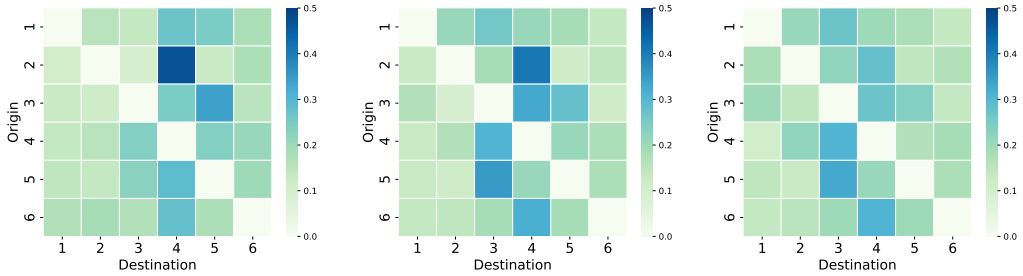

(a) $t = 6$ (7:00–7:10) **(b)** $t = 18$ (9:00–9:10) **(c)** $t = 36$ (12:00–12:10)

Figure 2.6. Trip Percentages

mobility vehicle allocation cost[2] for any $i \in \mathcal{M}$ is $c_i^k = 0.16$. The revenue per vehicle trip[3] is $h_{\mathrm{R}}^k = 0.4$ and the penalty cost per unsatisfied demand[4] is $h_{\mathrm{P}}^k = 0.1$. The relocation cost per relocated vehicle[5] is $h_{\mathrm{L}}^k = 0.12$ and the idle cost per idling vehicle[6] is $h_{\mathrm{I}}^k = 0.06$. The transfer cost per vehicle[7] is $h_{\mathrm{T}} = 0.12$. Given a budget limit to allocate vehicles in $\mathcal{M}$, we set $\hat{x}^k = 1500$, which is sufficiently large because the number of vehicles that each firm eventually allocates is less than $\hat{x}^k$.

The upper bound $\bar{x}_i$ of the total number of vehicles allocated by the two firms in $\mathcal{K}$ in each region $i \in \mathcal{M}$, i.e., *initial vehicle allocation quota*, is not available in the data. Nevertheless, we have $\max\{\sum_{i\in\mathcal{M}} \hat{D}_{i,t} \mid \forall t \in \mathcal{T}\} = 358$. To have a proper number of vehicles in the area to satisfy the trip demands of both firms while not creating traffic chaos on the street, we set $\sum_{i\in\mathcal{M}} \bar{x}_i = 360$. Given the total number of trips originating from region i in period t, $\hat{D}_{i,t}$, for any $i \in \mathcal{M}$ and $t \in \mathcal{T}$, we further set $\bar{x}_i = 360 \times (\sum_{t\in\mathcal{T}} \hat{D}_{i,t})/(\sum_{i\in\mathcal{M}} \sum_{t\in\mathcal{T}} \hat{D}_{i,t})$ for any $i \in \mathcal{M}$. For any two regions $i, i' \in \mathcal{M}$ and $i \neq i'$,

[2]We follow Jin et al. (2023) to estimate the vehicle allocation cost by dividing 150 dollars over 300 operational days and multiplying by 48/144 (i.e., scaling down the cost to our operational horizon), leading to $150/300 \times (48/144) \approx 0.16$.

[3]We assume the revenue generated per trip in the area remains fixed, regardless of the trip's duration. This is because (i) Citi Bike charges a monthly fee of 17 from each consumer and allows this consumer to freely ride bikes for any trip in less than 45 minutes and (ii) all the trips in the area take less than 45 minutes. The revenue per trip is then estimated by assuming that each consumer has two rides per operational day, leading to $300/12 \times 2 = 50$ trips per month and $17/50 \approx 0.4$ per trip.

[4]We test different values of h_{P}^k from 0.1 to 1, and the results are presented in Appendix A.8. The entire system's performance remains relatively consistent across different penalty values. Therefore, we set $h_{\mathrm{P}}^k = 0.1$ for simplicity.

[5]Citi Bike's Bike Angels Rewards Program uses rewards to hire individual riders to relocate vehicles. Specifically, one point is rewarded after one relocation is completed, and every ten points can be exchanged for 1.2 dollars, leading to $1.2/10 = 0.12$ dollars per relocation.

[6]The hourly car-parking rate in Manhattan is usually 4 dollars, leading to $4/6 \approx 0.6$ dollars per period (i.e., 10 min). A car-parking spot is assumed to accommodate 10 micromobility vehicles, leading to $0.6/10 = 0.06$ per vehicle per period.

[7]The firm pays her opponent the transfer cost for receiving a vehicle to satisfy its demand. However, in cases where capacity sharing is not available, the firm may relocate a vehicle from another region to meet this demand. Thus, we assume that the transfer cost equals the relocation cost.

we set $r_{i,i'} = \ell_{i,i'}$.

We further generate scenarios in $\mathcal{S}$. We use a random parameter $\tilde{D}_{i,t}$ to represent the number of trips (i.e., market demands) originating from region $i \in \mathcal{M}$ in period $t \in \mathcal{T}$. We assume that $(\tilde{D}_{1,t}, \ldots, \tilde{D}_{M,t})^\top$ follows a multivariate normal distribution; that is, $(\tilde{D}_{1,t}, \ldots, \tilde{D}_{M,t})^\top \sim \mathcal{N}(\hat{\boldsymbol{D}}_t, \boldsymbol{\Sigma}_t)$, for any $t \in \mathcal{T}$, where $\hat{\boldsymbol{D}}_t = (\hat{D}_{1,t}, \ldots, \hat{D}_{M,t})^\top$ and $\boldsymbol{\Sigma}_t$ represents the corresponding covariance matrix estimated from the given data in each period t. Following this distribution, we randomly generate $1,000$ samples of trip demands and use k-means clustering to cluster them into three groups, where we use the center of each group to represent a demand scenario in $\mathcal{S}$ and thus set $|\mathcal{S}| = 3$. Note that we do not choose a large number of scenarios for two reasons. First, as our models, i.e., (2.9)–(2.10) and (2.13)–(2.14), are large-scale MIPs that can be difficult to solve, our model will become computationally intractable if using a large number of scenarios. Second, the real data shows an apparent demand trend, and thus a few scenarios can well represent the demand uncertainty. We will also discuss the impact of $|\mathcal{S}|$ on computational performance in detail in Section 2.4.2.

Now, given the market demand originating from region $i \in \mathcal{M}$ in period $t \in \mathcal{T}$ and scenario $s \in \mathcal{S}$, denoted by $\dot{D}_{i,t,s}$, we let $D_{i,i',t,t',s} = \dot{D}_{i,t,s}\phi_{i,t,i'}$ for any $(i, i', t, t') \in \mathcal{Z}_{\mathrm{R}}$ and $s \in \mathcal{S}$, representing the trip demand from region i in period t to region i' in period $t' = t + \ell_{i,i'}$ in scenario $s \in \mathcal{S}$. Then, given a percentage (α_k) of consumers who are loyal to each firm $k \in \mathcal{K}$, we have the number of firm k's loyal consumers $Y^k_{i,i',t,t',s} = \alpha_k D_{i,i',t,t',s}$ and the number of disloyal consumers $Y^0_{i,i',t,t',s} = (1-\alpha_A-\alpha_B)D_{i,i',t,t',s}$ over any $(i, i', t, t') \in \mathcal{Z}_{\mathrm{R}}$ and in any scenario $s \in \mathcal{S}$.

2.4.2 Computational Performance

We consider Problem (2.9) and examine the impact of $|\mathcal{S}|$ on its computational performance, thereby demonstrating that setting $|\mathcal{S}| = 3$ is effective enough. Given the multivariate normal distribution $\mathcal{N}(\hat{\boldsymbol{D}}_t, \boldsymbol{\Sigma}_t)$ for any $t \in \mathcal{T}$, we let Ω represent the number of samples that we randomly generate from this distribution. Here, we consider $\Omega \in \{100 \times i, \ \forall\, i \in [1, 10]_{\mathbb{Z}}\}$. Given Ω randomly generated samples, we solve two instances of Problem (2.9): (i) $\mathcal{S}$ collects all the samples, with each sample representing a separate scenario, i.e., $|\mathcal{S}| = \Omega$; (ii) we use k-means clustering to cluster these Ω samples into three groups, with the center of each group representing a separate scenario, i.e.,

$|\mathcal{S}| = 3$. For each $i \in \mathcal{M}$ and $k \in \mathcal{K}$, we let $\hat{x}_i^{k^*}$ (resp. $x_i^{k^*}$) represent firm k's optimal initial allocation decision in region i after solving the first (resp. second) instance above. For each firm $k \in \mathcal{K}$, we use $(\sum_{i\in\mathcal{M}}(x_i^{k^*} - \hat{x}_i^{k^*})^2/|\mathcal{M}|)^{1/2}$ to measure the *relative error* of the solutions (i.e., solution difference) between the above two instances. Figure 2.7 shows the results.

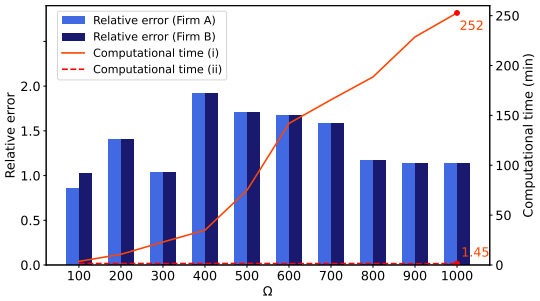

Figure 2.7. Relative Error and Computational Time

For each firm $k \in \mathcal{K}$, the *relative error* is around 1 and always less than 2, regardless of the value of Ω. Note that the optimal solutions of both the above two instances are to allocate 360 vehicles in all regions by the two firms, i.e., $\sum_{k\in\mathcal{K}}\sum_{i\in\mathcal{M}}\hat{x}_i^{k^*} = \sum_{k\in\mathcal{K}}\sum_{i\in\mathcal{M}}x_i^{k^*} = 360$, leading to 60 vehicles in each region on average. Thus, when the *relative error* is 1, it accounts for only 1.67% ($= 1/60 \times 100\%$) of all the allocated vehicles. Such a small error indicates that choosing three scenarios via clustering is effective and representative enough compared to choosing all the available samples. More importantly, Figure 2.7 shows that when $|\mathcal{S}|$ is larger, solving Problem (2.9) becomes more challenging. For instance, when $|\mathcal{S}| = 1,000$ in the first instance, the computational time (see the red solid line) is 252 minutes, while the computational time (see the red dashed line) is only 1.45 minutes when $|\mathcal{S}| = 3$ in the second instance. Thus, choosing three scenarios also helps us efficiently obtain the solutions, enabling practical applications in the industry. As a result, in the subsequent numerical experiments, we focus on using the three scenarios ($|\mathcal{S}| = 3$) we select in Section 2.4.1.

2.4.3 Impact of Initial Vehicle Allocation Quota

We examine the impact of the initial vehicle allocation quota on the firms' performance under the parameter settings in Section 2.4.1. We vary the quota for the entire area $\sum_{i\in\mathcal{M}}\bar{x}_i$ and the percentages of the two firms' loyal consumers (α_A, α_B), while keeping other parameters unchanged and not adopting capacity sharing. With $\sum_{i\in\mathcal{M}}\bar{x}_i$ given at

360, representing a proper-quota case, we also consider $\sum_{i\in\mathcal{M}} \bar{x}_i$ takes half and double of this quota, leading to 180 and 720, representing the low-quota and large-quota cases, respectively. When $\sum_{i\in\mathcal{M}} \bar{x}_i$ is given, we let $\bar{x}_i = \sum_{i\in\mathcal{M}} \bar{x}_i \times (\sum_{t\in\mathcal{T}} \hat{D}_{i,t})/(\sum_{i\in\mathcal{M}} \sum_{t\in\mathcal{T}} \hat{D}_{i,t})$ for any $i \in \mathcal{M}$.

First, we consider the two firms in $\mathcal{K}$ are symmetric with respect to (α_A, α_B), which can be $(0, 0)$, $(0.25, 0.25)$, and $(0.45, 0.45)$. Given $\bar{x}_i$ for any $i \in \mathcal{M}$ and (α_A, α_B), we solve Problem (2.9) (that minimizes the expected total demand loss) and Problem (2.10) (that minimizes the total number of allocated micromobility vehicles). Table 2.2 shows the equilibrium results. For each instance, we use a 3-tuple (*Firm A's result*, *Firm B's result*, *Summation of both firms' results*) to show both firms' performance in the initial vehicle allocation, profit, and service level.

Table 2.2. Impact of Initial Vehicle Allocation Quota on Symmetric Firms

		Allocation		Profit		Service Level (%)	
	(α_A, α_B)	Min. Demand Loss	Min. Allocation	Min. Demand Loss	Min. Allocation	Min. Demand Loss	Min. Allocation
Low (180)	(0, 0)	(0, 180, 180)	(0, 180, 180)	(0, 1801.5, 1801.5)	(0, 1801.5, 1801.5)	(-, 94.3, 94.3)	(-, 94.3, 94.3)
	(0.25, 0.25)	(90, 90, 180)	(90, 90, 180)	(900.3, 900.3, 1,800.6)	(900.3, 900.3, 1,800.6)	(94.3, 94.3, 94.3)	(94.3, 94.3, 94.3)
	(0.45, 0.45)	(90, 90, 180)	(90, 90, 180)	(900.2, 900.2, 1,800.4)	(900.2, 900.2, 1,800.4)	(94.3, 94.3, 94.3)	(94.3, 94.3, 94.3)
Proper (360)	(0, 0)	(0, 360, 360)	(0, 360, 360)	(0, 1,415.3, 1,415.3)	(0, 1,415.3, 1,415.3)	(-, 99.7, 99.7)	(-, 99.7, 99.7)
	(0.25, 0.25)	(180, 180, 360)	(180, 180, 360)	(707.7, 707.7, 1,415.4)	(707.7, 707.7, 1,415.4)	(99.7, 99.7, 99.7)	(99.7, 99.7, 99.7)
	(0.45, 0.45)	(180, 180, 360)	(180, 180, 360)	(707.7, 707.7, 1,415.4)	(707.7, 707.7, 1,415.4)	(99.7, 99.7, 99.7)	(99.7, 99.7, 99.7)
Large (720)	(0, 0)	(0, 720, 720)	(0, 720, 720)	(0, 329.4, 329.4)	(0, 329.4, 329.4)	(-, 100, 100)	(-, 100, 100)
	(0.25, 0.25)	(360, 360, 720)	(65, 65, 130)	(164.6, 164.6, 329.2)	(521.7, 521.7, 1043.4)	(100, 100, 100)	(97.3, 97.3, 97.3)
	(0.45, 0.45)	(360, 360, 720)	(83, 83, 166)	(164.6, 164.6, 329.2)	(830.9, 830.9, 1,661.8)	(100, 100, 100)	(94.2, 94.2, 94.2)

Table 2.2 suggests that setting a proper quota that approximates trip demands can help the firms achieve a high service level and profit simultaneously. Specifically, compared to the low-quota case, the service level of each firm is increased by around 5% under the proper-quota case regardless of the equilibrium criterion and loyal consumer percentages. Compared to the large-quota case, the proper-quota case performs better under different cases: (i) the profit of each firm is increased regardless of the equilibrium criterion when $\alpha_A \in \{0, 0.25\}$ and under the criterion of demand loss when $\alpha_A = 0.45$; (ii) the service level of each firm is also increased under the criterion of initial allocation when $\alpha_A \in \{0.25, 0.45\}$.

Both firms use up the quota under the low- and proper-quota cases regardless of the equilibrium criterion and loyal consumer percentages. For such cases, the number of disloyal consumers each firm can attract by allocating one more vehicle, i.e., $1/\sum_{i\in\mathcal{M}} \overline{x}_i$, is relatively large, motivating the firms to allocate as many vehicles as possible to attract disloyal consumers. Under the large-quota case with a large loyal consumer percentage (i.e., $\alpha_A \in \{0.25, 0.45\}$), both firms use up the quota under the criterion of demand

loss and use the quota partially under the other criterion. When the initial vehicle allocation quota is large, $1/\sum_{i\in\mathcal{M}}\overline{x}_i$ is relatively small, discouraging firms from allocating a large number of vehicles to attract disloyal consumers. Thus, when we aim to find an equilibrium minimizing the total number of allocated vehicles, we may not use up the quota, while a large number of vehicles may be required to achieve an equilibrium minimizing the expected total demand loss.

Table 2.3. Impact of Initial Vehicle Allocation Quota on Asymmetric Firms

	(α_A, α_B)	Allocation		Profit		Service Level (%)	
		Min. Demand Loss	Min. Allocation	Min. Demand Loss	Min. Allocation	Min. Demand Loss	Min. Allocation
Low (180)	(0.1, 0.15)	(72, 108, 180)	(72, 108, 180)	(719.5, 1,082.0, 1,801.5)	(719.5, 1,082.0, 1,801.5)	(94.3, 94.3, 94.3)	(94.3, 94.3, 94.3)
	(0.1, 0.45)	(33, 147, 180)	(49, 131, 180)	(327.3, 1,473.9, 1,801.2)	(386.2, 1,386.9, 1,773.1)	(94.3, 94.3, 94.3)	(96.3, 92.5, 93.3)
	(0.1, 0.8)	(20, 160, 180)	(20, 160, 180)	(200.0, 1,601.4, 1801.4)	(200.0, 1,601.4, 1801.4)	(94.2, 94.3, 94.3)	(94.2, 94.3, 94.3)
	(0.3, 0.4)	(76, 104, 180)	(80, 100, 180)	(771.5, 1,030.0, 1,801.5)	(763.3, 1,000.7, 1,764.0)	(94.3, 94.3, 94.3)	(93.5, 92.8, 93.1)
	(0.3, 0.6)	(60, 120, 180)	(65,115,180)	(600.2, 1,201.3, 1,801.5)	(602.2, 1,195.2, 1,797.4)	(94.3, 94.3, 94.3)	(95.2, 93.6, 94.1)
Proper (360)	(0.1, 0.15)	(151, 209, 360)	(103, 257, 360)	(582.2, 833.1, 1,415.3)	(471.7, 939.2, 1,410.9)	(99.7, 99.7, 99.7)	(99.2, 99.7, 99.5)
	(0.1, 0.45)	(69, 291, 360)	(55, 305, 360)	(258.1, 1157.2, 1,415.3)	(251.4, 1,159.9, 1,411.3)	(99.8, 99.7, 99.7)	(98.9, 99.7, 99.6)
	(0.1, 0.8)	(39, 321, 360)	(20, 161, 181)	(158.4, 1256.7, 1,415.1)	(189.9, 1,519.1, 1,709.0)	(99.7, 99.7, 99.7)	(95.2, 95.2, 95.2)
	(0.3, 0.4)	(156, 204, 360)	(87, 116, 203)	(605.0, 810.2, 1,415.2)	(651.0, 868.0, 1,519.0)	(99.7, 99.7, 99.7)	(97.9, 97.9, 97.9)
	(0.3, 0.6)	(131, 229, 360)	(60, 121, 181)	(447.8, 967.5, 1,415.3)	(569.7, 1,139.3, 1709.0)	(99.9, 99.6, 99.7)	(95.2, 95.2, 95.2)
Large (720)	(0.1, 0.15)	(343,377,720)	(35, 53, 88)	(108.7, 219.4, 328.1)	(231.9, 347.8, 579.7)	(100, 100, 100)	(98.7, 98.7, 98.7)
	(0.1, 0.45)	(77, 643, 720)	(26, 116, 142)	(137.8, 190.4, 328.3)	(205.1, 923.1, 1,128.2)	(100, 100, 100)	(97.4, 97.4, 97.4)
	(0.1, 0.8)	(43, 677, 720)	(19, 149, 168)	(134.4, 194.2, 328.6)	(184.9, 1479.1, 1,664.0)	(100, 100, 100)	(94.4, 94.4, 94.4)
	(0.3, 0.4)	(64, 86, 150)	(64, 86, 150)	(586.3, 781.8, 1368.1)	(586.3, 781.8, 1,368.1)	(95.7, 95.7,95.7)	(95.7, 95.7,95.7)
	(0.3, 0.6)	(56, 112, 168)	(56, 112, 168)	(554.6, 1109.3, 1663.9)	(554.6, 1109.3, 1,663.9)	(94.4,94.4,94.4)	(94.4,94.4,94.4)

Next, we consider the two firms in $\mathcal{K}$ are asymmetric with respect to (α_A, α_B), i.e., $\alpha_A \neq \alpha_B$. Table 2.3 shows the equilibrium results. We obtain the following results that are consistent with the symmetric case in Table 2.2: (i) under the proper-quota case, each firm can attain a high service level and profit; (ii) under the low-quota case, the firms use up the allocation quota; and (iii) under the large-quota case, the firms may not use up the quota, and the total number of allocated vehicles and profits increase with the loyal consumer percentage. We also obtain results that are inconsistent with the symmetric case. Specifically, under the proper-quota case, both firms do not use up the quota when $\alpha_A + \alpha_B$ is large (e.g., 0.7 and 0.9) under the equilibrium criterion of the initial allocation. This happens mainly because the market competitiveness under the asymmetric case when $\alpha_A + \alpha_B$ is large is weaker than that under the symmetric case, where neither firm dominates the market, and both firms have to halve the market equally. That is, under the symmetric case, both firms allocate as many vehicles as possible to attract disloyal consumers and thus use up the quota. In contrast, when $\alpha_A + \alpha_B$ is large under the asymmetric case, both firms are less willing to compete for limited disloyal consumers.

2.4.4 Impact of Competition

We examine the impact of competition by comparing the performance of the models with and without competition. Specifically, we consider Problems (2.9) and (2.10) as the models with competition. We let $\tilde{x}_i^k = \bar{x}_i \times \alpha_k/(\alpha_A + \alpha_B)$ for each firm $k \in \mathcal{K}$ in region $i \in \mathcal{M}$, and for each firm $k \in \mathcal{K}$, we define

$$\min_{\mathbf{x}^k} \left\{ {\mathbf{c}^k}^\top \mathbf{x}^k + \varphi^k\left(\mathbf{x}^k\right) \;\middle|\; \sum_{i\in\mathcal{M}} x_i^k \le \hat{x}^k; \quad x_i^k \le \tilde{x}_i^k,\ \forall\, i \in \mathcal{M}; \quad x_i^k \ge 0,\ \forall\, i \in \mathcal{M} \right\}$$

as the model without competition. Given an initial vehicle allocation quota and loyal consumer percentages, (i) we solve the above model and show the results in Table 2.4 (see the columns "W/O Competition"); (ii) we select the equilibrium result that yields the highest profit by Problems (2.9) and (2.10) (see the columns "W/ Competition" in Table 2.4). Note that here we consider the "*highest profit*" because the model without competition minimizes the total cost, i.e., maximizes the total profit, ensuring fair comparisons.

Table 2.4. Impact of Competition Under Asymmetric Cases

	(α_A, α_B)	Allocation		Profit		Service Level (%)	
		W/ Competition	W/O Competition	W/ Competition	W/O Competition	W/ Competition	W/O Competition
Low (180)	(0.1, 0.15)	(72, 108, 180)	(70, 110, 180)	(719.5, 1,082.0, 1,801.5)	(705.7, 1095.8, 1801.5)	(94.3, 94.3, 94.3)	(94.1, 94.3, 94.2)
	(0.1, 0.45)	(33, 147, 180)	(31, 149, 180)	(327.3, 1,473.9, 1,801.2)	(319.6, 1481.6, 1801.2)	(94.3, 94.3, 94.3)	(93.7, 94.4, 94.2)
	(0.1, 0.8)	(20, 160, 180)	(17, 163, 180)	(200.0, 1,601.4, 1801.4)	(195.3, 1603.8, 1799.1)	(94.2, 94.3, 94.3)	(91.2,94.5,94.2)
	(0.3, 0.4)	(76, 104, 180)	(74, 106, 180)	(771.5, 1,030.0, 1,801.5)	(762.4, 1038.3, 1800.7)	(94.3, 94.3, 94.3)	(93.7, 94.6, 94.2)
	(0.3, 0.6)	(60, 120, 180)	(59, 121,180)	(600.2, 1,201.3, 1,801.5)	(599.5, 1201.9, 1801.4)	(94.3, 94.3, 94.3)	(94.0, 94.4, 94.3)
Proper (360)	(0.1, 0.15)	(151, 209, 360)	(142, 218, 360)	(582.2, 833.1, 1,415.3)	(561.7, 853.7, 1415.3)	(99.7, 99.7, 99.7)	(99.7,99.7,99.7)
	(0.1, 0.45)	(69, 291, 360)	(64, 296, 360)	(258.1, 1157.2, 1,415.3)	(257.0, 1158.3, 1415.3)	(99.8, 99.7, 99.7)	(99.6, 99.7, 99.7)
	(0.1, 0.8)	(20, 161, 181)	(20, 161, 181)	(189.9, 1519.1, 1709.0)	(189.9, 1519.1, 1709.0)	(95.2, 95.2, 95.2)	(95.2, 95.2, 95.2)
	(0.3, 0.4)	(87, 116, 203)	(87, 116, 203)	(651.0, 868.0, 1519.0)	(651.0, 868.0, 1519.0)	(97.9, 97.9, 97.9)	(97.9, 97.9, 97.9)
	(0.3, 0.6)	(60, 121, 181)	(60, 121, 181)	(569.7, 1,139.3, 1709.0)	(569.7, 1,139.3, 1709.0)	(95.2, 95.2, 95.2)	(95.2, 95.2, 95.2)
Large (720)	(0.1, 0.15)	(35, 53, 88)	(35, 53, 88)	(231.9, 347.8, 579.7)	(231.9, 347.8, 579.7)	(98.7, 98.7, 98.7)	(98.7, 98.7, 98.7)
	(0.1, 0.45)	(26, 116, 142)	(26, 116, 142)	(205.1, 923.1, 1128.2)	(205.1, 923.1, 1128.2)	(97.4, 97.4, 97.4)	(97.4, 97.4, 97.4)
	(0.1, 0.8)	(19, 149, 168)	(19, 149, 168)	(184.9, 1479.1, 1,664.0)	(184.9, 1479.1, 1,664.0)	(94.4, 94.4, 94.4)	(94.4, 94.4, 94.4)
	(0.3, 0.4)	(64, 86, 150)	(64, 86, 150)	(586.3, 781.8, 1,368.1)	(586.3, 781.8, 1,368.1)	(95.7, 95.7,95.7)	(95.7, 95.7,95.7)
	(0.3, 0.6)	(56, 112, 168)	(56, 112, 168)	(554.6, 1109.3, 1663.9)	(554.6, 1109.3, 1663.9)	(94.4,94.4,94.4)	(94.4,94.4,94.4)

When $\alpha_A \neq \alpha_B$, we call the firm with a lower loyal consumer percentage the *weak* firm and the other the *strong* firm. For instance, when $(\alpha_A, \alpha_B) = (0.1, 0.45)$, Firm A is the weak firm and Firm B is the strong firm. Table 2.4 suggests that the weak firm benefits from the competition, which hurts the strong firm though. When no competition exists, the weak firm is given a small quota to allocate vehicles, while she has the opportunity to use the entire quota to allocate more vehicles and earns a higher profit after the competition is introduced. It follows that the strong firm is left with a smaller quota to allocate vehicles than before. Such changes after introducing the competition are more significant when the disloyal consumer percentage (i.e., $1 - \alpha_A - \alpha_B$) is large under the

proper-quota case. This is intuitive because more disloyal consumers lead to a more competitive market, where the competition will have a greater impact on the two firms.

We further analyze how each firm allocates vehicles in each region when the competition is present. For each instance of the model with competition described above, we let $x_i^{k^*}$ be the equilibrium allocation decision of firm $k \in \mathcal{K}$ in region $i \in \mathcal{M}$ that achieves the highest profit as mentioned above, and define $x_i^{k^*}/(x_i^{k^*} + x_i^{-k^*})$ as the allocation ratio of firm k in region i. For each firm $k \in \mathcal{K}$, we compare this ratio with $\alpha_k/(\alpha_A + \alpha_B)$, which defines the proportion of quota issued to firm k when there is no competition; a larger allocation ratio indicates that the competition facilitates more allocated vehicles. Specifically, we consider Problem (2.9) with $\alpha_B = 0.45$ and $\alpha_A \in \{0.1, 0.2, 0.3, 0.4\}$, where Firm A is the weak firm. Figure 2.8 shows the two firms' allocation ratios in every region (see the gray and white bars), where the red dashed line shows the value of $\alpha_A/(\alpha_A+\alpha_B)$. Thus, when the grey bar of region $i \in \mathcal{M}$ exceeds (i.e., is higher than) the red line, i.e., $x_i^{A^*}/(x_i^{A^*} + x_i^{B^*}) > \alpha_A/(\alpha_A + \alpha_B)$, we say the weak firm (i.e., Firm A) allocates more vehicles in region i after the competition is introduced.

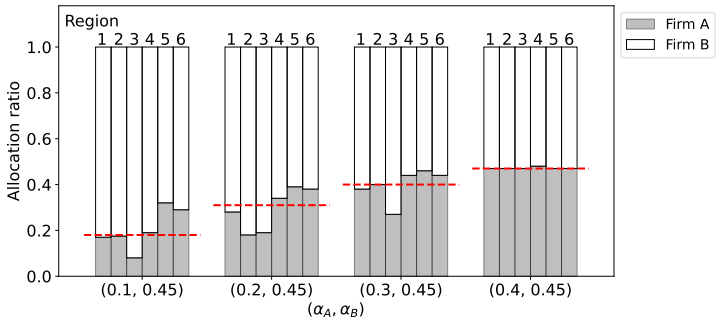

Figure 2.8. Initial Allocation in Each Region

Figure 2.8 shows that the weak firm allocates more vehicles in regions 5 and 6 and allocates less in regions 2 and 3 (i.e., the busiest regions with the largest consumer trips), compared to the case without competition. That is, regarding vehicle allocation in each region, the strong firm dominates the busy regions while the weak firm focuses on the non-busy ones. Note that allocating more vehicles in the busy regions is crucial to meet more trip demands, motivating the strong firm to prioritize the vehicle allocation there and allocate less in the non-busy regions. As a result, the weak firm allocates more vehicles to the non-busy regions. As α_A grows, Firm A becomes more comparably competitive with Firm B, which becomes more difficult to allocate vehicles in the busy regions, and eventually, the two firms' performance becomes similar.

2.4.5 Impact of Capacity Sharing

We investigate the impact of capacity sharing on firms' operations by comparing the results of Problem (2.9) (that does not consider capacity sharing) and Problem (2.13) (that considers capacity sharing). First, we consider the two firms in $\mathcal{K}$ are symmetric with respect to (α_A, α_B), i.e., $\alpha_A = \alpha_B \in \{10\% + i \times 5\%,\ \forall\, i \in [0,7]_{\mathbb{Z}}\}$. For any given α_A, we obtain the same symmetric equilibrium result after solving Problem (2.13) (see Table 2.5). In this equilibrium, neither firm would like to share vehicles with her opponent.

Table 2.5. Symmetric Equilibrium for Symmetric Firms

Allocation		Profit		Transfer		Demand		Service Level	
Firm A	Firm B	Firm A	Firm B	Firm A	Firm B	Firm A	Firm B	Firm A	Firm B
180	180	707.67	707.67	0	0	2724.04	2724.04	99.70	99.70

For any given α_A, we also obtain an asymmetric equilibrium (see Table 2.6). Firm A allocates fewer vehicles and has fewer total demands than Firm B. Despite fewer allocated vehicles, Firm A can receive vehicles transferred from Firm B due to the capacity-sharing agreement and thus achieves a high service level. Furthermore, when each firm has more loyal consumers, i.e., α_A is larger, the two firms' performance becomes closer, and the number of vehicles shared between the two firms drops. Thus, even when two firms are symmetric, one firm may act like a free rider that allocates fewer vehicles and asks for vehicles transferred from her opponent if needed.

Table 2.6. Asymmetric Equilibrium for Symmetric Firms

$\alpha_A(\alpha_B)$	Allocation		Profit ($)		Transfer		Demand		Service Level (%)	
	Firm A	Firm B	Firm A	Firm B	Firm A	Firm B	Firm A	Firm B	Firm A	Firm B
10%	74	286	193.35	1221.98	0	4.37	1440.72	4007.37	99.94	99.61
15%	108	252	409.07	1006.26	0	2.54	1961.31	3486.77	99.78	99.65
20%	150	210	554.64	860.69	0	1.95	2457.52	2990.57	99.80	99.61
25%	164	196	626.10	789.23	0	1.32	2601.46	2846.62	99.80	99.60
30%	171	189	650.22	765.11	0	1.02	2668.38	2779.71	99.72	99.67
35%	173	187	668.51	746.82	0	0.71	2693.76	2754.32	99.68	99.71
40%	176	184	687.50	727.83	0	0.51	2713.15	2734.94	99.73	99.67
45%	178	182	705.49	709.84	0	0.13	2719.91	2728.17	99.67	99.72

Next, we consider the two firms in $\mathcal{K}$ are asymmetric with respect to (α_A, α_B), i.e., $\alpha_A \neq \alpha_B$. We fix $\alpha_B = 45\%$ and vary α_A from 10% to 40%; that is, Firm B is the strong firm and Firm A is the weak firm. For ease of exposition, we define *Symmetry Level* (denoted by *SL*) as α_A/α_B, measuring the similarity between Firm A and Firm B. We further consider the factors that reflect the strong firm's ability to attract more loyal consumers. Specifically, the strong firm may use more advanced vehicles and provides

better services during operations, leading to a higher unit allocation cost and higher penalty, relocation, and idle costs, respectively. Thus, we set higher cost parameters for the strong firm in the following experiments by multiplying the strong firm's cost parameters (i.e., unit allocation, penalty, relocation, and idle costs) by a factor of $u \geq 1$. Detailed managerial insights are provided in the following sections.

Vehicle Transfers

First, we examine how the symmetry level SL and factor u affect the number of transferred vehicles. Figure 2.9 displays the number of transferred vehicles averaged over all the regions and periods with respect to different values of SL and u. No matter what u is, the number of transferred vehicles first increases and then decreases as SL increases. Specifically, when SL is small, i.e., α_A is small, the number of trip demands that Firm A should satisfy is small and can be mostly covered by her own allocated vehicles, leading to a small number of transferred vehicles. When SL grows, i.e., α_A increases, Firm A sees a larger demand to satisfy, leading to an increased need for available vehicles to satisfy demands and hence an increased number of transferred vehicles. When SL further grows, i.e., α_A becomes large, the number of disloyal consumers in the market shrinks. The weak firm, i.e., Firm A, becomes more comparable to her opponent and tends to build capacity to serve her loyal consumers. Meanwhile, the strong firm is reluctant to build a high capacity because the shrinkage of disloyal consumers in the market limits her benefits. It follows that both firms become less likely to share their vehicles.

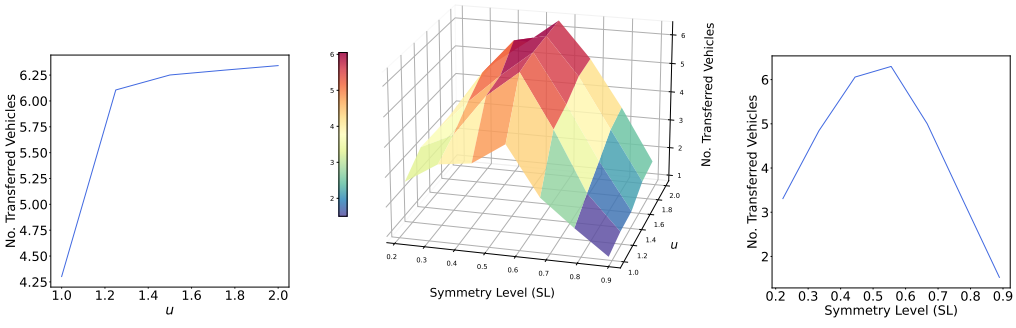

(a) $SL = 0.55$ **(b)** Various SL and u **(c)** $u = 1.75$

Figure 2.9. Number of Transferred Vehicles

Next, we examine the *temporal* and *spatial* features of transferred vehicles in detail. We consider $u = 1.25$ and $\alpha_A = 0.25$ and show the system's performance in Figures 2.10 and

2.11. Note that we choose $u = 1.25$ because shared micromobility firms do not have such large cost differences and choose $\alpha_A = 0.25$ because the number of transferred vehicles is significant (see Figure 2.9). Figure 2.10 shows the number of transferred vehicles averaged over all service regions during the entire operational horizon. The number of transferred vehicles is substantial during peak hours (i.e., $t \in [12, 18]_{\mathbb{Z}}$ or 8:00–9:00) and remains low during other periods, which is consistent with the trend of trip demands in Figure 2.4. A high trip demand indeed leads to a substantial need for available vehicles and an increased number of transferred vehicles, and vice versa.

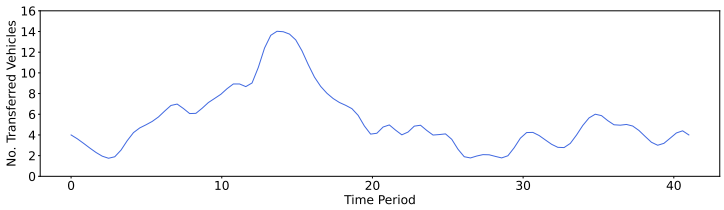

Figure 2.10. Vehicle Transfers

(a) $t = 6$ (7:00–7:10) **(b)** $t = 18$ (9:00–9:10) **(c)** $t = 36$ (12:00–12:10)

Figure 2.11. Spatial Features of Vehicle Transfers

Figure 2.11 shows the number of transferred vehicles in each region in periods $t \in \{6, 18, 36\}$. Regions 2 and 3 are the regions where most vehicles are shared and transferred between the two firms. Note that these two regions also have the largest trip demands that originate from them (see Figure 2.5). Therefore, in the period and region with high trip demands, we also see a large number of transferred vehicles. This indicates that capacity sharing can help firms to satisfy demands and potentially reduce traffic congestion on streets. We further examine the impacts of capacity sharing on firms' operations by comparing the results of Problem (2.9) and Problem (2.13) in the following three sections.

Impact on Relocation

We examine the benefits of capacity sharing in reducing the number of relocated vehicles (i.e., *relocation reduction*). When capacity sharing is adopted, one might expect a firm to

reduce her relocation because she can use vehicles from her opponent to satisfy demands instead of relocating her own vehicles. This expectation is confirmed by the results in Figure 2.12, showing that the total relocation reduction is positive and first increases then decreases with SL. This pattern with SL coincides with that in the number of transferred vehicles (see Figure 2.9). To obtain detailed insights into this pattern, we further investigate the *temporal* and *spatial* features of relocation reduction by fixing $u = 1.25$ and $\alpha_A = 0.25$.

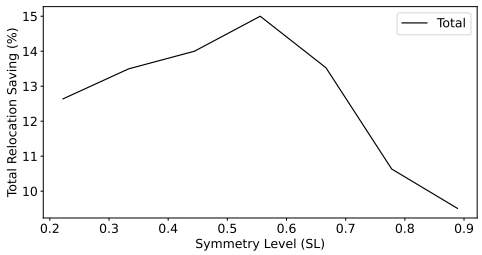

Figure 2.12. Impact of Capacity Sharing on Relocation Reduction

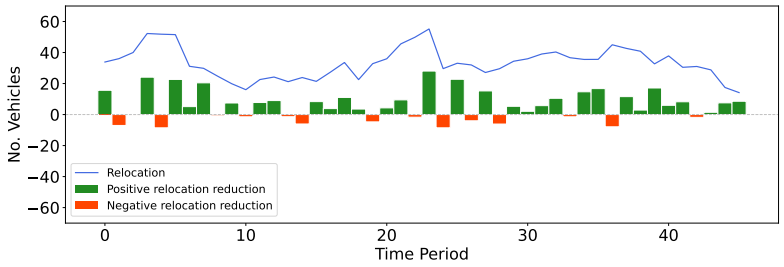

Figure 2.13. Impact of Capacity Sharing on Relocation Reduction in Each Period

Figure 2.13 shows the total number of relocated vehicles (i.e., *total relocation*) when capacity sharing is not considered (see the blue line) and the total relocation reduction (see the green/red bars) when capacity sharing is adopted in each period. The relocation reduction is positive in most periods and slightly negative in others. Meanwhile, the relocation reduction is limited during peak hours (i.e., $t \in [10, 20]_{\mathbb{Z}}$ or 7:40–9:20), but it is large right before and after the peak hours. To explain this phenomenon, we analyze the number of relocated vehicles that occur before, during, and after the peak hours when capacity sharing is not considered. (i) Before the peak hours, many vehicles are relocated, preparing for the upcoming high trip demands. After introducing capacity sharing, a firm can receive vehicles from her opponent to satisfy demands during peak hours (see many transferred vehicles during peak hours in Figure 2.10), by which the total relocation before the peak hours is reduced, i.e., the relocation reduction is significant. (ii) During the peak hours, the number of relocated vehicles is small because many vehicles

are used to satisfy the high demands and few vehicles can be relocated. Meanwhile, since the demands decrease significantly after the peak hours, a large-scale relocation during peak hours is unnecessary. Due to the small number of relocated vehicles, the relocation reduction by capacity sharing is also limited. (iii) After the peak hours, the number of relocated vehicles becomes large. This happens because vehicles can be clustered in some regions after many consumer trips are completed and must be relocated to other regions for the upcoming demands there. After introducing capacity sharing, a firm can receive vehicles from her opponent and hence does not need to relocate as many vehicles as when capacity sharing is not adopted, leading to significant relocation reduction again.

Figure 2.14(a) displays the number of relocated vehicles in each region averaged over all the periods when capacity sharing is not adopted. We focus on the demand features in three clusters of regions (see Figures 2.5 and 2.6) and the corresponding relocation features. (i) In the first cluster with regions 2 and 3, which are the busiest pick-up regions, many consumers need to travel from there and hence each firm relocates many vehicles to this cluster to satisfy demands. (ii) In the second cluster with regions 4 and 5, which are the busiest destination regions, vehicles are cluttered there and hence each firm relocates many vehicles from this cluster to other regions. (iii) In the third cluster with regions 1 and 6, which are neither the busiest pick-up regions nor the busiest destination regions, each firm relocates vehicles both from and to this cluster. Figure 2.14(b) shows the relocation reduction in each region averaged over all the periods after introducing capacity sharing. Clearly, the relocation reduction mainly occurs in the regions where the total relocation is high, which confirms that capacity sharing is a substitute for relocation.

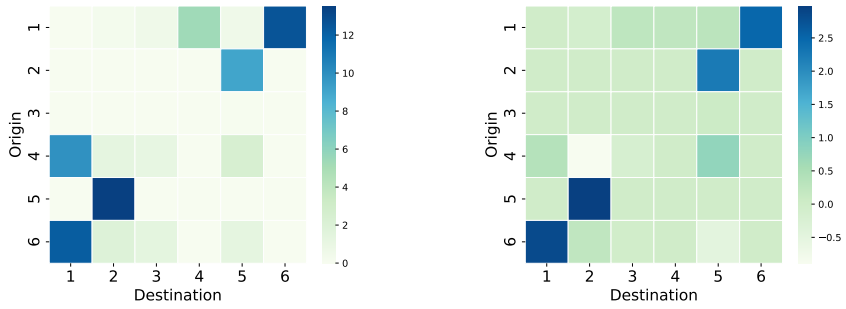

(a) Spatial Features of Relocation

(b) Spatial Features of Relocation Reduction

Figure 2.14. Impact of Capacity Sharing on Relocation in Each Region

Figure 2.15 provides an example to demonstrate how capacity sharing can substitute

for relocation. We consider a simplified case where Firm A operates in regions i and j from periods t to $t+3$. The number of trip demands from region j to i in period $t+1$ is d_1, and the numbers of trip demands from region i to j in periods $t+1$ and $t+2$ are d_2 and d_3, respectively. We assume that $d_3 \geq d_1 \geq d_2$ and show the number of vehicles on each arc in Figure 2.15. For example, in Figure 2.15(a), the number of vehicles on the arc from $n^A_{i,t+1}$ to $n^A_{j,t+2}$ is 0, while the trip demand from $n^A_{i,t+1}$ to $n^A_{j,t+2}$ is d_2.

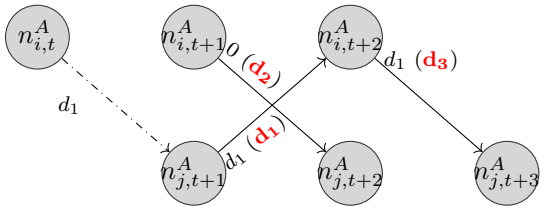

(a) An Optimal Solution without Capacity Sharing

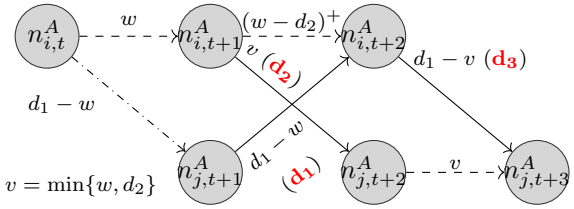

(b) A Feasible but Non-optimal Solution without Capacity Sharing

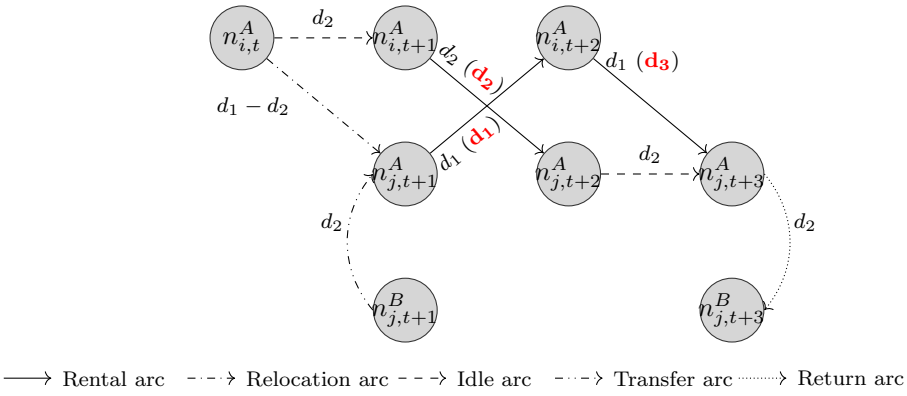

(c) An Optimal Solution with Capacity Sharing

Figure 2.15. Capacity Sharing Reduces Relocation

Figure 2.15(a) shows an optimal solution when capacity sharing is not adopted. Firm A relocates d_1 vehicles in advance from region i in period t to serve the d_1 consumers originating from region j in $t+1$. These vehicles are then reused to serve some of the d_3 consumers originating from region i in period $t+2$. Note that none of the d_2 consumers originating from region i in period $t+1$ is served. The total cost corresponding to this optimal solution $\text{cost}_\text{a} = h^A_\text{L} d_1 + h^A_\text{P}(d_2 + d_3 - d_1) - 2h^A_\text{R} d_1$. Figure 2.15(b) shows a solution with $d_1 - w$ vehicles relocated from region i in period t to region j when capacity sharing

is not adopted, where $0 \leq w \leq d_1$, leaving w vehicles idle in region i and period t. The total cost corresponding to this solution

$$\begin{aligned}\text{cost}_\text{b} &= h_\text{L}^A(d_1 - w) + h_\text{P}^A(w + d_3 - d_1 + d_2) + 2h_\text{I}^A w - h_\text{R}^A(d_1 - w + d_1) \\ &= \text{cost}_\text{a} + \left(h_\text{R}^A + h_\text{P}^A + 2h_\text{I}^A - h_\text{L}^A\right) w.\end{aligned}$$

As $h_\text{R}^A + h_\text{P}^A + 2h_\text{I}^A - h_\text{L}^A > 0$ by the parameter setting in Section 2.4.1, we have $\text{cost}_\text{b} > \text{cost}_\text{a}$. This explains why Firm A relocates d_1 vehicles, instead of fewer ones, from region i in period t when capacity sharing is not adopted. In addition, following the solution in Figure 2.15(a), Firm A serves $2d_1$ consumers in total, but she serves only $2d_1 - w$ consumers following the solution in Figure 2.15(b). Thus, a good relocation decision helps the firms serve more consumers and maximizes profit.

Figure 2.15(c) shows an optimal solution when capacity sharing is adopted. Firm A relocates $d_1 - d_2$ vehicles from region i in period t to region j, where $0 \leq d_2 \leq d_1$, and receives d_2 vehicles from her opponent (i.e., Firm B) to serve the d_1 consumers originating from j in $t + 1$. Some of the d_3 consumers originating from i in $t + 2$ are served, and the received d_2 vehicles are returned to Firm B in period $t + 3$. The total cost corresponding to this solution

$$\begin{aligned}\text{cost}_\text{c} &= h_\text{L}^A(d_1 - d_2) + h_\text{P}^A(d_3 - d_1) + 2h_\text{I}^A d_2 + h_\text{T} d_2 - h_\text{R}^A(2d_1 + d_2) \\ &= \text{cost}_\text{a} - (h_\text{R}^A + h_\text{P}^A - 2h_\text{I}^A + h_\text{L}^A - h_\text{T})d_2.\end{aligned}$$

As $h_\text{R}^A + h_\text{P}^A - 2h_\text{I}^A + h_\text{L}^A - h_\text{T} > 0$ by the parameter setting in Section 2.4.1, we have $\text{cost}_\text{c} < \text{cost}_\text{a}$. Therefore, by adopting capacity sharing, a firm can reduce the number of relocated vehicles while satisfying more consumers (i.e., $2d_1 + d_2$) than that (i.e., $2d_1$) when capacity sharing is not adopted.

Impact on Total Costs

We further examine the benefits of capacity sharing in saving the firms' costs. The cost saving by capacity sharing is defined as the difference between the minimum total cost (i.e., the maximum total profit) without capacity sharing and that with capacity sharing. A positive cost saving means that capacity sharing improves the firms' profitability.

Figure 2.16 shows that the total cost saving (i.e., the summation of cost savings for

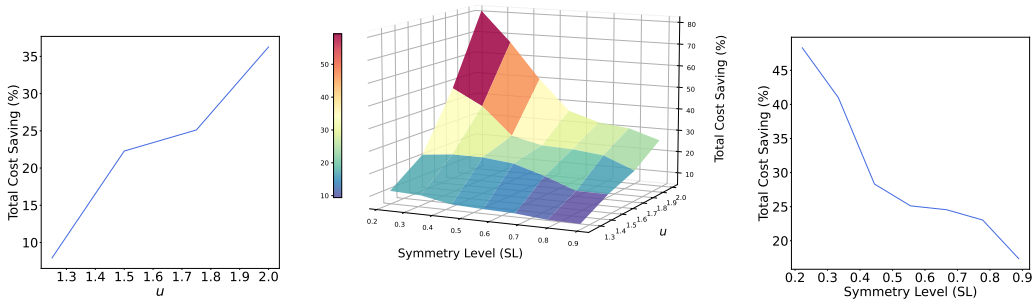

(a) $SL = 0.55$ **(b)** Various SL and u **(c)** $u = 1.75$

Figure 2.16. Impact of Capacity Sharing on Cost Saving

both firms) is always positive, regardless of SL and u. This confirms the effectiveness of capacity sharing in introducing cost savings to the industry. Meanwhile, the cost-saving benefit shrinks as the two firms become more symmetric (i.e., SL becomes larger). Specifically, as α_A becomes closer to α_B, the weak firm (i.e., Firm A) tends to build her own capacity to serve her loyal and disloyal consumers. Meanwhile, the strong firm is also reluctant to build a high capacity because the shrinkage of disloyal consumers limits the benefits. Thus, firms are less likely to share their capacities when they become more symmetric, and the benefit of the capacity-sharing scheme is insubstantial compared to the case without capacity sharing. The above observations demonstrate two effects that the capacity-sharing scheme brings: (i) *the demand uncertainty reduction effect*, i.e., capacity sharing can align the excessive supply and demand; (ii) *the free-rider effect*, i.e., a weak firm with fewer loyal consumers can free-ride the strong opponent's capacity to serve consumers, especially disloyal consumers. More importantly, we should promote the capacity-sharing agreement when the two firms have different numbers of loyal consumers, specifically when the discrepancy is large.

In addition, the cost saving increases with u. Note that capacity sharing can improve the two firms' operations, such as facilitating vehicle transfers (see Section 2.4.5) and reducing vehicle relocation (see Section 2.4.5). When the cost parameters of the strong firm increase, the cost that capacity sharing can reduce for her during the operation also increases. Thus, the cost-saving benefit is more significant as u increases, demonstrating that the unit cost of the strong firm affects the effectiveness of capacity sharing. We further investigate how capacity sharing affects each firm's total cost in detail. Specifically, we consider $u = 1.25$ and vary the value of SL.

Figure 2.17(a) continues to show that the total cost saving is positive and decreases with SL, whereas Figure 2.17(b) surprisingly shows that asymmetric firms cannot obtain better profitability simultaneously. Specifically, Firm A, the weak firm, has a negative cost saving, and Firm B, the strong firm, has a positive cost saving by capacity sharing. That is, capacity sharing benefits the strong firm and hurts the weak firm regarding cost reduction. Therefore, some interventions should be provided to incentivize both firms to reach a capacity-sharing agreement. For example, the strong firm that benefits may charge a lower transfer cost h_{T} from the weak firm. Moreover, the regulator may reduce some costs for the weak firm (i.e., Firm A), such as the plate registration cost (included by $\mathbf{c}^A$) and the idle cost (i.e., h_{I}^A), to incentivize the weak firm that suffers increased costs to reach the capacity-sharing agreement.

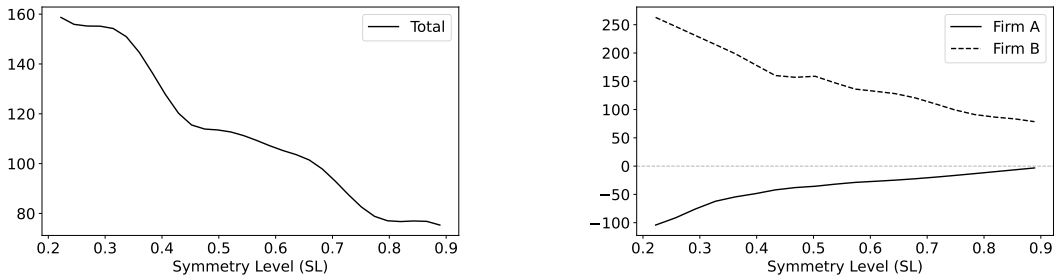

(a) Total Cost Saving **(b)** Individual Cost Saving

Figure 2.17. Impact of Capacity Sharing on Cost Saving When $u = 1.25$

Impact of Budget

In the above studies, we set $\hat{x}^k = 1500$, a sufficiently large limit for firm $k \in \mathcal{K}$ to allocate vehicles. Here we consider a budget limit that constrains the firms to allocate vehicles. Specifically, we vary the values of $\hat{x}^A$ and $\hat{x}^B$ and examine how they affect the firms' demand loss and the effectiveness of capacity sharing in reducing demand loss. We let $u = 1.25$ and $(\alpha_A, \alpha_B) = (0.15, 0.45)$ and compare the results of Problem (2.9) and Problem (2.13).

First, we fix $\hat{x}^A + \hat{x}^B = 360$ and vary the value of $\hat{x}^A$ from 160 to 60, by which $\hat{x}^B$ changes from 200 to 300. Figure 2.18 shows positive demand loss reduction, and such a reduction effect diminishes as $\hat{x}^B$ increases. Specifically, when $\hat{x}^B$ is small, Firm B, the strong firm, has large trip demands but is constrained from allocating enough vehicles to satisfy them, leading to significant demand losses. After capacity sharing is adopted, Firm

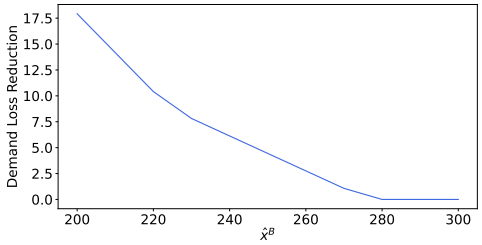

Figure 2.18. Demand Loss Reduction When $\hat{x}^A$ and $\hat{x}^B$ Change

B can receive vehicles from her opponent to satisfy the demands, leading to significant demand loss reduction. When $\hat{x}^B$ increases, Firm B is allowed to allocate more vehicles to satisfy her trip demands, reducing her reliance on capacity sharing and alleviating the demand loss reduction effect.

Next, we examine the impact of allocation budgets by fixing $\hat{x}^k$ fixed and varying the value of $\hat{x}^{-k}$. We consider $(\hat{x}^A, \hat{x}^B) = (60, 300)$ and the following two cases: (i) fixing $\hat{x}^B = 300$ and decreasing the value of $\hat{x}^A$ from 60 to 20; (i) fixing $\hat{x}^A = 60$ and decreasing the value of $\hat{x}^B$ from 300 to 260. Figure 2.19(a) shows the total demand loss of the two firms for the above two cases when capacity sharing is not adopted. Specifically, decreasing $\hat{x}^A$ only (the weak firm) results in a greater demand loss than decreasing $\hat{x}^B$ only (the strong firm). When capacity sharing is further adopted, the total demand loss is reduced only for the first case. Figure 2.19(b) shows the corresponding demand loss reduction for the first case, where the reduction increases as $\hat{x}^A$ decreases. This implies that when the weak firm's allocation budget is severely limited, adopting capacity sharing can significantly reduce the entire market's demand loss. Therefore, we should promote the capacity-sharing agreement when the two firms have different allocation budgets, specifically when the discrepancy is large.

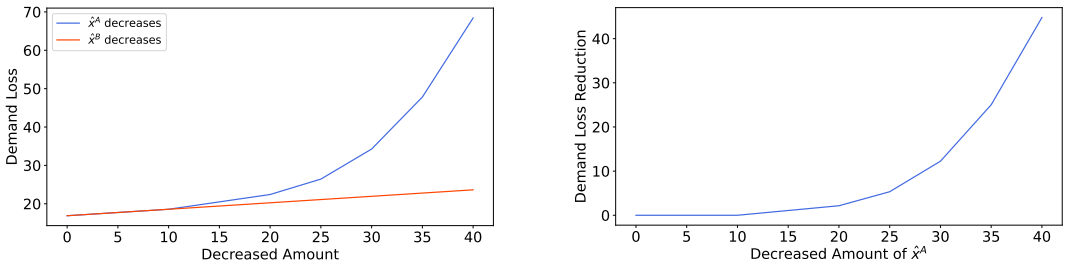

(a) Demand Loss **(b)** Demand Loss Reduction

Figure 2.19. Demand Loss When One Firm's Budget Changes

2.5 Conclusion

Different from other shared mobility systems, a shared micromobility system often (i) bears the high investment cost of heavy assets (e.g., micromobility vehicles) while charging a low rental price, (ii) offers the convenience of vehicle pick-ups and drop-offs that may lead to a severe imbalance between supply and demand under uncertain consumer demands though, and (iii) provides micromobility services not on an on-demand basis like ride-hailing, while the micromobility vehicles can be centrally managed and even shared with the competitors to serve demands. These three features draw attention to the initial allocation and subsequent operation of vehicles in the shared micromobility system. Currently, multiple shared micromobility firms operate in a city. The fierce competition among firms brings additional challenges to firms' decisions to allocate and relocate vehicles. Meanwhile, the city regulator (i) restricts the total number of vehicles in the market allocated to each service region to avoid traffic congestion on streets and (ii) expects to provide sustainable transportation services to as many city residents as possible. Such a restriction and expectation further challenge firms' vehicle allocation and relocation.

We consider two shared micromobility firms competing in the same service area with several service regions over an operational horizon. Each firm provides micromobility vehicles to satisfy the uncertain demands of two types of consumers: *loyal consumers* and *disloyal consumers*, capturing the demand heterogeneity in consumer loyalty. Each firm solves an integrated vehicle allocation and relocation problem, in which the total number of vehicles allocated by the two firms together in each service region is constrained by the city regulator, and provides a Nash equilibrium. Each firm's decision-making problem is formulated as a two-stage stochastic program on a spatial-temporal network, with the objective of maximizing her expected profit. In the capacity-development stage (1st stage), each firm decides initial vehicle allocation for service regions. In the operation stage (2nd stage), the firm makes subsequent vehicle relocation decisions as recourse across service regions to match supply with demand after the demands are realized in each period. Specifically, consumer demands depend on capacity decisions (i.e., the number of allocated vehicles), capturing the demand features in the shared micromobility market.

We explore the optimality condition of each firm's decision-making and provide a tractable optimization formulation to obtain the Nash equilibrium by optimizing certain objectives (i.e., criteria for selecting an equilibrium) over the joint optimality conditions

of both firms. In addition, to improve firms' operations with the limited number of allocated vehicles, we propose an innovative capacity-sharing agreement, under which a firm can share spare capacity for a fee with her opponent when both of them are competing in the same market. We prove that the capacity-sharing agreement between both firms benefits the entire system by reducing the expected total demand loss (see Proposition 1).

Based on real data collected from Citi Bike (2022), we perform numerical experiments to obtain managerial insights for the regulator and the firms with respect to two criteria for selecting an equilibrium: (i) minimizing the total demand loss of both firms and (ii) minimizing the total number of allocated vehicles. We discover the following insights that may provide valuable guidance for city regulations and for vehicle allocations and operations of shared micromobility firms in the competitive market.

(i) It is critical to set a proper initial vehicle allocation quota that approximates consumer trip demands, by which each firm can achieve a high service level and profit simultaneously. A small quota may restrict firms from serving consumers, leading to a low service level, and a large quota may push firms to allocate many vehicles, leading to a high cost and traffic congestion (see Section 2.4.3).

(ii) The competition benefits the weak firm with a few loyal consumers because she can allocate more vehicles to earn a higher profit than before when no competition exists. Such a benefit is more significant when the number of disloyal consumers is large and a proper quota for initial vehicle allocation is enforced. Regarding vehicle allocation in each region, the strong firm dominates the busy regions with high consumer demands, while the weak firm focuses on non-busy regions. When the weak firm becomes more comparably competitive with the strong firm, the two firms' performance becomes similar (see Section 2.4.4).

(iii) After introducing capacity sharing, one firm may act like a free rider that allocates fewer vehicles and asks for vehicles transferred from her opponent if needed when the two firms are symmetric. Meanwhile, many vehicles are shared in periods and regions with high trip demands. Capacity sharing can reduce the number of relocated vehicles by serving as a substitution for relocation and also improves the firms' profitability. However, the two firms cannot obtain better profitability simultaneously from the capacity-sharing agreement. Some interventions from the city regulator are needed to incentivize both

firms to reach the agreement. In addition, capacity sharing can reduce the entire market's demand loss when the firms' allocation budgets are limited (see Section 2.4.5).

Although our numerical experiments are based on Citi Bike (2022), our proposed models and solution approaches are general enough for any typical shared micromobility market with two or more competing firms, thereby offering valuable insights for other shared micromobility systems with similar operational and competitive features. Note that the number of consumers firm $k \in \mathcal{K}$ attracts depends on the total number of allocated vehicles divided by the initial vehicle allocation quota (i.e., $\sum_{i\in\mathcal{M}} x_i^k / \sum_{i\in\mathcal{M}} \bar{x}_i$ in constraints (2.2)) because the quota approximates the size of trip demands, thereby manifesting the firm's ability in attracting consumers. In addition, the loyal consumer percentages (α_A, α_B) are exogenously given because we focus on how the firms compete for disloyal consumers and further operate the system. It would be appealing to consider the decision to create loyal consumers. For instance, loyal consumers may be created by firms' advertising efforts and we can then endogenize the number of loyal consumers (Baye and Morgan 2009) in our models. We leave these for future research. Note that we consider no return cost in this study. Paying an additional positive return cost is equivalent to increasing the unit transfer cost h_{T}, because we assume the unit transfer cost remains fixed, regardless of the vehicle's transfer region or return period. We have conducted numerical tests to validate this equivalence. Our numerical results further demonstrate that a slight increase in transfer price does not significantly affect the operations of firms. Consequently, considering a positive return cost has no substantial impacts on the results. In future research, we plan to explore varying unit transfer costs across different regions. Additionally, we will consider a positive return cost that is dependent on the return period.

Chapter 3

Data-Driven Operations for Electric Vehicle-Sharing System with Vehicle-to-Grid Electricity Discharging

3.1 Introduction

A shared mobility system offers consumer services of picking up a vehicle nearby and dropping it off in any permitted service region at any time, offering short-term rental programs. Due to its flexibility and cost-effectiveness, the shared mobility system has gained popularity in numerous cities worldwide, with an annual growth rate of 30% (Soppert et al. 2022). Driven by the advances in electrical vehicles (EVs), which promise zero carbon emissions and low operation costs, EVs are transforming the shared mobility industry. Many car-sharing companies are transitioning from a fleet of fossil-fuel vehicles to a fleet comprised of EVs. For example, Zipcar, a leading car-sharing company, has allocated over 600 EVs across London and aims to upgrade its fleet to fully electric by 2025 (Zipcar 2024).

Despite the benefits, EVs introduce additional operational challenges for the system operator. The electric nature of EVs necessitates effective battery management to ensure they maintain sufficient capacity to meet trip demands. Managing the battery charging in the EV fleet operation poses a significant challenge because EVs can only be charged

at specific locations equipped with charging facilities, and the charging process is time-consuming, rendering EVs idle and unusable for serving consumer trips during this period. In addition to charging, EVs can also discharge stored electricity back to the power grid using vehicle-to-grid (V2G) technology, generating revenue for the system. However, this feature further adds complexity and challenges to the EV fleet operation. Consequently, the EV-sharing mobility system requires a reliable and advanced model to optimize its EV fleet management.

In addition to the above challenges posed by battery charging/discharging, the system operator also faces challenges from uncertain consumer trips. The uncertain consumer trips across all service regions and periods are dependent, leading to high-dimensional and correlated uncertainties. Consequently, estimating the exact probability distribution of uncertain trips requires a significant amount of historical data. However, such data is usually challenging to acquire in practice, especially considering EV-sharing mobility is a relatively new industry. Therefore, there is a need for an optimization method that can generate a reliable solution without requiring a large number of data. Distributionally robust optimization (DRO) takes into account certain information about the uncertain parameter, including its support, mean, and covariance. It can generate a reliable solution even when the optimization problem incorporates information with estimation errors. Furthermore, increasing the sample size in DRO problems improves its solution quality without increasing the problem size (Fathabad et al. 2020). These suggest that DRO is well-suited for addressing the above challenges in the EV-sharing mobility system. Because this system has limited available data, which may lead to estimation errors, and the problem size in this system is significant even in a deterministic scenario.

In this chapter, we focus on an EV-sharing mobility system incorporating V2G technology. In this system, an operator provides a fleet of EVs to satisfy consumer trips in a service area over an operational horizon, meanwhile, it needs to manage the charging/discharging of EVs during operations. The consumer trips across regions in all periods are uncertain and correlated. We jointly optimize vehicle initial allocation and subsequent operation, including charging and discharging, under uncertainties. To make a reliable solution under uncertainty with a limited amount of available data, we construct a two-stage DRO model. Our contributions and main results are summarized as follows:

(i) We present a formulation of operations in an EV-sharing mobility system incorporating V2G technology through a two-stage DRO model. In the first stage, we decide the initial vehicle allocation for the service regions, whereas in the second stage, we determine the subsequent charging and discharging operations over the horizon. In our DRO model, the true distribution of uncertain consumer trips lies in a set of distributions with known support and first- and second-moment information, which is estimated from historical data.

(ii) We introduce an exact semidefinite programming (SDP) reformulation of the two-stage DRO model. We derive outer and inner approximations for the DRO problem and propose algorithmic approaches to obtain high-quality solutions efficiently. Our numerical experiments based on data collected from TLC (2024) in New York City (NYC) suggest that our approaches yield high-quality solutions in a significantly short computational time. The outstanding performance of DRO, as compared to stochastic optimization and robust optimization, is demonstrated by the obtained results.

(iii) Our study yields the following managerial insights for the EV-sharing system incorporating V2G technology. EVs majorly charge electricity during the early hours when electricity prices and consumer trips are low. Conversely, they discharge electricity when prices are high. Faster charging reduces the number of allocated vehicles, improves the vehicle utilization rate, and decreases total costs. Comparing two pricing schemes for charging EVs, electricity-based and time-based, we observe more frequent charging and discharging under the time-based scheme than the electricity-based scheme.

After reviewing the related literature in Section 3.2, we formulate the problem in Sections 3.3 and 3.4. Section 3.5 proposes our approaches. Section 3.6 conducts numerical experiments to examine the performance of our proposed approaches and the mobility system. Section 3.7 concludes this chapter.

3.2 Related Literature

The field of shared mobility has drawn numerous attention because of its value in urban transportation and sustainability. In such a system, a customer can rent a vehicle from an individual vehicle owner for a short trip (e.g., Nair and Miller-Hooks 2011 and Benjaafar

et al. 2022b). Shu et al. (2013) develop two linear programming models to optimize bicycle allocation and bicycle fleet operation in a bicycle-sharing system. Lu et al. (2018) propose a two-stage stochastic model to optimize fossil-fuel vehicle allocation and fleet operation under uncertain demand.

Different from bicycle sharing or fossil-fuel vehicle sharing, EV sharing sees additional challenges in managing battery levels during operations. He et al. (2017) study a service region design problem by incorporating both the customer adoption rate for EVs and fleet operations, including charging, under uncertainty. He et al. (2021a) develop an optimization model to jointly plan battery charging plots and manage fleet charging operations in an EV-sharing mobility system. Dong et al. (2022) develop a Markov decision process model to dynamically employ EVs with a low battery level for charging and EVs with a high battery level for serving customers, aiming to minimize customer waiting time and customer loss. Abouee-Mehrizi et al. (2021) investigate a shared mobility system that incorporates both fossil-fuel vehicles and EVs, allowing customers to choose between the two. They develop a queueing model to examine in what conditions it is optimal to replace fossil-fuel vehicles with EVs.

Recently, some studies further extend the work in the EV-sharing system by incorporating V2G technology. Zhang et al. (2021) develop a two-stage stochastic program to optimize EV allocation and fleet operation in an EV-sharing mobility system with V2G. Their stochastic model considers a small number of discrete scenarios, whose correlations are omitted, and is solved by the sample average approximation approach. Qi et al. (2022) explore an EV-sharing mobility system connected with an urban microgrid through V2G. They formulate deterministic models to optimize EV fleet dispatch and electricity exchange. Our work further extends the existing studies on operations in the EV-sharing mobility system with V2G, providing a comprehensive consideration of uncertainty by capturing the correlations of uncertain trips across all service regions and periods.

Uncertainty poses challenges to decision making in many real-life problems. To overcome such challenges, advanced optimization approaches are proposed by existing studies. Among them, stochastic optimization (SO), robust optimization (RO), and DRO prevail nowadays (Fathabad et al. 2020). SO assumes knowledge of the probability distribution of uncertain parameters, which is hard to be precisely estimated in practice due to the

limited available data (Shapiro et al. 2021). RO assumes knowledge of the uncertainty set and hedges against the worst-case scenario within this set, leading to a conservative solution possibly (Ben-Tal et al. 2009). DRO relaxes the assumption of known probability distribution in SO and reduces the conservativeness of RO (Scarf 1958, Rahimian and Mehrotra 2019). It optimizes decisions against the worst-case distribution within a distributional ambiguity set. Delage and Ye (2010) propose a general moment-based DRO problem with an ambiguity set considering the information of support, mean, and covariance of uncertain parameters. They further reformulate the problem as a semidefinite program (SDP), which can be solved in polynomial time. Recognizing the benefits of DRO approach proved by existing studies, our study adopts this approach to effectively address the challenges posed by uncertainties in the EV-sharing mobility system with V2G.

3.3 Problem Formulation

Consider a shared electrical vehicle (EV) firm that operates an EV fleet, where each EV owns a range of state-of-charge (SoC) denoted by the set $\mathcal{S} = \{1, 2, \ldots, S\}$. The firm provides shared mobility service for a set of service regions $\mathcal{Z} = \{1, 2, \ldots, Z\}$ in each period $t \in \mathcal{T} = \{0, 1, \ldots, T\}$. We first study the movement of EVs with different SoC across service regions in the operation horizon and then construct an optimization model.

3.3.1 Vehicle Movement: A Time-Space-SoC Network

We model the movement of EVs with different SoC across regions and periods as the flow in a time-space-SoC network $\mathcal{G} = (\mathcal{N}, \mathcal{A})$, where $\mathcal{N}$ is the set of nodes and $\mathcal{A}$ is the set of directed arcs on the network as shown in Figure 3.1. A node $n_{z,t,s} \in \mathcal{N}$ represents region $z \in \mathcal{Z}$ in period $t \in \mathcal{T}$ and SoC $s \in \mathcal{S}$. The directed arc $(n_{z,t,s}, n_{z',t',s'}) \in \mathcal{A}$ represents the number of EVs moving from node $n_{z,t,s}$ to node $n_{z',t',s'}$.

Based on how EVs are moved between two nodes, we define five types of arcs in $\mathcal{A}$ in the time-space-SoC network:

(i) *Rental arcs*: The flow on each rental arc $(n_{z,t,s}, n_{z',t',s'}) \in \mathcal{A}^{\mathrm{R}}$ represents the number of EVs from region z in period t and SoC s to region $z' \neq z$ in period $t' = t + \ell_{z,z'}$ and SoC $s' = s - b_{z,z'}$ for rental trips, where $\ell_{z,z'}$ and $b_{z,z'}$ represent the number of

periods and number of SoC units an EV needs to move from region z to region z'. We have $(z, z', t, t', s, s') \in \mathcal{W}^{\mathrm{R}} := \{\mathcal{Z} \times \mathcal{Z} \times \mathcal{T} \times \mathcal{T} \times \mathcal{S} \times \mathcal{S} \mid (n_{z,t,s}, n_{z',t',s'}) \in \mathcal{A}^{\mathrm{R}}\}$.

(ii) *Idle arcs*: The flow of each idle arc $(n_{z,t,s}, n_{z,t+1,s}) \in \mathcal{A}^{\mathrm{I}}$ represents the number of idling EVs in region z from period t to period $t+1$. We have $(z, t, s) \in \mathcal{W}^{\mathrm{I}} := \{\mathcal{Z} \times \mathcal{T} \times \mathcal{S} \mid (n_{z,t,s}, n_{z,t+1,s}) \in \mathcal{A}^{\mathrm{I}}\}$.

(iii) *Relocation arcs*: The flow of each relocation arc $(n_{z,t,s}, n_{z',t',s}) \in \mathcal{A}^{\mathrm{L}}$ represents the number of EVs relocated from region z in period t and SoC s to region $z' \neq z$ in period $t' = t + \ell_{z,z'}$ and SoC s. We have $(z, z', t, t', s) \in \mathcal{W}^{\mathrm{L}} := \{\mathcal{Z} \times \mathcal{Z} \times \mathcal{T} \times \mathcal{T} \times \mathcal{S} \mid (n_{z,t,s}, n_{z',t',s}) \in \mathcal{A}^{\mathrm{L}}\}$.

(iv) *Charging arcs*: The flow of each charging arc $a = (n_{z,t,s}, n_{z,t+1,s'}) \in \mathcal{A}^{\mathrm{C}}$ represents the number of EVs in region z, period t, and SoC s charged to $s' = s + \delta^{\mathrm{C}}$ after one period, where δ^{C} represents the charging rate per period. We have $(z, t, s) \in \mathcal{W}^{\mathrm{C}} := \{\mathcal{Z} \times \mathcal{T} \times \mathcal{S} \mid (n_{z,t,s}, n_{z,t+1,s}) \in \mathcal{A}^{\mathrm{C}}\}$.

(v) *Discharging arcs*: The flow of each discharging arc $a = (n_{z,t,s}, n_{z,t+1,s'}) \in \mathcal{A}^{\mathrm{S}}$ represents the number of EVs in region z, period t, and SoC s discharged to $s' = s - \delta^{\mathrm{S}}$ after one period, where δ^{S} represents the discharging rate per period. We have $(z, t, s) \in \mathcal{W}^{\mathrm{S}} := \{\mathcal{Z} \times \mathcal{T} \times \mathcal{S} \mid (n_{z,t,s}, n_{z,t+1,s}) \in \mathcal{A}^{\mathrm{S}}\}$.

Hence, we have $\mathcal{A} = \mathcal{A}^{\mathrm{R}} \cup \mathcal{A}^{\mathrm{I}} \cup \mathcal{A}^{\mathrm{L}} \cup \mathcal{A}^{\mathrm{C}} \cup \mathcal{A}^{\mathrm{S}}$.

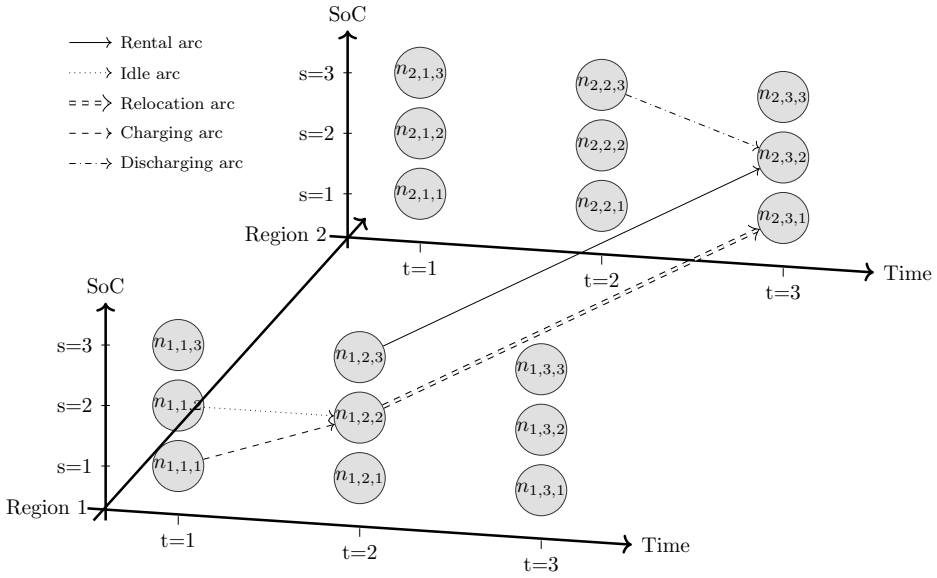

Figure 3.1. An Example of Time-Space-SoC Network

We formulate the problem as a two-stage model. In the first stage, we decide the initial number of EVs allocated to each service region. In the second stage, we decide EVs operations during the whole operational horizon.

3.3.2 First-stage Formulation

The operator is endowed with a budget that can afford at most $\overline{X}$ EVs. In the first stage, the operator makes the allocation decisions $x_{z,s}$ in region $z \in \mathcal{Z}$ with SoC $s \in \mathcal{S}$ so that

$$\sum_{z\in\mathcal{Z}}\sum_{s\in\mathcal{S}} x_{z,s} \leq \overline{X}. \tag{3.1}$$

A cost $c_s(\geq 0)$ is incurred for allocating an EV with SoC $s \in \mathcal{S}$ to any region. The government regulates parking spaces by establishing parking lots. These lots are categorized into three types: the lots without charging/discharging facilities (denoted by N), the lots with charging facilities (denoted by C), and the lots with discharging facilities (denoted by S). We denote the set of parking lots by $\mathcal{K} = \{\mathrm{N}, \mathrm{C}, \mathrm{S}\}$. We denote the number of parking lots $k \in \mathcal{K}$ in region $z \in \mathcal{Z}$ by X_z^k. Then due to the regulations on the parking space, we have

$$\sum_{s\in\mathcal{S}} x_{z,s} \leq \sum_{k\in\mathcal{K}} X_z^k, \ \forall\, z \in \mathcal{Z}. \tag{3.2}$$

Facing uncertain demands, the operator makes its initial vehicle allocation decisions in the first stage and subsequent operational decisions in the second stage to minimize its expected profit under a known distribution $\mathbb{P}$. Given the first-stage decisions $\mathbf{x} = (x_{z,s}, \forall\, z \in \mathcal{Z}, s \in \mathcal{S})^\top$ and a realization of uncertainty $\boldsymbol{\xi}$, we let $f(\mathbf{x}, \boldsymbol{\xi})$ denote the optimal operation costs in the second stage. The operator optimizes its allocation decisions by solving the following problem:

$$\min_{\mathbf{x}} \left\{ \sum_{z\in\mathcal{Z}}\sum_{s\in\mathcal{S}} c_s x_{z,s} + \mathbb{E}_{\mathbb{P}}\left[f\left(\mathbf{x}, \boldsymbol{\xi}\right)\right] \middle| (3.1) - (3.2) \right\}. \tag{$\mathcal{P}_0$}$$

3.3.3 Second-stage Formulation

At the beginning of the second stage, the uncertainty $\boldsymbol{\xi}$ is realized. Hence, the operator knows the time-space-dependent demands $d_{z,t,z'}(\boldsymbol{\xi})$ arriving at each region $z \in \mathcal{Z}$ at the start of each period $t \in \mathcal{T}$ and going to $z' \in \mathcal{Z}, z' \neq z$. We let $\mathcal{M} := \{(z,t,z') | \exists (n_{z,t,s}, n_{z',t',s'}) \in \mathcal{A}^{\mathrm{R}}\}$ denote the set of all trip demands. We introduce a con-

tinuous decision variable $w_a(\boldsymbol{\xi})$ to represent the number of vehicles on the flow $a \in \mathcal{A}$ with respect to realization $\boldsymbol{\xi}$. We let $[a,b]_{\mathbb{Z}}$ denote the set of all integers between any two nonnegative integers a and b, that is, $[a,b]_{\mathbb{Z}} = \{a, a+1, \ldots, b\}$ if $a \leq b$, and $[a,b]_{\mathbb{Z}} = \emptyset$ if $a > b$. Thus, given any node $n_{z,t,s} \in \mathcal{N}$, the number of EVs flowing into this node should be the same as the number of vehicles flowing out from this node:

$$\sum_{a \in \mathcal{A}_+(n_{z,0,s})} w_a(\boldsymbol{\xi}) = x_{z,s}, \ \forall\, z \in \mathcal{Z},\ s \in \mathcal{S}, \tag{3.3}$$

$$\sum_{a \in \mathcal{A}_+(n_{z,t,s})} w_a(\boldsymbol{\xi}) = \sum_{a \in \mathcal{A}_-(n_{z,t,s})} w_a(\boldsymbol{\xi}), \ \forall\, t \in [1, T-1]_{\mathbb{Z}},\ z \in \mathcal{Z},\ s \in \mathcal{S}, \tag{3.4}$$

$$\sum_{z \in \mathcal{Z}} \sum_{s \in \mathcal{S}} \sum_{a \in \mathcal{A}_-(n_{z,T,s})} w_a(\boldsymbol{\xi}) = \sum_{z \in \mathcal{Z}} \sum_{s \in \mathcal{S}} x_{z,s}, \tag{3.5}$$

where $\mathcal{A}_+(n_{z,t,s})$ and $\mathcal{A}_-(n_{z,t,s})$ denote the sets of arcs that originate and terminate at $n_{z,t,s} \in \mathcal{N}$, respectively. Constraints (3.3) state that in period $t = 0$, the *outflow* of $n_{z,0,s}$ equals the number of EVs with SoC $s \in \mathcal{S}$ initially allocated in region $z \in \mathcal{Z}$. Constraints (3.5) state that the sum of EVs in all regions with any SoC at the end equals the total number of EVs initially allocated.

For any trip demands $d_{z,t,z'}(\boldsymbol{\xi})$ where $(z,t,z') \in \mathcal{M}$, the operator can employ EVs with different SoC $s \in \mathcal{S}$ to serve them, represented by different rental arcs. For any $(z,t,z') \in \mathcal{M}$, we let $\hat{\mathcal{A}}^{\mathrm{R}}(z,t,z') := \{(n_{z,t,s}, n_{z',t',s'}) \in \mathcal{A}^{\mathrm{R}}\}$ denote the set of rental arcs for satisfying demands $d_{z,t,z'}(\boldsymbol{\xi})$. Thus, we have

$$\sum_{a \in \hat{\mathcal{A}}^{\mathrm{R}}(z,t,z')} w_a(\boldsymbol{\xi}) \leq d_{z,t,z'}(\boldsymbol{\xi}), \ \forall\, (z,t,z') \in \mathcal{M}. \tag{3.6}$$

Finally, we have the following constraints:

$$\sum_{s \in \mathcal{S}} \sum_{a \in \cup_{k \in \mathcal{K}} \mathcal{A}^k_+(n_{z,t,s})} w_a(\boldsymbol{\xi}) \leq \sum_{k \in \mathcal{K}} X^k_z, \ \forall\, z \in \mathcal{Z},\ t \in \mathcal{T}, \tag{3.7}$$

$$\sum_{s \in \mathcal{S}} \sum_{a \in \mathcal{A}^{\mathrm{C}}_+(n_{z,t,s})} w_a(\boldsymbol{\xi}) \leq X^{\mathrm{C}}_z + X^{\mathrm{S}}_z, \ \forall\, z \in \mathcal{Z},\ t \in \mathcal{T}, \tag{3.8}$$

$$\sum_{s \in \mathcal{S}} \sum_{a \in \mathcal{A}^{\mathrm{S}}_+(n_{z,t,s})} w_a(\boldsymbol{\xi}) \leq X^{\mathrm{S}}_z, \ \forall\, z \in \mathcal{Z},\ t \in \mathcal{T}, \tag{3.9}$$

$$w_a \geq 0, \ \forall\, a \in \mathcal{A}, \tag{3.10}$$

where $\mathcal{A}^k_+(n_{z,t,s})$ for any $k \in \mathcal{K}$ and $n_{z,t,s} \in \mathcal{N}$ denotes the set of arcs in $\mathcal{A}^k$ that origi-

nate at $n_{z,t,s}$. Constraints (3.7)–(3.9) ensure that the number of vehicles that stay idle, charging, and discharging in each region does not exceed the capacity of the respective parking lots. That is, the firm is prohibited from parking, charging, or discharging more vehicles than the available space allows in each region throughout the operational horizon. Constraints (3.10) ensure that the realized flow on each arc is non-negative.

We let $\mathbf{w} = \{w_a,\ \forall\, a \in \mathcal{A}\}$. Therefore, we have

$$f\left(\mathbf{x}, \boldsymbol{\xi}\right) = \min_{\mathbf{w}} \left\{ \sum_{a \in \mathcal{A}} c_a w_a(\boldsymbol{\xi}) + c_{\mathrm{P}} \sum_{(z,t,z') \in \mathcal{M}} \left(d_{z,t,z'}(\boldsymbol{\xi}) - \sum_{a \in \hat{\mathcal{A}}^{\mathrm{R}}(z,t,z')} w_a(\boldsymbol{\xi}) \right) \middle| (3.3) - (3.10) \right\}, \qquad (\mathcal{P}_2)$$

where c_a denotes the unit cost produced by flow $a \in \mathcal{A}$ and c_{P} denotes the unit penalty for unsatisfied trip demands. Specifically, (i) For rental arc $a = (n_{z,t,s}, n_{z',t',s'}) \in \mathcal{A}^{\mathrm{R}}$, we set $c_a = -c_{\mathrm{R}} \times \ell_{z,z'}$, where c_{R} is the unit revenue for rentals. (ii) For idle arc $a = (n_{z,t,s}, n_{z,t+1,s}) \in \mathcal{A}^{\mathrm{I}}$, we set $c_a = c_{\mathrm{I}}$, where c_{I} is the unit idle cost. (iii) For relocation arc $a = (n_{z,t,s}, n_{z',t',s}) \in \mathcal{A}^{\mathrm{L}}$, we set $c_a = c_{\mathrm{L}} \times \ell_{z,z'}$, where c_{L} is the unit relocation cost. (iv) For charging arc $a = (n_{z,t,s}, n_{z,t+1,s'}) \in \mathcal{A}^{\mathrm{C}}$, we set $c_a = c_t^{\mathrm{C}} = (P_t^{\mathrm{C}} + c_{\mathrm{deg}}) \times \delta^{\mathrm{C}}$, where P_t^{C} is the electricity charging price in period t and c_{deg} is the degeneration cost of battery. (v) For discharging arc $a = (n_{z,t,s}, n_{z,t+1,s'}) \in \mathcal{A}^{\mathrm{S}}$, we set $c_a = c_t^{\mathrm{S}} = (-P_t^{\mathrm{S}} + c_{\mathrm{deg}}) \times \delta^{\mathrm{S}}$, where P_t^{S} is the electricity selling price in period t.

3.4 Distributionally Robust Optimization Approach

The uncertain trip demands across all service regions and all periods are dependent. As a result, $\mathbf{d}(\boldsymbol{\xi}) = \{d_{z,t,z'}(\boldsymbol{\xi}),\ \forall\, (z,t,z') \in \mathcal{M}\}$, the vector of uncertain trip demands, has high dimensionality. For example, even if we cluster the area into $|\mathcal{N}| = 5$ service regions and consider a daily operation of $|\mathcal{T}| = 144$, $\mathbf{d}(\boldsymbol{\xi})$ is a random vector of dimension $2,880$. Consequently, to accurately estimate the joint distribution of $\mathbf{d}(\boldsymbol{\xi})$, a significant amount of historical data is necessary. However, such data is usually difficult to acquire in practice, if possible, especially considering that the EV sharing is a relatively new industry. Hence, we are confronted with the issue of limited information, which hampers our efforts to accurately estimate the distribution of demands. In this section, we address the issue of limited information by developing the framework of distributionally robust optimization (DRO).

DRO is a modeling framework that integrates the optimization method and statistical information about the uncertain parameters (Jiang et al. 2023). Under this framework, one can relax the assumption of the perfect knowledge of the true distribution, i.e., $\mathbb{P}$ in Problem ($\mathcal{P}_0$), and only assume that $\mathbb{P}$ runs in a distributional ambiguity set constructed based on the statistical information and then optimize decisions against the worst-case distribution within this set. In the following, we introduce how to apply DRO in our study in detail.

3.4.1 Ambiguity Set

The ambiguity set plays a crucial role in linking the optimization model with the statistical information, and it can significantly affect the performance of DRO (Esfahani and Kuhn 2017). The ambiguity sets can be categorized into two typical groups: moment-based and discrepancy-based ambiguity sets (Rahimian and Mehrotra 2019). Specifically, the moment-based ambiguity set includes all distributions whose mean and covariance satisfy the prescribed condition, and the discrepancy-based ambiguity set contains the distributions that are close to the empirical distribution in the sense of a discrepancy measure. While these two types of ambiguity sets have distinct properties and performances (for detailed information, we refer interested readers to Rahimian and Mehrotra (2019)), they both should (i) contain the true distribution $\mathbb{P}$ and (ii) keep as small as possible to control the conservatism of the problem.

In our study, the available data is limited, which may yield an unreliable empirical distribution with a significant discrepancy from the true distribution. This suggests that the discrepancy-based ambiguity set is not a proper choice in this study. Because in this case the discrepancy-based ambiguity set is required to be large enough to contain $\mathbb{P}$, potentially leading to a highly conservative solution. Conversely, a moment-based ambiguity set is a proper choice since reliable mean and covariance information of the uncertainty can be easily estimated, even with limited data. Consequently, the set can be small yet contain $\mathbb{P}$, controlling the conservatism of the problem. Furthermore, as noted in Delage and Ye (2010), using the moment information to construct the ambiguity set, one can obtain reliable solutions and formulate the DRO problem as a semidefinite program (SDP) which is efficiently solvable by commercial solvers including Mosek. Therefore, we

construct the moment-based ambiguity set in our study, which is defined below:

$$\mathcal{D}(\Omega, \boldsymbol{\mu}, \boldsymbol{\Sigma}, \gamma_1, \gamma_2) = \left\{ \mathbb{P} \;\middle|\; \begin{array}{l} \mathbb{P}\left(\boldsymbol{\xi} \in \Omega\right) = 1, \\ \left(\mathbb{E}_{\mathbb{P}}\left[\boldsymbol{\xi}\right] - \boldsymbol{\mu}\right)^{\top} \boldsymbol{\Sigma}^{-1} \left(\mathbb{E}_{\mathbb{P}}\left[\boldsymbol{\xi}\right] - \boldsymbol{\mu}\right) \leq \gamma_1, \\ \mathbb{E}_{\mathbb{P}}\left[\left(\boldsymbol{\xi} - \boldsymbol{\mu}\right)\left(\boldsymbol{\xi} - \boldsymbol{\mu}\right)^{\top}\right] \preceq \gamma_2 \boldsymbol{\Sigma} \end{array} \right\},$$

where Ω denotes the support set, $\boldsymbol{\mu}$ denotes the mean vector, and $\boldsymbol{\Sigma}$ denotes the covariance matrix, which is a positive definite matrix. Parameters $\gamma_1 \geq 0$ and $\gamma_2 \geq 1$ are obtained from historical data and used to control the size of the ambiguity set and the conservatism of optimal solutions. The three constraints in $\mathcal{D}$ state that (i) any $\boldsymbol{\xi}$ lies in support Ω; (ii) the mean of $\boldsymbol{\xi}$ lies in an ellipsoid of size γ_1 centered at $\boldsymbol{\mu}$; and (iii) the centered second-moment matrix is bounded by $\gamma_2\boldsymbol{\Sigma}$ in a PSD sense. We assume Ω is polyhedral, i.e., $\Omega = \{\boldsymbol{\xi} \in \mathbb{R}^{|\mathcal{M}|} \mid \mathbf{b}^{\text{lb}} \leq \mathbf{A}\boldsymbol{\xi} \leq \mathbf{b}^{\text{ub}}\}$, with at least one interior point.

3.4.2 Distributionally Robust Model and Its Reformulation

Given an ambiguity set of probability distributions $\mathcal{D}$, we may seek to minimize the worst-case expected cost over $\mathcal{D}$, instead of solving Problem ($\mathcal{P}_0$) with a given distribution. That is,

$$\Gamma = \min_{\mathbf{x}} \left\{ \sum_{z \in \mathcal{Z}} \sum_{s \in \mathcal{S}} c_s x_{z,s} + \max_{\mathbb{P} \in \mathcal{D}} \mathbb{E}_{\mathbb{P}}\left[f\left(\mathbf{x}, \boldsymbol{\xi}\right)\right] \;\middle|\; (3.1) - (3.2) \right\}. \tag{$\mathcal{P}_{\text{M}}$}$$

It is clear that in Problem ($\mathcal{P}_{\text{M}}$), we have an inner max-min problem, i.e., $\max_{\mathbb{P}\in\mathcal{D}} \mathbb{E}_{\mathbb{P}}[f(\mathbf{x}, \boldsymbol{\xi})]$. As such, it is not straightforward to solve Problem ($\mathcal{P}_{\text{M}}$) in its present form. Next, we derive an equivalent reformulation of Problem ($\mathcal{P}_{\text{M}}$) that is solvable. First, in Theorem 1, we introduce an equivalent reformulation of the inner max-min problem in ($\mathcal{P}_{\text{M}}$).

Theorem 1. $\max_{\mathbb{P}\in\mathcal{D}} \mathbb{E}_{\mathbb{P}}[f(\mathbf{x}, \boldsymbol{\xi})]$ *in* ($\mathcal{P}_{\text{M}}$) *is equivalent to*

$$\begin{aligned} \min_{\mathbf{Q}\succeq 0, \mathbf{q}, r} \;& r + \left(\gamma_2 \boldsymbol{\Sigma} + \boldsymbol{\mu}\boldsymbol{\mu}^{\top}\right) \bullet \mathbf{Q} + \boldsymbol{\mu}^{\top}\mathbf{q} + \sqrt{\gamma_1} \left\| \boldsymbol{\Sigma}^{\frac{1}{2}} \left(\mathbf{q} + 2\mathbf{Q}\boldsymbol{\mu}\right) \right\|_2 \\ \textit{s.t.} \;& r \geq f\left(\mathbf{x}, \boldsymbol{\xi}\right) - \boldsymbol{\xi}^{\top}\mathbf{Q}\boldsymbol{\xi} - \boldsymbol{\xi}^{\top}\mathbf{q}, \;\; \forall \boldsymbol{\xi} \in \Omega, \end{aligned} \tag{$\mathcal{P}_{\text{in}}$}$$

where $\mathbf{Q} \in \mathbb{R}^{|\mathcal{M}|\times|\mathcal{M}|}, \mathbf{q} \in \mathbb{R}^{|\mathcal{M}|}, r \in \mathbb{R}$ denote the dual variables associated with constraints in $\mathcal{D}$.

Proposition 2. *Problem* ($\mathcal{P}_{\text{in}}$) *is equivalent to*

$$\min_{\mathbf{Q}\succeq 0,\mathbf{q},r} \; r + \left(\gamma_2 \boldsymbol{\Sigma} + \boldsymbol{\mu}\boldsymbol{\mu}^\top\right) \bullet \mathbf{Q} + \boldsymbol{\mu}^\top \mathbf{q} + \sqrt{\gamma_1} \left\| \boldsymbol{\Sigma}^{\frac{1}{2}} \left(\mathbf{q} + 2\mathbf{Q}\boldsymbol{\mu}\right) \right\|_2 \tag{$\mathcal{P}'_{\text{in}}$}$$

$$s.t.\; r \geq \psi\left(\mathbf{x}, \boldsymbol{\pi}, \boldsymbol{\xi}\right) - \boldsymbol{\xi}^\top \mathbf{Q} \boldsymbol{\xi} - \boldsymbol{\xi}^\top \mathbf{q}, \;\; \forall\, \boldsymbol{\xi} \in \Omega, \boldsymbol{\pi} \in \mathit{vert}\left(\mathcal{Y}\right). \tag{3.11}$$

We let $\max_{\boldsymbol{\pi}\in\mathcal{Y}} \psi(\mathbf{x}, \boldsymbol{\pi}, \boldsymbol{\xi})$ denote the dual problem of the second-stage problem ($\mathcal{P}_2$). Specifically, $\boldsymbol{\pi}$, $\psi(\cdot)$, and $\mathcal{Y}$ denote the vector of variables, the objective function, and the feasible region of the dual problem of ($\mathcal{P}_2$), respectively. $\mathit{vert}(\mathcal{Y})$ denotes the set of all vertices of feasible region $\mathcal{Y}$ (see Appendix B.2 for details).

Problem ($\mathcal{P}'_{\text{in}}$) is not straightforward to solve, since constraints (3.11) in it consider any $\boldsymbol{\xi} \in \Omega$. Consequently, in Proposition 3, we transform problem ($\mathcal{P}'_{\text{in}}$) to an SDP formulation and combine it with the outer minimization problem in ($\mathcal{P}_{\text{M}}$), finally yielding the equivalent formulation of Problem ($\mathcal{P}_{\text{M}}$) that is solvable.

Proposition 3. *Problem* ($\mathcal{P}_{\text{M}}$) *is equivalent to*

$$\Gamma = \min_{\substack{\mathbf{x},\boldsymbol{\pi}\in \mathit{vert}(\mathcal{Y}) \\ \mathbf{Q}\succeq 0,\mathbf{q},r \\ \boldsymbol{\lambda}_1,\boldsymbol{\lambda}_2\geq \mathbf{0}}} \sum_{z\in\mathcal{Z}} \sum_{s\in\mathcal{S}} c_s x_{z,s} + r + \left(\gamma_2 \boldsymbol{\Sigma} + \boldsymbol{\mu}\boldsymbol{\mu}^\top\right) \bullet \mathbf{Q} + \boldsymbol{\mu}^\top \mathbf{q} + \sqrt{\gamma_1} \left\| \boldsymbol{\Sigma}^{\frac{1}{2}} \left(\mathbf{q} + 2\mathbf{Q}\boldsymbol{\mu}\right) \right\|_2 \tag{$\mathcal{P}_{\text{F}}$}$$

$$s.t.\; (3.1) - (3.2),$$

$$\begin{bmatrix} r - \psi_1\left(\mathbf{x}, \boldsymbol{\pi}\right) - \boldsymbol{\lambda}_1^\top \mathbf{b}^{\text{ub}} + \boldsymbol{\lambda}_2^\top \mathbf{b}^{\text{lb}} & \frac{1}{2}\left(\mathbf{q} + \mathbf{A}^\top\left(\boldsymbol{\lambda}_1 - \boldsymbol{\lambda}_2\right) - \psi_2\left(\boldsymbol{\pi}\right)\right)^\top \\ \frac{1}{2}\left(\mathbf{q} + \mathbf{A}^\top\left(\boldsymbol{\lambda}_1 - \boldsymbol{\lambda}_2\right) - \psi_2\left(\boldsymbol{\pi}\right)\right) & \mathbf{Q} \end{bmatrix} \succeq 0,$$

where $\psi_1(\mathbf{x}, \boldsymbol{\pi}) + \psi_2(\boldsymbol{\pi})^\top \boldsymbol{\xi} = \psi(\mathbf{x}, \boldsymbol{\pi}, \boldsymbol{\xi})$ *(see Appendix B.3 for details).*

3.5 Solution Approaches

Problem ($\mathcal{P}_{\text{F}}$) admits an SDP reformulation that is solvable. However, in practice, it is very challenging to solve Problem ($\mathcal{P}_{\text{F}}$), especially when we consider a large time-space-SoC network $\mathcal{G} = (\mathcal{N}, \mathcal{A})$. This is because it considers a large-size PSD matrix, a significant number of vertices in $\mathcal{Y}$, i.e., $|\mathit{vert}(\mathcal{Y})|$, and numerous decision variables. Therefore, we propose three approaches to boost the solving process: (i) We consider outer and inner approximations of ($\mathcal{P}_{\text{M}}$) (i.e., Problem ($\mathcal{P}_{\text{F}}$)) that have a PSD matrix with a small size and generate a high-quality solution. (ii) We adopt Algorithm 1 that considers only a small part of $\mathit{vert}(\mathcal{Y})$ and generates a high-quality solution. (iii) We

decompose $\mathcal{G} = (\mathcal{N}, \mathcal{A})$ into L sub-networks along the operational horizon, and each sub-network $l \in \{1, 2, \ldots, L\}$ has a shorter time horizon. Thus, we will solve a sequence of smaller SDP problems, each corresponding to a sub-network, in a backward manner from the last sub-network to the first one.

In the following, we derive an outer (resp. inner) approximation of Problem ($\mathcal{P}_{\mathrm{F}}$) (i.e., Problem ($\mathcal{P}_{\mathrm{M}}$)), leading to a lower (resp. upper) bound, in Section 3.5.1 (resp. Section 3.5.2). Then we present the details of the delayed constraint generation algorithm, i.e., Algorithm 1, and the temporal decomposition algorithm, i.e., Algorithm 2, in Section 3.5.3.

Before processing outer and inner approximations of Problem ($\mathcal{P}_{\mathrm{F}}$), we introduce a reformulation of Problem ($\mathcal{P}_{\mathrm{M}}$). We perform an eigenvalue decomposition on the covariance matrix, i.e., $\mathbf{\Sigma} \in \mathbb{R}^{|\mathcal{M}|\times|\mathcal{M}|}$, by $\mathbf{\Sigma} = \mathbf{U}\mathbf{\Lambda}\mathbf{U}^\top = \mathbf{U}\mathbf{\Lambda}^{1/2}(\mathbf{U}\mathbf{\Lambda}^{1/2})^\top$. Here, $\mathbf{U} \in \mathbb{R}^{|\mathcal{M}|\times|\mathcal{M}|}$ is an orthogonal transformation matrix and $\mathbf{\Lambda} \in \mathbb{R}^{|\mathcal{M}|\times|\mathcal{M}|}$ is a diagonal matrix whose diagonal elements are in decreasing order. By letting $\boldsymbol{\xi}_{\mathrm{I}} = (\mathbf{U}\mathbf{\Lambda}^{-1/2})^\top(\boldsymbol{\xi} - \boldsymbol{\mu})$, we reformulate Problem ($\mathcal{P}_{\mathrm{M}}$) as

$$\Gamma = \min_{\mathbf{x}} \left\{ \sum_{z\in\mathcal{Z}} \sum_{s\in\mathcal{S}} c_s x_{z,s} + \max_{\mathbb{P}_{\mathrm{I}}\in\mathcal{D}_{\mathrm{I}}} \mathbb{E}_{\mathbb{P}_{\mathrm{I}}} \left[f\left(\mathbf{x}, \mathbf{U}\mathbf{\Lambda}^{\frac{1}{2}}\boldsymbol{\xi}_{\mathrm{I}} + \boldsymbol{\mu}\right)\right] \middle| (3.1) - (3.2) \right\}, \tag{$\mathcal{P}_{\mathrm{I}}$}$$

where

$$\mathcal{D}_{\mathrm{I}}\left(\Omega_{\mathrm{I}}, \gamma_1, \gamma_2\right) = \left\{ \mathbb{P}_{\mathrm{I}} \;\middle|\; \begin{array}{l} \mathbb{P}_{\mathrm{I}}\left(\boldsymbol{\xi}_{\mathrm{I}} \in \Omega_{\mathrm{I}}\right) = 1 \\ \mathbb{E}_{\mathbb{P}_{\mathrm{I}}}\left[\boldsymbol{\xi}_{\mathrm{I}}^\top\right] \mathbb{E}_{\mathbb{P}_{\mathrm{I}}}\left[\boldsymbol{\xi}_{\mathrm{I}}\right] \leq \gamma_1 \\ \mathbb{E}_{\mathbb{P}_{\mathrm{I}}}\left[\boldsymbol{\xi}_{\mathrm{I}}\boldsymbol{\xi}_{\mathrm{I}}^\top\right] \preceq \gamma_2 \mathbf{I}_{|\mathcal{M}|} \end{array} \right\},$$

with $\Omega_{\mathrm{I}} := \{\boldsymbol{\xi}_{\mathrm{I}} \in \mathbb{R}^{|\mathcal{M}|} : \mathbf{U}\mathbf{\Lambda}^{1/2}\boldsymbol{\xi}_{\mathrm{I}} + \boldsymbol{\mu} \in \Omega\}$ and $\mathbf{I}_{|\mathcal{M}|}$ denoting an identity matrix of size $|\mathcal{M}|$.

3.5.1 Outer Approximation for DRO Problem

We use principal component analysis (PCA), which approximates a high-dimensional matrix to a low-dimensional one, to reduce the size of Problem ($\mathcal{P}_{\mathrm{F}}$) while maintaining a high solution quality. Specifically, we approximate $\boldsymbol{\xi}$ by capturing the major variability of $\mathbf{U}\mathbf{\Lambda}^{1/2}\boldsymbol{\xi}_{\mathrm{I}}$ by considering only the first m_1 random variables of $\boldsymbol{\xi}_{\mathrm{I}}$, i.e.,

$$\boldsymbol{\xi} = \mathbf{U}\mathbf{\Lambda}^{\frac{1}{2}}\boldsymbol{\xi}_{\mathrm{I}} + \boldsymbol{\mu} \approx \mathbf{U}\mathbf{\Lambda}^{\frac{1}{2}}[\boldsymbol{\xi}_{m_1}; \mathbf{0}_{|\mathcal{M}|-m_1}] + \boldsymbol{\mu} = \mathbf{U}_{|\mathcal{M}|\times m_1}\mathbf{\Lambda}_{m_1}^{\frac{1}{2}}\boldsymbol{\xi}_{m_1} + \boldsymbol{\mu},$$

where $\mathbf{0}_{|\mathcal{M}|-m_1}$ represents a zero vector of size $|\mathcal{M}|-m_1$, $\mathbf{U}_{|\mathcal{M}|\times m_1} \in \mathbb{R}^{|\mathcal{M}|\times m_1}$ and $\mathbf{\Lambda}_{m_1}^{1/2} \in \mathbb{R}^{m_1\times m_1}$ are upper-left submatrices of $\mathbf{U}$ and $\mathbf{\Lambda}^{1/2}$, respectively, and $\boldsymbol{\xi}_{m_1} \in \mathbb{R}^{m_1}$ consists of the first m_1 entries of $\boldsymbol{\xi}_{\mathrm{I}}$. As the uncertainty of the last $(|\mathcal{M}|-m_1)$ entries of $\boldsymbol{\xi}_{\mathrm{I}}$ vanishes, we have a relaxation of Problem ($\mathcal{P}_{\mathrm{M}}$):

$$\min_{\mathbf{x}} \left\{ \sum_{z\in\mathcal{Z}}\sum_{s\in\mathcal{S}} c_s x_{z,s} + \max_{\mathbb{P}_{m_1}\in\mathcal{D}_{m_1}} \mathbb{E}_{\mathbb{P}_{m_1}}\left[f\left(\mathbf{x}, \mathbf{U}_{|\mathcal{M}|\times m_1}\mathbf{\Lambda}_{m_1}^{\frac{1}{2}}\boldsymbol{\xi}_{m_1} + \boldsymbol{\mu}\right)\right] \middle| (3.1)-(3.2) \right\}, \tag{3.12}$$

where

$$\mathcal{D}_{m_1}(\Omega_{m_1},\gamma_1,\gamma_2) = \left\{ \mathbb{P}_{m_1} \middle| \begin{array}{l} \mathbb{P}_{m_1}\left(\boldsymbol{\xi}_{m_1}\in\Omega_{m_1}\right)=1 \\ \mathbb{E}_{\mathbb{P}_{m_1}}\left[\boldsymbol{\xi}_{m_1}^\top\right]\mathbb{E}_{\mathbb{P}_{m_1}}\left[\boldsymbol{\xi}_{m_1}\right] \le \gamma_1 \\ \mathbb{E}_{\mathbb{P}_{m_1}}\left[\boldsymbol{\xi}_{m_1}\boldsymbol{\xi}_{m_1}^\top\right] \preceq \gamma_2 \mathbf{I}_{m_1} \end{array} \right\},$$

with $\Omega_{m_1} := \{\boldsymbol{\xi}_{m_1}\in\mathbb{R}^{m_1} : \mathbf{U}_{|\mathcal{M}|\times m_1}\mathbf{\Lambda}_{m_1}^{1/2}\boldsymbol{\xi}_{m_1}+\boldsymbol{\mu}\in\Omega\}$.

Theorem 2. *Problem (3.12) has the same optimal value as the following problem:*

$$\begin{aligned} \min_{\mathbf{x},\mathbf{Q}_{m_1},\mathbf{q}_{m_1},r} \ & \sum_{z\in\mathcal{Z}}\sum_{s\in\mathcal{S}} c_s x_{z,s} + r + \gamma_2 I_{m_1}\bullet\mathbf{Q}_{m_1} + \sqrt{\gamma_1}\|\mathbf{q}_{m_1}\|_2 \qquad (3.13)\\ s.t.\ & (3.1)-(3.2), \\ & r \ge f\left(\mathbf{x}, \mathbf{U}_{|\mathcal{M}|\times m_1}\mathbf{\Lambda}_{m_1}^{\frac{1}{2}}\boldsymbol{\xi}_{m_1}+\boldsymbol{\mu}\right) - \boldsymbol{\xi}_{m_1}^\top\mathbf{Q}_{m_1}\boldsymbol{\xi}_{m_1} - \boldsymbol{\xi}_{m_1}^\top\mathbf{q}_{m_1},\ \forall\,\boldsymbol{\xi}_{m_1}\in\Omega_{m_1}, \\ & \mathbf{Q}_{m_1}\succeq 0, \end{aligned}$$

where $\mathbf{q}_{m_1}\in\mathbb{R}^{m_1}$ and $\mathbf{Q}_{m_1}\in\mathbb{R}^{m_1\times m_1}$. Furthermore, we have the following: (i) Problem (3.13) provides a lower bound for the optimal value of Problem ($\mathcal{P}_{\mathrm{M}}$); (ii) the optimal value of Problem (3.13) is nondecreasing in m_1; and (iii) if $m_1=|\mathcal{M}|$, then Problems (3.13) and ($\mathcal{P}_{\mathrm{M}}$) have the same optimal value.

Proposition 4. *Problem (3.13) has the same optimal value as the following SDP formu-*

lation

$$\min_{\substack{\mathbf{x},\boldsymbol{\pi}\in vert(\mathcal{Y})\\ \mathbf{Q}_{m_1}\succeq 0,\mathbf{q}_{m_1},r\\ \boldsymbol{\lambda}_1,\boldsymbol{\lambda}_2\geq \mathbf{0}}} \sum_{z\in\mathcal{Z}}\sum_{s\in\mathcal{S}} c_s x_{z,s} + r + \gamma_2 I_{m_1} \bullet \mathbf{Q}_{m_1} + \sqrt{\gamma_1}\|\mathbf{q}_{m_1}\|_2 \tag{3.14}$$

$$s.t.\ (3.1)-(3.2),$$

$$\begin{bmatrix} \mathbf{M}_1 & \mathbf{M}_2^\top \\ \mathbf{M}_2 & \mathbf{Q}_{m_1} \end{bmatrix} \succeq 0,$$

where $\mathbf{M}_1 = r - \psi_1(\mathbf{x},\boldsymbol{\pi}) - \boldsymbol{\lambda}_1^\top \mathbf{b}^{\text{ub}} + \boldsymbol{\lambda}_2^\top \mathbf{b}^{\text{lb}} - \psi_2(\boldsymbol{\pi})^\top \boldsymbol{\mu} + (\boldsymbol{\lambda}_1 - \boldsymbol{\lambda}_2)^\top \mathbf{A}\boldsymbol{\mu}$ *and* $\mathbf{M}_2 = 1/2 \times (\mathbf{q}_{m_1} + (\mathbf{U}_{|\mathcal{M}|\times m_1}\boldsymbol{\Lambda}_{m_1}^{1/2})^\top(\mathbf{A}^\top(\boldsymbol{\lambda}_1 - \boldsymbol{\lambda}_2) - \psi_2(\boldsymbol{\pi})))$.

Comparing Problem (3.14) (i.e., Problem (3.13)) with Problem ($\mathcal{P}_{\text{F}}$) (i.e., Problem ($\mathcal{P}_{\text{M}}$)) in terms of size, it can be noted that Problem (3.14) is significantly easier to solve than Problem ($\mathcal{P}_{\text{F}}$) because the size of PSD matrices in Problem (3.14) is significantly smaller than the one in Problem ($\mathcal{P}_{\text{F}}$), i.e., $(m_1+1)^2$ vs. $(|\mathcal{M}|+1)^2$.

3.5.2 Inner Approximation for DRO Problem

We further split the random vector $\boldsymbol{\xi}_{\text{I}}$ into several pieces to reduce the size of PSD matrices in Problem ($\mathcal{P}_{\text{F}}$). Specifically, we split $\boldsymbol{\xi}_{\text{I}}$ into U pieces, i.e., $\boldsymbol{\xi}_{\text{I}} = (\boldsymbol{\xi}_{\text{I}_1}^\top, \boldsymbol{\xi}_{\text{I}_2}^\top, \ldots, \boldsymbol{\xi}_{\text{I}_U}^\top)^\top$, where $\boldsymbol{\xi}_{\text{I}_i} \in \mathbb{R}^{m_i}$ for any $i \in [1,U]_{\mathbb{Z}}$, and $\sum_{i=1}^U m_i = |\mathcal{M}|$. Accordingly, we revise the second-moment constraint in $\mathcal{D}_{\text{I}}$ with respect to these smaller pieces, leading to the following ambiguity set:

$$\mathcal{D}_{\text{U}}(\Omega_{\text{I}},\gamma_1,\gamma_2) = \left\{ \mathbb{P}_{\text{U}} \;\middle|\; \begin{array}{l} \mathbb{P}_{\text{U}}(\boldsymbol{\xi}_{\text{I}} \in \Omega_{\text{I}}) = 1 \\ \mathbb{E}_{\mathbb{P}_{\text{U}}}[\boldsymbol{\xi}_{\text{I}}^\top]\,\mathbb{E}_{\mathbb{P}_{\text{U}}}[\boldsymbol{\xi}_{\text{I}}] \leq \gamma_1 \\ \mathbb{E}_{\mathbb{P}_{\text{U}}}[\boldsymbol{\xi}_{\text{I}_i}\boldsymbol{\xi}_{\text{I}_i}^\top] \preceq \gamma_2 \mathbf{I}_{m_i},\ \forall i \in [1,U]_{\mathbb{Z}} \end{array} \right\}.$$

The set $\mathcal{D}_{\text{U}}$ is a superset of $\mathcal{D}_{\text{I}}$ because we ignore the correlations among $\boldsymbol{\xi}_{\text{I}_i}$ and $\boldsymbol{\xi}_{\text{I}_j}$ for any $i,j \in [1,U]_{\mathbb{Z}}$ with $i \neq j$. This leads to the following inner approximation of Problem ($\mathcal{P}_{\text{M}}$):

$$\min_{\mathbf{x}} \left\{ \sum_{z\in\mathcal{Z}}\sum_{s\in\mathcal{S}} c_s x_{z,s} + \max_{\mathbb{P}_{\text{U}}\in\mathcal{D}_{\text{U}}} \mathbb{E}_{\mathbb{P}_{\text{U}}}\left[f\left(\mathbf{x}, \mathbf{U}\boldsymbol{\Lambda}^{\frac{1}{2}}\boldsymbol{\xi}_{\text{I}} + \boldsymbol{\mu}\right)\right] \middle| (3.1)-(3.2) \right\}. \tag{3.15}$$

Theorem 3. *Problem (3.15) has the same optimal value as the following problem:*

$$\begin{aligned}
\min_{\mathbf{x},\mathbf{Q}_i,\mathbf{q},r} \ & \sum_{z\in\mathcal{Z}}\sum_{s\in\mathcal{S}} c_s x_{z,s} + r + \gamma_2 \sum_{i=1}^{U} I_{m_i} \bullet \mathbf{Q}_i + \sqrt{\gamma_1}\|\mathbf{q}\|_2 \qquad (3.16)\\
s.t.\ & (3.1)-(3.2),\\
& r \geq f\left(\mathbf{x}, \mathbf{U}\boldsymbol{\Lambda}^{\frac{1}{2}}\boldsymbol{\xi}_{\mathrm{I}} + \boldsymbol{\mu}\right) - \sum_{i=1}^{U} \boldsymbol{\xi}_{\mathrm{I}_i}^{\top}\mathbf{Q}_i\boldsymbol{\xi}_{\mathrm{I}_i} - \boldsymbol{\xi}_{\mathrm{I}}^{\top}\mathbf{q},\ \forall \boldsymbol{\xi}_{\mathrm{I}} \in \Omega_{\mathrm{I}},\\
& \mathbf{Q}_i \succeq 0,\ \forall i \in [1,U]_{\mathbb{Z}},
\end{aligned}$$

where $\mathbf{q} \in \mathbb{R}^{|\mathcal{M}|}$ *and* $\mathbf{Q}_i \in \mathbb{R}^{m_i \times m_i}$ *for any* $i \in [1,U]_{\mathbb{Z}}$. *Furthermore, Problem (3.16) provides an upper bound for the optimal value of Problem* ($\mathcal{P}_{\mathrm{M}}$).

Proposition 5. *Problem (3.16) has the same optimal value as the following SDP formulation*

$$\begin{aligned}
\min_{\substack{\mathbf{x},\boldsymbol{\pi}\in vert(\mathcal{Y})\\ \mathbf{Q}_i,\mathbf{q}_i,\mathbf{q},r_i,r\\ \boldsymbol{\lambda}_1,\boldsymbol{\lambda}_2\geq\mathbf{0}}} \ & \sum_{z\in\mathcal{Z}}\sum_{s\in\mathcal{S}} c_s x_{z,s} + r + \gamma_2 \sum_{i=1}^{U} I_{m_i} \bullet \mathbf{Q}_i + \sqrt{\gamma_1}\|\mathbf{q}\|_2 \qquad (3.17)\\
s.t.\ & (3.1)-(3.2),\\
& \begin{bmatrix} r_i & \mathbf{M}_2^{i^{\top}} \\ \mathbf{M}_2^{i} & \mathbf{Q}_i \end{bmatrix} \succeq 0,\ \forall i \in [1,U]_{\mathbb{Z}},\\
& \sum_{i=1}^{U} r_i = r - \psi_1(\mathbf{x},\boldsymbol{\pi}) - \boldsymbol{\lambda}_1^{\top}\mathbf{b}^{\mathrm{ub}} + \boldsymbol{\lambda}_2^{\top}\mathbf{b}^{\mathrm{lb}} - \psi_2(\boldsymbol{\pi})^{\top}\boldsymbol{\mu} + (\boldsymbol{\lambda}_1-\boldsymbol{\lambda}_2)^{\top}\mathbf{A}\boldsymbol{\mu},\\
& \mathbf{Q}_i \succeq 0,\ \forall i \in [1,U]_{\mathbb{Z}},
\end{aligned}$$

where $\mathbf{M}_2^i = 1/2 \times (\mathbf{q}_i + (\mathbf{U}_{|\mathcal{M}|\times m_i}\boldsymbol{\Lambda}_{m_i}^{1/2})^{\top}(\mathbf{A}^{\top}(\boldsymbol{\lambda}_1 - \boldsymbol{\lambda}_2) - \psi_2(\boldsymbol{\pi})))$, $\mathbf{q}_i \in \mathbb{R}^{m_i}$, $\mathbf{q} = (\mathbf{q}_1^{\top},\ldots,\mathbf{q}_U^{\top})^{\top}$, and $\mathbf{Q}_i \in \mathbb{R}^{m_i\times m_i}$ for any $i \in [1,U]_{\mathbb{Z}}$.

3.5.3 Solution Algorithms

It is not practical to enumerate all vertices of the feasible region, i.e., $vert(\mathcal{Y})$, in Problems ($\mathcal{P}_{\mathrm{F}}$), (3.14) and (3.17). To overcome this challenge, we adopt "Delayed Constraint Generation Algorithm" introduced in (Fathabad et al. 2020), which solves the problems by considering a reduced set of vertices, denoted by $\mathcal{V}_{\mathrm{r}} \subseteq vert(\mathcal{Y})$. In the following, we introduce this algorithm, which is designed to solve Problem ($\mathcal{P}_{\mathrm{F}}$). Similar ones can be developed to solve Problems (3.14) and (3.17).

Algorithm 1 Delayed Constraint Generation Algorithm

1: Find initial vertices of the feasible region $\mathcal{Y}$, denoted by $\boldsymbol{\pi}^*$. Set $\mathcal{V}_\mathrm{r} = \emptyset$.
2: **do**
3: $\quad \mathcal{V}_\mathrm{r} = \mathcal{V}_\mathrm{r} \cup \{\boldsymbol{\pi}^*\}$.
4: $\quad$ Solve Problem ($\mathcal{P}_\mathrm{F}$) considering the vertices only in $\mathcal{V}_\mathrm{r}$. Then, save the optimal value Γ^* and optimal solution $(r^*, \mathbf{Q}^*, \mathbf{q}^*, \mathbf{x}^*)$.
5: $\quad$ Solve the following biconvex problem using $(r^*, \mathbf{Q}^*, \mathbf{q}^*, \mathbf{x}^*)$:

$$\min_{\boldsymbol{\pi}\in\mathcal{Y},\ \boldsymbol{\xi}\in\Omega} r^* + \boldsymbol{\xi}^\top \mathbf{Q}^* \boldsymbol{\xi} + \boldsymbol{\xi}^\top \mathbf{q}^* - \psi\left(\mathbf{x}^*, \boldsymbol{\pi}, \boldsymbol{\xi}\right), \tag{3.18}$$

$\quad$ and save the optimal value as s^* and optimal solution as $\boldsymbol{\pi}^*$.
6: **while** $s^* < 0$
7: Γ^* is optimal for Problem ($\mathcal{P}_\mathrm{F}$).

Algorithm 1 initially solves a relaxation of the SDP problem by considering $\mathcal{V}_\mathrm{r}$, whose size is always significantly smaller than $vert(\mathcal{Y})$. Before converging, it iteratively adds vertices of $\mathcal{Y}$ to the reduced set $\mathcal{V}_\mathrm{r}$ and solves the SDP problem with $\mathcal{V}_\mathrm{r}$. Note that in the beginning, we can obtain the initial vertices of $\mathcal{Y}$ by solving linear programming problems that are subject to $\mathcal{Y}$ but have different objective functions. Problem (3.18) is nonlinear because of the bilinear terms in $\psi(\mathbf{x}^*, \boldsymbol{\pi}, \boldsymbol{\xi})$ (see Appendix B.2 for details). We can solve this problem to a near-optimal solution by using the alternating direction search algorithm or alternating direction method of multipliers (ADMM).

Algorithm 1 needs to solve Problem ($\mathcal{P}_\mathrm{F}$) with $\mathcal{V}_\mathrm{r}$ iteratively. Even though the size of $\mathcal{V}_\mathrm{r}$ is significantly smaller than $vert(\mathcal{Y})$, Problem ($\mathcal{P}_\mathrm{F}$) is still hard to get solved due to the large number of variables and constraints induced by the large time-space-SoC network $\mathcal{G} = (\mathcal{N}, \mathcal{A})$. We thus adopt a temporal decomposition approach introduced in (Jin et al. 2023) to iteratively solve a sequence of subproblem, each of which considers only a part of $\mathcal{G}$. Specifically, we decompose $\mathcal{G}$ into L sub-networks, each sub-network $l \in \{1, 2, \ldots, L\}$ has time horizon with T_l, where $\sum_{l=1}^{L} T_l = T$. For recording purposes, we name $\mathcal{T}_1 = \{0, \ldots, T_1\}$ and $\mathcal{T}_l = \{\sum_{i=1}^{l-1} T_i + 1, \ldots, \sum_{i=1}^{l} T_i\}$ for any $l \in \{2, \ldots, L\}$. Likewise, for any $l \in \{1, \ldots, L\}$, we name $\mathcal{N}_l = \{n_{z,t,s} \in \mathcal{N} | z \in \mathcal{Z}, t \in \mathcal{T}_l, s \in \mathcal{S}\}$, $\mathcal{A}_l = \{(n_{z,t,s}, n_{z',t',s'}) \in \mathcal{A} | n_{z,t,s}, n_{z',t',s'} \in \mathcal{N}_l\}$, and $\mathcal{G}_l = (\mathcal{N}_l, \mathcal{A}_l)$. For any sub-network $\mathcal{G}_l$, $l \in \{1, \ldots, L\}$, we name Problems ($\mathcal{P}_0$) and ($\mathcal{P}_\mathrm{F}$) based on it as ($\mathcal{P}_0{}^l$) and ($\mathcal{P}_\mathrm{F}{}^l$), respectively (see Appendix B.8 for details).

In Algorithm 2, we solve smaller and thus simpler SDP problems over each sub-network $l \in \{L, L-1, \ldots, 1\}$ in a backward sequence, from the last sub-network $l = L$ to the

Algorithm 2 Temporal Decomposition Algorithm

1: Use Algorithm 1 to solve Problem ($\mathcal{P}_{\mathrm{F}}{}^{L}$), and save the optimal solution as $\overline{\mathbf{x}}^{L}$.
2: **for** $l = L-1, \ldots, 1$ **do**
3: Add constraints $\sum_{z\in\mathcal{Z}}\sum_{s\in\mathcal{S}} x_{z,s} \geq \sum_{z\in\mathcal{Z}}\sum_{s\in\mathcal{S}} \overline{x}^{i+1}_{z,s},\ \forall\, i \in \{l, \ldots, L-1\}$ to Problem ($\mathcal{P}_{\mathrm{F}}{}^{l}$).
4: Use Algorithm 1 to solve the updated Problem ($\mathcal{P}_{\mathrm{F}}{}^{l}$), and save the optimal solution as $\overline{\mathbf{x}}^{l}$.
5: **end for**
6: Return $\overline{\mathbf{x}}^{1}$.

first $l = 1$. In each iteration $l \in \{L-1, \ldots, 1\}$, we add constraints $\sum_{z\in\mathcal{Z}}\sum_{s\in\mathcal{S}} x_{z,s} \geq \sum_{z\in\mathcal{Z}}\sum_{s\in\mathcal{S}} \overline{x}^{i+1}_{z,s},\ \forall\, i \in \{l, \ldots, L-1\}$ to Problem ($\mathcal{P}_{\mathrm{F}}{}^{l}$), i.e., the total initial allocation $\sum_{z\in\mathcal{Z}}\sum_{s\in\mathcal{S}} x_{z,s}$ of the sub-network l is lower bounded by $\max_{i\in\{l,\ldots,L-1\}}\sum_{z\in\mathcal{Z}}\sum_{s\in\mathcal{S}} \overline{x}^{i+1}_{z,s}$. The intuition behind such constraints is that (i) the vehicle allocation solution of the SDP problem over the sub-network l should approximate that over the sub-networks from l to L, (ii) the trip demand over the sub-network l is no less than that over the sub-networks from l to L, and (iii) the larger trip demand often needs more allocated vehicles. We finally obtain $\overline{\mathbf{x}}^{1}$ for Problem ($\mathcal{P}_{\mathrm{F}}$).

3.6 Numerical Experiments: A Case Study

We conduct numerical experiments with the real data of taxi trip demands in NYC. We first discuss parameter settings and then examine the computational performances of the approaches proposed in Section 3.5. We finally obtain managerial insights from various experiments based on the settings.

3.6.1 Parameter Settings

We have collected data from TLC (2024) in NYC from January 1, 2011 to February 29, 2020. We focus on Midtown and Lower Manhattan, a traffic-intensive area in NYC, and divide this area into $|\mathcal{Z}| = 5$ service regions, as shown in Figure 3.2. Based on the collected data, the average trip duration from one region to a neighboring one is approximately 10 minutes. For simplicity, we assume the traveling speed between any two neighboring regions is the same and set each period as 10 minutes (leading to $T = 144$ periods per day). Table 3.1 introduces the trip duration in terms of the number of periods (i.e., $\ell_{z,z'}$) between any two service regions $z, z' \in \mathcal{Z}$ and $z \neq z'$.

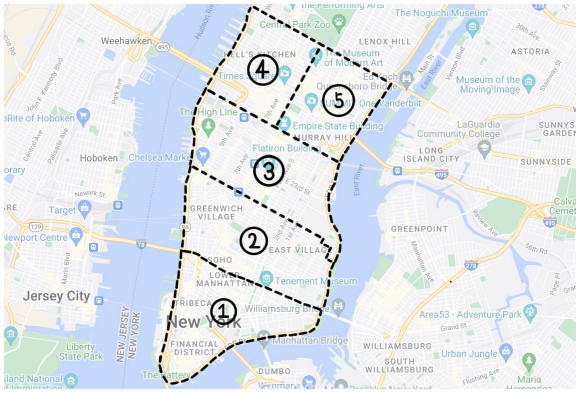

Figure 3.2. Service Regions in Manhattan

Regions	1	2	3	4	5
1	—	1	1	2	2
2	1	—	1	2	2
3	1	1	—	1	1
4	2	2	1	—	1
5	2	2	1	1	—

Table 3.1. Trip Duration Across Regions

Regions	1	2	3	4	5
1	—	1	1	2	2
2	1	—	1	2	2
3	1	1	—	1	1
4	2	2	1	—	1
5	2	2	1	1	—

Table 3.2. SoC Unit Usage Across Regions

Figure 3.3 shows the number of consumer trips throughout the day averaged over the service regions. It is observed that trip demands remain high for the majority of the day, except around 5:00 when they reach their lowest point. Figure 3.4 shows the number of trips across service regions averaged over the whole operational horizon.

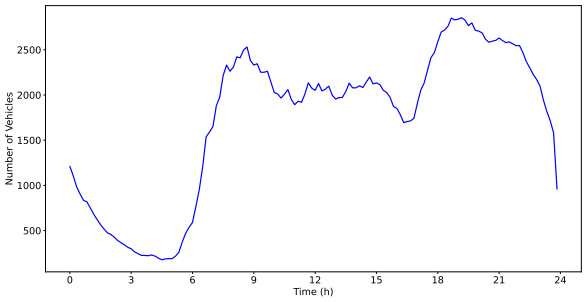

Figure 3.3. Average Consumer Trips Throughout The Day

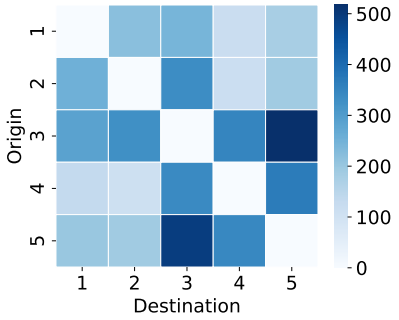

Figure 3.4. Average Consumer Trips Across Regions

We set the upper bound $\overline{X}$ of the total number of EVs allocated to all service regions as 4000. [1] In each region $z \in \mathcal{Z}$, the number X_z^{N} of parking stations, the number X_z^{C} of charging stations, and the number X_z^{S} of bi-directional charging stations are set as 800, 320, and 160, respectively. [2]

[1] We randomly select 30 samples from TLC (2024) and observe that the largest trip in one period among these 30 samples is 3928. Consequently, we set the upper bound as 4000.

[2] We assume the total number of parking stations equals the upper bound, i.e., $\sum_{z\in\mathcal{Z}} X_z^{\mathrm{N}} = \overline{X} = 4000$.

Each EV has a battery capacity of 40 kWh, allowing it to run for 6.5 hours or equivalently 38 periods. We assume that the vehicle's travel within 1 period consumes 1 SoC unit, leading to a maximum of 38 SoC units for each EV. Under this assumption, the SoC units usage in the travel between any two service regions $z, z' \in \mathcal{Z}$ and $z \neq z'$ (i.e., $b_{z,z'}$) remains consistent with the respective trip duration (i.e., $\ell_{z,z'}$), as shown in Table 3.2. We set the charging rate as 19 SoC units per period (i.e., $\delta^{\mathrm{C}} = 19$) and the discharging rate as 2 SoC units per period (i.e., $\delta^{\mathrm{S}} = 2$). [3]

We estimate cost parameters in USD. The EV allocation cost in any region $z \in \mathcal{Z}$ and SoC $s \in \mathcal{S}$ is $c_s = 21.6 + 0.1s$. [4] The revenue per EV trip per period is $c_{\mathrm{R}} = 2.8$, the penalty cost for an unsatisfied consumer trip is $c_{\mathrm{P}} = 3c_{\mathrm{R}}$, the relocation cost per relocated EV per period is $c_{\mathrm{L}} = 1.2$, the idle cost per idling EV per period is $c_{\mathrm{I}} = 0.01$, the battery degeneration cost per SoC unit is $c_{\mathrm{deg}} = 0.07$. We assume $P_t^{\mathrm{C}} = P_t^{\mathrm{S}}$ for any $t \in \mathcal{T}$. We collect the electricity price in Kansas Central from (Evergy 2022) to set $P_t^{\mathrm{C}}(P_t^{\mathrm{S}})$. They divide one day into four time intervals: super off-peak interval (0:00 – 6:00), off-peak interval (6:00–14:00 and 20:00–24:00), and peak interval (14:00–20:00), each having a distinct price. Specifically, $P_t^{\mathrm{C}}(P_t^{\mathrm{S}})$ is set as 0.1/kWh for $t \in [1, 36]_{\mathbb{Z}}$ (i.e., 0:00 – 6:00), 0.15/kWh for $t \in [37, 84]_{\mathbb{Z}} \cup [121, 144]_{\mathbb{Z}}$ (i.e., 6:00–14:00 and 20:00–24:00), and 0.27/kWh for $t \in [85, 120]_{\mathbb{Z}}$ (i.e., 14:00–20:00).

3.6.2 Computational Performance of Our Solution Approach

We perform all the numerical experiments on a computing node with 2.3-GHz Intel Xeon E5-2670 processor in a high-performance computing cluster using Mosek with C++ API under its default settings. In this section, we demonstrate the computational efficiency of our solution approach introduced in Section 3.5.

We then divide all the parking stations to each region equally, leading to $X_z^{\mathrm{N}} = 4000/5 = 800$ for any $z \in \mathcal{Z}$. NYC DOT (2021) state that 40% of urban parking spaces will be equipped with charging piles by 2030. Therefore, we set $X_z^{\mathrm{C}} = 0.4X_z^{\mathrm{N}} = 320$ for any $z \in \mathcal{Z}$. We observe that the number of bi-directional charging stations is smaller than the number of charging stations. We assume $X_z^{\mathrm{S}} = 0.5X_z^{\mathrm{C}} = 160$.

[3] Due to the popularity and rapidly increasing trend of fast chargers, we consider fast charging in our experiments. We consider a common fast-charging rate of 120 kW, which can charge a total of 120 kW $\times$ 1/6 hours = 20 kWh in one period. This amount is equivalent to $20/40 \times 38 = 19$ SoC units. We consider a common discharging rate of 15 kW, which can discharge a total of 15 kW $\times$ 1/6 hours = 2.5 kWh in one period. This amount is equivalent to $2.5/40 \times 38 \approx 2$ SoC units.

[4] The cost of allocating an EV with SoC $s \in \mathcal{S}$ to any service region $z \in \mathcal{Z}$ equals the EV purchasing cost, i.e., 21.6, plus the cost of charging the EV to SoC s, i.e., $0.1s$. We follow Jin et al. (2023) to estimate the EV purchasing cost by dividing 40000 dollars over $5 \times 365 = 1825$ days, leading to $40000/1825 \approx 21.6$. The electricity price at the beginning of the day is 0.1/kWh.

We compare the performances of the following approaches: (i) "Outer α:" Algorithm 1 combined with outer approximation with $m_1 = \lfloor \alpha |\mathcal{M}| \rfloor$, (ii) "Inner U:" Algorithm 1 combined with inner approximation with U pieces, (iii) "Sub L:" Temporal decomposition algorithm, i.e., Algorithm 2, with L sub-networks, and (iv) "Original:" Algorithm 1. We follow the setting in Section 3.6.1 and perform experiments to compare the optimal profit, allocation decision (i.e., $\mathbf{x}$), and computational time obtained by each approach.

Note that "Original" approach can only solve small instances to the optimality within 24 hours, we thus first consider a small instance with $|\mathcal{Z}| = 3$ and $|\mathcal{T}| = 6$ and show the results in Table 3.3. We set the results obtained by "Original" approach as the benchmark and subsequently calculate the gap between the benchmark results and the results obtained by the other approaches. For example, we calculate the profit gap between "Inner 2" and "Original" by

$$\frac{(\text{the profit by "Inner 2"}) - (\text{the profit by "Original"})}{(\text{the profit by "Original"})} \times 100\%.$$

Table 3.3 suggests that compared with "Original" approach, the "Inner 2," "Outer 80%," and "Sub 2" approaches can solve the instance with a significantly reduced computational time (reduced by more than 74.93%) and obtain very high-quality solutions (profit gap within 2.90% and allocation solution gap within 4.10%). Among these three approaches, "Sub 2" performs the best, reducing the most computational time (i.e., 96.12%) and achieving the smallest profit gap (i.e., 1.07%) and a very small solution gap (i.e., 3.26%). This suggests that our proposed approaches can all generate a high-quality solution with a dramatically reduced computational time. Notably, Algorithm 2 stands out as the best approach among the three, obtaining a very high-quality solution with the smallest computational time.

Table 3.3. Computational Performance When $|\mathcal{Z}| = 3$ and $|\mathcal{T}| = 6$

	Profit		$\mathbf{x}$		Time	
	Val ($)	Gap (%)	Val	Gap (%)	Val (s)	Gap (%)
Original	2621.77	0	463	0	11893	0
Inner 2	2697.85	2.90	454	1.94	1861	84.35
Outer 80%	2661.10	1.50	444	4.10	2982	74.93
Sub 2	2649.73	**1.07**	479	**3.46**	462	**96.12**

We next consider a larger case with $|\mathcal{Z}| = 3$ and $|\mathcal{T}| = 12$. Since "Original" approach cannot solve this instance to the optimality within 24 hours, we set the results obtained by "Sub 2" approach as the benchmark, as it demonstrates the best performance in the above

experiments. We show the results in Table 3.4. It can be observed that most approaches can solve the instance within 5 hours, with some even achieving it within 1 hour, e.g., "Sub 3" and "Sub 4" approaches. The approach with the smallest computational time is "Sub 4" approach, solving the instance in 776 seconds, approximately 13 minutes. In contrast, "Original" approach fails to solve the instance within 24 hours. Table 3.4 confirms the efficiency of the proposed approaches and points out the outstanding performance of Algorithm 2 in this new larger-scale instance. Table 3.4 also highlights that increasing the number of sub-networks in Algorithm 2, increasing the number of splitting pieces in inner approximation, and reducing the principle component considered in outer approximation all lead to shorter computational time.

Table 3.4. Computational Performance When $|\mathcal{Z}| = 3$ and $|\mathcal{T}| = 12$

	Profit		$\mathbf{x}$		Time	
	Val ($)	Gap (%)	Val	Gap (%)	Val (s)	Gap (%)
Sub 2	4211.15	0	432	0	15720	0
Sub 3	4052.81	-3.76	423	-2.08	2858	-81.82
Sub 4	4102.47	-2.58	454	5.09	776	-95.06
Inner 2	-	-	-	-	24h	-
Inner 3	3956.49	-6.05	406	-6.02	18157	15.50
Inner 4	3945.70	-6.30	433	0.23	3778	-75.97
Outer 40%	4448.02	5.62	417	-3.47	17550	11.64
Outer 60%	-	-	-	-	24h	-
Outer 80%	-	-	-	-	24h	-
Original	-	-	-	-	24h	-

In summary, our proposed approaches can all obtain a high-quality solution in a dramatically reduced computational time. This highlights their potential to support urban shared mobility operations. In the following sections, we investigate the out-of-sample performance of the problem with $|\mathcal{Z}| = 5$ and $|\mathcal{T}| = 144$ by using Algorithm 2 combined with outer and inner approximations and obtain managerial insights.

3.6.3 Comparison of Different Optimization Methods

We conduct a comparison between our proposed DRO model ($\mathcal{P}_{\mathrm{F}}$) with models that use stochastic optimization (referred to as "SO") and robust optimization (referred to as "RO") to model uncertainty. The SO model is solved using sample average approximation (SAA). SAA is widely known to be computationally expensive, especially for a large-scale model. In our numerical studies, we can only solve an SO model under 3 scenarios within 24 hours. To ensure that the 3 scenarios are adequately representative, we utilize K-means algorithm to cluster all consumer trip samples into 3 groups based on the size of the trip

and then randomly select one scenario from each group. We consider the RO model as a deterministic model under the scenario with the largest consumer trips. We first solve our proposed DRO model, SO model, and RO model based on the training data. Then we use the obtained vehicle allocations to check the out-of-sample performance of each model. Their out-of-sample performance is presented in Tables 3.5 and 3.6.

Table 3.5. Comparison of Different Methods Overview

	Costs ($)		
	Allocation	Operation	Total
DRO	181,080	-307,985	-126,905
SO	189,864	310,773	-120,909
RO	209,448	-314,055	-104,607

Table 3.5 presents the allocation costs (i.e., the cost of allocating vehicles), the operation costs (the cost minus the revenue generated in the operation stage), and the total costs (i.e., the summation of the allocation costs and operation costs). From Table 3.5, it is evident that DRO shows the best out-of-sample performance as it generates the lowest total costs. This signifies that DRO is able to provide more reliable decisions, i.e., vehicle allocation decisions, than both SO and RO. DRO outperforms the other two methods by taking into account all distributions in the constructed ambiguity set, whereas SO and RO have little information on distributions and consider a restricted number of scenarios. Table 3.5 also suggests that RO yields the most conservative decision as it generates the highest allocation costs and total costs.

Table 3.6. Comparison of Different Methods in Operations

	Service level (%)	Utilization rate	Costs ($)				
			Rental	Charging	Discharging	Relocation	Idle
DRO	99.8	34.9	-360,451	36,348.1	-802.9	12,583.6	609.6
SO	99.8	33.4	-361,041	35,409.9	-379.2	12,613.7	665.6
RO	99.9	30.4	-361,549	35,116.9	-767.3	11,790.2	921.7

Table 3.6 provides more details on the operation results of these three methods. We calculate the rental costs and discharging costs as negative revenues generated from vehicle rentals and discharging, respectively. A system with efficient operations should have a high expected service level $\mathbb{E}_{\mathbb{P}}[\sum_{m\in\mathcal{M}}\sum_{a\in\hat{\mathcal{A}}^{\mathrm{R}}(m)} w_a(\boldsymbol{\xi})/\sum_{m\in\mathcal{M}} d_m(\boldsymbol{\xi})]$ and a high expected utilization rate $\mathbb{E}_{\mathbb{P}}[\sum_{m\in\mathcal{M}}\sum_{a\in\hat{\mathcal{A}}^{\mathrm{R}}(m)} w_a(\boldsymbol{\xi})/\sum_{z\in\mathcal{Z}}\sum_{s\in\mathcal{S}} x_{z,s}]$. DRO model achieves a high service level that is almost identical to that in the other models, reaching nearly 100%. This is attributed to a higher utilization rate generated in DRO model. A higher utilization rate indicates that each vehicle is used more frequently, resulting in increased needs

for charging and relocation and reduced idle time during operations. Hence, DRO model generates higher charging costs and relocation costs, while also yielding lower idle costs, as validated by Table 3.6.

3.6.4 Operational Features of Charging and Discharging

We now examine the system's performance in charging (i.e., electricity from grid to vehicle) and discharging (i.e., electricity from vehicle to grid) over the whole operational horizon (i.e., one day).

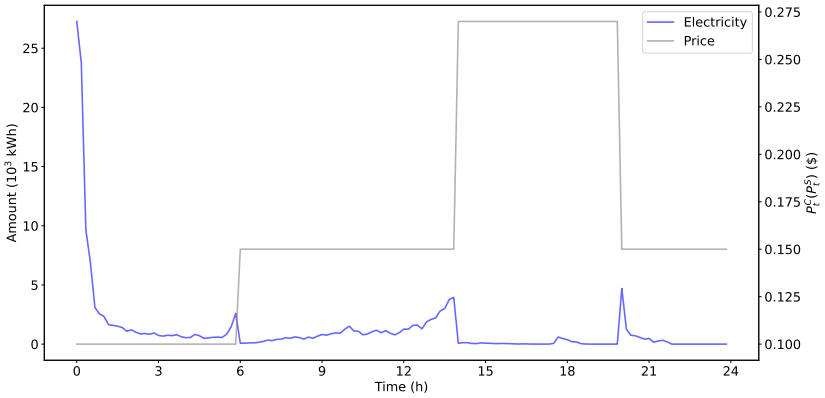

Figure 3.5. Charging in A Day

Figure 3.5 shows the amount of charging electricity and electricity prices over the operational horizon. It is clear that a substantial number of vehicles undergo charging during the early hours (i.e., 0:00 – 6:00), which finishes very rapidly, but are seldom charged afterward. During the early hours, both trip demands and charging prices remain low. Therefore, charging a significant number of vehicles during that period does not affect serving consumer trips and takes a low cost. This motivates the operator to charge a large number of vehicles during this time. Subsequently, both charging prices and consumer trips rise, resulting in higher charging costs and an increased number of vehicles being occupied with serving trips. As a result, the amount of charging stays limited. However, we can still observe some vehicles are charged before prices rise and after prices drop. This indicates that the electricity charged during early periods is insufficient for a full day of operation, necessitating the need for vehicles to get charged during the subsequent operation. EVs are charged several times with a small amount, instead of one time with a large amount. This is because consumer trips are high during operations which keep

most vehicles occupied and restrict the number of vehicles available for charging.

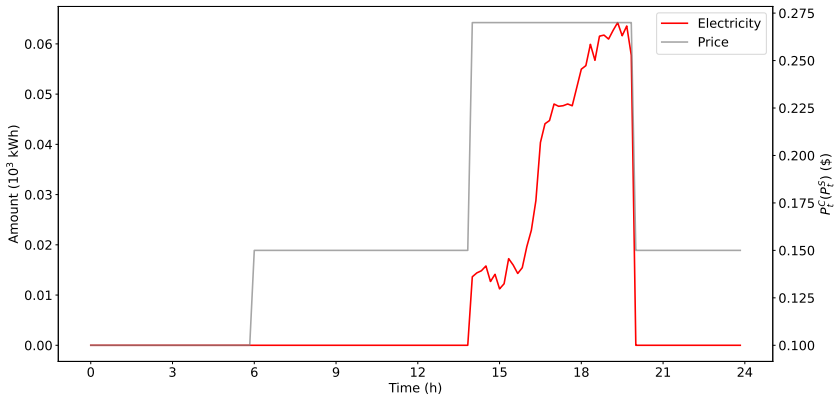

Figure 3.6. Discharging in A Day

Figure 3.6 shows the amount of discharging electricity and electricity prices over the operational horizon. It is evident that vehicles only sell electricity to the grid when discharging prices are at their peak, with the majority of electricity sales occurring during late periods when discharging prices are high. Delaying the sale of electricity minimizes the risk of electricity shortages that could impact consumer trip fulfillment.

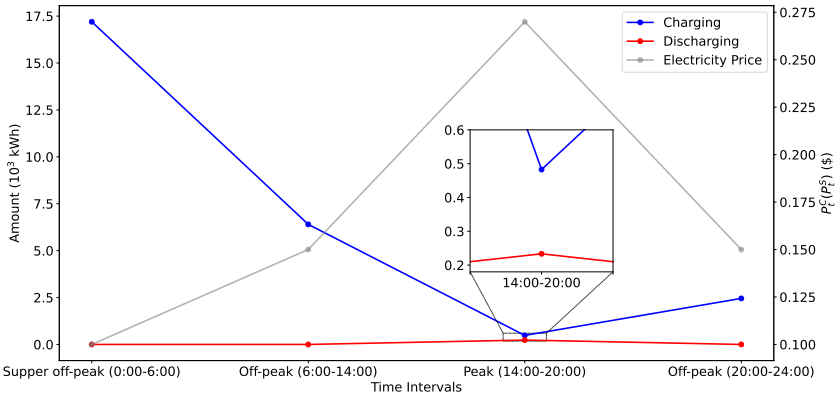

Figure 3.7. Overview of Charging and Discharging in A Day

In Figure 3.7, we provide an overview of the trends in amounts of charging and discharging electricity, as well as the changes in electricity price, over the operational horizon. We show the average amounts of charging and discharging electricity that occurred in each of the four time intervals introduced in Section 3.6.1. It is clear that charging exhibits an inverse correlation with prices, whereas discharging demonstrates a positive correlation with prices. Additionally, we can observe that the amount of discharging is obviously smaller than that of charging.

3.6.5 Impact of Charging Speed

In practice, it is common to see variations in charging speeds for electric vehicles due to different charger technologies. For instance, Tesla offers diverse charging options such as V2 Supercharger stations with a maximum power of 125 kW and Wall connectors with a maximum power of 11 kW (Tesla 2024a). We now examine the performance of the system when vehicles are charged at a low speed, i.e., 2 SoC per period, in this section.

Table 3.7. Comparison of Performances at Different Charging Speeds

	x	Service level (%)	Utilization rate	Costs ($)					
				Rental	Charging	Discharging	Relocation	Idle	Total
Fast	2,515	99.8	34.9	-360,451	36,348.1	-802.9	12,583.6	609.6	-126,905
Slow	2,783	99.9	31.8	-361,366	36,413.3	-1,493.8	12,004.2	918.1	-112,166

Table 3.7 compares the system performance at fast-charging and slow-charging speeds. It shows that a greater number of vehicles are allocated when using slow charging, leading to a slightly higher service level. However, the utilization rate is lower when the charging speed is slow. Benefiting from a larger fleet when the charging speed is slow, the system can generate higher revenues from renting vehicles and selling electricity to the grid. However, it has to spend higher costs on charging, relocation, and idling. Consequently, when considering the total cost, the system incurs higher expenses with slow charging compared to fast charging.

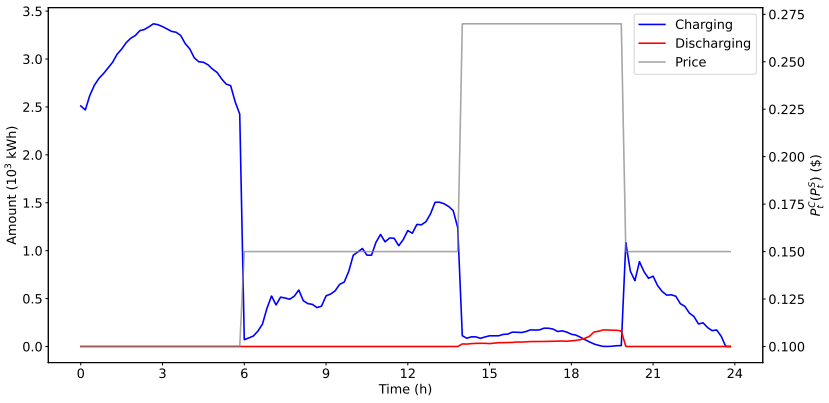

Figure 3.8. Charging and Discharging in Slow Speed

Figure 3.8 shows amounts of charging and discharging electricity, as well as electricity price levels, over the operational horizon. It shows that during periods of low charging prices, the amount of charging remains consistently high. This is very different from the performance in the fast-charging case, where the peak charging amount reaches a

significantly higher level (approximately 25×10^3 kWh) and the charging process has an obviously shorter duration. This discrepancy arises because slow charging can only charge a small amount of electricity in one period, so it requires more time to reach the same SoC compared to fast charging. Additionally, we can observe that the amount of charging electricity remains pronounced when prices are medium. This differs from the performance in the fast-charging case, where the amount of charging electricity becomes pronounced only before prices rise and after prices drop. This difference is also attributed to the longer time required for slow charging to reach the same SoC compared to fast charging. Regarding discharging, it is evident that the system sells electricity to the grid when the discharging prices are at their peak. Similarly to fast charging, in the case of slow charging, most electricity is discharged during later periods when discharging prices are high.

3.6.6 Impact of Pricing Scheme of Charging

It is common to see different pricing schemes for charging EVs in practice, including those based on electricity (i.e., measured in kWh) and those based on time (i.e., measured in minute) (Tesla 2024b). Having examined the system's performance under the electricity-based pricing scheme in the above, we next investigate its performance under the time-based pricing scheme. Given that the rate of fast charging is 19 SoC units per period and the charging electricity price per SoC unit is P_t^{C} at each period $t \in \mathcal{T}$, we can determine the charging electricity price per period P_t^{T} by multiplying the charging electricity price per SoC unit by 19, i.e., $P_t^{\mathrm{T}} = 19P_t^{\mathrm{C}}$.

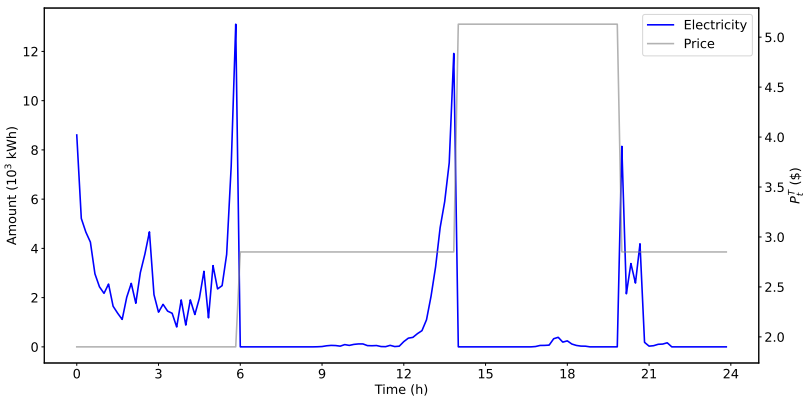

Figure 3.9. Charging in A Day Under Time-based Pricing Scheme

Figure 3.9 shows the amount of charging electricity over the operational horizon under the time-based pricing scheme. We can observe two significant peaks during the early hours (i.e., 0:00 – 6:00) when charging prices are low. Specifically, one peak occurs in the early periods while the other peak occurs in the late periods when charging prices are low. The charging pattern observed here differs from that under the electricity-based pricing scheme, where only one peak occurs during the early hours and the peak value is notably higher. After the early hours, we can observe that the amounts of charging electricity before the price rises and after the price drops are obviously higher under the time-based pricing scheme compared to the electricity-based pricing scheme.

To understand these performance discrepancies, it is helpful to note the *economies of scale in charging* under the time-based pricing scheme. Under this scheme, a fixed cost P_t^{T} is paid if a vehicle is charged at period $t \in \mathcal{T}$, regardless of the amount of SoC units it charges. Since we assume that charging will stop once the vehicle's SoC reaches its upper limit (i.e., 38), the amount of SoC units charged in a period may vary, depending on the vehicle's SoC before charging. Given that the rate of fast charging is 19 SoC units per period, the charged SoC units in a period may range from 1 to 19. It is obvious that charging 19 SoC units in a period leads to the lowest average cost per charged SoC unit, demonstrating the *economies of scale in charging*. In order to charge 19 SoC units in a period, the vehicle's SoC before charging should not exceed $38 - 19 = 19$. Consequently, in the case of the vehicle with an SoC greater than 19, it is more beneficial to use or sell some SoC units before its level drops to 19 or smaller and then proceed with charging. As a result, under the time-based pricing scheme, some vehicles are not charged initially until their SoC drops to a low level, leading to a smaller number of vehicles being charged initially and a larger number of vehicles being charged later. Therefore, under the time-based pricing scheme, we observe the first peak of charging becomes lower and a second peak of charging occurs after vehicles have been in operation for several hours. Additionally, the time-based pricing scheme incentivizes the system to charge more electricity than needed to serve consumer trips. This is because, under this scheme, charging small and large SoC units in a period costs the same, but charging larger SoC units can generate higher revenues by selling the excess electricity to the grid. Therefore, we can observe that amounts of charging before prices rise and after prices drop are obviously higher under the time-based pricing scheme compared to the electricity-based

pricing scheme. Additionally, from Figures 3.9 and 3.10, we can observe a large amount of charging and discharging electricity occurring before the electricity price rises at 14:00. Discharging before charging allows EVs to obtain revenue and charge more electricity in one period, pursuing *economies of scale in charging*. In Figure 3.10, we can also observe a large amount of discharging electricity occurring at the end of the day. This shows that under the time-based pricing scheme, EVs charge a large amount of excess electricity, which they finally need to sell.

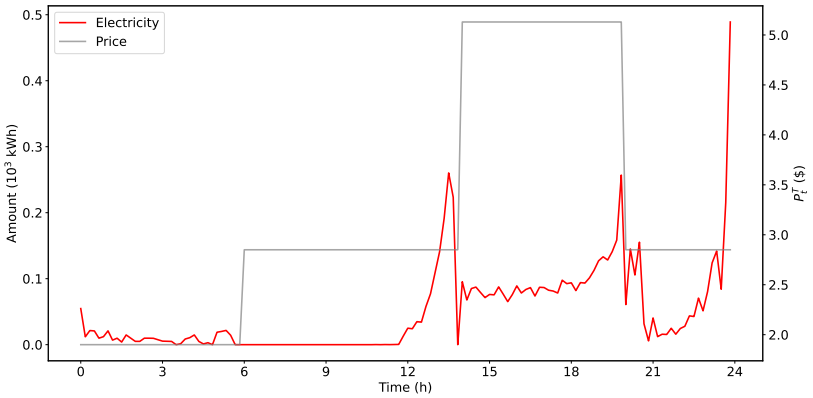

Figure 3.10. Discharging in A Day Under Time-based Pricing Scheme

3.7 Conclusion

In this chapter, we study an EV-sharing mobility system with V2G technology, which enables EVs to release their stored electricity back to the power grid. We formulate an integrated vehicle allocation and operation problem under consumer trip uncertainty as a two-stage DRO problem on a time-space-SoC network. The DRO approach only needs the support and first- and second-moment information of uncertain parameters. We reformulate the two-stage DRO problem as a SDP model. To deal with the significant computational difficulty of the SDP reformulation, we first introduce outer and inner approximations for it to reduce the size of PSD matrices. We then propose an algorithmic approach that incorporates time-based decomposition to further strengthen the solving process. Through numerical experiments using real-world data, we show that our proposed approaches can obtain high-quality solutions in significantly short computational time. Results also suggest that our DRO model outperforms SO and RO, generating a solution that incurs the lowest total cost. Our out-of-sample results re-

veal that most EVs charge electricity during the early hours of the day when electricity prices and trip demands are low. Conversely, EVs discharge electricity during periods of high electricity prices. Additionally, an increased charging speed contributes to a reduction in the number of allocated vehicles, an enhancement in the vehicle utilization rate, and a drop in total costs. We further compare two different pricing schemes for charging EVs: electricity-based and time-based pricing schemes. We find that EVs process charging and discharging more frequently under the time-based pricing scheme than the electricity-based pricing scheme. In the future, as the amount of available data increases, potentially yielding a more reliable empirical distribution, we may explore the adoption of a discrepancy-based ambiguity set. For example, we can consider an ambiguity set using the Wasserstein metric, as introduced in Esfahani and Kuhn (2017).

Chapter 4

Robust Grid-Vehicle Integration: A Machine Learning-Driven Optimization Approach

4.1 Introduction

Renewable energy sources (e.g., wind and solar) have become increasingly prevalent in the power grid system due to their economic and environmental advantages (Panwar et al. 2011). As of 2020, these sources contribute to a noteworthy 29% of global power generation, with an annual expansion rate of approximately 7% (IEA 2021a). Nevertheless, the inherent intermittency of renewable energy (e.g., wind energy's variable nature and solar energy's dependence on sunny weather) presents formidable challenges for grid operations. The unpredictable power load (i.e., demand) further exacerbates these complexities. Specifically, the power grid should decide whether generators start up a day ahead of real-time operations, considering the power load and renewable generation uncertainties. The escalating uncertainties amplify the intricacy of making day-ahead decisions. Meanwhile, the fluctuation pattern of the power load diverges from that of wind and solar energy. This misalignment in timing poses a significant operational challenge for the power grid, with the load peaking in the evening, while solar energy reaches its zenith at noon and diminishes by evening, and wind energy fluctuates irregularly throughout the day (CAISO 2016).

Addressing these challenges will ensure a seamless integration of renewable energy into

the power grid while maintaining its reliability. To that end, the grid may strategically invest in additional infrastructures to expand its generation and transmission capacity, enhancing overall flexibility and resilience. However, such investment requires substantial time and resources to construct facilities, which may be under low utilization during most operational hours. In addition, the grid can leverage regulation reserves (as a form of capacity provided by power generators) obtained from an ancillary service market (Huang et al. 2021a) to augment power generation (i.e., regulation-up reserves) or curtail it (i.e., regulation-down reserves) during real-time operations when facing the uncertainties. While this approach provides increased flexibility in adjusting generation levels, the remote transmission of regulation reserves over the geographically dispersed power network may lead to substantial energy loss and network congestion.

In this chapter, we consider integrating the power grid with increasing electric vehicles (EVs) to enhance the flexibility and resilience of the grid without incurring the drawbacks mentioned earlier. EVs rely on electricity charged from the grid, and their charging not only serves mobility demands whenever needed but also helps store excess electricity when the power generation exceeds the power load. Conversely, through the emerging *vehicle-to-grid (V2G)* technology, EVs can discharge electricity to supplement the grid's supply during periods of insufficient generation. More importantly, compared to the power generators often situated far from urban areas, the EVs are in much closer proximity to the power load, facilitating convenient power transfers without reliance on the power transmission network and minimizing energy loss and network congestion. This symbiotic relationship between EVs and the grid presents a promising avenue for bolstering flexibility and resilience without investing in additional power grid infrastructures.

EVs are increasingly popular globally, with 74.7% of new cars sold in Norway in 2020 being EVs (Wikipedia 2023). Despite a 16% drop in car sales due to the COVID-19 pandemic, EV sales expand by 41% worldwide in 2021 (IEA 2021b). Notably, 24 countries and leading car manufacturers committed to ending sales of fossil-fuel-powered vehicles by 2040 (The Guardian 2021). Shared mobility firms also embrace EVs, exemplified by Zipcar's commitment to upgrading their fleet to fully electric by 2025 (Zipcar 2024). The popularity of EVs has prompted power grids in various countries to initiate grid-vehicle integration through V2G. In China, State Grid launches a large V2G project in Baoding in 2021, with nearly 50 additional projects established in 15 provinces and cities across

China (Grasen 2021). In the U.S., Pacific Gas and Electric Company (PG&E) obtains regulatory approval to establish the nation's first V2G export rate (i.e., incentives) for commercial EVs in California in 2022 (Nasdaq 2022). In the U.K., E.ON, a major energy network operator, collaborates with Nissan to deploy 20 V2G points in Cranfield in 2020 (Zapmap 2020). Therefore, integrating the power grid with EVs is not only practical but also gaining momentum, and we term such an integration system *the grid-vehicle integration (GVI) system*.

Our primary focus centers on the operational dynamics of the GVI system across multiple periods under uncertainties. Specifically, we are interested in the following research questions: When integrated with EVs, how should the power grid strategically optimize its planning and operations to *robustly* align the power supply with demand, with the objective of minimizing costs, in the face of uncertain renewable generation, power load, and mobility trip demand? How does implementing V2G technology influence the power grid's decisions concerning initial generator start-up and subsequent power generation? With the V2G technology adopted, are there noteworthy temporal features in the power transfer dynamics (i.e., charging/discharging interactions) between the grid and EVs? How do system parameters (e.g., power load patterns) impact the GVI system's overall performance? To what extent can the GVI system contribute to sustainability, and can carbon neutrality be achieved within this system?

To answer the questions, we study a GVI system where the grid operates power generators to satisfy the power load, leveraging the assistance of EVs across an operational horizon with multiple periods. The renewable generation, power load, and EV trip demand in each period are uncertain. At the start of the horizon, the grid operator first decides whether a dispatchable (i.e., thermal) power generator starts up in each period before the uncertainty is realized. Subsequently, after the uncertainty is realized in each period, the grid determines power generation levels and charging/discharging interactions with EVs to satisfy the power load. Meanwhile, the mobility operator utilizes the EV fleet to execute charging/discharging operations and meet trip demands. To ensure the EVs' economic viability, the grid ensures that the EV fleet attains a predefined service level after fulfilling the requested power interactions; otherwise, the grid operator is obligated to provide subsidies to the other. To ensure power generation meets demand under any scenario of the random parameters while maintaining the reliability of the grid and EV

fleet, the GVI system should exhibit robustness against uncertainty. Thus, we employ a two-stage robust optimization model for the decision-making process, by which the power grid operator minimizes the worst-case total cost throughout the operational horizon. Note that solving a two-stage robust optimization model, which could be NP-hard (Ben-Tal and Nemirovski 1999), is significantly challenging. To address this challenge, we present an innovative machine learning-driven optimization approach as a pragmatic solution to overcome the computational hurdles. The main contributions of this chapter are summarized as follows:

(i) We present a novel formulation of the GVI system's operations through a two-stage robust mixed-integer programming (MIP) model. In the first stage, we decide whether each thermal generator starts up; in the second stage, we determine the subsequent power generation, charging/discharging interaction, and EV fleet operation over the horizon.

(ii) We introduce an innovative machine learning-driven optimization approach where we can first identify a worst-case scenario and then iteratively select a few more scenarios to derive a provably optimal solution efficiently. With theoretical guarantees, our numerical experiments, utilizing data from the New York Independent System Operator (NYISO)[1] and the Taxi and Limousine Commission (TLC) in New York City (NYC), show that our approach yields optimal solutions much more efficiently than a commercial solver.

(iii) Our study yields the following managerial insights for the GVI system. Introducing V2G technology effectively reduces the number of online generators and extends their operational periods, enhancing grid stability. The V2G helps stabilize the subsequent power generation by using EVs to "fill" the low power load and "shave" the peak across different periods. Furthermore, V2G contributes to sustainability by curbing carbon emissions, with the most significant impact observed during hours of moderate power load. The impacts of V2G are notably more pronounced under a bimodal power load pattern compared to a unimodal pattern. We also find that achieving carbon neutrality in this integration system is feasible yet challenging.

We organize the remainder of this chapter as follows. In Section 4.2, we review the related literature. In Section 4.3, we formulate the problem. In Section 4.4, we propose

[1]Website: https://www.nyiso.com/

the machine learning-driven optimization approach. In Section 4.5, we conduct numerical experiments to examine the performance of our proposed approach and the GVI system. In Section 4.6, we conclude this chapter. All proofs are presented in the Online Supplement.

4.2 Related Literature

This chapter is closely related to the Operations Management (OM)/Operations Research (OR) literature on power grid operations. Existing studies highlight the operational challenges posed by the increasing penetration of intermittent renewable generation into the power grid (Huang et al. 2022). To address such challenges, various studies consider expanding the grid infrastructures to hedge against uncertainties. Qi et al. (2015) design energy storage systems and transmission lines to optimize total cost and enhance system robustness under uncertain renewable generation. Salas and Powell (2018) optimize storage device distribution in the power system, and Zolan et al. (2021) design cost-effective microgrids with photovoltaic and battery storage systems to counter renewable uncertainty. Peng et al. (2021) investigate the relationships among fossil fuel, renewable, and battery storage capacities in a distributed power system, employing stochastic optimal control theory to explore their joint operations and investment relations. In addition, several studies utilize regulation reserves from the existing ancillary service market to address the uncertainty issue. For instance, Huang et al. (2021a,0) explore a stochastic problem co-optimizing power generation and regulation reserves, providing valuable insights via polyhedral study results.

As highlighted in Section 4.1, investing in additional infrastructures or soliciting regulation reserves to increase the power grid's capacity entails significant time and cost and causes potential energy loss and network congestion. In contrast, integrating the power grid with EVs avoids these drawbacks while presenting significant benefits. The following three papers consider deterministic grid-EV interactions. Tomić and Kempton (2007) evaluate the EV fleet's economic potential in ancillary service markets via charging and discharging. Both Saber and Venayagamoorthy (2010) and Ma et al. (2012) explore scenarios where EVs serve as loads, energy sources, or energy storage for the grid; the former examines how EV adoption can reduce grid costs and emissions, and the latter analyzes

the most efficient utilization of EV battery storage when supporting the power system. The above studies underscore the benefits of incorporating both regulation reserves and EVs in enhancing power grid operations. Our work builds upon these insights, addressing power grid operations under uncertainties by integrating both regulation reserves and EVs into our study.

Our work aligns more closely with studies on V2G. Early literature approached V2G from a social perspective, delving into social barriers, benefits, and net economic welfare associated with V2G (e.g., see Lund and Kempton 2008 and Sovacool and Hirsh 2009). Recently, V2G has gained attention in the OM/OR studies. Broneske and Wozabal (2017) examine the impacts of V2G contract parameters (e.g., plug-in duration) on the cooperation between EVs and the grid. Mak and Tang (2021) tackle a pricing optimization problem, studying how a platform operating a V2G network decides incentives for driver participation. Widrick et al. (2018) utilize the Markov decision process to optimize the number of batteries charged or discharged at an EV battery swap station during operations when V2G is involved. Zhang et al. (2021) focus on an EV-sharing mobility system with V2G, formulating a two-stage stochastic program to optimize EV allocation and fleet operation. Qi et al. (2022) consider an urban microgrid connected with an EV-sharing mobility system, formulating deterministic models to optimize EV fleet dispatch and electricity exchange, thereby enhancing microgrid self-sufficiency and resilience. While these studies provide valuable insights into the value of V2G, primarily from the perspective of the EV-sharing mobility system, they generally do not incorporate the power grid's decisions in planning and operations. They often overlook uncertainties in the power grid. In contrast, this chapter focuses on power grid operations while considering uncertainties in renewable generation, power load, and EV trip demand.

This chapter also contributes to the literature on robust optimization (RO). Given an uncertainty set with some information of uncertain parameters, RO is to find a solution feasible for any realization within this set while optimizing for the worst-case scenario (Ben-Tal et al. 2009, Bertsimas et al. 2011). The degree of conservatism in the robust solution can be fine-tuned through the choice of the uncertainty set (Bertsimas and Sim 2004), rendering RO widely applicable in various fields, including power systems (e.g., see Lorca et al. 2016 and Yang et al. 2021) and network/transportation systems (e.g., see Atamtürk and Zhang 2007 and Erera et al. 2009). However, solving two-

stage (or multi-stage) RO models poses significant computational challenges. Thus, two existing schemes are provided: (i) the approximation scheme that employs affine policies or assumes decision variables in subproblems are simple functions of uncertainties (e.g., see Ben-Tal et al. 2004, Bertsimas et al. 2010, and Lorca et al. 2016), and (ii) the exact scheme (e.g., see Zeng and Zhao 2013 and Yang et al. 2021), exemplified by the cutting plane method in the decomposition framework, which dynamically creates cuts using primal/dual solutions of the subproblem and incorporates them into the master problem. This chapter opts for the second scheme. We improve this approach by incorporating machine learning techniques to quickly identify a sufficient yet small number of scenarios from the uncertainty set to construct a support set of the problem, thereby significantly reducing the number of added cuts and enhancing solving efficiency.

4.3 Problem Formulation

Consider a power grid network with a set of nodes (termed "power bus") $\mathcal{B}$ and a set of bidirectional power transmission lines $\mathcal{L}$, where each line links two buses. The power grid operator (she) manages a set of thermal generators $\mathcal{G}$ to provide electricity to the public and ancillary services to maintain the grid reliability in each period $t \in \mathcal{T} = \{1, 2, \ldots, T\}$. Meanwhile, she manages a set of renewable generators (i.e., wind and solar farms) that intermittently feed electricity via each bus $b \in \mathcal{B}$ and interacts with a mobility operator (he) that manages a fleet of electric vehicles (EVs) and provides shared mobility services to the public.

Figure 4.1 illustrates the sequence of events regarding the operations and demand arrivals of the power grid and mobility fleet in each period $t \in \mathcal{T}$: (i) At the start of period t, grid and mobility demands arrive and generation amounts of renewable generators are realized. (ii) Knowing the realized grid demands and renewable generation, the power grid operator determines the generation amount of each thermal generator (e.g., coal- and gas-fired ones) in the power grid and the amounts of electric power charged from and discharged to the EVs. (iii) Knowing the realized mobility demands and charging/discharging interactions with the power grid, the mobility operator determines the number of EVs to complete the charging/discharging operations and satisfy mobility demands, respectively. (iv) Any demand loss is observed, and the grid-vehicle integration

(GVI) system is updated for the period $t+1$.

Facing significant uncertainty and reliability requirements to supply electricity, the power grid operator makes initial generator commitment (i.e., on/off) and subsequent generator dispatch and interactions with the mobility fleet to minimize the worst possible total cost. We formulate the problem as a *two-stage robust optimization* model. In the first stage, we decide the commitment status of each thermal generator in the power grid. In the second stage, when time-dependent demands arrive, we decide the generator and EV dispatch and their interactions in each period for the entire operational horizon as a recourse against the worst possible scenario.

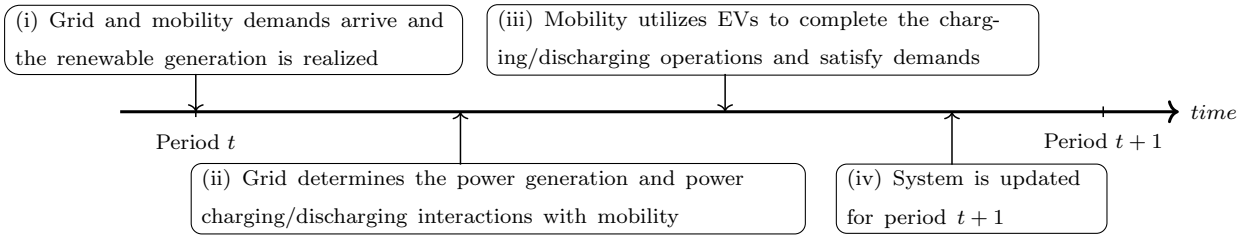

Figure 4.1. Sequence of Events

4.3.1 First-stage Formulation

For each generator $g \in \mathcal{G}$, the grid operator makes a decision u_t^g in each period $t \in \mathcal{T}$ to determine the generator starts up (i.e., $u_t^g = 1$) or not (i.e., $u_t^g = 0$). When a generator g starts up in period t, its commitment status becomes online in this period and may stay online during the coming periods. We define a binary variable y_t^g such that $y_t^g = 1$ if generator $g \in \mathcal{G}$ is online in period $t \in \mathcal{T}$ and $y_t^g = 0$ otherwise. Thus, if generator g is online in period t (i.e., $y_t^g = 1$) but not in period $t-1$ (i.e., $y_{t-1}^g = 0$), then clearly this generator starts up in period t (i.e., $u_t^g = 1$):

$$u_t^g - y_t^g + y_{t-1}^g \geq 0, \ \forall t \in \mathcal{T} \setminus \{1\}, g \in \mathcal{G}. \tag{4.1}$$

After staying online for several periods, a generator can shut down and its commitment status becomes offline. When generator $g \in \mathcal{G}$ starts up (resp. shuts down), a start-up cost SU^g (resp. a shut-down cost SD^g) is incurred and this generator has to stay online (resp. offline) for a minimum number of L^g (resp. ℓ^g) periods with $L^g,\ \ell^g \leq T-1$. Thus,

we have

$$\sum_{i=t-L^g+1}^{t} u_i^g \le y_t^g,\ \forall t \in [L^g+1, T]_{\mathbb{Z}}, g \in \mathcal{G}, \tag{4.2}$$

$$\sum_{i=t-\ell^g+1}^{t} u_i^g \le 1 - y_{t-\ell^g}^g,\ \forall t \in [\ell^g+1, T]_{\mathbb{Z}}, g \in \mathcal{G}, \tag{4.3}$$

where we let $[a,b]_{\mathbb{Z}}$ denote the set of all integers between any two nonnegative integers a and b; that is, $[a,b]_{\mathbb{Z}} = \{a, a+1, \ldots, b\}$ if $a \le b$, and $[a,b]_{\mathbb{Z}} = \emptyset$ if $a > b$. The above two constraints, i.e., minimum-up and minimum-down time limits, respectively, are respected due to physical limits and maintenance requirements. We further restrict u_t^g to be nonnegative:

$$u_t^g \ge 0,\ \forall t \in \mathcal{T} \setminus \{1\}, g \in \mathcal{G}, \tag{4.4}$$

and restrict u_t^g and y_t^g to be binary:

$$u_t^g \in \{0,1\},\ \forall t \in \mathcal{T} \setminus \{1\}, g \in \mathcal{G};\ y_t^g \in \{0,1\},\ \forall t \in \mathcal{T}, g \in \mathcal{G}. \tag{4.5}$$

Facing uncertain grid and EV demands and intermittent renewable generation in the second stage, the grid operator considers a set of possible scenarios of the random parameters, denoted by $\mathcal{S}$. Given the first-stage decisions $\mathbf{u} = (u_t^g,\ \forall t \in \mathcal{T} \setminus \{1\}, g \in \mathcal{G})^\top$ and $\mathbf{y} = (y_t^g,\ \forall t \in \mathcal{T}, g \in \mathcal{G})^\top$ and a realization $\boldsymbol{\xi} \in \mathcal{S}$, we let $\Psi(\mathbf{u}, \mathbf{y}, \boldsymbol{\xi})$ denote the optimal operational cost in the second stage. Thus, the grid operator makes its commitment decisions $(\mathbf{u}, \mathbf{y})$ and subsequent operational decisions in the second stage to minimize the total costs, including the first-stage and worst possible second-stage costs, by solving the following problem

$$\Theta = \min_{\mathbf{u},\mathbf{y}} \left\{ \sum_{g\in\mathcal{G}} \sum_{t=2}^{T} \left(\mathrm{SU}^g u_t^g + \mathrm{SD}^g (y_{t-1}^g - y_t^g + u_t^g) \right) + \max_{\boldsymbol{\xi}\in\mathcal{S}} \Psi(\mathbf{u}, \mathbf{y}, \boldsymbol{\xi}) \;\middle|\; (4.1) - (4.5) \right\}. \tag{$\mathcal{M}$}$$

Here the term "$\mathrm{SU}^g u_t^g$" (resp. "$\mathrm{SD}^g(y_{t-1}^g - y_t^g + u_t^g)$") represents the start-up (resp. shut-down) cost of generator g in period t. Constraints (4.1)–(4.2) and the minimization objective ensure that the shut-down cost SD^g is incurred in period t (i.e., $y_{t-1}^g - y_t^g + u_t^g = 1$) if and only if $y_{t-1}^g = 1$ and $y_t^g = 0$. In addition, $\max_{\boldsymbol{\xi}\in\mathcal{S}} \Psi(\mathbf{u}, \mathbf{y}, \boldsymbol{\xi})$ represents the worst possible operational cost in the second stage.

4.3.2 Second-stage Formulation

Given a realization $\boldsymbol{\xi} \in \mathcal{S}$, we let $p^{\mathrm{w}}_{b,t}$, $p^{\mathrm{s}}_{b,t}$, and $q_{b,t}$ denote the realized wind generation, solar generation, and power load (i.e., electric demand) in bus $b \in \mathcal{B}$ and period $t \in \mathcal{T}$, respectively, and let d_t denote the realized EV trip demand in period $t \in \mathcal{T}$. We then describe the power grid and EV fleet operations, respectively, in the following two sections.

Power Grid Operations

In each period $t \in \mathcal{T}$, when generator $g \in \mathcal{G}$ is online, i.e., $y^g_t = 0$, this generator has to generate a minimum amount of electricity (denoted by $\underline{C}^g$) and then the grid operator decides how much electricity (denoted by p^g_t) should be additionally generated; that is, the total generation amount is $\underline{C}^g + p^g_t$. To ensure that electricity can be supplied reliably to satisfy uncertain demands, when generator g is online in period t, the grid operator decides to reserve an amount of electricity (denoted by $r^{g^+}_t$) for potential real-time demand increase (termed "regulation-up") and an amount of electricity (denoted by $r^{g^-}_t$) for potential real-time demand decrease (termed "regulation-down"). The total generation amount of each generator is constrained by its minimum and maximum generation outputs $\underline{C}^g$ and $\overline{C}^g$, respectively:

$$p^g_t - r^{g^-}_t \geq 0, \ \forall t \in \mathcal{T}, g \in \mathcal{G}, \tag{4.6}$$

$$p^g_t + r^{g^+}_t \leq \big(\overline{C}^g - \underline{C}^g\big) y^g_t, \ \forall t \in \mathcal{T}, g \in \mathcal{G}, \tag{4.7}$$

where $\overline{C}^g > \underline{C}^g$ for any $g \in \mathcal{G}$.

In addition, when generator g increases (resp. decreases) its generation amount, termed "ramp up" (resp. "ramp down"), from period $t-1$ to period t, the increment (resp. decrement), termed "ramp-up rate" (resp. "ramp-down rate"), should be bounded due to physical constraints. Specifically, when generator g is online in periods $t-1$ and t, the ramp-up/-down rate limit is denoted by V^g; when generator g is online in one of the periods $t-1$ and t and offline in the other, i.e., starts up or shuts down in period t, the ramp-up/-down rate limit is denoted by $\overline{V}^g$. We assume that $\underline{C}^g < \overline{V}^g < \underline{C}^g + V^g$ for any $g \in \mathcal{G}$, which holds in most industrial settings (Pan et al. 2022). Considering each generator's power output and reserve amounts (i.e., regulation-up and regulation-down),

the ramping constraints (Carlson et al. 2012, Huang et al. 2021a) can be represented by

$$\left(p_t^g + \underline{C}^g y_t^g + r_t^{g+}\right) - \left(p_{t-1}^g + \underline{C}^g y_{t-1}^g\right) \leq V^g y_{t-1}^g + \overline{V}^g (1 - y_{t-1}^g),\ \forall t \in \mathcal{T} \setminus \{1\}, g \in \mathcal{G}, \tag{4.8}$$

$$\left(p_{t-1}^g + \underline{C}^g y_{t-1}^g\right) - \left(p_t^g + \underline{C}^g y_t^g - r_t^{g-}\right) \leq V^g y_t^g + \overline{V}^g (1 - y_t^g),\ \forall t \in \mathcal{T} \setminus \{1\}, g \in \mathcal{G}. \tag{4.9}$$

To ensure high system reliability, in each period t, the grid operator often reserves enough regulation-up and regulation-down amounts contributed by all the generators in $\mathcal{G}$:

$$\sum_{g \in \mathcal{G}} r_t^{g+} \geq R_t^+,\ \sum_{g \in \mathcal{G}} r_t^{g-} \geq R_t^-,\ \forall t \in \mathcal{T}, \tag{4.10}$$

where R_t^+ and R_t^- denote the minimum required regulation-up and regulation-down amounts in the power grid, respectively. A unit cost RU^g (resp. RD^g) is incurred when reserving regulation-up (resp. regulation-down) for each generator $g \in \mathcal{G}$.

Furthermore, the grid operator manages four energy sources to satisfy power load $q_{b,t}$ in each bus $b \in \mathcal{B}$ and period $t \in \mathcal{T}$. First, a set of thermal generators $\mathcal{G}_b \subseteq \mathcal{G}$ in each bus b generate electricity. Second, a set of renewable generators contribute $p_{b,t}^{\mathrm{w}}$ and $p_{b,t}^{\mathrm{s}}$ from wind and solar farms, respectively. Third, power generation flowing from any other buses in $\mathcal{B} \setminus \{b\}$ into bus b. Specifically, we use $\beta_{b,t}$ to denote the phase angle in each bus $b \in \mathcal{B}$ and period $t \in \mathcal{T}$ and $X_{b',b}$ the reactance of power transmission line $(b', b) \in \mathcal{L}$. Then the power flow from buses b' to b through line (b', b) can be calculated by $(\beta_{b',t} - \beta_{b,t})/X_{b',b}$. Fourth, the EV fleet discharges (resp. charges) an amount of electricity, denoted by v_t^+ (resp. v_t^-), into (resp. from) the power grid in each period $t \in \mathcal{G}$. Thus, the power load balance constraints can be represented by

$$\sum_{g \in \mathcal{G}_b} (p_t^g + \underline{C}^g y_t^g) + p_{b,t}^{\mathrm{w}} + p_{b,t}^{\mathrm{s}} + \sum_{\forall b' \in \mathcal{B}:\ (b',b) \in \mathcal{L}} \frac{\beta_{b',t} - \beta_{b,t}}{X_{b',b}} + v_t^+ - v_t^- = q_{b,t},$$
$$\forall t \in \mathcal{T}, b \in \mathcal{B}. \tag{4.11}$$

Each transmission line $(b', b) \in \mathcal{L}$ has a capacity $C_{b',b}$ on both directions:

$$-C_{b',b} \leq \frac{\beta_{b',t} - \beta_{b,t}}{X_{b',b}} \leq C_{b',b},\ \forall t \in \mathcal{T}, (b', b) \in \mathcal{L}. \tag{4.12}$$

In addition, we restrict all the decision variables within certain ranges:

$$p_t^g,\ r_t^{g+},\ r_t^{g-} \geq 0,\ \forall t \in \mathcal{T}, g \in \mathcal{G}, \tag{4.13}$$

$$v_t^+,\ v_t^- \geq 0,\ \forall t \in \mathcal{T};\quad \beta_{b,t} \in [-\pi, \pi],\ \forall b \in \mathcal{B}, t \in \mathcal{T}. \tag{4.14}$$

By constraints (4.6)–(4.7) and (4.13), when $y_t^g = 0$, i.e, generator g is offline in period t, we clearly have $p_t^g = r_t^{g+} = r_t^{g-} = 0$.

Finally, power generation cost f_t^g is incurred in each period $t \in \mathcal{T}$ when each thermal generator $g \in \mathcal{G}$ produces electricity:

$$f_t^g := \phi(p_t^g, y_t^g) = a^g \left(p_t^g + \underline{C}^g y_t^g\right)^2 + b^g \left(p_t^g + \underline{C}^g y_t^g\right) + c^g y_t^g,\ \forall t \in \mathcal{T}, g \in \mathcal{G}, \tag{4.15}$$

where a^g, b^g, and c^g are given cost parameters of generator $g \in \mathcal{G}$. Commonly, (4.15) is approximated by a piecewise linear function with H segments (Carrión and Arroyo 2006). Specifically, for each generator $g \in \mathcal{G}$, we consider $y_t^g = 1$ and divide the interval $[0, \overline{C}^g - \underline{C}^g]$ into H segments, each with length $\tau^g = (\overline{C}^g - \underline{C}^g)/H$. For any $h \in \mathcal{H} = \{1, 2, \ldots, H\}$, we approximate $\phi(p_t^g, 1)$ in the hth segment $[\sigma_{h-1}^g := (h-1)\tau^g, \sigma_h^g := h\tau^g]$ with a linear function passing through points $((h-1)\tau^g, \phi((h-1)\tau^g, 1))$ and $(h\tau^g, \phi(h\tau^g, 1))$. Let $\zeta_h^g = (\phi(h\tau^g, 1) - \phi((h-1)\tau^g, 1))/\tau^g$ denote the slope of this linear function. Therefore, because we would like to minimize the generation costs, constraints (4.15) can be approximated as follows:

$$f_t^g \geq \left(a^g (\underline{C}^g)^2 + b^g \underline{C}^g + c^g\right) y_t^g + \sum_{h \in \mathcal{H}} \zeta_h^g \bar{p}_{t,h}^g,\ \forall t \in \mathcal{T}, g \in \mathcal{G}, \tag{4.16}$$

$$0 \leq \bar{p}_{t,h}^g \leq \sigma_h^g - \sigma_{h-1}^g,\ \forall t \in \mathcal{T}, g \in \mathcal{G}, h \in \mathcal{H}, \tag{4.17}$$

$$p_t^g = \sum_{h \in \mathcal{H}} \bar{p}_{t,h}^g,\ \forall t \in \mathcal{T}, g \in \mathcal{G}, \tag{4.18}$$

where $\bar{p}_{t,h}^g$ indicates the generation amount in the segment $h \in \mathcal{H}$.

EV Fleet Operations

In each period $t \in \mathcal{T}$, knowing the power transfer requests v_t^+ and v_t^- from the power grid, the mobility operator schedules x_t^+ and x_t^- EVs to satisfy the requests, respectively, and meanwhile, schedules x_t^{r} EVs to satisfy the realized trip demand d_t. Unsatisfied demands

are lost. Given $\overline{X}$ EVs in total in the fleet, we have

$$x_t^{\mathrm{r}} + x_t^+ + x_t^- \leq \overline{X}, \quad x_t^{\mathrm{r}} \leq d_t, \ \forall t \in \mathcal{T}. \tag{4.19}$$

The discharging and charging amounts in each period are constrained by facility capacities:

$$x_t^+ \leq \overline{X}^+, \ x_t^- \leq \overline{X}^-, \ \forall t \in \mathcal{T}, \tag{4.20}$$

We define a variable s_t to denote the state of charge (SOC) of the EV fleet in each period $t \in \mathcal{T} \cup \{0\}$, where the fleet's initial SOC is given as S_0. When satisfying trip demands, the EV fleet consumes electricity at an amount of e^{r} per period. The EV fleet charges and discharges electricity at amounts of e^- and e^+ per period, respectively. We use δ to denote the time length of a period. Then, the following constraints illustrate the SOC balance between any two consecutive periods:

$$s_t = s_{t-1} + \left(-e^{\mathrm{r}} x_t^{\mathrm{r}} + e^- x_t^- - e^+ x_t^+\right) \delta, \ \forall t \in \mathcal{T}, \tag{4.21}$$

$$s_0 = S_0. \tag{4.22}$$

Clearly, the SOC level s_t is constrained by the EV battery capacity $\overline{S}$:

$$s_t \leq \overline{S}, \ \forall t \in \mathcal{T}. \tag{4.23}$$

When interacting with the mobility operator, the grid operator promises to ensure that the former can maintain a given service level $\alpha \in [0, 1]$, while the latter offers the mobility operator subsidies at a rate C_{sub} per unit of demand to compensate the service level discrepancy (denoted by o_t for each period $t \in \mathcal{T}$) if the mobility operator cannot reach the level α. Thus, we have

$$\frac{x_t^{\mathrm{r}}}{d_t} + o_t = \alpha, \ \forall t \in \mathcal{T}. \tag{4.24}$$

Through this mechanism, the mobility operator will fully satisfy the power transfer requests v_t^+ and v_t^- from the power grid:

$$v_t^+ = x_t^+ e^+ \delta, \ v_t^- = x_t^- e^- \delta, \ \forall t \in \mathcal{T}. \tag{4.25}$$

When the grid receives electricity from the EV fleet in period t, the grid operator pays the mobility operator at a unit price P_t^+. In contrast, when the EV fleet charges from the grid in period t, the mobility operator pays the grid operator at a unit price P_t^-. Note that constraints (4.25) link the number of EVs (e.g., x_t^+) to the power output level (e.g., v_t^+). Similarly, we introduce $v_t^{\mathrm{r}} = x_t^{\mathrm{r}} e^{\mathrm{r}} \delta$ for any $t \in \mathcal{T}$ to represent the power output level needed to satisfy EV trip demands. In addition, we restrict all the variables to be nonnegative:

$$x_t^{\mathrm{r}},\ x_t^+,\ x_t^-,\ s_t \geq 0,\ \forall t \in \mathcal{T}. \tag{4.26}$$

Finally, to keep consistent with the grid operations focusing on power output levels, we can reformulate the above constraints (4.19)–(4.26) as (4.22)–(4.23) and

$$\frac{v_t^{\mathrm{r}}}{e^{\mathrm{r}}\delta} + \frac{v_t^+}{e^+\delta} + \frac{v_t^-}{e^-\delta} \leq \overline{X},\quad \frac{v_t^{\mathrm{r}}}{e^{\mathrm{r}}\delta} \leq d_t,\quad \frac{v_t^+}{e^+\delta} \leq \overline{X}^+,\ \frac{v_t^-}{e^-\delta} \leq \overline{X}^-,\quad \forall t \in \mathcal{T}, \tag{4.27}$$

$$s_t = s_{t-1} - v_t^{\mathrm{r}} + v_t^- - v_t^+,\quad \frac{v_t^{\mathrm{r}}}{e^{\mathrm{r}}\delta d_t} + o_t = \alpha,\quad v_t^{\mathrm{r}} \geq 0,\quad s_t \geq 0,\ \forall t \in \mathcal{T}. \tag{4.28}$$

In the second stage, the power grid operator schedules thermal generators and interacts with the EV fleet to minimize the worst possible cost toward a robust power grid subject to uncertain grid and EV demands and intermittent renewable generation. We assume that there is a finite support for the joint distribution of the uncertain parameters across all the periods and accordingly re-define $\mathcal{S}$ as the set of scenario indices. For each scenario $j \in \mathcal{S}$, we reuse the above notation for the second-stage problem and add a subscript j to each decision variable and random parameter. We use bold symbols to represent vectors. For example, $\boldsymbol{\xi}_j = (p^{\mathrm{w}}_{b,t,j}, p^{\mathrm{s}}_{b,t,j}, q_{b,t,j}, d_{t,j}, \forall b \in \mathcal{B}, t \in \mathcal{T})^\top$ and $\mathbf{v}^+ = (v^+_{t,j}, \forall t \in \mathcal{T}, j \in \mathcal{S})^\top$. Given initial commitment decisions $(\mathbf{u}, \mathbf{y})$ and a scenario index $j \in \mathcal{S}$, $\Psi(\mathbf{u}, \mathbf{y}, \boldsymbol{\xi}_j)$ can be obtained by solving the following optimization problem:

$$\begin{aligned}\Psi(\mathbf{u}, \mathbf{y}, \boldsymbol{\xi}_j) \ = \ \min \ & \sum_{t\in\mathcal{T}} \left(\sum_{g\in\mathcal{G}} \left(f^g_{t,j} + \mathrm{RU}^g r^{g+}_{t,j} + \mathrm{RD}^g r^{g-}_{t,j} \right) + P_t^+ v^+_{t,j} - P_t^- v^-_{t,j} \right) \\ & + C_{\mathrm{sub}} \sum_{t\in\mathcal{T}} o_{t,j} d_{t,j} \\ \text{s.t. } & (4.6) - (4.14),\ (4.16) - (4.18),\ (4.22) - (4.23),\ (4.27) - (4.28).\end{aligned} \tag{$\mathcal{P}$}$$

Now, by introducing an auxiliary variable $z \in \mathbb{R}$, we can reformulate Problem ($\mathcal{M}$) into:

$$\Theta = \min \sum_{g\in\mathcal{G}} \sum_{t=2}^{T} \left(\mathrm{SU}^g u_t^g + \mathrm{SD}^g (y_{t-1}^g - y_t^g + u_t^g)\right) + z \tag{4.29}$$

$$\text{s.t. } (4.1) - (4.5),$$

$$z \geq \sum_{t\in\mathcal{T}} \left(\sum_{g\in\mathcal{G}} \left(f_{t,j}^g + \mathrm{RU}^g r_{t,j}^{g+} + \mathrm{RD}^g r_{t,j}^{g-} \right) + P_t^+ v_{t,j}^+ - P_t^- v_{t,j}^- \right) + C_{\text{sub}} \sum_{t\in\mathcal{T}} o_{t,j} d_{t,j}, \quad \forall j \in \mathcal{S}, \tag{4.30}$$

$$(4.6) - (4.14),\ (4.16) - (4.18),\ (4.22) - (4.23),\ (4.27) - (4.28),\ \forall j \in \mathcal{S}.$$

Constraints (4.30) are robust constraints because they are satisfied with respect to all the scenarios in $\mathcal{S}$. All the variables except z and $f_{t,j}^g$ ($\forall g \in \mathcal{G}, t \in \mathcal{T}, j \in \mathcal{S}$) in the feasible regions of the above model and its linear programming (LP) relaxation are clearly bounded, while the optimal values of z and $f_{t,j}^g$ ($\forall g \in \mathcal{G}, t \in \mathcal{T}, j \in \mathcal{S}$) are bounded because of the minimization objective and constraints (4.30).

4.4 Machine Learning-Driven Optimization

To ensure constraints (4.30) are satisfied for all the scenarios in $\mathcal{S}$, we are specifically concerned about the worst-case scenarios and the scenarios in the support set (see the following definitions).

Definition 1. *Let* $(\mathbf{u}^*, \mathbf{y}^*)$ *denote the optimal first-stage solution of Problem* ($\mathcal{M}$). *Scenario* $j \in \mathcal{S}$ *is a worst-case scenario if* $\Psi(\mathbf{u}^*, \mathbf{y}^*, \boldsymbol{\xi}_j) \geq \Psi(\mathbf{u}^*, \mathbf{y}^*, \boldsymbol{\xi}_{j'})$ *for any* $j' \in \mathcal{S}$.

Definition 2. *Let* $\Theta(\mathcal{S})$ *denote the optimal value of Problem* ($\mathcal{M}$) *when constraints* (4.30) *are satisfied with respect to all the scenarios in* $\mathcal{S}$. *A set* $\mathcal{S}_0 \subseteq \mathcal{S}$ *is a support set if* $\Theta(\mathcal{S}_0) = \Theta(\mathcal{S})$.

Once we have a support set $\mathcal{S}_0$ (preferably in a small size), constraints (4.30) should be satisfied with respect to the scenarios in $\mathcal{S}_0$ only, by which solving Problem ($\mathcal{M}$), i.e., Problem (4.29), becomes more efficient because $\mathcal{S}_0$ may include much fewer scenarios than $\mathcal{S}$. Thus, it would be appealing to have a support set $\mathcal{S}_0$ *before* solving Problem ($\mathcal{M}$). As any support set includes at least one worst-case scenario, we derive a machine learning approach to identify a worst-case scenario in $\mathcal{S}$ and an iterative optimization process

to construct a support set by selecting more scenarios from $\mathcal{S}$, leading to a *machine learning-driven optimization* approach as follows.

First, as the power grid and mobility systems have accumulated extensive data via historical operations, we use historical data to construct various instances of Problem ($\mathcal{M}$) considering various scenario samples in set $\mathcal{S}$. For each given instance of set $\mathcal{S}$, we derive an efficient algorithm in Section 4.4.1 to solve Problem ($\mathcal{M}$) offline and identify a worst-case scenario (note that we generally have a unique worst-case scenario based on the real data), by which we obtain a set of training data for the next step. Second, given offline input instances and output solutions, we perform linear regression to characterize the relationship between the statistical features of the worst-case scenario (i.e., output) and of the scenario samples in $\mathcal{S}$ (i.e., input). Given this linear regression relationship and a new instance of set $\mathcal{S}$, we identify a worst-case scenario j^* in this new set, after which we derive an efficient algorithm in Section 4.4.2 to solve Problem ($\mathcal{M}$) to optimality. Third, to further improve the efficiency of the derived algorithm in the previous step, we derive several families of strong valid inequalities in Section 4.4.3.

4.4.1 Alternating Direction Method of Multipliers for Training

We rewrite Problem ($\mathcal{M}$) in the following abstract form:

$$\Theta = \min_{\mathbf{u},\mathbf{y},z} \Big\{ \mathcal{F}(\mathbf{u},\mathbf{y}) + z \;\Big|\; \mathcal{H}^1(\mathbf{u},\mathbf{y}) \leq \mathbf{0},\ \mathbf{u} \in \{0,1\}^{(|\mathcal{T}|-1)\times|\mathcal{G}|},\ \mathbf{y} \in \{0,1\}^{|\mathcal{T}|\times|\mathcal{G}|};$$
$$\mathcal{H}^2(\mathbf{y}, z, \boldsymbol{\gamma}_j, \boldsymbol{\xi}_j) = \mathbf{0},\ \forall j \in \mathcal{S} \Big\}, \tag{$\mathcal{M}_1$}$$

where $\boldsymbol{\gamma}_j$ denotes all the second-stage variables with respect to scenario $j \in \mathcal{S}$. Specifically, for any $j \in \mathcal{S}$, $\boldsymbol{\gamma}_j = (\mathbf{f}_j,\ \mathbf{p}_j,\ \mathbf{p}'_j,\ \boldsymbol{\beta}_j,\ \mathbf{r}^+_j,\ \mathbf{r}^-_j,\ \mathbf{v}^+_j,\ \mathbf{v}^-_j,\ \mathbf{v}^{\mathrm{r}}_j,\ \mathbf{s}_j,\ \mathbf{o}_j, \boldsymbol{\kappa}_j)^\top$, where $\boldsymbol{\kappa}_j$ denotes slack variables that transform the inequalities into equalities. The inequality $\mathcal{H}^1(\mathbf{u},\mathbf{y}) \leq \mathbf{0}$ represents the first-stage constraints (4.1)–(4.4) and $\mathcal{H}^2(\mathbf{y}, z, \boldsymbol{\gamma}_j, \boldsymbol{\xi}_j) = \mathbf{0}$ represents the second-stage constraints (4.6)–(4.14), (4.16)–(4.18), (4.22)–(4.23), (4.27)–(4.28), and (4.30).

Consider a positive integer $N \leq |\mathcal{S}|$ and $\mathcal{N} = \{1, \ldots, N\}$. We divide $\mathcal{S}$ into N nonempty and disjoint subsets $\mathcal{S}_1, \ldots, \mathcal{S}_N$ such that $\mathcal{S}_n \subseteq \mathcal{S}$ $(n \in \mathcal{N})$ and $\cup_{n=1}^N \mathcal{S}_n = \mathcal{S}$. We further define $\mathbf{u}'_n = \mathbf{u}$, $\mathbf{y}'_n = \mathbf{y}$, and $z_n \in \mathbb{R}$ for any $n \in \mathcal{N}$ and then reformulate

Problem ($\mathcal{M}_1$) as follows:

$$\Theta = \min_{\mathbf{u},\mathbf{y},z} \Big\{ \mathcal{F}(\mathbf{u},\mathbf{y}) + z \;\Big|\; \mathcal{H}^1(\mathbf{u},\mathbf{y}) \le \mathbf{0},\ \mathbf{u} \in \{0,1\}^{(|\mathcal{T}|-1)\times|\mathcal{G}|},\ \mathbf{y} \in \{0,1\}^{|\mathcal{T}|\times|\mathcal{G}|},$$
$$\mathbf{u} = \mathbf{u}'_n,\ \mathbf{y} = \mathbf{y}'_n,\ z \ge z_n,\ \forall n \in \mathcal{N};$$
$$\mathcal{H}^2(\mathbf{y}'_n, z_n, \boldsymbol{\gamma}_j, \boldsymbol{\xi}_j) = \mathbf{0},\ \forall n \in \mathcal{N}, j \in \mathcal{S}_n \Big\}. \qquad (\mathcal{M}_2)$$

Note that the second-stage constraints are now separated in N groups and constraints $\mathbf{u} = \mathbf{u}'_n,\ \mathbf{y} = \mathbf{y}'_n$ $(n \in \mathcal{N})$ link these groups. By relaxing these linkage constraints, we have the augmented function for Problem ($\mathcal{M}_2$), $\mathcal{L}(\mathbf{u},\mathbf{y},z,\mathbf{u}',\mathbf{y}',\boldsymbol{\pi},\boldsymbol{\lambda}) :=$

$$\mathcal{F}(\mathbf{u},\mathbf{y}) + z + \sum_{n=1}^{N} \boldsymbol{\pi}_n^\top (\mathbf{u} - \mathbf{u}'_n) + \sum_{n=1}^{N} \boldsymbol{\lambda}_n^\top (\mathbf{y} - \mathbf{y}'_n) + \frac{\rho_1}{2} \sum_{n=1}^{N} \left\|\mathbf{u} - \mathbf{u}'_n\right\|^2 + \frac{\rho_2}{2} \sum_{n=1}^{N} \left\|\mathbf{y} - \mathbf{y}'_n\right\|^2, \qquad (4.31)$$

where $\boldsymbol{\pi}_n \in \mathbb{R}^{(|\mathcal{T}|-1)\times|\mathcal{G}|},\ \boldsymbol{\lambda}_n \in \mathbb{R}^{|\mathcal{T}|\times|\mathcal{G}|}$ are multiplier vectors, and $\rho_1,\ \rho_2 > 0$ are penalty parameters. We let $\mathbf{u}' = (\mathbf{u}'_n, \forall n \in \mathcal{N})^\top$, $\mathbf{y}' = (\mathbf{y}'_n, \forall n \in \mathcal{N})^\top$, $\boldsymbol{\pi} = (\boldsymbol{\pi}_n, \forall n \in \mathcal{N})^\top$, and $\boldsymbol{\lambda} = (\boldsymbol{\lambda}_n, \forall n \in \mathcal{N})^\top$. Then, we obtain the corresponding augmented Lagrangian problem (ALP) as follows:

$$\min \Big\{ \mathcal{L}(\mathbf{u},\mathbf{y},z,\mathbf{u}',\mathbf{y}',\boldsymbol{\pi},\boldsymbol{\lambda}) \;\Big|\; \mathcal{H}^1(\mathbf{u},\mathbf{y}) \le \mathbf{0},\ \mathbf{u} \in \{0,1\}^{(|\mathcal{T}|-1)\times|\mathcal{G}|},\ \mathbf{y} \in \{0,1\}^{|\mathcal{T}|\times|\mathcal{G}|},$$
$$z \ge z_n,\ \forall n \in \mathcal{N};$$
$$\mathcal{H}^2(\mathbf{y}'_n, z_n, \boldsymbol{\gamma}_j, \boldsymbol{\xi}_j) = \mathbf{0},\ \forall n \in \mathcal{N}, j \in \mathcal{S}_n \Big\}. \qquad \text{(ALP)}$$

To solve Problem (ALP), we apply the alternating direction method of multipliers (ADMM) and decompose Problem (ALP) into two subproblems, which will be solved iteratively toward convergence. The first subproblem is given by fixing $(z,\mathbf{u}',\mathbf{y}',\boldsymbol{\pi},\boldsymbol{\lambda}) = (\overline{z},\overline{\mathbf{u}}',\overline{\mathbf{y}}',\overline{\boldsymbol{\pi}},\overline{\boldsymbol{\lambda}})$:

$$\min \Big\{ \mathcal{L}(\mathbf{u},\mathbf{y},\overline{z},\overline{\mathbf{u}}',\overline{\mathbf{y}}',\overline{\boldsymbol{\pi}},\overline{\boldsymbol{\lambda}}) \;\Big|\; \mathcal{H}^1(\mathbf{u},\mathbf{y}) \le \mathbf{0},\ \mathbf{u} \in \{0,1\}^{(|\mathcal{T}|-1)\times|\mathcal{G}|},\ \mathbf{y} \in \{0,1\}^{|\mathcal{T}|\times|\mathcal{G}|} \Big\}, \qquad \text{(Fsub)}$$

and the second subproblem is given by fixing $(\mathbf{u},\mathbf{y},\boldsymbol{\pi},\boldsymbol{\lambda}) = (\overline{\mathbf{u}},\overline{\mathbf{y}},\overline{\boldsymbol{\pi}},\overline{\boldsymbol{\lambda}})$:

$$\min \Big\{ \mathcal{L}(\overline{\mathbf{u}},\overline{\mathbf{y}},z,\mathbf{u}',\mathbf{y}',\overline{\boldsymbol{\pi}},\overline{\boldsymbol{\lambda}}) \;\Big|\; z \ge z_n,\ \forall n \in \mathcal{N};$$
$$\mathcal{H}^2(\mathbf{y}'_n, z_n, \boldsymbol{\gamma}_j, \boldsymbol{\xi}_j) = \mathbf{0},\ \forall n \in \mathcal{N}, j \in \mathcal{S}_n \Big\}. \qquad \text{(Ssub)}$$

Theorem 4. *Problem* (Fsub) *has the same optimal solution as the following linear pro-*

gram:

$$\min \Bigg\{ \sum_{g\in\mathcal{G}} \sum_{t=2}^{T} \Big(SU^g u_t^g + SD^g \left(y_{t-1}^g - y_t^g + u_t^g \right) \Big) + \sum_{n\in\mathcal{N}} \sum_{g\in\mathcal{G}} \sum_{t=2}^{T} \Big(\overline{\pi}_{n,g,t} u_t^g + \frac{\rho_1}{2} \left(u_t^g - 2\overline{u}_{n,t}^{g\prime} u_t^g \right) \Big) + \sum_{n\in\mathcal{N}} \sum_{g\in\mathcal{G}} \sum_{t\in\mathcal{T}} \Big(\overline{\lambda}_{n,g,t} y_t^g + \frac{\rho_2}{2} \left(y_t^g - 2\overline{y}_{n,t}^{g\prime} y_t^g \right) \Big) \;\Big|\; (4.1)-(4.4) \Bigg\}. \tag{Fsub$_\mathrm{R}$}$$

Theorem 4 shows that Problem (Fsub), an integer program, can be solved as a linear program, which reduces the computational difficulty and facilitates the convergence of the ADMM algorithm. Meanwhile, with $(\mathbf{u}, \mathbf{y}) = (\overline{\mathbf{u}}, \overline{\mathbf{y}})$, Problem (Ssub) is separable with respect to each subset $\mathcal{S}_n$ $(n \in \mathcal{N})$, further reducing the computational difficulty. Specifically, for each $n \in \mathcal{N}$, we define $\mathcal{L}_n(\mathbf{u}, \mathbf{y}, z, \mathbf{u}'_n, \mathbf{y}'_n, \boldsymbol{\pi}_n, \boldsymbol{\lambda}_n) :=$

$$\mathcal{F}(\mathbf{u}, \mathbf{y}) + z + \boldsymbol{\pi}_n^\top \left(\mathbf{u} - \mathbf{u}'_n \right) + \boldsymbol{\lambda}_n^\top \left(\mathbf{y} - \mathbf{y}'_n \right) + \frac{\rho_1}{2} \left\| \mathbf{u} - \mathbf{u}'_n \right\|^2 + \frac{\rho_2}{2} \left\| \mathbf{y} - \mathbf{y}'_n \right\|^2,$$

by which the nth subproblem of Problem (Ssub) can be represented by

$$\min \Big\{ \mathcal{L}_n(\overline{\mathbf{u}}, \overline{\mathbf{y}}, z, \mathbf{u}'_n, \mathbf{y}'_n, \overline{\boldsymbol{\pi}}_n, \overline{\boldsymbol{\lambda}}_n) \;\Big|\; z \geq z_n,\ \mathcal{H}^2(\mathbf{y}'_n, z_n, \boldsymbol{\gamma}_j, \boldsymbol{\xi}_j) = \mathbf{0},\ \forall j \in \mathcal{S}_n \Big\}. \tag{Ssub$_n$}$$

With Problems (Fsub$_\mathrm{R}$) and (Ssub$_n$) $(n \in \mathcal{N})$, we present the details of the ADMM algorithm in Algorithm 3, where we use superscript m to denote the iteration step.

Algorithm 3 ADMM

Input: $\epsilon > 0$, ρ_1, ρ_2, iteration index $m = 0$, initial solutions $(\mathbf{u}^0, \mathbf{y}^0)$, and multipliers $(\boldsymbol{\pi}^0, \boldsymbol{\lambda}^0)$.
Output: Optimal solution $(\mathbf{u}^*, \mathbf{y}^*)$.

1: **do**
2: Set $(\overline{\mathbf{u}}, \overline{\mathbf{y}}, \overline{\boldsymbol{\pi}}_n, \overline{\boldsymbol{\lambda}}_n) = (\mathbf{u}^m, \mathbf{y}^m, \boldsymbol{\pi}_n^m, \boldsymbol{\lambda}_n^m),\ \forall n \in \mathcal{N}$.
3: Solve Problem (Ssub$_n$) to obtain an optimal solution $(z^{m+1}, z_n^{m+1}, \mathbf{u}_n'^{\,m+1}, \mathbf{y}_n'^{\,m+1}, \boldsymbol{\gamma}_j^{m+1}, \forall j \in \mathcal{S}_n)$ for any $n \in \mathcal{N}$.
4: Set $\overline{\mathbf{u}}' = (\mathbf{u}_1'^{\,m+1}, \ldots, \mathbf{u}_N'^{\,m+1})^\top$, $\overline{\mathbf{y}}' = (\mathbf{y}_1'^{\,m+1}, \ldots, \mathbf{y}_N'^{\,m+1})^\top$, and $\overline{z} = \max\{z_1^{m+1}, \ldots, z_N^{m+1}\}$.
5: Solve Problem (Fsub$_\mathrm{R}$) to obtain an optimal solution $(\mathbf{u}^{m+1}, \mathbf{y}^{m+1})$.
6: Set $\boldsymbol{\pi}_n^{m+1} = \boldsymbol{\pi}_n^m + \rho_1(\mathbf{u}^{m+1} - \mathbf{u}_n'^{\,m+1})$ and $\boldsymbol{\lambda}_n^{m+1} = \boldsymbol{\lambda}_n^m + \rho_2(\mathbf{y}^{m+1} - \mathbf{y}_n'^{\,m+1})$ for any $n \in \mathcal{N}$.
7: Set $m = m + 1$.
8: **while** $\sum_{n=1}^{N} (\|\mathbf{u}^m - \mathbf{u}_n'^{\,m}\|^2 + \|\mathbf{y}^m - \mathbf{y}_n'^{\,m}\|^2) > \epsilon$.

Algorithm 3 generates a set of sequences: $\{(\mathbf{u}^m, \mathbf{y}^m),\ \forall m\}$ and $\{(\mathbf{u}_n'^{\,m}, \mathbf{y}_n'^{\,m}),\ \forall m\}$ for any $n \in \mathcal{N}$. Note that we can always set the upper bound of z to be a sufficiently large but finite value while not changing the optimal solution and value of Problem ($\mathcal{M}$). That is, we can consider the feasible region of Problem (ALP)'s LP relaxation is bounded. We have the following proposition holds.

Proposition 6. *If* $\sum_{m=1}^{\infty}\sum_{n=1}^{N}\|\boldsymbol{\pi}_n^{m+1}-\boldsymbol{\pi}_n^{m}\|^2<\infty$ *and* $\sum_{m=1}^{\infty}\sum_{n=1}^{N}\|\boldsymbol{\lambda}_n^{m+1}-\boldsymbol{\lambda}_n^{m}\|^2<\infty$, *then*

$$\left\|\mathbf{u}^m-\mathbf{u}^{m+1}\right\|^2\to 0,\ \left\|\mathbf{y}^m-\mathbf{y}^{m+1}\right\|^2\to 0,\quad as\ m\to\infty,$$
$$\left\|\mathbf{u}_n'^{\,m}-\mathbf{u}_n'^{\,m+1}\right\|^2\to 0,\ \left\|\mathbf{y}_n'^{\,m}-\mathbf{y}_n'^{\,m+1}\right\|^2\to 0,\ as\ m\to\infty,\ \forall n\in\mathcal{N}.$$

Let $\mathbf{e}_{\mathrm{u}}=(1,\ldots,1)^\top\in\mathbb{R}^{(|\mathcal{T}|-1)|\mathcal{G}|}$, $\mathbf{e}_{\mathrm{y}}=(1,\ldots,1)^\top\in\mathbb{R}^{|\mathcal{T}||\mathcal{G}|}$, $\mathcal{H}^{\mathrm{y}}(\mathbf{y},z,\boldsymbol{\gamma}_j,\boldsymbol{\xi}_j)=\mathbf{0}$ represent the second-stage constraints involving $\mathbf{y}$, i.e., (4.7)–(4.9), (4.11), and (4.16), $M_1=\sum_{g\in\mathcal{G}}(2|\mathcal{T}|-L^g-\ell^g)+2(|\mathcal{T}|-1)|\mathcal{G}|$ representing the number of constraints (4.2)–(4.4), and $M_2=4|\mathcal{T}||\mathcal{G}|-2|\mathcal{G}|+|\mathcal{T}||\mathcal{B}|$ representing the number of constraints represented by $\mathcal{H}^{\mathrm{y}}(\mathbf{y},z,\boldsymbol{\gamma}_j,\boldsymbol{\xi}_j)=\mathbf{0}$. Let $(\mathbf{u}^*,\mathbf{y}^*,\boldsymbol{\pi}^*,\boldsymbol{\lambda}^*)$ denote any accumulation point of sequence $\{(\mathbf{u}^m,\mathbf{y}^m,\boldsymbol{\pi}^m,\boldsymbol{\lambda}^m),\ \forall m\}$ generated by Algorithm 3. We show that $(\mathbf{u}^*,\mathbf{y}^*)$ satisfies certain conditions in the following theorem.

Theorem 5. *Assume* $\sum_{m=1}^{\infty}\sum_{n=1}^{N}\|\boldsymbol{\pi}_n^{m+1}-\boldsymbol{\pi}_n^{m}\|^2<\infty$, $\sum_{m=1}^{\infty}\sum_{n=1}^{N}\|\boldsymbol{\lambda}_n^{m+1}-\boldsymbol{\lambda}_n^{m}\|^2<\infty$, $\{(\boldsymbol{\pi}_n^m,\boldsymbol{\lambda}_n^m),\ \forall m\}$ *is bounded for any* $n\in\mathcal{N}$, *and the objective value of the dual problem of Problem* (Ssub$_n$) *for any* $n\in\mathcal{N}$ *is bounded. Then, there exist* $\boldsymbol{\theta}_{n,j}^*\in\mathbb{R}^{M_2}$ $(\forall n\in\mathcal{N},j\in\mathcal{S}_n)$ *and* $\boldsymbol{\eta}^*\in\mathbb{R}_+^{M_1}$ *such that*

$$\bigtriangledown_{\mathbf{u}}\mathcal{F}\left(\mathbf{u}^*,\mathbf{y}^*\right)+\frac{N\rho_1}{2}\left(\mathbf{e}_{\mathrm{u}}-2\mathbf{u}^*\right)+\left(\bigtriangledown_{\mathbf{u}}\mathcal{H}^1\left(\mathbf{u}^*,\mathbf{y}^*\right)\right)^\top\boldsymbol{\eta}^*=\mathbf{0},\tag{4.32}$$

$$\bigtriangledown_{\mathbf{y}}\mathcal{F}\left(\mathbf{u}^*,\mathbf{y}^*\right)+\frac{N\rho_2}{2}\left(\mathbf{e}_{\mathrm{y}}-2\mathbf{y}^*\right)+\left(\bigtriangledown_{\mathbf{y}}\mathcal{H}^1\left(\mathbf{u}^*,\mathbf{y}^*\right)\right)^\top\boldsymbol{\eta}^*+\mathcal{Q}^\top\sum_{n=1}^{N}\sum_{j\in\mathcal{S}_n}\boldsymbol{\theta}_{n,j}^*=\mathbf{0},\tag{4.33}$$

$$\boldsymbol{\eta}^*\odot\mathcal{H}^1\left(\mathbf{u}^*,\mathbf{y}^*\right)=\mathbf{0},\tag{4.34}$$

where $\mathcal{Q}:=\bigtriangledown_{\mathbf{y}_n'}\mathcal{H}^{\mathrm{y}}(\mathbf{y}_n',z_n,\boldsymbol{\gamma}_j,\boldsymbol{\xi}_j)$ *for any* $n\in\mathcal{N}$ *and* $j\in\mathcal{S}_n$ *and* $\odot$ *denotes the Hadamard product.*

4.4.2 Machine Learning for Optimality

For each instance of Problem ($\mathcal{M}$) solved by Algorithm 3 offline, we use $\mathbf{x}_{\mathrm{in}}\in\mathbb{R}^{d_{\mathrm{in}}}$ to denote the statistical information (e.g., expectation and standard deviation) of all the scenarios in $\mathcal{S}$ and $\mathbf{y}_{\mathrm{out}}\in\mathbb{R}^{d_{\mathrm{out}}}$ the statistical information of an obtained worst-case scenario, where d_{in} and d_{out} are appropriate dimensions. Thus, for any instance $n(=1,2,\ldots)$ of Problem ($\mathcal{M}$) with set $\mathcal{S}^n$, we collect a training data set $\{(\mathbf{x}_{\mathrm{in}}^n,\mathbf{y}_{\mathrm{out}}^n),\forall n=1,2,\ldots\}$, by which we construct a linear regression model $\mathbf{y}_{\mathrm{out}}=\mathbf{c}^\top\mathbf{x}_{\mathrm{in}}$. Given this

model and a new instance with the scenario information $\tilde{\mathbf{x}}_{\text{in}} \in \mathbb{R}^{d_{\text{in}}}$ of $\mathcal{S}$, we predict the information $\tilde{\mathbf{y}}_{\text{out}} \in \mathbb{R}^{d_{\text{out}}}$ of a worst-case scenario. By computing the statistical information of each scenario $j \in \mathcal{S}$ (denoted by $\tilde{\mathbf{y}}^j_{\text{out}} \in \mathbb{R}^{d_{\text{out}}}$), we identify this worst-case scenario $j^* = \arg\min_{j \in \tilde{\mathcal{S}}}(\sum_{i=1}^{d_{\text{out}}} |\tilde{y}^{j,i}_{\text{out}} - \tilde{y}^i_{\text{out}}|/\tilde{y}^i_{\text{out}})$, i.e., the scenario with information closest to our prediction.

With the above new instance of set $\mathcal{S}$ and the identified worst-case scenario j^*, we derive Algorithm 4 to solve Problem ($\mathcal{M}$). Algorithm 4 reuses the definition of $\boldsymbol{\gamma}_j$ for any $j \in \mathcal{S}$ in Section 4.4.1. The following theorem shows that Algorithm 4 iteratively improves the lower bound for Problem ($\mathcal{M}$) until converging to the optimal solution.

Algorithm 4 Machine Learning-Driven Optimization

Input: Scenario sample set $\mathcal{S}$, worst-case scenario j^*, and iteration index $m = 1$.
Output: Optimal solution $(\mathbf{u}^*, \mathbf{y}^*)$ and the optimal value Θ.

Set $\mathcal{S}^{\text{w}}_m = \{j^*\}$ and $\mathcal{S}^{\text{nw}}_m = \mathcal{S} \setminus \{j^*\}$.
Solve Problem ($\mathcal{M}$) with sample set $\mathcal{S}^{\text{w}}_m$ to obtain optimal solution $(\mathbf{u}^m, \mathbf{y}^m, \boldsymbol{\gamma}^m_j, \forall j \in \mathcal{S}^{\text{w}}_m)$ and the optimal value $\overline{\Theta}^m$.
Solve Problem ($\mathcal{P}$) with $(\mathbf{u}, \mathbf{y}) = (\mathbf{u}^m, \mathbf{y}^m)$ and ξ_j for any $j \in \mathcal{S}^{\text{nw}}_m$ to obtain the optimal value $\Psi(\mathbf{u}^m, \mathbf{y}^m, \boldsymbol{\xi}_j)$ and optimal solution $\boldsymbol{\gamma}^m_j$ for any $j \in \mathcal{S}^{\text{nw}}_m$.
Set $\mathcal{S}^{\text{f}}_m = \{j \in \mathcal{S}^{\text{nw}}_m \mid \mathcal{F}(\mathbf{u}^m, \mathbf{y}^m) + \Psi(\mathbf{u}^m, \mathbf{y}^m, \boldsymbol{\xi}_j) > \overline{\Theta}^m\}$.
while $\mathcal{S}^{\text{f}}_m \neq \emptyset$ **do**
    Randomly select a scenario $j^{\text{f}}_m \in \mathcal{S}^{\text{f}}_m$ and set $\mathcal{S}^{\text{nw}}_{m+1} = \mathcal{S}^{\text{nw}}_m \setminus \{j^{\text{f}}_m\}$ and $\mathcal{S}^{\text{w}}_{m+1} = \mathcal{S}^{\text{w}}_m \cup \{j^{\text{f}}_m\}$.
    Solve Problem ($\mathcal{M}$) with sample set $\mathcal{S}^{\text{w}}_{m+1}$ to obtain optimal solution $(\mathbf{u}^{m+1}, \mathbf{y}^{m+1}, \boldsymbol{\gamma}^{m+1}_j, \forall j \in \mathcal{S}^{\text{w}}_{m+1})$ and the optimal value $\overline{\Theta}^{m+1}$.
    Solve Problem ($\mathcal{P}$) with $(\mathbf{u}, \mathbf{y}) = (\mathbf{u}^{m+1}, \mathbf{y}^{m+1})$ and ξ_j for any $j \in \mathcal{S}^{\text{nw}}_{m+1}$ to obtain the optimal value $\Psi(\mathbf{u}^{m+1}, \mathbf{y}^{m+1}, \boldsymbol{\xi}_j)$ and optimal solution $\boldsymbol{\gamma}^{m+1}_j$for any $j \in \mathcal{S}^{\text{nw}}_{m+1}$.
    Set $\mathcal{S}^{\text{f}}_{m+1} = \{j \in \mathcal{S}^{\text{nw}}_{m+1} \mid \mathcal{F}(\mathbf{u}^{m+1}, \mathbf{y}^{m+1}) + \Psi(\mathbf{u}^{m+1}, \mathbf{y}^{m+1}, \boldsymbol{\xi}_j) > \overline{\Theta}^{m+1}\}$.
    Set $m = m + 1$.
end while
$(\mathbf{u}^*, \mathbf{y}^*) = (\mathbf{u}^m, \mathbf{y}^m)$ and $\Theta = \overline{\Theta}^m$.

Theorem 6. *For Algorithm 4, we have (i)* $\Theta \geq \overline{\Theta}^n \geq \overline{\Theta}^m$ *for any iteration* $n > m \geq 1$ *and (ii) when the algorithm terminates, the obtained solution* $(\mathbf{u}^*, \mathbf{y}^*)$ *is optimal to Problem* ($\mathcal{M}$).

At each step m, Algorithm 4 iteratively selects a scenario j^{f}_m from $\mathcal{S}^{\text{f}}_m$, a subset of $\mathcal{S}^{\text{nw}}_m$ such that $\mathcal{F}(\mathbf{u}^m, \mathbf{y}^m) + \Psi(\mathbf{u}^m, \mathbf{y}^m, \boldsymbol{\xi}_j) > \overline{\Theta}^m$. This condition helps collect enough scenarios to construct a support set efficiently and obtain an optimal solution of Problem ($\mathcal{M}$) correspondingly. Clearly, we can naively select a scenario j^{f}_m directly from $\mathcal{S}^{\text{nw}}_m$ (i.e., *naive selection*), while the size of this set can be much larger than that of $\mathcal{S}^{\text{f}}_m$ and hence the algorithmic convergence will be delayed. Meanwhile, at step m, because $\mathcal{S}^{\text{nw}}_m \setminus \mathcal{S}^{\text{f}}_m$ may also include a scenario in the support set that we will eventually have when

the algorithm terminates, we can strategically select a scenario from either $\mathcal{S}_m^{\mathrm{f}}$ or $\mathcal{S}_m^{\mathrm{nw}}$. However, making such a *strategic selection* between $\mathcal{S}_m^{\mathrm{f}}$ and $\mathcal{S}_m^{\mathrm{nw}}$ is difficult because we have limited information to determine which set contains a higher proportion of scenarios in the support set. Thus, we select a scenario j_m^{f} from $\mathcal{S}_m^{\mathrm{f}}$ consistently at each step.

Note that a practical and large-scale instance of Problem ($\mathcal{M}$) may satisfy certain conditions to help analyze the properties of the above *naive selection* and *strategic selection*. Specifically, we assume that Problem ($\mathcal{M}$) has a unique minimum support set $\mathcal{S}^*$ that has the smallest size among all the support sets, with $|\mathcal{S}^*| = K$. Hence, any support set contains $\mathcal{S}^*$. We also assume that (i) Problem ($\mathcal{M}$) with $\mathcal{S}$ has a unique optimal solution or (ii) Problem ($\mathcal{M}$) with $\mathcal{S}$ and Problem ($\mathcal{M}$) with any support set share the same set of optimal solutions. Thus, at each step m of Algorithm 4, we have the following two observations: (i) The size of $\mathcal{S}_m^{\mathrm{nw}}$ becomes $|\mathcal{S}| - m$ and hence at most $K/(|\mathcal{S}| - m)$ of the scenarios in $\mathcal{S}_m^{\mathrm{nw}}$ are from $\mathcal{S}^*$; (ii) The set $\mathcal{S}_m^{\mathrm{f}}$ contains at least one scenario from $\mathcal{S}^*$ and hence at least $1/|\mathcal{S}_m^{\mathrm{f}}|$ of the scenarios in $\mathcal{S}_m^{\mathrm{f}}$ are from $\mathcal{S}^*$. We then update the *strategic selection* as follows: At each step m of Algorithm 4, we randomly select a scenario from $\mathcal{S}_m^{\mathrm{f}}$ if $1/|\mathcal{S}_m^{\mathrm{f}}| \geq K/(|\mathcal{S}| - m)$ and from $\mathcal{S}_m^{\mathrm{nw}}$ otherwise. The following two results hold accordingly.

Lemma 1. *Algorithm 4 is expected to terminate after* $1 + (K-1)|\mathcal{S}|/K$ *steps if it adopts naive selection and there exists a unique worst-case scenario.*

Theorem 7. *Algorithm 4 is expected to terminate in fewer steps by adopting strategic selection than naive selection.*

Lemma 1 and Theorem 7 provide structural results on the expected number of steps for Algorithm 4 to terminate. Lemma 1 indicates that naive selection may not be efficient, though the algorithm is more efficient when K is smaller. Theorem 7 suggests that it is better to adopt strategic selection when we have some information on the minimum support set of Problem ($\mathcal{M}$). Note that determining the exact value of K can be challenging in practice, while an upper bound for K can be provided (Anderson and Zachary 2023), facilitating the application of strategic selection.

It's important to highlight that our proposed machine learning-driven optimization approach, i.e., Algorithm 4, exhibits general applicability across a wide range of stochastic problems. For example, Algorithm 4 is applicable for solving the target-oriented model

for robust optimization in the framework of robust satisficing, which is proposed by Long et al. (2023). We formulate the robust satisficing variant of Problem ($\mathcal{M}$) and introduce how to use Algorithm 4 to solve it in Section 4.6 and leave it for future study.

4.4.3 Strong Valid Inequalities for Efficiency

Algorithm 4 needs to solve Problem ($\mathcal{M}$) with the sample set $\mathcal{S}_m^{\mathrm{w}}$, which is an MILP and can be computationally challenging, at each step m. To improve the efficiency of solving the MILP, we derive several families of strong valid inequalities to tighten the linear relaxation of Problem (4.29). On the one hand, a tighter linear relaxation can often improve computational efficiency by reducing the amount of enumeration required to find and prove an optimal solution (Knueven et al. 2020). On the other hand, the derived inequalities can be used as cutting planes in the branch-and-cut framework to improve the computational efficiency (Wolsey and Nemhauser 1999).

We study the properties of an individual generator's feasible region, as strong valid inequalities for the physical constraints of each individual generator are valid for Problem (4.29) and can be used to tighten its linear relaxation. Thus, we drop the superscript g and subscript j here and consider the following set of physical constraints:

$$
\begin{aligned}
\mathcal{D} := \Big\{ & \left(\mathbf{p}, \mathbf{r}^+, \mathbf{r}^-, \mathbf{y}, \mathbf{u}\right) \in \mathbb{R}^T \times \mathbb{R}^T \times \mathbb{R}^T \times \{0,1\}^T \times \{0,1\}^{T-1} : \\
& \textstyle\sum_{s=t-L+1}^{t} u_s \leq y_t, \ \forall t \in [L+1, T]_{\mathbb{Z}}, && \text{(4.35a)} \\
& \textstyle\sum_{s=t-\ell+1}^{t} u_s \leq 1 - y_{t-\ell}, \ \forall t \in [\ell+1, T]_{\mathbb{Z}}, && \text{(4.35b)} \\
& -y_{t-1} + y_t - u_t \leq 0, \ \forall t \in \mathcal{T} \setminus \{1\}, && \text{(4.35c)} \\
& p_t - r_t^- \geq 0, \ \forall t \in \mathcal{T}, && \text{(4.35d)} \\
& p_t + r_t^+ \leq \left(\overline{C} - \underline{C}\right) y_t, \ \forall t \in \mathcal{T}, && \text{(4.35e)} \\
& \left(p_t + \underline{C} y_t + r_t^+\right) - \left(p_{t-1} + \underline{C} y_{t-1}\right) \leq V y_{t-1} + \overline{V}(1 - y_{t-1}), \ \forall t \in \mathcal{T} \setminus \{1\}, && \text{(4.35f)} \\
& \left(p_{t-1} + \underline{C} y_{t-1}\right) - \left(p_t + \underline{C} y_t - r_t^-\right) \leq V y_t + \overline{V}(1 - y_t), \ \forall t \in \mathcal{T} \setminus \{1\}, && \text{(4.35g)} \\
& p_t, \ r_t^+, \ r_t^- \geq 0, \ \forall t \in \mathcal{T} \Big\}. && \text{(4.35h)}
\end{aligned}
$$

We use $\mathrm{conv}(\mathcal{D})$ to denote the convex hull of $\mathcal{D}$. Clearly, a valid inequality for the polytope $\mathrm{conv}(\mathcal{D})$ is also valid for Problem (4.29) for any generator g in any scenario j. Hence, the strong valid inequalities developed for $\mathrm{conv}(\mathcal{D})$ can be used to tighten the formulation of Problem (4.29). We let $\sum_{t=a}^{b} p_t = \sum_{t=a}^{b} r_t^+ = \sum_{t=a}^{b} r_t^- = \sum_{t=a}^{b} y_t =$

$\sum_{t=a}^{b} u_t = 0$ if $a > b$ and $\varsigma = \lfloor (\overline{C} - \overline{V})/V \rfloor \geq 0$. The following lemmas provide some preliminary results that entail polyhedral properties of $\mathcal{D}$.

Lemma 2. *For any $k \in [1, L]_{\mathbb{Z}}$ and $t \in [k+1, T]_{\mathbb{Z}}$, we have $\sum_{s=t-k+1}^{t} u_s \leq y_t$.*

Lemma 3. *For any $k \in [1, \ell]_{\mathbb{Z}}$ and $t \in [k+1, T]_{\mathbb{Z}}$, we have $\sum_{s=t-k+1}^{t} u_s \leq 1 - y_{t-k}$.*

Lemmas 2 and 3 generalize the minimum-up and minimum-down constraints (4.35a) and (4.35b), respectively. They state that (i) a generator starts up at most once within an operational horizon up to L periods and (ii) if a generator is currently online, then it does not start up within the subsequent operational horizon up to ℓ periods. Thus, the following corollary holds.

Corollary 1. *For any $t \in [2, T]_{\mathbb{Z}}$, we have $y_t \geq u_t$, $y_{t-1} + u_t \leq 1$, and $y_t \geq \sum_{s=\max\{2, t-L+1\}}^{t} u_s$.*

Lemma 4. *For any $t \in [2, T]_{\mathbb{Z}}$, we have $p_t - p_{t-1} \leq V$.*

Lemma 4 shows that a generator's generation increment between any two consecutive periods is bounded by V regardless of this generator's online/offline status. With the above lemmas, we first present a family of strong valid inequalities that provide an upper bound on the total amount of generation regulation-up and regulation-down $r_t^+ + r_t^-$ for each period t.

Proposition 7. *For any $t \in [3, T]_{\mathbb{Z}}$, the inequality*

$$r_t^+ + r_t^- \leq \left(\overline{V} - \underline{C}\right) y_t + V \left(y_t - u_t\right) + \left(\underline{C} + V - \overline{V}\right) \left(y_{t-1} - u_{t-1}\right) \tag{4.36}$$

is valid for $\mathrm{conv}(\mathcal{D})$. Furthermore, it is facet-defining for $\mathrm{conv}(\mathcal{D})$ when $L = 1$ and $\overline{C} - \underline{C} > 2V$.

Inequality (4.36) links the generation regulation-up r_t^+ and regulation-down r_t^- that are not considered simultaneously in a single constraint in $\mathcal{D}$. Nevertheless, the inequality in the following proposition explicitly tightens the existing constraints (4.35e) in $\mathcal{D}$.

Proposition 8. *For each $k \in [1, \min\{L, \varsigma + 1\}]_{\mathbb{Z}}$ and $t \in [k+1, T]_{\mathbb{Z}}$, the inequality*

$$p_t + r_t^+ \leq \left(\overline{C} - \underline{C}\right) y_t - \sum_{s=0}^{k-1} \left(\overline{C} - \overline{V} - sV\right) u_{t-s} \tag{4.37}$$

is valid for $\mathrm{conv}(\mathcal{D})$. Furthermore, it is facet-defining for $\mathrm{conv}(\mathcal{D})$ when one of the following two conditions holds: (i) $L = 1$ and (ii) $k = L = 2$ and $\overline{V} + V \leq \overline{C} \leq \overline{V} + 2V$.

Inequality (4.37) is tighter than (4.35e) because $\sum_{s=0}^{k-1}(\overline{C}-\overline{V}-sV)u_{t-s} \geq 0$ and hence the right-hand side of (4.37) is not larger than that of (4.35e). The following proposition provides a family of strong valid inequalities to bound the potential generation increment from period $t-k$ to period t.

Proposition 9. *For each $t \in [2,T]_{\mathbb{Z}}$ and $k \in [1, \min\{t-1, \varsigma\}]_{\mathbb{Z}}$, the inequality*

$$p_t + r_t^+ - p_{t-k} \leq kVy_t - \sum_{s=0}^{\min\{L,k\}-1} \left(\underline{C} + (k-s)V - \overline{V}\right) u_{t-s} \tag{4.38}$$

is valid for $\operatorname{conv}(\mathcal{D})$. *Furthermore, it is facet-defining for* $\operatorname{conv}(\mathcal{D})$ *when* $L = 1$.

Finally, we derive a family of strong valid inequalities in the following proposition to bound the potential generation decrement from period $t-k$ to period t, while considering both the generation regulation-up r_{t-k}^+ and regulation-down r_t^-.

Proposition 10. *For each $k \in [1, \min\{T-2, \varsigma\}]_{\mathbb{Z}}$ and $t \in [k+2, T]_{\mathbb{Z}}$, the inequality*

$$\begin{aligned} p_{t-k} + r_{t-k}^+ - p_t + r_t^- \leq{}& \left(\overline{V} - \underline{C}\right) y_{t-k} + 2V\left(y_{t-k} - \sum_{s=\max\{2,t-k-L+1\}}^{t-k} u_s\right) \\ &+ \sum_{i=1}^{k-1} V\left(y_{t-i} - \sum_{s=\max\{2,t-i-L+1\}}^{t-i} u_s\right) + (\underline{C} + V - \overline{V})\left(y_t - \sum_{s=\max\{2,t-L+1\}}^{t} u_s\right) \\ &+ \sum_{s=\max\{2,t-k-L+1\}}^{t-k-1} (t-k-s)Vu_s \end{aligned} \tag{4.39}$$

is valid for $\operatorname{conv}(\mathcal{D})$.

4.5 Numerical Experiments

We conduct numerical experiments using real data in New York City (NYC) from January 1, 2020 to June 30, 2022 to demonstrate the daily operations of a GVI system, with each period representing one hour and hence $T = 24$. We first introduce parameter settings and then validate our proposed algorithms and obtain managerial insights via various experiments.

4.5.1 Parameter Settings

First, we introduce the power grid setting. As NYC includes five subdivisions (i.e., Staten Island, Manhattan, Bronx, Brooklyn, and Queens), we consider a 5-bus power grid with each bus representing a subdivision (see Figure 4.2), i.e., $\mathcal{B} = \{1, 2, \ldots, 5\}$.

We have collected daily power demand (load) data in NYC from New York Independent System Operator (NYISO). Note that nuclear power plants (e.g., R. E. Ginna Nuclear Power Plant and Nine Mile Point Nuclear Station) and hydroelectric generators (e.g., Robert Moses Niagara Hydroelectric Power Station) are always online near NYC to serve the base load (EIA 2023). These power generators, with a capacity larger than $5,000$MW, run in 7×24h. Thus, we operate the power grid to satisfy only the peak load (i.e., the total load minus the base load). Specifically, we set 99% of the minimum load during each day as its base load. Thus, we hereafter use the term "load" to denote the peak load. In each period, we set the load at each subdivision (bus) as the total load multiplying this subdivision's GDP portion over the entire NYC's GDP (see Figure 4.3).

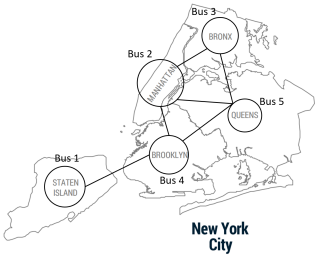

Figure 4.2. 5-Bus Power Grid in NYC

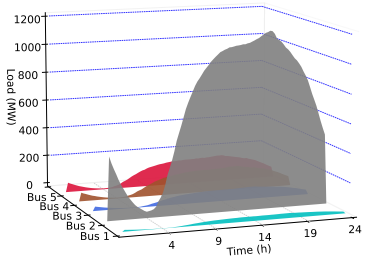

Figure 4.3. Power Load

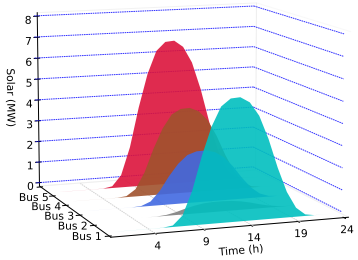

Figure 4.4. Solar Generation

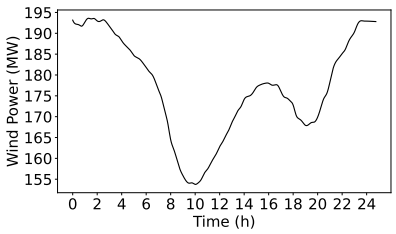

Figure 4.5. Wind Generation

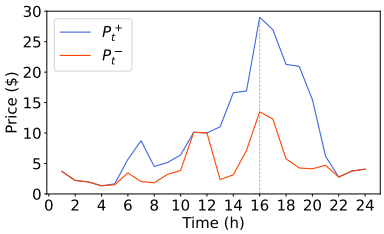

Figure 4.6. Power Price

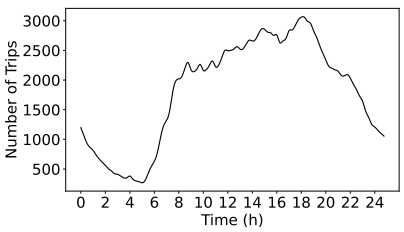

Figure 4.7. EV Trip Demands

We have also collected daily wind and solar power generation data from NYISO and Pennsylvania–New Jersey–Maryland Interconnection (PJM)[2], respectively. As the wind power is mainly produced by offshore wind farms (NYSERDA 2023), we assume that in each period $t \in \mathcal{T}$, each bus $b \in \mathcal{B}$ in Figure 4.2 contributes the same amount of wind power and shares 1/5 of the total wind power (see Figure 4.5), i.e., $p^{\mathrm{w}}_{b_1,t} = p^{\mathrm{w}}_{b_2,t}$

[2]Website: https://www.pjm.com/

for any $b_1, b_2 \in \mathcal{B}$. In addition, the PJM data provides the daily solar generation data in the Mid-Atlantic region, where the installed solar capacity is around $8,222.6$MW in 2020. As NY Solar Map (2023) provides the installed solar capacities in each subdivision (bus) of NYC, we set $p^{\mathrm{s}}_{b,t}$ as the total solar generation in period t divided by $8,222.6$ and multiplying the installed solar capacity in bus b (see Figure 4.4).

As shared mobility systems can serve as regulation-up/-down reserves for the power grid to help balance power supply and demand, we collect hourly market clearing prices of regulation-up/-down energy from the Electric Reliability Council of Texas (ERCOT)[3] to set the electricity purchasing/selling prices P^+_t/P^-_t. Specifically, we set P^+_t (resp. P^-_t) as the price of regulation-up (resp. regulation-down) reserve in each period $t \in \mathcal{T}$ (see Figure 4.6). In addition, ten thermal generators operating in NYC are considered to serve the 5-bus power grid, and we collect their physical parameters from EIA (2023) (see details in Appendix C.16).

Second, we introduce the EV fleet setting. We estimate EV trip demand d_t using the taxi trip demands from the NYC Taxi and Limousine Commission (TLC). As the NYC Department of Transportation (NYC DOT 2019) shows that 56% of all vehicles crossing into the CBD are private, and we assume that the remaining 44% are taxis, which are all promoted to be electrical in the near future for societal sustainability. Thus, we set d_t as the current taxi demands divided by 44% in each period $t \in \mathcal{T}$ (see Figure 4.7). We further set relevant cost parameters in USD: the unit rental price $C_{\mathrm{r}} = 12$ following the rental price of Zipcar (Zhang et al. 2021) and the penalty cost $C_{\mathrm{p}} = 12$ and the unit subsidy $C_{\mathrm{sub}} = C_{\mathrm{r}} + C_{\mathrm{p}} = 24$ for an unsatisfied trip demand. In addition, the number of allocated EVs $\overline{X} = 221,180$, and the corresponding charging/discharging facility capacity[4] upper bounds $\overline{X}^+ = \overline{X}^- = 20\% \times \overline{X}$. We set the EV fleet's battery capacity $\overline{S} = 22,118$MWh and initial SOC $S_0 = 50\% \times \overline{S}$. We also set $e^{\mathrm{r}} = 15$kW, $e^- = 170$kW, and $e^+ = 6$kW for each EV's electricity consumption, charging, and discharging rates[5], respectively. We set

[3]Website: https://www.ercot.com/

[4]Report (NY DMV 2018) suggests that there are 221,180 registered private vehicles in Manhattan. In addition, Qi et al. (2022) show that vehicle-share trip demands in Manhattan dominate in the city. Thus, we assume the total number of EVs is 221,180. Qi et al. (2022) show that charge and discharge plots account for 40% of all parking plots. We assume each EV has a parking plot and amounts of charge and discharge plots are equal, each of which thus accounts for 20% of total allocations.

[5]Most popular EVs (e.g., Tesla Model X and Volkswagen ID.6) equip a battery with a capacity ranging from 80kWh to 100kWh. Because the EV industry is developing quickly, we set each EV's battery capacity to be 100kWh, i.e., 0.1MWh. Several BYD EV models can easily keep a charging rate of 170kW and a discharging rate of 6kW. Tesla Model X 100D with a 100 kWh battery drives 295 miles in ideal condition, and the speed in urban areas generally is 30mph. Thus, the ideal average EV's

service level $\alpha = 0.97$ to ensure the EV fleet's profitability and the power grid's flexibility (see Appendix C.19 for details).

Therefore, we collect 912 data samples from January 1, 2020, to June 30, 2022, with each day representing a sample. For the random parameters $(\mathbf{p}^{\mathrm{w}}, \mathbf{p}^{\mathrm{s}}, \mathbf{q})$ in the power system (resp. $\mathbf{d}$ in the mobility system), we use $\mathcal{S}^{\mathrm{G}}$ (resp. $\mathcal{S}^{\mathrm{EV}}$) to collect all the relevant data samples we have. We use each data sample $(\mathbf{p}^{\mathrm{w}}, \mathbf{p}^{\mathrm{s}}, \mathbf{q}, \mathbf{d})$ to represent a single scenario in $\mathcal{S}$. We divide all these data samples into four groups: Group 1 (for constructing the linear regression model), Group 2 (for computational performance demonstration), Group 3 (for in-sample tests), and Group 4 (for out-of-sample tests). We randomly select 200 data samples from January 1, 2020 to July 31, 2021 (578 days) to construct Group 2, 60 data samples from January 1, 2020 to July 31, 2021 to construct Group 3, and 60 data samples from August 1, 2021 to Jun 30, 2022 (334 days) to construct Group 4. All the remaining 616 data samples go to Group 1.

Third, we introduce our computational setting. We perform all the experiments on a computing node with a 2.3-GHz Intel Xeon E5-2670 processor and a 64GB of memory using CPLEX 12.10 with C++ API under default settings as the optimization solver. We use the data in Group 1 to construct our linear regression model $\mathbf{y}_{\mathrm{out}} = \mathbf{c}^{\top}\mathbf{x}_{\mathrm{in}}$ introduced in Section 4.4.2 (see Appendix C.17 for the detailed setting), the data in Group 2 to show the computational performance of our proposed solution approaches (see Section 4.5.2), the data in Group 3 to compute the first-stage solution $(\mathbf{u}, \mathbf{y})$ by solving Problem $(\mathcal{M})$, and the data in Group 4 to perform out-of-sample tests by solving Problem $(\mathcal{P})$ with the above given $(\mathbf{u}, \mathbf{y})$ to obtain managerial insights.

4.5.2 Computational Performance

We demonstrate the computational efficiency of our proposed solution approaches, i.e., Algorithm 3 (ADMM) in Section 4.4.1 and Algorithm 4 (Machine Learning-Driven Optimization) in Section 4.4.2, for solving Problem $(\mathcal{M})$ by comparing them with benchmarks. Our derived strong valid inequalities in Section 4.4.3 are applied in Algorithm 4 to improve the solution process.

We perform experiments under various scenario sizes. Specifically, with the data in

electricity consumption rate is 100kWh / (295miles / 30mph) $\approx$ 10.2kW. Note that the ideal condition is rare to meet in practice. We hence consider a slightly larger electricity consumption rate in the trip at 15kW.

Group 2, we have 200 data samples from both $\mathcal{S}^{\mathrm{G}}$ and $\mathcal{S}^{\mathrm{EV}}$. We create an augmented scenario set $\mathcal{S}$ by defining $\mathcal{S} := \mathcal{S}^{\mathrm{G}} \times \mathcal{S}^{\mathrm{EV}} = \{(j^{\mathrm{G}}, j^{\mathrm{EV}}) \mid j^{\mathrm{G}} \in \mathcal{S}^{\mathrm{G}}, j^{\mathrm{EV}} \in \mathcal{S}^{\mathrm{EV}}\}$, leading to $40,000$ scenarios in $\mathcal{S}$ in total. By randomly selecting samples from $\mathcal{S}^{\mathrm{G}}$ and $\mathcal{S}^{\mathrm{EV}}$ (i.e., varying $|\mathcal{S}^{\mathrm{G}}|$ and $|\mathcal{S}^{\mathrm{EV}}|$) to create such an augmented set $\mathcal{S}$, we consider various instances of Problem ($\mathcal{M}$) with $\mathcal{S}$, with $|\mathcal{S}|$ ranging from 10 to $5,000$. For each computational run, the time limit is set as two hours when $|\mathcal{S}| < 5,000$ and three hours when $|\mathcal{S}| = 5,000$. We report the total cost, computational time in seconds, and optimality gap for each approach with respect to each instance.

First, we compare Algorithm 3 with the CPLEX solver under default settings, i.e., "ADMM" and "CPLEX" in Table 4.1. The CPLEX solver reports the terminating gap, i.e., "MIP Gap (%)," defined by the relative gap between the best lower and upper bounds. For each instance solved by the ADMM approach, we define

$$\text{ADMM Gap (\%)} = \frac{(\text{the cost by "ADMM"}) - (\text{the cost by "CPLEX"})}{(\text{the cost by "ADMM"})} \times 100\%.$$

As the ADMM does not return an optimal solution of Problem ($\mathcal{M}$) in general, we set $\epsilon = 0.001$ in Algorithm 3 to ensure a feasible $(\mathbf{u}^*, \mathbf{y}^*)$ to Problem ($\mathcal{M}$) is returned for each instance. Given $(\mathbf{u}^*, \mathbf{y}^*)$, we solve Problem ($\mathcal{M}$) to report its upper bound. Table 4.1 shows that the CPLEX approach solves all the instances to the optimality when $|\mathcal{S}| \leq 1,000$ (see Appendix C.18 for the results with small and medium instances). Our ADMM approach solves all these instances and returns the ADMM Gap within 0.9%, while it takes a much shorter computational time than the CPLEX. When $|\mathcal{S}| \geq 2,000$, the CPLEX cannot solve any instances to the optimality within the time limit and returns average terminating gaps at 69.093% ($|\mathcal{S}| = 2,000$) and 270.617% ($|\mathcal{S}| = 5,000$). In contrast, our ADMM approach solves all the instances within around one hour (resp. two hours) with an ADMM Gap at -1.095% (resp. -1.658%) when $|\mathcal{S}| = 2,000$ (resp. $|\mathcal{S}| = 5,000$). As the CPLEX does not obtain an optimal solution of Problem ($\mathcal{M}$) for these large instances, the ADMM Gap becomes negative, indicating that the upper bound obtained by the CPLEX is worse than that from the ADMM. Therefore, our ADMM approach can provide high-quality solutions very efficiently, which are further used as the training instances for our machine learning model.

Second, we demonstrate the effectiveness of machine learning in solving Problem ($\mathcal{M}$) by comparing the following three approaches: (i) the ADMM approach based on the

Table 4.1. Computational Performance of CPLEX and ADMM

$\|\mathcal{S}\|$	$\|\mathcal{S}^{\mathrm{G}}\|$	$\|\mathcal{S}^{\mathrm{EV}}\|$	CPLEX			ADMM		
			Cost ($)	**MIP Gap (%)**	**Time (s)**	**Cost ($)**	**ADMM Gap (%)**	**Time (s)**
500	50	10	453,343	0.009	852.7	457,903	0.990	635.7
	25	20	428,342	0	782.7	430,446	0.489	265.3
	20	25	428,342	0	788.8	430,900	0.594	215.8
	10	50	412,853	0.004	1,405.4	414,844	0.480	304.1
	Average		430,720	0.003	957.4	433,523	**0.638**	**355.2**
1,000	50	20	453,343	0.003	2,515.8	458,002	1.017	1,898.4
	40	25	453,307	0.007	2,185.7	458,253	1.079	1,179.8
	25	40	428,884	0	2,956.5	431,062	0.505	504.7
	20	50	428,884	0	2,563.3	432,364	0.805	1,028.6
	Average		441,105	0.003	2,555.4	444,920	**0.852**	**1,152.9**
2,000	100	20	498,508	270.617	7,200	492,608	-1.198	5,592.5
	50	40	463,498	2.226	7,200	458,556	-1.078	3,201.0
	40	50	453,307	0.019	7,200	458,279	1.085	2,275.2
	20	100	444,375	3.509	7,200	430,639	-3.190	5,469.7
	Average		464,922	69.093	7,200	460,021	**-1.095**	**4,134.6**
5,000	200	25	498,508	270.617	10,800	488,173	-2.073	7,950.0
	100	50	498,508	270.617	10,800	492,316	-1.242	8,503.6
	50	100	-	-	10,800	457,875	-	4,373.8
	25	200	-	-	10,800	430,808	-	9,770.6
	Average		498,508	270.617	10,800	467,293	**-1.658**	**7,649.5**
Average	-	-	458,814	84.929	5378.2	451,439	**-0.316**	**3323.05**

aforementioned setting; (ii) "Random Algorithm:" We adopt Algorithm 4 except that the input scenario j^* is a scenario *randomly* selected from $\mathcal{S}$, instead of the worst-case scenario returned by our machine learning model; (iii) "Learning Algorithm:" We adopt Algorithm 4 with a refinement applied to the scenario selection from $\mathcal{S}_m^{\mathrm{f}}$ (see line 6 in Algorithm 4) based on the construction of $\mathcal{S}$ as follows. At step m in Algorithm 4, the Learning Algorithm approach randomly selects a subset of scenarios $\mathcal{S}_m^{\mathrm{f}\,\prime}$ (instead of a single scenario) from $\mathcal{S}_m^{\mathrm{f}}$ such that (i) for any $j = (j^{\mathrm{G}}, j^{\mathrm{EV}}) \in \mathcal{S}_m^{\mathrm{f}}$, there exists and only exists one scenario $(j^{\mathrm{G}}, j^{\mathrm{EV}\prime}) \in \mathcal{S}_m^{\mathrm{f}\,\prime}$, and (ii) for any $j_n = (j_n^{\mathrm{G}}, j_n^{\mathrm{EV}}) \in \mathcal{S}_m^{\mathrm{f}\,\prime}$ and $j_l = (j_l^{\mathrm{G}}, j_l^{\mathrm{EV}}) \in \mathcal{S}_m^{\mathrm{f}\,\prime}$ with $j_n \neq j_l$, we have $j_n^{\mathrm{G}} \neq j_l^{\mathrm{G}}$. Such a refinement helps select more diversified scenarios from $\mathcal{S}_m^{\mathrm{f}}$ and reduce computational time significantly.

For the Random Algorithm and Learning Algorithm approaches, we report their performance when (i) only the initial scenario j^* is considered in Problem ($\mathcal{M}$) and (ii) the algorithm terminates. For case (i) (resp. case (ii)), we report the optimal value of Problem ($\mathcal{M}$), labeled "Initial Cost" (resp. "Final Cost"), terminating optimality gap, labeled "Initial Gap" (resp. "Final Gap"), and computational time, labeled "Initial Time" (resp. "Final Time"). Specifically, for each instance solved by each of the two approaches, we define

$$\text{Initial Gap (\%)} = \frac{(\text{"Initial Cost" by the given approach}) - (\text{the cost by "CPLEX"})}{(\text{"Initial Cost" by the given approach})} \times 100\%,$$

$$\text{Final Gap (\%)} = \frac{(\text{"Final Cost" by the given approach}) - (\text{the cost by "CPLEX"})}{(\text{"Final Cost" by the given approach})} \times 100\%.$$

Table 4.2 shows that when $|\mathcal{S}| \leq 1,000$, both the Random Algorithm and Learning Algorithm approaches solve all the instances to have a Final Gap within 0.01%, i.e., solved to the optimality under the CPLEX's optimality criteria. This result validates Theorem 6. When $|\mathcal{S}| \leq 2,000$, the Random Algorithm approach outperforms the ADMM approach because the former terminates with a better Final Gap and a shorter computational time, whereas the former performs worse when $|\mathcal{S}| = 5,000$ because too many scenarios added to Problem ($\mathcal{M}$) leads to a challenging solution process. The Learning Algorithm approach can find a lower bound with an Initial Gap at -1.573% for the optimal cost within 0.5 seconds on average and *solve any of the instances within* 34 *seconds on average using only around* 1% *of the computational time* by the above two approaches. The reasons are twofold. (i) Our machine learning model provides Algorithm 4 with an input scenario j^* that is very close to (even same as) a worst-case scenario of Problem ($\mathcal{M}$) (see Definition 1). (ii) With a good input scenario j^*, Algorithm 4 quickly finds enough (while not many) scenarios to construct a support set of Problem ($\mathcal{M}$) (see Definition 2). As a result, the value of Initial Cost is close to that of Final Cost and the computational time is very short, demonstrating *the value of machine learning*. In the following sections, we apply the Learning Algorithm approach to support the GVI system operations and obtain managerial insights via out-of-sample experiments.

Table 4.2. Computatinal Performance of Solution Approaches

$\|\mathcal{S}\|$	$\|\mathcal{S}^{\mathrm{G}}\|$	$\|\mathcal{S}^{\mathrm{EV}}\|$	ADMM			Random Algorithm						Learning Algorithm					
			Cost ($)	ADMM Gap (%)	Time (s)	Initial Cost ($)	Final Cost ($)	Initial Gap (%)	Final Gap (%)	Initial Time (s)	Final Time (s)	Initial Cost ($)	Final Cost ($)	Initial Gap (%)	Final Gap (%)	Initial Time (s)	Final Time (s)
500	50	10	457,903	0.990	635.7	411,803	453,343	-10.087	0	0.5	40.8	453,260	453,343	-0.018	0	0.6	9.4
	25	20	430,446	0.489	265.3	152,873	428,342	-180.195	0	0.8	393.2	428,321	428,342	-0.005	0	0.4	6.2
	20	25	430,900	0.594	215.8	402,154	428,342	-6.512	0	0.4	75.8	428,321	428,342	-0.005	0	0.4	7.3
	10	50	414,844	0.480	304.1	320,923	412,866	-28.646	0.003	0.9	583.2	412,173	412,866	-0.165	0.003	0.4	7.5
	Average		433,523	0.638	355.2	321,938	430,723	-56.360	0.001	0.7	273.2	430,519	430,723	**-0.048**	**0.001**	**0.4**	**7.6**
1,000	50	20	458,002	1.017	1,898.4	72,004	453,343	-529.610	0	1.3	1,769.1	453,260	453,343	-0.018	0	0.6	14.6
	40	25	458,253	1.079	1,179.8	317,065	453,307	-42.970	0	0.9	979.7	453,260	453,307	-0.010	0	0.6	12
	25	40	431,062	0.505	504.7	200,639	428,884	-113.759	0	0.5	772.8	428,321	428,884	-0.131	0	0.4	11.2
	20	50	432,364	0.805	1,028.6	314,202	428,884	-36.499	0	0.5	483.8	428,321	428,884	-0.131	0	0.4	11.1
	Average		444,920	0.852	1,152.9	225,977	441,105	-180.710	0	0.8	1,001.3	440,791	441,105	**-0.073**	**0**	**0.5**	**12.3**
2,000	100	20	492,608	-1.198	5,592.5	180,407	483,802	-176.324	-3.040	30.8	5,706.2	482,184	483,802	-3.385	-3.040	0.6	57.7
	50	40	458,556	-1.078	3,201.0	173,545	453,343	-167.077	-2.240	0.6	3,315.2	453,260	453,343	-2.259	-2.240	0.5	24.4
	40	50	458,279	1.085	2,275.2	317,065	453,307	-42.970	0	0.8	3,803.8	453,260	453,307	-0.010	0	0.6	22.4
	20	100	430,639	-3.190	5,469.7	302,429	428,884	-46.935	-3.612	0.4	2,800.1	428,321	428,884	-3.748	-3.612	0.4	21.5
	Average		460,021	-1.095	4,134.6	243,362	454,834	-108.326	-2.223	8.1	3,906.3	454,256	454,834	**-2.351**	**-2.223**	**0.5**	**31.5**
5,000	200	25	488,173	-2.073	7,950.0	348,969	-	-42.852	-	1.9	10,800	478,185	481,807	-4.250	-3.466	0.6	128.0
	100	50	492,316	-1.242	8,503.6	166,492	-	-199.419	-	1.4	10,800	482,184	483,802	-3.385	-3.040	0.7	93.4
	50	100	457,875	-	4,373.8	424,276	453,343	-	-	0.6	1,185.6	453,260	453,343	-	-	0.8	61.6
	25	200	430,808	-	9,770.6	201,116	-	-	-	0.5	10,800	428,321	428,884	-	-	0.5	55.9
	Average		467,293	-1.658	7,649.5	285,213	453,343	-121.135	-	1.1	7,856.4	460,488	461,959	**-3.818**	**-3.253**	**0.7**	**84.7**
Average	-	-	451,439	-0.316	3323.05	269,123	445,001	-116.633	-	2.7	3,259.3	446,514	447,155	**-1.573**	**-1.369**	**0.5**	**34.0**

4.5.3 Impact of V2G

We examine the impact of V2G on the system performance under the parameter settings in Section 4.5.1 by considering two strategies: (i) No V2G, i.e., Problem ($\mathcal{M}$) with $\mathbf{v}^+ = \mathbf{0}$, and (ii) V2G, i.e., Problem ($\mathcal{M}$). First, we study how the V2G technology affects the initial generator commitment decisions $(\mathbf{u}, \mathbf{y})$ (see Figure 4.8). We observe

that online generators are prepared in the morning with low power and mobility demands when V2G is adopted. Thus, the EV fleet saves more electricity into its batteries in the morning, which further feeds back to the power grid via V2G in the afternoon with high power demands, by which two fewer generators are online compared to the case of No V2G. As a result, the average online periods of each online generator when V2G is adopted (i.e., 16.8) is larger than the case of No V2G (i.e., 15.3), indicating a more stable grid operation because frequent generator start-up/shut-down may cause reliability issues in the power grid. Meanwhile, online generators start up later in the morning (e.g., $t = 9, \ldots, 12$) and shut down earlier in the afternoon (e.g., $t = 21, \ldots, 24$), by which the power generation cost is reduced when V2G is adopted. That is, *V2G ensures a more stable and cost-effective power grid operation with fewer online generators*. It follows that fewer carbon emissions are produced and more generators are standing by to address potential contingencies (e.g., natural disasters).

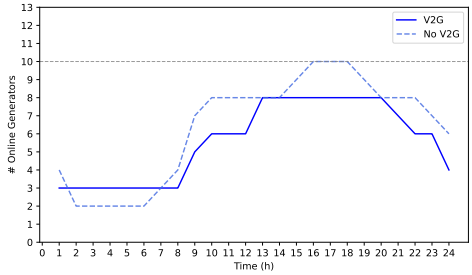

Figure 4.8. Total Number of Online Generators

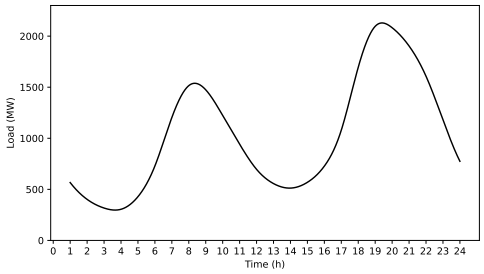

Figure 4.9. Bimodal Power Load

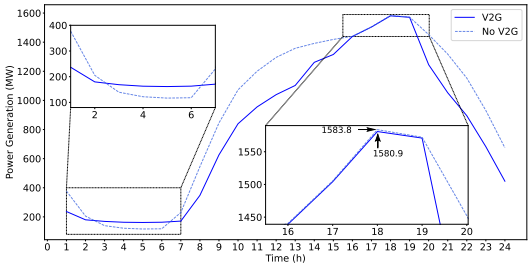

(a) All Samples

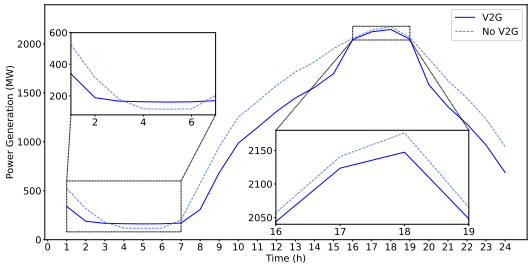

(b) High-power-load Samples

Figure 4.10. Power Generation

Second, we study how the V2G technology affects the subsequent generator dispatch and interactions $(\mathbf{p}, \mathbf{v}^+, \mathbf{v}^-)$ with the EV fleet. We investigate the out-of-sample performance over all the samples (see Figure 4.10(a)) and the three high-power-load samples $(j_i^{\mathrm{G}}, j_0^{\mathrm{EV}}) \in \mathcal{S}$ for $i \in [1, 3]_{\mathbb{Z}}$ (see Figure 4.10(b)), where j_1^{G}, j_2^{G}, and j_3^{G} have the highest average power loads in $\mathcal{S}^{\mathrm{G}}$ and j_0^{EV} is randomly selected from $\mathcal{S}^{\mathrm{EV}}$. During the *valley*

hours (i.e., low-power-load periods $t = 2, \ldots, 6$), we observe larger and more stable generations when V2G is adopted than the case of No V2G, leading to *valley-filling effect* driven explicitly by the following two factors. (i) Excess EVs can charge from the power grid because EV trip demands are low (see Figure 4.7) and the electricity purchase prices (P_t^-) are also low during the valley hours (see Figure 4.6), thereby saving enough electricity in the batteries to satisfy future trip demands or return back to the power grid. (ii) The power loads during the valley hours fluctuate significantly (see Figure 4.3) and hence require power generators to start up and shut down frequently, thereby increasing operational cost and causing potential reliability issues; that is, stable operations benefit the power grid.

During the *peak hours* (i.e., high-power-load periods $t = 16, \ldots, 19$), we observe smaller and more stable generations when V2G is adopted than the case of No V2G, leading to *peak-shaving effect*, even for the high-power-load samples (see Figure 4.10(b)). Specifically, excess EVs can discharge to the power grid through V2G, by which the latter turns on fewer thermal generators to satisfy the power loads, thereby saving the operational cost and increasing the system flexibility. Note that the peak-shaving effect is not as significant as the valley-filling effect due to the following two reasons. (i) The power transfer prices (P_t^+) for V2G are very high during the peak hours (see Figure 4.6), leading to a high cost when electricity is discharged from EVs. (ii) EV trip demands remain high during these hours (see Figure 4.7), limiting the number of EVs available for discharging. Thus, the grid operator purchases necessary electricity only towards turning on as a fewer number of generators as possible (see Figure 4.8). Note that power generation is also reduced by the V2G adoption during the other periods (i.e., $t = 7, \ldots, 15$ and $t = 20, \ldots, 24$), thereby enhancing the power grid's stability and reducing the operational cost.

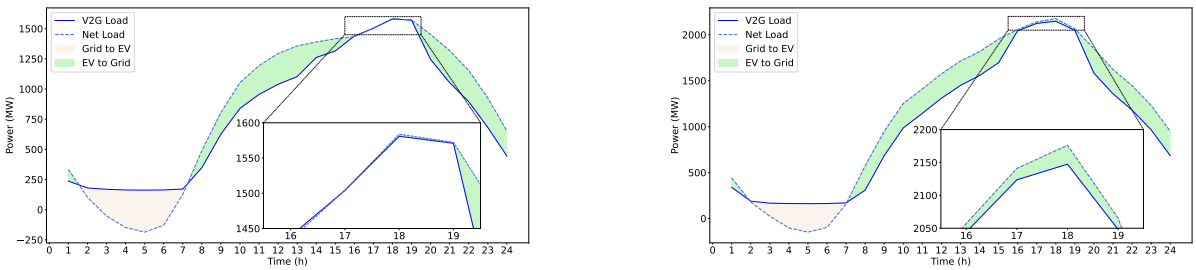

(a) All Samples **(b)** High-power-load Samples

Figure 4.11. Power Transfer

Third, we study the temporal features of power transfer $(\mathbf{v}^+, \mathbf{v}^-)$ when V2G is adopted. For each period $t \in \mathcal{T}$, we define Net Load $= \sum_{b\in\mathcal{B}}(q_{b,t} - p^{\mathrm{w}}_{b,t} - p^{\mathrm{s}}_{b,t})$ and V2G Load $=$ Net Load $+ v^-_t - v^+_t$; that is, the electric power is transferred from the power grid to the EV fleet when V2G Load $>$ Net Load and vice versa. Figure 4.11 shows power transfers from the power grid to the EV fleet during the valley hours and reverse power transfers during the non-valley hours, echoing the aforementioned valley-filling and peak-shaving effects. It follows the V2G Load is flatter than the Net Load, demonstrating the more stable power generation in Figure 4.10.

Finally, we study the V2G's potential to improve societal sustainability by reducing carbon emissions. We compute the emissions in each period $t \in \mathcal{T}$ (denoted by CE^1_t and CE^0_t for the cases of V2G and No V2G, respectively) by multiplying 0.433 by the total power generation in t (i.e., $\sum_{g\in\mathcal{G}}(p^g_t + \underline{C}^g y^g_t)$), which is a common formula proposed by EPA (2023). For each period $t \in \mathcal{T}$, we define *Emissions Reduction per Period (%)* $= (\mathrm{CE}^0_t - \mathrm{CE}^1_t)/\mathrm{CE}^0_t \times 100\%$ and *Cum. Emissions Reduction (%)* $= \sum_{i=1}^{t}\left(\mathrm{CE}^0_i - \mathrm{CE}^1_i\right) / \sum_{i=1}^{T}\mathrm{CE}^0_i \times 100\%$. Figure 4.12 shows that the V2G helps reduce carbon emissions by 21.66% by the end of the day (see the red lines), while the amount of reduced carbon emissions over the high-power-load samples (i.e., 2,647.04tons) is higher than over all the samples (i.e., 2,069.99tons). In addition, the carbon emissions are increased during the valley hours due to the valley-filling effect (see the blue bars), while significant carbon emissions are reduced during the non-valley and non-peak hours.

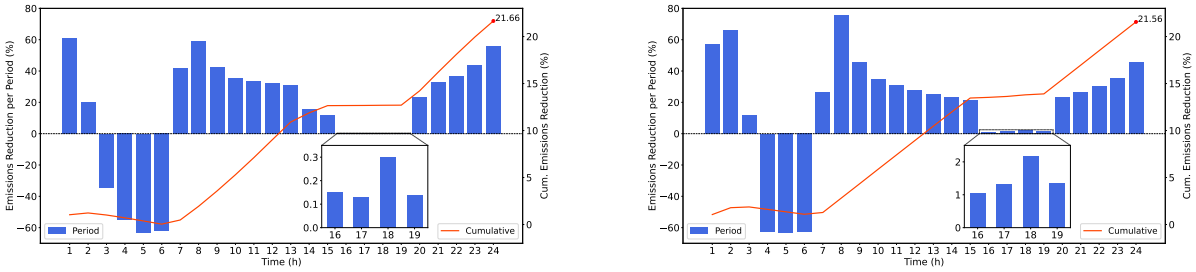

(a) All Samples **(b)** High-power-load Samples

Figure 4.12. Carbon Emission Reduction

4.5.4 Impact of Temporal Power Load Pattern

While the power load in NYC shows a unimodal pattern (see Figure 4.3), we observe a bimodal pattern in California. Thus, we examine the impact of temporal load pattern in this section. We have collected 180 data samples from California Independent System

Operator (CAISO)[6] from January 1, 2021, to March 31, 2021, and from January 1, 2022, to March 31, 2022, with each day representing a sample (scenario) of power load. We denote these samples from early to late by $\mathbf{q}'_1, \ldots, \mathbf{q}'_{180}$, where $\mathbf{q}'_j = (q'_{t,j}, \forall t \in \mathcal{T})^\top$ for any $j \in [1, 180]_{\mathbb{Z}}$. Note that the data samples of the NYC power load ($\mathbf{q}$) introduced in Section 4.5.1 are on a different scale from $\mathbf{q}'$ here. To see impacts caused only by the load pattern, we process the bimodal load samples ($\mathbf{q}'$) so that they are on the same scale as the unimodal load samples ($\mathbf{q}$). Specifically, we consider the new bimodal load samples $\tilde{\mathbf{q}}'$ as follows:

$$\tilde{q}'_{t,j} = q'_{t,j} \times \frac{\frac{1}{|\mathcal{S}^{\mathrm{G}}||\mathcal{T}|} \sum_{k \in \mathcal{S}^{\mathrm{G}}} \sum_{t \in \mathcal{T}} \sum_{b \in \mathcal{B}} q_{b,t,k}}{\frac{1}{180|\mathcal{T}|} \sum_{k=1}^{180} \sum_{t \in \mathcal{T}} q'_{t,k}}, \ \forall t \in \mathcal{T}, j \in [1, 180]_{\mathbb{Z}}.$$

Figure 4.9 shows $\tilde{\mathbf{q}}'$ averaged over all data samples. Following the parameter settings in Section 4.5.1, in each period $t \in \mathcal{T}$ and scenario $j \in [1, 180]_{\mathbb{Z}}$, we set the bimodal load at each subdivision (bus) as the total load ($\tilde{q}'_{t,j}$) multiplying this subdivision's GDP portion over the entire NYC's GDP. Meanwhile, we randomly select 60 samples from $\tilde{\mathbf{q}}'_1, \ldots, \tilde{\mathbf{q}}'_{90}$ (resp. $\tilde{\mathbf{q}}'_{91}, \ldots, \tilde{\mathbf{q}}'_{180}$) and combine them with the 60 data samples ($\mathbf{p}^{\mathrm{w}}, \mathbf{p}^{\mathrm{s}}, \mathbf{d}$) in Group 3 (resp. Group 4) in Section 4.5.1 to form a new data group for in-sample (resp. out-of-sample) tests under the bimodal load pattern.

First, we investigate power transfers under the bimodal load pattern. Figure 4.13 shows the valley-filling and peak-shaving effects under the bimodal pattern too. Specifically, the EV fleet charges significantly more power at noon than in the morning. The reasons are twofold. (i) The power load at noon fluctuates larger than in the morning, requiring more power to "fill" the valley. (ii) The EV trip and power demands during the second peak hours are higher than those during the first; hence, the EV fleet needs to first charge and prepare more power before the second peak comes and then return the power back to the power grid during the second peak hours.

Second, we compare the GVI system's operational efficiency and sustainability under the unimodal and bimodal patterns. We define the proportion of electricity consumption satisfied by *green power* (i.e., solar, wind, and EVs) as

$$\text{greenness}(\%) = \frac{\sum_{t \in \mathcal{T}} \left(\sum_{b \in \mathcal{B}} q_{b,t} + v^{\mathrm{r}}_t \right) - \sum_{t \in \mathcal{T}} \sum_{g \in \mathcal{G}} (p^g_t + \underline{C}^g y^g_t)}{\sum_{t \in \mathcal{T}} \left(\sum_{b \in \mathcal{B}} q_{b,t} + v^{\mathrm{r}}_t \right)} \times 100\%,$$

where the denominator calculates the total electricity consumption by the EV trip and

[6] Website: https://www.caiso.com/

power demands and the numerator calculates the electricity consumption satisfied by green power. A greenness value of 100% indicates the so-called *carbon neutrality*. Under each load pattern, we investigate the following three measures: (i) *#Online Generator Reduction (%)* $= \sum_{t\in\mathcal{T}}\sum_{g\in\mathcal{G}}(y_t^g$ with No V2G$-y_t^g$ with V2G$)/(\sum_{t\in\mathcal{T}}\sum_{g\in\mathcal{G}} y_t^g$ with No V2G$)\times$ 100%; (ii) *Cum. Emissions Reduction* defined in Section 4.5.3; (iii) *Greenness Improvement (%)* = (greenness with V2G$-$greenness with No V2G)/(greenness with No V2G)$\times$ 100%. Table 4.3 shows the following two insights. (i) The V2G technology reduces slightly more online generators under the bimodal pattern. This is because V2G reduces the number of online generators mainly during peak hours (see Figure 4.8) and the bimodal load has more peak hours than the unimodal load. (ii) V2G reduces carbon emissions and improves greenness more under the bimodal pattern than under the unimodal pattern. This is because the EV fleet stores electricity during the valley hours and returns it back to the power grid via V2G during the peak hours. With two valley hours, the bimodal pattern offers an additional opportunity for the EV fleet to perform the power transfers, thereby expanding the EV fleet's storage turnover rounds and enhancing its charging flexibility.

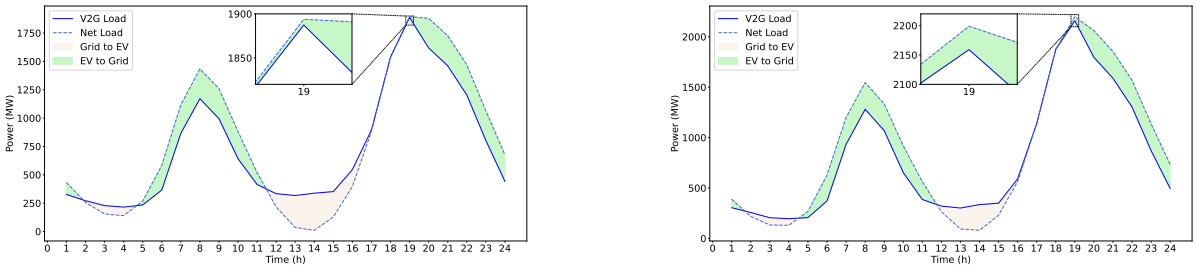

(a) All Samples **(b)** High-power-load Samples

Figure 4.13. Power Transfer under Bimodal Load Pattern

Table 4.3. Impact of Temporal Power Load Pattern

Load Pattern	#Online Generator Reduction	Cum. Emissions Reduction	Greenness Improvement
Unimodal	12.41%	21.66%	37.81%
Bimodal	12.79%	26.50%	49.17%

4.5.5 Toward Carbon Neutrality

Motivated by the significant potential of V2G in improving the greenness in Section 4.5.4, we examine the conditions under which the GVI system achieves carbon neutrality, i.e.,

greenness = 100%. Specifically, we consider the impacts of the renewable share (i.e., $(\sum_{b\in\mathcal{B}}\sum_{t\in\mathcal{T}} p^{\mathrm{w}}_{b,t} + p^{\mathrm{s}}_{b,t})/\sum_{b\in\mathcal{B}}\sum_{t\in\mathcal{T}} q_{b,t} \times 100\%$) and EV fleet size (i.e., $\overline{X}$) when V2G is adopted.

Figure 4.14 shows an increase in greenness with a higher renewable share or EV fleet size, while the increasing rate diminishes as these two parameters become larger. While achieving carbon neutrality by simply increasing the renewable share and EV fleet size is challenging, *a high level of greenness can be achieved easily*. For instance, a greenness of 0.72 can be achieved when the EV fleet size is 10^6 and the renewable share reaches 100% under the unimodal power load pattern (or 80% under the bimodal pattern). We also estimate the costs associated with various levels of greenness and find that achieving carbon neutrality incurs an extremely high cost (see Appendix C.20 for the details). This highlights the considerable challenge in achieving carbon neutrality.

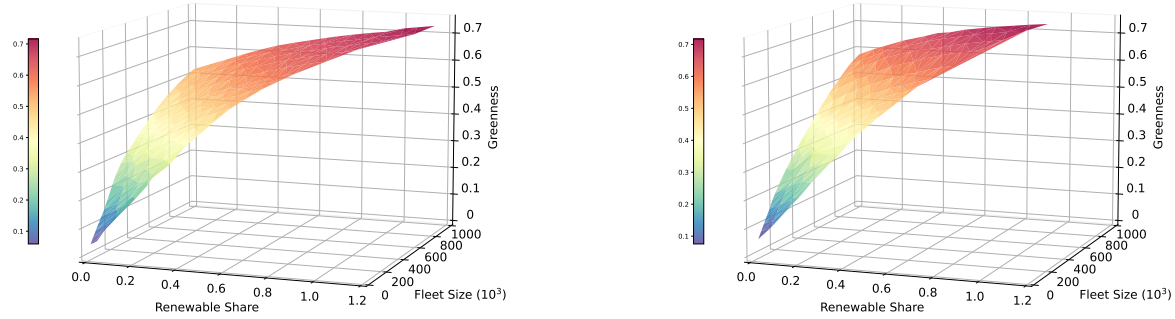

(a) Unimodal Power Load Pattern **(b)** Bimodal Power Load Pattern

Figure 4.14. Impacts of The Renewable Share and EV Fleet Size on Greenness

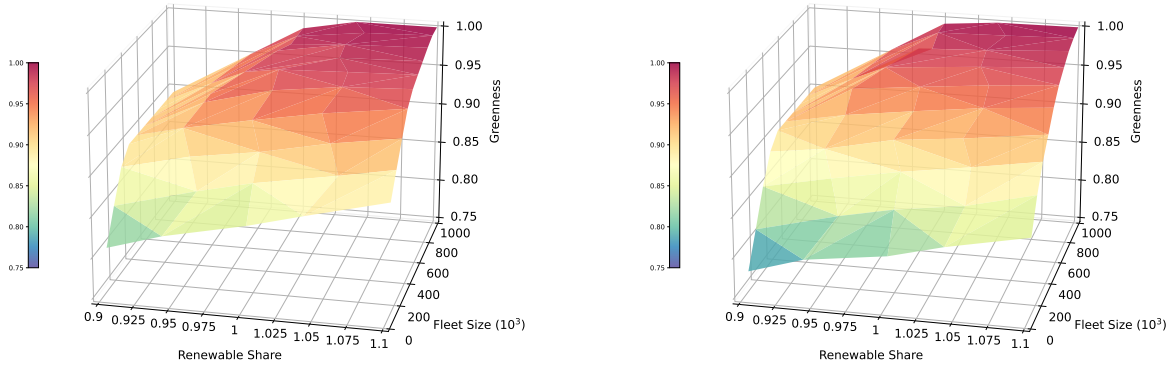

(a) Unimodal Power Load Pattern **(b)** Bimodal Power Load Pattern

Figure 4.15. Carbon Neutrality

To examine the condition of carbon neutrality, we consider a variant of Problem ($\mathcal{M}$) as follows. (i) We consider $|\mathcal{S}| = 1$, i.e., a deterministic case; (ii) The objective function

is to minimize the total generation contributed by all the thermal generators, where we exclude regulation reserves (i.e., $\mathbf{r}^- = \mathbf{r}^+ = \mathbf{R}^- = \mathbf{R}^+ = 0$), as carbon neutrality implies zero such power generation. (iii) We set the initial SOC of EVs as 0 (i.e., $S_0 = 0$), i.e., relying on solar and wind only as the energy sources. Thus, Problem ($\mathcal{M}$) can be rewritten as

$$\min \Bigg\{ \sum_{t\in\mathcal{T}} \sum_{g\in\mathcal{G}} (p_t^g + \underline{C}^g y_t^g) \;\Bigg|\; (4.1)-(4.14), (4.16)-(4.18), (4.22)-(4.23), (4.27)-(4.28), \\ r_t^{g-} = r_t^{g+} = 0,\ \forall t \in \mathcal{T}, g \in \mathcal{G} \Bigg\}.$$

Solving the above Problem ($\mathcal{M}$), we illustrate the results in Figure 4.15. We observe that carbon neutrality can be achieved when the renewable share is larger than 100% and the EV fleet size is 10^6 under either power load pattern. As the renewable generation and power load follow different temporal trends and dynamics, the renewable share should be larger than 100% here, where the EV fleet helps charge and discharge the electrical power if needed. Note that all the above results show significant challenges to achieving carbon neutrality in a GVI system. For instance, Norway, one of the world's most sustainable countries, has a renewable share of around 60% and around 6×10^5 EVs in use (IEA 2023, Wikipedia 2023), but this status-quo is still not enough. Although a considerable gap between industrial practices and global promises of carbon neutrality still exists, we believe the gap will quickly vanish because of the rapid growth of renewable generation, EVs with V2G, and other technologies.

4.6 Conclusion

The increasing prevalence of renewable energy presents significant challenges for power grid operations due to its inherent uncertainties. To address the challenges, the grid may invest in additional infrastructures to expand its capacity or utilize regulation reserves from an ancillary service market to help adjust power generation levels. However, these strategies may cause significant time/resource investment, energy loss, and network congestion. Thus, we consider integrating the power grid with EVs to enhance the grid's flexibility and resilience without incurring these drawbacks. EVs rely on electricity charged from the grid to serve mobility demands and help store excess electricity when

the power generation exceeds the power load. Conversely, through V2G technology, EVs can discharge electricity to supplement the grid's supply. Moreover, EVs are close to the power load, facilitating convenient power transfers and minimizing energy loss and network congestion. We term this integrated system "*the grid-vehicle integration (GVI) system*."

We formulate the GVI system's operations under uncertainties in renewable generation, power load, and EV trip demand as a two-stage robust MIP model (see Problem ($\mathcal{M}$)), which minimizes the worst-case total cost throughout the operational horizon. The first stage decides whether each thermal generator starts up, and the second stage decides the subsequent power generation, charging/discharging interaction, and the EV fleet operation over the horizon. Note that solving a robust optimization model is significantly challenging. Thus, we propose a machine learning-driven optimization approach, which initially uses a machine learning technique to identify a worst-case scenario (see Definition 1) from the uncertainty set $\mathcal{S}$ and iteratively construct a support set (see Definition 2) of the problem. This approach is derived as follows. First, we propose an ADMM algorithm to efficiently solve Problem ($\mathcal{M}$) offline (see Theorems 4–5 and Proposition 6) and identify a worst-case scenario, by which we obtain a set of data for the subsequent learning process. Second, given offline input instances and output solutions, we perform linear regression to characterize the relationship between the worst-case scenario (i.e., output) and the scenario samples in $\mathcal{S}$ (i.e., input). With this linear regression relationship, we derive an efficient algorithm to solve Problem ($\mathcal{M}$) to optimality (see Theorems 6–7 and Lemma 1). Third, we further derive several families of strong valid inequalities to tighten the linear relaxation of Problem (4.29) (i.e., Problem ($\mathcal{M}$)) (see Propositions 7–10). Numerical experiments suggest that our approach can find an optimal solution in a significantly shorter computational time than the CPLEX solver.

Based on the data set from NYISO and TLC in NYC, we investigate the impact of V2G and the GVI system's overall performance under various system parameters. We first solve the two-stage problem ($\mathcal{M}$) to obtain the online/offline status of thermal generators. Given the first-stage solution, we then solve the second-stage problem ($\mathcal{P}$) to determine out-of-sample operation decisions. We reveal the following insights that may shed light on the GVI system's operations and provide suggestions for improving sustainability in our society.

(i) V2G technology effectively reduces the number of online generators and extends their operational periods, thereby enhancing grid stability and reliability. In addition, V2G stabilizes the subsequent power generation through the *valley-filling effect* and *peak-shaving effect*. Specifically, we use EVs to store excess electricity in EV batteries during low-trip-demand hours and returning it to the grid when needed. V2G contributes to sustainability by curbing carbon emissions, with the most significant impact observed during hours of moderate power load (see Section 4.5.3).

(ii) The power load pattern impacts the GVI system performance with V2G adopted. Specifically, V2G reduces more online generators, decreases more carbon emissions, and improves more greenness under a bimodal power load pattern than a unimodal pattern (see Section 4.5.4).

(iii) A higher renewable share or EV fleet size increases the greenness, but the rate of increase diminishes as these two parameters become larger. We find that a greenness of 0.72 can be achieved when the EV fleet size is 10^6 and the renewable share reaches 100% under the unimodal power load pattern (or 80% under the bimodal pattern). However, achieving carbon neutrality by simply increasing the renewable share and EV fleet size is challenging. Considering a variant of Problem ($\mathcal{M}$), we find that carbon neutrality can be achieved when the renewable share is larger than 100% and the EV fleet size is 10^6 under either power load pattern (see Section 4.5.5).

Our model and approach are sufficiently general for any typical GVI systems and two-stage robust MIP problems. For example, we can use Algorithm 4 to solve the following robust satisficing variant of Problem ($\mathcal{M}$) with a prescribed target Z of the total cost and a given finite distribution set $\mathcal{W}$:

$$\begin{aligned}
&\min\ \omega \\
&\text{s.t.}\ \sum_{g\in\mathcal{G}}\sum_{t=2}^{T}\left(\mathrm{SU}^g u_t^g + \mathrm{SD}^g(y_{t-1}^g - y_t^g + u_t^g)\right) + \mathbb{E}_{\mathbb{P}}\left[\Psi\left(\mathbf{u},\mathbf{y},\boldsymbol{\xi}\right)\right] - Z \le \omega\Delta\left(\mathbb{P},\mathbb{P}_0\right),\ \forall \mathbb{P}\in\mathcal{W}, \\
&\quad (4.1)-(4.5),
\end{aligned}$$

where $\mathbb{P}_0$ denotes the empirical distribution based on observations in $\mathcal{S}$, i.e., $\mathbb{P}_0(\boldsymbol{\xi} = \boldsymbol{\xi}_j) = 1/|\mathcal{S}|$ for any $j \in \mathcal{S}$, and $\Delta\left(\mathbb{P},\mathbb{P}_0\right)$ measures the distance between $\mathbb{P}$ and $\mathbb{P}_0$. The

selection of Δ varies in different applications, and a popular choice is the Wasserstein metric (Esfahani and Kuhn 2017). By applying Algorithm 4, we can first predict the worst-case distribution in $\mathcal{W}$, and solve the robust satisfying problem with only the worst-case distribution. We can finally obtain its optimal solution by iteratively taking more distributions in $\mathcal{W}$ into consideration. As the data from NYISO and TLC in NYC is quite representative, we believe the above insights shall hold for other GVI systems with similar operational features. Furthermore, our study opens avenues for potential extensions in several directions. First, we can explore integrating the GVI system with other systems to further enhance the power grid's flexibility and resilience and easily achieve carbon neutrality. Second, we can incorporate additional ancillary service products of the power grid into the GVI system. Third, we may derive alternative machine learning techniques to further enhance the solving process. We leave these for future research.

Chapter 5

Conclusions

In this thesis, we present three studies on the shared mobility and electrical power grid, which are at the crux of smart city operations.

The first study considers the shared micromobility firms' operations under competition. Each firm provides micromobility vehicles to satisfy the uncertain demands of two types of consumers: *loyal consumers* and *disloyal consumers*, whose demands depend on capacity decisions. Each firm solves an integrated vehicle allocation and relocation problem, in which the total number of vehicles allocated by the two firms together in each service region is constrained by the city regulator, and provides a Nash equilibrium. Each firm's decision-making problem is formulated as a two-stage stochastic program on a spatial-temporal network, with the objective of maximizing her expected profit. To improve firms' operations with the limited number of allocated vehicles, we propose an innovative capacity-sharing agreement, under which a firm can share spare capacity for a fee with her opponent. Numerical results based on real data reveal that regulator restrictions impact firms' profitability and service level. Capacity sharing can reduce the number of relocated vehicles and also improve the firms' profitability. To promote the capacity-sharing agreement, the regulator should provide incentives to the firms.

The second study explores an EV-sharing mobility system incorporating V2G technology under high-dimensional and correlated uncertainties. The operator's EV planning and operation problem is formulated as a two-stage DRO problem on a time-space-soc network. We further reformulate the DRO problem as a SDP model. To deal with the significant computational difficulty of the SDP reformulation, we introduce outer and inner approximations for it to reduce the size of PSD matrices. We further propose an

algorithmic approach that incorporates time-based decomposition to further strengthen the solving process. Numerical results based on real data suggest that EVs majorly charge electricity during the early hours when electricity prices and consumer trips are low. Conversely, they discharge electricity when prices are high. Faster charging reduces the number of allocated vehicles, improves the vehicle utilization rate, and decreases total costs. Comparing two pricing schemes for charging EVs, electricity-based and time-based, we observe more frequent charging and discharging under the time-based scheme than the electricity-based scheme.

The third study considers a grid-vehicle integration (GVI) system employing V2G while managing uncertainties in renewable generation, power load, and EV trip demand. We formulate the problem of operating a GVI system as a two-stage robust mixed-integer program. To address a significant computational challenge, we propose a machine learning-driven optimization approach. Our approach outperforms a commercial solver in both computational time and solution quality for large-scale instances based on real data. Conducting out-of-sample tests with data from NYC, we reveal that V2G can reduce the number of required generators and stabilize power generation by "filling" the low power load and "shaving" the peak power load. Moreover, V2G helps achieve a substantial reduction in carbon emissions compared to the case without V2G. The impact of V2G is more pronounced under a bimodal power load pattern than a unimodal pattern. We also find that achieving carbon neutrality in this integration system is feasible yet challenging.

Appendix A

Supplements for Chapter 2

A.1 Table of Notation

Table A.1. Summary of Notation

Notation	Description
Sets:	
$\mathcal{K}$	set of shared micromobility firms $\mathcal{K} = \{A, B\}$
$\mathcal{M}$	set of service regions $\mathcal{M} = \{1, 2, \ldots, M\}$
$\mathcal{T}$	operational horizon $\mathcal{T} = \{0, 1, \ldots, T\}$
$\mathcal{G}$	time-space network $\mathcal{G} = (\mathcal{N}, \mathcal{E})$
$\mathcal{N}$	set of nodes on the network $\mathcal{G}$
$\mathcal{E}$	set of directed arcs on the network $\mathcal{G}$
$\mathcal{E}_{\mathrm{R}}^k, \mathcal{E}_{\mathrm{I}}^k, \mathcal{E}_{\mathrm{L}}^k$	rental arcs, idle arcs, relocation arcs for each firm $k \in \mathcal{K}$
$\mathcal{E}_{\mathrm{T}}^k, \mathcal{E}_{\mathrm{N}_\delta}^k$	transfer arcs, return arcs for each firm $k \in \mathcal{K}$ with $\delta \in \{1, 2, \ldots, \Delta\}$
$\mathcal{A}$	$\mathcal{A} = \{\mathrm{R}, \mathrm{I}, \mathrm{L}, \mathrm{T}, \mathrm{N}_\delta,\ \forall \delta = 1, 2, \ldots, \Delta\}$
$\mathcal{Z}_{\mathrm{R}}$	$\mathcal{Z}_{\mathrm{R}} = \{\mathcal{M} \times \mathcal{M} \times \mathcal{T} \times \mathcal{T} :\ i \neq i',\ t' = t + \ell_{i,i'}\}$
$\mathcal{Z}_{\mathrm{L}}$	$\mathcal{Z}_{\mathrm{L}} = \{\mathcal{M} \times \mathcal{M} \times \mathcal{T} \times \mathcal{T} :\ i \neq i',\ t' = t + r_{i,i'}\}$
$\mathcal{Z}_{\mathrm{I}}$	$\mathcal{Z}_{\mathrm{I}} = \{\mathcal{M} \times \mathcal{T} :\ t \in \mathcal{T} \setminus \{T\}\}$
$\mathcal{S}$	set of scenarios of uncertain demands in all the service regions across all the periods
$\mathcal{W}_0$	feasible region of problems (2.9) and (2.10)
$\mathcal{W}_1$	feasible region of problems (2.13) and (2.14)
Parameters:	
$\ell_{i,i'}$	duration for a rental trip from region $i \in \mathcal{M}$ to region $i' \in \mathcal{M}$
$r_{i,i'}$	duration to relocate a vehicle from region $i \in \mathcal{M}$ to region $i' \in \mathcal{M}$
α_k	the percentage of consumers who are loyal to firm $k \in \mathcal{K}$
$\hat{x}^k$	upper bound for the number of vehicles allocated by firm $k \in \mathcal{K}$
$\bar{x}_i$	upper bound for the number of vehicles allocated to region $i \in \mathcal{M}$ by both firms in set $\mathcal{K}$
h_{R}^k	revenue of firm $k \in \mathcal{K}$ for serving a consumer
h_{P}^k	penalty cost of firm $k \in \mathcal{K}$ per consumer lost
h_{I}^k	idle cost of firm $k \in \mathcal{K}$ (e.g., the maintenance cost of idle vehicles) for each idling vehicle
h_{L}^k	cost for relocation a vehicle for firm $k \in \mathcal{K}$

h_{T}	cost of receiving a vehicle for firm $k \in \mathcal{K}$ from firm $-k$
c_i^k	cost incurred for allocating a vehicle for firm $k \in \mathcal{K}$ to region $i \in \mathcal{M}$
$D_{i,i',t,t'}$	the total market demand over any given time-space range $(i, i', t, t') \in \mathcal{Z}_{\mathrm{R}}$
Y_e^k	the number of loyal consumers of firm $k \in \mathcal{K}$ on each rental arc $e = (n_{i,t}^k, n_{i',t'}^k) \in \mathcal{E}_{\mathrm{R}}^k$
$Y_{i,i',t,t'}^0$	the total number of disloyal consumers to both firms in set $\mathcal{K}$ over any given time-space range $(i, i', t, t') \in \mathcal{Z}_{\mathrm{R}}$
θ_s	probability of each scenario $s \in \mathcal{S}$
ϵ	the minimum service level provided by each firm on all rental arcs over the whole operational horizon
Variables:	
x_i^k	number of vehicles allocated to region $i \in \mathcal{M}$ by firm $k \in \mathcal{K}$
w_e	realized flow on each arc $e \in \mathcal{E}$
$\overline{w}_e^k$	consumer demand (the number of consumers) of firm $k \in \mathcal{K}$ from region i in period t to region i' in period $t + \ell_{i,i'}$ for each rental arc $e = (n_{i,t}^k, n_{i',t+\ell_{i,i'}}^k) \in \mathcal{E}_{\mathrm{R}}^k$
$\tau_k, \beta_{k,i}, \kappa_{k,i}$	dual multipliers with respect to constraints (2.1)
$\rho_{k,i,i',t,t',s}, \gamma_{k,i,t,s}$	dual multipliers with respect to constraints (2.2)–(2.3)
$\eta_{k,i,i',t,t',s}^{\mathrm{R}}, \eta_{k,i,t,s}^{\mathrm{I}}$	dual multipliers with respect to constraints (2.4)–(2.5)
$v_{k,i,i',t,t',s}^{\mathrm{R}}, v_{k,i,i',t,t',s}^{\mathrm{L}}$	dual multipliers with respect to constraints (2.6)–(2.7)
$v_{k,i,t,s}^{\mathrm{I}}$	dual multipliers with respect to constraint (2.8)
$\mathbf{\Lambda}_0$	vector of all variables associated with both firms in $\mathcal{K}$ in problems (2.9) and (2.10)
$\mathbf{\Lambda}_1$	vector of all variables associated with both firms in $\mathcal{K}$ in problems (2.13) and (2.14)
Objective:	
Ψ^k	the profit of each firm $k \in \mathcal{K}$
$\Gamma_0^{\mathrm{DL}}(\Gamma_0^{\mathrm{TA}})$	the total demand loss (allocated vehicles) of both firms when the capacity-sharing agreement is not adopted
$\Gamma_1^{\mathrm{DL}}(\Gamma_1^{\mathrm{TA}})$	the total demand loss (allocated vehicles) of both firms when the capacity-sharing agreement is adopted

A.2 KKT Conditions of Model $(\mathcal{D}^k(\mathbf{x}^{-k}))$, $\forall\, k \in \mathcal{K}$

First, we have the primal feasibility condition represented by the constraints (2.1)–(2.8). Second, to represent the dual feasibility condition, we define the following dual multipliers

with respect to constraints (2.1)–(2.8):

$$\tau_k \geq 0,\ \forall\, k \in \mathcal{K}, \tag{A.1}$$

$$\beta_{k,i} \geq 0,\ \forall\, k \in \mathcal{K},\ i \in \mathcal{M}, \tag{A.2}$$

$$\kappa_{k,i} \leq 0,\ \forall\, k \in \mathcal{K},\ i \in \mathcal{M}, \tag{A.3}$$

$$\rho_{k,i,i',t,t',s} \in \mathbb{R},\ \forall\, k \in \mathcal{K},\ (i,i',t,t') \in \mathcal{Z}_{\mathrm{R}},\ s \in \mathcal{S}, \tag{A.4}$$

$$\gamma_{k,i,0,s} \in \mathbb{R},\ \forall\, k \in \mathcal{K},\ i \in \mathcal{M},\ s \in \mathcal{S}, \tag{A.5}$$

$$\gamma_{k,i,t,s} \in \mathbb{R},\ \forall\, k \in \mathcal{K},\ i \in \mathcal{M},\ t \in [1, T-1]_{\mathbb{Z}},\ s \in \mathcal{S}, \tag{A.6}$$

$$\gamma_{k,i,T,s} \in \mathbb{R},\ \forall\, k \in \mathcal{K},\ i \in \mathcal{M},\ s \in \mathcal{S}, \tag{A.7}$$

$$\eta^{\mathrm{R}}_{k,i,i',t,t',s} \geq 0,\ \forall\, k \in \mathcal{K},\ (i,i',t,t') \in \mathcal{Z}_{\mathrm{R}},\ s \in \mathcal{S}, \tag{A.8}$$

$$\eta^{\mathrm{I}}_{k,i,t,s} \geq 0,\ \forall\, k \in \mathcal{K},\ i \in \mathcal{M},\ t \in [1, T-1]_{\mathbb{Z}},\ s \in \mathcal{S}, \tag{A.9}$$

$$v^{\mathrm{R}}_{k,i,i',t,t',s} \leq 0,\ \forall\, k \in \mathcal{K},\ (i,i',t,t') \in \mathcal{Z}_{\mathrm{R}},\ s \in \mathcal{S}, \tag{A.10}$$

$$v^{\mathrm{L}}_{k,i,i',t,t',s} \leq 0,\ \forall\, k \in \mathcal{K},\ (i,i',t,t') \in \mathcal{Z}_{\mathrm{L}},\ s \in \mathcal{S}, \tag{A.11}$$

$$v^{\mathrm{I}}_{k,i,t,s} \leq 0,\ \forall\, k \in \mathcal{K},\ i \in \mathcal{M},\ t \in [1, T-1]_{\mathbb{Z}},\ s \in \mathcal{S}. \tag{A.12}$$

Here, the multipliers defined in (A.1)–(A.9) correspond to constraints (2.1)–(2.7), respectively. The multipliers defined in (A.10)–(A.12), respectively, correspond to the following three parts of constraints (2.8): (i) $w_e \geq 0,\ \forall\, e \in \mathcal{E}^k_{\mathrm{R}},\ k \in \mathcal{K}$, (ii) $w_e \geq 0,\ \forall\, e \in \mathcal{E}^k_{\mathrm{L}},\ k \in \mathcal{K}$, and (iii) $w_e \geq 0,\ \forall\, e \in \mathcal{E}^k_{\mathrm{I}},\ k \in \mathcal{K}$.

Third, we have the following constraints to represent the complementary slackness condition:

$$\left(\sum_{i \in \mathcal{M}} x^k_i - \hat{x}^k\right) \tau_k = 0,\ \forall\, k \in \mathcal{K}, \tag{A.13}$$

$$\left(x^k_i + x^{-k}_i - \bar{x}_i\right) \beta_{k,i} = 0,\ \forall\, k \in \mathcal{K},\ i \in \mathcal{M}, \tag{A.14}$$

$$x^k_i \kappa_{k,i} = 0,\ \forall\, k \in \mathcal{K},\ i \in \mathcal{M}, \tag{A.15}$$

$$\left(w^{\mathrm{R}}_{k,i,i',t,t',s} - \overline{w}^{\mathrm{R}}_{k,i,i',t,t',s}\right) \eta^{\mathrm{R}}_{k,i,i',t,t',s} = 0,\ \forall\, k \in \mathcal{K},\ (i,i',t,t') \in \mathcal{Z}_{\mathrm{R}},\ s \in \mathcal{S}, \tag{A.16}$$

$$\left(w^{\mathrm{I}}_{k,i,t,s} - x^k_i\right) \eta^{\mathrm{I}}_{k,i,t,s} = 0,\ \forall\, k \in \mathcal{K},\ i \in \mathcal{M},\ t \in [1, T-1]_{\mathbb{Z}},\ s \in \mathcal{S}, \tag{A.17}$$

$$w^{\mathrm{R}}_{k,i,i',t,t',s} v^{\mathrm{R}}_{k,i,i',t,t',s} = 0,\ \forall\, k \in \mathcal{K},\ (i,i',t,t') \in \mathcal{Z}_{\mathrm{R}},\ s \in \mathcal{S}, \tag{A.18}$$

$$w^{\mathrm{L}}_{k,i,i',t,t',s} v^{\mathrm{L}}_{k,i,i',t,t',s} = 0,\ \forall\, k \in \mathcal{K},\ (i,i',t,t') \in \mathcal{Z}_{\mathrm{L}},\ s \in \mathcal{S}, \tag{A.19}$$

$$w^{\mathrm{I}}_{k,i,t,s} v^{\mathrm{I}}_{k,i,t,s} = 0,\ \forall\, k \in \mathcal{K},\ i \in \mathcal{M},\ t \in [1, T-1]_{\mathbb{Z}},\ s \in \mathcal{S}, \tag{A.20}$$

where we rewrite

$$w^{\mathrm{R}}_{k,i,i',t,t',s} := w^s_e,\ \forall\, k \in \mathcal{K},\ (i,i',t,t') \in \mathcal{Z}_{\mathrm{R}},\ s \in \mathcal{S},\ e = (n^k_{i,t}, n^k_{i',t'}) \in \mathcal{E}^k_{\mathrm{R}},$$
$$w^{\mathrm{L}}_{k,i,i',t,t',s} := w^s_e,\ \forall\, k \in \mathcal{K},\ (i,i',t,t') \in \mathcal{Z}_{\mathrm{L}},\ s \in \mathcal{S},\ e = (n^k_{i,t}, n^k_{i',t'}) \in \mathcal{E}^k_{\mathrm{L}},$$
$$w^{\mathrm{I}}_{k,i,t,s} := w^s_e,\ \forall\, k \in \mathcal{K},\ (i,t) \in \mathcal{Z}_{\mathrm{I}},\ s \in \mathcal{S},\ e = (n^k_{i,t}, n^k_{i,t+1}) \in \mathcal{E}^k_{\mathrm{I}}.$$

Fourth, we derive the Lagrangian stationarity conditions. Note that for each $k \in \mathcal{K}$, the Lagrangian function of model ($\mathcal{D}^k(\mathbf{x}^{-k})$) can be written as:

$$\begin{aligned}
\mathcal{L}^k = &\sum_{i\in\mathcal{M}} \left(c^k_i + \tau_k + \beta_{k,i} - \sum_{(i,i',t,t')\in\mathcal{Z}_{\mathrm{R}}} \sum_{s\in\mathcal{S}} \frac{Y^0_{i,i',t,t',s}}{\sum_{i\in\mathcal{M}} \bar{x}_i} \rho_{k,i,i',t,t',s} + \sum_{s\in\mathcal{S}} \left(\gamma_{k,i,T,s} - \gamma_{k,i,0,s} - \sum_{t=0}^{T-1} \eta^{\mathrm{I}}_{k,i,t,s} \right) + \kappa_{k,i} \right) x^k_i \\
&+ \sum_{(i,i',t,t')\in\mathcal{Z}_{\mathrm{R}}} \sum_{s\in\mathcal{S}} \left(\theta_s h^k_{\mathrm{P}} + \rho_{k,i,i',t,t',s} - \eta^{\mathrm{R}}_{k,i,i',t,t',s} \right) \overline{w}_{k,i,i',t,t',s} \\
&+ \sum_{(i,i',t,t')\in\mathcal{Z}_{\mathrm{R}}} \sum_{s\in\mathcal{S}} \left(-\theta_s h^k_{\mathrm{R}} - \theta_s h^k_{\mathrm{P}} + \gamma_{k,i,t,s} - \gamma_{k,i',t',s} + \eta^{\mathrm{R}}_{k,i,i',t,t',s} + v^{\mathrm{R}}_{k,i,i',t,t',s} \right) w^{\mathrm{R}}_{k,i,i',t,t',s} \\
&+ \sum_{(i,i',t,t')\in\mathcal{Z}_{\mathrm{L}}} \sum_{s\in\mathcal{S}} \left(\theta_s h^k_{\mathrm{L}} + \gamma_{k,i,t,s} - \gamma_{k,i',t',s} + v^{\mathrm{L}}_{k,i,i',t,t',s} \right) w^{\mathrm{L}}_{k,i,i',t,t',s} \\
&+ \sum_{(i,t)\in\mathcal{Z}_{\mathrm{I}}} \sum_{s\in\mathcal{S}} \left(\theta_s h^k_{\mathrm{I}} + \gamma_{k,i,t,s} - \gamma_{k,i,t+1,s} + \eta^{\mathrm{I}}_{k,i,t,s} + v^{\mathrm{I}}_{k,i,t,s} \right) w^{\mathrm{I}}_{k,i,t,s} \\
&- \hat{x}^k \tau_k + \sum_{i\in\mathcal{M}} \left(x^{-k}_i - \bar{x}_i \right) \beta_{k,i} - \sum_{(i,i',t,t')\in\mathcal{Z}_{\mathrm{R}}} \sum_{s\in\mathcal{S}} Y^k_{i,i',t,t',s} \rho_{k,i,i',t,t',s}. \qquad \text{(A.21)}
\end{aligned}$$

Thus, the stationarity conditions can be described by the following constraints:

$$\begin{aligned}
-c^k_i = \tau_k + \beta_{k,i} &- \sum_{(i,i',t,t')\in\mathcal{Z}_{\mathrm{R}}} \sum_{s\in\mathcal{S}} \frac{Y^0_{i,i',t,t',s}}{\sum_{i\in\mathcal{M}} \bar{x}_i} \rho_{k,i,i',t,t',s} \\
&+ \sum_{s\in\mathcal{S}} \left(\gamma_{k,i,T,s} - \gamma_{k,i,0,s} - \sum_{t=0}^{T-1} \eta^{\mathrm{I}}_{k,i,t,s} \right) + \kappa_{k,i}, \forall\, k \in \mathcal{K},\ i \in \mathcal{M}, \qquad \text{(A.22)}
\end{aligned}$$

$$-\theta_s h^k_{\mathrm{P}} = \rho_{k,i,i',t,t',s} - \eta^{\mathrm{R}}_{k,i,i',t,t',s},\ \forall\, k \in \mathcal{K},\ (i,i',t,t') \in \mathcal{Z}_{\mathrm{R}},\ s \in \mathcal{S}, \qquad \text{(A.23)}$$

$$\begin{aligned}
\theta_s h^k_{\mathrm{R}} + \theta_s h^k_{\mathrm{P}} = \gamma_{k,i,t,s} - \gamma_{k,i',t',s} + \eta^{\mathrm{R}}_{k,i,i',t,t',s} + v^{\mathrm{R}}_{k,i,i',t,t',s}, \\
\forall\, k \in \mathcal{K},\ (i,i',t,t') \in \mathcal{Z}_{\mathrm{R}},\ s \in \mathcal{S}, \qquad \text{(A.24)}
\end{aligned}$$

$$-\theta_s h^k_{\mathrm{L}} = \gamma_{k,i,t,s} - \gamma_{k,i',t',s} + v^{\mathrm{L}}_{k,i,i',t,t',s},\ \forall\, k \in \mathcal{K},\ (i,i',t,t') \in \mathcal{Z}_{\mathrm{L}},\ s \in \mathcal{S}, \qquad \text{(A.25)}$$

$$-\theta_s h^k_{\mathrm{I}} = \gamma_{k,i,t,s} - \gamma_{k,i,t+1,s} + \eta^{\mathrm{I}}_{k,i,t,s} + v^{\mathrm{I}}_{k,i,t,s},\ \forall\, k \in \mathcal{K},\ (i,t) \in \mathcal{Z}_{\mathrm{I}},\ s \in \mathcal{S}. \qquad \text{(A.26)}$$

We use $\mathcal{W}_0$ to denote the feasible region defined by the above KKT conditions, including (2.1) for any $k \in \mathcal{K}$, (2.2)–(2.8) for any $s \in \mathcal{S}$, (A.1)–(A.12), (A.13)–(A.20), and (A.22)–

(A.26). That is, $\mathcal{W}_0$ characterizes the set of possible equilibria of the Nash game between Firm A and Firm B.

Note that the complementary slackness conditions (A.13)–(A.20) are nonlinear. We can exactly linearize them for tractable computation. Specifically, we reformulate them into linear constraints by employing auxiliary binary variables. For example, for equation $x_i^k \kappa_{k,i} = 0$, given $k \in \mathcal{K},\ i \in \mathcal{M}$, we define a binary variable $z_{k,i}$ to indicate whether $\kappa_{k,i} = 0$ (i.e., $z_{k,i} = 1$) or $x_i^k = 0$ (i.e., $z_{k,i} = 0$). With an arbitrarily large positive number $G_{k,i}$, the equations $x_i^k \kappa_{k,i} = 0,\ \forall\, k \in \mathcal{K},\ i \in \mathcal{M}$ can be reformulated by the following linear constraints:

$$-G_{k,i} z_{k,i} \le x_i^k \le G_{k,i} z_{k,i},\ \forall\, k \in \mathcal{K},\ i \in \mathcal{M}, \tag{A.27}$$

$$-G_{k,i}(1 - z_{k,i}) \le \kappa_{k,i} \le G_{k,i}(1 - z_{k,i}),\ \forall\, k \in \mathcal{K},\ i \in \mathcal{M}, \tag{A.28}$$

$$z_{k,i} \in \{0, 1\},\ \forall\, k \in \mathcal{K},\ i \in \mathcal{M}. \tag{A.29}$$

Following the same way, we can also reformulate the remaining equations (A.13)–(A.20). We omit the details for simplicity.

A.3 Vector Definition for Problem (2.9)

For Problem (2.9), we let $\mathbf{x} = (x_i^k,\ \forall\, i \in \mathcal{M}, k \in \mathcal{K})^\top$ denote the vector of both firms' initial vehicle allocation decisions in all regions, and $\mathbf{w} = (w_e^s,\ \forall\, e \in \cup_{k\in\mathcal{K}} \mathcal{E}^k,\ \overline{w}_e^s,\ \forall\, e \in \cup_{k\in\mathcal{K}} \mathcal{E}_{\mathrm{R}}^k, s \in \mathcal{S})^\top$ denote the vector of both firms' subsequent operational decisions on all types of arcs and in all scenarios. We further let $\boldsymbol{\tau} = (\tau_k,\ \forall\, k \in \mathcal{K})^\top$ denote the vector of dual multipliers defined in constraints (A.1). For the other dual multipliers, we similarly let $\boldsymbol{\beta},\ \boldsymbol{\kappa},\ \boldsymbol{\rho},\ \boldsymbol{\gamma},\ \boldsymbol{\eta}^{\mathrm{R}},\ \boldsymbol{\eta}^{\mathrm{I}},\ \mathbf{v}^{\mathrm{R}},\ \mathbf{v}^{\mathrm{L}}$, and $\mathbf{v}^{\mathrm{I}}$ denote the vectors of dual multipliers defined in (A.2)–(A.12), respectively. In particular, the vectors $\boldsymbol{\beta},\ \boldsymbol{\kappa},\ \boldsymbol{\rho}$ denote the dual multipliers defined in (A.2)–(A.4), respectively. The vector $\boldsymbol{\gamma}$ denotes the dual multipliers defined in (A.5)–(A.7). The vectors $\boldsymbol{\eta}^{\mathrm{R}},\ \boldsymbol{\eta}^{\mathrm{I}},\ \mathbf{v}^{\mathrm{R}},\ \mathbf{v}^{\mathrm{L}}$, and $\mathbf{v}^{\mathrm{I}}$ denote the dual multipliers defined in (A.8)–(A.12), respectively. In addition, we let $\mathbf{y} = (\boldsymbol{\tau}, \boldsymbol{\beta}, \boldsymbol{\kappa}, \boldsymbol{\rho}, \boldsymbol{\eta}^{\mathrm{R}}, \boldsymbol{\eta}^{\mathrm{I}}, \mathbf{v}^{\mathrm{R}}, \mathbf{v}^{\mathrm{L}}, \mathbf{v}^{\mathrm{I}})^\top$ and $\boldsymbol{\Lambda}_0 = (\mathbf{x}, \mathbf{w}, \mathbf{y}, \boldsymbol{\gamma})^\top$. That is, we use $\boldsymbol{\Lambda}_0$ to denote a solution of Problem (2.9).

A.4 KKT Conditions of Model $(\mathcal{C}^k)$, $\forall\, k \in \mathcal{K}$

First, we have the primal feasibility condition represented by the constraints (2.1), (2.2)–(2.4) and (2.6)–(2.8) for any $s \in \mathcal{S}$, and (2.11)–(2.12). Second, to represent the dual feasibility condition, we continue to use the dual multipliers defined in (A.1)–(A.12), where $\gamma_{k,i,T,s} \in \mathbb{R},\ \forall\, k \in \mathcal{K},\ i \in \mathcal{M},\ s \in \mathcal{S}$ in constraints (A.7) now correspond to constraints (2.11) that are updated from (2.5). In addition, we introduce the following new dual multipliers:

$$\zeta_{k,t,s} \in \mathbb{R},\ \forall\, k \in \mathcal{K},\ t \in [1, T-1]_{\mathbb{Z}},\ s \in \mathcal{S}, \tag{A.30}$$

$$v^{\mathrm{T}}_{k,i,t,s} \leq 0,\ \forall\, k \in \mathcal{K},\ i \in \mathcal{M},\ t \in [1, T-1]_{\mathbb{Z}},\ s \in \mathcal{S}, \tag{A.31}$$

$$v^{\mathrm{E}}_{k,i,t,\delta,s} \leq 0,$$
$$\forall\, k \in \mathcal{K},\ i \in \mathcal{M},\ t \in [1, T-1]_{\mathbb{Z}},\ \delta \in [1, \min\{\Delta, T-t\}]_{\mathbb{Z}},\ s \in \mathcal{S}, \tag{A.32}$$

where the multipliers in (A.30) correspond to the new constraints (2.12), the multipliers in (A.31) correspond to a new part $w^s_e \geq 0,\ \forall\, e \in \mathcal{E}^k_{\mathrm{T}},\ s \in \mathcal{S}$ in the updated constraints (2.8) for any $s \in \mathcal{S}$, and the multipliers in (A.32) correspond to a new part $w^s_e \geq 0,\ \forall\, e \in \mathcal{E}^k_{\mathrm{N}_\delta},\ \delta \in [1, \min\{\Delta, T-t\}]_{\mathbb{Z}},\ t \in [1, T-1]_{\mathbb{Z}},\ k \in \mathcal{K},\ s \in \mathcal{S}$ in the updated constraints (2.8) for any $s \in \mathcal{S}$.

Third, to represent the complementary slackness condition, we continue to use constraints (A.13)–(A.20) and further introduce the following two constraints:

$$w^{\mathrm{T}}_{k,i,t,s} v^{\mathrm{T}}_{k,i,t,s} = 0,\ \forall\, k \in \mathcal{K},\ i \in \mathcal{M},\ t \in [1, T-1]_{\mathbb{Z}},\ s \in \mathcal{S}, \tag{A.33}$$

$$w^{\mathrm{E}}_{k,i,t,\delta,s} v^{\mathrm{E}}_{k,i,t,\delta,s} = 0,$$
$$\forall\, k \in \mathcal{K},\ i \in \mathcal{M},\ t \in [1, T-1]_{\mathbb{Z}},\ \delta \in [1, \min\{\Delta, T-t\}]_{\mathbb{Z}},\ s \in \mathcal{S}, \tag{A.34}$$

where

$$w^{\mathrm{T}}_{k,i,t,s} := w^s_e,\ \forall\, k \in \mathcal{K},\ i \in \mathcal{M},\ t \in [1, T-1]_{\mathbb{Z}},\ s \in \mathcal{S},\ e = (n^k_{i,t}, n^{-k}_{i,t}) \in \mathcal{E}^k_{\mathrm{T}},$$
$$w^{\mathrm{E}}_{k,i,t,\delta,s} := w^s_e,$$
$$\forall\, k \in \mathcal{K},\ i \in \mathcal{M},\ t \in [1, T-1]_{\mathbb{Z}},\ \delta \in [1, \min\{\Delta, T-t\}]_{\mathbb{Z}},\ s \in \mathcal{S},\ e = (n^k_{i,t}, n^{-k}_{i,t}) \in \mathcal{E}^k_{\mathrm{N}_\delta}.$$

Note that constraints (A.33)–(A.34) can also be reformulated as linear constraints following the same way in Appendix A.2.

Fourth, for the stationarity conditions, we continue to use constraints (A.22)–(A.26) and further introduce the following new constraints:

$$\theta_s h_{\mathrm{T}} = \gamma_{k,i,t,s} + v^{\mathrm{T}}_{k,i,t,s},\ \forall\, k \in \mathcal{K},\ i \in \mathcal{M},\ t \in [1, T-1]_{\mathbb{Z}},\ s \in \mathcal{S}, \tag{A.35}$$

$$0 = \gamma_{k,i,t+\delta,s} - \zeta_{k,t,s} + v^{\mathrm{E}}_{k,i,t,\delta,s},$$
$$\forall\, k \in \mathcal{K},\ i \in \mathcal{M},\ t \in [1, T-1]_{\mathbb{Z}},\ \delta \in [1, \min\{\Delta, T-t\}]_{\mathbb{Z}},\ s \in \mathcal{S}. \tag{A.36}$$

In summary, the KKT conditions of the model ($\mathcal{C}^k$) for any $k \in \mathcal{K}$ are represented by constraints (2.1), (2.2)–(2.4) and (2.6)–(2.8) for any $s \in \mathcal{S}$, (A.1)–(A.12), (A.13)–(A.20), (A.22)–(A.26), (2.11)–(2.12), and (A.30)–(A.36). We use $\mathcal{W}_1$ to denote the feasible region defined by these constraints.

A.5 Vector Definition for Problem (2.13)

For Problem (2.13), we adopt the vector definitions in A.3 and make the following additional definitions. We let $\mathbf{w}^{\mathrm{T}} = (w^s_e,\ \forall\, e \in \cup_{k\in\mathcal{K}} \mathcal{E}^k_{\mathrm{T}}, s \in \mathcal{S})^\top$ denote the vector of both firms' operational decisions on all transfer arcs and in all scenarios, and $\mathbf{w}^{\mathrm{E}} = (w^s_e,\ \forall\, e \in \cup_{k\in\mathcal{K},\delta\in\{1,\ldots,\Delta\}} \mathcal{E}^k_{\mathrm{N}_\delta}, s \in \mathcal{S})^\top$ denote the vector of both firms' operational decisions on all return arcs and in all scenarios. We further let $\boldsymbol{\zeta} = (\zeta_{k,t,s},\ \forall\, k \in \mathcal{K},\ t \in [1, T-1]_{\mathbb{Z}},\ s \in \mathcal{S})^\top$ denote the vector of dual multipliers defined in constraints (A.30). For the other dual multipliers, we similarly let $\boldsymbol{v}^{\mathrm{T}}$ and $\boldsymbol{v}^{\mathrm{E}}$ denote the vectors of dual multipliers defined in (A.31) and (A.32), respectively. In addition, we let $\boldsymbol{\Lambda}_1 = (\mathbf{x}, \mathbf{w}, \mathbf{y}, \boldsymbol{\gamma}, \mathbf{w}^{\mathrm{T}}, \mathbf{w}^{\mathrm{E}}, \boldsymbol{v}^{\mathrm{T}}, \boldsymbol{v}^{\mathrm{E}}, \boldsymbol{\zeta})^\top$. That is, we use $\boldsymbol{\Lambda}_1$ to denote a solution of Problem (2.13).

A.6 Proof of Proposition 1

Proof. Consider an optimal solution $\boldsymbol{\Lambda}^*_0 = (\mathbf{x}^*, \mathbf{w}^*, \mathbf{y}^*, \boldsymbol{\gamma}^*)^\top$ of Problem (2.9) with the corresponding optimal value Γ^{DL}_0. Based on this solution, we would like to construct a feasible solution $\hat{\boldsymbol{\Lambda}}_1 = (\hat{\mathbf{x}}, \hat{\mathbf{w}}, \hat{\mathbf{y}}, \hat{\boldsymbol{\gamma}}, \hat{\mathbf{w}}^{\mathrm{T}}, \hat{\mathbf{w}}^{\mathrm{E}}, \hat{\boldsymbol{v}}^{\mathrm{T}}, \hat{\boldsymbol{v}}^{\mathrm{E}}, \hat{\boldsymbol{\zeta}})^\top$ of Problem (2.13).

We let $\hat{\mathbf{x}} = \mathbf{x}^*,\ \hat{\mathbf{w}} = \mathbf{w}^*,\ \hat{\mathbf{y}} = \mathbf{y}^*$, and $\hat{\mathbf{w}}^{\mathrm{T}} = \hat{\mathbf{w}}^{\mathrm{E}} = \mathbf{0}$. We also let

$$\hat{\gamma}_{k,i,t,s} = \gamma^*_{k,i,t,s} + \lambda_{k,s},\ \forall\, k \in \mathcal{K},\ i \in \mathcal{M}, t \in \mathcal{T},\ s \in \mathcal{S}, \tag{A.37}$$

where

$$\lambda_{k,s} = \max_{\forall\, i\in\mathcal{M}, t\in[1,T-1]_{\mathbb{Z}}} (\theta_s h_{\mathrm{T}} - \gamma^*_{k,i,t,s})^+,\ \forall\, k\in\mathcal{K},\ s\in\mathcal{S}, \tag{A.38}$$

and let

$$\hat{v}^{\mathrm{T}}_{k,i,t,s} = \theta_s h_{\mathrm{T}} - \hat{\gamma}_{k,i,t,s},\ \forall\, k\in\mathcal{K},\ i\in\mathcal{M}, t\in[1,T-1]_{\mathbb{Z}},\ s\in\mathcal{S}, \tag{A.39}$$

$$\hat{\zeta}_{k,t,s} = \min_{\forall\, i\in\mathcal{M}, \delta\in[1,\min\{\Delta,T-t\}]} \hat{\gamma}_{k,i,t+\delta,s},\ \forall\, k\in\mathcal{K},\ t\in[1,T-1]_{\mathbb{Z}},\ s\in\mathcal{S}, \tag{A.40}$$

$$\hat{v}^{\mathrm{E}}_{k,i,t,\delta,s} = \hat{\zeta}_{k,t,s} - \hat{\gamma}_{k,i,t+\delta,s},$$
$$\forall\, k\in\mathcal{K},\ i\in\mathcal{M},\ t\in[1,T-1]_{\mathbb{Z}},\ \delta\in[1,\min\{\Delta,T-t\}]_{\mathbb{Z}},\ s\in\mathcal{S}. \tag{A.41}$$

It is easy to check that $\hat{\mathbf{\Lambda}}_1$ satisfies constraints (2.1) for any $k\in\mathcal{K}$, (2.2)–(2.4) and (2.6)–(2.8) for any $s\in\mathcal{S}$, (A.1)–(A.12), and (A.13)–(A.20). In addition, by (A.37), we have

$$\hat{\gamma}_{k,i,T,s} - \hat{\gamma}_{k,i,0,s} = \gamma^*_{k,i,T,s} + \lambda_{k,s} - \gamma^*_{k,i,0,s} - \lambda_{k,s} = \gamma^*_{k,i,T,s} - \gamma^*_{k,i,0,s},$$
$$\forall\, k\in\mathcal{K},\ i\in\mathcal{M},\ s\in\mathcal{S}, \tag{A.42}$$

$$\hat{\gamma}_{k,i,t,s} - \hat{\gamma}_{k,i',t',s} = \gamma^*_{k,i,t,s} + \lambda_{k,s} - \gamma^*_{k,i',t',s} - \lambda_{k,s} = \gamma^*_{k,i,t,s} - \gamma^*_{k,i',t',s},$$
$$\forall\, k\in\mathcal{K},\ (i,i',t,t')\in\mathcal{Z}_{\mathrm{R}},\ s\in\mathcal{S}, \tag{A.43}$$

$$\hat{\gamma}_{k,i,t,s} - \hat{\gamma}_{k,i,t+1,s} = \gamma^*_{k,i,t,s} + \lambda_{k,s} - \gamma^*_{k,i,t+1,s} - \lambda_{k,s} = \gamma^*_{k,i,t,s} - \gamma^*_{k,i,t+1,s},$$
$$\forall\, k\in\mathcal{K},\ (i,t)\in\mathcal{Z}_{\mathrm{I}},\ s\in\mathcal{S}. \tag{A.44}$$

With (A.42)–(A.44), we can clearly show that $\hat{\mathbf{\Lambda}}_1$ satisfies constraints (A.22)–(A.26). Moreover, as $\hat{\mathbf{w}}^{\mathrm{T}} = \hat{\mathbf{w}}^{\mathrm{E}} = \mathbf{0}$, clearly $\hat{\mathbf{\Lambda}}_1$ satisfies (2.11)–(2.12). It is trivial that $\hat{\mathbf{\Lambda}}_1$ satisfies constraints (A.30).

For any $k\in\mathcal{K},\ i\in\mathcal{M}, t\in[1,T-1]_{\mathbb{Z}},\ s\in\mathcal{S}$, we have

$$\begin{aligned}\hat{v}^{\mathrm{T}}_{k,i,t,s} &= \theta_s h_{\mathrm{T}} - \hat{\gamma}_{k,i,t,s} = \theta_s h_{\mathrm{T}} - \gamma^*_{k,i,t,s} - \lambda_{k,s} \le \theta_s h_{\mathrm{T}} - \gamma^*_{k,i,t,s} - (\theta_s h_{\mathrm{T}} - \gamma^*_{k,i,t,s})^+ \\ &= \begin{cases} 0, & \text{if } \theta_s h_{\mathrm{T}} - \gamma^*_{k,i,t,s} > 0 \\ \theta_s h_{\mathrm{T}} - \gamma^*_{k,i,t,s}, & \text{if } \theta_s h_{\mathrm{T}} - \gamma^*_{k,i,t,s} \le 0 \end{cases},\end{aligned} \tag{A.45}$$

where the first equality holds by (A.39), the second equality holds by (A.37) and $[1,T-1]_{\mathbb{Z}}\subseteq\mathcal{T}$, and the first inequality holds by (A.38). Clearly, (A.45) shows that $\hat{v}^{\mathrm{T}}_{k,i,t,s}\le 0,\ \forall\, k\in\mathcal{K},\ i\in\mathcal{M}, t\in[1,T-1]_{\mathbb{Z}},\ s\in\mathcal{S}$. Thus, $\hat{\mathbf{\Lambda}}_1$ satisfies constraints (A.31).

For any $k \in \mathcal{K},\ i \in \mathcal{M},\ t \in [1, T-1]_{\mathbb{Z}},\ \delta \in [1, \min\{\Delta, T-t\}]_{\mathbb{Z}},\ s \in \mathcal{S}$, we have

$$\hat{v}^{\mathrm{E}}_{k,i,t,\delta,s} = \hat{\zeta}_{k,t,s} - \hat{\gamma}_{k,i,t+\delta,s} = \min_{\forall\, i \in \mathcal{M}, \delta \in [1, \min\{\Delta, T-t\}]} \hat{\gamma}_{k,i,t+\delta,s} - \hat{\gamma}_{k,i,t+\delta,s} \leq 0,$$

where the first equality holds by (A.41) and the second equality holds by (A.40). Thus, $\hat{\mathbf{\Lambda}}_1$ satisfies constraints (A.32).

Since $\hat{\mathbf{w}}^{\mathrm{T}} = \hat{\mathbf{w}}^{\mathrm{E}} = \mathbf{0}$, it is trivial that $\hat{\mathbf{\Lambda}}_1$ satisfies constraints (A.33)–(A.34). By (A.39) and (A.41), we have $\hat{\mathbf{\Lambda}}_1$ satisfies constraints (A.35)–(A.36).

In summary, we have shown that $\hat{\mathbf{\Lambda}}_1$ satisfies all the constraints of Problem (2.13), including (2.1) for any $k \in \mathcal{K}$, (2.2)–(2.4) and (2.6)–(2.8) for any $s \in \mathcal{S}$, (A.1)–(A.12), (A.13)–(A.20), (A.22)–(A.26), (2.11)–(2.12), and (A.30)–(A.36). That is, $\hat{\mathbf{\Lambda}}_1$ is feasible to Problem (2.13), and the corresponding objective value equals

$$\sum_{k \in \mathcal{K}} \sum_{s \in \mathcal{S}} \theta_s \sum_{e \in \mathcal{E}^k_{\mathrm{R}}} \left(\hat{\overline{w}}^s_e - \hat{w}^s_e \right) = \sum_{k \in \mathcal{K}} \sum_{s \in \mathcal{S}} \theta_s \sum_{e \in \mathcal{E}^k_{\mathrm{R}}} \left(\overline{w}^{s^*}_e - w^{s^*}_e \right) = \Gamma^{\mathrm{DL}}_0.$$

Given that Problem (2.13) has a feasible solution $\hat{\mathbf{\Lambda}}_1$, we have that the feasible region $\mathcal{W}_1$ is non-empty. Meanwhile, $\mathcal{W}_1$ is clearly bounded. It follows that Problem (2.13) has an optimal solution with the corresponding optimal value Γ^{DL}_1. Because Problem (2.13) is a minimization problem, the optimal value Γ^{DL}_1 is no larger than the objective value Γ^{DL}_0 with respect to the feasible solution $\hat{\mathbf{\Lambda}}_1$, i.e., $\Gamma^{\mathrm{DL}}_1 \leq \Gamma^{\mathrm{DL}}_0$. □

A.7 Summary of All Trip Demands

Figure A.1 shows the summary of all the trip demands, where a subfigure in a cubic represents the trip demands from a region $i \in \mathcal{M}$ to another region $j \in \mathcal{M}$.

A.8 Impact of Penalty and Demand Level

We conduct experiments by varying the penalty cost (i.e., $h^k_{\mathrm{P}},\ k \in \mathcal{K}$) and demand level to examine how different penalty costs affect firms' performance under different demand sizes. The demand level refers to the extent to which the trip demand is increased. For example, a level of 10 corresponds to multiplying the trip demand set in Section 2.4.1 by 10. With $(\alpha_A, \alpha_B) = (0.1, 0.45)$ and $u = 1.25$, we solve Problem (2.9) and Problem

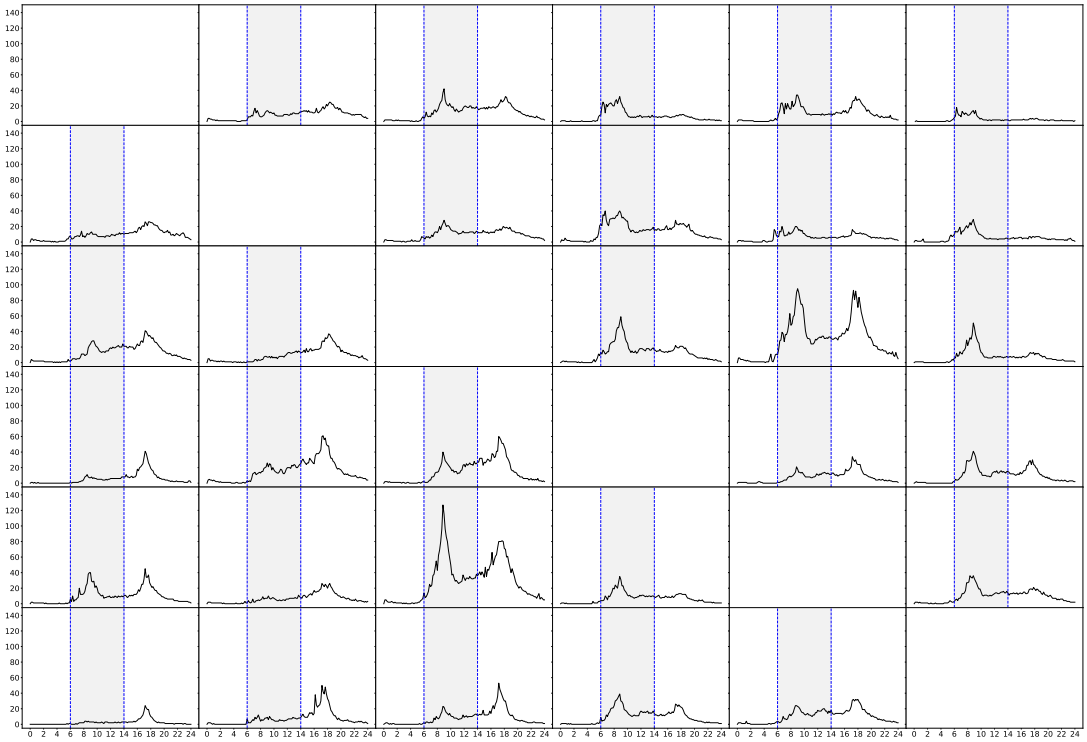

Figure A.1. The Sketch of Demand

(2.13) and show the results in Table A.2 and Table A.3, respectively. We define

$$\text{Gap}(\%) = \frac{|\text{the result when penalty is 0.1} - \text{the result when penalty is not 0.1}|}{\text{the result when penalty is 0.1}} \times 100\%,$$

with respect to each instance with a given demand level and penalty cost.

Table A.2 shows that when the demand level is 1 and the penalty cost varies from 0.1 to 1, the Gap (%) of allocation, profit, demand loss, or relocation remains within 1%. This suggests that varying the penalty cost has a limited impact on firms' performance when the demand level is 1 and capacity sharing is not adopted. We observe very similar results in Table A.3 where capacity sharing is adopted. The table shows that when the demand level is 1, the Gap (%) remains within 1.6% as the penalty cost varies.

When the demand level is 1, which aligns with the trip demand setting in Section 2.4.1, the two firms' performance is weakly affected by changes in penalty cost, no matter whether capacity sharing is adopted. Therefore, we set the penalty cost at 0.1 in numerical experiments for the sake of simplicity while ensuring the obtained results are promising and generalizable.

Table A.2 and Table A.3 also reveal that as the demand level increases, indicating trip demand rises, firms' performance is impacted by the penalty cost, specifically in terms of

vehicle relocation and transfer. Therefore, it is crucial to carefully estimate the penalty cost in the case where the trip demand is very large.

Table A.2. Performance Without Sharing

Level	Penalty	Allocation		Profit		Demand Loss		Relocation	
		Value	Gap (%)	Value ($)	Gap (%)	Value	Gap (%)	Value	Gap (%)
1	0.1	360	0	1250.32	0	16.88	0	75.00	0
	0.4	360	0	1246.86	0.28	16.88	0	75.29	0.39
	0.7	360	0	1243.20	0.57	16.88	0	75.31	0.42
	1	360	0	1241.51	0.71	16.88	0	75.44	0.58
4	0.1	1440	0	5000.32	0	67.53	0	305.38	0
	0.4	1440	0	4980.20	0.40	67.53	0	306.56	0.39
	0.7	1440	0	4950.80	0.99	67.53	0	307.06	0.55
	1	1440	0	4932.60	1.35	67.53	0	307.48	0.69
7	0.1	2520	0	8876.45	0	118.19	0	478.97	0
	0.4	2520	0	8720.34	1.76	118.19	0	468.19	2.25
	0.7	2520	0	8760.17	1.31	118.19	0	503.91	5.21
	1	2520	0	8770.05	1.20	118.19	0	506.95	5.84
10	0.1	3600	0	12621.60	0	168.84	0	707.32	0
	0.4	3600	0	12581.80	0.32	168.84	0	689.52	2.52
	0.7	3600	0	12488.30	1.06	168.84	0	677.07	4.28
	1	3600	0	12452.90	1.34	168.84	0	750.55	6.11

Table A.3. Performance With Sharing

Level	Penalty	Allocation		Profit		Demand Loss		Relocation		Transfer	
		Value	Gap (%)	Value ($)	Gap (%)	Value	Gap (%)	Value	Gap (%)	Value	Gap (%)
1	0.1	360	0	1408.69	0	16.88	0	64.58	0	3.29	0
	0.4	360	0	1407.07	0.12	16.88	0	64.63	0.06	3.31	0.61
	0.7	360	0	1402.81	0.42	16.88	0	64.00	0.91	3.31	0.61
	1	360	0	1392.20	1.17	16.88	0	65.21	0.96	3.34	1.52
4	0.1	1440	0	5640.85	0	67.53	0	273.19	0	16.13	0
	0.4	1440	0	5626.29	0.26	67.53	0	275.58	0.88	16.33	1.26
	0.7	1440	0	5605.46	0.63	67.53	0	277.29	1.50	16.04	0.57
	1	1440	0	5591.74	0.87	67.53	0	277.02	1.40	16.14	0.05
7	0.1	2520	0	9893.03	0	118.19	0	423.67	0	24.93	0
	0.4	2520	0	9858.58	0.35	118.19	0	431.29	1.80	26.13	4.80
	0.7	2520	0	9820.18	0.74	118.19	0	428.83	1.22	27.13	8.80
	1	2520	0	9787.94	1.06	118.19	0	432.10	1.99	26.59	6.63
10	0.1	3600	0	14130.90	0	168.84	0	610.08	0	34.91	0
	0.4	3600	0	14071.20	0.42	168.84	0	614.31	0.69	36.10	3.41
	0.7	3600	0	14024.30	0.75	168.84	0	621.88	1.93	38.05	9.00
	1	3600	0	13978.10	1.08	168.84	0	660.63	8.28	37.90	8.57

Appendix B

Supplements for Chapter 3

B.1 Proof of Theorem 1

Proof. This result is deduced from Lemma 1 in Delage and Ye (2010). □

B.2 Proof of Proposition 2

Proof. We define the following dual multipliers with respect to constraints (3.3)–(3.9):

$$\pi^0_{z,s} \in \mathbb{R},\ \forall\, z \in \mathcal{Z},\ s \in \mathcal{S},$$

$$\pi_{z,t,s} \in \mathbb{R},\ \forall\, z \in \mathcal{Z},\ t \in [1, T-1]_{\mathbb{Z}},\ s \in \mathcal{S},$$

$$\pi^{\mathrm{T}} \in \mathbb{R},$$

$$\omega_{z,t,z'} \leq 0,\ \forall\, (z, t, z') \in \mathcal{M},$$

$$\phi_{z,t} \leq 0,\ \forall\, z \in \mathcal{Z},\ t \in \mathcal{T},$$

$$\phi^{\mathrm{C}}_{z,t} \leq 0,\ \forall\, z \in \mathcal{Z},\ t \in \mathcal{T},$$

$$\phi^{\mathrm{S}}_{z,t} \leq 0,\ \forall\, z \in \mathcal{Z},\ t \in \mathcal{T}.$$

We use $\boldsymbol{\pi}$ to denote the vector of all the above dual variables.

With any given $(\mathbf{x}, \boldsymbol{\xi})$, we can formulate the dual problem of the second-stage problem

($\mathcal{P}_2$) as

$$
\begin{aligned}
f'(\mathbf{x},\boldsymbol{\xi})=\max\ & \sum_{z\in\mathcal{Z}}\sum_{s\in\mathcal{S}}\pi^0_{z,s}x_{z,s}+\pi^{\mathrm{T}}\sum_{z\in\mathcal{Z}}\sum_{s\in\mathcal{S}}x_{z,s}+\sum_{z\in\mathcal{Z}}\sum_{t\in\mathcal{T}}\phi_{z,t}\sum_{k\in\mathcal{K}}X^k_z && (\mathcal{P}_{\mathrm{d}})\\
& +\sum_{z\in\mathcal{Z}}\sum_{t\in\mathcal{T}}\phi^{\mathrm{C}}_{z,t}\left(X^{\mathrm{C}}_z+X^{\mathrm{S}}_z\right)+\sum_{z\in\mathcal{Z}}\sum_{t\in\mathcal{T}}\phi^{\mathrm{S}}_{z,t}X^{\mathrm{S}}_z\\
& +\sum_{(z,t,z')\in\mathcal{M}}d_{z,t,z'}(\boldsymbol{\xi})\omega_{z,t,z'}+c_{\mathrm{P}}\sum_{(z,t,z')\in\mathcal{M}}d_{z,t,z'}(\boldsymbol{\xi})\\
\text{s.t. }\ & \pi^0_{z,s}+\phi_{z,0}\le c_{\mathrm{I}},\ \forall\,(z,0,s)\in\mathcal{W}^{\mathrm{I}}, && (\text{B.1})\\
& \pi^0_{z,s}+\omega_{z,0,z'}\le -c_{\mathrm{R}}\ell_{z,z'}-c_{\mathrm{P}},\ \forall\,(z,z',0,t',s,s')\in\mathcal{W}^{\mathrm{R}}, && (\text{B.2})\\
& \pi^0_{z,s}\le c_{\mathrm{L}}\ell_{z,z'},\ \forall\,(z,z',0,t',s)\in\mathcal{W}^{\mathrm{L}}, && (\text{B.3})\\
& \pi^0_{z,s}+\phi_{z,0}+\phi^C_{z,0}\le c^{\mathrm{C}}_0,\ \forall\,(z,0,s)\in\mathcal{W}^{\mathrm{C}}, && (\text{B.4})\\
& \pi^0_{z,s}+\phi_{z,0}+\phi^S_{z,0}\le -c^{\mathrm{S}}_0,\ \forall\,(z,0,s)\in\mathcal{W}^{\mathrm{S}}, && (\text{B.5})\\
& \pi_{z,t,s}-\pi_{z',t',s'}+\omega_{z,t,z'}\le -c_{\mathrm{R}}\ell_{z,z'}-c_{\mathrm{P}},\\
& \qquad\qquad \forall\,t'\in[2,T-1]_{\mathbb{Z}},\ (z,z',t,t',s,s')\in\mathcal{W}^{\mathrm{R}}, && (\text{B.6})\\
& \pi_{z,t,s}-\pi_{z,t+1,s}+\phi_{z,t}\le c_{\mathrm{I}},\ \forall\,t\in[1,T-2]_{\mathbb{Z}},\ (z,t,s)\in\mathcal{W}^{\mathrm{I}}, && (\text{B.7})\\
& \pi_{z,t,s}-\pi_{z',t',s}\le c_{\mathrm{L}}\ell_{z,z'},\ \forall\,t'\in[2,T-1]_{\mathbb{Z}},\ (z,z',t,t',s)\in\mathcal{W}^{\mathrm{L}}, && (\text{B.8})\\
& \pi_{z,t,s}-\pi_{z,t+1,s'}+\phi_{z,t}+\phi^{\mathrm{C}}_{z,t}\le c^{\mathrm{C}}_t,\\
& \qquad\qquad \forall\,t\in[1,T-2]_{\mathbb{Z}},\ (z,t,s)\in\mathcal{W}^{\mathrm{C}}, && (\text{B.9})\\
& \pi_{z,t,s}-\pi_{z,t+1,s'}+\phi_{z,t}+\phi^{\mathrm{S}}_{z,t}\le -c^{\mathrm{S}}_t,\\
& \qquad\qquad \forall\,t\in[1,T-2]_{\mathbb{Z}},\ (z,t,s)\in\mathcal{W}^{\mathrm{S}}, && (\text{B.10})\\
& \pi^{\mathrm{T}}+\omega_{z,T-\ell_{z,z'},z'}\le -c_{\mathrm{R}}\ell_{z,z'}-c_{\mathrm{P}},\\
& \qquad\qquad \forall\,(z,z',T-\ell_{z,z'},T,s,s')\in\mathcal{W}^{\mathrm{R}}, && (\text{B.11})\\
& \pi^{\mathrm{T}}+\phi_{z,T-1}\le c_{\mathrm{I}},\ \forall\,(z,T-1,s)\in\mathcal{W}^{\mathrm{I}}, && (\text{B.12})\\
& \pi^{\mathrm{T}}\le c_{\mathrm{L}}\ell_{z,z'},\ \forall\,(z,z',T-\ell_{z,z'},T,s)\in\mathcal{W}^{\mathrm{L}}, && (\text{B.13})\\
& \pi^{\mathrm{T}}+\phi_{z,T-1}+\phi^{\mathrm{C}}_{z,T-1}\le c^{\mathrm{C}}_{T-1},\ \forall\,(z,T-1,s)\in\mathcal{W}^{\mathrm{C}}, && (\text{B.14})\\
& \pi^{\mathrm{T}}+\phi_{z,T-1}+\phi^{\mathrm{S}}_{z,T-1}\le -c^{\mathrm{S}}_{T-1},\ \forall\,(z,T-1,s)\in\mathcal{W}^{\mathrm{S}}, && (\text{B.15})\\
& \omega_{z,t,z'}\le 0,\ \forall\,(z,t,z')\in\mathcal{M};\ \phi_{z,t},\ \phi^{\mathrm{C}}_{z,t},\ \phi^{\mathrm{S}}_{z,t}\le 0,\ \forall\,z\in\mathcal{Z},\ t\in\mathcal{T}. && (\text{B.16})
\end{aligned}
$$

Thus, we define

$$\psi(\mathbf{x},\boldsymbol{\pi},\boldsymbol{\xi}) = \sum_{z\in\mathcal{Z}}\sum_{s\in\mathcal{S}}\pi^0_{z,s}x_{z,s} + \pi^{\mathrm{T}}\sum_{z\in\mathcal{Z}}\sum_{s\in\mathcal{S}}x_{z,s} + \sum_{z\in\mathcal{Z}}\sum_{t\in\mathcal{T}}\phi_{z,t}\sum_{k\in\mathcal{K}}X^k_z + \sum_{z\in\mathcal{Z}}\sum_{t\in\mathcal{T}}\phi^{\mathrm{C}}_{z,t}\left(X^{\mathrm{C}}_z + X^{\mathrm{S}}_z\right)$$
$$+ \sum_{z\in\mathcal{Z}}\sum_{t\in\mathcal{T}}\phi^{\mathrm{S}}_{z,t}X^{\mathrm{S}}_z + \sum_{(z,t,z')\in\mathcal{M}}d_{z,t,z'}(\boldsymbol{\xi})\omega_{z,t,z'} + c_{\mathrm{P}}\sum_{(z,t,z')\in\mathcal{M}}d_{z,t,z'}(\boldsymbol{\xi}), \tag{B.17}$$

and use $\mathcal{Y}$ to denote the feasible region defined by constraints (B.1)–(B.16). Then we can write problem ($\mathcal{P}_{\mathrm{d}}$) in the abstract form: $\max_{\boldsymbol{\pi}\in\mathcal{Y}}\psi(\mathbf{x},\boldsymbol{\pi},\boldsymbol{\xi})$.

By the strong duality theorem, we have $f(\mathbf{x},\boldsymbol{\xi}) = f'(\mathbf{x},\boldsymbol{\xi}) = \max_{\boldsymbol{\pi}\in\mathcal{Y}}\psi(\mathbf{x},\boldsymbol{\pi},\boldsymbol{\xi})$, with any given $(\mathbf{x},\boldsymbol{\xi})$. Therefore, we can equivalently rewrite Problem ($\mathcal{P}_{\mathrm{in}}$) as

$$\min_{\mathbf{Q}\succeq 0,\mathbf{q},r}\ r + \left(\gamma_2\boldsymbol{\Sigma} + \boldsymbol{\mu}\boldsymbol{\mu}^\top\right)\bullet\mathbf{Q} + \boldsymbol{\mu}^\top\mathbf{q} + \sqrt{\gamma_1}\left\|\boldsymbol{\Sigma}^{\frac{1}{2}}\left(\mathbf{q}+2\mathbf{Q}\boldsymbol{\mu}\right)\right\|_2$$
$$\text{s.t. } r \geq \max_{\boldsymbol{\pi}\in\mathcal{Y}}\psi(\mathbf{x},\boldsymbol{\pi},\boldsymbol{\xi}) - \boldsymbol{\xi}^\top\mathbf{Q}\boldsymbol{\xi} - \boldsymbol{\xi}^\top\mathbf{q},\ \forall\boldsymbol{\xi}\in\Omega.$$

It is well known that the optimal solution of a linear programming problem with a non-empty and compact feasible set is adopted at a vertex (Esfahani and Kuhn 2017). This means $\max_{\boldsymbol{\pi}\in\mathcal{Y}}\psi(\mathbf{x},\boldsymbol{\pi},\boldsymbol{\xi}) = \max_{\boldsymbol{\pi}\in vert(\mathcal{Y})}\psi(\mathbf{x},\boldsymbol{\pi},\boldsymbol{\xi})$. Thus, we have Proposition 2 holds. □

B.3 Proof of Proposition 3

Proof. Constraints (3.11) in Problem ($\mathcal{P}'_{\mathrm{in}}$) are equivalent to $\min_{\boldsymbol{\xi}\in\Omega}\ g(\boldsymbol{\xi},\boldsymbol{\pi})\geq 0$ for any $\boldsymbol{\pi}\in vert(\mathcal{Y})$, where $g(\boldsymbol{\xi},\boldsymbol{\pi}) = r - \psi(\mathbf{x},\boldsymbol{\pi},\boldsymbol{\xi}) + \boldsymbol{\xi}^\top\mathbf{Q}\boldsymbol{\xi} + \boldsymbol{\xi}^\top\mathbf{q}$. Given that $\Omega = \{\boldsymbol{\xi}\in\mathbb{R}^{|\mathcal{M}|}\mid \mathbf{b}^{\mathrm{lb}}\leq\mathbf{A}\boldsymbol{\xi}\leq\mathbf{b}^{\mathrm{ub}}\}$, we consider the Lagrange dual problem of $\min_{\boldsymbol{\xi}\in\Omega}\ g(\boldsymbol{\xi},\boldsymbol{\pi})$, i.e., $\max_{\boldsymbol{\lambda}_1,\boldsymbol{\lambda}_2\geq\mathbf{0}}\min_{\boldsymbol{\xi}\in\mathbb{R}^{|\mathcal{M}|}}\ g(\boldsymbol{\xi},\boldsymbol{\pi}) + \boldsymbol{\lambda}_1^\top(\mathbf{A}\boldsymbol{\xi}-\mathbf{b}^{\mathrm{ub}}) - \boldsymbol{\lambda}_2^\top(\mathbf{A}\boldsymbol{\xi}-\mathbf{b}^{\mathrm{lb}})$. Note that $g(\boldsymbol{\xi},\boldsymbol{\pi})$ is convex in $\boldsymbol{\xi}$ because $\mathbf{Q}\succeq 0$. It follows that constraints (3.11) are equivalent to the following ones:

$$\max_{\boldsymbol{\lambda}_1,\boldsymbol{\lambda}_2\geq\mathbf{0}}\min_{\boldsymbol{\xi}\in\mathbb{R}^{|\mathcal{M}|}}\ g(\boldsymbol{\xi},\boldsymbol{\pi}) + \boldsymbol{\lambda}_1^\top\left(\mathbf{A}\boldsymbol{\xi}-\mathbf{b}^{\mathrm{ub}}\right) - \boldsymbol{\lambda}_2^\top\left(\mathbf{A}\boldsymbol{\xi}-\mathbf{b}^{\mathrm{lb}}\right)\geq 0,\ \forall\boldsymbol{\pi}\in vert(\mathcal{Y}),$$

which are further equivalent to the following constraints:

$$\exists\boldsymbol{\lambda}_1,\boldsymbol{\lambda}_2\geq\mathbf{0},\ r - \psi(\mathbf{x},\boldsymbol{\pi},\boldsymbol{\xi}) + \boldsymbol{\xi}^\top\mathbf{Q}\boldsymbol{\xi} + \boldsymbol{\xi}^\top\mathbf{q} + \boldsymbol{\lambda}_1^\top\left(\mathbf{A}\boldsymbol{\xi}-\mathbf{b}^{\mathrm{ub}}\right) - \boldsymbol{\lambda}_2^\top\left(\mathbf{A}\boldsymbol{\xi}-\mathbf{b}^{\mathrm{lb}}\right)\geq 0,$$
$$\forall\boldsymbol{\xi}\in\mathbb{R}^{|\mathcal{M}|},\ \boldsymbol{\pi}\in vert(\mathcal{Y}). \tag{B.18}$$

By definition of $\psi(\mathbf{x}, \boldsymbol{\pi}, \boldsymbol{\xi})$, i.e., (B.17), we can rewrite (B.18) as:

$$\begin{aligned}\exists \boldsymbol{\lambda}_1, \boldsymbol{\lambda}_2 \geq \mathbf{0},\ r - \sum_{z\in\mathcal{Z}}\sum_{s\in\mathcal{S}} \pi^0_{z,s} x_{z,s} - \pi^{\mathrm{T}} \sum_{z\in\mathcal{Z}}\sum_{s\in\mathcal{S}} x_{z,s} - \sum_{z\in\mathcal{Z}}\sum_{t\in\mathcal{T}} \phi_{z,t} \sum_{k\in\mathcal{K}} X^k_z - \sum_{z\in\mathcal{Z}}\sum_{t\in\mathcal{T}} \phi^{\mathrm{C}}_{z,t}\left(X^{\mathrm{C}}_z + X^{\mathrm{S}}_z\right) \\ - \sum_{z\in\mathcal{Z}}\sum_{t\in\mathcal{T}} \phi^{\mathrm{S}}_{z,t} X^{\mathrm{S}}_z - \sum_{(z,t,z')\in\mathcal{M}} d_{z,t,z'}(\boldsymbol{\xi})\omega_{z,t,z'} - c_{\mathrm{P}} \sum_{(z,t,z')\in\mathcal{M}} d_{z,t,z'}(\boldsymbol{\xi}) + \boldsymbol{\xi}^\top \mathbf{Q}\boldsymbol{\xi} + \boldsymbol{\xi}^\top \mathbf{q} \\ + \boldsymbol{\lambda}_1^\top \left(\mathbf{A}\boldsymbol{\xi} - \mathbf{b}^{\mathrm{ub}}\right) - \boldsymbol{\lambda}_2^\top \left(\mathbf{A}\boldsymbol{\xi} - \mathbf{b}^{\mathrm{lb}}\right) \geq 0,\ \forall \boldsymbol{\xi} \in \mathbb{R}^{|\mathcal{M}|},\ \boldsymbol{\pi} \in vert\left(\mathcal{Y}\right),\end{aligned}$$

which are equivalent to

$$\begin{aligned}\exists \boldsymbol{\lambda}_1, \boldsymbol{\lambda}_2 \geq \mathbf{0},\ \boldsymbol{\xi}^\top \mathbf{Q}\boldsymbol{\xi} + r - \psi_1(\mathbf{x}, \boldsymbol{\pi}) - \boldsymbol{\lambda}_1^\top \mathbf{b}^{\mathrm{ub}} + \boldsymbol{\lambda}_2^\top \mathbf{b}^{\mathrm{lb}} + \left(\mathbf{q} + \mathbf{A}^\top(\boldsymbol{\lambda}_1 - \boldsymbol{\lambda}_2) - \psi_2(\boldsymbol{\pi})\right)^\top \boldsymbol{\xi} \geq 0, \\ \forall \boldsymbol{\xi} \in \mathbb{R}^{|\mathcal{M}|},\ \boldsymbol{\pi} \in vert\left(\mathcal{Y}\right), \qquad \text{(B.19)}\end{aligned}$$

where

$$\begin{aligned}\psi_1(\mathbf{x}, \boldsymbol{\pi}) = \sum_{z\in\mathcal{Z}}\sum_{s\in\mathcal{S}} \pi^0_{z,s} x_{z,s} + \pi^{\mathrm{T}} \sum_{z\in\mathcal{Z}}\sum_{s\in\mathcal{S}} x_{z,s} + \sum_{z\in\mathcal{Z}}\sum_{t\in\mathcal{T}} \phi_{z,t} \sum_{k\in\mathcal{K}} X^k_z + \sum_{z\in\mathcal{Z}}\sum_{t\in\mathcal{T}} \phi^{\mathrm{C}}_{z,t}\left(X^{\mathrm{C}}_z + X^{\mathrm{S}}_z\right) \\ + \sum_{z\in\mathcal{Z}}\sum_{t\in\mathcal{T}} \phi^{\mathrm{S}}_{z,t} X^{\mathrm{S}}_z, \\ \psi_2(\boldsymbol{\pi}) = \boldsymbol{\omega} + \mathbf{c}_{\mathrm{P}}.\end{aligned}$$

Thus, we have

$$\begin{aligned}\text{(B.19)} &\Leftrightarrow \exists \boldsymbol{\lambda}_1, \boldsymbol{\lambda}_2 \geq \mathbf{0},\ \left(1, \boldsymbol{\xi}^\top\right) \mathbf{V} \left(1, \boldsymbol{\xi}^\top\right)^\top \geq 0,\ \forall \boldsymbol{\xi} \in \mathbb{R}^{|\mathcal{M}|},\ \boldsymbol{\pi} \in vert\left(\mathcal{Y}\right), \qquad \text{(B.20)} \\ &\Leftrightarrow \exists \boldsymbol{\lambda}_1, \boldsymbol{\lambda}_2 \geq \mathbf{0}, \mathbf{V} \succeq 0,\ \forall \boldsymbol{\pi} \in vert\left(\mathcal{Y}\right), \qquad \text{(B.21)}\end{aligned}$$

where

$$\mathbf{V} = \begin{bmatrix} r - \psi_1(\mathbf{x}, \boldsymbol{\pi}) - \boldsymbol{\lambda}_1^\top \mathbf{b}^{\mathrm{ub}} + \boldsymbol{\lambda}_2^\top \mathbf{b}^{\mathrm{lb}} & \frac{1}{2}\left(\mathbf{q} + \mathbf{A}^\top(\boldsymbol{\lambda}_1 - \boldsymbol{\lambda}_2) - \psi_2(\boldsymbol{\pi})\right)^\top \\ \frac{1}{2}\left(\mathbf{q} + \mathbf{A}^\top(\boldsymbol{\lambda}_1 - \boldsymbol{\lambda}_2) - \psi_2(\boldsymbol{\pi})\right) & \mathbf{Q} \end{bmatrix}.$$

The first equivalence (B.20) holds due to the definition of $\mathbf{V}$. For the second equivalence, $\Leftarrow$ follows from the definition of a positive semidefinite (PSD) matrix. To prove $\Rightarrow$, we consider an arbitrary vector $(\zeta_0 \in \mathbb{R}, \boldsymbol{\zeta}^\top \in \mathbb{R}^{|\mathcal{M}|})^\top \in \mathbb{R}^{|\mathcal{M}|+1}$: (1) if $\zeta_0 = 0$, then $(\zeta_0, \boldsymbol{\zeta}^\top)\mathbf{V}(\zeta_0, \boldsymbol{\zeta}^\top)^\top = \boldsymbol{\zeta}^\top \mathbf{Q}\boldsymbol{\zeta} \geq 0$ because $\mathbf{Q}$ is PSD; (2) if $\zeta_0 \neq 0$, then we have $(\zeta_0, \boldsymbol{\zeta}^\top)\mathbf{V}(\zeta_0, \boldsymbol{\zeta}^\top)^\top = \zeta_0^2(1, \boldsymbol{\zeta}^\top/\zeta_0)\mathbf{V}(1, \boldsymbol{\zeta}^\top/\zeta_0)^\top \geq 0$, because of (B.20). Therefore, $\Rightarrow$

holds.

We obtain Problem ($\mathcal{P}_{\mathrm{F}}$) by replacing constraints (3.11) in Problem ($\mathcal{P}'_{\mathrm{in}}$) with (B.21) and further combine Problem ($\mathcal{P}'_{\mathrm{in}}$) with the outer minimization problem in ($\mathcal{P}_{\mathrm{M}}$).

□

B.4 Proof of Theorem 2

Proof. The proof of the reformulation (3.13) is the same as that of Theorem 1 and thus is omitted here. By Theorem 2 in Cheramin et al. (2022), we have

$$\max_{\mathbb{P}_{m_1}\in\mathcal{D}_{m_1}} \mathbb{E}_{\mathbb{P}_{m_1}}\left[f\left(\mathbf{x}, \mathbf{U}_{|\mathcal{M}|\times m_1}\mathbf{\Lambda}_{m_1}^{\frac{1}{2}}\boldsymbol{\xi}_{m_1}+\boldsymbol{\mu}\right)\right] \leq \max_{\mathbb{P}\in\mathcal{D}} \mathbb{E}_{\mathbb{P}}\left[f\left(\mathbf{x},\boldsymbol{\xi}\right)\right],$$

for any $\mathbf{x}$. This follows that

$$\sum_{z\in\mathcal{Z}}\sum_{s\in\mathcal{S}} c_s x_{z,s} + \max_{\mathbb{P}_{m_1}\in\mathcal{D}_{m_1}} \mathbb{E}_{\mathbb{P}_{m_1}}\left[f\left(\mathbf{x}, \mathbf{U}_{|\mathcal{M}|\times m_1}\mathbf{\Lambda}_{m_1}^{\frac{1}{2}}\boldsymbol{\xi}_{m_1}+\boldsymbol{\mu}\right)\right] \leq \sum_{z\in\mathcal{Z}}\sum_{s\in\mathcal{S}} c_s x_{z,s} + \max_{\mathbb{P}\in\mathcal{D}} \mathbb{E}_{\mathbb{P}}\left[f\left(\mathbf{x},\boldsymbol{\xi}\right)\right],$$

for any $\mathbf{x}$ satisfying constraints (3.1) – (3.2).

Therefore,

$$\begin{aligned}
&\min_{\mathbf{x}}\left\{\sum_{z\in\mathcal{Z}}\sum_{s\in\mathcal{S}} c_s x_{z,s} + \max_{\mathbb{P}_{m_1}\in\mathcal{D}_{m_1}} \mathbb{E}_{\mathbb{P}_{m_1}}\left[f\left(\mathbf{x}, \mathbf{U}_{|\mathcal{M}|\times m_1}\mathbf{\Lambda}_{m_1}^{\frac{1}{2}}\boldsymbol{\xi}_{m_1}+\boldsymbol{\mu}\right)\right] \middle| (3.1)-(3.2)\right\} \\
&\leq \min_{\mathbf{x}}\left\{\sum_{z\in\mathcal{Z}}\sum_{s\in\mathcal{S}} c_s x_{z,s} + \max_{\mathbb{P}\in\mathcal{D}} \mathbb{E}_{\mathbb{P}}\left[f\left(\mathbf{x},\boldsymbol{\xi}\right)\right] \middle| (3.1)-(3.2)\right\}.
\end{aligned}$$

Therefore, the optimal value of Problem (3.12) (i.e., Problem (3.13)) provides a lower bound for the optimal value of Problem ($\mathcal{P}_{\mathrm{M}}$).

By Theorem 2 in Cheramin et al. (2022), we have $\mathcal{D}_{m_1} \subset \mathcal{D}_{m_2}$ for $m_1 < m_2$. This follows that

$$\max_{\mathbb{P}_{m_1}\in\mathcal{D}_{m_1}} \mathbb{E}_{\mathbb{P}_{m_1}}\left[f\left(\mathbf{x}, \mathbf{U}_{|\mathcal{M}|\times m_1}\mathbf{\Lambda}_{m_1}^{\frac{1}{2}}\boldsymbol{\xi}_{m_1}+\boldsymbol{\mu}\right)\right] \leq \max_{\mathbb{P}_{m_2}\in\mathcal{D}_{m_2}} \mathbb{E}_{\mathbb{P}_{m_2}}\left[f\left(\mathbf{x}, \mathbf{U}_{|\mathcal{M}|\times m_2}\mathbf{\Lambda}_{m_2}^{\frac{1}{2}}\boldsymbol{\xi}_{m_2}+\boldsymbol{\mu}\right)\right]$$

for any $\mathbf{x}$. Therefore, we have

$$\begin{aligned}
&\min_{\mathbf{x}}\left\{\sum_{z\in\mathcal{Z}}\sum_{s\in\mathcal{S}} c_s x_{z,s} + \max_{\mathbb{P}_{m_1}\in\mathcal{D}_{m_1}} \mathbb{E}_{\mathbb{P}_{m_1}}\left[f\left(\mathbf{x}, \mathbf{U}_{|\mathcal{M}|\times m_1}\mathbf{\Lambda}_{m_1}^{\frac{1}{2}}\boldsymbol{\xi}_{m_1}+\boldsymbol{\mu}\right)\right] \middle| (3.1)-(3.2)\right\} \\
&\leq \min_{\mathbf{x}}\left\{\sum_{z\in\mathcal{Z}}\sum_{s\in\mathcal{S}} c_s x_{z,s} + \max_{\mathbb{P}_{m_2}\in\mathcal{D}_{m_2}} \mathbb{E}_{\mathbb{P}_{m_2}}\left[f\left(\mathbf{x}, \mathbf{U}_{|\mathcal{M}|\times m_2}\mathbf{\Lambda}_{m_2}^{\frac{1}{2}}\boldsymbol{\xi}_{m_2}+\boldsymbol{\mu}\right)\right] \middle| (3.1)-(3.2)\right\}.
\end{aligned}$$

That is, the optimal value of Problem (3.13) is nondecreasing in m_1.

Finally, Problem (3.12) is equivalent to Problem ($\mathcal{P}_{\mathrm{I}}$) (i.e., Problem ($\mathcal{P}_{\mathrm{M}}$)) when $m_1 = |\mathcal{M}|$. Then, Problems (3.13) and ($\mathcal{P}_{\mathrm{M}}$) have the same optimal value. □

B.5 Proof of Proposition 4

Proof. The proof is similar with that of Propositions 2 and 3 and thus is omitted here. □

B.6 Proof of Theorem 3

Proof. The proof of the reformulation (3.16) is the same as that of Theorem 1 and thus is omitted here. By Theorem 4 in Cheramin et al. (2022), we have $\mathcal{D}_{\mathrm{I}} \subset \mathcal{D}_{\mathrm{U}}$. Therefore, for any $\mathbf{x}$, we have

$$\max_{\mathbb{P}_{\mathrm{I}} \in \mathcal{D}_{\mathrm{I}}} \mathbb{E}_{\mathbb{P}_{\mathrm{I}}} \left[f\left(\mathbf{x}, \mathbf{U}\boldsymbol{\Lambda}^{\frac{1}{2}}\boldsymbol{\xi}_{\mathrm{I}} + \boldsymbol{\mu}\right)\right] \leq \max_{\mathbb{P}_{\mathrm{U}} \in \mathcal{D}_{\mathrm{U}}} \mathbb{E}_{\mathbb{P}_{\mathrm{U}}} \left[f\left(\mathbf{x}, \mathbf{U}\boldsymbol{\Lambda}^{\frac{1}{2}}\boldsymbol{\xi}_{\mathrm{I}} + \boldsymbol{\mu}\right)\right].$$

This follows that

$$\sum_{z\in\mathcal{Z}}\sum_{s\in\mathcal{S}} c_s x_{z,s} + \max_{\mathbb{P}_{\mathrm{I}} \in \mathcal{D}_{\mathrm{I}}} \mathbb{E}_{\mathbb{P}_{\mathrm{I}}} \left[f\left(\mathbf{x}, \mathbf{U}\boldsymbol{\Lambda}^{\frac{1}{2}}\boldsymbol{\xi}_{\mathrm{I}} + \boldsymbol{\mu}\right)\right] \leq \sum_{z\in\mathcal{Z}}\sum_{s\in\mathcal{S}} c_s x_{z,s} + \max_{\mathbb{P}_{\mathrm{U}} \in \mathcal{D}_{\mathrm{U}}} \mathbb{E}_{\mathbb{P}_{\mathrm{U}}} \left[f\left(\mathbf{x}, \mathbf{U}\boldsymbol{\Lambda}^{\frac{1}{2}}\boldsymbol{\xi}_{\mathrm{I}} + \boldsymbol{\mu}\right)\right],$$

for any $\mathbf{x}$ satisfying constraints (3.1) – (3.2). Therefore,

$$\begin{aligned}
&\min_{\mathbf{x}} \left\{ \sum_{z\in\mathcal{Z}}\sum_{s\in\mathcal{S}} c_s x_{z,s} + \max_{\mathbb{P}_{\mathrm{I}} \in \mathcal{D}_{\mathrm{I}}} \mathbb{E}_{\mathbb{P}_{\mathrm{I}}} \left[f\left(\mathbf{x}, \mathbf{U}\boldsymbol{\Lambda}^{\frac{1}{2}}\boldsymbol{\xi}_{\mathrm{I}} + \boldsymbol{\mu}\right)\right] \middle| (3.1) - (3.2) \right\} \\
&\leq \min_{\mathbf{x}} \left\{ \sum_{z\in\mathcal{Z}}\sum_{s\in\mathcal{S}} c_s x_{z,s} + \max_{\mathbb{P}_{\mathrm{U}} \in \mathcal{D}_{\mathrm{U}}} \mathbb{E}_{\mathbb{P}_{\mathrm{U}}} \left[f\left(\mathbf{x}, \mathbf{U}\boldsymbol{\Lambda}^{\frac{1}{2}}\boldsymbol{\xi}_{\mathrm{I}} + \boldsymbol{\mu}\right)\right] \middle| (3.1) - (3.2) \right\}.
\end{aligned}$$

Therefore, the optimal value of Problem (3.15) (i.e., Problem (3.16)) provides an upper bound for the optimal value of Problem ($\mathcal{P}_{\mathrm{I}}$) (i.e., Problem ($\mathcal{P}_{\mathrm{M}}$)). □

B.7 Proof of Proposition 5

Proof. This result is deduced from Proposition 5 in Cheramin et al. (2022). □

B.8 Formulations of Problems in Algorithm 2

For any sub-network $\mathcal{G}_l$, $l \in \{1, \ldots, L\}$, we formulate Problem $({\mathcal{P}_0}^l)$ based on it as the following:

$$\min_{\mathbf{x}} \left\{ \sum_{z\in\mathcal{Z}} \sum_{s\in\mathcal{S}} c_s x_{z,s} + \mathbb{E}_{\mathbb{P}} \left[f_l \left(\mathbf{x}, \boldsymbol{\xi} \right) \right] \middle| (3.1) - (3.2) \right\},$$

where

$$\begin{aligned}
f_l \left(\mathbf{x}, \boldsymbol{\xi} \right) = \min_{\mathbf{w}} \ & \sum_{a\in\mathcal{A}_l} c_a w_a(\boldsymbol{\xi}) + c_{\mathrm{P}} \sum_{(z,t,z')\in\mathcal{M}_l} \left(d_{z,t,z'}(\boldsymbol{\xi}) - \sum_{a\in\hat{\mathcal{A}}_l^{\mathrm{R}}(z,t,z')} w_a(\boldsymbol{\xi}) \right) \\
\text{s.t.} \ & \sum_{a\in\mathcal{A}_{l+}(n_{z,t_0,s})} w_a(\boldsymbol{\xi}) = x_{z,s}, \ \forall\, z \in \mathcal{Z},\ s \in \mathcal{S}, \\
& \sum_{a\in\mathcal{A}_{l+}(n_{z,t,s})} w_a(\boldsymbol{\xi}) = \sum_{a\in\mathcal{A}_{l-}(n_{z,t,s})} w_a(\boldsymbol{\xi}), \ \forall\, t \in [t_0+1, t'-1]_{\mathbb{Z}},\ z \in \mathcal{Z},\ s \in \mathcal{S}, \\
& \sum_{z\in\mathcal{Z}} \sum_{s\in\mathcal{S}} \sum_{a\in\mathcal{A}_{l-}(n_{z,t',s})} w_a(\boldsymbol{\xi}) = \sum_{z\in\mathcal{Z}} \sum_{s\in\mathcal{S}} x_{z,s}, \\
& \sum_{a\in\hat{\mathcal{A}}_l^{\mathrm{R}}(z,t,z')} w_a(\boldsymbol{\xi}) \le d_{z,t,z'}(\boldsymbol{\xi}), \ \forall\, (z,t,z') \in \mathcal{M}_l, \\
& \sum_{s\in\mathcal{S}} \sum_{a\in\cup_{k\in\mathcal{K}}\mathcal{A}_{l+}^k(n_{z,t,s})} w_a(\boldsymbol{\xi}) \le \sum_{k\in\mathcal{K}} X_z^k, \ \forall\, z \in \mathcal{Z},\ t \in \mathcal{T}_l, \\
& \sum_{s\in\mathcal{S}} \sum_{a\in\mathcal{A}_{l+}^{\mathrm{C}}(n_{z,t,s})} w_a(\boldsymbol{\xi}) \le X_z^{\mathrm{C}} + X_z^{\mathrm{S}}, \ \forall\, z \in \mathcal{Z},\ t \in \mathcal{T}_l, \\
& \sum_{s\in\mathcal{S}} \sum_{a\in\mathcal{A}_{l+}^{\mathrm{S}}(n_{z,t,s})} w_a(\boldsymbol{\xi}) \le X_z^{\mathrm{S}}, \ \forall\, z \in \mathcal{Z},\ t \in \mathcal{T}_l, \\
& w_a \ge 0, \ \forall\, a \in \mathcal{A}_l,
\end{aligned}$$

where $t_0 = 0$ if $l = 1$ and $t_0 = \sum_{i=1}^{l-1} T_i + 1$ otherwise, and $t' = \sum_{i=1}^{l} T_i$.

Appendix C

Supplements for Chapter 4

C.1 Table of Notation

Table C.1. Summary of Notation

Notation	Description
Sets:	
$\mathcal{S}$	set of scenarios
$\mathcal{T}$	operational horizon $\mathcal{T} = \{1, 2, \ldots, T\}$
$\mathcal{B}$	set of nodes (termed "power bus") in the power grid system
$\mathcal{L}$	set of bidirectional power transmission lines in the power grid system
$\mathcal{G}$	set of thermal generators in the power grid system
Parameters:	
SU^g, SD^g	start-up and shut-down costs of generator $g \in \mathcal{G}$, respectively
L^g, ℓ^g	minimum-up/-down time limits of generator $g \in \mathcal{G}$
$p^{\mathrm{w}}_{b,t}$, $p^{\mathrm{s}}_{b,t}$, $q_{b,t}$	wind generation, solar generation, and power load in bus $b \in \mathcal{B}$ and period $t \in \mathcal{T}$, respectively
$\underline{C}^g$, $\overline{C}^g$	generation lower/upper bounds of generator $g \in \mathcal{G}$
V^g, $\overline{V}^g$	ramp-up/down rate limit of generator $g \in \mathcal{G}$ when it is online and starts up/shuts down, respectively
R^+_t, R^-_t	minimum required regulation-up and regulation-down amounts in period $t \in \mathcal{T}$, respectively
$X_{b',b}$, $C_{b',b}$	reactance and capacity of power transmission line $(b', b) \in \mathcal{L}$
a^g, b^g, c^g	cost parameters of generator $g \in \mathcal{G}$
RU^g, RD^g	regulation-up and regulation-down cost of $g \in \mathcal{G}$, respectively
P^+_t, P^-_t	unit price the grid pays to the EV fleet and the EV fleet pays to the grid in period $t \in \mathcal{T}$, respectively
C_{sub}	unit subsidy offered by the grid system to the mobility system
$\overline{X}$, S_0	the EV fleet's size and initial SOC, respectively
d_t	EV trip demand in period $t \in \mathcal{T}$
$\overline{X}^+$, $\overline{X}^-$	discharging and charging amounts limits, respectively
$\overline{S}$	EV battery capacity
α	service level promised by the grid system to the mobility system
e^-, e^+, e^{r}	electricity consumed in charging, discharging, and satisfying trip demands in a period, respectively
δ	time length of a period
Variables:	
u^g_t	$u^g_t = 1$ if generator $g \in \mathcal{G}$ starts up in period $t \in \mathcal{T}$ and $u^g_t = 0$ otherwise

y_t^g	$y_t^g = 1$ if generator $g \in \mathcal{G}$ is online in period $t \in \mathcal{T}$ and $y_t^g = 0$ otherwise
p_t^g	amount of electricity generated by generator $g \in \mathcal{G}$ in period $t \in \mathcal{T}$
$r_t^{g^+}$, $r_t^{g^-}$	regulation-up and regulation-down amounts reserved by generator $g \in \mathcal{G}$ in period $t \in \mathcal{T}$, respectively
$\beta_{b,t}$	phase angle in bus $b \in \mathcal{B}$ and period $t \in \mathcal{T}$
v_t^+, v_t^-	amounts of electricity the EV fleet discharges to the power grid and the EV fleet charges from the power grid in period $t \in \mathcal{T}$, respectively
f_t^g	power generation cost of generator $g \in \mathcal{G}$ in period $t \in \mathcal{T}$
x_t^{r}	number of EVs to satisfy the realized trip demand d_t in period $t \in \mathcal{T}$
x_t^+, x_t^-	number of EVs to satisfy the power transfer requests from the power grid in period $t \in \mathcal{T}$
s_t	SOC level of the EV fleet in period $t \in \mathcal{T}$
o_t	service level discrepancy between the realized level and the promised level (α) in period $t \in \mathcal{T}$
v_t^{r}	power output level needed to satisfy EV trip demands in period $t \in \mathcal{T}$
Abbreviations:	
EV	electric vehicle
V2G	vehicle-to-grid
GVI	grid-vehicle integration
RO	robust optimization
MIP	mixed-integer programming
LP	linear programming
MILP	mixed-integer linear programming
ADMM	alternating direction method of multipliers

C.2 Proof of Theorem 4

Proof. For any $g \in \mathcal{G}$, we have $(u_t^g)^2 = u_t^g$ for any $t \in \mathcal{T} \setminus \{1\}$ and $(y_t^g)^2 = y_t^g$ for any $t \in \mathcal{T}$ when $u_t^g \in \{0,1\}$ and $y_t^g \in \{0,1\}$. Thus, the objective function of Problem (Fsub) can be rewritten as

$$\begin{aligned}\mathcal{L}\left(\mathbf{u},\mathbf{y},\overline{z},\overline{\mathbf{u}}',\overline{\mathbf{y}}',\overline{\boldsymbol{\pi}},\overline{\boldsymbol{\lambda}}\right) = &\sum_{g\in\mathcal{G}}\sum_{t=2}^{T}\left(\mathrm{SU}^g u_t^g + \mathrm{SD}^g\left(y_{t-1}^g - y_t^g + u_t^g\right)\right) + \overline{z} \\ &+ \sum_{n\in\mathcal{N}}\sum_{g\in\mathcal{G}}\sum_{t=2}^{T}\overline{\pi}_{n,g,t}\left(u_t^g - \overline{u}_{n,t}^{g\prime}\right) + \frac{\rho_1}{2}\sum_{n\in\mathcal{N}}\sum_{g\in\mathcal{G}}\sum_{t=2}^{T}\left(u_t^g - 2\overline{u}_{n,t}^{g\prime}u_t^g + \overline{u}_{n,t}^{g\prime\,2}\right) \\ &+ \sum_{n\in\mathcal{N}}\sum_{g\in\mathcal{G}}\sum_{t\in\mathcal{T}}\overline{\lambda}_{n,g,t}\left(y_t^g - \overline{y}_{n,t}^{g\prime}\right) + \frac{\rho_2}{2}\sum_{n\in\mathcal{N}}\sum_{g\in\mathcal{G}}\sum_{t\in\mathcal{T}}\left(y_t^g - 2\overline{y}_{n,t}^{g\prime}y_t^g + \overline{y}_{n,t}^{g\prime\,2}\right).\end{aligned}$$

By rearranging the terms in $\mathcal{L}(\mathbf{u}, \mathbf{y}, \overline{z}, \overline{\mathbf{u}}', \overline{\mathbf{y}}', \overline{\boldsymbol{\pi}}, \overline{\boldsymbol{\lambda}})$, we can rewrite Problem (Fsub) as

$$\min \Bigg\{ \sum_{g\in\mathcal{G}} \sum_{t=2}^{T} \left(\mathrm{SU}^g u_t^g + \mathrm{SD}^g \left(y_{t-1}^g - y_t^g + u_t^g\right)\right) + \overline{z} + \sum_{n\in\mathcal{N}} \sum_{g\in\mathcal{G}} \sum_{t=2}^{T} \left(\overline{\pi}_{n,g,t} u_t^g + \frac{\rho_1}{2}\left(u_t^g - 2\overline{u}_{n,t}^{g\prime} u_t^g\right)\right)$$
$$+ \sum_{n\in\mathcal{N}} \sum_{g\in\mathcal{G}} \sum_{t\in\mathcal{T}} \left(\overline{\lambda}_{n,g,t} y_t^g + \frac{\rho_2}{2}\left(y_t^g - 2\overline{y}_{n,t}^{g\prime} y_t^g\right)\right) - \sum_{n\in\mathcal{N}} \sum_{g\in\mathcal{G}} \sum_{t=2}^{T} \left(\overline{\pi}_{n,g,t}\overline{u}_{n,t}^{g\prime} - \frac{\rho_1}{2}\overline{u}_{n,t}^{g\prime\,2}\right)$$
$$- \sum_{n\in\mathcal{N}} \sum_{g\in\mathcal{G}} \sum_{t\in\mathcal{T}} \left(\overline{\lambda}_{n,g,t}\overline{y}_{n,t}^{g\prime} - \frac{\rho_2}{2}\overline{y}_{n,t}^{g\prime\,2}\right) \;\Big|\; (4.1) - (4.5) \Bigg\}. \tag{C.1}$$

Because $\rho_1, \rho_2, \overline{z}, \overline{u}_{n,t}^{g\prime}, \overline{\pi}_{n,g,t}$ for any $n \in \mathcal{N}$, $g \in \mathcal{G}$, and $t \in \mathcal{T} \setminus \{1\}$, and $\overline{y}_{n,t}^{g\prime}, \overline{\lambda}_{n,g,t}$ for any $n \in \mathcal{N}$, $g \in \mathcal{G}$, and $t \in \mathcal{T}$ are all given parameters, solving Problem (C.1) is equivalent to solving the following problem:

$$\min \Bigg\{ \sum_{g\in\mathcal{G}} \sum_{t=2}^{T} \left(\mathrm{SU}^g u_t^g + \mathrm{SD}^g \left(y_{t-1}^g - y_t^g + u_t^g\right)\right) + \sum_{n\in\mathcal{N}} \sum_{g\in\mathcal{G}} \sum_{t=2}^{T} \left(\overline{\pi}_{n,g,t} u_t^g + \frac{\rho_1}{2}\left(u_t^g - 2\overline{u}_{n,t}^{g\prime} u_t^g\right)\right)$$
$$+ \sum_{n\in\mathcal{N}} \sum_{g\in\mathcal{G}} \sum_{t\in\mathcal{T}} \left(\overline{\lambda}_{n,g,t} y_t^g + \frac{\rho_2}{2}\left(y_t^g - 2\overline{y}_{n,t}^{g\prime} y_t^g\right)\right) \;\Big|\; (4.1) - (4.5) \Bigg\}. \tag{C.2}$$

Theorem 2.10 in Rajan et al. (2005) shows that (4.1)–(4.4) define the convex hull of (4.1)–(4.5). Note that the objective function of Problem (C.2) is linear in u_t^g for any $t \in \mathcal{T} \setminus \{1\}$ and $g \in \mathcal{G}$ and y_t^g for any $t \in \mathcal{T}$ and $g \in \mathcal{G}$. Thus, Problem (C.2) is equivalent to the following problem:

$$\min \Bigg\{ \sum_{g\in\mathcal{G}} \sum_{t=2}^{T} \left(\mathrm{SU}^g u_t^g + \mathrm{SD}^g \left(y_{t-1}^g - y_t^g + u_t^g\right)\right) + \sum_{n\in\mathcal{N}} \sum_{g\in\mathcal{G}} \sum_{t=2}^{T} \left(\overline{\pi}_{n,g,t} u_t^g + \frac{\rho_1}{2}\left(u_t^g - 2\overline{u}_{n,t}^{g\prime} u_t^g\right)\right)$$
$$+ \sum_{n\in\mathcal{N}} \sum_{g\in\mathcal{G}} \sum_{t\in\mathcal{T}} \left(\overline{\lambda}_{n,g,t} y_t^g + \frac{\rho_2}{2}\left(y_t^g - 2\overline{y}_{n,t}^{g\prime} y_t^g\right)\right) \;\Big|\; (4.1) - (4.4) \Bigg\},$$

which is Problem ($\mathrm{Fsub_R}$). □

C.3 Proof of Proposition 6

Proof. We consider the augmented Lagrangian functions $\mathcal{L}(\mathbf{u}, \mathbf{y}, z, \mathbf{u}', \mathbf{y}', \boldsymbol{\pi}, \boldsymbol{\lambda})$ for Problem ($\mathcal{M}_2$) and $\mathcal{L}_n(\mathbf{u}, \mathbf{y}, z, \mathbf{u}'_n, \mathbf{y}'_n, \boldsymbol{\pi}_n, \boldsymbol{\lambda}_n)$ for Problem (Ssub_n) with each $n \in \mathcal{N}$ and examine how the values of these functions update after each iteration.

First, for any $n \in \mathcal{N}$ and iteration step $m \geq 1$, $(z^m, z_n^m, \mathbf{u}_n'^{\,m}, \mathbf{y}_n'^{\,m}, \boldsymbol{\gamma}_j^m, \forall j \in \mathcal{S}_n)$ and $(z^{m+1}, z_n^{m+1}, \mathbf{u}_n'^{\,m+1}, \mathbf{y}_n'^{\,m+1}, \boldsymbol{\gamma}_j^{m+1}, \forall j \in \mathcal{S}_n)$ solve Problem (Ssub_n), which is convex, in the

iteration steps $m-1$ and m, respectively. By the first-order optimality condition of a convex optimization problem, we have

$$\begin{aligned}
&\bigtriangledown_z \mathcal{L}_n \left(\mathbf{u}^m, \mathbf{y}^m, z^{m+1}, \mathbf{u}_n'^{\,m+1}, \mathbf{y}_n'^{\,m+1}, \boldsymbol{\pi}_n^m, \boldsymbol{\lambda}_n^m\right)^\top \left(z^m - z^{m+1}\right) \\
&+ \bigtriangledown_{\mathbf{u}_n'} \mathcal{L}_n \left(\mathbf{u}^m, \mathbf{y}^m, z^{m+1}, \mathbf{u}_n'^{\,m+1}, \mathbf{y}_n'^{\,m+1}, \boldsymbol{\pi}_n^m, \boldsymbol{\lambda}_n^m\right)^\top \left(\mathbf{u}_n'^{\,m} - \mathbf{u}_n'^{\,m+1}\right) \\
&+ \bigtriangledown_{\mathbf{y}_n'} \mathcal{L}_n \left(\mathbf{u}^m, \mathbf{y}^m, z^{m+1}, \mathbf{u}_n'^{\,m+1}, \mathbf{y}_n'^{\,m+1}, \boldsymbol{\pi}_n^m, \boldsymbol{\lambda}_n^m\right)^\top \left(\mathbf{y}_n'^{\,m} - \mathbf{y}_n'^{\,m+1}\right) \geq 0, \ \forall n \in \mathcal{N}. \quad \text{(C.3)}
\end{aligned}$$

The derivative terms in (C.3) correspond to variables z, $\mathbf{u}_n'$, and $\mathbf{y}_n'$ for any $n \in \mathcal{N}$, respectively. To better represent these derivative terms, for any $n \in \mathcal{N}$, we define

$$\begin{aligned}
\mathcal{U}\left(\mathbf{u}, \mathbf{u}_n', \boldsymbol{\pi}_n\right) &= \boldsymbol{\pi}_n^\top (\mathbf{u} - \mathbf{u}_n') + \frac{\rho_1}{2} \left\|\mathbf{u} - \mathbf{u}_n'\right\|^2, \\
\mathcal{Y}\left(\mathbf{y}, \mathbf{y}_n', \boldsymbol{\lambda}_n\right) &= \boldsymbol{\lambda}_n^\top \left(\mathbf{y} - \mathbf{y}_n'\right) + \frac{\rho_2}{2} \left\|\mathbf{y} - \mathbf{y}_n'\right\|^2, \ \mathcal{Z}(z) = z,
\end{aligned}$$

and rewrite $\mathcal{L}_n(\cdot)$ as follows:

$$\mathcal{L}_n \left(\mathbf{u}, \mathbf{y}, z, \mathbf{u}', \mathbf{y}', \boldsymbol{\pi}_n, \boldsymbol{\lambda}_n\right) = \mathcal{F}(\mathbf{u}, \mathbf{y}) + \mathcal{U}\left(\mathbf{u}, \mathbf{u}_n', \boldsymbol{\pi}_n\right) + \mathcal{Y}\left(\mathbf{y}, \mathbf{y}_n', \boldsymbol{\lambda}_n\right) + \mathcal{Z}(z).$$

Thus, we can rewrite (C.3) as

$$\begin{aligned}
&\bigtriangledown_z \mathcal{Z}\left(z^{m+1}\right)^\top \left(z^m - z^{m+1}\right) + \bigtriangledown_{\mathbf{u}_n'} \mathcal{U}\left(\mathbf{u}^m, \mathbf{u}_n'^{\,m+1}, \boldsymbol{\pi}_n^m\right)^\top \left(\mathbf{u}_n'^{\,m} - \mathbf{u}_n'^{\,m+1}\right) \\
&\qquad + \bigtriangledown_{\mathbf{y}_n'} \mathcal{Y}\left(\mathbf{y}^m, \mathbf{y}_n'^{\,m+1}, \boldsymbol{\lambda}_n^m\right)^\top \left(\mathbf{y}_n'^{\,m} - \mathbf{y}_n'^{\,m+1}\right) \geq 0, \ \forall n \in \mathcal{N}. \quad \text{(C.4)}
\end{aligned}$$

Note that $\mathcal{Z}(z)$ is convex in z and $\mathcal{U}(\mathbf{u}, \mathbf{u}_n', \boldsymbol{\pi}_n)$ and $\mathcal{Y}(\mathbf{y}, \mathbf{y}_n', \boldsymbol{\lambda}_n)$ are strongly convex in $\mathbf{u}_n'$ and $\mathbf{y}_n'$, respectively, for any $n \in \mathcal{N}$. Therefore, there exist $\epsilon_1 > 0$ and $\epsilon_2 > 0$ such that

$$\begin{aligned}
&\mathcal{Z}\left(z^m\right) - \mathcal{Z}\left(z^{m+1}\right) \geq \bigtriangledown_z \mathcal{Z}\left(z^{m+1}\right)^\top \left(z^m - z^{m+1}\right), \\
&\mathcal{U}\left(\mathbf{u}^m, \mathbf{u}_n'^{\,m}, \boldsymbol{\pi}_n^m\right) - \mathcal{U}\left(\mathbf{u}^m, \mathbf{u}_n'^{\,m+1}, \boldsymbol{\pi}_n^m\right) \geq \bigtriangledown_{\mathbf{u}_n'} \mathcal{U}\left(\mathbf{u}^m, \mathbf{u}_n'^{\,m+1}, \boldsymbol{\pi}_n^m\right)^\top \left(\mathbf{u}_n'^{\,m} - \mathbf{u}_n'^{\,m+1}\right) \\
&\qquad\qquad + \epsilon_1 \left\|\mathbf{u}_n'^{\,m} - \mathbf{u}_n'^{\,m+1}\right\|^2, \\
&\mathcal{Y}\left(\mathbf{y}^m, \mathbf{y}_n'^{\,m}, \boldsymbol{\lambda}_n^m\right) - \mathcal{Y}\left(\mathbf{y}^m, \mathbf{y}_n'^{\,m+1}, \boldsymbol{\lambda}_n^m\right) \geq \bigtriangledown_{\mathbf{y}_n'} \mathcal{Y}\left(\mathbf{y}^m, \mathbf{y}_n'^{\,m+1}, \boldsymbol{\lambda}_n^m\right)^\top \left(\mathbf{y}_n'^{\,m} - \mathbf{y}_n'^{\,m+1}\right) \\
&\qquad\qquad + \epsilon_2 \left\|\mathbf{y}_n'^{\,m} - \mathbf{y}_n'^{\,m+1}\right\|^2.
\end{aligned}$$

It follows that

$$
\begin{aligned}
&\mathcal{L}_n\left(\mathbf{u}^m, \mathbf{y}^m, z^m, \mathbf{u}_n'^m, \mathbf{y}_n'^m, \boldsymbol{\pi}_n^m, \boldsymbol{\lambda}_n^m\right) - \mathcal{L}_n\left(\mathbf{u}^m, \mathbf{y}^m, z^{m+1}, \mathbf{u}_n'^{m+1}, \mathbf{y}_n'^{m+1}, \boldsymbol{\pi}_n^m, \boldsymbol{\lambda}_n^m\right) \\
&= \mathcal{Z}\left(z^m\right) + \mathcal{U}\left(\mathbf{u}^m, \mathbf{u}_n'^m, \boldsymbol{\pi}_n^m\right) + \mathcal{Y}\left(\mathbf{y}^m, \mathbf{y}_n'^m, \boldsymbol{\lambda}_n^m\right) \\
&\quad - \mathcal{Z}\left(z^{m+1}\right) - \mathcal{U}\left(\mathbf{u}^m, \mathbf{u}_n'^{m+1}, \boldsymbol{\pi}_n^m\right) - \mathcal{Y}\left(\mathbf{y}^m, \mathbf{y}_n'^{m+1}, \boldsymbol{\lambda}_n^m\right) \\
&\geq \bigtriangledown_z \mathcal{Z}\left(z^{m+1}\right)^\top \left(z^m - z^{m+1}\right) + \bigtriangledown_{\mathbf{u}_n'} \mathcal{U}\left(\mathbf{u}^m, \mathbf{u}_n'^{m+1}, \boldsymbol{\pi}_n^m\right)^\top \left(\mathbf{u}_n'^m - \mathbf{u}_n'^{m+1}\right) + \epsilon_1 \left\|\mathbf{u}_n'^m - \mathbf{u}_n'^{m+1}\right\|^2 \\
&\quad + \bigtriangledown_{\mathbf{y}_n'} \mathcal{Y}\left(\mathbf{y}^m, \mathbf{y}_n'^{m+1}, \boldsymbol{\lambda}_n^m\right)^\top \left(\mathbf{y}_n'^m - \mathbf{y}_n'^{m+1}\right) + \epsilon_2 \left\|\mathbf{y}_n'^m - \mathbf{y}_n'^{m+1}\right\|^2 \\
&\geq \epsilon_1 \left\|\mathbf{u}_n'^m - \mathbf{u}_n'^{m+1}\right\|^2 + \epsilon_2 \left\|\mathbf{y}_n'^m - \mathbf{y}_n'^{m+1}\right\|^2,
\end{aligned}
$$

where the second inequality holds by (C.4). Thus, we further have

$$
\begin{aligned}
&\mathcal{L}\left(\mathbf{u}^m, \mathbf{y}^m, z^m, \mathbf{u}'^m, \mathbf{y}'^m, \boldsymbol{\pi}^m, \boldsymbol{\lambda}^m\right) - \mathcal{L}\left(\mathbf{u}^m, \mathbf{y}^m, z^{m+1}, \mathbf{u}'^{m+1}, \mathbf{y}'^{m+1}, \boldsymbol{\pi}^m, \boldsymbol{\lambda}^m\right) \\
&= z^m - z^{m+1} + \sum_{n=1}^N \left(\boldsymbol{\pi}_n^{m\top}\left(\mathbf{u}^m - \mathbf{u}_n'^m\right) + \boldsymbol{\lambda}_n^{m\top}\left(\mathbf{y}^m - \mathbf{y}_n'^m\right) + \frac{\rho_1}{2}\left\|\mathbf{u}^m - \mathbf{u}_n'^m\right\|^2 + \frac{\rho_2}{2}\left\|\mathbf{y}^m - \mathbf{y}_n'^m\right\|^2\right) \\
&\quad - \sum_{n=1}^N \left(\boldsymbol{\pi}_n^{m\top}\left(\mathbf{u}^m - \mathbf{u}_n'^{m+1}\right) + \boldsymbol{\lambda}_n^{m\top}\left(\mathbf{y}^m - \mathbf{y}_n'^{m+1}\right) + \frac{\rho_1}{2}\left\|\mathbf{u}^m - \mathbf{u}_n'^{m+1}\right\|^2 + \frac{\rho_2}{2}\left\|\mathbf{y}^m - \mathbf{y}_n'^{m+1}\right\|^2\right) \\
&= \sum_{n=1}^N \left(\mathcal{L}_n\left(\mathbf{u}^m, \mathbf{y}^m, z_n^m, \mathbf{u}_n'^m, \mathbf{y}_n'^m, \boldsymbol{\pi}_n^m, \boldsymbol{\lambda}_n^m\right) - \mathcal{L}_n\left(\mathbf{u}^m, \mathbf{y}^m, z_n^{m+1}, \mathbf{u}_n'^{m+1}, \mathbf{y}_n'^{m+1}, \boldsymbol{\pi}_n^m, \boldsymbol{\lambda}_n^m\right)\right) \\
&\quad - \sum_{n=1}^N \left(z_n^m - z_n^{m+1}\right) + z^m - z^{m+1} \\
&\geq \sum_{n=1}^N \left(\epsilon_1 \left\|\mathbf{u}_n'^m - \mathbf{u}_n'^{m+1}\right\|^2 + \epsilon_2 \left\|\mathbf{y}_n'^m - \mathbf{y}_n'^{m+1}\right\|^2\right) - \sum_{n=1}^N \left(z_n^m - z_n^{m+1}\right) + z^m - z^{m+1}, \qquad \text{(C.5)}
\end{aligned}
$$

where $z^m = \max_{n\in\mathcal{N}}\{z_n^m\}$ and $z^{m+1} = \max_{n\in\mathcal{N}}\{z_n^{m+1}\}$. The inequality (C.5) suggests how the objective value of Problem (Ssub) is updated after we solve Problems (Ssub$_n$) for any $n \in \mathcal{N}$ in each iteration step m.

Second, as $(\mathbf{u}^{m+1}, \mathbf{y}^{m+1})$ solves Problem (Fsub$_\mathrm{R}$) in the iteration step m and $(\mathbf{u}^m, \mathbf{y}^m)$ is feasible to Problem (Fsub$_\mathrm{R}$), we have

$$
\begin{aligned}
&\mathcal{L}\left(\mathbf{u}^m, \mathbf{y}^m, z^{m+1}, \mathbf{u}'^{m+1}, \mathbf{y}'^{m+1}, \boldsymbol{\pi}^m, \boldsymbol{\lambda}^m\right) \\
&\qquad - \mathcal{L}\left(\mathbf{u}^{m+1}, \mathbf{y}^{m+1}, z^{m+1}, \mathbf{u}'^{m+1}, \mathbf{y}'^{m+1}, \boldsymbol{\pi}^m, \boldsymbol{\lambda}^m\right) \geq 0. \qquad \text{(C.6)}
\end{aligned}
$$

Note that Algorithm 3 updates $\boldsymbol{\pi}_n^{m+1} = \boldsymbol{\pi}_n^m + \rho_1(\mathbf{u}^{m+1} - \mathbf{u}_n'^{m+1})$ and $\boldsymbol{\lambda}_n^{m+1} = \boldsymbol{\lambda}_n^m +$

$\rho_2(\mathbf{y}^{m+1} - \mathbf{y}_n'^{m+1})$ for any $n \in \mathcal{N}$ in the iteration step m. Thus, we have

$$
\begin{aligned}
&\mathcal{L}\left(\mathbf{u}^{m+1}, \mathbf{y}^{m+1}, z^{m+1}, \mathbf{u}'^{m+1}, \mathbf{y}'^{m+1}, \boldsymbol{\pi}^{m}, \boldsymbol{\lambda}^{m}\right) - \mathcal{L}\left(\mathbf{u}^{m+1}, \mathbf{y}^{m+1}, z^{m+1}, \mathbf{u}'^{m+1}, \mathbf{y}'^{m+1}, \boldsymbol{\pi}^{m+1}, \boldsymbol{\lambda}^{m+1}\right) \\
&= \sum_{n=1}^{N} \boldsymbol{\pi}_n^{m\top}\left(\mathbf{u}^{m+1} - \mathbf{u}_n'^{m+1}\right) + \sum_{n=1}^{N} \boldsymbol{\lambda}_n^{m\top}\left(\mathbf{y}^{m+1} - \mathbf{y}_n'^{m+1}\right) \\
&\quad - \sum_{n=1}^{N} \boldsymbol{\pi}_n^{m+1\top}\left(\mathbf{u}^{m+1} - \mathbf{u}_n'^{m+1}\right) - \sum_{n=1}^{N} \boldsymbol{\lambda}_n^{m+1\top}\left(\mathbf{y}^{m+1} - \mathbf{y}_n'^{m+1}\right) \\
&= \sum_{n=1}^{N} \left(\left(\boldsymbol{\pi}_n^{m} - \boldsymbol{\pi}_n^{m+1}\right)^{\top}\left(\mathbf{u}^{m+1} - \mathbf{u}_n'^{m+1}\right) + \left(\boldsymbol{\lambda}_n^{m} - \boldsymbol{\lambda}_n^{m+1}\right)^{\top}\left(\mathbf{y}^{m+1} - \mathbf{y}_n'^{m+1}\right)\right) \\
&= -\sum_{n=1}^{N} \left(\frac{1}{\rho_1}\left\|\boldsymbol{\pi}_n^{m} - \boldsymbol{\pi}_n^{m+1}\right\|^2 + \frac{1}{\rho_2}\left\|\boldsymbol{\lambda}_n^{m} - \boldsymbol{\lambda}_n^{m+1}\right\|^2\right). \qquad \text{(C.7)}
\end{aligned}
$$

The inequality (C.6) suggests how the objective value of Problem (Fsub_R) is updated in the iteration step m. The equality (C.7) suggests how the value of $\mathcal{L}(\cdot)$ is updated after we update multipliers $\boldsymbol{\pi}^m$ and $\boldsymbol{\lambda}^m$ to $\boldsymbol{\pi}^{m+1}$ and $\boldsymbol{\lambda}^{m+1}$ in the iteration step m.

Third, by (C.5), (C.6), and (C.7), for any iteration step $m \geq 1$, we have

$$
\begin{aligned}
&\mathcal{L}\left(\mathbf{u}^{m}, \mathbf{y}^{m}, z^{m}, \mathbf{u}'^{m}, \mathbf{y}'^{m}, \boldsymbol{\pi}^{m}, \boldsymbol{\lambda}^{m}\right) - \mathcal{L}\left(\mathbf{u}^{m+1}, \mathbf{y}^{m+1}, z^{m+1}, \mathbf{u}'^{m+1}, \mathbf{y}'^{m+1}, \boldsymbol{\pi}^{m+1}, \boldsymbol{\lambda}^{m+1}\right) \\
&= \mathcal{L}\left(\mathbf{u}^{m}, \mathbf{y}^{m}, z^{m}, \mathbf{u}'^{m}, \mathbf{y}'^{m}, \boldsymbol{\pi}^{m}, \boldsymbol{\lambda}^{m}\right) - \mathcal{L}\left(\mathbf{u}^{m}, \mathbf{y}^{m}, z^{m+1}, \mathbf{u}'^{m+1}, \mathbf{y}'^{m+1}, \boldsymbol{\pi}^{m}, \boldsymbol{\lambda}^{m}\right) \\
&\quad + \mathcal{L}\left(\mathbf{u}^{m}, \mathbf{y}^{m}, z^{m+1}, \mathbf{u}'^{m+1}, \mathbf{y}'^{m+1}, \boldsymbol{\pi}^{m}, \boldsymbol{\lambda}^{m}\right) - \mathcal{L}\left(\mathbf{u}^{m+1}, \mathbf{y}^{m+1}, z^{m+1}, \mathbf{u}'^{m+1}, \mathbf{y}'^{m+1}, \boldsymbol{\pi}^{m}, \boldsymbol{\lambda}^{m}\right) \\
&\quad + \mathcal{L}\left(\mathbf{u}^{m+1}, \mathbf{y}^{m+1}, z^{m+1}, \mathbf{u}'^{m+1}, \mathbf{y}'^{m+1}, \boldsymbol{\pi}^{m}, \boldsymbol{\lambda}^{m}\right) - \mathcal{L}\left(\mathbf{u}^{m+1}, \mathbf{y}^{m+1}, z^{m+1}, \mathbf{u}'^{m+1}, \mathbf{y}'^{m+1}, \boldsymbol{\pi}^{m+1}, \boldsymbol{\lambda}^{m+1}\right) \\
&\geq \sum_{n=1}^{N} \left(\epsilon_1\left\|\mathbf{u}_n'^{m} - \mathbf{u}_n'^{m+1}\right\|^2 + \epsilon_2\left\|\mathbf{y}_n'^{m} - \mathbf{y}_n'^{m+1}\right\|^2\right) - \sum_{n=1}^{N}\left(z_n^{m} - z_n^{m+1}\right) + z^{m} - z^{m+1} \\
&\qquad - \sum_{n=1}^{N} \left(\frac{1}{\rho_1}\left\|\boldsymbol{\pi}_n^{m} - \boldsymbol{\pi}_n^{m+1}\right\|^2 + \frac{1}{\rho_2}\left\|\boldsymbol{\lambda}_n^{m} - \boldsymbol{\lambda}_n^{m+1}\right\|^2\right).
\end{aligned}
$$

Summing up both sides of the above inequality from $m = 1$ to $m = \infty$, we have

$$
\begin{aligned}
&\mathcal{L}\left(\mathbf{u}^{1}, \mathbf{y}^{1}, z^{1}, \mathbf{u}'^{1}, \mathbf{y}'^{1}, \boldsymbol{\pi}^{1}, \boldsymbol{\lambda}^{1}\right) - \mathcal{L}\left(\mathbf{u}^{\infty}, \mathbf{y}^{\infty}, z^{\infty}, \mathbf{u}'^{\infty}, \mathbf{y}'^{\infty}, \boldsymbol{\pi}^{\infty}, \boldsymbol{\lambda}^{\infty}\right) \\
&\geq \sum_{m=1}^{\infty}\sum_{n=1}^{N} \left(\epsilon_1\left\|\mathbf{u}_n'^{m} - \mathbf{u}_n'^{m+1}\right\|^2 + \epsilon_2\left\|\mathbf{y}_n'^{m} - \mathbf{y}_n'^{m+1}\right\|^2\right) - \sum_{n=1}^{N}\left(z_n^{1} - z_n^{\infty}\right) + z^{1} - z^{\infty} \\
&\qquad - \sum_{m=1}^{\infty}\sum_{n=1}^{N} \left(\frac{1}{\rho_1}\left\|\boldsymbol{\pi}_n^{m} - \boldsymbol{\pi}_n^{m+1}\right\|^2 + \frac{1}{\rho_2}\left\|\boldsymbol{\lambda}_n^{m} - \boldsymbol{\lambda}_n^{m+1}\right\|^2\right).
\end{aligned}
$$

That is,

$$\begin{aligned}
&\mathcal{L}\left(\mathbf{u}^1, \mathbf{y}^1, z^1, \mathbf{u}'^1, \mathbf{y}'^1, \boldsymbol{\pi}^1, \boldsymbol{\lambda}^1\right) - \mathcal{L}\left(\mathbf{u}^\infty, \mathbf{y}^\infty, z^\infty, \mathbf{u}'^\infty, \mathbf{y}'^\infty, \boldsymbol{\pi}^\infty, \boldsymbol{\lambda}^\infty\right) + \sum_{n=1}^{N}\left(z_n^1 - z_n^\infty\right) - z^1 + z^\infty \\
&\quad + \sum_{m=1}^{\infty}\sum_{n=1}^{N}\left(\frac{1}{\rho_1}\left\|\boldsymbol{\pi}_n^m - \boldsymbol{\pi}_n^{m+1}\right\|^2 + \frac{1}{\rho_2}\left\|\boldsymbol{\lambda}_n^m - \boldsymbol{\lambda}_n^{m+1}\right\|^2\right) \\
&\geq \sum_{m=1}^{\infty}\sum_{n=1}^{N}\left(\epsilon_1\left\|\mathbf{u}_n'^{\,m} - \mathbf{u}_n'^{\,m+1}\right\|^2 + \epsilon_2\left\|\mathbf{y}_n'^{\,m} - \mathbf{y}_n'^{\,m+1}\right\|^2\right) \geq 0. \qquad \text{(C.8)}
\end{aligned}$$

As the feasible region of Problem (ALP)'s LP relaxation is bounded, we have $\mathbf{u}^m$, $\mathbf{y}^m$, $\mathbf{u}'^m$, $\mathbf{y}'^m$, z^m, and z_n^m for any $n \in \mathcal{N}$ and $m \geq 1$ are all bounded. Meanwhile, by the assumption that $\sum_{m=1}^{\infty}\sum_{n=1}^{N}\|\boldsymbol{\pi}_n^{m+1} - \boldsymbol{\pi}_n^m\|^2 < \infty$ and $\sum_{m=1}^{\infty}\sum_{n=1}^{N}\|\boldsymbol{\lambda}_n^{m+1} - \boldsymbol{\lambda}_n^m\|^2 < \infty$, we have $\boldsymbol{\pi}_n^m$ and $\boldsymbol{\lambda}_n^m$ for any $n \in \mathcal{N}$ and $m \geq 1$ are also bounded. Thus, $\mathcal{L}(\mathbf{u}^m, \mathbf{y}^m, z^m, \mathbf{u}'^m, \mathbf{y}'^m, \boldsymbol{\pi}^m, \boldsymbol{\lambda}^m)$ is bounded for any iteration step m and the left-hand side of (C.8) is bounded. It follows that

$$\infty > \sum_{m=1}^{\infty}\sum_{n=1}^{N}\left(\epsilon_1\left\|\mathbf{u}_n'^{\,m} - \mathbf{u}_n'^{\,m+1}\right\|^2 + \epsilon_2\left\|\mathbf{y}_n'^{\,m} - \mathbf{y}_n'^{\,m+1}\right\|^2\right) \geq 0, \qquad \text{(C.9)}$$

which implies that

$$\left\|\mathbf{u}_n'^{\,m} - \mathbf{u}_n'^{\,m+1}\right\|^2 \to 0,\ \left\|\mathbf{y}_n'^{\,m} - \mathbf{y}_n'^{\,m+1}\right\|^2 \to 0,\ \text{as } m \to \infty,\ \forall n \in \mathcal{N}. \qquad \text{(C.10)}$$

As $\sum_{m=1}^{\infty}\sum_{n=1}^{N}\|\boldsymbol{\pi}_n^{m+1} - \boldsymbol{\pi}_n^m\|^2 < \infty$ and $\sum_{m=1}^{\infty}\sum_{n=1}^{N}\|\boldsymbol{\lambda}_n^{m+1} - \boldsymbol{\lambda}_n^m\|^2 < \infty$, we further have

$$\left\|\boldsymbol{\pi}_n^{m+1} - \boldsymbol{\pi}_n^m\right\|^2 \to 0,\ \left\|\boldsymbol{\lambda}_n^{m+1} - \boldsymbol{\lambda}_n^m\right\|^2 \to 0,\ \text{as } m \to \infty,\ \forall n \in \mathcal{N},$$

which indicates that

$$\left\|\mathbf{u}^{m+1} - \mathbf{u}_n'^{\,m+1}\right\|^2 = \frac{1}{\rho_1^2}\left\|\boldsymbol{\pi}_n^{m+1} - \boldsymbol{\pi}_n^m\right\|^2 \to 0,\ \text{as } m \to \infty,\ \forall n \in \mathcal{N}, \qquad \text{(C.11)}$$

$$\left\|\mathbf{y}^{m+1} - \mathbf{y}_n'^{\,m+1}\right\|^2 = \frac{1}{\rho_2^2}\left\|\boldsymbol{\lambda}_n^{m+1} - \boldsymbol{\lambda}_n^m\right\|^2 \to 0,\ \text{as } m \to \infty,\ \forall n \in \mathcal{N}. \qquad \text{(C.12)}$$

By the triangular inequality, we have

$$\left\|\mathbf{u}^m - \mathbf{u}^{m+1}\right\|^2 \leq \left\|\mathbf{u}^m - \mathbf{u}_n'^{\,m}\right\|^2 + \left\|\mathbf{u}_n'^{\,m} - \mathbf{u}_n'^{\,m+1}\right\|^2 + \left\|\mathbf{u}_n'^{\,m+1} - \mathbf{u}^{m+1}\right\|^2,\ \forall n \in \mathcal{N},$$

which, by (C.10) and (C.11), indicates that $\|\mathbf{u}^m - \mathbf{u}^{m+1}\|^2 \to 0$ as $m \to \infty$. Similarly, we

can show $\|\mathbf{y}^m - \mathbf{y}^{m+1}\|^2 \to 0$ as $m \to \infty$. □

C.4 Boundedness of Dual Multipliers of Problems (Fsub_R) and (Ssub_n) for any $n \in \mathcal{N}$

To prove Theorem 5, we discuss the boundedness of dual multipliers of Problems (Fsub_R) and (Ssub_n) for any $n \in \mathcal{N}$ in this section. First, we consider Problem (Fsub_R). Note that Problem (Fsub_R) is separable with respect to each generator $g \in \mathcal{G}$. It suffices to drop the superscript g here and consider the following problem:

$$
\begin{aligned}
\min \quad & \sum_{t=2}^{T} \left(\text{SU} u_t + \text{SD}\left(y_{t-1} - y_t + u_t\right)\right) + \sum_{n\in\mathcal{N}} \sum_{t=2}^{T} \left(\overline{\pi}_{n,t} u_t + \frac{\rho_1}{2}\left(u_t - 2\overline{u}'_{n,t} u_t\right)\right) \\
& + \sum_{n\in\mathcal{N}} \sum_{t\in\mathcal{T}} \left(\overline{\lambda}_{n,t} y_t + \frac{\rho_2}{2}\left(y_t - 2\overline{y}'_{n,t} y_t\right)\right) \\
\text{s.t.} \quad & u_t - y_t + y_{t-1} \geq 0, \ \forall t \in \mathcal{T} \setminus \{1\}, && \text{(C.13a)} \\
& \sum_{i=t-L+1}^{t} u_i - y_t \leq 0, \ \forall t \in [L+1, T]_\mathbb{Z}, && \text{(C.13b)} \\
& \sum_{i=t-\ell+1}^{t} u_i + y_{t-\ell} \leq 1, \ \forall t \in [\ell+1, T]_\mathbb{Z}, && \text{(C.13c)} \\
& u_t \geq 0, \ \forall t \in \mathcal{T} \setminus \{1\}. && \text{(C.13d)}
\end{aligned}
$$

We use $\eta_t^1 \leq 0$ ($\forall t \in \mathcal{T} \setminus \{1\}$), $\eta_t^2 \geq 0$ ($\forall t \in [L+1, T]_\mathbb{Z}$), $\eta_t^3 \geq 0$ ($\forall t \in [\ell+1, T]_\mathbb{Z}$), and $\eta_t^4 \leq 0$ ($\forall t \in \mathcal{T} \setminus \{1\}$) to denote the dual multipliers with respect to constraints (C.13a)–(C.13d), respectively. We use the above four groups of notations with a superscript $*$ to denote the corresponding optimal dual multipliers when Problem (C.13) is solved. We have the following proposition holds.

Proposition 11. *Given bounded $\overline{\mathbf{u}}'$, $\overline{\mathbf{y}}'$, $\overline{\boldsymbol{\pi}}$, and $\overline{\boldsymbol{\lambda}}$, we have η_t^{1*} ($\forall t \in \mathcal{T} \setminus \{1\}$), η_t^{2*} ($\forall t \in [L+1, T]_\mathbb{Z}$), η_t^{3*} ($\forall t \in [\ell+1, T]_\mathbb{Z}$), and η_t^{4*} ($\forall t \in \mathcal{T} \setminus \{1\}$) are bounded.*

Proof. First, we consider η_t^{3*} for any $t \in [\ell+1, T]_\mathbb{Z}$. Note that the dual problem's objective value equals $\sum_{t\in[\ell+1,T]_\mathbb{Z}} \eta_t^{3*}$, which is bounded by strong duality. Thus, η_t^{3*} is bounded for any $t \in [\ell+1, T]_\mathbb{Z}$.

Second, we consider η_t^{1*} for any $t \in \mathcal{T} \setminus \{1\}$. Note that the stationary condition with

respect to y_1 is

$$\mathrm{SD} + \sum_{n\in\mathcal{N}} \left(\overline{\lambda}_{n,1} + \frac{\rho_2}{2}\left(1 - 2\overline{y}'_{n,1}\right)\right) + \eta_2^{1^*} + {\eta_{\ell+1}^3}^* = 0.$$

Because ${\eta_{\ell+1}^3}^*$ is bounded and the given parameters, i.e., $\overline{\boldsymbol{\lambda}}$ and $\overline{\mathbf{y}}'$, are bounded, we have $\eta_2^{1^*}$ is bounded. For any $t \in \mathcal{T} \setminus \{1, T\}$, the stationary condition with respect to y_t can be formulated as

$${\eta_{t+1}^1}^* - \eta_t^{1^*} = \mathcal{W}^2(t) - \mathcal{W}^3(t) - \sum_{n\in\mathcal{N}} \left(\overline{\lambda}_{n,t} + \frac{\rho_2}{2}\left(1 - 2\overline{y}'_{n,t}\right)\right) := \delta'(t)$$

where $\mathcal{W}^2(t) = \eta_t^{2^*}$ if $t \in [L+1, T]_{\mathbb{Z}}$ and $\mathcal{W}^2(t) = 0$ otherwise, and $\mathcal{W}^3(t) = {\eta_{t+\ell}^3}^*$ if $t \in [1, T-\ell]_{\mathbb{Z}}$ and $\mathcal{W}^3(t) = 0$ otherwise. Clearly, $\delta'(t) > -\infty$ for any $t \in \mathcal{T} \setminus \{1, T\}$. Thus, we have ${\eta_{t+1}^1}^* = \eta_2^{1^*} + \sum_{s=2}^{t} \delta'(s) > -\infty$ for any $t \in \mathcal{T} \setminus \{1, T\}$. That is, $\eta_t^{1^*}$ is bounded for any $t \in \mathcal{T} \setminus \{1\}$.

Third, we consider $\eta_t^{2^*}$ for any $t \in [L+1, T]_{\mathbb{Z}}$. With respect to y_t for any $t \in [L+1, T-1]_{\mathbb{Z}}$, the stationary condition is

$$\eta_t^{2^*} = \sum_{n\in\mathcal{N}} \left(\overline{\lambda}_{n,t} + \frac{\rho_2}{2}\left(1 - 2\overline{y}'_{n,t}\right)\right) + {\eta_{t+1}^1}^* - \eta_t^{1^*} + \mathcal{W}^3(t),$$

which follows that $\eta_t^{2^*}$ is bounded for any $t \in [L+1, T-1]_{\mathbb{Z}}$. In addition, with respect to y_T, the stationary condition is

$${\eta_T^2}^* = -\mathrm{SD} + \sum_{n\in\mathcal{N}} \left(\overline{\lambda}_{n,T} + \frac{\rho_2}{2}\left(1 - 2\overline{y}'_{n,T}\right)\right) - \eta_T^{1^*},$$

which follows that ${\eta_T^2}^*$ is bounded.

Fourth, we consider $\eta_t^{4^*}$ for any $t \in \mathcal{T} \setminus \{1\}$. With respect to u_t for any $t \in \mathcal{T} \setminus \{1\}$, the stationary condition is

$$\mathrm{SU} + \mathrm{SD} + \sum_{n\in\mathcal{N}} \left(\overline{\pi}_{n,t} + \frac{\rho_1}{2}\left(1 - 2\overline{u}'_{n,t}\right)\right) + \eta_t^{1^*} + \sum_{s=\max\{t,L+1\}}^{\min\{t+L-1,T\}} \eta_s^{2^*} + \sum_{s=\max\{t,\ell+1\}}^{\min\{t+\ell-1,T\}} \eta_s^{3^*} = -\eta_t^{4^*}.$$

As all the terms on the left-hand side of the above equation are bounded, we conclude that $\eta_t^{4^*}$ is bounded for any $t \in \mathcal{T} \setminus \{1\}$. □

Next, we consider Problem (Ssub$_n$) for any $n \in \mathcal{N}$. For any $n \in \mathcal{N}$, we let $\mathcal{S}'$ denote the set $\mathcal{S}_n$ and z' denote the variable z in Problem (Ssub$_n$), by which we rewrite Problem

(Ssub$_n$) as

$$\min \left\{ \mathcal{L}_n(\overline{\mathbf{u}}, \overline{\mathbf{y}}, z', \mathbf{u}'_n, \mathbf{y}'_n, \overline{\boldsymbol{\pi}}_n, \overline{\boldsymbol{\lambda}}_n) \;\middle|\; z' \geq z_n,\ \mathcal{H}^2(\mathbf{y}'_n, z_n, \boldsymbol{\gamma}_j, \boldsymbol{\xi}_j) = \mathbf{0},\ \forall j \in \mathcal{S}' \right\}.$$

For simplicity, we drop the subscript n and then the problem becomes

$$\min\ \mathcal{F}(\overline{\mathbf{u}}, \overline{\mathbf{y}}) + z' + \overline{\boldsymbol{\pi}}^\top \left(\overline{\mathbf{u}} - \mathbf{u}'\right) + \overline{\boldsymbol{\lambda}}^\top \left(\overline{\mathbf{y}} - \mathbf{y}'\right) + \frac{\rho_1}{2} \left\|\overline{\mathbf{u}} - \mathbf{u}'\right\|^2 + \frac{\rho_2}{2} \left\|\overline{\mathbf{y}} - \mathbf{y}'\right\|^2 \quad \text{(C.14a)}$$

$$\text{s.t.}\ \ z' \geq z, \quad \text{(C.14b)}$$

$$\mathcal{H}^2(\mathbf{y}', z, \boldsymbol{\gamma}_j, \boldsymbol{\xi}_j) = \mathbf{0},\ \forall j \in \mathcal{S}'.$$

Thus, it suffices to study the dual multipliers of Problem (C.14). Specifically, we focus on the multipliers corresponding to the constraints involving $\mathbf{y}'$, i.e., constraints (4.7)–(4.9), (4.11), and (4.16) applied for any $j \in \mathcal{S}'$. For ease of exposition, we list such constraints as follows:

$$p^g_{t,j} + r^{g+}_{t,j} - \left(\overline{C}^g - \underline{C}^g\right) y^{g'}_t \leq 0,\ \forall t \in \mathcal{T}, g \in \mathcal{G}, j \in \mathcal{S}',$$

$$p^g_{t,j} + r^{g+}_{t,j} - p^g_{t-1,j} - \left(V^g + \underline{C}^g - \overline{V}^g\right) y^{g'}_{t-1} + \underline{C}^g y^{g'}_t \leq \overline{V}^g,\ \forall t \in \mathcal{T} \setminus \{1\}, g \in \mathcal{G}, j \in \mathcal{S}',$$

$$p^g_{t-1,j} - p^g_{t,j} + r^{g-}_{t,j} - \left(V^g + \underline{C}^g - \overline{V}^g\right) y^{g'}_t + \underline{C}^g y^{g'}_{t-1} \leq \overline{V}^g,\ \forall t \in \mathcal{T} \setminus \{1\}, g \in \mathcal{G}, j \in \mathcal{S}',$$

$$\sum_{g \in \mathcal{G}_b} \underline{C}^g y^{g'}_t + \sum_{g \in \mathcal{G}_b} p^g_{t,j} + \sum_{\forall b' \in \mathcal{B}:\ (b',b) \in \mathcal{L}} \frac{\beta_{b',t,j} - \beta_{b,t,j}}{X_{b',b}} + v^+_{t,j} - v^-_{t,j} = q_{b,t,j} - p^{\mathrm{w}}_{b,t,j} - p^{\mathrm{s}}_{b,t,j},$$

$$\forall b \in \mathcal{B}, t \in \mathcal{T}, j \in \mathcal{S}',$$

$$f^g_{t,j} - \left(a^g (\underline{C}^g)^2 + b^g \underline{C}^g + c^g\right) y^{g'}_t - \sum_{h \in \mathcal{H}} \zeta^g_h \overline{p}^g_{t,h,j} \geq 0,\ \forall t \in \mathcal{T}, g \in \mathcal{G}, j \in \mathcal{S}'.$$

We define $\theta^1_{t,g,j} \geq 0$ ($\forall t \in \mathcal{T}, g \in \mathcal{G}, j \in \mathcal{S}'$), $\theta^2_{t,g,j} \geq 0$ ($\forall t \in \mathcal{T} \setminus \{1\}, g \in \mathcal{G}, j \in \mathcal{S}'$), $\theta^3_{t,g,j} \geq 0$ ($\forall t \in \mathcal{T} \setminus \{1\}, g \in \mathcal{G}, j \in \mathcal{S}'$), $\theta^4_{b,t,j}$ ($\forall b \in \mathcal{B}, t \in \mathcal{T}, j \in \mathcal{S}'$), and $\theta^5_{t,g,j} \leq 0$ ($\forall t \in \mathcal{T}, g \in \mathcal{G}, j \in \mathcal{S}'$) to represent the dual multipliers corresponding to the above five groups of constraints, respectively. We use the above five groups of notations with a superscript $*$ to denote the corresponding optimal dual multipliers when Problem (C.14) is solved, where the optimal primal solution is $\mathbf{y}'^*$. We have the following proposition holds.

Proposition 12. *Given bounded $\overline{\mathbf{u}}$, $\overline{\mathbf{y}}$, $\overline{\boldsymbol{\pi}}$, and $\overline{\boldsymbol{\lambda}}$, if the objective value of Problem (Ssub$_n$)'s dual problem is bounded for any $n \in \mathcal{N}$, then $\theta^{1*}_{t,g,j}$ ($\forall t \in \mathcal{T}, g \in \mathcal{G}, j \in \mathcal{S}'$), $\theta^{2*}_{t,g,j}$ ($\forall t \in \mathcal{T} \setminus \{1\}, g \in \mathcal{G}, j \in \mathcal{S}'$), $\theta^{3*}_{t,g,j}$ ($\forall t \in \mathcal{T} \setminus \{1\}, g \in \mathcal{G}, j \in \mathcal{S}'$), $\theta^{4*}_{b,t,j}$ ($\forall b \in \mathcal{B}, t \in \mathcal{T}, j \in \mathcal{S}'$), and $\theta^{5*}_{t,g,j}$ ($\forall t \in \mathcal{T}, g \in \mathcal{G}, j \in \mathcal{S}'$) are bounded.*

Proof. For any $t \in \mathcal{T} \setminus \{T\}$ and $g \in \mathcal{G}$, we write the stationary condition with respect to $y_t^{g'}$ as

$$
\begin{aligned}
&-\overline{\lambda}_{t,g} - \rho_2 \left(\overline{y}_t^g - y_t^{g'^*}\right) - \left(\overline{C}^g - \underline{C}^g\right) \sum_{j \in \mathcal{S}'} \theta_{t,g,j}^{1^*} + \underline{C}^g \sum_{j \in \mathcal{S}'} \theta_{t,g,j}^{2^*} - \left(V^g + \underline{C}^g - \overline{V}^g\right) \sum_{j \in \mathcal{S}'} \theta_{t+1,g,j}^{2^*} \\
&\quad - \left(V^g + \underline{C}^g - \overline{V}^g\right) \sum_{j \in \mathcal{S}'} \theta_{t,g,j}^{3^*} + \underline{C}^g \sum_{j \in \mathcal{S}'} \theta_{t+1,g,j}^{3^*} + \underline{C}^g \sum_{j \in \mathcal{S}'} \theta_{\omega(g),t,j}^{4^*} \\
&\quad - \left(a^g (\underline{C}^g)^2 + b^g \underline{C}^g + c^g\right) \sum_{j \in \mathcal{S}'} \theta_{t,g,j}^{5^*} = 0, \qquad \text{(C.15)}
\end{aligned}
$$

where $\omega(g) = b$ if $g \in \mathcal{G}_b$ for any $g \in \mathcal{G}$. Because each generator $g \in \mathcal{G}$ locates in only one bus, $\omega(g)$ returns a unique value in $\mathcal{B}$. For any $g \in \mathcal{G}$, we write the stationary condition with respect to $y_T^{g'}$ as follows

$$
\begin{aligned}
&-\overline{\lambda}_{T,g} - \rho_2 \left(\overline{y}_T^g - y_T^{g'^*}\right) - \left(\overline{C}^g - \underline{C}^g\right) \sum_{j \in \mathcal{S}'} \theta_{T,g,j}^{1^*} + \underline{C}^g \sum_{j \in \mathcal{S}'} \theta_{T,g,j}^{2^*} - \left(V^g + \underline{C}^g - \overline{V}^g\right) \sum_{j \in \mathcal{S}'} \theta_{T,g,j}^{3^*} \\
&\quad + \underline{C}^g \sum_{j \in \mathcal{S}'} \theta_{\omega(g),T,j}^{4^*} - \left(a^g (\underline{C}^g)^2 + b^g \underline{C}^g + c^g\right) \sum_{j \in \mathcal{S}'} \theta_{T,g,j}^{5^*} = 0. \qquad \text{(C.16)}
\end{aligned}
$$

First, we consider $\theta_{t,g,j}^{5^*}$ for any $t \in \mathcal{T}$, $g \in \mathcal{G}$, and $j \in \mathcal{S}'$. With respect to constraint (C.14b), we define a dual multiplier $\theta^{z'} \leq 0$. Then the stationary condition with respect to z' is $1 + \theta^{z'^*} = 0$, i.e., $\theta^{z'^*} = -1$. With respect to constraints (4.30) for any $j \in \mathcal{S}'$, we define a dual multiplier $\theta_j^z \leq 0$. Then the stationary condition with respect to z is $-\theta^{z'^*} + \sum_{j \in \mathcal{S}'} \theta_j^{z^*} = 0$, i.e., $\sum_{j \in \mathcal{S}'} \theta_j^{z^*} = \theta^{z'^*} = -1$. Thus, $\theta_j^{z^*}$ is bounded for any $j \in \mathcal{S}'$. Now, for any $t \in \mathcal{T}$, $g \in \mathcal{G}$, and $j \in \mathcal{S}'$, we write the stationary condition with respect to $f_{t,j}^g$ as $\theta_{t,g,j}^{5^*} - \theta_j^{z^*} = 0$, indicating that $\theta_{t,g,j}^{5^*}$ is bounded.

Second, note that the right-hand sides of constraints (4.8)–(4.9) and (4.11) include non-negative constants. By the assumption that the objective value of Problem (Ssub_n)'s dual problem is bounded for any $n \in \mathcal{N}$, we have $\theta_{t,g,j}^{2^*}$ $(\forall t \in \mathcal{T} \setminus \{1\}, g \in \mathcal{G}, j \in \mathcal{S}')$, $\theta_{t,g,j}^{3^*}$ $(\forall t \in \mathcal{T} \setminus \{1\}, g \in \mathcal{G}, j \in \mathcal{S}')$, and $\theta_{b,t,j}^{4^*}$ $(\forall b \in \mathcal{B}, t \in \mathcal{T}, j \in \mathcal{S}')$ are bounded.

Third, in (C.15) and (C.16), as all the terms except those involving $\theta_{t,g,j}^{1^*}$ for any $t \in \mathcal{T}$, $g \in \mathcal{G}$, and $j \in \mathcal{S}'$ are bounded, we have $\theta_{t,g,j}^{1^*}$ is also bounded. □

C.5 Proof of Theorem 5

Proof. By Proposition 6 and the conditions of Theorem 5, there exists a subsequence $\{(\mathbf{u}^m, \mathbf{y}^m, \boldsymbol{\pi}^m, \boldsymbol{\lambda}^m),\ \forall m \in \mathcal{K}\}$ that converges to $(\mathbf{u}^*, \mathbf{y}^*, \boldsymbol{\pi}^*, \boldsymbol{\lambda}^*)$ as $m \to \infty$ and $m \in \mathcal{K}$.

By (C.11) and (C.12), we also have $\{(\mathbf{u}_n'^{\,m}, \mathbf{y}_n'^{\,m}),\ \forall m \in \mathcal{K}\}$ converges to $(\mathbf{u}^*, \mathbf{y}^*)$ as $m \to \infty$ and $m \in \mathcal{K}$ for any $n \in \mathcal{N}$. Now, we analyze the stationary and complementary slackness conditions of Problems (Fsub_R) and (Ssub_n) for any $n \in \mathcal{N}$. First, we consider Problem (Fsub_R) and rewrite it in the following abstract form:

$$\begin{aligned} &\min\ \mathcal{F}(\mathbf{u}, \mathbf{y}) + \sum_{n=1}^{N} \overline{\boldsymbol{\pi}}_n^\top \mathbf{u} + \sum_{n=1}^{N} \overline{\boldsymbol{\lambda}}_n^\top \mathbf{y} + \frac{\rho_1}{2} \sum_{n=1}^{N} \left(\mathbf{e}_\text{u} - 2\overline{\mathbf{u}}_n'\right)^\top \mathbf{u} + \frac{\rho_2}{2} \sum_{n=1}^{N} \left(\mathbf{e}_\text{y} - 2\overline{\mathbf{y}}_n'\right)^\top \mathbf{y} \qquad \text{(C.17)} \\ &\text{s.t. } \mathcal{H}^1(\mathbf{u}, \mathbf{y}) \leq \mathbf{0}, \end{aligned}$$

where $\mathbf{e}_\text{u} = (1, \ldots, 1)^\top \in \mathbb{R}^{(|\mathcal{T}|-1)|\mathcal{G}|}$ and $\mathbf{e}_\text{y} = (1, \ldots, 1)^\top \in \mathbb{R}^{|\mathcal{T}||\mathcal{G}|}$.

In the iteration step m of Algorithm 3, $(\mathbf{u}^{m+1}, \mathbf{y}^{m+1})$ solves Problem (Fsub_R), i.e., Problem (C.17), when $(\overline{\mathbf{u}}_n', \overline{\mathbf{y}}_n') = (\mathbf{u}_n'^{\,m+1}, \mathbf{y}_n'^{\,m+1})$, $\overline{\boldsymbol{\pi}}_n = \boldsymbol{\pi}_n^m$, and $\overline{\boldsymbol{\lambda}}_n = \boldsymbol{\lambda}_n^m$ for any $n \in \mathcal{N}$. Thus, there exists $\boldsymbol{\eta}^m \in \mathbb{R}_+^{M_1}$ such that

$$\begin{aligned} &\nabla_\mathbf{u} \mathcal{F}\left(\mathbf{u}^{m+1}, \mathbf{y}^{m+1}\right) + \sum_{n=1}^{N} \boldsymbol{\pi}_n^m + \frac{\rho_1}{2} \sum_{n=1}^{N} \left(\mathbf{e}_\text{u} - 2\mathbf{u}_n'^{\,m+1}\right) \\ &\qquad + \left(\nabla_\mathbf{u} \mathcal{H}^1\left(\mathbf{u}^{m+1}, \mathbf{y}^{m+1}\right)\right)^\top \boldsymbol{\eta}^m = \mathbf{0}, \qquad \text{(C.18a)} \\ &\nabla_\mathbf{y} \mathcal{F}\left(\mathbf{u}^{m+1}, \mathbf{y}^{m+1}\right) + \sum_{n=1}^{N} \boldsymbol{\lambda}_n^m + \frac{\rho_2}{2} \sum_{n=1}^{N} \left(\mathbf{e}_\text{y} - 2\mathbf{y}_n'^{\,m+1}\right) \\ &\qquad + \left(\nabla_\mathbf{y} \mathcal{H}^1\left(\mathbf{u}^{m+1}, \mathbf{y}^{m+1}\right)\right)^\top \boldsymbol{\eta}^m = \mathbf{0}, \qquad \text{(C.18b)} \\ &\boldsymbol{\eta}^m \odot \mathcal{H}^1\left(\mathbf{u}^{m+1}, \mathbf{y}^{m+1}\right) = \mathbf{0}, \qquad \text{(C.18c)} \end{aligned}$$

where $\odot$ denotes the Hadamard product (or elementary-wise product). Note that $\overline{\mathbf{u}}_n'$ and $\overline{\mathbf{y}}_n'$ are bounded for any $n \in \mathcal{N}$. We also have $\overline{\boldsymbol{\pi}}_n$ and $\overline{\boldsymbol{\lambda}}_n$ are bounded for any $n \in \mathcal{N}$ by our assumption. Therefore, Proposition 11 shows that $\boldsymbol{\eta}^m$ is bounded. By assuming that $\boldsymbol{\eta}^m \to \boldsymbol{\eta}^*$ as $m \to \infty$ and $m \in \mathcal{K}$ and taking limits for $m \in \mathcal{K}$ on (C.18a)–(C.18c), we obtain

$$\begin{aligned} &\nabla_\mathbf{u} \mathcal{F}(\mathbf{u}^*, \mathbf{y}^*) + \sum_{n=1}^{N} \boldsymbol{\pi}_n^* + \frac{N\rho_1}{2} (\mathbf{e}_\text{u} - 2\mathbf{u}^*) + \left(\nabla_\mathbf{u} \mathcal{H}^1(\mathbf{u}^*, \mathbf{y}^*)\right)^\top \boldsymbol{\eta}^* = \mathbf{0}, \qquad \text{(C.19a)} \\ &\nabla_\mathbf{y} \mathcal{F}(\mathbf{u}^*, \mathbf{y}^*) + \sum_{n=1}^{N} \boldsymbol{\lambda}_n^* + \frac{N\rho_2}{2} (\mathbf{e}_\text{y} - 2\mathbf{y}^*) + \left(\nabla_\mathbf{y} \mathcal{H}^1(\mathbf{u}^*, \mathbf{y}^*)\right)^\top \boldsymbol{\eta}^* = \mathbf{0}, \qquad \text{(C.19b)} \\ &\boldsymbol{\eta}^* \odot \mathcal{H}^1(\mathbf{u}^*, \mathbf{y}^*) = \mathbf{0}. \qquad \text{(C.19c)} \end{aligned}$$

Next, we consider Problem (Ssub_n) for any $n \in \mathcal{N}$. In Problem (Ssub_n) for any $n \in \mathcal{N}$, the constraints involving $\mathbf{y}_n'$ are represented by $\mathcal{H}^\text{y}(\mathbf{y}_n', z_n, \boldsymbol{\gamma}_j, \boldsymbol{\xi}_j) = \mathbf{0}$ for any $j \in \mathcal{S}_n$. For any $n \in \mathcal{N}$ and $j \in \mathcal{S}_n$, let $\boldsymbol{\theta}_{n,j} \in \mathbb{R}^{M_2}$ denote the dual mul-

tipliers with respect to constraints represented by $\mathcal{H}^{\mathrm{y}}(\mathbf{y}'_n, z_n, \boldsymbol{\gamma}_j, \boldsymbol{\xi}_j) = \mathbf{0}$. We have $(z^{m+1}, z_n^{m+1}, \mathbf{u}_n'^{\,m+1}, \mathbf{y}_n'^{\,m+1}, \boldsymbol{\gamma}_j^{m+1}, \forall j \in \mathcal{S}_n)$ solves Problem (Ssub$_n$) for any $n \in \mathcal{N}$ when $(\overline{\mathbf{u}}, \overline{\mathbf{y}}) = (\mathbf{u}^m, \mathbf{y}^m)$, $\overline{\boldsymbol{\pi}}_n = \boldsymbol{\pi}_n^m$, and $\overline{\boldsymbol{\lambda}}_n = \boldsymbol{\lambda}_n^m$ in the iteration step m of Algorithm 3. It follows that

$$\nabla_{\mathbf{u}'_n} \mathcal{L}_n \left(\mathbf{u}^m, \mathbf{y}^m, z^{m+1}, \mathbf{u}_n'^{\,m+1}, \mathbf{y}_n'^{\,m+1}, \boldsymbol{\pi}_n^m, \boldsymbol{\lambda}_n^m\right) = -\boldsymbol{\pi}_n^m - \rho_1 \left(\mathbf{u}^m - \mathbf{u}_n'^{\,m+1}\right) = \mathbf{0}, \ \forall n \in \mathcal{N}, \tag{C.20a}$$

$$\begin{aligned}&\nabla_{\mathbf{y}'_n} \mathcal{L}_n \left(\mathbf{u}^m, \mathbf{y}^m, z^{m+1}, \mathbf{u}_n'^{\,m+1}, \mathbf{y}_n'^{\,m+1}, \boldsymbol{\pi}_n^m, \boldsymbol{\lambda}_n^m\right) + \sum_{j \in \mathcal{S}_n} \left(\nabla_{\mathbf{y}'_n} \mathcal{H}^{\mathrm{y}} \left(\mathbf{y}_n'^{\,m+1}, z_n^{m+1}, \boldsymbol{\gamma}_j^{\,m+1}, \boldsymbol{\xi}_j\right)\right)^{\top} \boldsymbol{\theta}_{n,j}^m \\ &= -\boldsymbol{\lambda}_n^m - \rho_2 \left(\mathbf{y}^m - \mathbf{y}_n'^{\,m+1}\right) + \sum_{j \in \mathcal{S}_n} \left(\nabla_{\mathbf{y}'_n} \mathcal{H}^{\mathrm{y}} \left(\mathbf{y}_n'^{\,m+1}, z_n^{m+1}, \boldsymbol{\gamma}_j^{\,m+1}, \boldsymbol{\xi}_j\right)\right)^{\top} \boldsymbol{\theta}_{n,j}^m = \mathbf{0}, \ \forall n \in \mathcal{N}.\end{aligned} \tag{C.20b}$$

For ease of exposition, we define

$$\mathcal{Q} := \nabla_{\mathbf{y}'_n} \mathcal{H}^{\mathrm{y}} \left(\mathbf{y}_n'^{\,m+1}, z_n^{m+1}, \boldsymbol{\gamma}_j^{\,m+1}, \boldsymbol{\xi}_j\right), \ \forall n \in \mathcal{N}, j \in \mathcal{S}_n.$$

Note that $\overline{\mathbf{u}}$ and $\overline{\mathbf{y}}$ are bounded. We also have $\overline{\boldsymbol{\pi}}_n$ and $\overline{\boldsymbol{\lambda}}_n$ are bounded for any $n \in \mathcal{N}$ and the objective value of Problem (Ssub$_n$)'s dual problem is bounded for any $n \in \mathcal{N}$ by our assumption. Therefore, Proposition 12 shows that $\boldsymbol{\theta}_{n,j}^m$ is bounded for any $n \in \mathcal{N}$ and $j \in \mathcal{S}_n$. By assuming that $\boldsymbol{\theta}_{n,j}^m \to \boldsymbol{\theta}_{n,j}^*$ for any $n \in \mathcal{N}$ and $j \in \mathcal{S}_n$ as $m \to \infty$ and $m \in \mathcal{K}$ and taking limits for $m \in \mathcal{K}$ on (C.20a)–(C.20b), we obtain

$$\begin{aligned}&-\boldsymbol{\pi}_n^* - \rho_1 \lim_{m \to \infty} \left(\mathbf{u}^m - \mathbf{u}_n'^{\,m+1}\right) = \mathbf{0}, \ \forall n \in \mathcal{N}, \\ &-\boldsymbol{\lambda}_n^* - \rho_2 \lim_{m \to \infty} \left(\mathbf{y}^m - \mathbf{y}_n'^{\,m+1}\right) + \mathcal{Q}^{\top} \sum_{j \in \mathcal{S}_n} \boldsymbol{\theta}_{n,j}^* = 0, \ \forall n \in \mathcal{N},\end{aligned}$$

which, by Proposition 6, (C.11), and (C.12), indicate

$$\boldsymbol{\pi}_n^* = 0, \ \forall n \in \mathcal{N}, \tag{C.21a}$$

$$-\boldsymbol{\lambda}_n^* + \mathcal{Q}^{\top} \sum_{j \in \mathcal{S}_n} \boldsymbol{\theta}_{n,j}^* = 0, \ \forall n \in \mathcal{N}. \tag{C.21b}$$

Finally, combining (C.19a)–(C.19c) and (C.21a)–(C.21b) leads to

$$\begin{aligned}&\nabla_{\mathbf{u}} \mathcal{F}\left(\mathbf{u}^*, \mathbf{y}^*\right) + \frac{N\rho_1}{2} \left(\mathbf{e}_{\mathrm{u}} - 2\mathbf{u}^*\right) + \left(\nabla_{\mathbf{u}} \mathcal{H}^1\left(\mathbf{u}^*, \mathbf{y}^*\right)\right)^{\top} \boldsymbol{\eta}^* = \mathbf{0}, \\ &\nabla_{\mathbf{y}} \mathcal{F}\left(\mathbf{u}^*, \mathbf{y}^*\right) + \mathcal{Q}^{\top} \sum_{n=1}^{N} \sum_{j \in \mathcal{S}_n} \boldsymbol{\theta}_{n,j}^* + \frac{N\rho_2}{2} \left(\mathbf{e}_{\mathrm{y}} - 2\mathbf{y}^*\right) + \left(\nabla_{\mathbf{y}} \mathcal{H}^1\left(\mathbf{u}^*, \mathbf{y}^*\right)\right)^{\top} \boldsymbol{\eta}^* = \mathbf{0}, \\ &\boldsymbol{\eta}^* \odot \mathcal{H}^1\left(\mathbf{u}^*, \mathbf{y}^*\right) = \mathbf{0},\end{aligned}$$

which completes the proof. □

C.6 Proof of Theorem 6

Proof. First, for any $n > m \geq 1$, we have $\mathcal{S}_m^{\mathrm{w}} \subseteq \mathcal{S}_n^{\mathrm{w}} \subseteq \mathcal{S}$, indicating that $\overline{\Theta}^m \leq \overline{\Theta}^n \leq \Theta$. Next, consider Algorithm 4 terminates at step $m \leq |\mathcal{S}|$, where $(\mathbf{u}^m, \mathbf{y}^m, \boldsymbol{\gamma}_j^m, \forall j \in \mathcal{S}_m^{\mathrm{w}})$ solves Problem $(\mathcal{M})$ with sample set $\mathcal{S}_m^{\mathrm{w}}$ and $\boldsymbol{\gamma}_j^m$ solves Problem $(\mathcal{P})$ with $(\mathbf{u}, \mathbf{y}) = (\mathbf{u}^m, \mathbf{y}^m)$ and ξ_j for any $j \in \mathcal{S}_m^{\mathrm{nw}}$. By the terminating condition, we have $\mathcal{S}_m^{\mathrm{f}} = \emptyset$. This implies $\mathcal{F}(\mathbf{u}^m, \mathbf{y}^m) + \Psi(\mathbf{u}^m, \mathbf{y}^m, \boldsymbol{\xi}_j) \leq \overline{\Theta}^m$ for any $j \in \mathcal{S}_m^{\mathrm{nw}}$. Meanwhile, because $(\mathbf{u}^m, \mathbf{y}^m, \boldsymbol{\gamma}_j^m, \forall j \in \mathcal{S}_m^{\mathrm{w}})$ solves Problem $(\mathcal{M})$ with sample set $\mathcal{S}_m^{\mathrm{w}}$, we have $\mathcal{F}(\mathbf{u}^m, \mathbf{y}^m) + \Psi(\mathbf{u}^m, \mathbf{y}^m, \boldsymbol{\xi}_j) \leq \overline{\Theta}^m$ for any $j \in \mathcal{S}_m^{\mathrm{w}}$. Therefore, $\mathcal{F}(\mathbf{u}^m, \mathbf{y}^m) + \Psi(\mathbf{u}^m, \mathbf{y}^m, \boldsymbol{\xi}_j) \leq \overline{\Theta}^m$ for any $j \in \mathcal{S}$, as $\mathcal{S}_m^{\mathrm{w}} \cup \mathcal{S}_m^{\mathrm{nw}} = \mathcal{S}$.

Now let $z^m = \overline{\Theta}^m - \mathcal{F}(\mathbf{u}^m, \mathbf{y}^m)$. Then, $(\mathbf{u}^m, \mathbf{y}^m, z^m, \boldsymbol{\gamma}_j^m, \forall j \in \mathcal{S})$ is feasible to Problem (4.29), which reformulates Problem $(\mathcal{M})$. This feasible solution realizes an objective value at $\overline{\Theta}^m$. Because Problem $(\mathcal{M})$ (i.e., Problem (4.29)) is a minimization problem, we have $\overline{\Theta}^m \geq \Theta$. Note that we have $\overline{\Theta}^n \leq \Theta$ for any $n \geq 1$. Thus, $\overline{\Theta}^m = \Theta$. That is, $(\mathbf{u}^*, \mathbf{y}^*) = (\mathbf{u}^m, \mathbf{y}^m)$ is optimal to Problem $(\mathcal{M})$. □

C.7 Proof of Lemma 1

Proof. First, we show that Algorithm 4 terminates if and only if a support set is obtained. On the one hand, Theorem 6 suggests that Algorithm 4 terminates with an optimal solution of Problem $(\mathcal{M})$. That is, a support set is obtained when the algorithm terminates. On the other hand, if a support set is obtained at step m, i.e., $\mathcal{S}_m^{\mathrm{w}}$ is a support set, then the solution obtained at step m, i.e., $(\mathbf{u}^m, \mathbf{y}^m)$, is optimal to Problem $(\mathcal{M})$ with $\mathcal{S}$ and $\overline{\Theta}^m = \Theta(\mathcal{S})$. This is because we assume that (i) Problem $(\mathcal{M})$ with $\mathcal{S}$ has a unique optimal solution or (ii) Problem $(\mathcal{M})$ with $\mathcal{S}$ and Problem $(\mathcal{M})$ with any support set share the same set of optimal solutions. It follows that $\mathcal{S}_m^{\mathrm{f}} = \emptyset$ and Algorithm 4 terminates.

Note that $\mathcal{S}^*$ is a unique minimum support set; that is, a support set is obtained if and only if all the elements (i.e., scenarios) in $\mathcal{S}^*$ are obtained. Thus, Algorithm 4 terminates if and only if all the elements in $\mathcal{S}^*$ are obtained. It follows that the expected number of steps for Algorithm 4 to terminate equals the expected number of steps to collect all the

K scenarios in $\mathcal{S}^*$.

Next, we note that there exists a unique worst-case scenario j^*. That is, $\Psi(\mathbf{u}^*, \mathbf{y}^*, \boldsymbol{\xi}_{j^*}) > \Psi(\mathbf{u}^*, \mathbf{y}^*, \boldsymbol{\xi}_{j'})$ for any $j' \in \mathcal{S}$ and $j' \neq j^*$, where $(\mathbf{u}^*, \mathbf{y}^*)$ is the optimal first-stage solution of Problem ($\mathcal{M}$) with $\mathcal{S}$. We show that $j^* \in \mathcal{S}^*$. By contradiction, suppose that $j^* \notin \mathcal{S}^*$. We can solve Problem ($\mathcal{M}$) with $\mathcal{S}^*$ and obtain the optimal first-stage solution $(\mathbf{u}^*, \mathbf{y}^*)$ and $\Theta(\mathcal{S}^*)$. Clearly, there exists $j_0 \in \mathcal{S}^*$ such that $j_0 \neq j^*$ (because $j^* \notin \mathcal{S}^*$) and $\Psi(\mathbf{u}^*, \mathbf{y}^*, \boldsymbol{\xi}_{j_0}) = \Theta(\mathcal{S}^*) = \Theta(\mathcal{S})$, where the second equality holds because $\mathcal{S}^*$ is a support set. It follows that $\Psi(\mathbf{u}^*, \mathbf{y}^*, \boldsymbol{\xi}_{j^*}) \leq \Theta(\mathcal{S}) = \Psi(\mathbf{u}^*, \mathbf{y}^*, \boldsymbol{\xi}_{j_0})$, leading to a contradiction.

Because Algorithm 4 selects the worst-case scenario initially, we only need to collect the remaining $K-1$ scenarios in $\mathcal{S}^*$ before the algorithm terminates. Thus, it suffices to calculate the expected number of steps to collect the remaining $K-1$ scenarios in $\mathcal{S}^*$ from all the $|\mathcal{S}|-1$ scenarios in $\mathcal{S} \setminus \{j^*\}$. To complete this calculation, we transform it into the following problem.

> ***Select red balls (SRB):*** *Given a set of $K-1$ red balls and $|\mathcal{S}|-K$ black balls, we randomly select a ball from the set at each step until all $|\mathcal{S}|-1$ balls are selected. Let n^{o} represent the number of balls in total from the first selected ball to the last selected red ball, inclusive of both. What is $\mathbb{E}[n^{\text{o}}]$?*

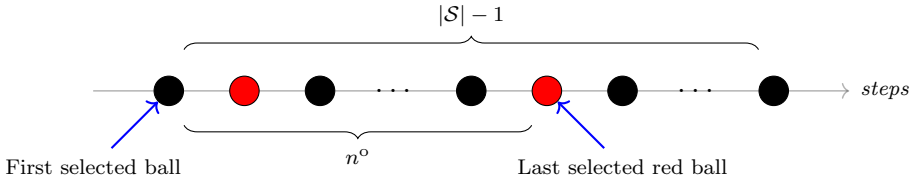

Figure C.1. Problem SRB

Here we show that $\mathbb{E}[n^{\text{o}}]$ in the Problem SRB equals the expected number of steps to collect the $K-1$ scenarios from all the $|\mathcal{S}|-1$ scenarios as mentioned above. Specifically, the $K-1$ red balls (resp. $|\mathcal{S}|-K$ black balls) in the Problem SRB can be considered the $K-1$ scenarios in $\mathcal{S}^*$ (resp. $|\mathcal{S}|-K$ scenarios in $\mathcal{S} \setminus \mathcal{S}^*$). Randomly selecting a ball at each step in the Problem SRB is equivalent to randomly selecting a scenario in Algorithm 4 with *naive selection*.

Clearly, the smallest possible value of n^{o} is $K-1$ and the actual realization of n^{o} (increases based on $K-1$) depends on the number of selected black balls when selecting the $K-1$ red balls. We consider that all the $K-1$ red balls are sequentially aligned over a

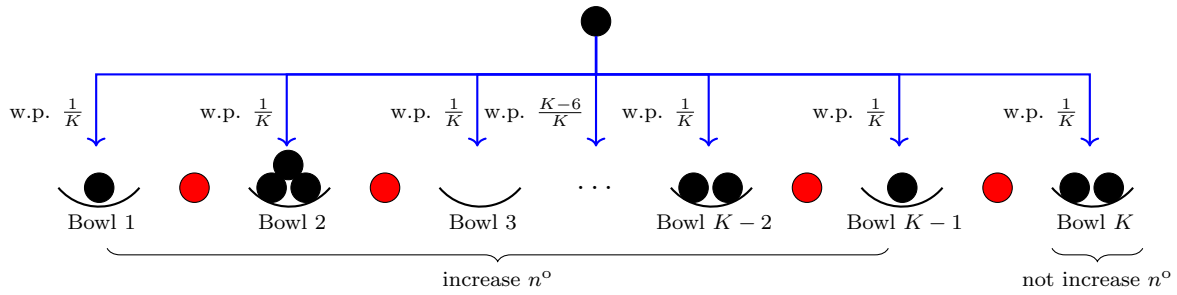

Figure C.2. A Black Ball Falls into A Bowl

horizonal line (see Figures C.1 and C.2) and there is a bowl before and after each red ball to collect the selected black balls, leading to a total of K bowls. Because we randomly select a ball at each step, i.e., each ball has the same probability of being selected at each step, then a black ball falls into each bowl with the same probability at $1/K$. If a black ball falls into the first $K-1$ bowls, i.e., Bowl 1 to Bowl $K-1$ in Figure C.2, then the value of n^{o} increases by 1. Otherwise, i.e., the black ball falls into Bowl K, then the value of n^{o} remains unchanged.

We define a random variable Y_j to represent the increase in n^{o} due to a possibly selected black ball $j = 1, \ldots, |\mathcal{S}| - K$. We have

$$Y_j = \begin{cases} 1, & \text{with probability } \frac{K-1}{K} \\ 0, & \text{with probability } \frac{1}{K} \end{cases}, \ \forall j = 1, \ldots, |\mathcal{S}| - K.$$

Thus, $\mathbb{E}[n^{\text{o}}] = 1 + (K-1) + \mathbb{E}[\sum_{j=1}^{|\mathcal{S}|-K} Y_j] = K + \sum_{j=1}^{|\mathcal{S}|-K} \mathbb{E}[Y_j] = K + \sum_{j=1}^{|\mathcal{S}|-K}(1 \times (K-1)/K + 0 \times 1/K) = K + (|\mathcal{S}| - K) \times (K-1)/K = 1 + |\mathcal{S}| \times (K-1)/K$. This completes the proof. □

C.8 Proof of Theorem 7

Proof. Note that the expected number of steps for Algorithm 4 to terminate equals the expected number of steps to collect all the K scenarios in $\mathcal{S}^*$ when using either of the naive selection and strategic selection (see the proof of Lemma 1). At any iteration step $i > 0$ of Algorithm 4, we use (i) a binary variable X_i to denote whether a scenario in $\mathcal{S}^*$ is selected at this step ($X_i = 1$) or not ($X_i = 0$) and (ii) an integer variable S_i to denote the number of scenarios in $\mathcal{S}^*$ that have not been selected until this step. Clearly, $S_0 = K$ and $S_j = S_i - \sum_{n=i+1}^{j} X_n$ for any $j > i \geq 0$.

Now, we use two parts to complete the proof. In the first part, we construct a binary tree to describe the process of randomly selecting a scenario at each step until collecting all the K scenarios in $\mathcal{S}^*$ from all the $|\mathcal{S}|$ scenarios in $\mathcal{S}$. In the second part, based on the constructed binary tree, we compare the expected number of steps to collect all the K scenarios under the naive selection with that under strategic selection.

First, we construct a binary tree (see Figure C.3) with each node describing the status of the random process until the current step. Specifically, each node at each iteration step $i \geq 0$ on the tree denotes the numbers of scenarios in $\mathcal{S}$ and $\mathcal{S}^*$ that have not been selected until the step i by $(|\mathcal{S}|-i, S_i)$. For instance, at step i_0 in Figure C.3, the bottom node shows that $|\mathcal{S}| - i_0$ scenarios in $\mathcal{S}$ and $S^*_{i_0}$ scenarios in $\mathcal{S}^*$ have not be selected. We use $\mathcal{V}$ to denote the set of all the nodes on the tree.

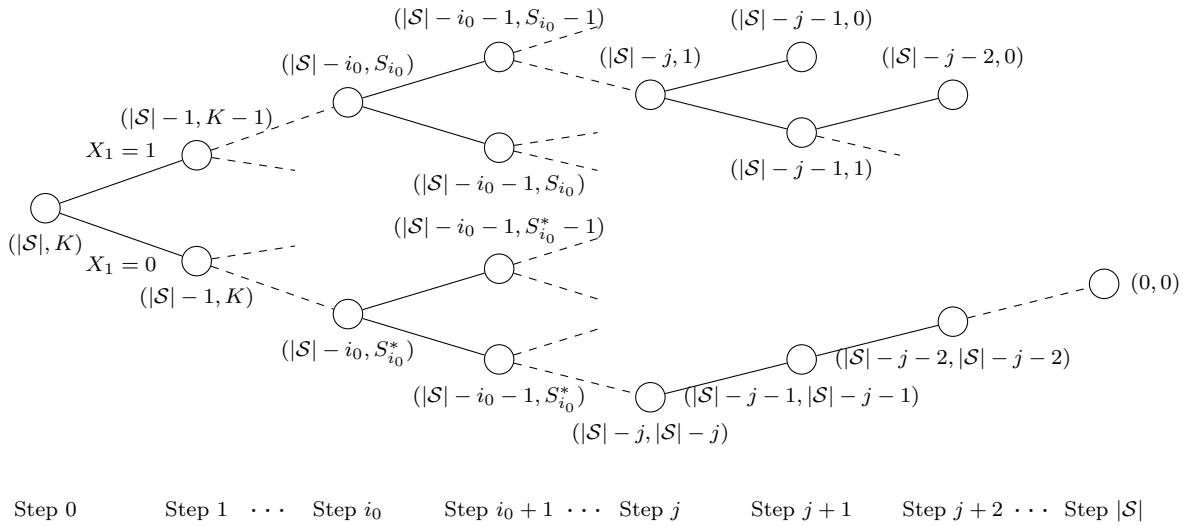

Figure C.3. The Constructed Binary Tree

Each node in the tree has up to two branches (child nodes) to describe the status at the next step. If a node has two child nodes, then one child node specifies that a scenario in $\mathcal{S}^*$ is selected at the next step and the other specifies that a scenario in $\mathcal{S} \setminus \mathcal{S}^*$ is selected. More specifically, at each step $i \geq 1$, each node satisfies one of the following three conditions:

- $S_i = 0$. All the scenarios in $\mathcal{S}^*$ have been selected until this step. Such a node hence has no child node. We define $\mathcal{V}_1 = \{(|\mathcal{S}|-i, S_i) \in \mathcal{V} \mid S_i = 0, i \geq 0\}$ to collect all such nodes.

- $|\mathcal{S}| - i = S_i > 0$. Some scenarios in $\mathcal{S}^*$ have not been selected and all the scenarios in $\mathcal{S} \setminus \mathcal{S}^*$ have been selected until this step. Such a node hence has only one child

node: $(|\mathcal{S}|-i-1, S_i-1)$. We define $\mathcal{V}_2 := \{(|\mathcal{S}|-i, S_i) \in \mathcal{V} \mid |\mathcal{S}|-i = S_i > 0, i \geq 0\}$ to collect all such nodes.

- $|\mathcal{S}| - i > S_i > 0$. Some scenarios in both $\mathcal{S}^*$ and $\mathcal{S} \setminus \mathcal{S}^*$ have not been selected until this step. Such a node hence has two child nodes: $(|\mathcal{S}| - i - 1, S_i - 1)$ and $(|\mathcal{S}| - i - 1, S_i)$. We define $\mathcal{V}_3 := \{(|\mathcal{S}| - i, S_i) \in \mathcal{V} \mid |\mathcal{S}| - i > S_i > 0, i \geq 0\}$ to collect all such nodes.

Clearly, $\cup_{i=1}^{3}\mathcal{V}_i = \mathcal{V}$ and $\mathcal{V}_i \cap \mathcal{V}_j = \emptyset$ for any $i, j \in \{1, 2, 3\}$ and $i \neq j$. The root node is $(|\mathcal{S}|, K)$ and $\mathcal{V}_1$ also represents the set of all leaf nodes of the constructed tree.

Note that we go from a node in the tree to this node's child node after we select a scenario from $\mathcal{S}$. For instance, we go from node $(|\mathcal{S}| - i, S_i)$ to node $(|\mathcal{S}| - i - 1, S_i - 1)$ (resp. $(|\mathcal{S}| - i - 1, S_i)$) if a scenario in $\mathcal{S}^*$ (resp. a scenario in $\mathcal{S} \setminus \mathcal{S}^*$) is selected at step $i \geq 0$, i.e., $X_i = 1$ (resp. $X_i = 0$). We let $\mathbb{P}$ denote the transition probability measure that returns the probability of transitioning from a node in $\mathcal{V}_2 \cup \mathcal{V}_3$ (i.e., the set of non-leaf nodes) to one of its child nodes. For instance, $\mathbb{P}((|\mathcal{S}|-i, S_i), (|\mathcal{S}|-i-1, S_{i+1}))$ measures the probability that node $(|\mathcal{S}| - i, S_i) \in \mathcal{V}_2 \cup \mathcal{V}_3$ transitions to its child node $(|\mathcal{S}| - i - 1, S_{i+1})$. The following properties hold:

$$\begin{aligned}
&\mathbb{P}\left((|\mathcal{S}| - i, S_i), (|\mathcal{S}| - i - 1, S_i - 1)\right) = 1, \ \forall (|\mathcal{S}| - i, S_i) \in \mathcal{V}_2, \\
&\mathbb{P}\left((|\mathcal{S}| - i, S_i), (|\mathcal{S}| - i - 1, S_i)\right) + \mathbb{P}\left((|\mathcal{S}| - i, S_i), (|\mathcal{S}| - i - 1, S_i - 1)\right) = 1, \\
&\qquad\qquad \forall (|\mathcal{S}| - i, S_i) \in \mathcal{V}_2 \cup \mathcal{V}_3. \qquad \text{(C.22)}
\end{aligned}$$

Based on the constructed binary tree and given $0 \leq i < j$, we define a sequence of nodes $\{(|\mathcal{S}|-i, S_i), (|\mathcal{S}|-i-1, S_{i+1}), \ldots, (|\mathcal{S}|-j, S_j)\}$ as a path if the following conditions are satisfied: (i) $(|\mathcal{S}| - n, S_n) \in \mathcal{V}$ for any n such that $i \leq n \leq j$, (ii) $S_j = 0$, and (iii) $S_n - S_{n+1} \in \{0, 1\}$ for any n such that $i \leq n \leq j - 1$. Clearly, the number of paths is limited because the number of nodes is limited, i.e., $|\mathcal{V}| < \infty$. We define the length of a path as the number of transitions along the path. For instance, the length of the path $\{(|\mathcal{S}| - i, S_i), (|\mathcal{S}| - i - 1, S_{i+1}), \ldots, (|\mathcal{S}| - j, S_j)\}$ is $j - i$. In addition, we define function $\mu : \mathcal{V} \to \mathbb{R}$ to return the expected length of all the paths that start from a node $(|\mathcal{S}| - i, S_i) \in \mathcal{V}$. As no path starts from any node $(|\mathcal{S}| - i, S_i) \in \mathcal{V}_1$, we have $\mu((|\mathcal{S}| - i, S_i)) = 0$.

Note that the process of collecting all the scenarios in $\mathcal{S}^*$ can be represented by a path

from the root node $(|\mathcal{S}|, K)$ to a leaf node of the tree. Thus, to calculate the expected number of steps for Algorithm 4 to terminate, it suffices to calculate the expected length of all the paths starting from the root node. Figure C.4 shows an instance of the constructed binary tree with $(|\mathcal{S}|, K) = (4, 2)$, all possible paths starting from $(|\mathcal{S}|, K)$, and their expected length.

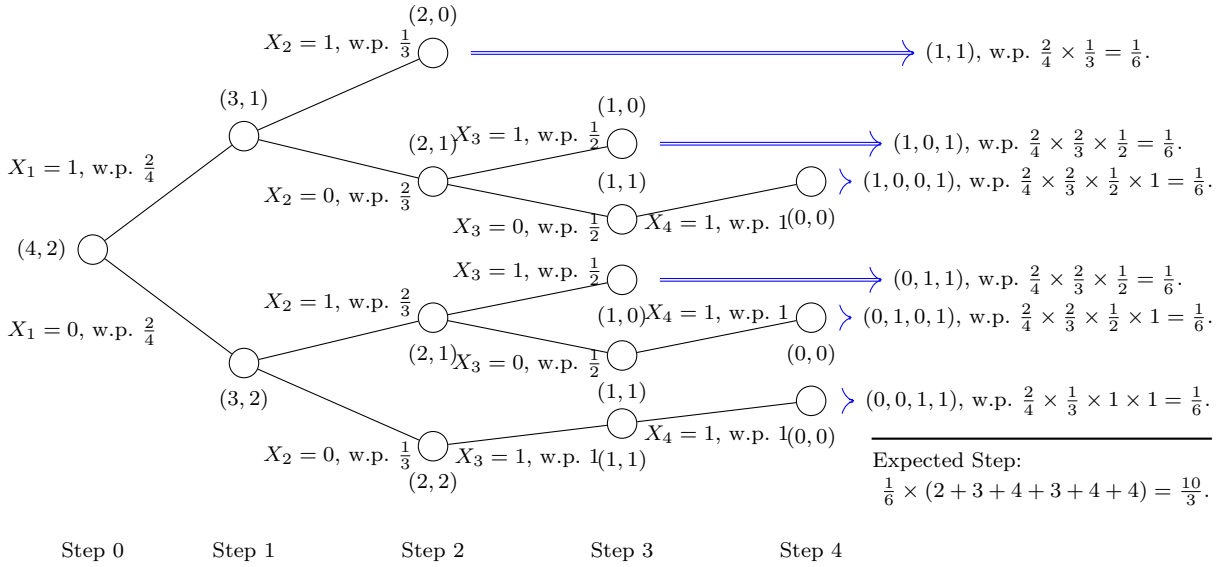

Figure C.4. Paths of a Binary Tree

Second, based on the constructed binary tree above, we now compare the expected number of steps to collect all the K scenarios in $\mathcal{S}^*$ under the naive selection with that under strategic selection. To differentiate the transition probability measure $\mathbb{P}$ under these two selection methods, we use $\mathbb{P}_{\mathrm{n}}$ (resp. $\mathbb{P}_{\mathrm{s}}$) to denote the transition probability measure when the naive selection (resp. strategic selection) is adopted. Correspondingly, we use μ_{n} (resp. μ_{s}) to denote the function μ that returns the expected length of all the paths starting from a node in $\mathcal{V}$ under $\mathbb{P}_{\mathrm{n}}$ (resp. $\mathbb{P}_{\mathrm{s}}$). Therefore, $\mu_{\mathrm{n}}((|\mathcal{S}|, K))$ (resp. $\mu_{\mathrm{s}}((|\mathcal{S}|, K))$) represents the expected number of steps for Algorithm 4 to terminate under the naive selection (resp. strategic selection).

Recall that under strategic selection, at any step $i \geq 0$, we randomly select a scenario from $\mathcal{S}_i^{\mathrm{f}}$ if $1/|\mathcal{S}_i^{\mathrm{f}}| \geq K/(|\mathcal{S}| - i)$ and from $\mathcal{S}_i^{\mathrm{nw}}$ otherwise. Note that at any step $i \geq 0$ before Algorithm 4 terminates, $\mathcal{S}_i^{\mathrm{f}}$ includes at least one scenario in $\mathcal{S}^*$. Hence, the probability that a selected scenario from $\mathcal{S}_i^{\mathrm{f}}$ belongs to $\mathcal{S}^*$ is no smaller than $1/|\mathcal{S}_i^{\mathrm{f}}|$. Thus, at any step $i \geq 0$ with $(|\mathcal{S}| - i, S_i) \in \mathcal{V}_2 \cup \mathcal{V}_3$ before Algorithm 4 terminates, if $1/|\mathcal{S}_i^{\mathrm{f}}| \geq K/(|\mathcal{S}| - i)$,

then

$$\mathbb{P}_{\mathrm{s}}\left((|\mathcal{S}|-i,S_i),(|\mathcal{S}|-i-1,S_i-1)\right) \geq \frac{1}{|\mathcal{S}_i^{\mathrm{f}}|} \geq \frac{K}{|\mathcal{S}|-i} \geq \frac{S_i}{|\mathcal{S}|-i} = \mathbb{P}_{\mathrm{n}}\left((|\mathcal{S}|-i,S_i),(|\mathcal{S}|-i-1,S_i-1)\right);$$

otherwise, then $\mathbb{P}_{\mathrm{s}}((|\mathcal{S}|-i,S_i),(|\mathcal{S}|-i-1,S_i-1)) = \mathbb{P}_{\mathrm{n}}((|\mathcal{S}|-i,S_i),(|\mathcal{S}|-i-1,S_i-1))$. That is,

$$\mathbb{P}_{\mathrm{n}}\left((|\mathcal{S}|-i,S_i),(|\mathcal{S}|-i-1,S_i-1)\right) \leq \mathbb{P}_{\mathrm{s}}\left((|\mathcal{S}|-i,S_i),(|\mathcal{S}|-i-1,S_i-1)\right), \quad \forall (|\mathcal{S}|-i,S_i) \in \mathcal{V}_2 \cup \mathcal{V}_3. \tag{C.23}$$

We complete the proof by induction. We define $\mathcal{C} \subseteq \mathcal{V}_2 \cup \mathcal{V}_3$ to collect all the nodes $(|\mathcal{S}|-i,S_i) \in \mathcal{V}_2 \cup \mathcal{V}_3$ satisfying $\mathbb{P}_{\mathrm{n}}((|\mathcal{S}|-i,S_i),(|\mathcal{S}|-i-1,S_i-1)) < \mathbb{P}_{\mathrm{s}}((|\mathcal{S}|-i,S_i),(|\mathcal{S}|-i-1,S_i-1))$. By (C.23), we have $\mathbb{P}_{\mathrm{n}}((|\mathcal{S}|-i,S_i),(|\mathcal{S}|-i-1,S_i-1)) = \mathbb{P}_{\mathrm{s}}((|\mathcal{S}|-i,S_i),(|\mathcal{S}|-i-1,S_i-1))$ for any $(|\mathcal{S}|-i,S_i) \in \mathcal{V}_2 \cup \mathcal{V}_3 \setminus \mathcal{C}$. Note that any node $(|\mathcal{S}|-i,S_i) \in \mathcal{V}_2$ has only one child node $(|\mathcal{S}|-i-1,S_i-1)$, indicating that $\mathbb{P}_{\mathrm{n}}((|\mathcal{S}|-i,S_i),(|\mathcal{S}|-i-1,S_i-1)) = \mathbb{P}_{\mathrm{s}}((|\mathcal{S}|-i,S_i),(|\mathcal{S}|-i-1,S_i-1)) = 1$ for any node $(|\mathcal{S}|-i,S_i) \in \mathcal{V}_2$. Thus, $\mathcal{C} \cap \mathcal{V}_2 = \emptyset$ and $\mathcal{C} \subseteq \mathcal{V}_2 \cup \mathcal{V}_3 \setminus \mathcal{V}_2 = \mathcal{V}_3$. More specifically, any node $(|\mathcal{S}|-i,S_i) \in \mathcal{V}_3$ has two child nodes: $(|\mathcal{S}|-i-1,S_i-1)$ and $(|\mathcal{S}|-i-1,S_i)$; that is, the probability that $(|\mathcal{S}|-i,S_i)$ transitions to $(|\mathcal{S}|-i-1,S_i-1)$ may vary depending on the naive or strategic selection. Thus, it is possible that $\mathbb{P}_{\mathrm{n}}((|\mathcal{S}|-i,S_i),(|\mathcal{S}|-i-1,S_i-1)) < \mathbb{P}_{\mathrm{s}}((|\mathcal{S}|-i,S_i),(|\mathcal{S}|-i-1,S_i-1))$ for any node $(|\mathcal{S}|-i,S_i) \in \mathcal{V}_3$. It follows that $\mathcal{C}$ may contain all the nodes in $\mathcal{V}_3$ and the maximum possible value of $|\mathcal{C}|$ equals to $|\mathcal{V}_3| < \infty$.

We perform induction on $|\mathcal{C}|$. First, we consider $|\mathcal{C}| = 0$, i.e., $\mathcal{C} = \emptyset$. Thus, $\mathbb{P}_{\mathrm{n}}((|\mathcal{S}|-i,S_i),(|\mathcal{S}|-i-1,S_i-1)) = \mathbb{P}_{\mathrm{s}}((|\mathcal{S}|-i,S_i),(|\mathcal{S}|-i-1,S_i-1))$ for any $(|\mathcal{S}|-i,S_i) \in \mathcal{V}_2 \cup \mathcal{V}_3$, indicating that $\mu_{\mathrm{n}}((|\mathcal{S}|,K)) = \mu_{\mathrm{s}}((|\mathcal{S}|,K))$.

Second, we consider $|\mathcal{C}| = 1$. Without loss of generality, we assume $\mathcal{C} = \{(|\mathcal{S}|-i_0,S_{i_0}^*)\}$,

where $(|\mathcal{S}| - i_0, S^*_{i_0})$ is an arbitrary node in $\mathcal{V}_2 \cup \mathcal{V}_3$. In this case, we have

$$
\begin{aligned}
\mu_{\mathrm{n}}\left((|\mathcal{S}| - i_0, S^*_{i_0})\right) &= \mu_{\mathrm{n}}\left((|\mathcal{S}| - i_0 - 1, S^*_{i_0} - 1)\right) \mathbb{P}_{\mathrm{n}}\left((|\mathcal{S}| - i_0, S^*_{i_0}), (|\mathcal{S}| - i_0 - 1, S^*_{i_0} - 1)\right) \\
&\quad + \mu_{\mathrm{n}}\left((|\mathcal{S}| - i_0 - 1, S^*_{i_0})\right) \mathbb{P}_{\mathrm{n}}\left((|\mathcal{S}| - i_0, S^*_{i_0}), (|\mathcal{S}| - i_0 - 1, S^*_{i_0})\right) + 1 \\
&= \mu_{\mathrm{n}}\left((|\mathcal{S}| - i_0 - 1, S^*_{i_0} - 1)\right) \mathbb{P}_{\mathrm{n}}\left((|\mathcal{S}| - i_0, S^*_{i_0}), (|\mathcal{S}| - i_0 - 1, S^*_{i_0} - 1)\right) \\
&\quad + \mu_{\mathrm{n}}\left((|\mathcal{S}| - i_0 - 1, S^*_{i_0})\right) \left(1 - \mathbb{P}_{\mathrm{n}}\left((|\mathcal{S}| - i_0, S^*_{i_0}), (|\mathcal{S}| - i_0 - 1, S^*_{i_0} - 1)\right)\right) + 1 \\
&= \mu_{\mathrm{n}}\left((|\mathcal{S}| - i_0 - 1, S^*_{i_0} - 1)\right) \mathbb{P}_{\mathrm{n}}\left((|\mathcal{S}| - i_0, S^*_{i_0}), (|\mathcal{S}| - i_0 - 1, S^*_{i_0} - 1)\right) \\
&\quad - \mu_{\mathrm{n}}\left((|\mathcal{S}| - i_0 - 1, S^*_{i_0})\right) \mathbb{P}_{\mathrm{n}}\left((|\mathcal{S}| - i_0, S^*_{i_0}), (|\mathcal{S}| - i_0 - 1, S^*_{i_0} - 1)\right) \\
&\quad + \mu_{\mathrm{n}}\left((|\mathcal{S}| - i_0 - 1, S^*_{i_0})\right) + 1 \\
&> \mu_{\mathrm{n}}\left((|\mathcal{S}| - i_0 - 1, S^*_{i_0} - 1)\right) \mathbb{P}_{\mathrm{s}}\left((|\mathcal{S}| - i_0, S^*_{i_0}), (|\mathcal{S}| - i_0 - 1, S^*_{i_0} - 1)\right) \\
&\quad - \mu_{\mathrm{n}}\left((|\mathcal{S}| - i_0 - 1, S^*_{i_0})\right) \mathbb{P}_{\mathrm{s}}\left((|\mathcal{S}| - i_0, S^*_{i_0}), (|\mathcal{S}| - i_0 - 1, S^*_{i_0} - 1)\right) \\
&\quad + \mu_{\mathrm{n}}\left((|\mathcal{S}| - i_0 - 1, S^*_{i_0})\right) + 1 \qquad \text{(C.24)} \\
&= \mu_{\mathrm{s}}\left((|\mathcal{S}| - i_0 - 1, S^*_{i_0} - 1)\right) \mathbb{P}_{\mathrm{s}}\left((|\mathcal{S}| - i_0, S^*_{i_0}), (|\mathcal{S}| - i_0 - 1, S^*_{i_0} - 1)\right) \\
&\quad - \mu_{\mathrm{s}}\left((|\mathcal{S}| - i_0 - 1, S^*_{i_0})\right) \mathbb{P}_{\mathrm{s}}\left((|\mathcal{S}| - i_0, S^*_{i_0}), (|\mathcal{S}| - i_0 - 1, S^*_{i_0} - 1)\right) \\
&\quad + \mu_{\mathrm{s}}\left((|\mathcal{S}| - i_0 - 1, S^*_{i_0})\right) + 1 \qquad \text{(C.25)} \\
&= \mu_{\mathrm{s}}\left((|\mathcal{S}| - i_0 - 1, S^*_{i_0} - 1)\right) \mathbb{P}_{\mathrm{s}}\left((|\mathcal{S}| - i_0, S^*_{i_0}), (|\mathcal{S}| - i_0 - 1, S^*_{i_0} - 1)\right) \\
&\quad + \mu_{\mathrm{s}}\left((|\mathcal{S}| - i_0 - 1, S^*_{i_0})\right) \mathbb{P}_{\mathrm{s}}\left((|\mathcal{S}| - i_0, S^*_{i_0}), (|\mathcal{S}| - i_0 - 1, S^*_{i_0})\right) + 1 \\
&= \mu_{\mathrm{s}}\left((|\mathcal{S}| - i_0, S^*_{i_0})\right), \qquad \text{(C.26)}
\end{aligned}
$$

where the reasons why (C.24)–(C.25) hold are described as follows. Specifically, (C.24) holds because $\mu_{\mathrm{n}}((|\mathcal{S}| - i_0 - 1, S^*_{i_0} - 1)) < \mu_{\mathrm{n}}((|\mathcal{S}| - i_0 - 1, S^*_{i_0}))$ due to Lemma 1 and $\mathbb{P}_{\mathrm{n}}((|\mathcal{S}| - i_0, S^*_{i_0}), (|\mathcal{S}| - i_0 - 1, S^*_{i_0} - 1)) < \mathbb{P}_{\mathrm{s}}((|\mathcal{S}| - i_0, S^*_{i_0}), (|\mathcal{S}| - i_0 - 1, S^*_{i_0} - 1))$. To show (C.25) holds, we note that the paths starting from nodes $(|\mathcal{S}| - i_0 - 1, S^*_{i_0} - 1)$ and $(|\mathcal{S}| - i_0 - 1, S^*_{i_0})$ at step $i_0 + 1$, which are the child nodes of $(|\mathcal{S}| - i_0, S^*_{i_0})$, do not pass $(|\mathcal{S}| - i_0, S^*_{i_0})$ (see Figure C.3). Thus, we have $\mu_{\mathrm{n}}((|\mathcal{S}| - i_0 - 1, S^*_{i_0} - 1)) = \mu_{\mathrm{s}}((|\mathcal{S}| - i_0 - 1, S^*_{i_0} - 1))$ and $\mu_{\mathrm{n}}((|\mathcal{S}| - i_0 - 1, S^*_{i_0})) = \mu_{\mathrm{s}}((|\mathcal{S}| - i_0 - 1, S^*_{i_0}))$, as $\mathbb{P}_{\mathrm{n}}((|\mathcal{S}| - i, S_i), (|\mathcal{S}| - i - 1, S_i - 1)) = \mathbb{P}_{\mathrm{s}}((|\mathcal{S}| - i, S_i), (|\mathcal{S}| - i - 1, S_i - 1))$ for any $(|\mathcal{S}| - i, S_i) \in \mathcal{V}_2 \cup \mathcal{V}_3 \setminus \{(|\mathcal{S}| - i_0, S^*_{i_0})\}$.

We let $\mu_{\mathrm{n}}((|\mathcal{S}|, K) \mid (|\mathcal{S}| - i, S_i))$ (resp. $\mu_{\mathrm{s}}((|\mathcal{S}|, K) \mid (|\mathcal{S}| - i, S_i))$) for any $(|\mathcal{S}| - i, S_i) \in \mathcal{V}_2 \cup \mathcal{V}_3$ denote the conditional expected length of the paths starting from $(|\mathcal{S}|, K)$ under $\mathbb{P}_{\mathrm{n}}$ (resp. $\mathbb{P}_{\mathrm{s}}$), given that the paths pass $(|\mathcal{S}| - i, S_i)$ at step i. By the law of total expectation, we have $\mu_{\mathrm{n}}((|\mathcal{S}|, K)) = \mathbb{E}_{\mathbb{P}_{\mathrm{n}}}[\mu((|\mathcal{S}|, K) \mid (|\mathcal{S}| - i, S_i))]$ and $\mu_{\mathrm{s}}((|\mathcal{S}|, K)) = \mathbb{E}_{\mathbb{P}_{\mathrm{s}}}[\mu((|\mathcal{S}|, K) \mid (|\mathcal{S}| - i, S_i))]$. Meanwhile, for any $(|\mathcal{S}| - i, S_i) \in \mathcal{V}_2 \cup \mathcal{V}_3$, it is clear

that $S_i \geq K - i$ because $K - i$ is achieved only when a scenario in $\mathcal{S}^*$ is selected at every step from 1 to i. Moreover, we have $S_i \leq K$ and $S_i \leq |\mathcal{S}| - i$. It follows that $S_i \in \{K - i, \ldots, \min\{K, |\mathcal{S}| - i\}\}$. For any $(|\mathcal{S}| - i, S_i) \in \mathcal{V}_2 \cup \mathcal{V}_3$, we let $\mathbb{P}'_{\mathrm{n}}((|\mathcal{S}| - i, S_i))$ (resp. $\mathbb{P}'_{\mathrm{s}}((|\mathcal{S}| - i, S_i))$) denote the probability of starting from $(|\mathcal{S}|, K)$ and passing node $(|\mathcal{S}| - i, S_i)$ at step i under $\mathbb{P}_{\mathrm{n}}$ (resp. $\mathbb{P}_{\mathrm{s}}$). Thus, we have

$$
\begin{aligned}
\mu_{\mathrm{s}}\left((|\mathcal{S}|, K)\right) &= \mathbb{E}_{\mathbb{P}_{\mathrm{s}}}\left[\mu_{\mathrm{s}}\left((|\mathcal{S}|, K)|(|\mathcal{S}| - i_0, S_{i_0})\right)\right] \\
&= \sum_{S_{i_0} \in \{K - i_0, \ldots, \min\{K, |\mathcal{S}| - i_0\}\}} \mathbb{P}'_{\mathrm{s}}\left((|\mathcal{S}| - i_0, S_{i_0})\right) \mu_{\mathrm{s}}\left((|\mathcal{S}|, K)|(|\mathcal{S}| - i_0, S_{i_0})\right) \\
&= \sum_{S_{i_0} \in \{K - i_0, \ldots, \min\{K, |\mathcal{S}| - i_0\}\}} \mathbb{P}'_{\mathrm{s}}\left((|\mathcal{S}| - i_0, S_{i_0})\right) \left(i_0 + \mu_{\mathrm{s}}\left((|\mathcal{S}| - i_0, S_{i_0})\right)\right) \\
&= i_0 + \sum_{S_{i_0} \in \{K - i_0, \ldots, \min\{K, |\mathcal{S}| - i_0\}\} \setminus \{S^*_{i_0}\}} \mathbb{P}'_{\mathrm{s}}\left((|\mathcal{S}| - i_0, S_{i_0})\right) \mu_{\mathrm{s}}\left((|\mathcal{S}| - i_0, S_{i_0})\right) \\
&\qquad + \mathbb{P}'_{\mathrm{s}}\left(\left(|\mathcal{S}| - i_0, S^*_{i_0}\right)\right) \mu_{\mathrm{s}}\left(\left(|\mathcal{S}| - i_0, S^*_{i_0}\right)\right) \\
&< i_0 + \sum_{S_{i_0} \in \{K - i_0, \ldots, \min\{K, |\mathcal{S}| - i_0\}\} \setminus \{S^*_{i_0}\}} \mathbb{P}'_{\mathrm{s}}\left((|\mathcal{S}| - i_0, S_{i_0})\right) \mu_{\mathrm{s}}\left((|\mathcal{S}| - i_0, S_{i_0})\right) \\
&\qquad + \mathbb{P}'_{\mathrm{s}}\left(\left(|\mathcal{S}| - i_0, S^*_{i_0}\right)\right) \mu_{\mathrm{n}}\left(\left(|\mathcal{S}| - i_0, S^*_{i_0}\right)\right) \qquad \text{(C.27)} \\
&= i_0 + \sum_{S_{i_0} \in \{K - i_0, \ldots, \min\{K, |\mathcal{S}| - i_0\}\} \setminus \{S^*_{i_0}\}} \mathbb{P}'_{\mathrm{n}}\left((|\mathcal{S}| - i_0, S_{i_0})\right) \mu_{\mathrm{n}}\left((|\mathcal{S}| - i_0, S_{i_0})\right) \\
&\qquad + \mathbb{P}'_{\mathrm{n}}\left(\left(|\mathcal{S}| - i_0, S^*_{i_0}\right)\right) \mu_{\mathrm{n}}\left(\left(|\mathcal{S}| - i_0, S^*_{i_0}\right)\right) \qquad \text{(C.28)} \\
&= \sum_{S_{i_0} \in \{K - i_0, \ldots, \min\{K, |\mathcal{S}| - i_0\}\}} \mathbb{P}'_{\mathrm{n}}\left((|\mathcal{S}| - i_0, S_{i_0})\right) \left(i_0 + \mu_{\mathrm{n}}\left((|\mathcal{S}| - i_0, S_{i_0})\right)\right) \\
&= \mu_{\mathrm{n}}\left((|\mathcal{S}|, K)\right),
\end{aligned}
$$

where (C.27) holds by (C.26). To show (C.28) holds, we note that for any node $(|\mathcal{S}| - i_0, S_{i_0}) \in \mathcal{V}_2 \cup \mathcal{V}_3$, any paths that start from $(|\mathcal{S}|, K)$ and pass $(|\mathcal{S}| - i_0, S_{i_0})$ at step i_0 do not pass $(|\mathcal{S}| - i_0, S^*_{i_0})$ before step i_0 (see Figure C.3). As a result, $\mathbb{P}'_{\mathrm{s}}((|\mathcal{S}| - i_0, S_{i_0})) = \mathbb{P}'_{\mathrm{n}}((|\mathcal{S}| - i_0, S_{i_0}))$ for any $(|\mathcal{S}| - i_0, S_{i_0}) \in \mathcal{V}_2 \cup \mathcal{V}_3$, because $\mathbb{P}_{\mathrm{n}}((|\mathcal{S}| - i, S_i), (|\mathcal{S}| - i - 1, S_i - 1)) = \mathbb{P}_{\mathrm{s}}((|\mathcal{S}| - i, S_i), (|\mathcal{S}| - i - 1, S_i - 1))$ for any $(|\mathcal{S}| - i, S_i) \in \mathcal{V}_2 \cup \mathcal{V}_3 \setminus \{(|\mathcal{S}| - i_0, S^*_{i_0})\}$. Meanwhile, for any node $(|\mathcal{S}| - i_0, S_{i_0}) \in \mathcal{V}_2 \cup \mathcal{V}_3 \setminus \{(|\mathcal{S}| - i_0, S^*_{i_0})\}$, the path starting from this node clearly does not pass its parent node $(|\mathcal{S}| - i_0, S^*_{i_0})$ (see Figure C.3). Thus, $\mu_{\mathrm{s}}((|\mathcal{S}| - i_0, S_{i_0})) = \mu_{\mathrm{n}}((|\mathcal{S}| - i_0, S_{i_0}))$ for any $(|\mathcal{S}| - i_0, S_{i_0}) \in \mathcal{V}_2 \cup \mathcal{V}_3 \setminus \{(|\mathcal{S}| - i_0, S^*_{i_0})\}$, indicating that (C.28) holds. Therefore, we have $\mu_{\mathrm{n}}((|\mathcal{S}|, K)) > \mu_{\mathrm{s}}((|\mathcal{S}|, K))$ when $|\mathcal{C}| = 1$.

Third, we assume that $\mu_{\mathrm{n}}((|\mathcal{S}|, K)) > \mu_{\mathrm{s}}((|\mathcal{S}|, K))$ when $|\mathcal{C}| = M$ and $1 \leq M \leq |\mathcal{V}_3| - 1$.

We further consider $|\mathcal{C}| = M+1$. For notational brevity, we use a superscript index that equals $|\mathcal{C}|$ to distinguish $\mathcal{C}$, $\mathbb{P}$, $\mathbb{P}'$, and μ across different induction cases with respect to $|\mathcal{C}|$. Without loss of generality, we assume $\mathcal{C}^{M+1} \backslash \mathcal{C}^M = \{(|\mathcal{S}|-i_M, S^*_{i_M})\}$, where $(|\mathcal{S}|-i_M, S^*_{i_M})$ is an arbitrary node in $\mathcal{V}_2 \cup \mathcal{V}_3 \setminus \mathcal{C}^M$. The only difference between the cases $|\mathcal{C}| = M$ and $|\mathcal{C}| = M+1$ is the probability of transitioning from $(|\mathcal{S}|-i_M, S^*_{i_M})$ to $(|\mathcal{S}|-i_M-1, S^*_{i_M}-1)$ or $(|\mathcal{S}|-i_M-1, S^*_{i_M})$ under strategic selection. Thus, for any $(|\mathcal{S}|-i, S_i) \in \mathcal{V}_2 \cup \mathcal{V}_3$, we have $\mathbb{P}_{\mathrm{n}}^{M+1}((|\mathcal{S}|-i, S_i), (|\mathcal{S}|-i-1, S_i-1)) = \mathbb{P}_{\mathrm{n}}^{M}((|\mathcal{S}|-i, S_i), (|\mathcal{S}|-i-1, S_i-1))$, indicating that $\mu_{\mathrm{n}}^{M+1}((|\mathcal{S}|, K)) = \mu_{\mathrm{n}}^{M}((|\mathcal{S}|, K))$. For any $(|\mathcal{S}|-i, S_i) \in \mathcal{V}_2 \cup \mathcal{V}_3 \setminus \{(|\mathcal{S}|-i_M, S^*_{i_M})\}$, we have $\mathbb{P}_{\mathrm{s}}^{M+1}((|\mathcal{S}|-i, S_i), (|\mathcal{S}|-i-1, S_i-1)) = \mathbb{P}_{\mathrm{s}}^{M}((|\mathcal{S}|-i, S_i), (|\mathcal{S}|-i-1, S_i-1))$. For $(|\mathcal{S}|-i_M, S^*_{i_M})$, we have

$$\begin{aligned}
\mathbb{P}_{\mathrm{s}}^{M+1}\left((|\mathcal{S}|-i_M, S^*_{i_M}), (|\mathcal{S}|-i_M-1, S^*_{i_M}-1)\right) &> \mathbb{P}_{\mathrm{n}}^{M+1}\left((|\mathcal{S}|-i_M, S^*_{i_M}), (|\mathcal{S}|-i_M-1, S^*_{i_M}-1)\right) \\
&= \mathbb{P}_{\mathrm{n}}^{M}\left((|\mathcal{S}|-i_M, S^*_{i_M}), (|\mathcal{S}|-i_M-1, S^*_{i_M}-1)\right) \\
&= \mathbb{P}_{\mathrm{s}}^{M}\left((|\mathcal{S}|-i_M, S^*_{i_M}), (|\mathcal{S}|-i_M-1, S^*_{i_M}-1)\right),
\end{aligned}$$

where the inequality holds because $(|\mathcal{S}|-i_M, S^*_{i_M}) \in \mathcal{C}^{M+1}$ and the last equality holds because $(|\mathcal{S}|-i_M, S^*_{i_M}) \notin \mathcal{C}^M$.

Similar to the case $|\mathcal{C}| = 1$, we can now show that $\mu_{\mathrm{s}}^{M}((|\mathcal{S}|, K)) > \mu_{\mathrm{s}}^{M+1}((|\mathcal{S}|, K))$. Specifically,

$$\begin{aligned}
\mu_{\mathrm{s}}^{M}\left((|\mathcal{S}|-i_M, S^*_{i_M})\right) &= \mu_{\mathrm{s}}^{M}\left((|\mathcal{S}|-i_M-1, S^*_{i_M}-1)\right)\mathbb{P}_{\mathrm{s}}^{M}\left((|\mathcal{S}|-i_M, S^*_{i_M}), (|\mathcal{S}|-i_M-1, S^*_{i_M}-1)\right) \\
&\quad - \mu_{\mathrm{s}}^{M}\left((|\mathcal{S}|-i_M-1, S^*_{i_M})\right)\mathbb{P}_{\mathrm{s}}^{M}\left((|\mathcal{S}|-i_M, S^*_{i_M}), (|\mathcal{S}|-i_M-1, S^*_{i_M}-1)\right) \\
&\quad + \mu_{\mathrm{s}}^{M}\left((|\mathcal{S}|-i_M-1, S^*_{i_M})\right) + 1 \\
&> \mu_{\mathrm{s}}^{M}\left((|\mathcal{S}|-i_M-1, S^*_{i_M}-1)\right)\mathbb{P}_{\mathrm{s}}^{M+1}\left((|\mathcal{S}|-i_M, S^*_{i_M}), (|\mathcal{S}|-i_M-1, S^*_{i_M}-1)\right) \\
&\quad - \mu_{\mathrm{s}}^{M}\left((|\mathcal{S}|-i_M-1, S^*_{i_M})\right)\mathbb{P}_{\mathrm{s}}^{M+1}\left((|\mathcal{S}|-i_M, S^*_{i_M}), (|\mathcal{S}|-i_M-1, S^*_{i_M}-1)\right) \\
&\quad + \mu_{\mathrm{s}}^{M}\left((|\mathcal{S}|-i_M-1, S^*_{i_M})\right) + 1 \\
&= \mu_{\mathrm{s}}^{M+1}\left((|\mathcal{S}|-i_M-1, S^*_{i_M}-1)\right)\mathbb{P}_{\mathrm{s}}^{M+1}\left((|\mathcal{S}|-i_M, S^*_{i_M}), (|\mathcal{S}|-i_M-1, S^*_{i_M}-1)\right) \\
&\quad - \mu_{\mathrm{s}}^{M+1}\left((|\mathcal{S}|-i_M-1, S^*_{i_M})\right)\mathbb{P}_{\mathrm{s}}^{M+1}\left((|\mathcal{S}|-i_M, S^*_{i_M}), (|\mathcal{S}|-i_M-1, S^*_{i_M}-1)\right) \\
&\quad + \mu_{\mathrm{s}}^{M+1}\left((|\mathcal{S}|-i_M-1, S^*_{i_M})\right) + 1 \\
&= \mu_{\mathrm{s}}^{M+1}\left((|\mathcal{S}|-i_M, S^*_{i_M})\right).
\end{aligned}$$

Based on this result, we can show that

$$\begin{aligned}
\mu_{\mathrm{s}}^{M+1}\left(\left(|\mathcal{S}|,K\right)\right) &= i_M + \sum_{S_{i_M}\in\{K-i_M,\ldots,\min\{K,|\mathcal{S}|-i_M\}\}\setminus\{S_{i_M}^*\}} \mathbb{P}_{\mathrm{s}}^{M+1'}\left(\left(|\mathcal{S}|-i_M,S_{i_M}\right)\right)\mu_{\mathrm{s}}^{M+1}\left(\left(|\mathcal{S}|-i_M,S_{i_M}\right)\right) \\
&\qquad + \mathbb{P}_{\mathrm{s}}^{M+1'}\left(\left(|\mathcal{S}|-i_M,S_{i_M}^*\right)\right)\mu_{\mathrm{s}}^{M+1}\left(\left(|\mathcal{S}|-i_M,S_{i_M}^*\right)\right) \\
&< i_M + \sum_{S_{i_M}\in\{K-i_M,\ldots,\min\{K,|\mathcal{S}|-i_M\}\}\setminus\{S_{i_M}^*\}} \mathbb{P}_{\mathrm{s}}^{M+1'}\left(\left(|\mathcal{S}|-i_M,S_{i_M}\right)\right)\mu_{\mathrm{s}}^{M+1}\left(\left(|\mathcal{S}|-i_M,S_{i_M}\right)\right) \\
&\qquad + \mathbb{P}_{\mathrm{s}}^{M+1'}\left(\left(|\mathcal{S}|-i_M,S_{i_M}^*\right)\right)\mu_{\mathrm{s}}^{M}\left(\left(|\mathcal{S}|-i_M,S_{i_M}^*\right)\right) \\
&= i_M + \sum_{S_{i_M}\in\{K-i_M,\ldots,\min\{K,|\mathcal{S}|-i_M\}\}\setminus\{S_{i_M}^*\}} \mathbb{P}_{\mathrm{s}}^{M'}\left(\left(|\mathcal{S}|-i_M,S_{i_M}\right)\right)\mu_{\mathrm{s}}^{M}\left(\left(|\mathcal{S}|-i_M,S_{i_M}\right)\right) \\
&\qquad + \mathbb{P}_{\mathrm{s}}^{M'}\left(\left(|\mathcal{S}|-i_M,S_{i_M}^*\right)\right)\mu_{\mathrm{s}}^{M}\left(\left(|\mathcal{S}|-i_M,S_{i_M}^*\right)\right) \\
&= \mu_{\mathrm{s}}^{M}\left(\left(|\mathcal{S}|,K\right)\right).
\end{aligned}$$

Therefore, we have $\mu_{\mathrm{s}}^{M+1}((|\mathcal{S}|,K)) < \mu_{\mathrm{s}}^{M}((|\mathcal{S}|,K)) < \mu_{\mathrm{n}}^{M}((|\mathcal{S}|,K)) = \mu_{\mathrm{n}}^{M+1}((|\mathcal{S}|,K))$, where the second inequality holds by induction. It follows that $\mu_{\mathrm{n}}^{M}((|\mathcal{S}|,K)) > \mu_{\mathrm{s}}^{M}((|\mathcal{S}|,K))$ for any $|\mathcal{C}| = M \in [1,|\mathcal{V}_3|]_{\mathbb{Z}}$. That is, $\mu_{\mathrm{n}}((|\mathcal{S}|,K)) \geq \mu_{\mathrm{s}}((|\mathcal{S}|,K))$ and Algorithm 4 terminates in fewer steps by adopting strategic selection than naive selection. □

C.9 Proof of Lemma 2

Proof. When $t \in [L+1,T]_{\mathbb{Z}}$, we have $y_t \geq \sum_{s=t-L+1}^{t} u_s = \sum_{s=t-L+1}^{t-k} u_s + \sum_{s=t-k+1}^{t} u_s \geq \sum_{s=t-k+1}^{t} u_s$, where the first inequality holds by (4.35a) and the second inequality holds because $u_s \geq 0$ for any $s \in [2,T]_{\mathbb{Z}}$. When $t \in [k+1,L]_{\mathbb{Z}}$, we have $y_t = \sum_{s=t}^{L}(y_s - y_{s+1} + u_{s+1}) + (y_{L+1} - \sum_{s=0}^{L-1} u_{L+1-s}) + \sum_{s=2}^{t} u_s \geq \sum_{s=2}^{t} u_s = \sum_{s=2}^{t-k} u_s + \sum_{s=t-k+1}^{t} u_s \geq \sum_{s=t-k+1}^{t} u_s$, where the first inequality holds by (4.35a) and (4.35c) and the second inequality holds because $u_s \geq 0$ for any $s \in [2,T]_{\mathbb{Z}}$. □

C.10 Proof of Lemma 3

Proof. When $t-k+\ell \leq T$, we have $y_{t-k}+\sum_{s=t-k+1}^{t} u_s \leq y_{t-k}+\sum_{s=t-k+1}^{t} u_s+\sum_{s=t+1}^{t-k+\ell} u_s \leq 1$, where the first inequality holds because $u_s \geq 0$ for any $s \in [2,T]_{\mathbb{Z}}$ and the second inequality holds by (4.35b). When $t-k+\ell \geq T+1$, we have $y_{t-k} + \sum_{s=t-k+1}^{t} u_s \leq y_{t-k} + \sum_{s=t-k+1}^{T} u_s = (y_{T-\ell} + \sum_{s=T-\ell+1}^{T} u_s) + \sum_{s=T-\ell+1}^{t-k}(y_s - y_{s-1} - u_s) \leq 1$, where the first inequality holds because $u_s \geq 0$ for any $s \in [2,T]_{\mathbb{Z}}$ and the second inequality holds

by (4.35b) and (4.35c). □

C.11 Proof of Lemma 4

Proof. Consider any $t \in [2, T]_{\mathbb{Z}}$. As $y_t \in \{0, 1\}$ for any $t \in \mathcal{T}$, we divide the analysis into the following three possible cases.

Case 1: $y_t = 0$. We have $p_t = 0$ by (4.35e) and (4.35h). Clearly, $p_t - p_{t-1} = -p_{t-1} \leq V$ because $p_{t-1} \geq 0$ by (4.35h).

Case 2: $(y_{t-1}, y_t) = (0, 1)$. We have $p_t - p_{t-1} \leq p_t + r_t^+ - p_{t-1} \leq \overline{V} - \underline{C} < V$, where the first inequality holds because $r_t^+ \geq 0$, the second inequality holds by the ramp-up constraint (4.35f) at t, and the third inequality holds by the problem setting in Section 4.3.2.

Case 3: $(y_{t-1}, y_t) = (1, 1)$. We have $p_t - p_{t-1} \leq p_t + r_t^+ - p_{t-1} \leq V$, where the first inequality holds because $r_t^+ \geq 0$ and the second inequality holds by the ramp-up constraint (4.35f) at t. □

C.12 Proof of Proposition 7

Proof. To prove that inequality (4.36) is valid for $\text{conv}(\mathcal{D})$ for any $t \in [3, T]_{\mathbb{Z}}$, it suffices to show that it is valid for $\mathcal{D}$ for any $t \in [3, T]_{\mathbb{Z}}$. Consider any element $(\mathbf{p}, \mathbf{r}^+, \mathbf{r}^-, \mathbf{y}, \mathbf{u})$ of $\mathcal{D}$ and any $t \in [3, T]_{\mathbb{Z}}$. We show that $(\mathbf{p}, \mathbf{r}^+, \mathbf{r}^-, \mathbf{y}, \mathbf{u})$ satisfies (4.36). We divide the analysis into the following four possible cases.

Case 1: $y_t = 0$. By the problem setting in Section 4.3.2, we have $\overline{V} - \underline{C} \geq 0$ and $\underline{C} + V - \overline{V} \geq 0$. By Corollary 1, we have $y_t - u_t \geq 0$ and $y_{t-1} - u_{t-1} \geq 0$. Thus, the right-hand side of inequality (4.36) is nonnegative. Because $y_t = 0$, by (4.35d), (4.35e), and (4.35h), we have $r_t^+ = r_t^- = 0$. Therefore, in this case, $(\mathbf{p}, \mathbf{r}^+, \mathbf{r}^-, \mathbf{y}, \mathbf{u})$ satisfies (4.36).

Case 2: $y_t = 1$ and $u_t = 1$. By Corollary 1, we have $y_{t-1} \leq 1 - u_t = 0$, implying that $y_{t-1} = 0$. It further implies that $u_{t-1} = 0$ because $y_{t-1} \geq u_{t-1}$ by Corollary 1 and that $p_{t-1} = 0$ by (4.35e) and (4.35h). Thus, the right-hand side of inequality (4.36) is $\overline{V} - \underline{C}$. Because $p_{t-1} = y_{t-1} = 0$ and $y_t = 1$, by (4.35f), we have $p_t + r_t^+ \leq \overline{V} - \underline{C}$. Thus, $r_t^+ + r_t^- \leq r_t^+ + p_t \leq \overline{V} - \underline{C}$, where the first inequality holds by (4.35d). Therefore, in this case, $(\mathbf{p}, \mathbf{r}^+, \mathbf{r}^-, \mathbf{y}, \mathbf{u})$ satisfies (4.36).

Case 3: $y_t = 1$, $u_t = 0$, and $u_{t-1} = 1$. We have $y_{t-1} \geq u_{t-1} = 1$ and $y_{t-2} \leq 1 - u_{t-1} = 0$ by Corollary 1, implying that $y_{t-1} = 1$ and $y_{t-2} = 0$. Thus, the right-hand side of inequality (4.36) is $\overline{V} - \underline{C} + V$. Because $y_{t-2} = 0$, we have $p_{t-2} = 0$ by (4.35e) and (4.35h). Because $y_{t-1} = 1$ and $y_{t-2} = p_{t-2} = 0$, by (4.35f) at $t-1$, we have $p_{t-1} + r^+_{t-1} \leq \overline{V} - \underline{C}$, implying that $p_{t-1} \leq \overline{V} - \underline{C}$ because $r^+_{t-1} \geq 0$. Because $y_{t-1} = y_t = 1$, by (4.35f) at t, we have $p_t + r^+_t - p_{t-1} \leq V$. Thus, $r^+_t + r^-_t \leq r^+_t + p_t \leq p_{t-1} + V \leq \overline{V} - \underline{C} + V$, where the first inequality holds by (4.35d). Therefore, in this case, $(\mathbf{p}, \mathbf{r}^+, \mathbf{r}^-, \mathbf{y}, \mathbf{u})$ satisfies (4.36).

Case 4: $y_t = 1$, $u_t = 0$, and $u_{t-1} = 0$. We have $y_{t-1} \geq y_t - u_t = 1$ by (4.35c), implying that $y_{t-1} = 1$. Thus, the right-hand side of inequality (4.36) is $2V$. Because $y_{t-1} = y_t = 1$, (i) by (4.35f) at t, we have $p_t + r^+_t - p_{t-1} \leq V$, and (ii) by (4.35h) at t, we have $p_{t-1} + r^-_t - p_t \leq V$. It follows that $r^+_t + r^-_t = (p_t + r^+_t - p_{t-1}) + (p_{t-1} + r^-_t - p_t) \leq 2V$. Therefore, in this case, $(\mathbf{p}, \mathbf{r}^+, \mathbf{r}^-, \mathbf{y}, \mathbf{u})$ satisfies (4.36).

Coonsider any $t \in [3, T]_{\mathbb{Z}}$. To prove inequality (4.36) is facet-defining for $\text{conv}(\mathcal{D})$ when $\overline{C} - \underline{C} > 2V$ and $L = 1$, it suffices to create $5T - 1$ affinely independent points in $\text{conv}(\mathcal{D})$ that satisfy (4.36) at equality. Because $\mathbf{0} \in \text{conv}(\mathcal{D})$ and $\mathbf{0}$ satisfies (4.36) at equality, it suffices to create the remaining $5T - 2$ nonzero linearly independent points. We let $\grave{\boldsymbol{\theta}} = (\grave{\mathbf{p}}, \grave{\mathbf{r}}^+, \grave{\mathbf{r}}^-, \grave{\mathbf{y}}, \grave{\mathbf{u}})$ and denote the sth component of $\grave{\mathbf{p}}$, $\grave{\mathbf{r}}^+$, $\grave{\mathbf{r}}^-$, $\grave{\mathbf{y}}$, and $\grave{\mathbf{u}}$ by $\grave{p}_s$, $\grave{r}^+_s$, $\grave{r}^-_s$, $\grave{y}_s$, and $\grave{u}_s$. Similarly, we define $\acute{\boldsymbol{\theta}}$, $\hat{\boldsymbol{\theta}}$, $\overline{\boldsymbol{\theta}}$, and $\dot{\boldsymbol{\theta}}$. We denote the $5T - 2$ nonzero linearly independent points by $\grave{\boldsymbol{\theta}}^\alpha$ for $\alpha \in \mathcal{T}$, $\acute{\boldsymbol{\theta}}^\alpha$ for $\alpha \in \mathcal{T} \setminus \{t\}$, $\hat{\boldsymbol{\theta}}^\alpha$ for $\alpha \in \mathcal{T}$, $\overline{\boldsymbol{\theta}}^\alpha$ for $\alpha \in \mathcal{T}$, and $\dot{\boldsymbol{\theta}}^\alpha$ for $\alpha \in \mathcal{T} \setminus \{1\}$. We let $\epsilon = \min\{\underline{C} + V - \overline{V},\ \overline{V} - \underline{C},\ \overline{C} - \underline{C} - 2V\} > 0$ and divide the $5T - 2$ points into the following 16 groups.

(A1) For each $\alpha \in [1, t-1]_{\mathbb{Z}}$, we create a point $\grave{\boldsymbol{\theta}}^\alpha$ as follows:

$$\grave{p}^\alpha_s = \begin{cases} \overline{V} - \underline{C}, & s \in [1, \alpha]_{\mathbb{Z}} \\ 0, & s \in [\alpha + 1, T]_{\mathbb{Z}} \end{cases}, \quad \grave{y}^\alpha_s = \begin{cases} 1, & s \in [1, \alpha]_{\mathbb{Z}} \\ 0, & s \in [\alpha + 1, T]_{\mathbb{Z}} \end{cases},$$

$\grave{r}^{+,\alpha}_s = \grave{r}^{-,\alpha}_s = 0$ for any $s \in \mathcal{T}$, and $\grave{u}^\alpha_s = 0$ for any $s \in \mathcal{T} \setminus \{1\}$. It is easy to verify that $\grave{\boldsymbol{\theta}}^\alpha$ satisfies (4.35a)–(4.35h). Thus, $\grave{\boldsymbol{\theta}}^\alpha \in \text{conv}(\mathcal{D})$. It is also easy to verify that $\grave{\boldsymbol{\theta}}^\alpha$ satisfies (4.36) at equality.

(A2) For $\alpha = t$, we create a point $\grave{\boldsymbol{\theta}}^{\alpha}$ as follows:

$$\grave{p}_s^{\alpha} = \begin{cases} V, & s \in [1, t-2]_{\mathbb{Z}} \\ V + \epsilon, & s = t-1 \\ \overline{V} - \underline{C}, & s = t \\ 0, & \text{otherwise (o.w.)} \end{cases}, \quad \grave{r}_s^{+,\alpha} = \begin{cases} 2V - \overline{V} + \underline{C} + \epsilon, & s = t \\ 0, & \text{o.w.} \end{cases},$$

$$\grave{r}_s^{-,\alpha} = \begin{cases} \overline{V} - \underline{C} - \epsilon, & s = t \\ 0, & \text{o.w.} \end{cases},$$

$\grave{y}_s^{\alpha} = 1$ for any $s \in [1, t]_{\mathbb{Z}}$ and $\grave{y}_s^{\alpha} = 0$ otherwise, and $\grave{u}_s^{\alpha} = 0$ for any $s \in \mathcal{T} \setminus \{1\}$. Note that $\overline{C} - \underline{C} > 2V$ and $\underline{C} < \overline{V} < \underline{C} + V$. Thus, $\grave{\boldsymbol{\theta}}^{\alpha}$ satisfies (4.35a)–(4.35h), i.e., $\grave{\boldsymbol{\theta}}^{\alpha} \in \text{conv}(\mathcal{D})$. It is also easy to verify that $\grave{\boldsymbol{\theta}}^{\alpha}$ satisfies (4.36) at equality.

(A3) For each $\alpha \in [t+1, T]_{\mathbb{Z}}$, we create a point $\grave{\boldsymbol{\theta}}^{\alpha}$ as follows:

$$\grave{p}_s^{\alpha} = \begin{cases} V, & s \in [1, t-1]_{\mathbb{Z}} \\ \overline{V} - \underline{C}, & s \in [t, \alpha]_{\mathbb{Z}} \\ 0, & \text{o.w.} \end{cases}, \quad \grave{r}_s^{+,\alpha} = \begin{cases} 2V - \overline{V} + \underline{C}, & s = t \\ 0, & \text{o.w.} \end{cases}, \quad \grave{r}_s^{-,\alpha} = \begin{cases} \overline{V} - \underline{C}, & s = t \\ 0, & \text{o.w.} \end{cases},$$

$\grave{y}_s^{\alpha} = 1$ for any $s \in [1, \alpha]_{\mathbb{Z}}$ and $\grave{y}_s^{\alpha} = 0$ otherwise, and $\grave{u}_s^{\alpha} = 0$ for any $s \in \mathcal{T} \setminus \{1\}$. It is easy to verify that $\grave{\boldsymbol{\theta}}^{\alpha}$ satisfies (4.35a)–(4.35h). Thus, $\grave{\boldsymbol{\theta}}^{\alpha} \in \text{conv}(\mathcal{D})$. It is also easy to verify that $\grave{\boldsymbol{\theta}}^{\alpha}$ satisfies (4.36) at equality.

(A4) For each $\alpha \in [1, t-1]_{\mathbb{Z}}$, we create a point $\acute{\boldsymbol{\theta}}^{\alpha}$ as follows:

$$\acute{p}_s^{\alpha} = \begin{cases} \overline{V} - \underline{C}, & s \in [1, \alpha]_{\mathbb{Z}} \\ 0, & \text{o.w.} \end{cases}, \quad \acute{r}_s^{+,\alpha} = \begin{cases} \overline{V} - \underline{C}, & s \in [1, \alpha]_{\mathbb{Z}} \\ 0, & \text{o.w.} \end{cases},$$

$\acute{r}_s^{-,\alpha} = 0$ for any $s \in \mathcal{T}$, $\acute{y}_s^{\alpha} = 1$ for any $s \in [1, \alpha]_{\mathbb{Z}}$ and $\acute{y}_s^{\alpha} = 0$ otherwise, and $\acute{u}_s^{\alpha} = 0$ for any $s \in \mathcal{T} \setminus \{1\}$. It is easy to verify that $\acute{\boldsymbol{\theta}}^{\alpha}$ satisfies (4.35a)–(4.35d) and (4.35f)–(4.35h). Note that $0 < 2\overline{V} - 2\underline{C} < 2(\underline{C} + V) - 2\underline{C} = 2V < \overline{C} - \underline{C}$. Thus, $\acute{\boldsymbol{\theta}}^{\alpha}$ also satisfies (4.35e), implying that $\acute{\boldsymbol{\theta}}^{\alpha} \in \text{conv}(\mathcal{D})$. It is also easy to verify that $\acute{\boldsymbol{\theta}}^{\alpha}$ satisfies (4.36) at equality.

(A5) For each $\alpha \in [t+1, T]_{\mathbb{Z}}$, we create a point $\acute{\boldsymbol{\theta}}^{\alpha}$ as follows:

$$\acute{p}_s^{\alpha} = \begin{cases} V, & s \in [1, t-1]_{\mathbb{Z}} \\ \overline{V} - \underline{C}, & s \in [t, \alpha]_{\mathbb{Z}} \\ 0, & \text{o.w.} \end{cases}, \quad \acute{r}_s^{+,\alpha} = \begin{cases} \overline{V} - \underline{C}, & s \in [1, \alpha]_{\mathbb{Z}} \setminus \{t\} \\ 2V - \overline{V} + \underline{C}, & s = t \\ 0, & \text{o.w.} \end{cases},$$

$$\acute{r}_s^{-,\alpha} = \begin{cases} \overline{V} - \underline{C}, & s = t \\ 0, & \text{o.w.} \end{cases},$$

$\acute{y}_s^{\alpha} = 1$ for any $s \in [1, \alpha]_{\mathbb{Z}}$ and $\acute{y}_s^{\alpha} = 0$ otherwise, and $\acute{u}_s^{\alpha} = 0$ for any $s \in \mathcal{T} \setminus \{1\}$. It is easy to verify that $\acute{\boldsymbol{\theta}}^{\alpha}$ satisfies (4.35a)–(4.35d) and (4.35f)–(4.35h). Note that $V + \overline{V} - \underline{C} < V + (\underline{C} + V) - \underline{C} = 2V < \overline{C} - \underline{C}$. Thus, $\acute{\boldsymbol{\theta}}^{\alpha}$ also satisfies (4.35e), implying that $\acute{\boldsymbol{\theta}}^{\alpha} \in \text{conv}(\mathcal{D})$. It is also easy to verify that $\acute{\boldsymbol{\theta}}^{\alpha}$ satisfies (4.36) at equality.

(A6) For $\alpha = 1$, we create a point $\hat{\boldsymbol{\theta}}^{\alpha}$ as follows:

$$\hat{p}_s^{\alpha} = \begin{cases} \overline{V} - \underline{C}, & s = 1 \\ 0, & \text{o.w.} \end{cases}, \quad \hat{r}_s^{-,\alpha} = \begin{cases} \overline{V} - \underline{C}, & s = 1 \\ 0, & \text{o.w.} \end{cases}, \quad \hat{y}_s^{\alpha} = \begin{cases} 1, & s = 1 \\ 0, & \text{o.w.} \end{cases},$$

$\hat{r}_s^{+,\alpha} = 0$ for any $s \in \mathcal{T}$, and $\hat{u}_s^{+,\alpha} = 0$ for any $s \in \mathcal{T} \setminus \{1\}$. It is easy to verify that $\hat{\boldsymbol{\theta}}^{\alpha}$ satisfies (4.35a)–(4.35h). Thus, $\hat{\boldsymbol{\theta}}^{\alpha} \in \text{conv}(\mathcal{D})$. It is also easy to verify that $\hat{\boldsymbol{\theta}}^{\alpha}$ satisfies (4.36) at equality.

(A7) For each $\alpha \in [2, t-2]_{\mathbb{Z}}$, we create a point $\hat{\boldsymbol{\theta}}^{\alpha}$ as follows:

$$\hat{p}_s^{\alpha} = \hat{r}_s^{-,\alpha} = \begin{cases} \overline{V} - \underline{C}, & s = \alpha \\ 0, & \text{o.w.} \end{cases}, \quad \hat{y}_s^{\alpha} = \hat{u}_s^{\alpha} = \begin{cases} 1, & s = \alpha \\ 0, & \text{o.w.} \end{cases},$$

and $\hat{r}_s^{+,\alpha} = 0$ for any $s \in \mathcal{T}$. It is easy to verify that $\hat{\boldsymbol{\theta}}^{\alpha}$ satisfies (4.35a)–(4.35h) because $L = 1$. Thus, $\hat{\boldsymbol{\theta}}^{\alpha} \in \text{conv}(\mathcal{D})$. It is also easy to verify that $\hat{\boldsymbol{\theta}}^{\alpha}$ satisfies (4.36) at equality.

(A8) For each $\alpha = t-1$, we create a point $\hat{\boldsymbol{\theta}}^{\alpha}$ as follows:

$$\hat{p}_s^{\alpha} = \begin{cases} \overline{V} - \underline{C}, & s \in [t-1, \min\{t+1, T\}]_{\mathbb{Z}} \setminus \{t\} \\ \overline{V} + V - \underline{C}, & s = t \\ 0, & \text{o.w.} \end{cases}, \quad \hat{r}_s^{-,\alpha} = \begin{cases} \overline{V} - \underline{C}, & s = t-1 \\ \overline{V} + V - \underline{C}, & s = t \\ 0, & \text{o.w.} \end{cases},$$

$$\hat{y}_s^{\alpha} = \begin{cases} 1, & s \in [t-1, \min\{t+1, T\}]_{\mathbb{Z}} \\ 0, & \text{o.w.} \end{cases}, \quad \hat{u}_s^{\alpha} = \begin{cases} 1, & s = t-1 \\ 0, & \text{o.w.} \end{cases},$$

and $\hat{r}_s^{+,\alpha} = 0$ for any $s \in \mathcal{T}$. Note that $\overline{V} + V - \underline{C} < (\underline{C} + V) + V - \underline{C} = 2V < \overline{C} - \underline{C}$. Thus, $\hat{\boldsymbol{\theta}}^{\alpha}$ satisfies (4.35a)–(4.35h) and $\hat{\boldsymbol{\theta}}^{\alpha} \in \text{conv}(\mathcal{D})$. It is also easy to verify that $\hat{\boldsymbol{\theta}}^{\alpha}$ satisfies (4.36) at equality.

(A9) For each $\alpha = t$, we create a point $\hat{\boldsymbol{\theta}}^{\alpha}$ as follows:

$$\hat{p}_s^{\alpha} = \begin{cases} \overline{V} - \underline{C} - \epsilon, & s = t \\ 0, & \text{o.w.} \end{cases}, \quad \hat{r}_s^{+,\alpha} = \begin{cases} \epsilon, & s = t \\ 0, & \text{o.w.} \end{cases}, \quad \hat{r}_s^{-,\alpha} = \begin{cases} \overline{V} - \underline{C} - \epsilon, & s = t \\ 0, & \text{o.w.} \end{cases},$$

and $\hat{y}_s^{\alpha} = \hat{u}_s^{\alpha} = 1$ for $s = t$ and $\hat{y}_s^{\alpha} = \hat{u}_s^{\alpha} = 0$ otherwise. It is clear that $\hat{\boldsymbol{\theta}}^{\alpha}$ satisfies (4.35a)–(4.35h) because $L = 1$. Thus, $\hat{\boldsymbol{\theta}}^{\alpha} \in \text{conv}(\mathcal{D})$. It is also easy to verify that $\hat{\boldsymbol{\theta}}^{\alpha}$ satisfies (4.36) at equality.

(A10) For each $\alpha \in [t+1, T]_{\mathbb{Z}}$, we create a point $\hat{\boldsymbol{\theta}}^{\alpha}$ as follows:

$$\hat{p}_s^{\alpha} = \begin{cases} \overline{V} - \underline{C}, & s = \alpha \\ 0, & \text{o.w.} \end{cases}, \quad \hat{r}_s^{-,\alpha} = \begin{cases} \overline{V} - \underline{C}, & s = \alpha \\ 0, & \text{o.w.} \end{cases}, \quad \hat{y}_s^{\alpha} = \hat{u}_s^{\alpha} = \begin{cases} 1, & s = \alpha \\ 0, & \text{o.w.} \end{cases},$$

and $\hat{r}_s^{+,\alpha} = 0$ for any $s \in \mathcal{T}$. It is easy to verify that $\hat{\boldsymbol{\theta}}^{\alpha}$ satisfies (4.35a)–(4.35h) because $L = 1$. Thus, $\hat{\boldsymbol{\theta}}^{\alpha} \in \text{conv}(\mathcal{D})$. It is also easy to verify that $\hat{\boldsymbol{\theta}}^{\alpha}$ satisfies (4.36) at equality.

(A11) For each $\alpha \in [1, t-1]_{\mathbb{Z}}$, we create a point $\overline{\boldsymbol{\theta}}^{\alpha}$ as follows:

$$\overline{p}_s^{\alpha} = \begin{cases} \overline{V} - \underline{C} - \epsilon, & s \in [1, \alpha]_{\mathbb{Z}} \\ 0, & \text{o.w.} \end{cases}, \ \overline{y}_s^{\alpha} = \begin{cases} 1, & s \in [1, \alpha]_{\mathbb{Z}} \\ 0, & \text{o.w.} \end{cases},$$

$\overline{r}_s^{+,\alpha} = \overline{r}_s^{-,\alpha} = 0$ for any $s \in \mathcal{T}$, and $\overline{u}_s^{\alpha} = 0$ for any $s \in \mathcal{T} \setminus \{1\}$. It is easy to verify that $\overline{\boldsymbol{\theta}}^{\alpha}$ satisfies (4.35a)–(4.35h). Thus, $\overline{\boldsymbol{\theta}}^{\alpha} \in \text{conv}(\mathcal{D})$. It is also easy to verify that $\overline{\boldsymbol{\theta}}^{\alpha}$ satisfies (4.36) at equality.

(A12) For each $\alpha \in [t, T]_{\mathbb{Z}}$, we create a point $\overline{\boldsymbol{\theta}}^{\alpha}$ as follows:

$$\bar{p}_s^{\alpha} = \begin{cases} V, & s \in [1, t-1]_{\mathbb{Z}} \\ \overline{V} - \underline{C} - \epsilon, & s \in [t, \alpha]_{\mathbb{Z}} \\ 0, & \text{o.w.} \end{cases}, \ \overline{r}_s^{+,\alpha} = \begin{cases} 2V - \overline{V} + \underline{C} + \epsilon, & s = t \\ 0, & \text{o.w.} \end{cases},$$

$$\overline{r}_s^{-,\alpha} = \begin{cases} \overline{V} - \underline{C} - \epsilon, & s = t \\ 0, & \text{o.w.} \end{cases},$$

$\overline{y}_s^{\alpha} = 1$ for any $s \in [1, \alpha]_{\mathbb{Z}}$ and $\overline{y}_s^{\alpha} = 0$ otherwise, and $\overline{u}_s^{\alpha} = 0$ for any $s \in \mathcal{T} \setminus \{1\}$. It is easy to verify that $\overline{\boldsymbol{\theta}}^{\alpha}$ satisfies (4.35a)–(4.35h) because $2V < \overline{C} - \underline{C}$. Thus, $\overline{\boldsymbol{\theta}}^{\alpha} \in \text{conv}(\mathcal{D})$. It is also easy to verify that $\overline{\boldsymbol{\theta}}^{\alpha}$ satisfies (4.36) at equality.

(A13) For each $\alpha \in [2, t-2]_{\mathbb{Z}}$, we create a point $\dot{\boldsymbol{\theta}}^{\alpha}$ as follows:

$$\dot{p}_s^{\alpha} = \begin{cases} \overline{V} - \underline{C}, & s = \alpha \\ 0, & \text{o.w.} \end{cases}, \ \dot{y}_s^{\alpha} = \dot{u}_s^{\alpha} = \begin{cases} 1, & s = \alpha \\ 0, & \text{o.w.} \end{cases},$$

and $\dot{r}_s^{+,\alpha} = \dot{r}_s^{-,\alpha} = 0$ for any $s \in \mathcal{T}$. It is easy to verify that $\dot{\boldsymbol{\theta}}^{\alpha}$ satisfies (4.35a)–(4.35h) because $L = 1$. Thus, $\dot{\boldsymbol{\theta}}^{\alpha} \in \text{conv}(\mathcal{D})$. It is also easy to verify that $\dot{\boldsymbol{\theta}}^{\alpha}$ satisfies (4.36) at equality.

(A14) For $\alpha = t-1$, we create a point $\dot{\boldsymbol{\theta}}^\alpha$ as follows:

$$\dot{p}_s^\alpha = \begin{cases} \overline{V} - \underline{C}, & s \in [t-1, \min\{t+1, T\}]_{\mathbb{Z}} \setminus \{t\} \\ \overline{V} + V - \underline{C}, & s = t \\ 0, & \text{o.w.} \end{cases}, \quad \dot{r}_s^{-,\alpha} = \begin{cases} \overline{V} + V - \underline{C}, & s = t \\ 0, & \text{o.w.} \end{cases},$$

$$\dot{y}_s^\alpha = \begin{cases} 1, & s \in [t-1, \min\{t+1, T\}]_{\mathbb{Z}} \\ 0, & \text{o.w.} \end{cases}, \text{ and } \dot{u}_s^\alpha = \begin{cases} 1, & s = t-1 \\ 0, & \text{o.w.} \end{cases},$$

and $\dot{r}_s^{+,\alpha} = 0$ for any $s \in \mathcal{T}$. Note that $\overline{V} + V - \underline{C} < (\underline{C} + V) + V - \underline{C} = 2V < \overline{C} - \underline{C}$. Thus, $\dot{\boldsymbol{\theta}}^\alpha$ satisfies (4.35a)–(4.35h) and $\dot{\boldsymbol{\theta}}^\alpha \in \text{conv}(\mathcal{D})$. It is also easy to verify that $\dot{\boldsymbol{\theta}}^\alpha$ satisfies (4.36) at equality.

(A15) For $\alpha = t$, we create a point $\dot{\boldsymbol{\theta}}^\alpha$ as follows:

$$\dot{p}_s^\alpha = \begin{cases} \overline{V} - \underline{C}, & s = t \\ 0, & \text{o.w.} \end{cases}, \quad \dot{r}_s^{-,\alpha} = \begin{cases} \overline{V} - \underline{C}, & s = t \\ 0, & \text{o.w.} \end{cases}, \quad \dot{y}_s^\alpha = \dot{u}_s^\alpha = \begin{cases} 1, & s = t \\ 0, & \text{o.w.} \end{cases},$$

and $\dot{r}_s^{+,\alpha} = 0$ for any $s \in \mathcal{T}$. It is easy to verify that $\dot{\boldsymbol{\theta}}^\alpha$ satisfies (4.35a)–(4.35h) because $L = 1$. Thus, $\dot{\boldsymbol{\theta}}^\alpha \in \text{conv}(\mathcal{D})$. It is also easy to verify that $\dot{\boldsymbol{\theta}}^\alpha$ satisfies (4.36) at equality.

(A16) For each $\alpha \in [t+1, T]_{\mathbb{Z}}$, we create a point $\dot{\boldsymbol{\theta}}^\alpha$ as follows:

$$\dot{p}_s^\alpha = \begin{cases} \overline{V} - \underline{C}, & s = \alpha \\ 0, & \text{o.w.} \end{cases}, \quad \dot{y}_s^\alpha = \dot{u}_s^\alpha = \begin{cases} 1, & s = \alpha \\ 0, & \text{o.w.} \end{cases},$$

and $\dot{r}_s^{+,\alpha} = \dot{r}_s^{-,\alpha} = 0$ for any $s \in \mathcal{T}$. It is easy to verify that $\dot{\boldsymbol{\theta}}^\alpha$ satisfies (4.35a)–(4.35h) because $L = 1$. Thus, $\dot{\boldsymbol{\theta}}^\alpha \in \text{conv}(\mathcal{D})$. It is also easy to verify that $\dot{\boldsymbol{\theta}}^\alpha$ satisfies (4.36) at equality.

Table C.2 shows a matrix with $5T - 2$ rows, where each row represents a point created above. This matrix can be transformed into the matrix in Table C.3 via the following Gaussian elimination process:

Table C.2. Matrix with The Rows Representing $5T-2$ Points in $\mathrm{conv}(\mathcal{D})$ That Satisfy Inequality (4.36) at Equality

Point	Group	Index α	$\mathbf{p}$									$\mathbf{r}^+$								$\mathbf{r}^-$								$\mathbf{y}$								$\mathbf{u}$							
			1	2	$\cdots$	$t-2$	$t-1$	t	$t+1$	$\cdots$	T	1	2	$\cdots$	$t-1$	t	$t+1$	$\cdots$	T	1	2	$\cdots$	$t-2$	$t-1$	t	$t+1$	$\cdots$	T	1	2	$\cdots$	$t-2$	$t-1$	t	$t+1$	$\cdots$	T	2	$\cdots$	$t-2$	$t-1$	t	$t+1$	$\cdots$	T
$\grave{\boldsymbol{\theta}}^{\alpha}$		1	$\overline{V}-\underline{C}$	0	$\cdots$	0	0	0	0	$\cdots$	0	0	0	$\cdots$	0	0	0	$\cdots$	0	0	0	$\cdots$	0	0	0	0	$\cdots$	0	1	0	$\cdots$	0	0	0	0	$\cdots$	0	0	$\cdots$	0	0	0	0	$\cdots$	0
	(A1)	2	$\overline{V}-\underline{C}$	$\overline{V}-\underline{C}$	$\cdots$	0	0	0	0	$\cdots$	0	0	0	$\cdots$	0	0	0	$\cdots$	0	0	0	$\cdots$	0	0	0	0	$\cdots$	0	1	1	$\cdots$	0	0	0	0	$\cdots$	0	0	$\cdots$	0	0	0	0	$\cdots$	0
		$\vdots$	$\vdots$	$\vdots$	$\ddots$	$\vdots$	$\vdots$	$\vdots$	$\vdots$	$\ddots$	$\vdots$	$\vdots$	$\vdots$	$\ddots$	$\vdots$	$\vdots$	$\vdots$	$\ddots$	$\vdots$	$\vdots$	$\vdots$	$\ddots$	$\vdots$	$\vdots$	$\vdots$	$\vdots$	$\ddots$	$\vdots$	$\vdots$	$\vdots$	$\ddots$	$\vdots$	$\vdots$	$\vdots$	$\vdots$	$\ddots$	$\vdots$	$\vdots$	$\ddots$	$\vdots$	$\vdots$	$\vdots$	$\vdots$	$\ddots$	$\vdots$
		$t-1$	$\overline{V}-\underline{C}$	$\overline{V}-\underline{C}$	$\cdots$	$\overline{V}-\underline{C}$	$\overline{V}-\underline{C}$	0	0	$\cdots$	0	0	0	$\cdots$	0	0	0	$\cdots$	0	0	0	$\cdots$	0	0	0	0	$\cdots$	0	1	1	$\cdots$	1	1	0	0	$\cdots$	0	0	$\cdots$	0	0	0	0	$\cdots$	0
	(A2)	t	V	V	$\cdots$	V	$V+\epsilon$	$\overline{V}-\underline{C}$	0	$\cdots$	0	0	0	$\cdots$	0	$2V-\overline{V}+\underline{C}+\epsilon$	0	$\cdots$	0	0	0	$\cdots$	0	0	$\overline{V}-\underline{C}-\epsilon$	0	$\cdots$	0	1	1	$\cdots$	1	1	1	0	$\cdots$	0	0	$\cdots$	0	0	0	0	$\cdots$	0
		$t+1$	V	V	$\cdots$	V	V	$\overline{V}-\underline{C}$	$\overline{V}-\underline{C}$	$\cdots$	0	0	0	$\cdots$	0	$2V-\overline{V}+\underline{C}$	0	$\cdots$	0	0	0	$\cdots$	0	0	$\overline{V}-\underline{C}$	0	$\cdots$	0	1	1	$\cdots$	1	1	1	1	$\cdots$	0	0	$\cdots$	0	0	0	0	$\cdots$	0
	(A3)	$\vdots$	$\vdots$	$\vdots$	$\ddots$	$\vdots$	$\vdots$	$\vdots$	$\vdots$	$\ddots$	$\vdots$	$\vdots$	$\vdots$	$\ddots$	$\vdots$	$\vdots$	$\vdots$	$\ddots$	$\vdots$	$\vdots$	$\vdots$	$\ddots$	$\vdots$	$\vdots$	$\vdots$	$\vdots$	$\ddots$	$\vdots$	$\vdots$	$\vdots$	$\ddots$	$\vdots$	$\vdots$	$\vdots$	$\vdots$	$\ddots$	$\vdots$	$\vdots$	$\ddots$	$\vdots$	$\vdots$	$\vdots$	$\vdots$	$\ddots$	$\vdots$
		T	V	V	$\cdots$	V	V	$\overline{V}-\underline{C}$	$\overline{V}-\underline{C}$	$\cdots$	$\overline{V}-\underline{C}$	0	0	$\cdots$	0	$2V-\overline{V}+\underline{C}$	0	$\cdots$	0	0	0	$\cdots$	0	0	$\overline{V}-\underline{C}$	0	$\cdots$	0	1	1	$\cdots$	1	1	1	1	$\cdots$	1	0	$\cdots$	0	0	0	0	$\cdots$	0
$\hat{\boldsymbol{\theta}}^{\alpha}$		1	$\overline{V}-\underline{C}$	0	$\cdots$	0	0	0	0	$\cdots$	0	$\overline{V}-\underline{C}$	0	$\cdots$	0	0	0	$\cdots$	0	0	0	$\cdots$	0	0	0	0	$\cdots$	0	1	0	$\cdots$	0	0	0	0	$\cdots$	0	0	$\cdots$	0	0	0	0	$\cdots$	0
	(A4)	2	$\overline{V}-\underline{C}$	$\overline{V}-\underline{C}$	$\cdots$	0	0	0	0	$\cdots$	0	$\overline{V}-\underline{C}$	$\overline{V}-\underline{C}$	$\cdots$	0	0	0	$\cdots$	0	0	0	$\cdots$	0	0	0	0	$\cdots$	0	1	1	$\cdots$	0	0	0	0	$\cdots$	0	0	$\cdots$	0	0	0	0	$\cdots$	0
		$\vdots$	$\vdots$	$\vdots$	$\ddots$	$\vdots$	$\vdots$	$\vdots$	$\vdots$	$\ddots$	$\vdots$	$\vdots$	$\vdots$	$\ddots$	$\vdots$	$\vdots$	$\vdots$	$\ddots$	$\vdots$	$\vdots$	$\vdots$	$\ddots$	$\vdots$	$\vdots$	$\vdots$	$\vdots$	$\ddots$	$\vdots$	$\vdots$	$\vdots$	$\ddots$	$\vdots$	$\vdots$	$\vdots$	$\vdots$	$\ddots$	$\vdots$	$\vdots$	$\ddots$	$\vdots$	$\vdots$	$\vdots$	$\vdots$	$\ddots$	$\vdots$
		$t-1$	$\overline{V}-\underline{C}$	$\overline{V}-\underline{C}$	$\cdots$	$\overline{V}-\underline{C}$	$\overline{V}-\underline{C}$	0	0	$\cdots$	0	$\overline{V}-\underline{C}$	$\overline{V}-\underline{C}$	$\cdots$	$\overline{V}-\underline{C}$	0	0	$\cdots$	0	0	0	$\cdots$	0	0	0	0	$\cdots$	0	1	1	$\cdots$	1	1	0	0	$\cdots$	0	0	$\cdots$	0	0	0	0	$\cdots$	0
	(A5)	$t+1$	V	V	$\cdots$	V	V	$\overline{V}-\underline{C}$	$\overline{V}-\underline{C}$	$\cdots$	0	$\overline{V}-\underline{C}$	$\overline{V}-\underline{C}$	$\cdots$	$\overline{V}-\underline{C}$	$2V-\overline{V}+\underline{C}$	$\overline{V}-\underline{C}$	$\cdots$	0	0	0	$\cdots$	0	0	$\overline{V}-\underline{C}$	0	$\cdots$	0	1	1	$\cdots$	1	1	1	1	$\cdots$	0	0	$\cdots$	0	0	0	0	$\cdots$	0
		$\vdots$	$\vdots$	$\vdots$	$\ddots$	$\vdots$	$\vdots$	$\vdots$	$\vdots$	$\ddots$	$\vdots$	$\vdots$	$\vdots$	$\ddots$	$\vdots$	$\vdots$	$\vdots$	$\ddots$	$\vdots$	$\vdots$	$\vdots$	$\ddots$	$\vdots$	$\vdots$	$\vdots$	$\vdots$	$\ddots$	$\vdots$	$\vdots$	$\vdots$	$\ddots$	$\vdots$	$\vdots$	$\vdots$	$\vdots$	$\ddots$	$\vdots$	$\vdots$	$\ddots$	$\vdots$	$\vdots$	$\vdots$	$\vdots$	$\ddots$	$\vdots$
		T	V	V	$\cdots$	V	V	$\overline{V}-\underline{C}$	$\overline{V}-\underline{C}$	$\cdots$	$\overline{V}-\underline{C}$	$\overline{V}-\underline{C}$	$\overline{V}-\underline{C}$	$\cdots$	$\overline{V}-\underline{C}$	$2V-\overline{V}+\underline{C}$	$\overline{V}-\underline{C}$	$\cdots$	$\overline{V}-\underline{C}$	0	0	$\cdots$	0	0	$\overline{V}-\underline{C}$	0	$\cdots$	0	1	1	$\cdots$	1	1	1	1	$\cdots$	1	0	$\cdots$	0	0	0	0	$\cdots$	0
$\grave{\boldsymbol{\theta}}^{\alpha}$	(A6)	1	$\overline{V}-\underline{C}$	0	$\cdots$	0	0	0	0	$\cdots$	0	0	0	$\cdots$	0	0	0	$\cdots$	0	$\overline{V}-\underline{C}$	0	$\cdots$	0	0	0	0	$\cdots$	0	1	0	$\cdots$	0	0	0	0	$\cdots$	0	0	$\cdots$	0	0	0	0	$\cdots$	0
	(A7)	2	0	$\overline{V}-\underline{C}$	$\cdots$	0	0	0	0	$\cdots$	0	0	0	$\cdots$	0	0	0	$\cdots$	0	0	$\overline{V}-\underline{C}$	$\cdots$	0	0	0	0	$\cdots$	0	0	1	$\cdots$	0	0	0	0	$\cdots$	0	1	$\cdots$	0	0	0	0	$\cdots$	0
		$\vdots$	$\vdots$	$\vdots$	$\ddots$	$\vdots$	$\vdots$	$\vdots$	$\vdots$	$\ddots$	$\vdots$	$\vdots$	$\vdots$	$\ddots$	$\vdots$	$\vdots$	$\vdots$	$\ddots$	$\vdots$	$\vdots$	$\vdots$	$\ddots$	$\vdots$	$\vdots$	$\vdots$	$\vdots$	$\ddots$	$\vdots$	$\vdots$	$\vdots$	$\ddots$	$\vdots$	$\vdots$	$\vdots$	$\vdots$	$\ddots$	$\vdots$	$\vdots$	$\ddots$	$\vdots$	$\vdots$	$\vdots$	$\vdots$	$\ddots$	$\vdots$
		$t-2$	0	0	$\cdots$	$\overline{V}-\underline{C}$	0	0	0	$\cdots$	0	0	0	$\cdots$	0	0	0	$\cdots$	0	0	0	$\cdots$	$\overline{V}-\underline{C}$	0	0	0	$\cdots$	0	0	0	$\cdots$	1	0	0	0	$\cdots$	0	0	$\cdots$	1	0	0	0	$\cdots$	0
	(A8)	$t-1$	0	0	$\cdots$	0	$\overline{V}-\underline{C}$	$\overline{V}+V-\underline{C}$	$\overline{V}-\underline{C}$	$\cdots$	0	0	0	$\cdots$	0	0	0	$\cdots$	0	0	0	$\cdots$	0	$\overline{V}-\underline{C}$	$\overline{V}+V-\underline{C}$	0	$\cdots$	0	0	0	$\cdots$	0	1	1	1	$\cdots$	0	0	$\cdots$	0	1	0	0	$\cdots$	0
	(A9)	t	0	0	$\cdots$	0	0	$\overline{V}-\underline{C}-\epsilon$	0	$\cdots$	0	0	0	$\cdots$	0	ϵ	0	$\cdots$	0	0	0	$\cdots$	0	0	$\overline{V}-\underline{C}-\epsilon$	0	$\cdots$	0	0	0	$\cdots$	0	0	1	0	$\cdots$	0	0	$\cdots$	0	0	1	0	$\cdots$	0
		$t+1$	0	0	$\cdots$	0	0	0	$\overline{V}-\underline{C}$	$\cdots$	0	0	0	$\cdots$	0	0	0	$\cdots$	0	0	0	$\cdots$	0	0	0	$\overline{V}-\underline{C}$	$\cdots$	0	0	0	$\cdots$	0	0	0	1	$\cdots$	0	0	$\cdots$	0	0	0	1	$\cdots$	0
	(A10)	$\vdots$	$\vdots$	$\vdots$	$\ddots$	$\vdots$	$\vdots$	$\vdots$	$\vdots$	$\ddots$	$\vdots$	$\vdots$	$\vdots$	$\ddots$	$\vdots$	$\vdots$	$\vdots$	$\ddots$	$\vdots$	$\vdots$	$\vdots$	$\ddots$	$\vdots$	$\vdots$	$\vdots$	$\vdots$	$\ddots$	$\vdots$	$\vdots$	$\vdots$	$\ddots$	$\vdots$	$\vdots$	$\vdots$	$\vdots$	$\ddots$	$\vdots$	$\vdots$	$\ddots$	$\vdots$	$\vdots$	$\vdots$	$\vdots$	$\ddots$	$\vdots$
		T	0	0	$\cdots$	0	0	0	0	$\cdots$	$\overline{V}-\underline{C}$	0	0	$\cdots$	0	0	0	$\cdots$	0	0	0	$\cdots$	0	0	0	0	$\cdots$	$\overline{V}-\underline{C}$	0	0	$\cdots$	0	0	0	0	$\cdots$	1	0	$\cdots$	0	0	0	0	$\cdots$	1
$\overline{\boldsymbol{\theta}}^{\alpha}$		1	$\overline{V}-\underline{C}-\epsilon$	0	$\cdots$	0	0	0	0	$\cdots$	0	0	0	$\cdots$	0	0	0	$\cdots$	0	0	0	$\cdots$	0	0	0	0	$\cdots$	0	1	0	$\cdots$	0	0	0	0	$\cdots$	0	0	$\cdots$	0	0	0	0	$\cdots$	0
	(A11)	2	$\overline{V}-\underline{C}-\epsilon$	$\overline{V}-\underline{C}-\epsilon$	$\cdots$	0	0	0	0	$\cdots$	0	0	0	$\cdots$	0	0	0	$\cdots$	0	0	0	$\cdots$	0	0	0	0	$\cdots$	0	1	1	$\cdots$	0	0	0	0	$\cdots$	0	0	$\cdots$	0	0	0	0	$\cdots$	0
		$\vdots$	$\vdots$	$\vdots$	$\ddots$	$\vdots$	$\vdots$	$\vdots$	$\vdots$	$\ddots$	$\vdots$	$\vdots$	$\vdots$	$\ddots$	$\vdots$	$\vdots$	$\vdots$	$\ddots$	$\vdots$	$\vdots$	$\vdots$	$\ddots$	$\vdots$	$\vdots$	$\vdots$	$\vdots$	$\ddots$	$\vdots$	$\vdots$	$\vdots$	$\ddots$	$\vdots$	$\vdots$	$\vdots$	$\vdots$	$\ddots$	$\vdots$	$\vdots$	$\ddots$	$\vdots$	$\vdots$	$\vdots$	$\vdots$	$\ddots$	$\vdots$
		$t-1$	$\overline{V}-\underline{C}-\epsilon$	$\overline{V}-\underline{C}-\epsilon$	$\cdots$	$\overline{V}-\underline{C}-\epsilon$	$\overline{V}-\underline{C}-\epsilon$	0	0	$\cdots$	0	0	0	$\cdots$	0	0	0	$\cdots$	0	0	0	$\cdots$	0	0	0	0	$\cdots$	0	1	1	$\cdots$	1	1	0	0	$\cdots$	0	0	$\cdots$	0	0	0	0	$\cdots$	0
	(A12)	t	V	V	$\cdots$	V	V	$\overline{V}-\underline{C}-\epsilon$	0	$\cdots$	0	0	0	$\cdots$	0	$2V-\overline{V}+\underline{C}+\epsilon$	0	$\cdots$	0	0	0	$\cdots$	0	0	$\overline{V}-\underline{C}-\epsilon$	0	$\cdots$	0	1	1	$\cdots$	1	1	1	0	$\cdots$	0	0	$\cdots$	0	0	0	0	$\cdots$	0
		$t+1$	V	V	$\cdots$	V	V	$\overline{V}-\underline{C}-\epsilon$	$\overline{V}-\underline{C}-\epsilon$	$\cdots$	0	0	0	$\cdots$	0	$2V-\overline{V}+\underline{C}+\epsilon$	0	$\cdots$	0	0	0	$\cdots$	0	0	$\overline{V}-\underline{C}-\epsilon$	0	$\cdots$	0	1	1	$\cdots$	1	1	1	1	$\cdots$	0	0	$\cdots$	0	0	0	0	$\cdots$	0
		$\vdots$	$\vdots$	$\vdots$	$\ddots$	$\vdots$	$\vdots$	$\vdots$	$\vdots$	$\ddots$	$\vdots$	$\vdots$	$\vdots$	$\ddots$	$\vdots$	$\vdots$	$\vdots$	$\ddots$	$\vdots$	$\vdots$	$\vdots$	$\ddots$	$\vdots$	$\vdots$	$\vdots$	$\vdots$	$\ddots$	$\vdots$	$\vdots$	$\vdots$	$\ddots$	$\vdots$	$\vdots$	$\vdots$	$\vdots$	$\ddots$	$\vdots$	$\vdots$	$\ddots$	$\vdots$	$\vdots$	$\vdots$	$\vdots$	$\ddots$	$\vdots$
		T	V	V	$\cdots$	V	V	$\overline{V}-\underline{C}-\epsilon$	$\overline{V}-\underline{C}-\epsilon$	$\cdots$	$\overline{V}-\underline{C}-\epsilon$	0	0	$\cdots$	0	$2V-\overline{V}+\underline{C}+\epsilon$	0	$\cdots$	0	0	0	$\cdots$	0	0	$\overline{V}-\underline{C}-\epsilon$	0	$\cdots$	0	1	1	$\cdots$	1	1	1	1	$\cdots$	1	0	$\cdots$	0	0	0	0	$\cdots$	0
$\hat{\boldsymbol{\theta}}^{\alpha}$		2	0	$\overline{V}-\underline{C}$	$\cdots$	0	0	0	0	$\cdots$	0	0	0	$\cdots$	0	0	0	$\cdots$	0	0	0	$\cdots$	0	0	0	0	$\cdots$	0	0	1	$\cdots$	0	0	0	0	$\cdots$	0	1	$\cdots$	0	0	0	0	$\cdots$	0
	(A13)	$\vdots$	$\vdots$	$\vdots$	$\ddots$	$\vdots$	$\vdots$	$\vdots$	$\vdots$	$\ddots$	$\vdots$	$\vdots$	$\vdots$	$\ddots$	$\vdots$	$\vdots$	$\vdots$	$\ddots$	$\vdots$	$\vdots$	$\vdots$	$\ddots$	$\vdots$	$\vdots$	$\vdots$	$\vdots$	$\ddots$	$\vdots$	$\vdots$	$\vdots$	$\ddots$	$\vdots$	$\vdots$	$\vdots$	$\vdots$	$\ddots$	$\vdots$	$\vdots$	$\ddots$	$\vdots$	$\vdots$	$\vdots$	$\vdots$	$\ddots$	$\vdots$
		$t-2$	0	0	$\cdots$	$\overline{V}-\underline{C}$	0	0	0	$\cdots$	0	0	0	$\cdots$	0	0	0	$\cdots$	0	0	0	$\cdots$	0	0	0	0	$\cdots$	0	0	0	$\cdots$	1	0	0	0	$\cdots$	0	0	$\cdots$	1	0	0	0	$\cdots$	0
	(A14)	$t-1$	0	0	$\cdots$	0	$\overline{V}-\underline{C}$	$\overline{V}+V-\underline{C}$	$\overline{V}-\underline{C}$	$\cdots$	0	0	0	$\cdots$	0	0	0	$\cdots$	0	0	0	$\cdots$	0	0	$\overline{V}+V-\underline{C}$	0	$\cdots$	0	0	0	$\cdots$	0	1	1	1	$\cdots$	0	0	$\cdots$	0	1	0	0	$\cdots$	0
	(A15)	t	0	0	$\cdots$	0	0	$\overline{V}-\underline{C}$	0	$\cdots$	0	0	0	$\cdots$	0	0	0	$\cdots$	0	0	0	$\cdots$	0	0	$\overline{V}-\underline{C}$	0	$\cdots$	0	0	0	$\cdots$	0	0	1	0	$\cdots$	0	0	$\cdots$	0	0	1	0	$\cdots$	0
		$t+1$	0	0	$\cdots$	0	0	0	$\overline{V}-\underline{C}$	$\cdots$	0	0	0	$\cdots$	0	0	0	$\cdots$	0	0	0	$\cdots$	0	0	0	0	$\cdots$	0	0	0	$\cdots$	0	0	0	1	$\cdots$	0	0	$\cdots$	0	0	0	1	$\cdots$	0
	(A16)	$\vdots$	$\vdots$	$\vdots$	$\ddots$	$\vdots$	$\vdots$	$\vdots$	$\vdots$	$\ddots$	$\vdots$	$\vdots$	$\vdots$	$\ddots$	$\vdots$	$\vdots$	$\vdots$	$\ddots$	$\vdots$	$\vdots$	$\vdots$	$\ddots$	$\vdots$	$\vdots$	$\vdots$	$\vdots$	$\ddots$	$\vdots$	$\vdots$	$\vdots$	$\ddots$	$\vdots$	$\vdots$	$\vdots$	$\vdots$	$\ddots$	$\vdots$	$\vdots$	$\ddots$	$\vdots$	$\vdots$	$\vdots$	$\vdots$	$\ddots$	$\vdots$
		T	0	0	$\cdots$	0	0	0	0	$\cdots$	$\overline{V}-\underline{C}$	0	0	$\cdots$	0	0	0	$\cdots$	0	0	0	$\cdots$	0	0	0	0	$\cdots$	$\overline{V}-\underline{C}$	0	0	$\cdots$	0	0	0	0	$\cdots$	1	0	$\cdots$	0	0	0	0	$\cdots$	1

Table C.3. Lower Triangular Matrix Obtained From Table C.2 via Gaussian Elimination

Point	Group	Index α	$\mathbf{p}$									$\mathbf{r}^+$									$\mathbf{r}^-$									$\mathbf{y}$									$\mathbf{u}$								
			1	2	$\cdots$	$t-2$	$t-1$	t	$t+1$	$\cdots$	T	1	2	$\cdots$	$t-1$	t	$t+1$	$\cdots$	T	1	2	$\cdots$	$t-2$	$t-1$	t	$t+1$	$\cdots$	T	1	2	$\cdots$	$t-2$	$t-1$	t	$t+1$	$\cdots$	T	2	$\cdots$	$t-2$	$t-1$	t	$t+1$	$\cdots$	T
$\underline{\hat{\theta}}^{\alpha}$	(B1)	1	ϵ	0	$\cdots$	0	0	0	0	$\cdots$	0	0	0	$\cdots$	0	0	0	$\cdots$	0	0	0	$\cdots$	0	0	0	0	$\cdots$	0	0	0	$\cdots$	0	0	0	0	$\cdots$	0	0	$\cdots$	0	0	0	0	$\cdots$	0
		2	ϵ	ϵ	$\cdots$	0	0	0	0	$\cdots$	0	0	0	$\cdots$	0	0	0	$\cdots$	0	0	0	$\cdots$	0	0	0	0	$\cdots$	0	0	0	$\cdots$	0	0	0	0	$\cdots$	0	0	$\cdots$	0	0	0	0	$\cdots$	0
		$\vdots$	$\vdots$	$\vdots$	$\ddots$	$\vdots$	$\vdots$	$\vdots$	$\vdots$	$\ddots$	$\vdots$	$\vdots$	$\vdots$	$\ddots$	$\vdots$	$\vdots$	$\vdots$	$\ddots$	$\vdots$	$\vdots$	$\vdots$	$\ddots$	$\vdots$	$\vdots$	$\vdots$	$\vdots$	$\ddots$	$\vdots$	$\vdots$	$\vdots$	$\ddots$	$\vdots$	$\vdots$	$\vdots$	$\vdots$	$\ddots$	$\vdots$	$\vdots$	$\ddots$	$\vdots$	$\vdots$	$\vdots$	$\vdots$	$\ddots$	$\vdots$
		$t-1$	ϵ	ϵ	$\cdots$	ϵ	ϵ	0	0	$\cdots$	0	0	0	$\cdots$	0	0	0	$\cdots$	0	0	0	$\cdots$	0	0	0	0	$\cdots$	0	0	0	$\cdots$	0	0	0	0	$\cdots$	0	0	$\cdots$	0	0	0	0	$\cdots$	0
		t	0	0	$\cdots$	0	ϵ	ϵ	0	$\cdots$	0	0	0	$\cdots$	0	0	0	$\cdots$	0	0	0	$\cdots$	0	0	0	0	$\cdots$	0	0	0	$\cdots$	0	0	0	0	$\cdots$	0	0	$\cdots$	0	0	0	0	$\cdots$	0
		$t+1$	0	0	$\cdots$	0	0	0	ϵ	$\cdots$	0	0	0	$\cdots$	0	0	0	$\cdots$	0	0	0	$\cdots$	0	0	0	0	$\cdots$	0	0	0	$\cdots$	0	0	0	0	$\cdots$	0	0	$\cdots$	0	0	0	0	$\cdots$	0
		$\vdots$	$\vdots$	$\vdots$	$\ddots$	$\vdots$	$\vdots$	$\vdots$	$\vdots$	$\ddots$	$\vdots$	$\vdots$	$\vdots$	$\ddots$	$\vdots$	$\vdots$	$\vdots$	$\ddots$	$\vdots$	$\vdots$	$\vdots$	$\ddots$	$\vdots$	$\vdots$	$\vdots$	$\vdots$	$\ddots$	$\vdots$	$\vdots$	$\vdots$	$\ddots$	$\vdots$	$\vdots$	$\vdots$	$\vdots$	$\ddots$	$\vdots$	$\vdots$	$\ddots$	$\vdots$	$\vdots$	$\vdots$	$\vdots$	$\ddots$	$\vdots$
		T	0	0	$\cdots$	0	0	0	ϵ	$\cdots$	ϵ	0	0	$\cdots$	0	0	0	$\cdots$	0	0	0	$\cdots$	0	0	0	0	$\cdots$	0	0	0	$\cdots$	0	0	0	0	$\cdots$	0	0	$\cdots$	0	0	0	0	$\cdots$	0
$\underline{\hat{\theta}}^{\alpha}$	(B2)	1	ϵ	0	$\cdots$	0	0	0	0	$\cdots$	0	$\overline{V}-\underline{C}$	0	$\cdots$	0	0	0	$\cdots$	0	0	0	$\cdots$	0	0	0	0	$\cdots$	0	0	0	0	$\cdots$	0	0	0	0	$\cdots$	0	0	$\cdots$	0	0	0	0	$\cdots$	0
		2	ϵ	ϵ	$\cdots$	0	0	0	0	$\cdots$	0	$\overline{V}-\underline{C}$	$\overline{V}-\underline{C}$	$\cdots$	0	0	0	$\cdots$	0	0	0	$\cdots$	0	0	0	0	$\cdots$	0	0	0	$\cdots$	0	0	0	0	$\cdots$	0	0	$\cdots$	0	0	0	0	$\cdots$	0
		$\vdots$	$\vdots$	$\vdots$	$\ddots$	$\vdots$	$\vdots$	$\vdots$	$\vdots$	$\ddots$	$\vdots$	$\vdots$	$\vdots$	$\ddots$	$\vdots$	$\vdots$	$\vdots$	$\ddots$	$\vdots$	$\vdots$	$\vdots$	$\ddots$	$\vdots$	$\vdots$	$\vdots$	$\vdots$	$\ddots$	$\vdots$	$\vdots$	$\vdots$	$\ddots$	$\vdots$	$\vdots$	$\vdots$	$\vdots$	$\ddots$	$\vdots$	$\vdots$	$\ddots$	$\vdots$	$\vdots$	$\vdots$	$\vdots$	$\ddots$	$\vdots$
		$t-1$	ϵ	ϵ	$\cdots$	ϵ	ϵ	0	0	$\cdots$	0	$\overline{V}-\underline{C}$	$\overline{V}-\underline{C}$	$\cdots$	$\overline{V}-\underline{C}$	0	0	$\cdots$	0	0	0	$\cdots$	0	0	0	0	$\cdots$	0	0	0	$\cdots$	0	0	0	0	$\cdots$	0	0	$\cdots$	0	0	0	0	$\cdots$	0
		$t+1$	0	0	$\cdots$	0	0	0	ϵ	$\cdots$	0	$\overline{V}-\underline{C}$	$\overline{V}-\underline{C}$	$\cdots$	$\overline{V}-\underline{C}$	0	$\overline{V}-\underline{C}$	$\cdots$	0	0	0	$\cdots$	0	0	0	0	$\cdots$	0	0	0	$\cdots$	0	0	0	0	$\cdots$	0	0	$\cdots$	0	0	0	0	$\cdots$	0
		$\vdots$	$\vdots$	$\vdots$	$\ddots$	$\vdots$	$\vdots$	$\vdots$	$\vdots$	$\ddots$	$\vdots$	$\vdots$	$\vdots$	$\ddots$	$\vdots$	$\vdots$	$\vdots$	$\ddots$	$\vdots$	$\vdots$	$\vdots$	$\ddots$	$\vdots$	$\vdots$	$\vdots$	$\vdots$	$\ddots$	$\vdots$	$\vdots$	$\vdots$	$\ddots$	$\vdots$	$\vdots$	$\vdots$	$\vdots$	$\ddots$	$\vdots$	$\vdots$	$\ddots$	$\vdots$	$\vdots$	$\vdots$	$\vdots$	$\ddots$	$\vdots$
		T	0	0	$\cdots$	0	0	0	ϵ	$\cdots$	ϵ	$\overline{V}-\underline{C}$	$\overline{V}-\underline{C}$	$\cdots$	$\overline{V}-\underline{C}$	0	$\overline{V}-\underline{C}$	$\cdots$	$\overline{V}-\underline{C}$	0	0	$\cdots$	0	0	0	0	$\cdots$	0	0	0	$\cdots$	0	0	0	0	$\cdots$	0	0	$\cdots$	0	0	0	0	$\cdots$	0
$\underline{\hat{\theta}}^{\alpha}$	(B3)	1	ϵ	0	$\cdots$	0	0	0	0	$\cdots$	0	0	0	$\cdots$	0	0	0	$\cdots$	0	$\overline{V}-\underline{C}$	0	$\cdots$	0	0	0	0	$\cdots$	0	0	0	$\cdots$	0	0	0	0	$\cdots$	0	0	$\cdots$	0	0	0	0	$\cdots$	0
		2	0	0	$\cdots$	0	0	0	0	$\cdots$	0	0	0	$\cdots$	0	0	0	$\cdots$	0	0	$\overline{V}-\underline{C}$	$\cdots$	0	0	0	0	$\cdots$	0	0	0	$\cdots$	0	0	0	0	$\cdots$	0	0	$\cdots$	0	0	0	0	$\cdots$	0
		$\vdots$	$\vdots$	$\vdots$	$\ddots$	$\vdots$	$\vdots$	$\vdots$	$\vdots$	$\ddots$	$\vdots$	$\vdots$	$\vdots$	$\ddots$	$\vdots$	$\vdots$	$\vdots$	$\ddots$	$\vdots$	$\vdots$	$\vdots$	$\ddots$	$\vdots$	$\vdots$	$\vdots$	$\vdots$	$\ddots$	$\vdots$	$\vdots$	$\vdots$	$\ddots$	$\vdots$	$\vdots$	$\vdots$	$\vdots$	$\ddots$	$\vdots$	$\vdots$	$\ddots$	$\vdots$	$\vdots$	$\vdots$	$\vdots$	$\ddots$	$\vdots$
		$t-2$	0	0	$\cdots$	0	0	0	0	$\cdots$	0	0	0	$\cdots$	0	0	0	$\cdots$	0	0	0	$\cdots$	$\overline{V}-\underline{C}$	0	0	0	$\cdots$	0	0	0	$\cdots$	0	0	0	0	$\cdots$	0	0	$\cdots$	0	0	0	0	$\cdots$	0
		$t-1$	0	0	$\cdots$	0	0	0	0	$\cdots$	0	0	0	$\cdots$	0	0	0	$\cdots$	0	0	0	$\cdots$	0	$\overline{V}-\underline{C}$	0	0	$\cdots$	0	0	0	$\cdots$	0	0	0	0	$\cdots$	0	0	$\cdots$	0	0	0	0	$\cdots$	0
		t	0	0	$\cdots$	0	0	$-\epsilon$	0	$\cdots$	0	0	0	$\cdots$	0	ϵ	0	$\cdots$	0	0	0	$\cdots$	0	0	0	$-\epsilon$	0	$\cdots$	0	0	0	$\cdots$	0	0	0	0	$\cdots$	0	0	$\cdots$	0	0	0	0	$\cdots$	0
		$t+1$	0	0	$\cdots$	0	0	0	0	$\cdots$	0	0	0	$\cdots$	0	0	0	$\cdots$	0	0	0	$\cdots$	0	0	0	0	$\overline{V}-\underline{C}$	$\cdots$	0	0	0	$\cdots$	0	0	0	0	$\cdots$	0	0	$\cdots$	0	0	0	0	$\cdots$	0
		$\vdots$	$\vdots$	$\vdots$	$\ddots$	$\vdots$	$\vdots$	$\vdots$	$\vdots$	$\ddots$	$\vdots$	$\vdots$	$\vdots$	$\ddots$	$\vdots$	$\vdots$	$\vdots$	$\ddots$	$\vdots$	$\vdots$	$\vdots$	$\ddots$	$\vdots$	$\vdots$	$\vdots$	$\vdots$	$\ddots$	$\vdots$	$\vdots$	$\vdots$	$\ddots$	$\vdots$	$\vdots$	$\vdots$	$\vdots$	$\ddots$	$\vdots$	$\vdots$	$\ddots$	$\vdots$	$\vdots$	$\vdots$	$\vdots$	$\ddots$	$\vdots$
		T	0	0	$\cdots$	0	0	0	0	$\cdots$	0	0	0	$\cdots$	0	0	0	$\cdots$	0	0	0	$\cdots$	0	0	0	0	$\cdots$	$\overline{V}-\underline{C}$	0	0	$\cdots$	0	0	0	0	$\cdots$	0	0	$\cdots$	0	0	0	0	$\cdots$	0
$\bar{\underline{\theta}}^{\alpha}$	(B4)	1	$\overline{V}-\underline{C}-\epsilon$	0	$\cdots$	0	0	0	0	$\cdots$	0	0	0	$\cdots$	0	0	0	$\cdots$	0	0	0	$\cdots$	0	0	0	0	$\cdots$	0	0	0	$\cdots$	0	0	0	0	$\cdots$	0	0	$\cdots$	0	0	0	0	$\cdots$	0
		2	$\overline{V}-\underline{C}-\epsilon$	$\overline{V}-\underline{C}-\epsilon$	$\cdots$	0	0	0	0	$\cdots$	0	0	0	$\cdots$	0	0	0	$\cdots$	0	0	0	$\cdots$	0	0	0	0	$\cdots$	0	0	0	$\cdots$	0	0	0	0	$\cdots$	0	0	$\cdots$	0	0	0	0	$\cdots$	0
		$\vdots$	$\vdots$	$\vdots$	$\ddots$	$\vdots$	$\vdots$	$\vdots$	$\vdots$	$\ddots$	$\vdots$	$\vdots$	$\vdots$	$\ddots$	$\vdots$	$\vdots$	$\vdots$	$\ddots$	$\vdots$	$\vdots$	$\vdots$	$\ddots$	$\vdots$	$\vdots$	$\vdots$	$\vdots$	$\ddots$	$\vdots$	$\vdots$	$\vdots$	$\ddots$	$\vdots$	$\vdots$	$\vdots$	$\vdots$	$\ddots$	$\vdots$	$\vdots$	$\ddots$	$\vdots$	$\vdots$	$\vdots$	$\vdots$	$\ddots$	$\vdots$
		$t-1$	$\overline{V}-\underline{C}-\epsilon$	$\overline{V}-\underline{C}-\epsilon$	$\cdots$	$\overline{V}-\underline{C}-\epsilon$	$\overline{V}-\underline{C}-\epsilon$	0	0	$\cdots$	0	0	0	$\cdots$	0	0	0	$\cdots$	0	0	0	$\cdots$	0	0	0	0	$\cdots$	0	0	1	1	$\cdots$	1	1	0	0	$\cdots$	0	0	$\cdots$	0	0	0	0	$\cdots$	0
		t	V	V	$\cdots$	V	V	$\overline{V}-\underline{C}-\epsilon$	0	$\cdots$	0	0	0	$\cdots$	0	$2V-\overline{V}+\underline{C}+\epsilon$	0	$\cdots$	0	0	0	$\cdots$	0	0	$\overline{V}-\underline{C}-\epsilon$	0	$\cdots$	0	1	1	$\cdots$	1	1	1	0	$\cdots$	0	0	$\cdots$	0	0	0	0	$\cdots$	0
		$t+1$	V	V	$\cdots$	V	V	$\overline{V}-\underline{C}-\epsilon$	$\overline{V}-\underline{C}-\epsilon$	$\cdots$	0	0	0	$\cdots$	0	$2V-\overline{V}+\underline{C}+\epsilon$	0	$\cdots$	0	0	0	$\cdots$	0	0	$\overline{V}-\underline{C}-\epsilon$	0	$\cdots$	0	1	1	$\cdots$	1	1	1	1	$\cdots$	0	0	$\cdots$	0	0	0	0	$\cdots$	0
		$\vdots$	$\vdots$	$\vdots$	$\ddots$	$\vdots$	$\vdots$	$\vdots$	$\vdots$	$\ddots$	$\vdots$	$\vdots$	$\vdots$	$\ddots$	$\vdots$	$\vdots$	$\vdots$	$\ddots$	$\vdots$	$\vdots$	$\vdots$	$\ddots$	$\vdots$	$\vdots$	$\vdots$	$\vdots$	$\ddots$	$\vdots$	$\vdots$	$\vdots$	$\ddots$	$\vdots$	$\vdots$	$\vdots$	$\vdots$	$\ddots$	$\vdots$	$\vdots$	$\ddots$	$\vdots$	$\vdots$	$\vdots$	$\vdots$	$\ddots$	$\vdots$
		T	V	V	$\cdots$	V	V	$\overline{V}-\underline{C}-\epsilon$	$\overline{V}-\underline{C}-\epsilon$	$\cdots$	$\overline{V}-\underline{C}-\epsilon$	0	0	$\cdots$	0	$2V-\overline{V}+\underline{C}+\epsilon$	0	$\cdots$	0	0	0	$\cdots$	0	0	$\overline{V}-\underline{C}-\epsilon$	0	$\cdots$	0	1	1	$\cdots$	1	1	1	1	$\cdots$	1	0	$\cdots$	0	0	0	0	$\cdots$	0
$\bar{\underline{\theta}}^{\alpha}$	(B5)	2	0	$\overline{V}-\underline{C}$	$\cdots$	0	0	0	0	$\cdots$	0	0	0	$\cdots$	0	0	0	$\cdots$	0	0	0	$\cdots$	0	0	0	0	$\cdots$	0	0	1	$\cdots$	0	0	0	0	$\cdots$	0	1	$\cdots$	0	0	0	0	$\cdots$	0
		$\vdots$	$\vdots$	$\vdots$	$\ddots$	$\vdots$	$\vdots$	$\vdots$	$\vdots$	$\ddots$	$\vdots$	$\vdots$	$\vdots$	$\ddots$	$\vdots$	$\vdots$	$\vdots$	$\ddots$	$\vdots$	$\vdots$	$\vdots$	$\ddots$	$\vdots$	$\vdots$	$\vdots$	$\vdots$	$\ddots$	$\vdots$	$\vdots$	$\vdots$	$\ddots$	$\vdots$	$\vdots$	$\vdots$	$\vdots$	$\ddots$	$\vdots$	$\vdots$	$\ddots$	$\vdots$	$\vdots$	$\vdots$	$\vdots$	$\ddots$	$\vdots$
		$t-2$	0	0	$\cdots$	$\overline{V}-\underline{C}$	0	0	0	$\cdots$	0	0	0	$\cdots$	0	0	0	$\cdots$	0	0	0	$\cdots$	0	0	0	0	$\cdots$	0	0	0	$\cdots$	1	0	0	0	$\cdots$	0	0	$\cdots$	1	0	0	0	$\cdots$	0
		$t-1$	0	0	$\cdots$	0	$\overline{V}-\underline{C}$	$\overline{V}+V-\underline{C}$	$\overline{V}-\underline{C}$	$\cdots$	0	0	0	$\cdots$	0	0	0	$\cdots$	0	0	0	$\cdots$	0	0	$\overline{V}+V-\underline{C}$	0	$\cdots$	0	0	0	$\cdots$	0	1	1	1	$\cdots$	0	0	$\cdots$	0	1	0	0	$\cdots$	0
		t	0	0	$\cdots$	0	0	$\overline{V}-\underline{C}$	0	$\cdots$	0	0	0	$\cdots$	0	0	0	$\cdots$	0	0	0	$\cdots$	0	0	$\overline{V}-\underline{C}$	0	$\cdots$	0	0	0	$\cdots$	0	0	1	0	$\cdots$	0	0	$\cdots$	0	0	1	0	$\cdots$	0
		$t+1$	0	0	$\cdots$	0	0	0	$\overline{V}-\underline{C}$	$\cdots$	0	0	0	$\cdots$	0	0	0	$\cdots$	0	0	0	$\cdots$	0	0	0	0	$\cdots$	0	0	0	$\cdots$	0	0	0	1	$\cdots$	0	0	$\cdots$	0	0	0	1	$\cdots$	0
		$\vdots$	$\vdots$	$\vdots$	$\ddots$	$\vdots$	$\vdots$	$\vdots$	$\vdots$	$\ddots$	$\vdots$	$\vdots$	$\vdots$	$\ddots$	$\vdots$	$\vdots$	$\vdots$	$\ddots$	$\vdots$	$\vdots$	$\vdots$	$\ddots$	$\vdots$	$\vdots$	$\vdots$	$\vdots$	$\ddots$	$\vdots$	$\vdots$	$\vdots$	$\ddots$	$\vdots$	$\vdots$	$\vdots$	$\vdots$	$\ddots$	$\vdots$	$\vdots$	$\ddots$	$\vdots$	$\vdots$	$\vdots$	$\vdots$	$\ddots$	$\vdots$
		T	0	0	$\cdots$	0	0	0	0	$\cdots$	$\overline{V}-\underline{C}$	0	0	$\cdots$	0	0	0	$\cdots$	0	0	0	$\cdots$	0	0	0	0	$\cdots$	0	0	0	$\cdots$	0	0	0	0	$\cdots$	1	0	$\cdots$	0	0	0	0	$\cdots$	1

(i) For each $\alpha \in [1,T]_{\mathbb{Z}}$, the point with index α in group (B1), denoted by $\underline{\grave{\boldsymbol{\theta}}}^{\alpha}$, is obtained by setting $\underline{\grave{\boldsymbol{\theta}}}^{\alpha} = \grave{\boldsymbol{\theta}}^{\alpha} - \overline{\boldsymbol{\theta}}^{\alpha}$ for any $\alpha \in [1,t]_{\mathbb{Z}}$, $\underline{\grave{\boldsymbol{\theta}}}^{\alpha} = \grave{\boldsymbol{\theta}}^{\alpha} - \overline{\boldsymbol{\theta}}^{\alpha} + \hat{\boldsymbol{\theta}}^{t} - \dot{\boldsymbol{\theta}}^{t}$ for any $\alpha \in [t+1,T]_{\mathbb{Z}}$ when $t < T$. Here $\grave{\boldsymbol{\theta}}^{\alpha}$ is the point with index α in groups (A1)–(A3), $\overline{\boldsymbol{\theta}}^{\alpha}$ is the point in groups (A11)–(A12), $\hat{\boldsymbol{\theta}}^{t}$ is the point in group (A9), and $\dot{\boldsymbol{\theta}}^{t}$ is the point in group (A15).

(ii) For each $\alpha \in [1,T]_{\mathbb{Z}} \setminus \{t\}$, the point with index α in group (B2), denoted by $\underline{\acute{\boldsymbol{\theta}}}^{\alpha}$, is obtained by setting $\underline{\acute{\boldsymbol{\theta}}}^{\alpha} = \acute{\boldsymbol{\theta}}^{\alpha} - \overline{\boldsymbol{\theta}}^{\alpha}$ for any $\alpha \in [1,t-1]_{\mathbb{Z}}$ and $\underline{\acute{\boldsymbol{\theta}}}^{\alpha} = \acute{\boldsymbol{\theta}}^{\alpha} - \overline{\boldsymbol{\theta}}^{\alpha} + \hat{\boldsymbol{\theta}}^{t} - \dot{\boldsymbol{\theta}}^{t}$ for any $\alpha \in [t+1,T]_{\mathbb{Z}}$ when $t < T$. Here $\acute{\boldsymbol{\theta}}^{\alpha}$ is the point in groups (A4)–(A5), $\overline{\boldsymbol{\theta}}^{\alpha}$ is the point in groups (A11)–(A12), $\hat{\boldsymbol{\theta}}^{t}$ is the point in group (A9), and $\dot{\boldsymbol{\theta}}^{t}$ is the point in group (A15).

(iii) For each $\alpha \in [1,T]_{\mathbb{Z}}$, the point with index α in group (B3), denoted by $\underline{\hat{\boldsymbol{\theta}}}^{\alpha}$, is obtained by setting $\underline{\hat{\boldsymbol{\theta}}}^{1} = \hat{\boldsymbol{\theta}}^{1} - \overline{\boldsymbol{\theta}}^{1}$ and $\underline{\hat{\boldsymbol{\theta}}}^{\alpha} = \hat{\boldsymbol{\theta}}^{\alpha} - \dot{\boldsymbol{\theta}}^{\alpha}$ for any $\alpha \in [2,T]_{\mathbb{Z}}$. Here $\hat{\boldsymbol{\theta}}^{\alpha}$ is the point in groups (A6)–(A10), $\overline{\boldsymbol{\theta}}^{1}$ is the point in group (A11), and $\dot{\boldsymbol{\theta}}^{\alpha}$ is the point in groups (A13)–(A16).

(iv) For each $\alpha \in [1,T]_{\mathbb{Z}}$, the point with index α in group (B4), denoted by $\underline{\overline{\boldsymbol{\theta}}}^{\alpha}$, is obtained by setting $\underline{\overline{\boldsymbol{\theta}}}^{\alpha} = \overline{\boldsymbol{\theta}}^{\alpha}$. Here $\overline{\boldsymbol{\theta}}^{\alpha}$ is the point in groups (A11)–(A12).

(v) For each $\alpha \in [2,T]_{\mathbb{Z}}$, the point with index α in group (B5), denoted by $\underline{\dot{\boldsymbol{\theta}}}^{\alpha}$, is obtained by setting $\underline{\dot{\boldsymbol{\theta}}}^{\alpha} = \dot{\boldsymbol{\theta}}^{\alpha}$. Here $\dot{\boldsymbol{\theta}}^{\alpha}$ is the point with index α in groups (A13)–(A16).

The matrix shown in Table C.3 is lower triangular; that is, the position of the last nonzero component of a row of the matrix is greater than the position of the last nonzero component of the previous row. This indicates that the $5T-2$ points in groups (A1)–(A16) are linearly independent. Therefore, inequality (4.36) is facet-defining for $\operatorname{conv}(\mathcal{D})$. □

C.13 Proof of Proposition 8

Proof. To prove that inequality (4.37) is valid for $\operatorname{conv}(\mathcal{D})$ for any $k \in [1, \min\{L, \varsigma+1\}]_{\mathbb{Z}}$ and $t \in [k+1,T]_{\mathbb{Z}}$, it suffices to show that it is valid for $\mathcal{D}$ for such k and t. Consider any element $(\mathbf{p}, \mathbf{r}^{+}, \mathbf{r}^{-}, \mathbf{y}, \mathbf{u})$ of $\mathcal{D}$ and any $k \in [1, \min\{L, \varsigma+1\}]_{\mathbb{Z}}$ and $t \in [k+1,T]_{\mathbb{Z}}$. We show that $(\mathbf{p}, \mathbf{r}^{+}, \mathbf{r}^{-}, \mathbf{y}, \mathbf{u})$ satisfies (4.37). We divide the analysis into the following three possible cases.

Case 1: $y_t = 0$. By Lemma 2, we have $\sum_{s=0}^{k-1} u_{t-s} = 0$ and hence $u_{t-s} = 0$ for any $s \in [0, k-1]_{\mathbb{Z}}$. Thus, the right-hand side of (4.37) is 0. Because $y_t = 0$, by (4.35e) and (4.35h), we have $p_t = r_t^+ = 0$. Therefore, in this case, $(\mathbf{p}, \mathbf{r}^+, \mathbf{r}^-, \mathbf{y}, \mathbf{u})$ satisfies (4.37).

Case 2: $y_t = 1$ and $u_{t-s} = 0$ for any $s \in [0, k-1]_{\mathbb{Z}}$. The right-hand side of (4.37) is $\overline{C} - \underline{C}$. Because $y_t = 1$, by (4.35e), we have $p_t + r_t^+ \leq \overline{C} - \underline{C}$. Therefore, in this case, $(\mathbf{p}, \mathbf{r}^+, \mathbf{r}^-, \mathbf{y}, \mathbf{u})$ satisfies (4.37).

Case 3: $y_t = 1$ and $u_{t-s'} = 1$ for some $s' \in [0, k-1]_{\mathbb{Z}}$. By Lemma 2, we have $u_{t-s} = 0$ for any $s \in [0, k-1]_{\mathbb{Z}} \setminus \{s'\}$. Thus, the right-hand side of (4.37) is $\overline{V} - \underline{C} + s'V$. For any $s \in [0, s']_{\mathbb{Z}}$, we have $y_t - y_{t-s} = y_t - y_{t-s} - \sum_{i=0}^{s-1} u_{t-i} = \sum_{i=0}^{s-1} (y_{t-i} - y_{t-i-1} - u_{t-i}) \leq 0$, where the first equality holds because $u_{t-i} = 0$ for any $i \in [0, k-1]_{\mathbb{Z}} \setminus \{s'\}$ and the inequality holds by (4.35c). Because $y_t = 1$, we have $y_{t-s} = 1$ for any $s \in [0, s']_{\mathbb{Z}}$. Because $u_{t-s'} = 1$, by Corollary 1, we have $y_{t-s'-1} = 0$, which, by (4.35e) and (4.35h), implies that $p_{t-s'-1} = 0$. Thus,

$$
\begin{aligned}
&p_t + r_t^+ = p_t + r_t^+ - p_{t-s'-1} \leq \sum_{s=t-s'}^{t} \left(p_s + r_s^+ - p_{s-1}\right) \\
&\leq \sum_{s=t-s'}^{t} \left(\overline{V} + \left(\underline{C} + V - \overline{V}\right) y_{s-1} - \underline{C} y_s\right) = (s'+1)\,\overline{V} + \sum_{i=1}^{s'+1} \left(\underline{C} + V - \overline{V}\right) y_{t-i} - \sum_{i=0}^{s'} \underline{C} y_{t-i} \\
&= (s'+1)\,\overline{V} + s'\left(\underline{C} + V - \overline{V}\right) - (s'+1)\,\underline{C} = \overline{V} - \underline{C} + s'V,
\end{aligned}
$$

where the first inequality holds by (4.35h) and the second inequality holds by the ramp-up constraints (4.35f). Therefore, in this case, $(\mathbf{p}, \mathbf{r}^+, \mathbf{r}^-, \mathbf{y}, \mathbf{u})$ satisfies (4.37).

Consider any $k \in [1, \min\{L, \varsigma + 1\}]_{\mathbb{Z}}$ and $t \in [k+1, T]_{\mathbb{Z}}$. To prove inequality (4.37) is facet-defining for $\mathrm{conv}(\mathcal{D})$ when one of the following two conditions holds: (i) $L = 1$ and (ii) $k = L = 2$ and $\overline{V} + V \leq \overline{C} \leq \overline{V} + 2V$, it suffices to create $5T - 1$ affinely independent points in $\mathrm{conv}(\mathcal{D})$ that satisfy (4.37) at equality. Because $\mathbf{0} \in \mathrm{conv}(\mathcal{D})$ and $\mathbf{0}$ satisfies (4.37) at equality, it suffices to create the remaining $5T - 2$ nonzero linearly independent points.

First, we consider $L = 1$, implying that $k = 1$. We let $\grave{\boldsymbol{\theta}} = (\grave{\mathbf{p}}, \grave{\mathbf{r}}^+, \grave{\mathbf{r}}^-, \grave{\mathbf{y}}, \grave{\mathbf{u}})$ and denote the sth component of $\grave{\mathbf{p}}$, $\grave{\mathbf{r}}^+$, $\grave{\mathbf{r}}^-$, $\grave{\mathbf{y}}$, and $\grave{\mathbf{u}}$ by $\grave{p}_s$, $\grave{r}_s^+$, $\grave{r}_s^-$, $\grave{y}_s$, and $\grave{u}_s$. Similarly, we define $\acute{\boldsymbol{\theta}}$, $\hat{\boldsymbol{\theta}}$, $\overline{\boldsymbol{\theta}}$, and $\dot{\boldsymbol{\theta}}$. We denote the $5T - 2$ nonzero linearly independent points by $\grave{\boldsymbol{\theta}}^{\alpha}$ for $\alpha \in \mathcal{T} \setminus \{t\}$, $\acute{\boldsymbol{\theta}}^{\alpha}$ for $\alpha \in \mathcal{T}$, $\hat{\boldsymbol{\theta}}^{\alpha}$ for $\alpha \in \mathcal{T}$, $\overline{\boldsymbol{\theta}}^{\alpha}$ for $\alpha \in \mathcal{T}$, and $\dot{\boldsymbol{\theta}}^{\alpha}$ for $\alpha \in \mathcal{T} \setminus \{1\}$. We let $\epsilon = \min\left\{\underline{C} + V - \overline{V},\ \overline{V} - \underline{C}\right\} > 0$ and divide the $5T - 2$ points into the following 11

groups.

(A1) For each $\alpha \in [1, t-1]_{\mathbb{Z}}$, we create a point $\grave{\boldsymbol{\theta}}^{\alpha}$ as follows:

$$\grave{p}_s^{\alpha} = \begin{cases} \overline{V} - \underline{C}, & s \in [1, \alpha]_{\mathbb{Z}} \\ 0, & \text{o.w.} \end{cases}, \ \grave{y}_s^{\alpha} = \begin{cases} 1, & s \in [1, \alpha]_{\mathbb{Z}} \\ 0, & \text{o.w.} \end{cases},$$

$\grave{r}_s^{+,\alpha} = \grave{r}_s^{-,\alpha} = 0$ for any $s \in \mathcal{T}$, and $\grave{u}_s^{\alpha} = 0$ for any $s \in \mathcal{T} \setminus \{1\}$. It is easy to verify that $\grave{\boldsymbol{\theta}}^{\alpha}$ satisfies (4.35a)–(4.35h). Thus, $\grave{\boldsymbol{\theta}}^{\alpha} \in \text{conv}(\mathcal{D})$. It is also easy to verify that $\grave{\boldsymbol{\theta}}^{\alpha}$ satisfies (4.37) at equality.

(A2) For each $\alpha \in [t+1, T]_{\mathbb{Z}}$, we create a point $\grave{\boldsymbol{\theta}}^{\alpha}$ as follows:

$$\grave{p}_s^{\alpha} = \begin{cases} \overline{V} - \underline{C}, & s \in [t, \alpha]_{\mathbb{Z}} \\ 0, & o.w. \end{cases}, \ \grave{y}_s^{\alpha} = \begin{cases} 1, & s \in [t, \alpha]_{\mathbb{Z}} \\ 0, & \text{o.w.} \end{cases}, \ \grave{u}_s^{\alpha} = \begin{cases} 1, & s = t \\ 0, & \text{o.w.} \end{cases},$$

and $\grave{r}_s^{+,\alpha} = \grave{r}_s^{-,\alpha} = 0$ for any $s \in \mathcal{T}$. It is easy to verify that $\grave{\boldsymbol{\theta}}^{\alpha}$ satisfies (4.35a)–(4.35h). Thus, $\grave{\boldsymbol{\theta}}^{\alpha} \in \text{conv}(\mathcal{D})$. It is also easy to verify that $\grave{\boldsymbol{\theta}}^{\alpha}$ satisfies (4.37) at equality.

(A3) For each $\alpha \in [1, t-1]_{\mathbb{Z}}$, we create a point $\acute{\boldsymbol{\theta}}^{\alpha}$ as follows:

$$\acute{p}_s^{\alpha} = \begin{cases} \overline{V} - \underline{C} - \epsilon, & s \in [1, \alpha]_{\mathbb{Z}} \\ 0, & \text{o.w.} \end{cases}, \ \acute{r}_s^{+,\alpha} = \begin{cases} \epsilon, & s = \alpha \\ 0, & \text{o.w.} \end{cases}, \ \acute{y}_s^{\alpha} = \begin{cases} 1, & s \in [1, \alpha]_{\mathbb{Z}} \\ 0, & \text{o.w.} \end{cases},$$

$\acute{r}_s^{-,\alpha} = 0$ for any $s \in \mathcal{T}$, and $\acute{u}_s^{\alpha} = 0$ for any $s \in \mathcal{T} \setminus \{1\}$. It is easy to verify that $\acute{\boldsymbol{\theta}}^{\alpha}$ satisfies (4.35a)–(4.35h). Thus, $\acute{\boldsymbol{\theta}}^{\alpha} \in \text{conv}(\mathcal{D})$. It is also easy to verify that $\acute{\boldsymbol{\theta}}^{\alpha}$ satisfies (4.37) at equality.

(A4) For $\alpha = t$, we create a point $\acute{\boldsymbol{\theta}}^{\alpha}$ as follows:

$$\acute{p}_s^{\alpha} = \begin{cases} \overline{V} - \underline{C} - \epsilon, & s = t \\ 0, & \text{o.w.} \end{cases}, \ \acute{r}_s^{+,\alpha} = \begin{cases} \epsilon, & s = t \\ 0, & \text{o.w.} \end{cases}, \ \acute{y}_s^{\alpha} = \acute{u}_s^{\alpha} = \begin{cases} 1, & s = t \\ 0, & \text{o.w.} \end{cases},$$

and $\acute{r}_s^{-,\alpha} = 0$ for any $s \in \mathcal{T}$. It is easy to verify that $\acute{\boldsymbol{\theta}}^{\alpha}$ satisfies (4.35a)–(4.35h). Thus, $\acute{\boldsymbol{\theta}}^{\alpha} \in \text{conv}(\mathcal{D})$. It is also easy to verify that $\acute{\boldsymbol{\theta}}^{\alpha}$ satisfies (4.37).

(A5) For each $\alpha \in [t+1, T]_{\mathbb{Z}}$, we create a point $\acute{\boldsymbol{\theta}}^{\alpha}$ as follows:

$$\acute{p}_s^{\alpha} = \begin{cases} \overline{V} - \underline{C}, & s = t, \\ \overline{V} - \underline{C} - \epsilon, & s \in [t+1, \alpha]_{\mathbb{Z}} \\ 0, & o.w. \end{cases}, \; \acute{r}_s^{+,\alpha} = \begin{cases} \epsilon, & s = \alpha \\ 0, & \text{o.w.} \end{cases}, \; \acute{y}_s^{\alpha} = \begin{cases} 1, & s \in [t, \alpha]_{\mathbb{Z}} \\ 0, & \text{o.w.} \end{cases},$$

$$\acute{u}_s^{\alpha} = \begin{cases} 1, & s = t \\ 0, & \text{o.w.} \end{cases},$$

and $\acute{r}_s^{-,\alpha} = 0$ for any $s \in \mathcal{T}$. It is easy to verify that $\acute{\boldsymbol{\theta}}^{\alpha}$ satisfies (4.35a)–(4.35h). Thus, $\acute{\boldsymbol{\theta}}^{\alpha} \in \text{conv}(\mathcal{D})$. It is also easy to verify that $\acute{\boldsymbol{\theta}}^{\alpha}$ satisfies (4.37) at equality.

(A6) For each $\alpha \in [1, t-1]_{\mathbb{Z}}$, we create a point $\hat{\boldsymbol{\theta}}^{\alpha}$ as follows:

$$\hat{p}_s^{\alpha} = \begin{cases} \overline{V} - \underline{C} - \epsilon, & s \in [1, \alpha]_{\mathbb{Z}} \\ 0, & \text{o.w.} \end{cases}, \; \hat{r}_s^{-,\alpha} = \begin{cases} \epsilon, & s = \alpha \\ 0, & \text{o.w.} \end{cases}, \; \hat{y}_s^{\alpha} = \begin{cases} 1, & s \in [1, \alpha]_{\mathbb{Z}} \\ 0, & \text{o.w.} \end{cases},$$

$\hat{r}_s^{+,\alpha} = 0$ for any $s \in \mathcal{T}$, and $\hat{u}_s^{\alpha} = 0$ for any $s \in \mathcal{T} \setminus \{1\}$. It is easy to verify that $\hat{\boldsymbol{\theta}}^{\alpha}$ satisfies (4.35a)–(4.35h). Thus, $\hat{\boldsymbol{\theta}}^{\alpha} \in \text{conv}(\mathcal{D})$. It is also easy to verify that $\hat{\boldsymbol{\theta}}^{\alpha}$ satisfies (4.37) at equality.

(A7) For each $\alpha \in [t, T]_{\mathbb{Z}}$, we create a point $\hat{\boldsymbol{\theta}}^{\alpha}$ as follows:

$$\hat{p}_s^{\alpha} = \begin{cases} \overline{V} - \underline{C}, & s = t \\ \overline{V} - \underline{C} - \epsilon, & s \in [t+1, \alpha]_{\mathbb{Z}}, \; t < T \\ 0, & \text{o.w.} \end{cases}, \; \hat{r}_s^{-,\alpha} = \begin{cases} \epsilon, & s = \alpha \\ 0, & \text{o.w.} \end{cases}, \; \hat{y}_s^{\alpha} = \begin{cases} 1, & s \in [t, \alpha]_{\mathbb{Z}} \\ 0, & \text{o.w.} \end{cases},$$

$\hat{r}_s^{+,\alpha} = 0$ for any $s \in \mathcal{T}$, and $\hat{u}_s^{\alpha} = 1$ for $s = t$ and $\hat{u}_s^{\alpha} = 0$ otherwise. It is clear that $\hat{\boldsymbol{\theta}}^{\alpha}$ satisfies (4.35a)–(4.35h). Thus, $\hat{\boldsymbol{\theta}}^{\alpha} \in \text{conv}(\mathcal{D})$. It is also easy to verify that $\hat{\boldsymbol{\theta}}^{\alpha}$ satisfies (4.37) at equality.

(A8) For each $\alpha \in [1, t-1]_{\mathbb{Z}}$, we create a point $\overline{\boldsymbol{\theta}}^{\alpha}$ as follows:

$$\overline{p}_s^{\alpha} = \begin{cases} \overline{V} - \underline{C} - \epsilon, & s \in [1, \alpha]_{\mathbb{Z}} \\ 0, & \text{o.w.} \end{cases}, \ \overline{y}_s^{\alpha} = \begin{cases} 1, & s \in [1, \alpha]_{\mathbb{Z}} \\ 0, & \text{o.w.} \end{cases},$$

$\overline{r}_s^{+,\alpha} = \overline{r}_s^{-,\alpha} = 0$ for any $s \in \mathcal{T}$, and $\overline{u}_s^{\alpha} = 0$ for any $s \in \mathcal{T} \setminus \{1\}$. It is easy to verify that $\overline{\boldsymbol{\theta}}^{\alpha}$ satisfies (4.35a)–(4.35h). Thus, $\overline{\boldsymbol{\theta}}^{\alpha} \in \text{conv}(\mathcal{D})$. It is also easy to verify that $\overline{\boldsymbol{\theta}}^{\alpha}$ satisfies (4.37) at equality.

(A9) For $\alpha = t$, we create a point $\overline{\boldsymbol{\theta}}^{\alpha}$ such that $\overline{p}_s^{\alpha} = \overline{C} - \underline{C}$, $\overline{r}_s^{+,\alpha} = \overline{r}_s^{-,\alpha} = 0$, and $\overline{y}_s^{\alpha} = 1$ for any $s \in \mathcal{T}$, and $\overline{u}_s^{\alpha} = 0$ for any $s \in \mathcal{T} \setminus \{1\}$. It is easy to verify that $\overline{\boldsymbol{\theta}}^{\alpha}$ satisfies (4.35a)–(4.35h). Thus, $\overline{\boldsymbol{\theta}}^{\alpha} \in \text{conv}(\mathcal{D})$. It is also easy to verify that $\overline{\boldsymbol{\theta}}^{\alpha}$ satisfies (4.37) at equality.

(A10) For each $\alpha \in [t+1, T]_{\mathbb{Z}}$, we create a point $\overline{\boldsymbol{\theta}}^{\alpha}$ as follows:

$$\overline{p}_s^{\alpha} = \begin{cases} \overline{V} - \underline{C}, & s = t \\ \overline{V} - \underline{C} - \epsilon, & s \in [t+1, \alpha]_{\mathbb{Z}} \\ 0, & \text{o.w.} \end{cases}, \ \overline{y}_s^{\alpha} = \begin{cases} 1, & s \in [t, \alpha]_{\mathbb{Z}} \\ 0, & \text{o.w.} \end{cases}, \ \overline{u}_s^{\alpha} = \begin{cases} 1, & s = t \\ 0, & \text{o.w.} \end{cases},$$

and $\overline{r}_s^{+,\alpha} = \overline{r}_s^{-,\alpha} = 0$ for any $s \in \mathcal{T}$. It is easy to verify that $\overline{\boldsymbol{\theta}}^{\alpha}$ satisfies (4.35a)–(4.35h). Thus, $\overline{\boldsymbol{\theta}}^{\alpha} \in \text{conv}(\mathcal{D})$. It is also easy to verify that $\overline{\boldsymbol{\theta}}^{\alpha}$ satisfies (4.37) at equality.

(A11) For each $\alpha \in [2, T]_{\mathbb{Z}}$, we create a point $\dot{\boldsymbol{\theta}}^{\alpha}$ as follows:

$$\dot{p}_s^{\alpha} = \begin{cases} \overline{V} - \underline{C}, & s = \alpha, \\ 0, & \text{o.w.} \end{cases}, \ \dot{y}_s^{\alpha} = \dot{u}_s^{\alpha} = \begin{cases} 1, & s = \alpha, \\ 0, & \text{o.w.} \end{cases},$$

and $\dot{r}_s^{+,\alpha} = \dot{r}_s^{-,\alpha} = 0$ for any $s \in \mathcal{T}$. It is easy to verify that $\dot{\boldsymbol{\theta}}^{\alpha}$ satisfies (4.35a)–(4.35h). Thus, $\dot{\boldsymbol{\theta}}^{\alpha} \in \text{conv}(\mathcal{D})$. It is also easy to verify that $\dot{\boldsymbol{\theta}}^{\alpha}$ satisfies (4.37) at equality.

Table C.4 shows a matrix with $5T - 2$ rows, where each row represents a point created above. This matrix can be transformed into the matrix in Table C.5 via the following

Gaussian elimination process:

(i) For each $\alpha \in [1,T]_{\mathbb{Z}} \setminus \{t\}$, the point with index α in group (B1), denoted by $\underline{\grave{\boldsymbol{\theta}}}^{\alpha}$, is obtained by setting $\underline{\grave{\boldsymbol{\theta}}}^{\alpha} = \grave{\boldsymbol{\theta}}^{\alpha} - \overline{\boldsymbol{\theta}}^{\alpha}$ for any $\alpha \in [1,T]_{\mathbb{Z}} \setminus \{t\}$. Here $\grave{\boldsymbol{\theta}}^{\alpha}$ is the point with index α in groups (A1)–(A2) and $\overline{\boldsymbol{\theta}}^{\alpha}$ is the point with index α in groups (A8) and (A10).

(ii) For each $\alpha \in [1,T]_{\mathbb{Z}}$, the point with index α in group (B2), denoted by $\underline{\acute{\boldsymbol{\theta}}}^{\alpha}$, is obtained by setting $\underline{\acute{\boldsymbol{\theta}}}^{\alpha} = \acute{\boldsymbol{\theta}}^{\alpha} - \overline{\boldsymbol{\theta}}^{\alpha}$ for any $\alpha \in [1,T]_{\mathbb{Z}} \setminus \{t\}$ and $\underline{\acute{\boldsymbol{\theta}}}^{t} = \acute{\boldsymbol{\theta}}^{t} - \dot{\boldsymbol{\theta}}^{t}$. Here $\acute{\boldsymbol{\theta}}^{\alpha}$ is the point with index α in groups (A3)–(A5), $\overline{\boldsymbol{\theta}}^{\alpha}$ is the point with index α in groups (A8) and (A10), and $\dot{\boldsymbol{\theta}}^{t}$ is the point in group (A11).

(iii) For each $\alpha \in [1,T]_{\mathbb{Z}}$, the point with index α in group (B3), denoted by $\underline{\hat{\boldsymbol{\theta}}}^{\alpha}$, is obtained by setting $\underline{\hat{\boldsymbol{\theta}}}^{\alpha} = \hat{\boldsymbol{\theta}}^{\alpha} - \overline{\boldsymbol{\theta}}^{\alpha}$ for any $\alpha \in [1,T]_{\mathbb{Z}} \setminus \{t\}$ and $\underline{\hat{\boldsymbol{\theta}}}^{t} = \hat{\boldsymbol{\theta}}^{t} - \dot{\boldsymbol{\theta}}^{t}$. Here $\hat{\boldsymbol{\theta}}^{\alpha}$ is the point with index α in groups (A6)–(A7), $\overline{\boldsymbol{\theta}}^{\alpha}$ is the point with index α in groups (A8) and (A10), and $\dot{\boldsymbol{\theta}}^{t}$ is the point in group (A11).

(iv) For each $\alpha \in [1,T]_{\mathbb{Z}}$, the point with index α in group (B4), denoted by $\underline{\overline{\boldsymbol{\theta}}}^{\alpha}$, is obtained by setting $\underline{\overline{\boldsymbol{\theta}}}^{\alpha} = \overline{\boldsymbol{\theta}}^{\alpha}$ for any $\alpha \in [1,t-1]_{\mathbb{Z}}$, $\underline{\overline{\boldsymbol{\theta}}}^{t} = \overline{\boldsymbol{\theta}}^{t}$ when $t = T$, $\underline{\overline{\boldsymbol{\theta}}}^{t} = \overline{\boldsymbol{\theta}}^{t} - \overline{\boldsymbol{\theta}}^{T} + \dot{\boldsymbol{\theta}}^{t} - \overline{\boldsymbol{\theta}}^{t-1}$ when $t < T$, and $\underline{\overline{\boldsymbol{\theta}}}^{\alpha} = \overline{\boldsymbol{\theta}}^{\alpha} - \dot{\boldsymbol{\theta}}^{t}$ for any $\alpha \in [t+1,T]_{\mathbb{Z}}$ when $t < T$. Here $\overline{\boldsymbol{\theta}}^{\alpha}$ is the point with index α in groups (A8), (A9), and (A10), and $\dot{\boldsymbol{\theta}}^{t}$ is the point in group (A11).

(v) For each $\alpha \in [2,T]_{\mathbb{Z}}$, the point with index α in group (B5), denoted by $\underline{\dot{\boldsymbol{\theta}}}^{\alpha}$, is obtained by setting $\underline{\dot{\boldsymbol{\theta}}}^{\alpha} = \dot{\boldsymbol{\theta}}^{\alpha}$. Here $\dot{\boldsymbol{\theta}}^{\alpha}$ is the point with index α in group (A11).

The matrix shown in Table C.5 is lower triangular; that is, the position of the last nonzero component of a row of the matrix is greater than the position of the last nonzero component of the previous row. This indicates that the $5T-2$ points in groups (A1)–(A11) are linearly independent. Therefore, inequality (4.37) is facet-defining for $\mathrm{conv}(\mathcal{D})$ when $L = 1$.

Table C.4. Matrix with The Rows Representing $5T-2$ Points in $\mathrm{conv}(\mathcal{D})$ That Satisfy Inequality (4.37) at Equality When $L=1$

Point	Group	Index α	$\mathbf{p}$								$\mathbf{r}^+$								$\mathbf{r}^-$								$\mathbf{y}$								$\mathbf{u}$							
			1	2	$\cdots$	$t-1$	t	$t+1$	$\cdots$	T	1	2	$\cdots$	$t-1$	t	$t+1$	$\cdots$	T	1	2	$\cdots$	$t-1$	t	$t+1$	$\cdots$	T	1	2	$\cdots$	$t-1$	t	$t+1$	$\cdots$	T	2	$\cdots$	$t-1$	t	$t+1$	$\cdots$	T
$\hat{\boldsymbol{\theta}}^{\alpha}$	(A1)	1	$\overline{V}-\underline{C}$	0	$\cdots$	0	0	0	$\cdots$	0	0	0	$\cdots$	0	0	0	$\cdots$	0	0	0	$\cdots$	0	0	0	$\cdots$	0	1	0	$\cdots$	0	0	0	$\cdots$	0	0	$\cdots$	0	0	0	$\cdots$	0
		2	$\overline{V}-\underline{C}$	$\overline{V}-\underline{C}$	$\cdots$	0	0	0	$\cdots$	0	0	0	$\cdots$	0	0	0	$\cdots$	0	0	0	$\cdots$	0	0	0	$\cdots$	0	1	1	$\cdots$	0	0	0	$\cdots$	0	0	$\cdots$	0	0	0	$\cdots$	0
		$\vdots$	$\vdots$	$\vdots$	$\ddots$	$\vdots$	$\vdots$	$\vdots$	$\ddots$	$\vdots$	$\vdots$	$\vdots$	$\ddots$	$\vdots$	$\vdots$	$\vdots$	$\ddots$	$\vdots$	$\vdots$	$\vdots$	$\ddots$	$\vdots$	$\vdots$	$\vdots$	$\ddots$	$\vdots$	$\vdots$	$\vdots$	$\ddots$	$\vdots$	$\vdots$	$\vdots$	$\ddots$	$\vdots$	$\vdots$	$\ddots$	$\vdots$	$\vdots$	$\vdots$	$\ddots$	$\vdots$
		$t-1$	$\overline{V}-\underline{C}$	$\overline{V}-\underline{C}$	$\cdots$	$\overline{V}-\underline{C}$	0	0	$\cdots$	0	0	0	$\cdots$	0	0	0	$\cdots$	0	0	0	$\cdots$	0	0	0	$\cdots$	0	1	1	$\cdots$	1	0	0	$\cdots$	0	0	$\cdots$	0	0	0	$\cdots$	0
	(A2)	$t+1$	0	0	$\cdots$	0	$\overline{V}-\underline{C}$	$\overline{V}-\underline{C}$	$\cdots$	0	0	0	$\cdots$	0	0	0	$\cdots$	0	0	0	$\cdots$	0	0	0	$\cdots$	0	0	0	$\cdots$	0	1	1	$\cdots$	0	0	$\cdots$	0	1	0	$\cdots$	0
		$\vdots$	$\vdots$	$\vdots$	$\ddots$	$\vdots$	$\vdots$	$\vdots$	$\ddots$	$\vdots$	$\vdots$	$\vdots$	$\ddots$	$\vdots$	$\vdots$	$\vdots$	$\ddots$	$\vdots$	$\vdots$	$\vdots$	$\ddots$	$\vdots$	$\vdots$	$\vdots$	$\ddots$	$\vdots$	$\vdots$	$\vdots$	$\ddots$	$\vdots$	$\vdots$	$\vdots$	$\ddots$	$\vdots$	$\vdots$	$\ddots$	$\vdots$	$\vdots$	$\vdots$	$\ddots$	$\vdots$
		T	0	0	$\cdots$	0	$\overline{V}-\underline{C}$	$\overline{V}-\underline{C}$	$\cdots$	$\overline{V}-\underline{C}$	0	0	$\cdots$	0	0	0	$\cdots$	0	0	0	$\cdots$	0	0	0	$\cdots$	0	0	0	$\cdots$	0	1	1	$\cdots$	1	0	$\cdots$	0	1	0	$\cdots$	0
$\hat{\boldsymbol{\theta}}^{\alpha}$	(A3)	1	$\overline{V}-\underline{C}-\epsilon$	0	$\cdots$	0	0	0	$\cdots$	0	ϵ	0	$\cdots$	0	0	0	$\cdots$	0	0	0	$\cdots$	0	0	0	$\cdots$	0	1	0	$\cdots$	0	0	0	$\cdots$	0	0	$\cdots$	0	0	0	$\cdots$	0
		2	$\overline{V}-\underline{C}-\epsilon$	$\overline{V}-\underline{C}-\epsilon$	$\cdots$	0	0	0	$\cdots$	0	0	ϵ	$\cdots$	0	0	0	$\cdots$	0	0	0	$\cdots$	0	0	0	$\cdots$	0	1	1	$\cdots$	0	0	0	$\cdots$	0	0	$\cdots$	0	0	0	$\cdots$	0
		$\vdots$	$\vdots$	$\vdots$	$\ddots$	$\vdots$	$\vdots$	$\vdots$	$\ddots$	$\vdots$	$\vdots$	$\vdots$	$\ddots$	$\vdots$	$\vdots$	$\vdots$	$\ddots$	$\vdots$	$\vdots$	$\vdots$	$\ddots$	$\vdots$	$\vdots$	$\vdots$	$\ddots$	$\vdots$	$\vdots$	$\vdots$	$\ddots$	$\vdots$	$\vdots$	$\vdots$	$\ddots$	$\vdots$	$\vdots$	$\ddots$	$\vdots$	$\vdots$	$\vdots$	$\ddots$	$\vdots$
		$t-1$	$\overline{V}-\underline{C}-\epsilon$	$\overline{V}-\underline{C}-\epsilon$	$\cdots$	$\overline{V}-\underline{C}-\epsilon$	0	0	$\cdots$	0	0	0	$\cdots$	ϵ	0	0	$\cdots$	0	0	0	$\cdots$	0	0	0	$\cdots$	0	1	1	$\cdots$	1	0	0	$\cdots$	0	0	$\cdots$	0	0	0	$\cdots$	0
	(A4)	t	0	0	$\cdots$	0	$\overline{V}-\underline{C}-\epsilon$	0	$\cdots$	0	0	0	$\cdots$	0	ϵ	0	$\cdots$	0	0	0	$\cdots$	0	0	0	$\cdots$	0	0	0	$\cdots$	0	1	0	$\cdots$	0	0	$\cdots$	0	1	0	$\cdots$	0
	(A5)	$t+1$	0	0	$\cdots$	0	$\overline{V}-\underline{C}$	$\overline{V}-\underline{C}-\epsilon$	$\cdots$	0	0	0	$\cdots$	0	0	ϵ	$\cdots$	0	0	0	$\cdots$	0	0	0	$\cdots$	0	0	0	$\cdots$	0	1	1	$\cdots$	0	0	$\cdots$	0	1	0	$\cdots$	0
		$\vdots$	$\vdots$	$\vdots$	$\ddots$	$\vdots$	$\vdots$	$\vdots$	$\ddots$	$\vdots$	$\vdots$	$\vdots$	$\ddots$	$\vdots$	$\vdots$	$\vdots$	$\ddots$	$\vdots$	$\vdots$	$\vdots$	$\ddots$	$\vdots$	$\vdots$	$\vdots$	$\ddots$	$\vdots$	$\vdots$	$\vdots$	$\ddots$	$\vdots$	$\vdots$	$\vdots$	$\ddots$	$\vdots$	$\vdots$	$\ddots$	$\vdots$	$\vdots$	$\vdots$	$\ddots$	$\vdots$
		T	0	0	$\cdots$	0	$\overline{V}-\underline{C}$	$\overline{V}-\underline{C}-\epsilon$	$\cdots$	$\overline{V}-\underline{C}-\epsilon$	0	0	$\cdots$	0	0	0	$\cdots$	ϵ	0	0	$\cdots$	0	0	0	$\cdots$	0	0	0	$\cdots$	0	1	1	$\cdots$	1	0	$\cdots$	0	1	0	$\cdots$	0
$\hat{\boldsymbol{\theta}}^{\alpha}$	(A6)	1	$\overline{V}-\underline{C}-\epsilon$	0	$\cdots$	0	0	0	$\cdots$	0	0	0	$\cdots$	0	0	0	$\cdots$	0	ϵ	0	$\cdots$	0	0	0	$\cdots$	0	1	0	$\cdots$	0	0	0	$\cdots$	0	0	$\cdots$	0	0	0	$\cdots$	0
		2	$\overline{V}-\underline{C}-\epsilon$	$\overline{V}-\underline{C}-\epsilon$	$\cdots$	0	0	0	$\cdots$	0	0	0	$\cdots$	0	0	0	$\cdots$	0	0	ϵ	$\cdots$	0	0	0	$\cdots$	0	1	1	$\cdots$	0	0	0	$\cdots$	0	0	$\cdots$	0	0	0	$\cdots$	0
		$\vdots$	$\vdots$	$\vdots$	$\ddots$	$\vdots$	$\vdots$	$\vdots$	$\ddots$	$\vdots$	$\vdots$	$\vdots$	$\ddots$	$\vdots$	$\vdots$	$\vdots$	$\ddots$	$\vdots$	$\vdots$	$\vdots$	$\ddots$	$\vdots$	$\vdots$	$\vdots$	$\ddots$	$\vdots$	$\vdots$	$\vdots$	$\ddots$	$\vdots$	$\vdots$	$\vdots$	$\ddots$	$\vdots$	$\vdots$	$\ddots$	$\vdots$	$\vdots$	$\vdots$	$\ddots$	$\vdots$
		$t-1$	$\overline{V}-\underline{C}-\epsilon$	$\overline{V}-\underline{C}-\epsilon$	$\cdots$	$\overline{V}-\underline{C}-\epsilon$	0	0	$\cdots$	0	0	0	$\cdots$	0	0	0	$\cdots$	0	0	0	$\cdots$	ϵ	0	0	$\cdots$	0	1	1	$\cdots$	1	0	0	$\cdots$	0	0	$\cdots$	0	0	0	$\cdots$	0
	(A7)	t	0	0	$\cdots$	0	$\overline{V}-\underline{C}$	0	$\cdots$	0	0	0	$\cdots$	0	0	0	$\cdots$	0	0	0	$\cdots$	0	ϵ	0	$\cdots$	0	0	0	$\cdots$	0	1	0	$\cdots$	0	0	$\cdots$	0	1	0	$\cdots$	0
		$t+1$	0	0	$\cdots$	0	$\overline{V}-\underline{C}$	$\overline{V}-\underline{C}-\epsilon$	$\cdots$	0	0	0	$\cdots$	0	0	0	$\cdots$	0	0	0	$\cdots$	0	0	ϵ	$\cdots$	0	0	0	$\cdots$	0	1	1	$\cdots$	0	0	$\cdots$	0	1	0	$\cdots$	0
		$\vdots$	$\vdots$	$\vdots$	$\ddots$	$\vdots$	$\vdots$	$\vdots$	$\ddots$	$\vdots$	$\vdots$	$\vdots$	$\ddots$	$\vdots$	$\vdots$	$\vdots$	$\ddots$	$\vdots$	$\vdots$	$\vdots$	$\ddots$	$\vdots$	$\vdots$	$\vdots$	$\ddots$	$\vdots$	$\vdots$	$\vdots$	$\ddots$	$\vdots$	$\vdots$	$\vdots$	$\ddots$	$\vdots$	$\vdots$	$\ddots$	$\vdots$	$\vdots$	$\vdots$	$\ddots$	$\vdots$
		T	0	0	$\cdots$	0	$\overline{V}-\underline{C}$	$\overline{V}-\underline{C}-\epsilon$	$\cdots$	$\overline{V}-\underline{C}-\epsilon$	0	0	$\cdots$	0	0	0	$\cdots$	0	0	0	$\cdots$	0	0	0	$\cdots$	ϵ	0	0	$\cdots$	0	1	1	$\cdots$	1	0	$\cdots$	0	1	0	$\cdots$	0
$\overline{\boldsymbol{\theta}}^{\alpha}$	(A8)	1	$\overline{V}-\underline{C}-\epsilon$	0	$\cdots$	0	0	0	$\cdots$	0	0	0	$\cdots$	0	0	0	$\cdots$	0	0	0	$\cdots$	0	0	0	$\cdots$	0	1	0	$\cdots$	0	0	0	$\cdots$	0	0	$\cdots$	0	0	0	$\cdots$	0
		2	$\overline{V}-\underline{C}-\epsilon$	$\overline{V}-\underline{C}-\epsilon$	$\cdots$	0	0	0	$\cdots$	0	0	0	$\cdots$	0	0	0	$\cdots$	0	0	0	$\cdots$	0	0	0	$\cdots$	0	1	1	$\cdots$	0	0	0	$\cdots$	0	0	$\cdots$	0	0	0	$\cdots$	0
		$\vdots$	$\vdots$	$\vdots$	$\ddots$	$\vdots$	$\vdots$	$\vdots$	$\ddots$	$\vdots$	$\vdots$	$\vdots$	$\ddots$	$\vdots$	$\vdots$	$\vdots$	$\ddots$	$\vdots$	$\vdots$	$\vdots$	$\ddots$	$\vdots$	$\vdots$	$\vdots$	$\ddots$	$\vdots$	$\vdots$	$\vdots$	$\ddots$	$\vdots$	$\vdots$	$\vdots$	$\ddots$	$\vdots$	$\vdots$	$\ddots$	$\vdots$	$\vdots$	$\vdots$	$\ddots$	$\vdots$
		$t-1$	$\overline{V}-\underline{C}-\epsilon$	$\overline{V}-\underline{C}-\epsilon$	$\cdots$	$\overline{V}-\underline{C}-\epsilon$	0	0	$\cdots$	0	0	0	$\cdots$	0	0	0	$\cdots$	0	0	0	$\cdots$	0	0	0	$\cdots$	0	1	1	$\cdots$	1	0	0	$\cdots$	0	0	$\cdots$	0	0	0	$\cdots$	0
	(A9)	t	$\overline{C}-\underline{C}$	$\overline{C}-\underline{C}$	$\cdots$	$\overline{C}-\underline{C}$	$\overline{C}-\underline{C}$	$\overline{C}-\underline{C}$	$\cdots$	$\overline{C}-\underline{C}$	0	0	$\cdots$	0	0	0	$\cdots$	0	0	0	$\cdots$	0	0	0	$\cdots$	0	1	1	$\cdots$	1	1	1	$\cdots$	1	0	$\cdots$	0	0	0	$\cdots$	0
	(A10)	$t+1$	0	0	$\cdots$	0	$\overline{V}-\underline{C}$	$\overline{V}-\underline{C}-\epsilon$	$\cdots$	0	0	0	$\cdots$	0	0	0	$\cdots$	0	0	0	$\cdots$	0	0	0	$\cdots$	0	0	0	$\cdots$	0	1	1	$\cdots$	0	0	$\cdots$	0	1	0	$\cdots$	0
		$\vdots$	$\vdots$	$\vdots$	$\ddots$	$\vdots$	$\vdots$	$\vdots$	$\ddots$	$\vdots$	$\vdots$	$\vdots$	$\ddots$	$\vdots$	$\vdots$	$\vdots$	$\ddots$	$\vdots$	$\vdots$	$\vdots$	$\ddots$	$\vdots$	$\vdots$	$\vdots$	$\ddots$	$\vdots$	$\vdots$	$\vdots$	$\ddots$	$\vdots$	$\vdots$	$\vdots$	$\ddots$	$\vdots$	$\vdots$	$\ddots$	$\vdots$	$\vdots$	$\vdots$	$\ddots$	$\vdots$
		T	0	0	$\cdots$	0	$\overline{V}-\underline{C}$	$\overline{V}-\underline{C}-\epsilon$	$\cdots$	$\overline{V}-\underline{C}-\epsilon$	0	0	$\cdots$	0	0	0	$\cdots$	0	0	0	$\cdots$	0	0	0	$\cdots$	0	0	0	$\cdots$	0	1	1	$\cdots$	1	0	$\cdots$	0	1	0	$\cdots$	0
$\hat{\boldsymbol{\theta}}^{\alpha}$	(A11)	2	0	$\overline{V}-\underline{C}$	$\cdots$	0	0	0	$\cdots$	0	0	0	$\cdots$	0	0	0	$\cdots$	0	0	0	$\cdots$	0	0	0	$\cdots$	0	0	1	$\cdots$	0	0	0	$\cdots$	0	1	$\cdots$	0	0	0	$\cdots$	0
		$\vdots$	$\vdots$	$\vdots$	$\ddots$	$\vdots$	$\vdots$	$\vdots$	$\ddots$	$\vdots$	$\vdots$	$\vdots$	$\ddots$	$\vdots$	$\vdots$	$\vdots$	$\ddots$	$\vdots$	$\vdots$	$\vdots$	$\ddots$	$\vdots$	$\vdots$	$\vdots$	$\ddots$	$\vdots$	$\vdots$	$\vdots$	$\ddots$	$\vdots$	$\vdots$	$\vdots$	$\ddots$	$\vdots$	$\vdots$	$\ddots$	$\vdots$	$\vdots$	$\vdots$	$\ddots$	$\vdots$
		T	0	0	$\cdots$	0	0	0	$\cdots$	$\overline{V}-\underline{C}$	0	0	$\cdots$	0	0	0	$\cdots$	0	0	0	$\cdots$	0	0	0	$\cdots$	0	0	0	$\cdots$	0	0	0	$\cdots$	1	0	$\cdots$	0	0	0	$\cdots$	1

Table C.5. Lower Triangular Matrix Obtained From Table C.4 via Gaussian Elimination

Point	Group	Index α	$\mathbf{p}$								$\mathbf{r}^+$								$\mathbf{r}^-$								$\mathbf{y}$								$\mathbf{u}$							
			1	2	$\cdots$	$t-1$	t	$t+1$	$\cdots$	T	1	2	$\cdots$	$t-1$	t	$t+1$	$\cdots$	T	1	2	$\cdots$	$t-1$	t	$t+1$	$\cdots$	T	1	2	$\cdots$	$t-1$	t	$t+1$	$\cdots$	T	2	$\cdots$	$t-1$	t	$t+1$	$\cdots$	T
$\underline{\grave{\boldsymbol{\theta}}}^{\alpha}$	(B1)	1	ϵ	0	$\cdots$	0	0	0	$\cdots$	0	0	0	$\cdots$	0	0	0	$\cdots$	0	0	0	$\cdots$	0	0	0	$\cdots$	0	0	0	$\cdots$	0	0	0	$\cdots$	0	0	$\cdots$	0	0	0	$\cdots$	0
		2	ϵ	ϵ	$\cdots$	0	0	0	$\cdots$	0	0	0	$\cdots$	0	0	0	$\cdots$	0	0	0	$\cdots$	0	0	0	$\cdots$	0	0	0	$\cdots$	0	0	0	$\cdots$	0	0	$\cdots$	0	0	0	$\cdots$	0
		$\vdots$	$\vdots$	$\vdots$	$\ddots$	$\vdots$	$\vdots$	$\vdots$	$\ddots$	$\vdots$	$\vdots$	$\vdots$	$\ddots$	$\vdots$	$\vdots$	$\vdots$	$\ddots$	$\vdots$	$\vdots$	$\vdots$	$\ddots$	$\vdots$	$\vdots$	$\vdots$	$\ddots$	$\vdots$	$\vdots$	$\vdots$	$\ddots$	$\vdots$	$\vdots$	$\vdots$	$\ddots$	$\vdots$	$\vdots$	$\ddots$	$\vdots$	$\vdots$	$\vdots$	$\ddots$	$\vdots$
		$t-1$	ϵ	ϵ	$\cdots$	ϵ	0	0	$\cdots$	0	0	0	$\cdots$	0	0	0	$\cdots$	0	0	0	$\cdots$	0	0	0	$\cdots$	0	0	0	$\cdots$	0	0	0	$\cdots$	0	0	$\cdots$	0	0	0	$\cdots$	0
		$t+1$	0	0	$\cdots$	0	0	ϵ	$\cdots$	0	0	0	$\cdots$	0	0	0	$\cdots$	0	0	0	$\cdots$	0	0	0	$\cdots$	0	0	0	$\cdots$	0	0	0	$\cdots$	0	0	$\cdots$	0	0	0	$\cdots$	0
		$\vdots$	$\vdots$	$\vdots$	$\ddots$	$\vdots$	$\vdots$	$\vdots$	$\ddots$	$\vdots$	$\vdots$	$\vdots$	$\ddots$	$\vdots$	$\vdots$	$\vdots$	$\ddots$	$\vdots$	$\vdots$	$\vdots$	$\ddots$	$\vdots$	$\vdots$	$\vdots$	$\ddots$	$\vdots$	$\vdots$	$\vdots$	$\ddots$	$\vdots$	$\vdots$	$\vdots$	$\ddots$	$\vdots$	$\vdots$	$\ddots$	$\vdots$	$\vdots$	$\vdots$	$\ddots$	$\vdots$
		T	0	0	$\cdots$	0	0	ϵ	$\cdots$	ϵ	0	0	$\cdots$	0	0	0	$\cdots$	0	0	0	$\cdots$	0	0	0	$\cdots$	0	0	0	$\cdots$	0	0	0	$\cdots$	0	0	$\cdots$	0	0	0	$\cdots$	0
$\underline{\grave{\boldsymbol{\theta}}}^{\alpha}$	(B2)	1	0	0	$\cdots$	0	0	0	$\cdots$	0	ϵ	0	$\cdots$	0	0	0	$\cdots$	0	0	0	$\cdots$	0	0	0	$\cdots$	0	0	0	$\cdots$	0	0	0	$\cdots$	0	0	$\cdots$	0	0	0	$\cdots$	0
		2	0	0	$\cdots$	0	0	0	$\cdots$	0	0	ϵ	$\cdots$	0	0	0	$\cdots$	0	0	0	$\cdots$	0	0	0	$\cdots$	0	0	0	$\cdots$	0	0	0	$\cdots$	0	0	$\cdots$	0	0	0	$\cdots$	0
		$\vdots$	$\vdots$	$\vdots$	$\ddots$	$\vdots$	$\vdots$	$\vdots$	$\ddots$	$\vdots$	$\vdots$	$\vdots$	$\ddots$	$\vdots$	$\vdots$	$\vdots$	$\ddots$	$\vdots$	$\vdots$	$\vdots$	$\ddots$	$\vdots$	$\vdots$	$\vdots$	$\ddots$	$\vdots$	$\vdots$	$\vdots$	$\ddots$	$\vdots$	$\vdots$	$\vdots$	$\ddots$	$\vdots$	$\vdots$	$\ddots$	$\vdots$	$\vdots$	$\vdots$	$\ddots$	$\vdots$
		$t-1$	0	0	$\cdots$	0	0	0	$\cdots$	0	0	0	$\cdots$	ϵ	0	0	$\cdots$	0	0	0	$\cdots$	0	0	0	$\cdots$	0	0	0	$\cdots$	0	0	0	$\cdots$	0	0	$\cdots$	0	0	0	$\cdots$	0
		t	0	0	$\cdots$	0	$-\epsilon$	0	$\cdots$	0	0	0	$\cdots$	0	ϵ	0	$\cdots$	0	0	0	$\cdots$	0	0	0	$\cdots$	0	0	0	$\cdots$	0	0	0	$\cdots$	0	0	$\cdots$	0	0	0	$\cdots$	0
		$t+1$	0	0	$\cdots$	0	0	0	$\cdots$	0	0	0	$\cdots$	0	0	ϵ	$\cdots$	0	0	0	$\cdots$	0	0	0	$\cdots$	0	0	0	$\cdots$	0	0	0	$\cdots$	0	0	$\cdots$	0	0	0	$\cdots$	0
		$\vdots$	$\vdots$	$\vdots$	$\ddots$	$\vdots$	$\vdots$	$\vdots$	$\ddots$	$\vdots$	$\vdots$	$\vdots$	$\ddots$	$\vdots$	$\vdots$	$\vdots$	$\ddots$	$\vdots$	$\vdots$	$\vdots$	$\ddots$	$\vdots$	$\vdots$	$\vdots$	$\ddots$	$\vdots$	$\vdots$	$\vdots$	$\ddots$	$\vdots$	$\vdots$	$\vdots$	$\ddots$	$\vdots$	$\vdots$	$\ddots$	$\vdots$	$\vdots$	$\vdots$	$\ddots$	$\vdots$
		T	0	0	$\cdots$	0	0	0	$\cdots$	0	0	0	$\cdots$	0	0	0	$\cdots$	ϵ	0	0	$\cdots$	0	0	0	$\cdots$	0	0	0	$\cdots$	0	0	0	$\cdots$	0	0	$\cdots$	0	0	0	$\cdots$	0
$\underline{\hat{\boldsymbol{\theta}}}^{\alpha}$	(B3)	1	0	0	$\cdots$	0	0	0	$\cdots$	0	0	0	$\cdots$	0	0	0	$\cdots$	0	ϵ	0	$\cdots$	0	0	0	$\cdots$	0	0	0	$\cdots$	0	0	0	$\cdots$	0	0	$\cdots$	0	0	0	$\cdots$	0
		2	0	0	$\cdots$	0	0	0	$\cdots$	0	0	0	$\cdots$	0	0	0	$\cdots$	0	0	ϵ	$\cdots$	0	0	0	$\cdots$	0	0	0	$\cdots$	0	0	0	$\cdots$	0	0	$\cdots$	0	0	0	$\cdots$	0
		$\vdots$	$\vdots$	$\vdots$	$\ddots$	$\vdots$	$\vdots$	$\vdots$	$\ddots$	$\vdots$	$\vdots$	$\vdots$	$\ddots$	$\vdots$	$\vdots$	$\vdots$	$\ddots$	$\vdots$	$\vdots$	$\vdots$	$\ddots$	$\vdots$	$\vdots$	$\vdots$	$\ddots$	$\vdots$	$\vdots$	$\vdots$	$\ddots$	$\vdots$	$\vdots$	$\vdots$	$\ddots$	$\vdots$	$\vdots$	$\ddots$	$\vdots$	$\vdots$	$\vdots$	$\ddots$	$\vdots$
		$t-1$	0	0	$\cdots$	0	0	0	$\cdots$	0	0	0	$\cdots$	0	0	0	$\cdots$	0	0	0	$\cdots$	ϵ	0	0	$\cdots$	0	0	0	$\cdots$	0	0	0	$\cdots$	0	0	$\cdots$	0	0	0	$\cdots$	0
		t	0	0	$\cdots$	0	0	0	$\cdots$	0	0	0	$\cdots$	0	0	0	$\cdots$	0	0	0	$\cdots$	0	ϵ	0	$\cdots$	0	0	0	$\cdots$	0	0	0	$\cdots$	0	0	$\cdots$	0	0	0	$\cdots$	0
		$t+1$	0	0	$\cdots$	0	0	0	$\cdots$	0	0	0	$\cdots$	0	0	0	$\cdots$	0	0	0	$\cdots$	0	0	ϵ	$\cdots$	0	0	0	$\cdots$	0	0	0	$\cdots$	0	0	$\cdots$	0	0	0	$\cdots$	0
		$\vdots$	$\vdots$	$\vdots$	$\ddots$	$\vdots$	$\vdots$	$\vdots$	$\ddots$	$\vdots$	$\vdots$	$\vdots$	$\ddots$	$\vdots$	$\vdots$	$\vdots$	$\ddots$	$\vdots$	$\vdots$	$\vdots$	$\ddots$	$\vdots$	$\vdots$	$\vdots$	$\ddots$	$\vdots$	$\vdots$	$\vdots$	$\ddots$	$\vdots$	$\vdots$	$\vdots$	$\ddots$	$\vdots$	$\vdots$	$\ddots$	$\vdots$	$\vdots$	$\vdots$	$\ddots$	$\vdots$
		T	0	0	$\cdots$	0	0	0	$\cdots$	0	0	0	$\cdots$	0	0	0	$\cdots$	0	0	0	$\cdots$	0	0	0	$\cdots$	ϵ	0	0	$\cdots$	0	0	0	$\cdots$	0	0	$\cdots$	0	0	0	$\cdots$	0
$\underline{\bar{\boldsymbol{\theta}}}^{\alpha}$	(B4)	1	$\overline{V}-\underline{C}-\epsilon$	0	$\cdots$	0	0	0	$\cdots$	0	0	0	$\cdots$	0	0	0	$\cdots$	0	0	0	$\cdots$	0	0	0	$\cdots$	0	1	0	$\cdots$	0	0	0	$\cdots$	0	0	$\cdots$	0	0	0	$\cdots$	0
		2	$\overline{V}-\underline{C}-\epsilon$	$\overline{V}-\underline{C}-\epsilon$	$\cdots$	0	0	0	$\cdots$	0	0	0	$\cdots$	0	0	0	$\cdots$	0	0	0	$\cdots$	0	0	0	$\cdots$	0	1	1	$\cdots$	0	0	0	$\cdots$	0	0	$\cdots$	0	0	0	$\cdots$	0
		$\vdots$	$\vdots$	$\vdots$	$\ddots$	$\vdots$	$\vdots$	$\vdots$	$\ddots$	$\vdots$	$\vdots$	$\vdots$	$\ddots$	$\vdots$	$\vdots$	$\vdots$	$\ddots$	$\vdots$	$\vdots$	$\vdots$	$\ddots$	$\vdots$	$\vdots$	$\vdots$	$\ddots$	$\vdots$	$\vdots$	$\vdots$	$\ddots$	$\vdots$	$\vdots$	$\vdots$	$\ddots$	$\vdots$	$\vdots$	$\ddots$	$\vdots$	$\vdots$	$\vdots$	$\ddots$	$\vdots$
		$t-1$	$\overline{V}-\underline{C}-\epsilon$	$\overline{V}-\underline{C}-\epsilon$	$\cdots$	$\overline{V}-\underline{C}-\epsilon$	0	0	$\cdots$	0	0	0	$\cdots$	0	0	0	$\cdots$	0	0	0	$\cdots$	0	0	0	$\cdots$	0	1	1	$\cdots$	1	0	0	$\cdots$	0	0	$\cdots$	0	0	0	$\cdots$	0
		t	$\overline{C}-\overline{V}+\epsilon$	$\overline{C}-\overline{V}+\epsilon$	$\cdots$	$\overline{C}-\overline{V}+\epsilon$	$\overline{C}-\underline{C}$	$\overline{C}-\overline{V}+\epsilon$	$\cdots$	$\overline{C}-\overline{V}+\epsilon$	0	0	$\cdots$	0	0	0	$\cdots$	0	0	0	$\cdots$	0	0	0	$\cdots$	0	0	0	$\cdots$	0	1	0	$\cdots$	0	0	$\cdots$	0	0	0	$\cdots$	0
		$t+1$	0	0	$\cdots$	0	0	$\overline{V}-\underline{C}-\epsilon$	$\cdots$	0	0	0	$\cdots$	0	0	0	$\cdots$	0	0	0	$\cdots$	0	0	0	$\cdots$	0	0	0	$\cdots$	0	0	1	$\cdots$	0	0	$\cdots$	0	0	0	$\cdots$	0
		$\vdots$	$\vdots$	$\vdots$	$\ddots$	$\vdots$	$\vdots$	$\vdots$	$\ddots$	$\vdots$	$\vdots$	$\vdots$	$\ddots$	$\vdots$	$\vdots$	$\vdots$	$\ddots$	$\vdots$	$\vdots$	$\vdots$	$\ddots$	$\vdots$	$\vdots$	$\vdots$	$\ddots$	$\vdots$	$\vdots$	$\vdots$	$\ddots$	$\vdots$	$\vdots$	$\vdots$	$\ddots$	$\vdots$	$\vdots$	$\ddots$	$\vdots$	$\vdots$	$\vdots$	$\ddots$	$\vdots$
		T	0	0	$\cdots$	0	0	$\overline{V}-\underline{C}-\epsilon$	$\cdots$	$\overline{V}-\underline{C}-\epsilon$	0	0	$\cdots$	0	0	0	$\cdots$	0	0	0	$\cdots$	0	0	0	$\cdots$	0	0	0	$\cdots$	0	0	1	$\cdots$	1	0	$\cdots$	0	0	0	$\cdots$	0
$\underline{\hat{\boldsymbol{\theta}}}^{\alpha}$	(B5)	2	0	$\overline{V}-\underline{C}$	$\cdots$	0	0	0	$\cdots$	0	0	0	$\cdots$	0	0	0	$\cdots$	0	0	0	$\cdots$	0	0	0	$\cdots$	0	0	1	$\cdots$	0	0	0	$\cdots$	0	1	$\cdots$	0	0	0	$\cdots$	0
		$\vdots$	$\vdots$	$\vdots$	$\ddots$	$\vdots$	$\vdots$	$\vdots$	$\ddots$	$\vdots$	$\vdots$	$\vdots$	$\ddots$	$\vdots$	$\vdots$	$\vdots$	$\ddots$	$\vdots$	$\vdots$	$\vdots$	$\ddots$	$\vdots$	$\vdots$	$\vdots$	$\ddots$	$\vdots$	$\vdots$	$\vdots$	$\ddots$	$\vdots$	$\vdots$	$\vdots$	$\ddots$	$\vdots$	$\vdots$	$\ddots$	$\vdots$	$\vdots$	$\vdots$	$\ddots$	$\vdots$
		T	0	0	$\cdots$	0	0	0	$\cdots$	$\overline{V}-\underline{C}$	0	0	$\cdots$	0	0	0	$\cdots$	0	0	0	$\cdots$	0	0	0	$\cdots$	0	0	0	$\cdots$	0	0	0	$\cdots$	1	0	$\cdots$	0	0	0	$\cdots$	1

Next, we consider $k = L = 2$ and $\overline{V} + V \leq \overline{C} \leq \overline{V} + 2V$. We let $\grave{\boldsymbol{\theta}} = (\grave{\mathbf{p}}, \grave{\mathbf{r}}^+, \grave{\mathbf{r}}^-, \grave{\mathbf{y}}, \grave{\mathbf{u}})$ and denote the sth component of $\grave{\mathbf{p}}$, $\grave{\mathbf{r}}^+$, $\grave{\mathbf{r}}^-$, $\grave{\mathbf{y}}$, and $\grave{\mathbf{u}}$ by $\grave{p}_s$, $\grave{r}_s^+$, $\grave{r}_s^-$, $\grave{y}_s$, and $\grave{u}_s$. Similarly, we define $\acute{\boldsymbol{\theta}}$, $\hat{\boldsymbol{\theta}}$, $\overline{\boldsymbol{\theta}}$, and $\dot{\boldsymbol{\theta}}$. We denote the $5T-2$ nonzero linearly independent points by $\grave{\boldsymbol{\theta}}^\alpha$ for $\alpha \in \mathcal{T} \setminus \{t\}$, $\acute{\boldsymbol{\theta}}^\alpha$ for $\alpha \in \mathcal{T}$, $\hat{\boldsymbol{\theta}}^\alpha$ for $\alpha \in \mathcal{T}$, $\overline{\boldsymbol{\theta}}^\alpha$ for $\alpha \in \mathcal{T}$, and $\dot{\boldsymbol{\theta}}^\alpha$ for $\alpha \in \mathcal{T} \setminus \{1\}$. We let $\epsilon = \min\left\{\underline{C} + V - \overline{V},\ \overline{V} - \underline{C}\right\} > 0$ and create the $5T-2$ points as follows.

For each $\alpha \in \mathcal{T} \setminus \{t,\ t+1\}$, we create the same point $\grave{\boldsymbol{\theta}}^\alpha$ as in groups (A1) and (A2). For each $\alpha \in \mathcal{T} \setminus \{t\}$, we create the same point $\acute{\boldsymbol{\theta}}^\alpha$ as in groups (A3) and (A5), For each $\alpha \in \mathcal{T} \setminus \{t\}$, we create the same point $\hat{\boldsymbol{\theta}}^\alpha$ as in groups (A6) and (A7), For each $\alpha \in \mathcal{T} \setminus \{t,\ t+1\}$, we create the same point $\overline{\boldsymbol{\theta}}^\alpha$ as in groups (A8) and (A10). We further create the following points.

(N1) For $\alpha = t+1$, we create a point $\grave{\boldsymbol{\theta}}^\alpha$ as follows:

$$\grave{p}_s^\alpha = \begin{cases} \overline{V} - \underline{C}, & s = t \\ \overline{V} - \underline{C} - \epsilon, & s = t+1 \\ 0, & o.w. \end{cases}, \ \grave{y}_s^\alpha = \begin{cases} 1, & s \in [t, t+1]_{\mathbb{Z}} \\ 0, & \text{o.w.} \end{cases}, \ \grave{u}_s^\alpha = \begin{cases} 1, & s = t \\ 0, & \text{o.w.} \end{cases},$$

and $\grave{r}_s^{+,\alpha} = \grave{r}_s^{-,\alpha} = 0$ for any $s \in \mathcal{T}$. It is easy to verify that $\grave{\boldsymbol{\theta}}^\alpha$ satisfies (4.35a)–(4.35h). Thus, $\grave{\boldsymbol{\theta}}^\alpha \in \text{conv}(\mathcal{D})$. It is also easy to verify that $\grave{\boldsymbol{\theta}}^\alpha$ satisfies (4.37) at equality.

(N2) For $\alpha = t$, we create a point $\acute{\boldsymbol{\theta}}^\alpha$ as follows:

$$\acute{p}_s^\alpha = \begin{cases} \overline{V} - \underline{C} - \epsilon, & s \in [t, \min\{t+1, T\}]_{\mathbb{Z}} \\ 0, & \text{o.w.} \end{cases}, \ \acute{r}_s^{+,\alpha} = \begin{cases} \epsilon, & s = t \\ 0, & \text{o.w.} \end{cases},$$

$$\acute{y}_s^\alpha = \begin{cases} 1, & s \in [t, \min\{t+1, T\}]_{\mathbb{Z}} \\ 0, & \text{o.w.} \end{cases},$$

$\acute{r}_s^{-,\alpha} = 0$ for any $s \in \mathcal{T}$, and $\acute{u}_s^\alpha = 1$ for $s = t$ and $\acute{u}_s^\alpha = 0$ otherwise. It is easy to verify that $\acute{\boldsymbol{\theta}}^\alpha$ satisfies (4.35a)–(4.35h). Thus, $\acute{\boldsymbol{\theta}}^\alpha \in \text{conv}(\mathcal{D})$. It is also easy to verify that $\acute{\boldsymbol{\theta}}^\alpha$ satisfies (4.37).

(N3) For $\alpha = t$, we create a point $\hat{\boldsymbol{\theta}}^\alpha$ as follows:

$$\hat{p}_s^\alpha = \begin{cases} \overline{V} - \underline{C}, & s = t \\ \overline{V} - \underline{C} - \epsilon, & s = t+1,\ t < T \\ 0, & \text{o.w.} \end{cases},\ \hat{r}_s^{-,\alpha} = \begin{cases} \epsilon, & s = \alpha \\ 0, & \text{o.w.} \end{cases},\ \hat{y}_s^\alpha = \begin{cases} 1, & s \in [t, \min\{t+1, T\}]_{\mathbb{Z}} \\ 0, & \text{o.w.} \end{cases},$$

$\hat{r}_s^{+,\alpha} = 0$ for any $s \in \mathcal{T}$, and $\hat{u}_s^\alpha = 1$ for $s = t$ and $\hat{u}_s^\alpha = 0$ otherwise. It is clear that $\hat{\boldsymbol{\theta}}^t$ satisfies (4.35a)–(4.35h). Thus, $\hat{\boldsymbol{\theta}}^t \in \mathrm{conv}(\mathcal{D})$. It is also easy to verify that $\hat{\boldsymbol{\theta}}^t$ satisfies (4.37) at equality.

(N4) For $\alpha = t$, we create a point $\overline{\boldsymbol{\theta}}^\alpha$ as follows:

$$\overline{p}_s^\alpha = \begin{cases} \overline{C} - \underline{C} - V, & s \in [1, t-1]_{\mathbb{Z}} \\ \overline{V} - \underline{C}, & s = t \\ 0, & \text{o.w.} \end{cases},\ \overline{r}_s^{+,\alpha} = \begin{cases} \overline{C} - \overline{V}, & s = t \\ 0, & \text{o.w.} \end{cases},\ \overline{y}_s^\alpha = \begin{cases} 1, & s \in [1, t]_{\mathbb{Z}} \\ 0, & \text{o.w.} \end{cases},$$

$\overline{r}_s^{-,\alpha} = 0$ for any $s \in \mathcal{T}$, and $\overline{u}_s^\alpha = 0$ for any $s \in \mathcal{T} \setminus \{1\}$. It is easy to verify that $\overline{\boldsymbol{\theta}}^\alpha$ satisfies (4.35a)–(4.35f). Note that $(\overline{C} - \underline{C} - V) - (\overline{V} - \underline{C}) = \overline{C} - V - \overline{V} \leq (\overline{V} + 2V) - V - \overline{V} = V$, where the first inequality holds by the assumption. Thus, $\overline{\boldsymbol{\theta}}^\alpha$ satisfies (4.35g). Note also that $\overline{C} - \underline{C} - V \geq (\overline{V} + V) - \underline{C} - V = \overline{V} - \underline{C} > 0$, where the first inequality holds by the assumption. Thus, $\overline{\boldsymbol{\theta}}^\alpha$ satisfies (4.35h) and $\overline{\boldsymbol{\theta}}^\alpha \in \mathrm{conv}(\mathcal{D})$. It is also easy to verify that $\overline{\boldsymbol{\theta}}^\alpha$ satisfies (4.37) at equality.

(N5) For $\alpha = t+1$, we create a point $\overline{\boldsymbol{\theta}}^\alpha$ such that $\overline{p}_s^\alpha = \overline{C} - \underline{C}$, $\overline{r}_s^{+,\alpha} = \overline{r}_s^{-,\alpha} = 0$, and $\overline{y}_s^\alpha = 1$ for any $s \in \mathcal{T}$, and $\overline{u}_s^\alpha = 0$ for any $s \in \mathcal{T} \setminus \{1\}$. It is easy to verify that $\overline{\boldsymbol{\theta}}^\alpha$ satisfies (4.35a)–(4.35h). Thus, $\overline{\boldsymbol{\theta}}^\alpha \in \mathrm{conv}(\mathcal{D})$. It is also easy to verify that $\overline{\boldsymbol{\theta}}^\alpha$ satisfies (4.37) at equality.

(N6) For each $\alpha \in [2, t-2]_{\mathbb{Z}}$, we create a point $\dot{\boldsymbol{\theta}}^\alpha$ as follows:

$$\dot{p}_s^\alpha = \begin{cases} \overline{V} - \underline{C}, & s \in [\alpha, \alpha+1]_{\mathbb{Z}}, \\ 0, & \text{o.w.} \end{cases},\ \dot{y}_s^\alpha = \begin{cases} 1, & s \in [\alpha, \alpha+1]_{\mathbb{Z}}, \\ 0, & \text{o.w.} \end{cases},\ \dot{u}_s^{+,\alpha} = \begin{cases} 1, & s = \alpha \\ 0, & \text{o.w.} \end{cases},$$

and $\overline{r}_s^{+,\alpha} = \overline{r}_s^{-,\alpha} = 0$ for any $s \in \mathcal{T}$. It is easy to verify that $\dot{\boldsymbol{\theta}}^\alpha$ satisfies (4.35a)–

(4.35h). Thus, $\dot{\boldsymbol{\theta}}^{\alpha} \in \mathrm{conv}(\mathcal{D})$. It is also easy to verify that $\dot{\boldsymbol{\theta}}^{\alpha}$ satisfies (4.37) at equality.

(N7) For each $\alpha = t-1$, we create a point $\dot{\boldsymbol{\theta}}^{\alpha}$ as follows:

$$\dot{p}_s^{\alpha} = \begin{cases} \overline{V} - \underline{C}, & s \in [t-1, \min\{t+1, T\}]_{\mathbb{Z}} \setminus \{t\}, \\ \overline{V} - \underline{C} + V, & s = t, \\ 0, & \text{o.w.} \end{cases}, \quad \dot{y}_s^{\alpha} = \begin{cases} 1, & s \in [t-1, \min\{t+1, T\}]_{\mathbb{Z}}, \\ 0, & \text{o.w.} \end{cases},$$

$\dot{r}_s^{+,\alpha} = \dot{r}_s^{-,\alpha} = 0$ for any $s \in \mathcal{T}$, $\dot{u}_s^{+,\alpha} = 1$ for $s = t-1$ and $\dot{u}_s^{+,\alpha} = 0$ otherwise. Note that $\overline{V} - \underline{C} + V \leq \overline{C} - \underline{C}$. Thus, $\dot{\boldsymbol{\theta}}^{\alpha}$ satisfies (4.35a)–(4.35h) and $\dot{\boldsymbol{\theta}}^{\alpha} \in \mathrm{conv}(\mathcal{D})$. It is also easy to verify that $\dot{\boldsymbol{\theta}}^{\alpha}$ satisfies (4.37) at equality.

(N8) For each $\alpha \in [t, T]_{\mathbb{Z}}$, we create a point $\dot{\boldsymbol{\theta}}^{\alpha}$ as follows:

$$\dot{p}_s^{\alpha} = \begin{cases} \overline{V} - \underline{C}, & s \in [\alpha, \min\{\alpha+1, T\}]_{\mathbb{Z}}, \\ 0, & \text{o.w.} \end{cases}, \quad \dot{y}_s^{\alpha} = \begin{cases} 1, & s \in [\alpha, \min\{\alpha+1, T\}]_{\mathbb{Z}}, \\ 0, & \text{o.w.} \end{cases},$$

$\dot{r}_s^{+,\alpha} = \dot{r}_s^{-,\alpha} = 0$ for any $s \in \mathcal{T}$, and $\dot{u}_s^{+,\alpha} = 1$ for $s = \alpha$ and $\dot{u}_s^{+,\alpha} = 0$ otherwise. It is clear that $\dot{\boldsymbol{\theta}}^{\alpha}$ satisfies (4.35a)–(4.35h). Thus, $\dot{\boldsymbol{\theta}}^{\alpha} \in \mathrm{conv}(\mathcal{D})$. It is also cleare that $\dot{\boldsymbol{\theta}}^{\alpha}$ satisfies (4.37) at equality.

Table C.6 shows a matrix with $5T-2$ rows, where each row represents a point created by above. This matrix can be transformed into the matrix in Table C.7 via the following Gaussian elimination process:

(i) For each $\alpha \in [1, T]_{\mathbb{Z}} \setminus \{t\}$, the point with index α in group (B1), denoted by $\underline{\grave{\boldsymbol{\theta}}}^{\alpha}$, is obtained by setting $\underline{\grave{\boldsymbol{\theta}}}^{\alpha} = \grave{\boldsymbol{\theta}}^{\alpha} - \overline{\boldsymbol{\theta}}^{\alpha}$ for any $\alpha \in \mathcal{T} \setminus \{t,\ t+1\}$, $\underline{\grave{\boldsymbol{\theta}}}^{t+1} = \grave{\boldsymbol{\theta}}^{t+1} - \dot{\boldsymbol{\theta}}^{t}$ when $t < T$. Here $\grave{\boldsymbol{\theta}}^{\alpha}$ with $\alpha \in [1, T]_{\mathbb{Z}} \setminus \{t,\ t+1\}$ is the point with index α in groups (A1) and (A2), $\grave{\boldsymbol{\theta}}^{t+1}$ with $t < T$ is the point in group (N1), $\overline{\boldsymbol{\theta}}^{\alpha}$ with $\alpha \in [1, t-1]_{\mathbb{Z}}$ is the point with index α in group (A8), $\overline{\boldsymbol{\theta}}^{\alpha}$ with $\alpha \in [t+2, T]_{\mathbb{Z}}$ and $t \leq T-2$ is the point in group (A10), and $\dot{\boldsymbol{\theta}}^{t}$ is the point in group (N8).

(ii) For each $\alpha \in [1, T]_{\mathbb{Z}}$, the point with index α in group (B2), denoted by $\underline{\acute{\boldsymbol{\theta}}}^{\alpha}$, is obtained by setting $\underline{\acute{\boldsymbol{\theta}}}^{\alpha} = \acute{\boldsymbol{\theta}}^{\alpha} - \overline{\boldsymbol{\theta}}^{\alpha}$ for any $\alpha \in [1, T]_{\mathbb{Z}} \setminus \{t,\ t+1\}$, $\underline{\acute{\boldsymbol{\theta}}}^{\alpha} = \acute{\boldsymbol{\theta}}^{\alpha} - \dot{\boldsymbol{\theta}}^{t}$ for any $\alpha \in [t, \min\{t+1, T\}]_{\mathbb{Z}}$. Here $\acute{\boldsymbol{\theta}}^{\alpha}$ with $\alpha \in [1, T]_{\mathbb{Z}} \setminus \{t\}$ is the point with index

α in group (A3) and (A5), $\acute{\boldsymbol{\theta}}^t$ is the point in group (N2), $\overline{\boldsymbol{\theta}}^\alpha$ with $\alpha \in [1, t-1]_{\mathbb{Z}}$ is the point with index α in group (A8), $\overline{\boldsymbol{\theta}}^\alpha$ with $\alpha \in [t+2, T]_{\mathbb{Z}}$ and $t \leq T-2$ is the point in group (A10), and $\dot{\boldsymbol{\theta}}^t$ is the point in group (N8).

Table C.6. Matrix with The Rows Representing $5T-2$ Points in $\mathrm{conv}(\mathcal{D})$ That Satisfy Inequality (4.37) at Equality When $L=2$

Point	Group	Index α	$\mathbf{p}$								$\mathbf{r}^+$								$\mathbf{r}^-$								$\mathbf{y}$								$\mathbf{u}$							
			1	2	$\cdots$	$t-1$	t	$t+1$	$\cdots$	T	1	2	$\cdots$	$t-1$	t	$t+1$	$\cdots$	T	1	2	$\cdots$	$t-1$	t	$t+1$	$\cdots$	T	1	2	$\cdots$	$t-1$	t	$t+1$	$t+2$	$\cdots$	T	2	$\cdots$	$t-1$	t	$t+1$	$\cdots$	T
$\grave{\boldsymbol{\theta}}^{\alpha}$		1	$\overline{V}-\underline{C}$	0	$\cdots$	0	0	0	$\cdots$	0	0	0	$\cdots$	0	0	0	$\cdots$	0	0	0	$\cdots$	0	0	0	$\cdots$	0	1	0	$\cdots$	0	0	0	0	$\cdots$	0	0	$\cdots$	0	0	0	$\cdots$	0
		2	$\overline{V}-\underline{C}$	$\overline{V}-\underline{C}$	$\cdots$	0	0	0	$\cdots$	0	0	0	$\cdots$	0	0	0	$\cdots$	0	0	0	$\cdots$	0	0	0	$\cdots$	0	1	1	$\cdots$	0	0	0	0	$\cdots$	0	0	$\cdots$	0	0	0	$\cdots$	0
	(A1)	$\vdots$	$\vdots$	$\vdots$	$\ddots$	$\vdots$	$\vdots$	$\vdots$	$\ddots$	$\vdots$	$\vdots$	$\vdots$	$\ddots$	$\vdots$	$\vdots$	$\vdots$	$\ddots$	$\vdots$	$\vdots$	$\vdots$	$\ddots$	$\vdots$	$\vdots$	$\vdots$	$\ddots$	$\vdots$	$\vdots$	$\vdots$	$\ddots$	$\vdots$	$\vdots$	$\vdots$	$\vdots$	$\ddots$	$\vdots$	$\vdots$	$\ddots$	$\vdots$	$\vdots$	$\vdots$	$\ddots$	$\vdots$
		$t-1$	$\overline{V}-\underline{C}$	$\overline{V}-\underline{C}$	$\cdots$	$\overline{V}-\underline{C}$	0	0	$\cdots$	0	0	0	$\cdots$	0	0	0	$\cdots$	0	0	0	$\cdots$	0	0	0	$\cdots$	0	1	1	$\cdots$	1	0	0	0	$\cdots$	0	0	$\cdots$	0	0	0	$\cdots$	0
	(N1)	$t+1$	0	0	$\cdots$	0	$\overline{V}-\underline{C}$	$\overline{V}-\underline{C}-\epsilon$	$\cdots$	0	0	0	$\cdots$	0	0	0	$\cdots$	0	0	0	$\cdots$	0	0	0	$\cdots$	0	0	0	$\cdots$	0	1	1	0	$\cdots$	0	0	$\cdots$	0	1	0	$\cdots$	0
		$t+2$	0	0	$\cdots$	0	$\overline{V}-\underline{C}$	$\overline{V}-\underline{C}$	$\cdots$	0	0	0	$\cdots$	0	0	0	$\cdots$	0	0	0	$\cdots$	0	0	0	$\cdots$	0	0	0	$\cdots$	0	1	1	1	$\cdots$	0	0	$\cdots$	0	1	0	$\cdots$	0
	(A2)	$\vdots$	$\vdots$	$\vdots$	$\ddots$	$\vdots$	$\vdots$	$\vdots$	$\ddots$	$\vdots$	$\vdots$	$\vdots$	$\ddots$	$\vdots$	$\vdots$	$\vdots$	$\ddots$	$\vdots$	$\vdots$	$\vdots$	$\ddots$	$\vdots$	$\vdots$	$\vdots$	$\ddots$	$\vdots$	$\vdots$	$\vdots$	$\ddots$	$\vdots$	$\vdots$	$\vdots$	$\vdots$	$\ddots$	$\vdots$	$\vdots$	$\ddots$	$\vdots$	$\vdots$	$\vdots$	$\ddots$	$\vdots$
		T	0	0	$\cdots$	0	$\overline{V}-\underline{C}$	$\overline{V}-\underline{C}$	$\cdots$	$\overline{V}-\underline{C}$	0	0	$\cdots$	0	0	0	$\cdots$	0	0	0	$\cdots$	0	0	0	$\cdots$	0	0	0	$\cdots$	0	1	1	1	$\cdots$	1	0	$\cdots$	0	1	0	$\cdots$	0
$\hat{\boldsymbol{\theta}}^{\alpha}$		1	$\overline{V}-\underline{C}-\epsilon$	0	$\cdots$	0	0	0	$\cdots$	0	ϵ	0	$\cdots$	0	0	0	$\cdots$	0	0	0	$\cdots$	0	0	0	$\cdots$	0	1	0	$\cdots$	0	0	0	0	$\cdots$	0	0	$\cdots$	0	0	0	$\cdots$	0
		2	$\overline{V}-\underline{C}-\epsilon$	$\overline{V}-\underline{C}-\epsilon$	$\cdots$	0	0	0	$\cdots$	0	0	ϵ	$\cdots$	0	0	0	$\cdots$	0	0	0	$\cdots$	0	0	0	$\cdots$	0	1	1	$\cdots$	0	0	0	0	$\cdots$	0	0	$\cdots$	0	0	0	$\cdots$	0
	(A3)	$\vdots$	$\vdots$	$\vdots$	$\ddots$	$\vdots$	$\vdots$	$\vdots$	$\ddots$	$\vdots$	$\vdots$	$\vdots$	$\ddots$	$\vdots$	$\vdots$	$\vdots$	$\ddots$	$\vdots$	$\vdots$	$\vdots$	$\ddots$	$\vdots$	$\vdots$	$\vdots$	$\ddots$	$\vdots$	$\vdots$	$\vdots$	$\ddots$	$\vdots$	$\vdots$	$\vdots$	$\vdots$	$\ddots$	$\vdots$	$\vdots$	$\ddots$	$\vdots$	$\vdots$	$\vdots$	$\ddots$	$\vdots$
		$t-1$	$\overline{V}-\underline{C}-\epsilon$	$\overline{V}-\underline{C}-\epsilon$	$\cdots$	$\overline{V}-\underline{C}-\epsilon$	0	0	$\cdots$	0	0	0	$\cdots$	ϵ	0	0	$\cdots$	0	0	0	$\cdots$	0	0	0	$\cdots$	0	1	0	$\cdots$	1	0	0	0	$\cdots$	0	0	$\cdots$	0	0	0	$\cdots$	0
	(N2)	t	0	0	$\cdots$	0	$\overline{V}-\underline{C}-\epsilon$	$\overline{V}-\underline{C}-\epsilon$	$\cdots$	0	0	0	$\cdots$	0	ϵ	0	$\cdots$	0	0	0	$\cdots$	0	0	0	$\cdots$	0	0	0	$\cdots$	0	1	1	0	$\cdots$	0	0	$\cdots$	0	1	0	$\cdots$	0
		$t+1$	0	0	$\cdots$	0	$\overline{V}-\underline{C}$	$\overline{V}-\underline{C}-\epsilon$	$\cdots$	0	0	0	$\cdots$	0	0	ϵ	$\cdots$	0	0	0	$\cdots$	0	0	0	$\cdots$	0	0	0	$\cdots$	0	1	1	0	$\cdots$	0	0	$\cdots$	0	1	0	$\cdots$	0
	(A5)	$\vdots$	$\vdots$	$\vdots$	$\ddots$	$\vdots$	$\vdots$	$\vdots$	$\ddots$	$\vdots$	$\vdots$	$\vdots$	$\ddots$	$\vdots$	$\vdots$	$\vdots$	$\ddots$	$\vdots$	$\vdots$	$\vdots$	$\ddots$	$\vdots$	$\vdots$	$\vdots$	$\ddots$	$\vdots$	$\vdots$	$\vdots$	$\ddots$	$\vdots$	$\vdots$	$\vdots$	$\vdots$	$\ddots$	$\vdots$	$\vdots$	$\ddots$	$\vdots$	$\vdots$	$\vdots$	$\ddots$	$\vdots$
		T	0	0	$\cdots$	0	$\overline{V}-\underline{C}$	$\overline{V}-\underline{C}-\epsilon$	$\cdots$	$\overline{V}-\underline{C}-\epsilon$	0	0	$\cdots$	0	0	0	$\cdots$	ϵ	0	0	$\cdots$	0	0	0	$\cdots$	0	0	0	$\cdots$	0	1	1	1	$\cdots$	1	0	$\cdots$	0	1	0	$\cdots$	0
$\check{\boldsymbol{\theta}}^{\alpha}$		1	$\overline{V}-\underline{C}-\epsilon$	0	$\cdots$	0	0	0	$\cdots$	0	ϵ	0	$\cdots$	0	0	0	$\cdots$	0	0	0	$\cdots$	0	0	0	$\cdots$	0	1	0	$\cdots$	0	0	0	0	$\cdots$	0	0	$\cdots$	0	0	0	$\cdots$	0
		2	$\overline{V}-\underline{C}-\epsilon$	$\overline{V}-\underline{C}-\epsilon$	$\cdots$	0	0	0	$\cdots$	0	0	ϵ	$\cdots$	0	0	0	$\cdots$	0	0	0	$\cdots$	0	0	0	$\cdots$	0	1	1	$\cdots$	0	0	0	0	$\cdots$	0	0	$\cdots$	0	0	0	$\cdots$	0
	(A6)	$\vdots$	$\vdots$	$\vdots$	$\ddots$	$\vdots$	$\vdots$	$\vdots$	$\ddots$	$\vdots$	$\vdots$	$\vdots$	$\ddots$	$\vdots$	$\vdots$	$\vdots$	$\ddots$	$\vdots$	$\vdots$	$\vdots$	$\ddots$	$\vdots$	$\vdots$	$\vdots$	$\ddots$	$\vdots$	$\vdots$	$\vdots$	$\ddots$	$\vdots$	$\vdots$	$\vdots$	$\vdots$	$\ddots$	$\vdots$	$\vdots$	$\ddots$	$\vdots$	$\vdots$	$\vdots$	$\ddots$	$\vdots$
		$t-1$	$\overline{V}-\underline{C}-\epsilon$	$\overline{V}-\underline{C}-\epsilon$	$\cdots$	$\overline{V}-\underline{C}-\epsilon$	0	0	$\cdots$	0	0	0	$\cdots$	0	0	0	$\cdots$	0	0	0	$\cdots$	ϵ	0	0	$\cdots$	0	1	0	$\cdots$	1	0	0	0	$\cdots$	0	0	$\cdots$	0	0	0	$\cdots$	0
	(N3)	t	0	0	$\cdots$	0	$\overline{V}-\underline{C}$	$\overline{V}-\underline{C}-\epsilon$	$\cdots$	0	0	0	$\cdots$	0	0	0	$\cdots$	0	0	0	$\cdots$	0	ϵ	0	$\cdots$	0	0	0	$\cdots$	0	1	1	0	$\cdots$	0	0	$\cdots$	0	1	0	$\cdots$	0
		$t+1$	0	0	$\cdots$	0	$\overline{V}-\underline{C}$	$\overline{V}-\underline{C}-\epsilon$	$\cdots$	0	0	0	$\cdots$	0	0	0	$\cdots$	0	0	0	$\cdots$	0	0	ϵ	$\cdots$	0	0	0	$\cdots$	0	1	1	0	$\cdots$	0	0	$\cdots$	0	1	0	$\cdots$	0
	(A7)	$\vdots$	$\vdots$	$\vdots$	$\ddots$	$\vdots$	$\vdots$	$\vdots$	$\ddots$	$\vdots$	$\vdots$	$\vdots$	$\ddots$	$\vdots$	$\vdots$	$\vdots$	$\ddots$	$\vdots$	$\vdots$	$\vdots$	$\ddots$	$\vdots$	$\vdots$	$\vdots$	$\ddots$	$\vdots$	$\vdots$	$\vdots$	$\ddots$	$\vdots$	$\vdots$	$\vdots$	$\vdots$	$\ddots$	$\vdots$	$\vdots$	$\ddots$	$\vdots$	$\vdots$	$\vdots$	$\ddots$	$\vdots$
		T	0	0	$\cdots$	0	$\overline{V}-\underline{C}$	$\overline{V}-\underline{C}-\epsilon$	$\cdots$	$\overline{V}-\underline{C}-\epsilon$	0	0	$\cdots$	0	0	0	$\cdots$	0	0	0	$\cdots$	0	0	0	$\cdots$	ϵ	0	0	$\cdots$	0	1	1	1	$\cdots$	1	0	$\cdots$	0	1	0	$\cdots$	0
$\overline{\boldsymbol{\theta}}^{\alpha}$		1	$\overline{V}-\underline{C}-\epsilon$	0	$\cdots$	0	0	0	$\cdots$	0	0	0	$\cdots$	0	0	0	$\cdots$	0	0	0	$\cdots$	0	0	0	$\cdots$	0	1	0	$\cdots$	0	0	0	0	$\cdots$	0	0	$\cdots$	0	0	0	$\cdots$	0
		2	$\overline{V}-\underline{C}-\epsilon$	$\overline{V}-\underline{C}-\epsilon$	$\cdots$	0	0	0	$\cdots$	0	0	0	$\cdots$	0	0	0	$\cdots$	0	0	0	$\cdots$	0	0	0	$\cdots$	0	1	1	$\cdots$	0	0	0	0	$\cdots$	0	0	$\cdots$	0	0	0	$\cdots$	0
	(A8)	$\vdots$	$\vdots$	$\vdots$	$\ddots$	$\vdots$	$\vdots$	$\vdots$	$\ddots$	$\vdots$	$\vdots$	$\vdots$	$\ddots$	$\vdots$	$\vdots$	$\vdots$	$\ddots$	$\vdots$	$\vdots$	$\vdots$	$\ddots$	$\vdots$	$\vdots$	$\vdots$	$\ddots$	$\vdots$	$\vdots$	$\vdots$	$\ddots$	$\vdots$	$\vdots$	$\vdots$	$\vdots$	$\ddots$	$\vdots$	$\vdots$	$\ddots$	$\vdots$	$\vdots$	$\vdots$	$\ddots$	$\vdots$
		$t-1$	$\overline{V}-\underline{C}-\epsilon$	$\overline{V}-\underline{C}-\epsilon$	$\cdots$	$\overline{V}-\underline{C}-\epsilon$	0	0	$\cdots$	0	0	0	$\cdots$	0	0	0	$\cdots$	0	0	0	$\cdots$	0	0	0	$\cdots$	0	1	0	$\cdots$	1	0	0	0	$\cdots$	0	0	$\cdots$	0	0	0	$\cdots$	0
	(N4)	t	$\overline{C}-\underline{C}-V$	$\overline{C}-\underline{C}-V$	$\cdots$	$\overline{C}-\underline{C}-V$	$\overline{V}-\underline{C}$	0	$\cdots$	0	0	0	$\cdots$	0	$\overline{C}-\overline{V}$	0	$\cdots$	0	0	0	$\cdots$	0	0	0	$\cdots$	0	1	1	$\cdots$	1	1	0	0	$\cdots$	0	0	$\cdots$	0	0	0	$\cdots$	0
	(N5)	$t+1$	$\overline{C}-\underline{C}$	$\overline{C}-\underline{C}$	$\cdots$	$\overline{C}-\underline{C}$	$\overline{C}-\underline{C}$	$\overline{C}-\underline{C}$	$\cdots$	$\overline{C}-\underline{C}$	0	0	$\cdots$	0	0	0	$\cdots$	0	0	0	$\cdots$	0	0	0	$\cdots$	0	1	1	$\cdots$	1	1	1	1	$\cdots$	1	0	$\cdots$	0	0	0	$\cdots$	0
		$t+2$	0	0	$\cdots$	0	$\overline{V}-\underline{C}$	$\overline{V}-\underline{C}-\epsilon$	$\cdots$	0	0	0	$\cdots$	0	0	0	$\cdots$	0	0	0	$\cdots$	0	0	0	$\cdots$	0	0	0	$\cdots$	0	1	1	1	$\cdots$	0	0	$\cdots$	0	1	0	$\cdots$	0
	(A10)	$\vdots$	$\vdots$	$\vdots$	$\ddots$	$\vdots$	$\vdots$	$\vdots$	$\ddots$	$\vdots$	$\vdots$	$\vdots$	$\ddots$	$\vdots$	$\vdots$	$\vdots$	$\ddots$	$\vdots$	$\vdots$	$\vdots$	$\ddots$	$\vdots$	$\vdots$	$\vdots$	$\ddots$	$\vdots$	$\vdots$	$\vdots$	$\ddots$	$\vdots$	$\vdots$	$\vdots$	$\vdots$	$\ddots$	$\vdots$	$\vdots$	$\ddots$	$\vdots$	$\vdots$	$\vdots$	$\ddots$	$\vdots$
		T	0	0	$\cdots$	0	$\overline{V}-\underline{C}$	$\overline{V}-\underline{C}-\epsilon$	$\cdots$	$\overline{V}-\underline{C}-\epsilon$	0	0	$\cdots$	0	0	0	$\cdots$	0	0	0	$\cdots$	0	0	0	$\cdots$	0	0	0	$\cdots$	0	1	1	1	$\cdots$	1	0	$\cdots$	0	1	0	$\cdots$	0
$\dot{\boldsymbol{\theta}}^{\alpha}$		2	0	$\overline{V}-\underline{C}$	$\cdots$	0	0	0	$\cdots$	0	0	0	$\cdots$	0	0	0	$\cdots$	0	0	0	$\cdots$	0	0	0	$\cdots$	0	0	1	$\cdots$	0	0	0	0	$\cdots$	0	1	$\cdots$	0	0	0	$\cdots$	0
	(N6)	$\vdots$	$\vdots$	$\vdots$	$\ddots$	$\vdots$	$\vdots$	$\vdots$	$\ddots$	$\vdots$	$\vdots$	$\vdots$	$\ddots$	$\vdots$	$\vdots$	$\vdots$	$\ddots$	$\vdots$	$\vdots$	$\vdots$	$\ddots$	$\vdots$	$\vdots$	$\vdots$	$\ddots$	$\vdots$	$\vdots$	$\vdots$	$\ddots$	$\vdots$	$\vdots$	$\vdots$	$\vdots$	$\ddots$	$\vdots$	$\vdots$	$\ddots$	$\vdots$	$\vdots$	$\vdots$	$\ddots$	$\vdots$
	(N7)	$t-1$	0	0	$\cdots$	$\overline{V}-\underline{C}$	$\overline{V}-\underline{C}+V$	$\overline{V}-\underline{C}$	$\cdots$	0	0	0	$\cdots$	0	0	0	$\cdots$	0	0	0	$\cdots$	0	0	0	$\cdots$	0	0	0	$\cdots$	1	1	1	0	$\cdots$	0	0	$\cdots$	1	0	0	$\cdots$	0
		t	0	0	$\cdots$	0	$\overline{V}-\underline{C}$	$\overline{V}-\underline{C}$	$\cdots$	0	0	0	$\cdots$	0	0	0	$\cdots$	0	0	0	$\cdots$	0	0	0	$\cdots$	0	0	0	$\cdots$	0	1	1	0	$\cdots$	0	0	$\cdots$	0	1	0	$\cdots$	0
	(N8)	$\vdots$	$\vdots$	$\vdots$	$\ddots$	$\vdots$	$\vdots$	$\vdots$	$\ddots$	$\vdots$	$\vdots$	$\vdots$	$\ddots$	$\vdots$	$\vdots$	$\vdots$	$\ddots$	$\vdots$	$\vdots$	$\vdots$	$\ddots$	$\vdots$	$\vdots$	$\vdots$	$\ddots$	$\vdots$	$\vdots$	$\vdots$	$\ddots$	$\vdots$	$\vdots$	$\vdots$	$\vdots$	$\ddots$	$\vdots$	$\vdots$	$\ddots$	$\vdots$	$\vdots$	$\vdots$	$\ddots$	$\vdots$
		T	0	0	$\cdots$	0	0	0	$\cdots$	$\overline{V}-\underline{C}$	0	0	$\cdots$	0	0	0	$\cdots$	0	0	0	$\cdots$	0	0	0	$\cdots$	0	0	0	$\cdots$	0	0	0	0	$\cdots$	1	0	$\cdots$	0	0	0	$\cdots$	1

Table C.7. Lower Triangular Matrix Obtained From Table C.6 via Gaussian Elimination

Point	Group	Index α	$\mathbf{p}$								$\mathbf{r}^+$								$\mathbf{r}^-$								$\mathbf{y}$									$\mathbf{u}$							
			1	2	$\cdots$	$t-1$	t	$t+1$	$\cdots$	T	1	2	$\cdots$	$t-1$	t	$t+1$	$\cdots$	T	1	2	$\cdots$	$t-1$	t	$t+1$	$\cdots$	T	1	2	$\cdots$	$t-1$	t	$t+1$	$t+2$	$\cdots$	T	2	$\cdots$	$t-1$	t	$t+1$	$\cdots$	T
$\underline{\grave{\boldsymbol{\theta}}}^{\alpha}$	(B1)	1	ϵ	0	$\cdots$	0	0	0	$\cdots$	0	0	0	$\cdots$	0	0	0	$\cdots$	0	0	0	$\cdots$	0	0	0	$\cdots$	0	0	0	$\cdots$	0	0	0	0	$\cdots$	0	0	$\cdots$	0	0	0	$\cdots$	0
		2	ϵ	ϵ	$\cdots$	0	0	0	$\cdots$	0	0	0	$\cdots$	0	0	0	$\cdots$	0	0	0	$\cdots$	0	0	0	$\cdots$	0	0	0	$\cdots$	0	0	0	0	$\cdots$	0	0	$\cdots$	0	0	0	$\cdots$	0
		$\vdots$	$\vdots$	$\vdots$	$\ddots$	$\vdots$	$\vdots$	$\vdots$	$\ddots$	$\vdots$	$\vdots$	$\vdots$	$\ddots$	$\vdots$	$\vdots$	$\vdots$	$\ddots$	$\vdots$	$\vdots$	$\vdots$	$\ddots$	$\vdots$	$\vdots$	$\vdots$	$\ddots$	$\vdots$	$\vdots$	$\vdots$	$\ddots$	$\vdots$	$\vdots$	$\vdots$	$\vdots$	$\ddots$	$\vdots$	$\vdots$	$\ddots$	$\vdots$	$\vdots$	$\vdots$	$\ddots$	$\vdots$
		$t-1$	ϵ	ϵ	$\cdots$	ϵ	0	0	$\cdots$	0	0	0	$\cdots$	0	0	0	$\cdots$	0	0	0	$\cdots$	0	0	0	$\cdots$	0	0	0	$\cdots$	0	0	0	0	$\cdots$	0	0	$\cdots$	0	0	0	$\cdots$	0
		$t+1$	0	0	$\cdots$	0	0	$-\epsilon$	$\cdots$	0	0	0	$\cdots$	0	0	0	$\cdots$	0	0	0	$\cdots$	0	0	0	$\cdots$	0	0	0	$\cdots$	0	0	0	0	$\cdots$	0	0	$\cdots$	0	0	0	$\cdots$	0
		$\vdots$	$\vdots$	$\vdots$	$\ddots$	$\vdots$	$\vdots$	$\vdots$	$\ddots$	$\vdots$	$\vdots$	$\vdots$	$\ddots$	$\vdots$	$\vdots$	$\vdots$	$\ddots$	$\vdots$	$\vdots$	$\vdots$	$\ddots$	$\vdots$	$\vdots$	$\vdots$	$\ddots$	$\vdots$	$\vdots$	$\vdots$	$\ddots$	$\vdots$	$\vdots$	$\vdots$	$\vdots$	$\ddots$	$\vdots$	$\vdots$	$\ddots$	$\vdots$	$\vdots$	$\vdots$	$\ddots$	$\vdots$
		T	0	0	$\cdots$	0	0	ϵ	$\cdots$	ϵ	0	0	$\cdots$	0	0	0	$\cdots$	0	0	0	$\cdots$	0	0	0	$\cdots$	0	0	0	$\cdots$	0	0	0	0	$\cdots$	0	0	$\cdots$	0	0	0	$\cdots$	0
$\underline{\grave{\boldsymbol{\theta}}}^{\alpha}$	(B2)	1	0	0	$\cdots$	0	0	0	$\cdots$	0	ϵ	0	$\cdots$	0	0	0	$\cdots$	0	0	0	$\cdots$	0	0	0	$\cdots$	0	0	0	$\cdots$	0	0	0	0	$\cdots$	0	0	$\cdots$	0	0	0	$\cdots$	0
		2	0	0	$\cdots$	0	0	0	$\cdots$	0	0	ϵ	$\cdots$	0	0	0	$\cdots$	0	0	0	$\cdots$	0	0	0	$\cdots$	0	0	0	$\cdots$	0	0	0	0	$\cdots$	0	0	$\cdots$	0	0	0	$\cdots$	0
		$\vdots$	$\vdots$	$\vdots$	$\ddots$	$\vdots$	$\vdots$	$\vdots$	$\ddots$	$\vdots$	$\vdots$	$\vdots$	$\ddots$	$\vdots$	$\vdots$	$\vdots$	$\ddots$	$\vdots$	$\vdots$	$\vdots$	$\ddots$	$\vdots$	$\vdots$	$\vdots$	$\ddots$	$\vdots$	$\vdots$	$\vdots$	$\ddots$	$\vdots$	$\vdots$	$\vdots$	$\vdots$	$\ddots$	$\vdots$	$\vdots$	$\ddots$	$\vdots$	$\vdots$	$\vdots$	$\ddots$	$\vdots$
		$t-1$	0	0	$\cdots$	0	0	0	$\cdots$	0	0	0	$\cdots$	ϵ	0	0	$\cdots$	0	0	0	$\cdots$	0	0	0	$\cdots$	0	0	0	$\cdots$	0	0	0	0	$\cdots$	0	0	$\cdots$	0	0	0	$\cdots$	0
		t	0	0	$\cdots$	0	$-\epsilon$	$-\epsilon$	$\cdots$	0	0	0	$\cdots$	0	ϵ	0	$\cdots$	0	0	0	$\cdots$	0	0	0	$\cdots$	0	0	0	$\cdots$	0	0	0	0	$\cdots$	0	0	$\cdots$	0	0	0	$\cdots$	0
		$t+1$	0	0	$\cdots$	0	0	$-\epsilon$	$\cdots$	0	0	0	$\cdots$	0	0	ϵ	$\cdots$	0	0	0	$\cdots$	0	0	0	$\cdots$	0	0	0	$\cdots$	0	0	0	0	$\cdots$	0	0	$\cdots$	0	0	0	$\cdots$	0
		$\vdots$	$\vdots$	$\vdots$	$\ddots$	$\vdots$	$\vdots$	$\vdots$	$\ddots$	$\vdots$	$\vdots$	$\vdots$	$\ddots$	$\vdots$	$\vdots$	$\vdots$	$\ddots$	$\vdots$	$\vdots$	$\vdots$	$\ddots$	$\vdots$	$\vdots$	$\vdots$	$\ddots$	$\vdots$	$\vdots$	$\vdots$	$\ddots$	$\vdots$	$\vdots$	$\vdots$	$\vdots$	$\ddots$	$\vdots$	$\vdots$	$\ddots$	$\vdots$	$\vdots$	$\vdots$	$\ddots$	$\vdots$
		T	0	0	$\cdots$	0	0	0	$\cdots$	0	0	0	$\cdots$	0	0	0	$\cdots$	ϵ	0	0	$\cdots$	0	0	0	$\cdots$	0	0	0	$\cdots$	0	0	0	0	$\cdots$	0	0	$\cdots$	0	0	0	$\cdots$	0
$\underline{\hat{\boldsymbol{\theta}}}^{\alpha}$	(B3)	1	0	0	$\cdots$	0	0	0	$\cdots$	0	0	0	$\cdots$	0	0	0	$\cdots$	0	ϵ	0	$\cdots$	0	0	0	$\cdots$	0	0	0	$\cdots$	0	0	0	0	$\cdots$	0	0	$\cdots$	0	0	0	$\cdots$	0
		2	0	0	$\cdots$	0	0	0	$\cdots$	0	0	0	$\cdots$	0	0	0	$\cdots$	0	0	ϵ	$\cdots$	0	0	0	$\cdots$	0	0	0	$\cdots$	0	0	0	0	$\cdots$	0	0	$\cdots$	0	0	0	$\cdots$	0
		$\vdots$	$\vdots$	$\vdots$	$\ddots$	$\vdots$	$\vdots$	$\vdots$	$\ddots$	$\vdots$	$\vdots$	$\vdots$	$\ddots$	$\vdots$	$\vdots$	$\vdots$	$\ddots$	$\vdots$	$\vdots$	$\vdots$	$\ddots$	$\vdots$	$\vdots$	$\vdots$	$\ddots$	$\vdots$	$\vdots$	$\vdots$	$\ddots$	$\vdots$	$\vdots$	$\vdots$	$\vdots$	$\ddots$	$\vdots$	$\vdots$	$\ddots$	$\vdots$	$\vdots$	$\vdots$	$\ddots$	$\vdots$
		$t-1$	0	0	$\cdots$	0	0	0	$\cdots$	0	0	0	$\cdots$	0	0	0	$\cdots$	0	0	0	$\cdots$	ϵ	0	0	$\cdots$	0	0	0	$\cdots$	0	0	0	0	$\cdots$	0	0	$\cdots$	0	0	0	$\cdots$	0
		t	0	0	$\cdots$	0	0	$-\epsilon$	$\cdots$	0	0	0	$\cdots$	0	0	0	$\cdots$	0	0	0	$\cdots$	0	ϵ	0	$\cdots$	0	0	0	$\cdots$	0	0	0	0	$\cdots$	0	0	$\cdots$	0	0	0	$\cdots$	0
		$t+1$	0	0	$\cdots$	0	0	$-\epsilon$	$\cdots$	0	0	0	$\cdots$	0	0	0	$\cdots$	0	0	0	$\cdots$	0	0	ϵ	$\cdots$	0	0	0	$\cdots$	0	0	0	0	$\cdots$	0	0	$\cdots$	0	0	0	$\cdots$	0
		$\vdots$	$\vdots$	$\vdots$	$\ddots$	$\vdots$	$\vdots$	$\vdots$	$\ddots$	$\vdots$	$\vdots$	$\vdots$	$\ddots$	$\vdots$	$\vdots$	$\vdots$	$\ddots$	$\vdots$	$\vdots$	$\vdots$	$\ddots$	$\vdots$	$\vdots$	$\vdots$	$\ddots$	$\vdots$	$\vdots$	$\vdots$	$\ddots$	$\vdots$	$\vdots$	$\vdots$	$\vdots$	$\ddots$	$\vdots$	$\vdots$	$\ddots$	$\vdots$	$\vdots$	$\vdots$	$\ddots$	$\vdots$
		T	0	0	$\cdots$	0	0	0	$\cdots$	0	0	0	$\cdots$	0	0	0	$\cdots$	0	0	0	$\cdots$	0	0	0	$\cdots$	ϵ	0	0	$\cdots$	0	0	0	0	$\cdots$	0	0	$\cdots$	0	0	0	$\cdots$	0
$\underline{\bar{\boldsymbol{\theta}}}^{\alpha}$	(B4)	1	$\overline{V}-\underline{C}-\epsilon$	0	$\cdots$	0	0	0	$\cdots$	0	0	0	$\cdots$	0	0	0	$\cdots$	0	0	0	$\cdots$	0	0	0	$\cdots$	0	1	0	$\cdots$	0	0	0	0	$\cdots$	0	0	$\cdots$	0	0	0	$\cdots$	0
		2	$\overline{V}-\underline{C}-\epsilon$	$\overline{V}-\underline{C}-\epsilon$	$\cdots$	0	0	0	$\cdots$	0	0	0	$\cdots$	0	0	0	$\cdots$	0	0	0	$\cdots$	0	0	0	$\cdots$	0	1	1	$\cdots$	0	0	0	0	$\cdots$	0	0	$\cdots$	0	0	0	$\cdots$	0
		$\vdots$	$\vdots$	$\vdots$	$\ddots$	$\vdots$	$\vdots$	$\vdots$	$\ddots$	$\vdots$	$\vdots$	$\vdots$	$\ddots$	$\vdots$	$\vdots$	$\vdots$	$\ddots$	$\vdots$	$\vdots$	$\vdots$	$\ddots$	$\vdots$	$\vdots$	$\vdots$	$\ddots$	$\vdots$	$\vdots$	$\vdots$	$\ddots$	$\vdots$	$\vdots$	$\vdots$	$\vdots$	$\ddots$	$\vdots$	$\vdots$	$\ddots$	$\vdots$	$\vdots$	$\vdots$	$\ddots$	$\vdots$
		$t-1$	$\overline{V}-\underline{C}-\epsilon$	$\overline{V}-\underline{C}-\epsilon$	$\cdots$	$\overline{V}-\underline{C}-\epsilon$	0	0	$\cdots$	0	0	0	$\cdots$	0	0	0	$\cdots$	0	0	0	$\cdots$	0	0	0	$\cdots$	0	1	1	$\cdots$	1	0	0	0	$\cdots$	0	0	$\cdots$	0	0	0	$\cdots$	0
		t	$\overline{C}-\underline{C}-V$	$\overline{C}-\underline{C}-V$	$\cdots$	$\overline{C}-\underline{C}-V$	$\overline{V}-\underline{C}$	0	$\cdots$	0	0	0	$\cdots$	0	$\overline{C}-\overline{V}$	0	$\cdots$	0	0	0	$\cdots$	0	0	0	$\cdots$	0	1	1	$\cdots$	1	1	0	0	$\cdots$	0	0	$\cdots$	0	0	0	$\cdots$	0
		$t+1$	$\overline{C}-\underline{C}$	$\overline{C}-\underline{C}$	$\cdots$	$\overline{C}-\underline{C}$	$\overline{C}-\underline{C}$	$\overline{C}-\underline{C}+\epsilon$	$\cdots$	$\overline{C}-\overline{V}+\epsilon$	0	0	$\cdots$	0	0	0	$\cdots$	0	0	0	$\cdots$	0	0	0	$\cdots$	0	1	1	$\cdots$	1	1	1	0	$\cdots$	0	0	$\cdots$	0	0	0	$\cdots$	0
		$t+2$	0	0	$\cdots$	0	0	$-\epsilon$	$\cdots$	0	0	0	$\cdots$	0	0	0	$\cdots$	0	0	0	$\cdots$	0	0	0	$\cdots$	0	0	0	$\cdots$	0	0	0	1	$\cdots$	0	0	$\cdots$	0	0	0	$\cdots$	0
		$\vdots$	$\vdots$	$\vdots$	$\ddots$	$\vdots$	$\vdots$	$\vdots$	$\ddots$	$\vdots$	$\vdots$	$\vdots$	$\ddots$	$\vdots$	$\vdots$	$\vdots$	$\ddots$	$\vdots$	$\vdots$	$\vdots$	$\ddots$	$\vdots$	$\vdots$	$\vdots$	$\ddots$	$\vdots$	$\vdots$	$\vdots$	$\ddots$	$\vdots$	$\vdots$	$\vdots$	$\vdots$	$\ddots$	$\vdots$	$\vdots$	$\ddots$	$\vdots$	$\vdots$	$\vdots$	$\ddots$	$\vdots$
		T	0	0	$\cdots$	0	0	$-\epsilon$	$\cdots$	$\overline{V}-\underline{C}-\epsilon$	0	0	$\cdots$	0	0	0	$\cdots$	0	0	0	$\cdots$	0	0	0	$\cdots$	0	0	0	$\cdots$	0	0	0	1	$\cdots$	1	0	$\cdots$	0	0	0	$\cdots$	0
$\underline{\dot{\boldsymbol{\theta}}}^{\alpha}$	(B5)	2	0	$\overline{V}-\underline{C}$	$\cdots$	0	0	0	$\cdots$	0	0	0	$\cdots$	0	0	0	$\cdots$	0	0	0	$\cdots$	0	0	0	$\cdots$	0	0	1	$\cdots$	0	0	0	0	$\cdots$	0	1	$\cdots$	0	0	0	$\cdots$	0
		$\vdots$	$\vdots$	$\vdots$	$\ddots$	$\vdots$	$\vdots$	$\vdots$	$\ddots$	$\vdots$	$\vdots$	$\vdots$	$\ddots$	$\vdots$	$\vdots$	$\vdots$	$\ddots$	$\vdots$	$\vdots$	$\vdots$	$\ddots$	$\vdots$	$\vdots$	$\vdots$	$\ddots$	$\vdots$	$\vdots$	$\vdots$	$\ddots$	$\vdots$	$\vdots$	$\vdots$	$\vdots$	$\ddots$	$\vdots$	$\vdots$	$\ddots$	$\vdots$	$\vdots$	$\vdots$	$\ddots$	$\vdots$
		$t-1$	0	0	$\cdots$	$\overline{V}-\underline{C}$	$\overline{V}-\underline{C}+V$	$\overline{V}-\underline{C}$	$\cdots$	0	0	0	$\cdots$	0	0	0	$\cdots$	0	0	0	$\cdots$	0	0	0	$\cdots$	0	0	0	$\cdots$	1	1	1	0	$\cdots$	0	0	$\cdots$	1	0	0	$\cdots$	0
		t	0	0	$\cdots$	0	$\overline{V}-\underline{C}$	$\overline{V}-\underline{C}$	$\cdots$	0	0	0	$\cdots$	0	0	0	$\cdots$	0	0	0	$\cdots$	0	0	0	$\cdots$	0	0	0	$\cdots$	0	1	1	0	$\cdots$	0	0	$\cdots$	0	1	0	$\cdots$	0
		$\vdots$	$\vdots$	$\vdots$	$\ddots$	$\vdots$	$\vdots$	$\vdots$	$\ddots$	$\vdots$	$\vdots$	$\vdots$	$\ddots$	$\vdots$	$\vdots$	$\vdots$	$\ddots$	$\vdots$	$\vdots$	$\vdots$	$\ddots$	$\vdots$	$\vdots$	$\vdots$	$\ddots$	$\vdots$	$\vdots$	$\vdots$	$\ddots$	$\vdots$	$\vdots$	$\vdots$	$\vdots$	$\ddots$	$\vdots$	$\vdots$	$\ddots$	$\vdots$	$\vdots$	$\vdots$	$\ddots$	$\vdots$
		T	0	0	$\cdots$	0	0	0	$\cdots$	$\overline{V}-\underline{C}$	0	0	$\cdots$	0	0	0	$\cdots$	0	0	0	$\cdots$	0	0	0	$\cdots$	0	0	0	$\cdots$	0	0	0	0	$\cdots$	1	0	$\cdots$	0	0	0	$\cdots$	1

(iii) For each $\alpha \in [1,T]_{\mathbb{Z}}$, the point with index α in group (B3), denoted by $\underline{\hat{\boldsymbol{\theta}}}^{\alpha}$, is obtained by setting $\underline{\hat{\boldsymbol{\theta}}}^{\alpha} = \hat{\boldsymbol{\theta}}^{\alpha} - \overline{\boldsymbol{\theta}}^{\alpha}$ for any $\alpha \in [1,T]_{\mathbb{Z}} \setminus \{t,\ t+1\}$, $\underline{\hat{\boldsymbol{\theta}}}^{\alpha} = \hat{\boldsymbol{\theta}}^{\alpha} - \dot{\boldsymbol{\theta}}^{t}$ for any $\alpha \in [t, \min\{t+1,T\}]_{\mathbb{Z}}$. Here $\hat{\boldsymbol{\theta}}^{\alpha}$ with $\alpha \in [1,T]_{\mathbb{Z}} \setminus \{t\}$ is the point with index α in group (A6) and (A7), $\hat{\boldsymbol{\theta}}^{t}$ is the point in group (N3), $\overline{\boldsymbol{\theta}}^{\alpha}$ with $\alpha \in [1,t-1]_{\mathbb{Z}}$ is the point with index α in group (A8), $\overline{\boldsymbol{\theta}}^{\alpha}$ with $\alpha \in [t+2,T]_{\mathbb{Z}}$ and $t \leq T-2$ is the point in group (A10), and $\dot{\boldsymbol{\theta}}^{t}$ is the point in group (N8).

(iv) For each $\alpha \in [1,T]_{\mathbb{Z}}$, the point with index α in group (B4), denoted by $\underline{\overline{\boldsymbol{\theta}}}^{\alpha}$, is obtained by setting (i) $\underline{\overline{\boldsymbol{\theta}}}^{\alpha} = \overline{\boldsymbol{\theta}}^{\alpha}$ for any $\alpha \in [1,t]_{\mathbb{Z}}$, where $\overline{\boldsymbol{\theta}}^{\alpha}$ with $\alpha \in [1,t-1]_{\mathbb{Z}}$ is the point with index α in group (A8), $\overline{\boldsymbol{\theta}}^{t}$ is the point in group (N4), (ii) $\underline{\overline{\boldsymbol{\theta}}}^{t+1} = \overline{\boldsymbol{\theta}}^{t+1}$ when $t = T-1$, where $\overline{\boldsymbol{\theta}}^{t+1}$ is the point in group (N5), $\underline{\overline{\boldsymbol{\theta}}}^{t+1} = \overline{\boldsymbol{\theta}}^{t+1} - \overline{\boldsymbol{\theta}}^{T} + \dot{\boldsymbol{\theta}}^{t}$ when $t \leq T-2$, where $\overline{\boldsymbol{\theta}}^{t+1}$ and $\overline{\boldsymbol{\theta}}^{T}$ are points in group (N5) and group (A10), respectively, and (iii) $\underline{\overline{\boldsymbol{\theta}}}^{\alpha} = \overline{\boldsymbol{\theta}}^{\alpha} - \dot{\boldsymbol{\theta}}^{t}$ for any $\alpha \in [t+2,T]_{\mathbb{Z}}$ when $t \leq T-2$, where $\overline{\boldsymbol{\theta}}^{\alpha}$ is the point in group (A10). Here $\dot{\boldsymbol{\theta}}^{t}$ is the point in group (N8).

(v) For each $\alpha \in [2,T]_{\mathbb{Z}}$, the point with index α in group (B5), denoted by $\underline{\dot{\boldsymbol{\theta}}}^{\alpha}$, is obtained by setting $\underline{\dot{\boldsymbol{\theta}}}^{\alpha} = \dot{\boldsymbol{\theta}}^{\alpha}$. Here $\dot{\boldsymbol{\theta}}^{\alpha}$ is the point with index α in groups (N6)–(N8).

The matrix shown in Table C.7 is lower triangular; that is, the position of the last nonzero component of a row of the matrix is greater than the position of the last nonzero component of the previous row. This indicates that the $5T-2$ points created above are linearly independent. Therefore, inequality (4.37) is facet-defining for $\operatorname{conv}(\mathcal{D})$ when $k = L = 2$ and $\overline{V} + V \leq \overline{C} \leq \overline{V} + 2V$. □

C.14 Proof of Proposition 9

Proof. To prove that inequality (4.38) is valid for $\operatorname{conv}(\mathcal{D})$ for any $t \in [2,T]_{\mathbb{Z}}$ and $k \in [1, \min\{t-1,\varsigma\}]_{\mathbb{Z}}$, it suffices to show that it is valid for $\mathcal{D}$ for such t and k. Consider any element $(\mathbf{p},\mathbf{r}^{+},\mathbf{r}^{-},\mathbf{y},\mathbf{u})$ of $\mathcal{D}$ and any $t \in [2,T]_{\mathbb{Z}}$ and $k \in [1, \min\{t-1,\varsigma\}]_{\mathbb{Z}}$. We show that $(\mathbf{p},\mathbf{r}^{+},\mathbf{r}^{-},\mathbf{y},\mathbf{u})$ satisfies (4.38).

First, we show $\sum_{s=0}^{\min\{L,k\}-1} u_{t-s} \leq y_t$. Specifically, when $k \geq L$, we have $\sum_{s=0}^{\min\{L,k\}-1} u_{t-s} = \sum_{s=0}^{L-1} u_{t-s} = \sum_{s=t-L+1}^{t} u_s \leq y_t$, where the inequality holds by (4.35a). When $k < L$, we have $\sum_{s=0}^{\min\{L,k\}-1} u_{t-s} = \sum_{s=0}^{k-1} u_{t-s} = \sum_{s=t-k+1}^{t} u_s \leq y_t$, where the inequality holds by

Lemma 2. Next, we divide the analysis into the following three possible cases.

Case 1: $y_t = 0$. Because $\sum_{s=0}^{\min\{L,k\}-1} u_{t-s} \leq y_t$, we have $\sum_{s=0}^{\min\{L,k\}-1} u_{t-s} = 0$, implying that $u_{t-s} = 0$ for any $s \in [0, \min\{L,k\} - 1]_{\mathbb{Z}}$. Thus, the right-hand side of (4.38) is 0. Because $y_t = 0$, by (4.35e) and (4.35h), we have $p_t = r_t^+ = 0$. Therefore, in this case, $(\mathbf{p}, \mathbf{r}^+, \mathbf{r}^-, \mathbf{y}, \mathbf{u})$ satisfies (4.38).

Case 2: $y_t = 1$ and $u_{t-s} = 0$ for any $s \in [0, \min\{L,k\} - 1]_{\mathbb{Z}}$. The right-hand side of (4.38) is kV. By (4.35c), we have $y_{t-1} = 1$. Therefore, we have $p_t + r_t^+ - p_{t-k} = p_t + r_t^+ - p_{t-1} + \sum_{s=1}^{k-1} (p_{t-s} - p_{t-s-1}) \leq V + \sum_{s=1}^{k-1} (p_{t-s} - p_{t-s-1}) \leq kV$, where the first inequality holds by (4.35f) and the last inequality holds by Lemma 4. Therefore, in this case, $(\mathbf{p}, \mathbf{r}^+, \mathbf{r}^-, \mathbf{y}, \mathbf{u})$ satisfies (4.38).

Case 3: $y_t = 1$ and $u_{t-s'} = 1$ for some $s' \in [0, \min\{L,k\} - 1]_{\mathbb{Z}}$. By Lemma 2, we have $u_{t-s} = 0$ for any $s \in [0, k-1]_{\mathbb{Z}} \backslash \{s'\}$. Thus, the right-hand side of (4.38) is $\overline{V} - \underline{C} + s'V$. For any $s \in [0, s']_{\mathbb{Z}}$, we have $y_t - y_{t-s} = y_t - y_{t-s} - \sum_{i=0}^{s-1} u_{t-i} = \sum_{i=0}^{s-1} (y_{t-i} - y_{t-i-1} - u_{t-i}) \leq 0$, where the first equality holds because $u_{t-i} = 0$ for any $i \in [0, k-1]_{\mathbb{Z}} \setminus \{s'\}$ and the inequality holds by (4.35c). Because $y_t = 1$, we have $y_{t-s} = 1$ for any $s \in [0, s']_{\mathbb{Z}}$. Because $u_{t-s'} = 1$, by Corollary 1, we have $y_{t-s'-1} = 0$, which, by (4.35e) and (4.35h), implies that $p_{t-s'-1} = 0$. Thus,

$$
\begin{aligned}
&p_t + r_t^+ - p_{t-k} \leq p_t + r_t^+ = p_t + r_t^+ - p_{t-s'-1} \leq \sum_{s=t-s'}^{t} \left(p_s + r_s^+ - p_{s-1}\right) \\
&\leq \sum_{s=t-s'}^{t} \left(\overline{V} + \left(\underline{C} + V - \overline{V}\right) y_{s-1} - \underline{C} y_s\right) = (s'+1)\,\overline{V} + \sum_{i=1}^{s'+1} \left(\underline{C} + V - \overline{V}\right) y_{t-i} - \sum_{i=0}^{s'} \underline{C} y_{t-i} \\
&= (s'+1)\,\overline{V} + s' \left(\underline{C} + V - \overline{V}\right) - (s'+1)\,\underline{C} = \overline{V} - \underline{C} + s'V,
\end{aligned}
$$

where the first and second inequalities hold by (4.35h) and the third inequality holds by the ramp-up constraints (4.35f). Therefore, in this case, $(\mathbf{p}, \mathbf{r}^+, \mathbf{r}^-, \mathbf{y}, \mathbf{u})$ satisfies (4.38).

Consider any $t \in [2, T]_{\mathbb{Z}}$ and $k \in [1, \min\{t-1, \varsigma\}]_{\mathbb{Z}}$. To prove (4.38) is facet-defining for $\mathrm{conv}(\mathcal{D})$ when $L = 1$, it suffices to create $5T - 1$ affinely independent points in $\mathrm{conv}(\mathcal{D})$ that satisfy (4.38) at equality. Because $\mathbf{0} \in \mathrm{conv}(\mathcal{D})$ and $\mathbf{0}$ satisfies (4.36) at equality, it suffices to create the remaining $5T - 2$ nonzero linearly independent points. We let $\grave{\boldsymbol{\theta}} = (\grave{\mathbf{p}}, \grave{\mathbf{r}}^+, \grave{\mathbf{r}}^-, \grave{\mathbf{y}}, \grave{\mathbf{u}})$ and denote the sth component of $\grave{\mathbf{p}}$, $\grave{\mathbf{r}}^+$, $\grave{\mathbf{r}}^-$, $\grave{\mathbf{y}}$, and $\grave{\mathbf{u}}$ by $\grave{p}_s$, $\grave{r}_s^+$, $\grave{r}_s^-$, $\grave{y}_s$, and $\grave{u}_s$. Similarly, we define $\acute{\boldsymbol{\theta}}$, $\hat{\boldsymbol{\theta}}$, $\overline{\boldsymbol{\theta}}$, and $\dot{\boldsymbol{\theta}}$. We denote the $5T - 2$ nonzero linearly independent points by $\grave{\boldsymbol{\theta}}^\alpha$ for $\alpha \in \mathcal{T} \setminus \{t-k\}$, $\acute{\boldsymbol{\theta}}^\alpha$ for $\alpha \in \mathcal{T}$, $\hat{\boldsymbol{\theta}}^\alpha$ for $\alpha \in \mathcal{T}$, $\overline{\boldsymbol{\theta}}^\alpha$ for $\alpha \in \mathcal{T}$,

and $\dot{\boldsymbol{\theta}}^{\alpha}$ for $\alpha \in \mathcal{T} \setminus \{1\}$. We let $\epsilon = \min\left\{\underline{C} + V - \overline{V},\ \overline{V} - \underline{C}\right\} > 0$ and divide the $5T-2$ points into the following 14 groups.

(A1) For each $\alpha \in [1, t-1]_{\mathbb{Z}} \setminus \{t-k\}$, we create a point $\grave{\boldsymbol{\theta}}^{\alpha}$ as follows:

$$\grave{p}_s^{\alpha} = \begin{cases} \overline{V} - \underline{C}, & s \in [1, \alpha]_{\mathbb{Z}} \setminus \{t-k\} \\ 0, & \text{o.w.} \end{cases},\ \grave{y}_s^{\alpha} = \begin{cases} 1, & s \in [1, \alpha]_{\mathbb{Z}} \\ 0, & \text{o.w.} \end{cases},$$

$\grave{r}_s^{+,\alpha} = \grave{r}_s^{-,\alpha} = 0$ for any $s \in \mathcal{T}$, and $\grave{u}_s^{\alpha} = 0$ for any $s \in \mathcal{T} \setminus \{1\}$. It is easy to verify that $\grave{\boldsymbol{\theta}}^{\alpha}$ satisfies (4.35a)–(4.35h). Thus, $\grave{\boldsymbol{\theta}}^{\alpha} \in \operatorname{conv}(\mathcal{D})$. It is also easy to verify that $\grave{\boldsymbol{\theta}}^{\alpha}$ satisfies (4.38) at equality.

(A2) For $\alpha = t$, we create a point $\grave{\boldsymbol{\theta}}^{\alpha}$ as follows:

$$\grave{p}_s^{\alpha} = \begin{cases} \overline{V} - \underline{C}, & s \in [1, t-k]_{\mathbb{Z}} \\ \overline{V} - \underline{C} + (s - t + k)V, & s \in [t-k+1, t]_{\mathbb{Z}} \\ \overline{V} - \underline{C} + kV, & \text{o.w.} \end{cases},$$

$\grave{r}_s^{+,\alpha} = \grave{r}_s^{-,\alpha} = 0$ for any $s \in \mathcal{T}$, $\grave{y}_s^{\alpha} = 1$ for any $s \in \mathcal{T}$, and $\grave{u}_s^{\alpha} = 0$ for any $s \in \mathcal{T} \setminus \{1\}$. Note that $k \leq (\overline{C} - \overline{V})/V$ and hence $\overline{V} - \underline{C} + kV \leq \overline{C} - \underline{C}$. Thus, $\grave{\boldsymbol{\theta}}^{\alpha}$ satisfies (4.35a)–(4.35h) and $\grave{\boldsymbol{\theta}}^{\alpha} \in \operatorname{conv}(\mathcal{D})$. It is also easy to verify that $\grave{\boldsymbol{\theta}}^{\alpha}$ satisfies (4.38) at equality.

(A3) For each $\alpha \in [t+1, T]_{\mathbb{Z}}$, we create a point $\grave{\boldsymbol{\theta}}^{\alpha}$ as follows:

$$\grave{p}_s^{\alpha} = \begin{cases} \overline{V} - \underline{C}, & s \in [t, \alpha]_{\mathbb{Z}} \\ 0, & \text{o.w.} \end{cases},\ \grave{y}_s^{\alpha} = \begin{cases} 1, & s \in [t, \alpha]_{\mathbb{Z}} \\ 0, & \text{o.w.} \end{cases},\ \grave{u}_s^{\alpha} = \begin{cases} 1, & s = t \\ 0, & \text{o.w.} \end{cases},$$

and $\grave{r}_s^{+,\alpha} = \grave{r}_s^{-,\alpha} = 0$ for any $s \in \mathcal{T}$. It is easy to verify that $\grave{\boldsymbol{\theta}}^{\alpha}$ satisfies (4.35a)–(4.35h). Thus, $\grave{\boldsymbol{\theta}}^{\alpha} \in \operatorname{conv}(\mathcal{D})$. It is also easy to verify that $\grave{\boldsymbol{\theta}}^{\alpha}$ satisfies (4.38) at equality.

(A4) For each $\alpha \in [1, t-1]_{\mathbb{Z}}$, we create a point $\acute{\boldsymbol{\theta}}^{\alpha}$ as follows:

$$\acute{p}_s^{\alpha} = \begin{cases} \overline{V} - \underline{C} - \epsilon, & s \in [1, \alpha]_{\mathbb{Z}} \setminus \{t-k\} \\ 0, & \text{o.w.} \end{cases}, \quad \acute{r}_s^{+,\alpha} = \begin{cases} \epsilon, & s = \alpha \\ 0, & \text{o.w.} \end{cases}, \quad \acute{y}_s^{\alpha} = \begin{cases} 1, & s \in [1, \alpha]_{\mathbb{Z}} \\ 0, & \text{o.w.} \end{cases},$$

$\acute{r}_s^{-,\alpha} = 0$ for any $s \in \mathcal{T}$, and $\acute{u}_s^{\alpha} = 0$ for any $s \in \mathcal{T} \setminus \{1\}$. It is easy to verify that $\acute{\boldsymbol{\theta}}^{\alpha}$ satisfies (4.35a)–(4.35h). Thus, $\acute{\boldsymbol{\theta}}^{\alpha} \in \text{conv}(\mathcal{D})$. It is also easy to verify that $\acute{\boldsymbol{\theta}}^{\alpha}$ satisfies (4.38) at equality.

(A5) For each $\alpha \in [t, T]_{\mathbb{Z}}$, we create a point $\acute{\boldsymbol{\theta}}^{\alpha}$ as follows:

$$\acute{p}_s^{\alpha} = \begin{cases} \overline{V} - \underline{C}, & s \in [t, \alpha-1]_{\mathbb{Z}} \\ \overline{V} - \underline{C} - \epsilon, & s = \alpha \\ 0, & \text{o.w.} \end{cases}, \quad \acute{r}_s^{+,\alpha} = \begin{cases} \epsilon, & s = \alpha \\ 0, & \text{o.w.} \end{cases}, \quad \acute{y}_s^{\alpha} = \begin{cases} 1, & s \in [t, \alpha]_{\mathbb{Z}} \\ 0, & \text{o.w.} \end{cases},$$

$$\acute{u}_s^{\alpha} = \begin{cases} 1, & s = t \\ 0, & \text{o.w.} \end{cases},$$

and $\acute{r}_s^{-,\alpha} = 0$ for any $s \in \mathcal{T}$. It is easy to verify that $\acute{\boldsymbol{\theta}}^{\alpha}$ satisfies (4.35a)–(4.35h). Thus, $\acute{\boldsymbol{\theta}}^{\alpha} \in \text{conv}(\mathcal{D})$. It is also easy to verify that $\acute{\boldsymbol{\theta}}^{\alpha}$ satisfies (4.38) at equality.

(A6) For each $\alpha \in [1, t-1]_{\mathbb{Z}} \setminus \{t-k\}$, we create a point $\hat{\boldsymbol{\theta}}^{\alpha}$ as follows:

$$\hat{p}_s^{\alpha} = \begin{cases} \overline{V} - \underline{C} - \epsilon, & s \in [1, \alpha]_{\mathbb{Z}} \setminus \{t-k\} \\ 0, & \text{o.w.} \end{cases}, \quad \hat{r}_s^{-,\alpha} = \begin{cases} \epsilon, & s = \alpha \\ 0, & \text{o.w.} \end{cases}, \quad \hat{y}_s^{\alpha} = \begin{cases} 1, & s \in [1, \alpha]_{\mathbb{Z}} \\ 0, & \text{o.w.} \end{cases},$$

$\hat{r}_s^{+,\alpha} = 0$ for any $s \in \mathcal{T}$, and $\hat{u}_s^{\alpha} = 0$ for any $s \in \mathcal{T} \setminus \{1\}$. It is easy to verify that $\hat{\boldsymbol{\theta}}^{\alpha}$ satisfies (4.35a)–(4.35h). Thus, $\hat{\boldsymbol{\theta}}^{\alpha} \in \text{conv}(\mathcal{D})$. It is also easy to verify that $\hat{\boldsymbol{\theta}}^{\alpha}$ satisfies (4.38) at equality.

(A7) For $\alpha = t-k$, we create a point $\hat{\boldsymbol{\theta}}^\alpha$ as follows:

$$\hat{p}_s^\alpha = \begin{cases} \overline{V} - \underline{C}, & s \in [1, t-k]_{\mathbb{Z}} \\ \overline{V} - \underline{C} + (s-t+k)V, & s \in [t-k+1, t]_{\mathbb{Z}} \\ \overline{V} - \underline{C} + kV, & \text{o.w.} \end{cases}, \quad \hat{r}_s^{-,\alpha} = \begin{cases} \epsilon, & s = t-k \\ 0, & \text{o.w.} \end{cases},$$

$\hat{r}_s^{+,\alpha} = 0$ for any $s \in \mathcal{T}$, $\hat{y}_s^\alpha = 1$ for any $s \in \mathcal{T}$, and $\hat{u}_s^\alpha = 0$ for any $s \in \mathcal{T} \setminus \{1\}$. It is easy to verify that $\hat{\boldsymbol{\theta}}^\alpha$ satisfies (4.35a)–(4.35h). Thus, $\hat{\boldsymbol{\theta}}^\alpha \in \text{conv}(\mathcal{D})$. It is also easy to verify that $\hat{\boldsymbol{\theta}}^\alpha$ satisfies (4.38) at equality.

(A8) For $\alpha = t$, we create a point $\hat{\boldsymbol{\theta}}^\alpha$ as follows:

$$\hat{p}_s^\alpha = \begin{cases} \overline{V} - \underline{C}, & s = t \\ 0, & \text{o.w.} \end{cases}, \quad \hat{r}_s^{-,\alpha} = \begin{cases} \epsilon, & s = t \\ 0, & \text{o.w.} \end{cases}, \quad \hat{y}_s^\alpha = \begin{cases} 1, & s = t \\ 0, & \text{o.w.} \end{cases}, \quad \hat{u}_s^\alpha = \begin{cases} 1, & s = t \\ 0, & \text{o.w.} \end{cases},$$

and $\hat{r}_s^{+,\alpha} = 0$ for any $s \in \mathcal{T}$. It is easy to verify that $\hat{\boldsymbol{\theta}}^\alpha$ satisfies (4.35a)–(4.35h). Thus, $\hat{\boldsymbol{\theta}}^\alpha \in \text{conv}(\mathcal{D})$. It is also easy to verify that $\hat{\boldsymbol{\theta}}^\alpha$ satisfies (4.38) at equality.

(A9) For each $\alpha \in [t+1, T]_{\mathbb{Z}}$, we create a point $\hat{\boldsymbol{\theta}}^\alpha$ as follows:

$$\hat{p}_s^\alpha = \begin{cases} \overline{V} - \underline{C}, & s \in [t, \alpha-1]_{\mathbb{Z}} \\ \overline{V} - \underline{C} - \epsilon, & s = \alpha \\ 0, & \text{o.w.} \end{cases}, \quad \hat{r}_s^{-,\alpha} = \begin{cases} \epsilon, & s = \alpha \\ 0, & \text{o.w.} \end{cases}, \quad \hat{y}_s^\alpha = \begin{cases} 1, & s \in [t, \alpha]_{\mathbb{Z}} \\ 0, & \text{o.w.} \end{cases},$$

$$\hat{u}_s^\alpha = \begin{cases} 1, & s = t \\ 0, & \text{o.w.} \end{cases},$$

and $\hat{r}_s^{+,\alpha} = 0$ for any $s \in \mathcal{T}$. It is easy to verify that $\hat{\boldsymbol{\theta}}^\alpha$ satisfies (4.35a)–(4.35h). Thus, $\hat{\boldsymbol{\theta}}^\alpha \in \text{conv}(\mathcal{D})$. It is also easy to verify that $\hat{\boldsymbol{\theta}}^\alpha$ satisfies (4.38) at equality.

(A10) For each $\alpha \in [1, t-1]_{\mathbb{Z}}$, we create a point $\overline{\boldsymbol{\theta}}^\alpha$ as follows:

$$\overline{p}_s^\alpha = \begin{cases} \overline{V} - \underline{C} - \epsilon, & s \in [1, \alpha]_{\mathbb{Z}} \setminus \{t-k\} \\ 0, & \text{o.w.} \end{cases}, \quad \overline{y}_s^\alpha = \begin{cases} 1, & s \in [1, \alpha]_{\mathbb{Z}} \\ 0, & \text{o.w.} \end{cases},$$

$\overline{r}_s^{+,\alpha} = \overline{r}_s^{-,\alpha} = 0$ for any $s \in \mathcal{T}$, and $\overline{u}_s^{\alpha} = 0$ for any $s \in \mathcal{T} \setminus \{1\}$. It is easy to verify that $\overline{\boldsymbol{\theta}}^{\alpha}$ satisfies (4.35a)–(4.35h). Thus, $\overline{\boldsymbol{\theta}}^{\alpha} \in \mathrm{conv}(\mathcal{D})$. It is also easy to verify that $\overline{\boldsymbol{\theta}}^{\alpha}$ satisfies (4.38) at equality.

(A11) For $\alpha = t$, we create a point $\overline{\boldsymbol{\theta}}^{\alpha}$ as follows:

$$\overline{p}_s^{\alpha} = \begin{cases} (s-t+k)V, & s \in [t-k+1, t]_{\mathbb{Z}} \\ kV, & s \in [t+1, T]_{\mathbb{Z}} \\ 0, & \text{o.w.} \end{cases},$$

$\overline{r}_s^{+,\alpha} = \overline{r}_s^{-,\alpha} = 0$ for any $s \in \mathcal{T}$, $\overline{y}_s^{\alpha} = 1$ for any $s \in \mathcal{T}$, and $\overline{u}_s^{\alpha} = 0$ for any $s \in \mathcal{T} \setminus \{1\}$. Note that $\underline{C} < \overline{V}$ and $k \leq (\overline{C} - \overline{V})/V$, we have $k < (\overline{C} - \underline{C})/V$, i.e., $kV < \overline{C} - \underline{C}$. Thus, $\overline{\boldsymbol{\theta}}^{\alpha}$ satisfies (4.35a)–(4.35h) and $\overline{\boldsymbol{\theta}}^{\alpha} \in \mathrm{conv}(\mathcal{D})$. It is also easy to verify that $\overline{\boldsymbol{\theta}}^{\alpha}$ satisfies (4.38) at equality.

(A12) For each $\alpha \in [t+1, T]_{\mathbb{Z}}$, we create a point $\overline{\boldsymbol{\theta}}^{\alpha}$ as follows:

$$\overline{p}_s^{\alpha} = \begin{cases} \overline{V} - \underline{C}, & s \in [t, \alpha-1]_{\mathbb{Z}} \\ \overline{V} - \underline{C} - \epsilon, & s = \alpha \\ 0, & \text{o.w.} \end{cases}, \ \overline{y}_s^{\alpha} = \begin{cases} 1, & s \in [t, \alpha]_{\mathbb{Z}} \\ 0, & \text{o.w.} \end{cases}, \ \overline{u}_s^{\alpha} = \begin{cases} 1, & s = t \\ 0, & \text{o.w.} \end{cases},$$

and $\overline{r}_s^{+,\alpha} = \overline{r}_s^{-,\alpha} = 0$ for any $s \in \mathcal{T}$. It is easy to verify that $\overline{\boldsymbol{\theta}}^{\alpha}$ satisfies (4.35a)–(4.35h). Thus, $\overline{\boldsymbol{\theta}}^{\alpha} \in \mathrm{conv}(\mathcal{D})$. It is also easy to verify that $\overline{\boldsymbol{\theta}}^{\alpha}$ satisfies (4.38) at equality.

(A13) For each $\alpha \in [2, T]_{\mathbb{Z}} \setminus \{t-k\}$, we create a point $\dot{\boldsymbol{\theta}}^{\alpha}$ as follows:

$$\dot{p}_s^{\alpha} = \begin{cases} \overline{V} - \underline{C}, & s = \alpha \\ 0, & \text{o.w.} \end{cases}, \ \dot{y}_s^{\alpha} = \begin{cases} 1, & s = \alpha \\ 0, & \text{o.w.} \end{cases}, \ \dot{u}_s^{\alpha} = \begin{cases} 1, & s = \alpha \\ 0, & \text{o.w.} \end{cases},$$

and $\dot{r}_s^{+,\alpha} = \dot{r}_s^{-,\alpha} = 0$ for any $s \in \mathcal{T}$. It is easy to verify that $\dot{\boldsymbol{\theta}}^{\alpha}$ satisfies (4.35a)–(4.35h) when $L = 1$. Thus, $\dot{\boldsymbol{\theta}}^{\alpha} \in \mathrm{conv}(\mathcal{D})$. It is also easy to verify that $\dot{\boldsymbol{\theta}}^{\alpha}$ satisfies (4.38) at equality.

(A14) For $\alpha = t - k \in [2, T]_{\mathbb{Z}}$, we create a point $\dot{\boldsymbol{\theta}}^{\alpha}$ such that $\dot{p}_s^{\alpha} = \dot{r}_s^{+,\alpha} = \dot{r}_s^{-,\alpha} = 0$ for

any $s \in \mathcal{T}$ and $\dot{y}_s^\alpha = \dot{u}_s^\alpha = 1$ for $s = t - k$ and $\dot{y}_s^\alpha = \dot{u}_s^\alpha = 0$ otherwise. It is easy to verify that $\dot{\boldsymbol{\theta}}^\alpha$ satisfies (4.35a)–(4.35h). Thus, $\dot{\boldsymbol{\theta}}^\alpha \in \text{conv}(\mathcal{D})$. It is also easy to verify that $\dot{\boldsymbol{\theta}}^\alpha$ satisfies (4.38) at equality.

Tables C.8–C.10 show matrices with $5T - 2$ rows, where each row represents a point created above, when $k = 1$, $k = 2$, and $k \geq 3$, respectively. These matrices can be transformed into the matrices in Tables C.11–C.13 via the following Gaussian elimination process:

(i) For each $\alpha \in [1, T]_{\mathbb{Z}} \setminus \{t - k\}$, the point with index α in group (B1), denoted by $\grave{\underline{\boldsymbol{\theta}}}^\alpha$, is obtained by setting $\grave{\underline{\boldsymbol{\theta}}}^\alpha = \grave{\boldsymbol{\theta}}^\alpha - \overline{\boldsymbol{\theta}}^\alpha$ for any $\alpha \in [1, T]_{\mathbb{Z}} \setminus \{t - k,\ t\}$, $\grave{\underline{\boldsymbol{\theta}}}^t = \grave{\boldsymbol{\theta}}^t - \overline{\boldsymbol{\theta}}^t - ((\overline{V} - \underline{C})/\epsilon) \sum_{n=t+1}^{T} (\grave{\boldsymbol{\theta}}^n - \overline{\boldsymbol{\theta}}^n)$ when $t < T$, and $\grave{\underline{\boldsymbol{\theta}}}^t = \grave{\boldsymbol{\theta}}^t - \overline{\boldsymbol{\theta}}^t$ when $t = T$. Here $\grave{\boldsymbol{\theta}}^\alpha$ is the point with index α in groups (A1)–(A3) and $\overline{\boldsymbol{\theta}}^\alpha$ is the point with index α in groups (A10) and (A12).

Table C.8. Matrix with The rows Representing $5T-2$ Points in $\mathrm{conv}(\mathcal{D})$ That Satisfy Inequality (4.38) at Equality When $k=1$

Point	Group	Index α	$\mathbf{p}$								$\mathbf{r}^+$								$\mathbf{r}^-$								$\mathbf{y}$								$\mathbf{u}$							
			1	2	$\cdots$	$t-1$	t	$t+1$	$\cdots$	T	1	2	$\cdots$	$t-1$	t	$\cdots$	T		1	2	$\cdots$	$t-1$	t	$t+1$	$\cdots$	T		1	2	$\cdots$	$t-1$	t	$t+1$	$\cdots$	T		2	$\cdots$	$t-1$	t	$t+1$	$\cdots$	T
$\grave{\boldsymbol{\theta}}^{\alpha}$	(A1)	1	$\overline{V}-\underline{C}$	0	$\cdots$	0	0	0	$\cdots$	0	0	0	$\cdots$	0	0	$\cdots$	0		0	0	$\cdots$	0	0	0	$\cdots$	0		1	0	$\cdots$	0	0	0	$\cdots$	0		0	$\cdots$	0	0	0	$\cdots$	0
		2	$\overline{V}-\underline{C}$	$\overline{V}-\underline{C}$	$\cdots$	0	0	0	$\cdots$	0	0	0	$\cdots$	0	0	$\cdots$	0		0	0	$\cdots$	0	0	0	$\cdots$	0		1	1	$\cdots$	0	0	0	$\cdots$	0		0	$\cdots$	0	0	0	$\cdots$	0
		$\vdots$	$\vdots$	$\vdots$	$\ddots$	$\vdots$	$\vdots$	$\vdots$	$\ddots$	$\vdots$	$\vdots$	$\vdots$	$\ddots$	$\vdots$	$\vdots$	$\ddots$	$\vdots$		$\vdots$	$\vdots$	$\ddots$	$\vdots$	$\vdots$	$\vdots$	$\ddots$	$\vdots$		$\vdots$	$\vdots$	$\ddots$	$\vdots$	$\vdots$	$\vdots$	$\ddots$	$\vdots$		$\vdots$	$\ddots$	$\vdots$	$\vdots$	$\vdots$	$\ddots$	$\vdots$
		$t-2$	$\overline{V}-\underline{C}$	$\overline{V}-\underline{C}$	$\cdots$	0	0	0	$\cdots$	0	0	0	$\cdots$	0	0	$\cdots$	0		0	0	$\cdots$	0	0	0	$\cdots$	0		1	1	$\cdots$	0	0	0	$\cdots$	0		0	$\cdots$	0	0	0	$\cdots$	0
	(A2)	t	$\overline{V}-\underline{C}$	$\overline{V}-\underline{C}$	$\cdots$	$\overline{V}-\underline{C}$	$\overline{V}-\underline{C}+V$	$\overline{V}-\underline{C}+V$	$\cdots$	$\overline{V}-\underline{C}+V$	0	0	$\cdots$	0	0	$\cdots$	0		0	0	$\cdots$	0	0	0	$\cdots$	0		1	1	$\cdots$	1	1	1	$\cdots$	1		0	$\cdots$	0	0	0	$\cdots$	0
	(A3)	$t+1$	0	0	$\cdots$	0	$\overline{V}-\underline{C}$	$\overline{V}-\underline{C}$	$\cdots$	0	0	0	$\cdots$	0	0	$\cdots$	0		0	0	$\cdots$	0	0	0	$\cdots$	0		0	0	$\cdots$	0	1	1	$\cdots$	0		0	$\cdots$	0	1	0	$\cdots$	0
		$\vdots$	$\vdots$	$\vdots$	$\ddots$	$\vdots$	$\vdots$	$\vdots$	$\ddots$	$\vdots$	$\vdots$	$\vdots$	$\ddots$	$\vdots$	$\vdots$	$\ddots$	$\vdots$		$\vdots$	$\vdots$	$\ddots$	$\vdots$	$\vdots$	$\vdots$	$\ddots$	$\vdots$		$\vdots$	$\vdots$	$\ddots$	$\vdots$	$\vdots$	$\vdots$	$\ddots$	$\vdots$		$\vdots$	$\ddots$	$\vdots$	$\vdots$	$\vdots$	$\ddots$	$\vdots$
		T	0	0	$\cdots$	0	$\overline{V}-\underline{C}$	$\overline{V}-\underline{C}$	$\cdots$	$\overline{V}-\underline{C}$	0	0	$\cdots$	0	0	$\cdots$	0		0	0	$\cdots$	0	0	0	$\cdots$	0		0	0	$\cdots$	0	1	1	$\cdots$	1		0	$\cdots$	0	1	0	$\cdots$	0
$\hat{\boldsymbol{\theta}}^{\alpha}$	(A4)	1	$\overline{V}-\underline{C}-\epsilon$	0	$\cdots$	0	0	0	$\cdots$	0	ϵ	0	$\cdots$	0	0	$\cdots$	0		0	0	$\cdots$	0	0	0	$\cdots$	0		1	0	$\cdots$	0	0	0	$\cdots$	0		0	$\cdots$	0	0	0	$\cdots$	0
		2	$\overline{V}-\underline{C}-\epsilon$	$\overline{V}-\underline{C}-\epsilon$	$\cdots$	0	0	0	$\cdots$	0	0	ϵ	$\cdots$	0	0	$\cdots$	0		0	0	$\cdots$	0	0	0	$\cdots$	0		1	1	$\cdots$	0	0	0	$\cdots$	0		0	$\cdots$	0	0	0	$\cdots$	0
		$\vdots$	$\vdots$	$\vdots$	$\ddots$	$\vdots$	$\vdots$	$\vdots$	$\ddots$	$\vdots$	$\vdots$	$\vdots$	$\ddots$	$\vdots$	$\vdots$	$\ddots$	$\vdots$		$\vdots$	$\vdots$	$\ddots$	$\vdots$	$\vdots$	$\vdots$	$\ddots$	$\vdots$		$\vdots$	$\vdots$	$\ddots$	$\vdots$	$\vdots$	$\vdots$	$\ddots$	$\vdots$		$\vdots$	$\ddots$	$\vdots$	$\vdots$	$\vdots$	$\ddots$	$\vdots$
		$t-1$	$\overline{V}-\underline{C}-\epsilon$	$\overline{V}-\underline{C}-\epsilon$	$\cdots$	$\overline{V}-\underline{C}-\epsilon$	0	0	$\cdots$	0	0	0	$\cdots$	ϵ	0	$\cdots$	0		0	0	$\cdots$	0	0	0	$\cdots$	0		1	1	$\cdots$	1	0	0	$\cdots$	0		0	$\cdots$	0	0	0	$\cdots$	0
	(A5)	t	0	0	$\cdots$	0	$\overline{V}-\underline{C}-\epsilon$	0	$\cdots$	0	0	0	$\cdots$	0	ϵ	$\cdots$	0		0	0	$\cdots$	0	0	0	$\cdots$	0		0	0	$\cdots$	0	1	0	$\cdots$	0		0	$\cdots$	0	1	0	$\cdots$	0
		$\vdots$	$\vdots$	$\vdots$	$\ddots$	$\vdots$	$\vdots$	$\vdots$	$\ddots$	$\vdots$	$\vdots$	$\vdots$	$\ddots$	$\vdots$	$\vdots$	$\ddots$	$\vdots$		$\vdots$	$\vdots$	$\ddots$	$\vdots$	$\vdots$	$\vdots$	$\ddots$	$\vdots$		$\vdots$	$\vdots$	$\ddots$	$\vdots$	$\vdots$	$\vdots$	$\ddots$	$\vdots$		$\vdots$	$\ddots$	$\vdots$	$\vdots$	$\vdots$	$\ddots$	$\vdots$
		T	0	0	$\cdots$	0	$\overline{V}-\underline{C}$	$\overline{V}-\underline{C}$	$\cdots$	$\overline{V}-\underline{C}-\epsilon$	0	0	$\cdots$	0	0	$\cdots$	ϵ		0	0	$\cdots$	0	0	0	$\cdots$	0		0	0	$\cdots$	0	1	1	$\cdots$	1		0	$\cdots$	0	1	0	$\cdots$	0
$\check{\boldsymbol{\theta}}^{\alpha}$	(A6)	1	$\overline{V}-\underline{C}-\epsilon$	0	$\cdots$	0	0	0	$\cdots$	0	0	0	$\cdots$	0	0	$\cdots$	0		ϵ	0	$\cdots$	0	0	0	$\cdots$	0		1	0	$\cdots$	0	0	0	$\cdots$	0		0	$\cdots$	0	0	0	$\cdots$	0
		2	$\overline{V}-\underline{C}-\epsilon$	$\overline{V}-\underline{C}-\epsilon$	$\cdots$	0	0	0	$\cdots$	0	0	0	$\cdots$	0	0	$\cdots$	0		0	ϵ	$\cdots$	0	0	0	$\cdots$	0		1	1	$\cdots$	0	0	0	$\cdots$	0		0	$\cdots$	0	0	0	$\cdots$	0
		$\vdots$	$\vdots$	$\vdots$	$\ddots$	$\vdots$	$\vdots$	$\vdots$	$\ddots$	$\vdots$	$\vdots$	$\vdots$	$\ddots$	$\vdots$	$\vdots$	$\ddots$	$\vdots$		$\vdots$	$\vdots$	$\ddots$	$\vdots$	$\vdots$	$\vdots$	$\ddots$	$\vdots$		$\vdots$	$\vdots$	$\ddots$	$\vdots$	$\vdots$	$\vdots$	$\ddots$	$\vdots$		$\vdots$	$\ddots$	$\vdots$	$\vdots$	$\vdots$	$\ddots$	$\vdots$
	(A7)	$t-1$	$\overline{V}-\underline{C}$	$\overline{V}-\underline{C}$	$\cdots$	$\overline{V}-\underline{C}$	$\overline{V}-\underline{C}+V$	$\overline{V}-\underline{C}+V$	$\cdots$	$\overline{V}-\underline{C}+V$	0	0	$\cdots$	0	0	$\cdots$	0		0	0	$\cdots$	ϵ	0	0	$\cdots$	0		1	1	$\cdots$	1	1	1	$\cdots$	1		0	$\cdots$	0	0	0	$\cdots$	0
	(A8)	t	0	0	$\cdots$	0	$\overline{V}-\underline{C}$	0	$\cdots$	0	0	0	$\cdots$	0	0	$\cdots$	0		0	0	$\cdots$	0	ϵ	0	$\cdots$	0		0	0	$\cdots$	0	1	0	$\cdots$	0		0	$\cdots$	0	1	0	$\cdots$	0
	(A9)	$t+1$	0	0	$\cdots$	0	$\overline{V}-\underline{C}$	$\overline{V}-\underline{C}-\epsilon$	$\cdots$	0	0	0	$\cdots$	0	0	$\cdots$	0		0	0	$\cdots$	0	0	ϵ	$\cdots$	0		0	0	$\cdots$	0	1	1	$\cdots$	0		0	$\cdots$	0	1	0	$\cdots$	0
		$\vdots$	$\vdots$	$\vdots$	$\ddots$	$\vdots$	$\vdots$	$\vdots$	$\ddots$	$\vdots$	$\vdots$	$\vdots$	$\ddots$	$\vdots$	$\vdots$	$\ddots$	$\vdots$		$\vdots$	$\vdots$	$\ddots$	$\vdots$	$\vdots$	$\vdots$	$\ddots$	$\vdots$		$\vdots$	$\vdots$	$\ddots$	$\vdots$	$\vdots$	$\vdots$	$\ddots$	$\vdots$		$\vdots$	$\ddots$	$\vdots$	$\vdots$	$\vdots$	$\ddots$	$\vdots$
		T	0	0	$\cdots$	0	$\overline{V}-\underline{C}$	$\overline{V}-\underline{C}$	$\cdots$	$\overline{V}-\underline{C}-\epsilon$	0	0	$\cdots$	0	0	$\cdots$	0		0	0	$\cdots$	0	0	0	$\cdots$	ϵ		0	0	$\cdots$	0	1	1	$\cdots$	1		0	$\cdots$	0	1	0	$\cdots$	0
$\overline{\boldsymbol{\theta}}^{\alpha}$		1	$\overline{V}-\underline{C}-\epsilon$	0	$\cdots$	0	0	0	$\cdots$	0	0	0	$\cdots$	0	0	$\cdots$	0		0	0	$\cdots$	0	0	0	$\cdots$	0		1	0	$\cdots$	0	0	0	$\cdots$	0		0	$\cdots$	0	0	0	$\cdots$	0
	(A10)	2	$\overline{V}-\underline{C}-\epsilon$	$\overline{V}-\underline{C}-\epsilon$	$\cdots$	0	0	0	$\cdots$	0	0	0	$\cdots$	0	0	$\cdots$	0		0	0	$\cdots$	0	0	0	$\cdots$	0		1	1	$\cdots$	0	0	0	$\cdots$	0		0	$\cdots$	0	0	0	$\cdots$	0
		$\vdots$	$\vdots$	$\vdots$	$\ddots$	$\vdots$	$\vdots$	$\vdots$	$\ddots$	$\vdots$	$\vdots$	$\vdots$	$\ddots$	$\vdots$	$\vdots$	$\ddots$	$\vdots$		$\vdots$	$\vdots$	$\ddots$	$\vdots$	$\vdots$	$\vdots$	$\ddots$	$\vdots$		$\vdots$	$\vdots$	$\ddots$	$\vdots$	$\vdots$	$\vdots$	$\ddots$	$\vdots$		$\vdots$	$\ddots$	$\vdots$	$\vdots$	$\vdots$	$\ddots$	$\vdots$
		$t-1$	$\overline{V}-\underline{C}-\epsilon$	$\overline{V}-\underline{C}-\epsilon$	$\cdots$	0	0	0	$\cdots$	0	0	0	$\cdots$	0	0	$\cdots$	0		0	0	$\cdots$	0	0	0	$\cdots$	0		1	1	$\cdots$	1	0	0	$\cdots$	0		0	$\cdots$	0	0	0	$\cdots$	0
	(A11)	t	0	0	$\cdots$	0	V	V	$\cdots$	V	0	0	$\cdots$	0	0	$\cdots$	0		0	0	$\cdots$	0	0	0	$\cdots$	0		1	1	$\cdots$	1	1	1	$\cdots$	1		0	$\cdots$	0	0	0	$\cdots$	0
	(A12)	$t+1$	0	0	$\cdots$	0	$\overline{V}-\underline{C}$	$\overline{V}-\underline{C}-\epsilon$	$\cdots$	0	0	0	$\cdots$	0	0	$\cdots$	0		0	0	$\cdots$	0	0	0	$\cdots$	0		0	0	$\cdots$	0	1	1	$\cdots$	0		0	$\cdots$	0	1	0	$\cdots$	0
		$\vdots$	$\vdots$	$\vdots$	$\ddots$	$\vdots$	$\vdots$	$\vdots$	$\ddots$	$\vdots$	$\vdots$	$\vdots$	$\ddots$	$\vdots$	$\vdots$	$\ddots$	$\vdots$		$\vdots$	$\vdots$	$\ddots$	$\vdots$	$\vdots$	$\vdots$	$\ddots$	$\vdots$		$\vdots$	$\vdots$	$\ddots$	$\vdots$	$\vdots$	$\vdots$	$\ddots$	$\vdots$		$\vdots$	$\ddots$	$\vdots$	$\vdots$	$\vdots$	$\ddots$	$\vdots$
		T	0	0	$\cdots$	0	$\overline{V}-\underline{C}$	$\overline{V}-\underline{C}$	$\cdots$	$\overline{V}-\underline{C}-\epsilon$	0	0	$\cdots$	0	0	$\cdots$	0		0	0	$\cdots$	0	0	0	$\cdots$	0		0	0	$\cdots$	0	1	1	$\cdots$	1		0	$\cdots$	0	1	0	$\cdots$	0
$\grave{\boldsymbol{\theta}}^{\alpha}$	(A13)	2	0	$\overline{V}-\underline{C}$	$\cdots$	0	0	0	$\cdots$	0	0	0	$\cdots$	0	0	$\cdots$	0		0	0	$\cdots$	0	0	0	$\cdots$	0		0	1	$\cdots$	0	0	0	$\cdots$	0		1	$\cdots$	0	0	0	$\cdots$	0
		$\vdots$	$\vdots$	$\vdots$	$\ddots$	$\vdots$	$\vdots$	$\vdots$	$\ddots$	$\vdots$	$\vdots$	$\vdots$	$\ddots$	$\vdots$	$\vdots$	$\ddots$	$\vdots$		$\vdots$	$\vdots$	$\ddots$	$\vdots$	$\vdots$	$\vdots$	$\ddots$	$\vdots$		$\vdots$	$\vdots$	$\ddots$	$\vdots$	$\vdots$	$\vdots$	$\ddots$	$\vdots$		$\vdots$	$\ddots$	$\vdots$	$\vdots$	$\vdots$	$\ddots$	$\vdots$
	(A14)	$t-1$	0	0	$\cdots$	0	0	0	$\cdots$	0	0	0	$\cdots$	0	0	$\cdots$	0		0	0	$\cdots$	0	0	0	$\cdots$	0		0	0	$\cdots$	1	0	0	$\cdots$	0		0	$\cdots$	1	0	0	$\cdots$	0
$\check{\boldsymbol{\theta}}^{\alpha}$		t	0	0	$\cdots$	0	$\overline{V}-\underline{C}$	0	$\cdots$	0	0	0	$\cdots$	0	0	$\cdots$	0		0	0	$\cdots$	0	0	0	$\cdots$	0		0	0	$\cdots$	0	1	0	$\cdots$	0		0	$\cdots$	0	1	0	$\cdots$	0
		$t+1$	0	0	$\cdots$	0	0	$\overline{V}-\underline{C}$	$\cdots$	0	0	0	$\cdots$	0	0	$\cdots$	0		0	0	$\cdots$	0	0	0	$\cdots$	0		0	0	$\cdots$	0	0	1	$\cdots$	0		0	$\cdots$	0	0	1	$\cdots$	0
	(A13)	$\vdots$	$\vdots$	$\vdots$	$\ddots$	$\vdots$	$\vdots$	$\vdots$	$\ddots$	$\vdots$	$\vdots$	$\vdots$	$\ddots$	$\vdots$	$\vdots$	$\ddots$	$\vdots$		$\vdots$	$\vdots$	$\ddots$	$\vdots$	$\vdots$	$\vdots$	$\ddots$	$\vdots$		$\vdots$	$\vdots$	$\ddots$	$\vdots$	$\vdots$	$\vdots$	$\ddots$	$\vdots$		$\vdots$	$\ddots$	$\vdots$	$\vdots$	$\vdots$	$\ddots$	$\vdots$
		T	0	0	$\cdots$	0	0	0	$\cdots$	$\overline{V}-\underline{C}$	0	0	$\cdots$	0	0	$\cdots$	0		0	0	$\cdots$	0	0	0	$\cdots$	0		0	0	$\cdots$	0	0	0	$\cdots$	1		0	$\cdots$	0	0	0	$\cdots$	1

Table C.9. Matrix with The Rows Representing $5T-2$ Points in $\mathrm{conv}(\mathcal{D})$ That Satisfy Inequality (4.38) at Equality When $k=2$

Point	Group	Index α	$\mathbf{p}$									$\mathbf{r}^+$								$\mathbf{r}^-$								$\mathbf{y}$								$\mathbf{u}$							
			1	2	$\cdots$	$t-2$	$t-1$	t	$t+1$	$\cdots$	T	1	2	$\cdots$	$t-1$	t	$t+1$	$\cdots$	T	1	2	$\cdots$	$t-2$	$t-1$	t	$t+1$	$\cdots$	T	1	2	$\cdots$	$t-1$	t	$t+1$	$\cdots$	T	2	$\cdots$	$t-2$	$t-1$	t	$t+1$	$\cdots$	T
$\grave{\boldsymbol{\theta}}^\alpha$		1	$\overline{V}-\underline{C}$	0	$\cdots$	0	0	0	0	$\cdots$	0	0	0	$\cdots$	0	0	0	$\cdots$	0	0	0	$\cdots$	0	0	0	0	$\cdots$	0	1	0	$\cdots$	0	0	0	$\cdots$	0	0	$\cdots$	0	0	0	0	$\cdots$	0
		2	$\overline{V}-\underline{C}$	$\overline{V}-\underline{C}$	$\cdots$	0	0	0	0	$\cdots$	0	0	0	$\cdots$	0	0	0	$\cdots$	0	0	0	$\cdots$	0	0	0	0	$\cdots$	0	1	1	$\cdots$	0	0	0	$\cdots$	0	0	$\cdots$	0	0	0	0	$\cdots$	0
	(A1)	$\vdots$	$\vdots$	$\vdots$	$\ddots$	$\vdots$	$\vdots$	$\vdots$	$\vdots$	$\ddots$	$\vdots$	$\vdots$	$\vdots$	$\ddots$	$\vdots$	$\vdots$	$\vdots$	$\ddots$	$\vdots$	$\vdots$	$\vdots$	$\ddots$	$\vdots$	$\vdots$	$\vdots$	$\vdots$	$\ddots$	$\vdots$	$\vdots$	$\vdots$	$\ddots$	$\vdots$	$\vdots$	$\vdots$	$\ddots$	$\vdots$	$\vdots$	$\ddots$	$\vdots$	$\vdots$	$\vdots$	$\vdots$	$\ddots$	$\vdots$
		$t-1$	$\overline{V}-\underline{C}$	$\overline{V}-\underline{C}$	$\cdots$	0	$\overline{V}-\underline{C}$	0	0	$\cdots$	0	0	0	$\cdots$	0	0	0	$\cdots$	0	0	0	$\cdots$	0	0	0	0	$\cdots$	0	1	1	$\cdots$	1	0	0	$\cdots$	0	0	$\cdots$	0	0	0	0	$\cdots$	0
	(A2)	t	$\overline{V}-\underline{C}$	$\overline{V}-\underline{C}$	$\cdots$	$\overline{V}-\underline{C}$	$\overline{V}-\underline{C}+V$	$\overline{V}-\underline{C}+2V$	$\overline{V}-\underline{C}+2V$	$\cdots$	$\overline{V}-\underline{C}+2V$	0	0	$\cdots$	0	0	0	$\cdots$	0	0	0	$\cdots$	0	0	0	0	$\cdots$	0	1	1	$\cdots$	1	1	1	$\cdots$	1	0	$\cdots$	0	0	0	0	$\cdots$	0
		$t+1$	0	0	$\cdots$	0	0	$\overline{V}-\underline{C}$	$\overline{V}-\underline{C}$	$\cdots$	0	0	0	$\cdots$	0	0	0	$\cdots$	0	0	0	$\cdots$	0	0	0	0	$\cdots$	0	0	0	$\cdots$	0	1	1	$\cdots$	0	0	$\cdots$	0	0	1	0	$\cdots$	0
	(A3)	$\vdots$	$\vdots$	$\vdots$	$\ddots$	$\vdots$	$\vdots$	$\vdots$	$\vdots$	$\ddots$	$\vdots$	$\vdots$	$\vdots$	$\ddots$	$\vdots$	$\vdots$	$\vdots$	$\ddots$	$\vdots$	$\vdots$	$\vdots$	$\ddots$	$\vdots$	$\vdots$	$\vdots$	$\vdots$	$\ddots$	$\vdots$	$\vdots$	$\vdots$	$\ddots$	$\vdots$	$\vdots$	$\vdots$	$\ddots$	$\vdots$	$\vdots$	$\ddots$	$\vdots$	$\vdots$	$\vdots$	$\vdots$	$\ddots$	$\vdots$
		T	0	0	$\cdots$	0	0	$\overline{V}-\underline{C}$	$\overline{V}-\underline{C}$	$\cdots$	$\overline{V}-\underline{C}$	0	0	$\cdots$	0	0	0	$\cdots$	0	0	0	$\cdots$	0	0	0	0	$\cdots$	0	0	1	$\cdots$	1	1	1	$\cdots$	1	0	$\cdots$	0	0	1	0	$\cdots$	0
$\hat{\boldsymbol{\theta}}^\alpha$		1	$\overline{V}-\underline{C}-\epsilon$	0	$\cdots$	0	0	0	0	$\cdots$	0	ϵ	0	$\cdots$	0	0	0	$\cdots$	0	0	0	$\cdots$	0	0	0	0	$\cdots$	0	1	0	$\cdots$	0	0	0	$\cdots$	0	0	$\cdots$	0	0	0	0	$\cdots$	0
		2	$\overline{V}-\underline{C}-\epsilon$	$\overline{V}-\underline{C}-\epsilon$	$\cdots$	0	0	0	0	$\cdots$	0	0	ϵ	$\cdots$	0	0	0	$\cdots$	0	0	0	$\cdots$	0	0	0	0	$\cdots$	0	1	1	$\cdots$	0	0	0	$\cdots$	0	0	$\cdots$	0	0	0	0	$\cdots$	0
	(A4)	$\vdots$	$\vdots$	$\vdots$	$\ddots$	$\vdots$	$\vdots$	$\vdots$	$\vdots$	$\ddots$	$\vdots$	$\vdots$	$\vdots$	$\ddots$	$\vdots$	$\vdots$	$\vdots$	$\ddots$	$\vdots$	$\vdots$	$\vdots$	$\ddots$	$\vdots$	$\vdots$	$\vdots$	$\vdots$	$\ddots$	$\vdots$	$\vdots$	$\vdots$	$\ddots$	$\vdots$	$\vdots$	$\vdots$	$\ddots$	$\vdots$	$\vdots$	$\ddots$	$\vdots$	$\vdots$	$\vdots$	$\vdots$	$\ddots$	$\vdots$
		$t-1$	$\overline{V}-\underline{C}-\epsilon$	$\overline{V}-\underline{C}-\epsilon$	$\cdots$	0	$\overline{V}-\underline{C}-\epsilon$	0	0	$\cdots$	0	0	0	$\cdots$	ϵ	0	0	$\cdots$	0	0	0	$\cdots$	0	0	0	0	$\cdots$	0	1	1	$\cdots$	1	0	0	$\cdots$	0	0	$\cdots$	0	0	0	0	$\cdots$	0
		t	0	0	$\cdots$	0	0	$\overline{V}-\underline{C}-\epsilon$	0	$\cdots$	0	0	0	$\cdots$	0	ϵ	0	$\cdots$	0	0	0	$\cdots$	0	0	0	0	$\cdots$	0	0	0	$\cdots$	0	1	0	$\cdots$	0	0	$\cdots$	0	0	1	0	$\cdots$	0
	(A5)	$t+1$	0	0	$\cdots$	0	0	$\overline{V}-\underline{C}$	$\overline{V}-\underline{C}-\epsilon$	$\cdots$	0	0	0	$\cdots$	0	0	ϵ	$\cdots$	0	0	0	$\cdots$	0	0	0	0	$\cdots$	0	0	0	$\cdots$	0	1	1	$\cdots$	0	0	$\cdots$	0	0	1	0	$\cdots$	0
		$\vdots$	$\vdots$	$\vdots$	$\ddots$	$\vdots$	$\vdots$	$\vdots$	$\vdots$	$\ddots$	$\vdots$	$\vdots$	$\vdots$	$\ddots$	$\vdots$	$\vdots$	$\vdots$	$\ddots$	$\vdots$	$\vdots$	$\vdots$	$\ddots$	$\vdots$	$\vdots$	$\vdots$	$\vdots$	$\ddots$	$\vdots$	$\vdots$	$\vdots$	$\ddots$	$\vdots$	$\vdots$	$\vdots$	$\ddots$	$\vdots$	$\vdots$	$\ddots$	$\vdots$	$\vdots$	$\vdots$	$\vdots$	$\ddots$	$\vdots$
		T	0	0	$\cdots$	0	0	$\overline{V}-\underline{C}$	$\overline{V}-\underline{C}$	$\cdots$	$\overline{V}-\underline{C}-\epsilon$	0	0	$\cdots$	0	0	0	$\cdots$	ϵ	0	0	$\cdots$	0	0	0	0	$\cdots$	0	0	0	$\cdots$	0	1	1	$\cdots$	1	0	$\cdots$	0	0	1	0	$\cdots$	0
$\check{\boldsymbol{\theta}}^\alpha$		1	$\overline{V}-\underline{C}-\epsilon$	0	$\cdots$	0	0	0	0	$\cdots$	0	0	0	$\cdots$	0	0	0	$\cdots$	0	ϵ	0	$\cdots$	0	0	0	0	$\cdots$	0	1	0	$\cdots$	0	0	0	$\cdots$	0	0	$\cdots$	0	0	0	0	$\cdots$	0
		2	$\overline{V}-\underline{C}-\epsilon$	$\overline{V}-\underline{C}-\epsilon$	$\cdots$	0	0	0	0	$\cdots$	0	0	0	$\cdots$	0	0	0	$\cdots$	0	0	ϵ	$\cdots$	0	0	0	0	$\cdots$	0	1	1	$\cdots$	0	0	0	$\cdots$	0	0	$\cdots$	0	0	0	0	$\cdots$	0
	(A6)	$\vdots$	$\vdots$	$\vdots$	$\ddots$	$\vdots$	$\vdots$	$\vdots$	$\vdots$	$\ddots$	$\vdots$	$\vdots$	$\vdots$	$\ddots$	$\vdots$	$\vdots$	$\vdots$	$\ddots$	$\vdots$	$\vdots$	$\vdots$	$\ddots$	$\vdots$	$\vdots$	$\vdots$	$\vdots$	$\ddots$	$\vdots$	$\vdots$	$\vdots$	$\ddots$	$\vdots$	$\vdots$	$\vdots$	$\ddots$	$\vdots$	$\vdots$	$\ddots$	$\vdots$	$\vdots$	$\vdots$	$\vdots$	$\ddots$	$\vdots$
	(A7)	$t-2$	$\overline{V}-\underline{C}$	$\overline{V}-\underline{C}$	$\cdots$	$\overline{V}-\underline{C}$	$\overline{V}-\underline{C}+V$	$\overline{V}-\underline{C}+2V$	$\overline{V}-\underline{C}+2V$	$\cdots$	$\overline{V}-\underline{C}+2V$	0	0	$\cdots$	0	0	0	$\cdots$	0	0	0	$\cdots$	ϵ	0	0	0	$\cdots$	0	1	1	$\cdots$	1	1	1	$\cdots$	1	0	$\cdots$	0	0	0	0	$\cdots$	0
$\check{\boldsymbol{\theta}}^\alpha$	(A6)	$t-1$	$\overline{V}-\underline{C}-\epsilon$	$\overline{V}-\underline{C}-\epsilon$	$\cdots$	0	$\overline{V}-\underline{C}-\epsilon$	0	0	$\cdots$	0	0	0	$\cdots$	0	0	0	$\cdots$	0	0	0	$\cdots$	0	ϵ	0	0	$\cdots$	0	1	1	$\cdots$	1	0	0	$\cdots$	0	0	$\cdots$	0	0	0	0	$\cdots$	0
	(A8)	t	0	0	$\cdots$	0	0	$\overline{V}-\underline{C}$	0	$\cdots$	0	0	0	$\cdots$	0	0	0	$\cdots$	0	0	0	$\cdots$	0	0	ϵ	0	$\cdots$	0	0	0	$\cdots$	0	1	0	$\cdots$	0	0	$\cdots$	0	0	1	0	$\cdots$	0
		$t+1$	0	0	$\cdots$	0	0	$\overline{V}-\underline{C}$	$\overline{V}-\underline{C}-\epsilon$	$\cdots$	0	0	0	$\cdots$	0	0	0	$\cdots$	0	0	0	$\cdots$	0	0	0	ϵ	$\cdots$	0	0	0	$\cdots$	0	1	1	$\cdots$	0	0	$\cdots$	0	0	1	0	$\cdots$	0
	(A9)	$\vdots$	$\vdots$	$\vdots$	$\ddots$	$\vdots$	$\vdots$	$\vdots$	$\vdots$	$\ddots$	$\vdots$	$\vdots$	$\vdots$	$\ddots$	$\vdots$	$\vdots$	$\vdots$	$\ddots$	$\vdots$	$\vdots$	$\vdots$	$\ddots$	$\vdots$	$\vdots$	$\vdots$	$\vdots$	$\ddots$	$\vdots$	$\vdots$	$\vdots$	$\ddots$	$\vdots$	$\vdots$	$\vdots$	$\ddots$	$\vdots$	$\vdots$	$\ddots$	$\vdots$	$\vdots$	$\vdots$	$\vdots$	$\ddots$	$\vdots$
		T	0	0	$\cdots$	0	0	$\overline{V}-\underline{C}$	$\overline{V}-\underline{C}$	$\cdots$	$\overline{V}-\underline{C}-\epsilon$	0	0	$\cdots$	0	0	0	$\cdots$	0	0	0	$\cdots$	0	0	0	0	$\cdots$	ϵ	0	0	$\cdots$	0	1	1	$\cdots$	1	0	$\cdots$	0	0	1	0	$\cdots$	0
$\overline{\boldsymbol{\theta}}^\alpha$		1	$\overline{V}-\underline{C}-\epsilon$	0	$\cdots$	0	0	0	0	$\cdots$	0	0	0	$\cdots$	0	0	0	$\cdots$	0	0	0	$\cdots$	0	0	0	0	$\cdots$	0	1	0	$\cdots$	0	0	0	$\cdots$	0	0	$\cdots$	0	0	0	0	$\cdots$	0
		2	$\overline{V}-\underline{C}-\epsilon$	$\overline{V}-\underline{C}-\epsilon$	$\cdots$	0	0	0	0	$\cdots$	0	0	0	$\cdots$	0	0	0	$\cdots$	0	0	0	$\cdots$	0	0	0	0	$\cdots$	0	1	1	$\cdots$	0	0	0	$\cdots$	0	0	$\cdots$	0	0	0	0	$\cdots$	0
	(A10)	$\vdots$	$\vdots$	$\vdots$	$\ddots$	$\vdots$	$\vdots$	$\vdots$	$\vdots$	$\ddots$	$\vdots$	$\vdots$	$\vdots$	$\ddots$	$\vdots$	$\vdots$	$\vdots$	$\ddots$	$\vdots$	$\vdots$	$\vdots$	$\ddots$	$\vdots$	$\vdots$	$\vdots$	$\vdots$	$\ddots$	$\vdots$	$\vdots$	$\vdots$	$\ddots$	$\vdots$	$\vdots$	$\vdots$	$\ddots$	$\vdots$	$\vdots$	$\ddots$	$\vdots$	$\vdots$	$\vdots$	$\vdots$	$\ddots$	$\vdots$
		$t-1$	$\overline{V}-\underline{C}-\epsilon$	$\overline{V}-\underline{C}-\epsilon$	$\cdots$	0	$\overline{V}-\underline{C}-\epsilon$	0	0	$\cdots$	0	0	0	$\cdots$	0	0	0	$\cdots$	0	0	0	$\cdots$	0	0	0	0	$\cdots$	0	1	1	$\cdots$	1	0	0	$\cdots$	0	0	$\cdots$	0	0	0	0	$\cdots$	0
	(A11)	t	0	0	$\cdots$	0	V	$2V$	$2V$	$\cdots$	$2V$	0	0	$\cdots$	0	0	0	$\cdots$	0	0	0	$\cdots$	0	0	0	0	$\cdots$	0	1	1	$\cdots$	1	1	1	$\cdots$	1	0	$\cdots$	0	0	0	0	$\cdots$	0
		$t+1$	0	0	$\cdots$	0	0	$\overline{V}-\underline{C}$	$\overline{V}-\underline{C}-\epsilon$	$\cdots$	0	0	0	$\cdots$	0	0	0	$\cdots$	0	0	0	$\cdots$	0	0	0	0	$\cdots$	0	0	0	$\cdots$	0	1	1	$\cdots$	0	0	$\cdots$	0	0	1	0	$\cdots$	0
	(A12)	$\vdots$	$\vdots$	$\vdots$	$\ddots$	$\vdots$	$\vdots$	$\vdots$	$\vdots$	$\ddots$	$\vdots$	$\vdots$	$\vdots$	$\ddots$	$\vdots$	$\vdots$	$\vdots$	$\ddots$	$\vdots$	$\vdots$	$\vdots$	$\ddots$	$\vdots$	$\vdots$	$\vdots$	$\vdots$	$\ddots$	$\vdots$	$\vdots$	$\vdots$	$\ddots$	$\vdots$	$\vdots$	$\vdots$	$\ddots$	$\vdots$	$\vdots$	$\ddots$	$\vdots$	$\vdots$	$\vdots$	$\vdots$	$\ddots$	$\vdots$
		T	0	0	$\cdots$	0	0	$\overline{V}-\underline{C}$	$\overline{V}-\underline{C}$	$\cdots$	$\overline{V}-\underline{C}-\epsilon$	0	0	$\cdots$	0	0	0	$\cdots$	0	0	0	$\cdots$	0	0	0	0	$\cdots$	0	0	0	$\cdots$	0	1	1	$\cdots$	1	0	$\cdots$	0	0	1	0	$\cdots$	0
$\hat{\boldsymbol{\theta}}^\alpha$		2	0	$\overline{V}-\underline{C}$	$\cdots$	0	0	0	0	$\cdots$	0	0	0	$\cdots$	0	0	0	$\cdots$	0	0	0	$\cdots$	0	0	0	0	$\cdots$	0	0	1	$\cdots$	0	0	0	$\cdots$	0	1	$\cdots$	0	0	0	0	$\cdots$	0
	(A13)	$\vdots$	$\vdots$	$\vdots$	$\ddots$	$\vdots$	$\vdots$	$\vdots$	$\vdots$	$\ddots$	$\vdots$	$\vdots$	$\vdots$	$\ddots$	$\vdots$	$\vdots$	$\vdots$	$\ddots$	$\vdots$	$\vdots$	$\vdots$	$\ddots$	$\vdots$	$\vdots$	$\vdots$	$\vdots$	$\ddots$	$\vdots$	$\vdots$	$\vdots$	$\ddots$	$\vdots$	$\vdots$	$\vdots$	$\ddots$	$\vdots$	$\vdots$	$\ddots$	$\vdots$	$\vdots$	$\vdots$	$\vdots$	$\ddots$	$\vdots$
	(A14)	$t-2$	0	0	$\cdots$	0	0	0	0	$\cdots$	0	0	0	$\cdots$	0	0	0	$\cdots$	0	0	0	$\cdots$	0	0	0	0	$\cdots$	0	0	0	$\cdots$	0	0	0	$\cdots$	0	0	$\cdots$	1	0	0	0	$\cdots$	0
$\hat{\boldsymbol{\theta}}^\alpha$		$t-1$	0	0	$\cdots$	0	$\overline{V}-\underline{C}$	0	0	$\cdots$	0	0	0	$\cdots$	0	0	0	$\cdots$	0	0	0	$\cdots$	0	0	0	0	$\cdots$	0	0	0	$\cdots$	1	0	0	$\cdots$	0	0	$\cdots$	0	1	0	0	$\cdots$	0
		t	0	0	$\cdots$	0	0	$\overline{V}-\underline{C}$	0	$\cdots$	0	0	0	$\cdots$	0	0	0	$\cdots$	0	0	0	$\cdots$	0	0	0	0	$\cdots$	0	0	0	$\cdots$	0	1	0	$\cdots$	0	0	$\cdots$	0	0	1	0	$\cdots$	0
	(A13)	$t+1$	0	0	$\cdots$	0	0	0	$\overline{V}-\underline{C}$	$\cdots$	0	0	0	$\cdots$	0	0	0	$\cdots$	0	0	0	$\cdots$	0	0	0	0	$\cdots$	0	0	0	$\cdots$	0	0	1	$\cdots$	0	0	$\cdots$	0	0	0	1	$\cdots$	0
		$\vdots$	$\vdots$	$\vdots$	$\ddots$	$\vdots$	$\vdots$	$\vdots$	$\vdots$	$\ddots$	$\vdots$	$\vdots$	$\vdots$	$\ddots$	$\vdots$	$\vdots$	$\vdots$	$\ddots$	$\vdots$	$\vdots$	$\vdots$	$\ddots$	$\vdots$	$\vdots$	$\vdots$	$\vdots$	$\ddots$	$\vdots$	$\vdots$	$\vdots$	$\ddots$	$\vdots$	$\vdots$	$\vdots$	$\ddots$	$\vdots$	$\vdots$	$\ddots$	$\vdots$	$\vdots$	$\vdots$	$\vdots$	$\ddots$	$\vdots$
		T	0	0	$\cdots$	0	0	0	0	$\cdots$	$\overline{V}-\underline{C}$	0	0	$\cdots$	0	0	0	$\cdots$	0	0	0	$\cdots$	0	0	0	0	$\cdots$	0	0	0	$\cdots$	0	0	0	$\cdots$	1	0	$\cdots$	0	0	0	0	$\cdots$	1

Table C.10. Matrix with the Rows Representing $5T-2$ Points in $\mathrm{conv}(\mathcal{D})$ That Satisfy Inequality (4.38) at Equality When $k \geq 3$

Point	Group	Index α	$\mathbf{p}$							$\mathbf{r}^+$				$\mathbf{r}^-$				$\mathbf{y}$							$\mathbf{u}$						
			1	2	$\cdots$	$t-k$	$\cdots$	t	$\cdots$	T	1	$\cdots$	t	$\cdots$	T	1	$\cdots$	$t-k$	$\cdots$	t	$\cdots$	T	1	2	$\cdots$	$t-k$	$\cdots$	t	$\cdots$	T	2	$\cdots$	$t-k$	$\cdots$	t	$\cdots$	T
$\grave{\boldsymbol{\theta}}^{\alpha}$	(A1)	1	$\overline{V}-\underline{C}$	0	$\cdots$	0	$\cdots$	0	$\cdots$	0	0	$\cdots$	0	$\cdots$	0	0	$\cdots$	0	$\cdots$	0	$\cdots$	0	1	0	$\cdots$	0	$\cdots$	0	$\cdots$	0	0	$\cdots$	0	$\cdots$	0	$\cdots$	0
		$\vdots$	$\vdots$	$\vdots$	$\ddots$	$\vdots$	$\ddots$	$\vdots$	$\ddots$	$\vdots$	$\vdots$	$\ddots$	$\vdots$	$\ddots$	$\vdots$	$\vdots$	$\ddots$	$\vdots$	$\ddots$	$\vdots$	$\ddots$	$\vdots$	$\vdots$	$\vdots$	$\ddots$	$\vdots$	$\ddots$	$\vdots$	$\ddots$	$\vdots$	$\vdots$	$\ddots$	$\vdots$	$\ddots$	$\vdots$	$\ddots$	$\vdots$
	(A2)	t	$\overline{V}-\underline{C}$	$\overline{V}-\underline{C}$	$\cdots$	$\overline{V}-\underline{C}$	$\cdots$	$\overline{V}-\underline{C}+kV$	$\cdots$	$\overline{V}-\underline{C}+kV$	0	$\cdots$	0	$\cdots$	0	0	$\cdots$	0	$\cdots$	0	$\cdots$	0	1	1	$\cdots$	1	$\cdots$	1	$\cdots$	1	0	$\cdots$	0	$\cdots$	0	$\cdots$	0
	(A3)	$\vdots$	$\vdots$	$\vdots$	$\ddots$	$\vdots$	$\ddots$	$\vdots$	$\ddots$	$\vdots$	$\vdots$	$\ddots$	$\vdots$	$\ddots$	$\vdots$	$\vdots$	$\ddots$	$\vdots$	$\ddots$	$\vdots$	$\ddots$	$\vdots$	$\vdots$	$\vdots$	$\ddots$	$\vdots$	$\ddots$	$\vdots$	$\ddots$	$\vdots$	$\vdots$	$\ddots$	$\vdots$	$\ddots$	$\vdots$	$\ddots$	$\vdots$
		T	0	0	$\cdots$	0	$\cdots$	$\overline{V}-\underline{C}$	$\cdots$	$\overline{V}-\underline{C}$	0	$\cdots$	0	$\cdots$	0	0	$\cdots$	0	$\cdots$	0	$\cdots$	0	0	0	$\cdots$	0	$\cdots$	1	$\cdots$	1	0	$\cdots$	0	$\cdots$	1	$\cdots$	0
$\hat{\boldsymbol{\theta}}^{\alpha}$	(A4)	1	$\overline{V}-\underline{C}-\epsilon$	0	$\cdots$	0	$\cdots$	0	$\cdots$	0	ϵ	$\cdots$	0	$\cdots$	0	0	$\cdots$	0	$\cdots$	0	$\cdots$	0	1	0	$\cdots$	0	$\cdots$	0	$\cdots$	0	0	$\cdots$	0	$\cdots$	0	$\cdots$	0
		$\vdots$	$\vdots$	$\vdots$	$\ddots$	$\vdots$	$\ddots$	$\vdots$	$\ddots$	$\vdots$	$\vdots$	$\ddots$	$\vdots$	$\ddots$	$\vdots$	$\vdots$	$\ddots$	$\vdots$	$\ddots$	$\vdots$	$\ddots$	$\vdots$	$\vdots$	$\vdots$	$\ddots$	$\vdots$	$\ddots$	$\vdots$	$\ddots$	$\vdots$	$\vdots$	$\ddots$	$\vdots$	$\ddots$	$\vdots$	$\ddots$	$\vdots$
	(A5)	t	0	0	$\cdots$	0	$\cdots$	$\overline{V}-\underline{C}-\epsilon$	$\cdots$	0	0	$\cdots$	ϵ	$\cdots$	0	0	$\cdots$	0	$\cdots$	0	$\cdots$	0	0	0	$\cdots$	0	$\cdots$	1	$\cdots$	0	0	$\cdots$	0	$\cdots$	1	$\cdots$	0
		$\vdots$	$\vdots$	$\vdots$	$\ddots$	$\vdots$	$\ddots$	$\vdots$	$\ddots$	$\vdots$	$\vdots$	$\ddots$	$\vdots$	$\ddots$	$\vdots$	$\vdots$	$\ddots$	$\vdots$	$\ddots$	$\vdots$	$\ddots$	$\vdots$	$\vdots$	$\vdots$	$\ddots$	$\vdots$	$\ddots$	$\vdots$	$\ddots$	$\vdots$	$\vdots$	$\ddots$	$\vdots$	$\ddots$	$\vdots$	$\ddots$	$\vdots$
		T	0	0	$\cdots$	0	$\cdots$	$\overline{V}-\underline{C}$	$\cdots$	$\overline{V}-\underline{C}-\epsilon$	0	$\cdots$	0	$\cdots$	ϵ	0	$\cdots$	0	$\cdots$	0	$\cdots$	0	0	0	$\cdots$	0	$\cdots$	1	$\cdots$	1	0	$\cdots$	0	$\cdots$	1	$\cdots$	0
$\hat{\boldsymbol{\theta}}^{\alpha}$	(A6)	1	$\overline{V}-\underline{C}-\epsilon$	0	$\cdots$	0	$\cdots$	0	$\cdots$	0	0	$\cdots$	0	$\cdots$	0	ϵ	$\cdots$	0	$\cdots$	0	$\cdots$	0	1	0	$\cdots$	0	$\cdots$	0	$\cdots$	0	0	$\cdots$	0	$\cdots$	0	$\cdots$	0
		$\vdots$	$\vdots$	$\vdots$	$\ddots$	$\vdots$	$\ddots$	$\vdots$	$\ddots$	$\vdots$	$\vdots$	$\ddots$	$\vdots$	$\ddots$	$\vdots$	$\vdots$	$\ddots$	$\vdots$	$\ddots$	$\vdots$	$\ddots$	$\vdots$	$\vdots$	$\vdots$	$\ddots$	$\vdots$	$\ddots$	$\vdots$	$\ddots$	$\vdots$	$\vdots$	$\ddots$	$\vdots$	$\ddots$	$\vdots$	$\ddots$	$\vdots$
	(A7)	$t-k$	$\overline{V}-\underline{C}$	$\overline{V}-\underline{C}$	$\cdots$	$\overline{V}-\underline{C}$	$\cdots$	$\overline{V}-\underline{C}+kV$	$\cdots$	$\overline{V}-\underline{C}+kV$	0	$\cdots$	0	$\cdots$	0	0	$\cdots$	ϵ	$\cdots$	0	$\cdots$	0	1	1	$\cdots$	1	$\cdots$	1	$\cdots$	1	0	$\cdots$	0	$\cdots$	0	$\cdots$	0
	(A6)	$\vdots$	$\vdots$	$\vdots$	$\ddots$	$\vdots$	$\ddots$	$\vdots$	$\ddots$	$\vdots$	$\vdots$	$\ddots$	$\vdots$	$\ddots$	$\vdots$	$\vdots$	$\ddots$	$\vdots$	$\ddots$	$\vdots$	$\ddots$	$\vdots$	$\vdots$	$\vdots$	$\ddots$	$\vdots$	$\ddots$	$\vdots$	$\ddots$	$\vdots$	$\vdots$	$\ddots$	$\vdots$	$\ddots$	$\vdots$	$\ddots$	$\vdots$
	(A8)	t	0	0	$\cdots$	0	$\cdots$	$\overline{V}-\underline{C}$	$\cdots$	0	0	$\cdots$	0	$\cdots$	0	0	$\cdots$	0	$\cdots$	ϵ	$\cdots$	0	0	0	$\cdots$	0	$\cdots$	1	$\cdots$	0	0	$\cdots$	0	$\cdots$	1	$\cdots$	0
	(A9)	$\vdots$	$\vdots$	$\vdots$	$\ddots$	$\vdots$	$\ddots$	$\vdots$	$\ddots$	$\vdots$	$\vdots$	$\ddots$	$\vdots$	$\ddots$	$\vdots$	$\vdots$	$\ddots$	$\vdots$	$\ddots$	$\vdots$	$\ddots$	$\vdots$	$\vdots$	$\vdots$	$\ddots$	$\vdots$	$\ddots$	$\vdots$	$\ddots$	$\vdots$	$\vdots$	$\ddots$	$\vdots$	$\ddots$	$\vdots$	$\ddots$	$\vdots$
		T	0	0	$\cdots$	0	$\cdots$	$\overline{V}-\underline{C}$	$\cdots$	$\overline{V}-\underline{C}-\epsilon$	0	$\cdots$	0	$\cdots$	0	0	$\cdots$	0	$\cdots$	0	$\cdots$	ϵ	0	0	$\cdots$	0	$\cdots$	1	$\cdots$	1	0	$\cdots$	0	$\cdots$	1	$\cdots$	0
$\overline{\boldsymbol{\theta}}^{\alpha}$	(A10)	1	$\overline{V}-\underline{C}-\epsilon$	0	$\cdots$	0	$\cdots$	0	$\cdots$	0	0	$\cdots$	0	$\cdots$	0	0	$\cdots$	0	$\cdots$	0	$\cdots$	0	1	0	$\cdots$	0	$\cdots$	0	$\cdots$	0	0	$\cdots$	0	$\cdots$	0	$\cdots$	0
		$\vdots$	$\vdots$	$\vdots$	$\ddots$	$\vdots$	$\ddots$	$\vdots$	$\ddots$	$\vdots$	$\vdots$	$\ddots$	$\vdots$	$\ddots$	$\vdots$	$\vdots$	$\ddots$	$\vdots$	$\ddots$	$\vdots$	$\ddots$	$\vdots$	$\vdots$	$\vdots$	$\ddots$	$\vdots$	$\ddots$	$\vdots$	$\ddots$	$\vdots$	$\vdots$	$\ddots$	$\vdots$	$\ddots$	$\vdots$	$\ddots$	$\vdots$
	(A11)	t	0	0	$\cdots$	0	$\cdots$	kV	$\cdots$	kV	0	$\cdots$	0	$\cdots$	0	0	$\cdots$	0	$\cdots$	0	$\cdots$	0	1	1	$\cdots$	1	$\cdots$	1	$\cdots$	1	0	$\cdots$	0	$\cdots$	0	$\cdots$	0
	(A12)	$t+1$	0	0	$\cdots$	0	$\cdots$	$\overline{V}-\underline{C}$	$\cdots$	0	0	$\cdots$	0	$\cdots$	0	0	$\cdots$	0	$\cdots$	0	$\cdots$	0	0	0	$\cdots$	0	$\cdots$	1	$\cdots$	0	0	$\cdots$	0	$\cdots$	1	$\cdots$	0
		$\vdots$	$\vdots$	$\vdots$	$\ddots$	$\vdots$	$\ddots$	$\vdots$	$\ddots$	$\vdots$	$\vdots$	$\ddots$	$\vdots$	$\ddots$	$\vdots$	$\vdots$	$\ddots$	$\vdots$	$\ddots$	$\vdots$	$\ddots$	$\vdots$	$\vdots$	$\vdots$	$\ddots$	$\vdots$	$\ddots$	$\vdots$	$\ddots$	$\vdots$	$\vdots$	$\ddots$	$\vdots$	$\ddots$	$\vdots$	$\ddots$	$\vdots$
		T	0	0	$\cdots$	0	$\cdots$	$\overline{V}-\underline{C}$	$\cdots$	$\overline{V}-\underline{C}-\epsilon$	0	$\cdots$	0	$\cdots$	0	0	$\cdots$	0	$\cdots$	0	$\cdots$	0	0	0	$\cdots$	0	$\cdots$	1	$\cdots$	1	0	$\cdots$	0	$\cdots$	1	$\cdots$	0
$\dot{\boldsymbol{\theta}}^{\alpha}$	(A13)	2	0	$\overline{V}-\underline{C}$	$\cdots$	0	$\cdots$	0	$\cdots$	0	0	$\cdots$	0	$\cdots$	0	0	$\cdots$	0	$\cdots$	0	$\cdots$	0	0	1	$\cdots$	0	$\cdots$	0	$\cdots$	0	1	$\cdots$	0	$\cdots$	0	$\cdots$	0
		$\vdots$	$\vdots$	$\vdots$	$\ddots$	$\vdots$	$\ddots$	$\vdots$	$\ddots$	$\vdots$	$\vdots$	$\ddots$	$\vdots$	$\ddots$	$\vdots$	$\vdots$	$\ddots$	$\vdots$	$\ddots$	$\vdots$	$\ddots$	$\vdots$	$\vdots$	$\vdots$	$\ddots$	$\vdots$	$\ddots$	$\vdots$	$\ddots$	$\vdots$	$\vdots$	$\ddots$	$\vdots$	$\ddots$	$\vdots$	$\ddots$	$\vdots$
	(A14)	$t-k$	0	0	$\cdots$	0	$\cdots$	0	$\cdots$	0	0	$\cdots$	0	$\cdots$	0	0	$\cdots$	0	$\cdots$	0	$\cdots$	0	0	0	$\cdots$	1	$\cdots$	0	$\cdots$	0	0	$\cdots$	1	$\cdots$	0	$\cdots$	0
	(A13)	$\vdots$	$\vdots$	$\vdots$	$\ddots$	$\vdots$	$\ddots$	$\vdots$	$\ddots$	$\vdots$	$\vdots$	$\ddots$	$\vdots$	$\ddots$	$\vdots$	$\vdots$	$\ddots$	$\vdots$	$\ddots$	$\vdots$	$\ddots$	$\vdots$	$\vdots$	$\vdots$	$\ddots$	$\vdots$	$\ddots$	$\vdots$	$\ddots$	$\vdots$	$\vdots$	$\ddots$	$\vdots$	$\ddots$	$\vdots$	$\ddots$	$\vdots$
		T	0	0	$\cdots$	0	$\cdots$	0	$\cdots$	$\overline{V}-\underline{C}$	0	$\cdots$	0	$\cdots$	0	0	$\cdots$	0	$\cdots$	0	$\cdots$	0	0	0	$\cdots$	0	$\cdots$	0	$\cdots$	1	0	$\cdots$	0	$\cdots$	0	$\cdots$	1

Table C.11. Lower Triangular Matrix Obtained From Table C.8 via Gaussian Elimination

Point	Group	Index α	$\mathbf{p}$								$\mathbf{r}^+$								$\mathbf{r}^-$								$\mathbf{y}$								$\mathbf{u}$							
			1	2	$\cdots$	$t-1$	t	$t+1$	$\cdots$	T	1	2	$\cdots$	$t-1$	t	$\cdots$	T		1	2	$\cdots$	$t-1$	t	$t+1$	$\cdots$	T		1	2	$\cdots$	$t-1$	t	$t+1$	$\cdots$	T		2	$\cdots$	$t-1$	t	$t+1$	$\cdots$	T
$\underline{\dot{\boldsymbol{\theta}}}^{\alpha}$	(B1)	1	ϵ	0	$\cdots$	0	0	0	$\cdots$	0	0	0	$\cdots$	0	0	$\cdots$	0		0	0	$\cdots$	0	0	0	$\cdots$	0		0	0	$\cdots$	0	0	0	$\cdots$	0		0	$\cdots$	0	0	0	$\cdots$	0
		2	ϵ	ϵ	$\cdots$	0	0	0	$\cdots$	0	0	0	$\cdots$	0	0	$\cdots$	0		0	0	$\cdots$	0	0	0	$\cdots$	0		0	0	$\cdots$	0	0	0	$\cdots$	0		0	$\cdots$	0	0	0	$\cdots$	0
		$\vdots$	$\vdots$	$\vdots$	$\ddots$	$\vdots$	$\vdots$	$\vdots$	$\ddots$	$\vdots$	$\vdots$	$\vdots$	$\ddots$	$\vdots$	$\vdots$	$\ddots$	$\vdots$		$\vdots$	$\vdots$	$\ddots$	$\vdots$	$\vdots$	$\vdots$	$\ddots$	$\vdots$		$\vdots$	$\vdots$	$\ddots$	$\vdots$	$\vdots$	$\vdots$	$\ddots$	$\vdots$		$\vdots$	$\ddots$	$\vdots$	$\vdots$	$\vdots$	$\ddots$	$\vdots$
		t	$\overline{V}-\underline{C}$	$\overline{V}-\underline{C}$	$\cdots$	$\overline{V}-\underline{C}$	$\overline{V}-\underline{C}$	0	$\cdots$	0	0	0	$\cdots$	0	0	$\cdots$	0		0	0	$\cdots$	0	0	0	$\cdots$	0		0	0	$\cdots$	0	0	0	$\cdots$	0		0	$\cdots$	0	0	0	$\cdots$	0
		$t+1$	0	0	$\cdots$	0	0	ϵ	$\cdots$	0	0	0	$\cdots$	0	0	$\cdots$	0		0	0	$\cdots$	0	0	0	$\cdots$	0		0	0	$\cdots$	0	0	0	$\cdots$	0		0	$\cdots$	0	0	0	$\cdots$	0
		$\vdots$	$\vdots$	$\vdots$	$\ddots$	$\vdots$	$\vdots$	$\vdots$	$\ddots$	$\vdots$	$\vdots$	$\vdots$	$\ddots$	$\vdots$	$\vdots$	$\ddots$	$\vdots$		$\vdots$	$\vdots$	$\ddots$	$\vdots$	$\vdots$	$\vdots$	$\ddots$	$\vdots$		$\vdots$	$\vdots$	$\ddots$	$\vdots$	$\vdots$	$\vdots$	$\ddots$	$\vdots$		$\vdots$	$\ddots$	$\vdots$	$\vdots$	$\vdots$	$\ddots$	$\vdots$
		T	0	0	$\cdots$	0	0	0	$\cdots$	ϵ	0	0	$\cdots$	0	0	$\cdots$	0		0	0	$\cdots$	0	0	0	$\cdots$	0		0	0	$\cdots$	0	0	0	$\cdots$	0		0	$\cdots$	0	0	0	$\cdots$	0
$\underline{\dot{\boldsymbol{\theta}}}^{\alpha}$	(B2)	1	0	0	$\cdots$	0	0	0	$\cdots$	0	ϵ	0	$\cdots$	0	0	$\cdots$	0		0	0	$\cdots$	0	0	0	$\cdots$	0		0	0	$\cdots$	0	0	0	$\cdots$	0		0	$\cdots$	0	0	0	$\cdots$	0
		2	0	0	$\cdots$	0	0	0	$\cdots$	0	0	ϵ	$\cdots$	0	0	$\cdots$	0		0	0	$\cdots$	0	0	0	$\cdots$	0		0	0	$\cdots$	0	0	0	$\cdots$	0		0	$\cdots$	0	0	0	$\cdots$	0
		$\vdots$	$\vdots$	$\vdots$	$\ddots$	$\vdots$	$\vdots$	$\vdots$	$\ddots$	$\vdots$	$\vdots$	$\vdots$	$\ddots$	$\vdots$	$\vdots$	$\ddots$	$\vdots$		$\vdots$	$\vdots$	$\ddots$	$\vdots$	$\vdots$	$\vdots$	$\ddots$	$\vdots$		$\vdots$	$\vdots$	$\ddots$	$\vdots$	$\vdots$	$\vdots$	$\ddots$	$\vdots$		$\vdots$	$\ddots$	$\vdots$	$\vdots$	$\vdots$	$\ddots$	$\vdots$
		$t-1$	0	0	$\cdots$	0	0	0	$\cdots$	0	0	0	$\cdots$	ϵ	0	$\cdots$	0		0	0	$\cdots$	0	0	0	$\cdots$	0		0	0	$\cdots$	0	0	0	$\cdots$	0		0	$\cdots$	0	0	0	$\cdots$	0
		t	0	0	$\cdots$	0	$-\epsilon$	0	$\cdots$	0	0	0	$\cdots$	0	ϵ	$\cdots$	0		0	0	$\cdots$	0	0	0	$\cdots$	0		0	0	$\cdots$	0	0	0	$\cdots$	0		0	$\cdots$	0	0	0	$\cdots$	0
		$\vdots$	$\vdots$	$\vdots$	$\ddots$	$\vdots$	$\vdots$	$\vdots$	$\ddots$	$\vdots$	$\vdots$	$\vdots$	$\ddots$	$\vdots$	$\vdots$	$\ddots$	$\vdots$		$\vdots$	$\vdots$	$\ddots$	$\vdots$	$\vdots$	$\vdots$	$\ddots$	$\vdots$		$\vdots$	$\vdots$	$\ddots$	$\vdots$	$\vdots$	$\vdots$	$\ddots$	$\vdots$		$\vdots$	$\ddots$	$\vdots$	$\vdots$	$\vdots$	$\ddots$	$\vdots$
		T	0	0	$\cdots$	0	0	0	$\cdots$	0	0	0	$\cdots$	0	0	$\cdots$	ϵ		0	0	$\cdots$	0	0	0	$\cdots$	0		0	0	$\cdots$	0	0	0	$\cdots$	0		0	$\cdots$	0	0	0	$\cdots$	0
$\underline{\dot{\boldsymbol{\theta}}}^{\alpha}$	(B3)	1	0	0	$\cdots$	0	0	0	$\cdots$	0	0	0	$\cdots$	0	0	$\cdots$	0		ϵ	0	$\cdots$	0	0	0	$\cdots$	0		0	0	$\cdots$	0	0	0	$\cdots$	0		0	$\cdots$	0	0	0	$\cdots$	0
		2	0	0	$\cdots$	0	0	0	$\cdots$	0	0	0	$\cdots$	0	0	$\cdots$	0		0	ϵ	$\cdots$	0	0	0	$\cdots$	0		0	0	$\cdots$	0	0	0	$\cdots$	0		0	$\cdots$	0	0	0	$\cdots$	0
		$\vdots$	$\vdots$	$\vdots$	$\ddots$	$\vdots$	$\vdots$	$\vdots$	$\ddots$	$\vdots$	$\vdots$	$\vdots$	$\ddots$	$\vdots$	$\vdots$	$\ddots$	$\vdots$		$\vdots$	$\vdots$	$\ddots$	$\vdots$	$\vdots$	$\vdots$	$\ddots$	$\vdots$		$\vdots$	$\vdots$	$\ddots$	$\vdots$	$\vdots$	$\vdots$	$\ddots$	$\vdots$		$\vdots$	$\ddots$	$\vdots$	$\vdots$	$\vdots$	$\ddots$	$\vdots$
		$t-1$	$\overline{V}-\underline{C}$	$\overline{V}-\underline{C}$	$\cdots$	$\overline{V}-\underline{C}$	$\overline{V}-\underline{C}$	$\overline{V}-\underline{C}$	$\cdots$	$\overline{V}-\underline{C}$	0	0	$\cdots$	0	0	$\cdots$	0		0	0	$\cdots$	ϵ	0	0	$\cdots$	0		0	0	$\cdots$	0	0	0	$\cdots$	0		0	$\cdots$	0	0	0	$\cdots$	0
		t	0	0	$\cdots$	0	0	0	$\cdots$	0	0	0	$\cdots$	0	0	$\cdots$	0		0	0	$\cdots$	0	ϵ	0	$\cdots$	0		0	0	$\cdots$	0	0	0	$\cdots$	0		0	$\cdots$	0	0	0	$\cdots$	0
		$t+1$	0	0	$\cdots$	0	0	0	$\cdots$	0	0	0	$\cdots$	0	0	$\cdots$	0		0	0	$\cdots$	0	0	ϵ	$\cdots$	0		0	0	$\cdots$	0	0	0	$\cdots$	0		0	$\cdots$	0	0	0	$\cdots$	0
		$\vdots$	$\vdots$	$\vdots$	$\ddots$	$\vdots$	$\vdots$	$\vdots$	$\ddots$	$\vdots$	$\vdots$	$\vdots$	$\ddots$	$\vdots$	$\vdots$	$\ddots$	$\vdots$		$\vdots$	$\vdots$	$\ddots$	$\vdots$	$\vdots$	$\vdots$	$\ddots$	$\vdots$		$\vdots$	$\vdots$	$\ddots$	$\vdots$	$\vdots$	$\vdots$	$\ddots$	$\vdots$		$\vdots$	$\ddots$	$\vdots$	$\vdots$	$\vdots$	$\ddots$	$\vdots$
		T	0	0	$\cdots$	0	0	0	$\cdots$	0	0	0	$\cdots$	0	0	$\cdots$	0		0	0	$\cdots$	0	0	0	$\cdots$	ϵ		0	0	$\cdots$	0	0	0	$\cdots$	0		0	$\cdots$	0	0	0	$\cdots$	0
$\overline{\dot{\boldsymbol{\theta}}}^{\alpha}$	(B4)	1	$\overline{V}-\underline{C}-\epsilon$	0	$\cdots$	0	0	0	$\cdots$	0	0	0	$\cdots$	0	0	$\cdots$	0		0	0	$\cdots$	0	0	0	$\cdots$	0		1	0	$\cdots$	0	0	0	$\cdots$	0		0	$\cdots$	0	0	0	$\cdots$	0
		2	$\overline{V}-\underline{C}-\epsilon$	$\overline{V}-\underline{C}-\epsilon$	$\cdots$	0	0	0	$\cdots$	0	0	0	$\cdots$	0	0	$\cdots$	0		0	0	$\cdots$	0	0	0	$\cdots$	0		1	1	$\cdots$	0	0	0	$\cdots$	0		0	$\cdots$	0	0	0	$\cdots$	0
		$\vdots$	$\vdots$	$\vdots$	$\ddots$	$\vdots$	$\vdots$	$\vdots$	$\ddots$	$\vdots$	$\vdots$	$\vdots$	$\ddots$	$\vdots$	$\vdots$	$\ddots$	$\vdots$		$\vdots$	$\vdots$	$\ddots$	$\vdots$	$\vdots$	$\vdots$	$\ddots$	$\vdots$		$\vdots$	$\vdots$	$\ddots$	$\vdots$	$\vdots$	$\vdots$	$\ddots$	$\vdots$		$\vdots$	$\ddots$	$\vdots$	$\vdots$	$\vdots$	$\ddots$	$\vdots$
		$t-1$	$\overline{V}-\underline{C}-\epsilon$	$\overline{V}-\underline{C}-\epsilon$	$\cdots$	0	0	0	$\cdots$	0	0	0	$\cdots$	0	0	$\cdots$	0		0	0	$\cdots$	0	0	0	$\cdots$	0		1	1	$\cdots$	1	0	0	$\cdots$	0		0	$\cdots$	0	0	0	$\cdots$	0
		t	0	0	$\cdots$	0	V	$V-\overline{V}+\underline{C}$	$\cdots$	$V-\overline{V}+\underline{C}+\epsilon$	0	0	$\cdots$	0	0	$\cdots$	0		0	0	$\cdots$	0	0	0	$\cdots$	0		1	1	$\cdots$	1	1	0	$\cdots$	0		0	$\cdots$	0	0	0	$\cdots$	0
		$t+1$	0	0	$\cdots$	0	0	$\overline{V}-\underline{C}-\epsilon$	$\cdots$	0	0	0	$\cdots$	0	0	$\cdots$	0		0	0	$\cdots$	0	0	0	$\cdots$	0		0	0	$\cdots$	0	0	1	$\cdots$	0		0	$\cdots$	0	0	0	$\cdots$	0
		$\vdots$	$\vdots$	$\vdots$	$\ddots$	$\vdots$	$\vdots$	$\vdots$	$\ddots$	$\vdots$	$\vdots$	$\vdots$	$\ddots$	$\vdots$	$\vdots$	$\ddots$	$\vdots$		$\vdots$	$\vdots$	$\ddots$	$\vdots$	$\vdots$	$\vdots$	$\ddots$	$\vdots$		$\vdots$	$\vdots$	$\ddots$	$\vdots$	$\vdots$	$\vdots$	$\ddots$	$\vdots$		$\vdots$	$\ddots$	$\vdots$	$\vdots$	$\vdots$	$\ddots$	$\vdots$
		T	0	0	$\cdots$	0	0	$\overline{V}-\underline{C}$	$\cdots$	$\overline{V}-\underline{C}-\epsilon$	0	0	$\cdots$	0	0	$\cdots$	0		0	0	$\cdots$	0	0	0	$\cdots$	0		0	0	$\cdots$	0	0	1	$\cdots$	1		0	$\cdots$	0	0	0	$\cdots$	0
$\underline{\dot{\boldsymbol{\theta}}}^{\alpha}$	(B5)	2	0	$\overline{V}-\underline{C}$	$\cdots$	0	0	0	$\cdots$	0	0	0	$\cdots$	0	0	$\cdots$	0		0	0	$\cdots$	0	0	0	$\cdots$	0		0	1	$\cdots$	0	0	0	$\cdots$	0		1	$\cdots$	0	0	0	$\cdots$	0
		$\vdots$	$\vdots$	$\vdots$	$\ddots$	$\vdots$	$\vdots$	$\vdots$	$\ddots$	$\vdots$	$\vdots$	$\vdots$	$\ddots$	$\vdots$	$\vdots$	$\ddots$	$\vdots$		$\vdots$	$\vdots$	$\ddots$	$\vdots$	$\vdots$	$\vdots$	$\ddots$	$\vdots$		$\vdots$	$\vdots$	$\ddots$	$\vdots$	$\vdots$	$\vdots$	$\ddots$	$\vdots$		$\vdots$	$\ddots$	$\vdots$	$\vdots$	$\vdots$	$\ddots$	$\vdots$
		$t-1$	0	0	$\cdots$	0	0	0	$\cdots$	0	0	0	$\cdots$	0	0	$\cdots$	0		0	0	$\cdots$	0	0	0	$\cdots$	0		0	0	$\cdots$	1	0	0	$\cdots$	0		0	$\cdots$	1	0	0	$\cdots$	0
		t	0	0	$\cdots$	0	$\overline{V}-\underline{C}$	0	$\cdots$	0	0	0	$\cdots$	0	0	$\cdots$	0		0	0	$\cdots$	0	0	0	$\cdots$	0		0	0	$\cdots$	0	1	0	$\cdots$	0		0	$\cdots$	0	1	0	$\cdots$	0
		$t+1$	0	0	$\cdots$	0	0	$\overline{V}-\underline{C}$	$\cdots$	0	0	0	$\cdots$	0	0	$\cdots$	0		0	0	$\cdots$	0	0	0	$\cdots$	0		0	0	$\cdots$	0	0	1	$\cdots$	0		0	$\cdots$	0	0	1	$\cdots$	0
		$\vdots$	$\vdots$	$\vdots$	$\ddots$	$\vdots$	$\vdots$	$\vdots$	$\ddots$	$\vdots$	$\vdots$	$\vdots$	$\ddots$	$\vdots$	$\vdots$	$\ddots$	$\vdots$		$\vdots$	$\vdots$	$\ddots$	$\vdots$	$\vdots$	$\vdots$	$\ddots$	$\vdots$		$\vdots$	$\vdots$	$\ddots$	$\vdots$	$\vdots$	$\vdots$	$\ddots$	$\vdots$		$\vdots$	$\ddots$	$\vdots$	$\vdots$	$\vdots$	$\ddots$	$\vdots$
		T	0	0	$\cdots$	0	0	0	$\cdots$	$\overline{V}-\underline{C}$	0	0	$\cdots$	0	0	$\cdots$	0		0	0	$\cdots$	0	0	0	$\cdots$	0		0	0	$\cdots$	0	0	0	$\cdots$	1		0	$\cdots$	0	0	0	$\cdots$	1

Table C.12. Lower Triangular Matrix Obtained From Table C.9 via Gaussian Elimination

Point	Group	Index α	$\mathbf{p}$									$\mathbf{r}^+$									$\mathbf{r}^-$									$\mathbf{y}$									$\mathbf{u}$								
			1	2	$\cdots$	$t-2$	$t-1$	t	$t+1$	$\cdots$	T	1	2	$\cdots$	$t-1$	t	$t+1$	$\cdots$	T	1	2	$\cdots$	$t-2$	$t-1$	t	$t+1$	$\cdots$	T	1	2	$\cdots$	$t-1$	t	$t+1$	$\cdots$	T	2	$\cdots$	$t-2$	$t-1$	t	$t+1$	$\cdots$	T
$\underline{\dot{\boldsymbol{\theta}}}^{\alpha}$	(B1)	1	ϵ	0	$\cdots$	0	0	0	0	$\cdots$	0	0	0	$\cdots$	0	0	0	$\cdots$	0	0	0	$\cdots$	0	0	0	0	$\cdots$	0	0	0	$\cdots$	0	0	0	$\cdots$	0	0	$\cdots$	0	0	0	0	$\cdots$	0
		2	ϵ	ϵ	$\cdots$	0	0	0	0	$\cdots$	0	0	0	$\cdots$	0	0	0	$\cdots$	0	0	0	$\cdots$	0	0	0	0	$\cdots$	0	0	0	$\cdots$	0	0	0	$\cdots$	0	0	$\cdots$	0	0	0	0	$\cdots$	0
		$\vdots$	$\vdots$	$\vdots$	$\ddots$	$\vdots$	$\vdots$	$\vdots$	$\vdots$	$\ddots$	$\vdots$	$\vdots$	$\vdots$	$\ddots$	$\vdots$	$\vdots$	$\vdots$	$\ddots$	$\vdots$	$\vdots$	$\vdots$	$\ddots$	$\vdots$	$\vdots$	$\vdots$	$\vdots$	$\ddots$	$\vdots$	$\vdots$	$\vdots$	$\ddots$	$\vdots$	$\vdots$	$\vdots$	$\ddots$	$\vdots$	$\vdots$	$\ddots$	$\vdots$	$\vdots$	$\vdots$	$\vdots$	$\ddots$	$\vdots$
		$t-1$	ϵ	ϵ	$\cdots$	0	ϵ	0	0	$\cdots$	0	0	0	$\cdots$	0	0	0	$\cdots$	0	0	0	$\cdots$	0	0	0	0	$\cdots$	0	0	0	$\cdots$	0	0	0	$\cdots$	0	0	$\cdots$	0	0	0	0	$\cdots$	0
		t	$\overline{V}-\underline{C}$	$\overline{V}-\underline{C}$	$\cdots$	$\overline{V}-\underline{C}$	$\overline{V}-\underline{C}$	$\overline{V}-\underline{C}$	0	$\cdots$	0	0	0	$\cdots$	0	0	0	$\cdots$	0	0	0	$\cdots$	0	0	0	0	$\cdots$	0	0	0	$\cdots$	0	0	0	$\cdots$	0	0	$\cdots$	0	0	0	0	$\cdots$	0
		$t+1$	0	0	$\cdots$	0	0	0	ϵ	$\cdots$	0	0	0	$\cdots$	0	0	0	$\cdots$	0	0	0	$\cdots$	0	0	0	0	$\cdots$	0	0	0	$\cdots$	0	0	0	$\cdots$	0	0	$\cdots$	0	0	0	0	$\cdots$	0
		$\vdots$	$\vdots$	$\vdots$	$\ddots$	$\vdots$	$\vdots$	$\vdots$	$\vdots$	$\ddots$	$\vdots$	$\vdots$	$\vdots$	$\ddots$	$\vdots$	$\vdots$	$\vdots$	$\ddots$	$\vdots$	$\vdots$	$\vdots$	$\ddots$	$\vdots$	$\vdots$	$\vdots$	$\vdots$	$\ddots$	$\vdots$	$\vdots$	$\vdots$	$\ddots$	$\vdots$	$\vdots$	$\vdots$	$\ddots$	$\vdots$	$\vdots$	$\ddots$	$\vdots$	$\vdots$	$\vdots$	$\vdots$	$\ddots$	$\vdots$
		T	0	0	$\cdots$	0	0	0	0	$\cdots$	ϵ	0	0	$\cdots$	0	0	0	$\cdots$	0	0	0	$\cdots$	0	0	0	0	$\cdots$	0	0	0	$\cdots$	0	0	0	$\cdots$	0	0	$\cdots$	0	0	0	0	$\cdots$	0
$\underline{\dot{\boldsymbol{\theta}}}^{\alpha}$	(B2)	1	0	0	$\cdots$	0	0	0	0	$\cdots$	0	ϵ	0	$\cdots$	0	0	0	$\cdots$	0	0	0	$\cdots$	0	0	0	0	$\cdots$	0	0	0	$\cdots$	0	0	0	$\cdots$	0	0	$\cdots$	0	0	0	0	$\cdots$	0
		2	0	0	$\cdots$	0	0	0	0	$\cdots$	0	0	ϵ	$\cdots$	0	0	0	$\cdots$	0	0	0	$\cdots$	0	0	0	0	$\cdots$	0	0	0	$\cdots$	0	0	0	$\cdots$	0	0	$\cdots$	0	0	0	0	$\cdots$	0
		$\vdots$	$\vdots$	$\vdots$	$\ddots$	$\vdots$	$\vdots$	$\vdots$	$\vdots$	$\ddots$	$\vdots$	$\vdots$	$\vdots$	$\ddots$	$\vdots$	$\vdots$	$\vdots$	$\ddots$	$\vdots$	$\vdots$	$\vdots$	$\ddots$	$\vdots$	$\vdots$	$\vdots$	$\vdots$	$\ddots$	$\vdots$	$\vdots$	$\vdots$	$\ddots$	$\vdots$	$\vdots$	$\vdots$	$\ddots$	$\vdots$	$\vdots$	$\ddots$	$\vdots$	$\vdots$	$\vdots$	$\vdots$	$\ddots$	$\vdots$
		$t-1$	0	0	$\cdots$	0	0	0	0	$\cdots$	0	0	0	$\cdots$	ϵ	0	0	$\cdots$	0	0	0	$\cdots$	0	0	0	0	$\cdots$	0	0	0	$\cdots$	0	0	0	$\cdots$	0	0	$\cdots$	0	0	0	0	$\cdots$	0
		t	0	0	$\cdots$	0	0	$-\epsilon$	0	$\cdots$	0	0	0	$\cdots$	0	ϵ	0	$\cdots$	0	0	0	$\cdots$	0	0	0	0	$\cdots$	0	0	0	$\cdots$	0	0	0	$\cdots$	0	0	$\cdots$	0	0	0	0	$\cdots$	0
		$t+1$	0	0	$\cdots$	0	0	0	0	$\cdots$	0	0	0	$\cdots$	0	0	ϵ	$\cdots$	0	0	0	$\cdots$	0	0	0	0	$\cdots$	0	0	0	$\cdots$	0	0	0	$\cdots$	0	0	$\cdots$	0	0	0	0	$\cdots$	0
		$\vdots$	$\vdots$	$\vdots$	$\ddots$	$\vdots$	$\vdots$	$\vdots$	$\vdots$	$\ddots$	$\vdots$	$\vdots$	$\vdots$	$\ddots$	$\vdots$	$\vdots$	$\vdots$	$\ddots$	$\vdots$	$\vdots$	$\vdots$	$\ddots$	$\vdots$	$\vdots$	$\vdots$	$\vdots$	$\ddots$	$\vdots$	$\vdots$	$\vdots$	$\ddots$	$\vdots$	$\vdots$	$\vdots$	$\ddots$	$\vdots$	$\vdots$	$\ddots$	$\vdots$	$\vdots$	$\vdots$	$\vdots$	$\ddots$	$\vdots$
		T	0	0	$\cdots$	0	0	0	0	$\cdots$	0	0	0	$\cdots$	0	0	0	$\cdots$	ϵ	0	0	$\cdots$	0	0	0	0	$\cdots$	0	0	0	$\cdots$	0	0	0	$\cdots$	0	0	$\cdots$	0	0	0	0	$\cdots$	0
$\underline{\dot{\boldsymbol{\theta}}}^{\alpha}$	(B3)	1	0	0	$\cdots$	0	0	0	0	$\cdots$	0	0	0	$\cdots$	0	0	0	$\cdots$	0	ϵ	0	$\cdots$	0	0	0	0	$\cdots$	0	0	0	$\cdots$	0	0	0	$\cdots$	0	0	$\cdots$	0	0	0	0	$\cdots$	0
		2	0	0	$\cdots$	0	0	0	0	$\cdots$	0	0	0	$\cdots$	0	0	0	$\cdots$	0	0	ϵ	$\cdots$	0	0	0	0	$\cdots$	0	0	0	$\cdots$	0	0	0	$\cdots$	0	0	$\cdots$	0	0	0	0	$\cdots$	0
		$\vdots$	$\vdots$	$\vdots$	$\ddots$	$\vdots$	$\vdots$	$\vdots$	$\vdots$	$\ddots$	$\vdots$	$\vdots$	$\vdots$	$\ddots$	$\vdots$	$\vdots$	$\vdots$	$\ddots$	$\vdots$	$\vdots$	$\vdots$	$\ddots$	$\vdots$	$\vdots$	$\vdots$	$\vdots$	$\ddots$	$\vdots$	$\vdots$	$\vdots$	$\ddots$	$\vdots$	$\vdots$	$\vdots$	$\ddots$	$\vdots$	$\vdots$	$\ddots$	$\vdots$	$\vdots$	$\vdots$	$\vdots$	$\ddots$	$\vdots$
		$t-2$	$\overline{V}-\underline{C}$	$\overline{V}-\underline{C}$	$\cdots$	$\overline{V}-\underline{C}$	$\overline{V}-\underline{C}$	$\overline{V}-\underline{C}$	$\overline{V}-\underline{C}$	$\cdots$	$\overline{V}-\underline{C}$	0	0	$\cdots$	0	0	0	$\cdots$	0	0	0	$\cdots$	ϵ	0	0	0	$\cdots$	0	0	0	$\cdots$	0	0	0	$\cdots$	0	0	$\cdots$	0	0	0	0	$\cdots$	0
		$t-1$	0	0	$\cdots$	0	0	0	0	$\cdots$	0	0	0	$\cdots$	0	0	0	$\cdots$	0	0	0	$\cdots$	0	ϵ	0	0	$\cdots$	0	0	0	$\cdots$	0	0	0	$\cdots$	0	0	$\cdots$	0	0	0	0	$\cdots$	0
		t	0	0	$\cdots$	0	0	0	0	$\cdots$	0	0	0	$\cdots$	0	0	0	$\cdots$	0	0	0	$\cdots$	0	0	ϵ	0	$\cdots$	0	0	0	$\cdots$	0	0	0	$\cdots$	0	0	$\cdots$	0	0	0	0	$\cdots$	0
		$t+1$	0	0	$\cdots$	0	0	0	0	$\cdots$	0	0	0	$\cdots$	0	0	0	$\cdots$	0	0	0	$\cdots$	0	0	0	ϵ	$\cdots$	0	0	0	$\cdots$	0	0	0	$\cdots$	0	0	$\cdots$	0	0	0	0	$\cdots$	0
		$\vdots$	$\vdots$	$\vdots$	$\ddots$	$\vdots$	$\vdots$	$\vdots$	$\vdots$	$\ddots$	$\vdots$	$\vdots$	$\vdots$	$\ddots$	$\vdots$	$\vdots$	$\vdots$	$\ddots$	$\vdots$	$\vdots$	$\vdots$	$\ddots$	$\vdots$	$\vdots$	$\vdots$	$\vdots$	$\ddots$	$\vdots$	$\vdots$	$\vdots$	$\ddots$	$\vdots$	$\vdots$	$\vdots$	$\ddots$	$\vdots$	$\vdots$	$\ddots$	$\vdots$	$\vdots$	$\vdots$	$\vdots$	$\ddots$	$\vdots$
		T	0	0	$\cdots$	0	0	0	0	$\cdots$	0	0	0	$\cdots$	0	0	0	$\cdots$	0	0	0	$\cdots$	0	0	0	0	$\cdots$	ϵ	0	0	$\cdots$	0	0	0	$\cdots$	0	0	$\cdots$	0	0	0	0	$\cdots$	0
$\overline{\dot{\boldsymbol{\theta}}}^{\alpha}$	(B4)	1	$\overline{V}-\underline{C}-\epsilon$	0	$\cdots$	0	0	0	0	$\cdots$	0	0	0	$\cdots$	0	0	0	$\cdots$	0	0	0	$\cdots$	0	0	0	0	$\cdots$	0	0	0	$\cdots$	0	0	0	$\cdots$	0	1	0	$\cdots$	0	0	0	0	$\cdots$	0
		2	$\overline{V}-\underline{C}-\epsilon$	$\overline{V}-\underline{C}-\epsilon$	$\cdots$	0	0	0	0	$\cdots$	0	0	0	$\cdots$	0	0	0	$\cdots$	0	0	0	$\cdots$	0	0	0	0	$\cdots$	0	0	0	$\cdots$	0	0	0	$\cdots$	0	1	1	$\cdots$	0	0	0	0	$\cdots$	0
		$\vdots$	$\vdots$	$\vdots$	$\ddots$	$\vdots$	$\vdots$	$\vdots$	$\vdots$	$\ddots$	$\vdots$	$\vdots$	$\vdots$	$\ddots$	$\vdots$	$\vdots$	$\vdots$	$\ddots$	$\vdots$	$\vdots$	$\vdots$	$\ddots$	$\vdots$	$\vdots$	$\vdots$	$\vdots$	$\ddots$	$\vdots$	$\vdots$	$\vdots$	$\ddots$	$\vdots$	$\vdots$	$\vdots$	$\ddots$	$\vdots$	$\vdots$	$\ddots$	$\vdots$	$\vdots$	$\vdots$	$\vdots$	$\ddots$	$\vdots$
		$t-1$	$\overline{V}-\underline{C}-\epsilon$	$\overline{V}-\underline{C}-\epsilon$	$\cdots$	0	$\overline{V}-\underline{C}-\epsilon$	0	0	$\cdots$	0	0	0	$\cdots$	0	0	0	$\cdots$	0	0	0	$\cdots$	0	0	0	0	$\cdots$	0	0	0	$\cdots$	0	0	0	$\cdots$	0	1	1	$\cdots$	1	0	0	$\cdots$	0
		t	0	0	$\cdots$	0	V	$2V$	$2V-\overline{V}+\underline{C}$	$\cdots$	$2V-\overline{V}+\underline{C}+\epsilon$	0	0	$\cdots$	0	0	0	$\cdots$	0	0	0	$\cdots$	0	0	0	0	$\cdots$	0	0	0	$\cdots$	0	0	0	$\cdots$	0	1	1	$\cdots$	1	1	0	$\cdots$	0
		$t+1$	0	0	$\cdots$	0	0	0	$\overline{V}-\underline{C}-\epsilon$	$\cdots$	0	0	0	$\cdots$	0	0	0	$\cdots$	0	0	0	$\cdots$	0	0	0	0	$\cdots$	0	0	0	$\cdots$	0	0	0	$\cdots$	0	0	0	$\cdots$	0	0	1	$\cdots$	0
		$\vdots$	$\vdots$	$\vdots$	$\ddots$	$\vdots$	$\vdots$	$\vdots$	$\vdots$	$\ddots$	$\vdots$	$\vdots$	$\vdots$	$\ddots$	$\vdots$	$\vdots$	$\vdots$	$\ddots$	$\vdots$	$\vdots$	$\vdots$	$\ddots$	$\vdots$	$\vdots$	$\vdots$	$\vdots$	$\ddots$	$\vdots$	$\vdots$	$\vdots$	$\ddots$	$\vdots$	$\vdots$	$\vdots$	$\ddots$	$\vdots$	$\vdots$	$\ddots$	$\vdots$	$\vdots$	$\vdots$	$\vdots$	$\ddots$	$\vdots$
		T	0	0	$\cdots$	0	0	0	$\overline{V}-\underline{C}$	$\cdots$	$\overline{V}-\underline{C}-\epsilon$	0	0	$\cdots$	0	0	0	$\cdots$	0	0	0	$\cdots$	0	0	0	0	$\cdots$	0	0	0	$\cdots$	0	0	0	$\cdots$	0	0	0	$\cdots$	0	0	1	$\cdots$	1
$\underline{\dot{\boldsymbol{\theta}}}^{\alpha}$	(B5)	2	0	$\overline{V}-\underline{C}$	$\cdots$	0	0	0	0	$\cdots$	0	0	0	$\cdots$	0	0	0	$\cdots$	0	0	0	$\cdots$	0	0	0	0	$\cdots$	0	0	0	$\cdots$	0	0	0	$\cdots$	0	0	1	$\cdots$	0	0	0	0	$\cdots$	0
		$\vdots$	$\vdots$	$\vdots$	$\ddots$	$\vdots$	$\vdots$	$\vdots$	$\vdots$	$\ddots$	$\vdots$	$\vdots$	$\vdots$	$\ddots$	$\vdots$	$\vdots$	$\vdots$	$\ddots$	$\vdots$	$\vdots$	$\vdots$	$\ddots$	$\vdots$	$\vdots$	$\vdots$	$\vdots$	$\ddots$	$\vdots$	$\vdots$	$\vdots$	$\ddots$	$\vdots$	$\vdots$	$\vdots$	$\ddots$	$\vdots$	$\vdots$	$\ddots$	$\vdots$	$\vdots$	$\vdots$	$\vdots$	$\ddots$	$\vdots$
		$t-2$	0	0	$\cdots$	0	0	0	0	$\cdots$	0	0	0	$\cdots$	0	0	0	$\cdots$	0	0	0	$\cdots$	0	0	0	0	$\cdots$	0	0	0	$\cdots$	0	0	0	$\cdots$	0	0	$\cdots$	1	0	0	0	$\cdots$	0
		$t-1$	0	0	$\cdots$	0	$\overline{V}-\underline{C}$	0	0	$\cdots$	0	0	0	$\cdots$	0	0	0	$\cdots$	0	0	0	$\cdots$	0	0	0	0	$\cdots$	0	0	0	$\cdots$	0	1	0	$\cdots$	0	0	$\cdots$	0	1	0	0	$\cdots$	0
		t	0	0	$\cdots$	0	0	$\overline{V}-\underline{C}$	0	$\cdots$	0	0	0	$\cdots$	0	0	0	$\cdots$	0	0	0	$\cdots$	0	0	0	0	$\cdots$	0	0	0	$\cdots$	0	0	1	$\cdots$	0	0	$\cdots$	0	0	1	0	$\cdots$	0
		$t+1$	0	0	$\cdots$	0	0	0	$\overline{V}-\underline{C}$	$\cdots$	0	0	0	$\cdots$	0	0	0	$\cdots$	0	0	0	$\cdots$	0	0	0	0	$\cdots$	0	0	0	$\cdots$	0	0	0	$\cdots$	1	0	$\cdots$	0	0	0	1	$\cdots$	0
		$\vdots$	$\vdots$	$\vdots$	$\ddots$	$\vdots$	$\vdots$	$\vdots$	$\vdots$	$\ddots$	$\vdots$	$\vdots$	$\vdots$	$\ddots$	$\vdots$	$\vdots$	$\vdots$	$\ddots$	$\vdots$	$\vdots$	$\vdots$	$\ddots$	$\vdots$	$\vdots$	$\vdots$	$\vdots$	$\ddots$	$\vdots$	$\vdots$	$\vdots$	$\ddots$	$\vdots$	$\vdots$	$\vdots$	$\ddots$	$\vdots$	$\vdots$	$\ddots$	$\vdots$	$\vdots$	$\vdots$	$\vdots$	$\ddots$	$\vdots$
		T	0	0	$\cdots$	0	0	0	0	$\cdots$	$\overline{V}-\underline{C}$	0	0	$\cdots$	0	0	0	$\cdots$	0	0	0	$\cdots$	0	0	0	0	$\cdots$	1	0	0	$\cdots$	0	0	0	$\cdots$	0	0	$\cdots$	0	0	0	0	$\cdots$	1

Table C.13. Lower Triangular Matrix Obtained From Table C.10 via Gaussian Elimination

Point	Group	Index α	$\mathbf{p}$					$\mathbf{r}^+$				$\mathbf{r}^-$					$\mathbf{y}$				$\mathbf{u}$				
			1	$\cdots$	t	$\cdots$	T	1	$\cdots$	t	$\cdots$	T	1	$\cdots$	$t-k$	$\cdots$	t	$\cdots$	T	1	$\cdots$	t	$\cdots$	T	2	$\cdots$	$t-k$	$\cdots$	T
$\underline{\dot{\boldsymbol{\theta}}}^{\alpha}$	(B1)	1	ϵ	$\cdots$	0	$\cdots$	0	0	$\cdots$	0	$\cdots$	0	0	$\cdots$	0	$\cdots$	0	$\cdots$	0	0	$\cdots$	0	$\cdots$	0	0	$\cdots$	0	$\cdots$	0
		$\vdots$	$\vdots$	$\ddots$	$\vdots$	$\ddots$	$\vdots$	$\vdots$	$\ddots$	$\vdots$	$\ddots$	$\vdots$	$\vdots$	$\ddots$	$\vdots$	$\ddots$	$\vdots$	$\ddots$	$\vdots$	$\vdots$	$\ddots$	$\vdots$	$\ddots$	$\vdots$	$\vdots$	$\ddots$	$\vdots$	$\ddots$	$\vdots$
		t	$\overline{V}-\underline{C}$	$\cdots$	$\overline{V}-\underline{C}$	$\cdots$	0	0	$\cdots$	0	$\cdots$	0	0	$\cdots$	0	$\cdots$	0	$\cdots$	0	0	$\cdots$	0	$\cdots$	0	0	$\cdots$	0	$\cdots$	0
		$\vdots$	$\vdots$	$\ddots$	$\vdots$	$\ddots$	$\vdots$	$\vdots$	$\ddots$	$\vdots$	$\ddots$	$\vdots$	$\vdots$	$\ddots$	$\vdots$	$\ddots$	$\vdots$	$\ddots$	$\vdots$	$\vdots$	$\ddots$	$\vdots$	$\ddots$	$\vdots$	$\vdots$	$\ddots$	$\vdots$	$\ddots$	$\vdots$
		T	0	$\cdots$	0	$\cdots$	ϵ	0	$\cdots$	0	$\cdots$	0	0	$\cdots$	0	$\cdots$	0	$\cdots$	0	0	$\cdots$	0	$\cdots$	0	0	$\cdots$	0	$\cdots$	0
$\underline{\hat{\boldsymbol{\theta}}}^{\alpha}$	(B2)	1	0	$\cdots$	0	$\cdots$	0	ϵ	$\cdots$	0	$\cdots$	0	0	$\cdots$	0	$\cdots$	0	$\cdots$	0	0	$\cdots$	0	$\cdots$	0	0	$\cdots$	0	$\cdots$	0
		$\vdots$	$\vdots$	$\ddots$	$\vdots$	$\ddots$	$\vdots$	$\vdots$	$\ddots$	$\vdots$	$\ddots$	$\vdots$	$\vdots$	$\ddots$	$\vdots$	$\ddots$	$\vdots$	$\ddots$	$\vdots$	$\vdots$	$\ddots$	$\vdots$	$\ddots$	$\vdots$	$\vdots$	$\ddots$	$\vdots$	$\ddots$	$\vdots$
		t	0	$\cdots$	$-\epsilon$	$\cdots$	0	0	$\cdots$	ϵ	$\cdots$	0	0	$\cdots$	0	$\cdots$	0	$\cdots$	0	0	$\cdots$	0	$\cdots$	0	0	$\cdots$	0	$\cdots$	0
		$\vdots$	$\vdots$	$\ddots$	$\vdots$	$\ddots$	$\vdots$	$\vdots$	$\ddots$	$\vdots$	$\ddots$	$\vdots$	$\vdots$	$\ddots$	$\vdots$	$\ddots$	$\vdots$	$\ddots$	$\vdots$	$\vdots$	$\ddots$	$\vdots$	$\ddots$	$\vdots$	$\vdots$	$\ddots$	$\vdots$	$\ddots$	$\vdots$
		T	0	$\cdots$	0	$\cdots$	0	0	$\cdots$	0	$\cdots$	ϵ	0	$\cdots$	0	$\cdots$	0	$\cdots$	0	0	$\cdots$	0	$\cdots$	0	0	$\cdots$	0	$\cdots$	0
$\underline{\hat{\boldsymbol{\theta}}}^{\alpha}$	(B3)	1	0	$\cdots$	0	$\cdots$	0	0	$\cdots$	0	$\cdots$	0	ϵ	$\cdots$	0	$\cdots$	0	$\cdots$	0	0	$\cdots$	0	$\cdots$	0	0	$\cdots$	0	$\cdots$	0
		$\vdots$	$\vdots$	$\ddots$	$\vdots$	$\ddots$	$\vdots$	$\vdots$	$\ddots$	$\vdots$	$\ddots$	$\vdots$	$\vdots$	$\ddots$	$\vdots$	$\ddots$	$\vdots$	$\ddots$	$\vdots$	$\vdots$	$\ddots$	$\vdots$	$\ddots$	$\vdots$	$\vdots$	$\ddots$	$\vdots$	$\ddots$	$\vdots$
		$t-k$	$\overline{V}-\underline{C}$	$\cdots$	$\overline{V}-\underline{C}$	$\cdots$	$\overline{V}-\underline{C}$	0	$\cdots$	0	$\cdots$	0	0	$\cdots$	ϵ	$\cdots$	0	$\cdots$	0	0	$\cdots$	0	$\cdots$	0	0	$\cdots$	0	$\cdots$	0
		$\vdots$	$\vdots$	$\ddots$	$\vdots$	$\ddots$	$\vdots$	$\vdots$	$\ddots$	$\vdots$	$\ddots$	$\vdots$	$\vdots$	$\ddots$	$\vdots$	$\ddots$	$\vdots$	$\ddots$	$\vdots$	$\vdots$	$\ddots$	$\vdots$	$\ddots$	$\vdots$	$\vdots$	$\ddots$	$\vdots$	$\ddots$	$\vdots$
		t	0	$\cdots$	0	$\cdots$	0	0	$\cdots$	0	$\cdots$	0	0	$\cdots$	0	$\cdots$	ϵ	$\cdots$	0	0	$\cdots$	0	$\cdots$	0	0	$\cdots$	0	$\cdots$	0
		$\vdots$	$\vdots$	$\ddots$	$\vdots$	$\ddots$	$\vdots$	$\vdots$	$\ddots$	$\vdots$	$\ddots$	$\vdots$	$\vdots$	$\ddots$	$\vdots$	$\ddots$	$\vdots$	$\ddots$	$\vdots$	$\vdots$	$\ddots$	$\vdots$	$\ddots$	$\vdots$	$\vdots$	$\ddots$	$\vdots$	$\ddots$	$\vdots$
		T	0	$\cdots$	0	$\cdots$	0	0	$\cdots$	0	$\cdots$	0	0	$\cdots$	0	$\cdots$	0	$\cdots$	ϵ	0	$\cdots$	0	$\cdots$	0	0	$\cdots$	0	$\cdots$	0
$\underline{\overline{\boldsymbol{\theta}}}^{\alpha}$	(B4)	1	$\overline{V}-\underline{C}-\epsilon$	$\cdots$	0	$\cdots$	0	0	$\cdots$	0	$\cdots$	0	0	$\cdots$	0	$\cdots$	0	$\cdots$	0	1	$\cdots$	0	$\cdots$	0	0	$\cdots$	0	$\cdots$	0
		$\vdots$	$\vdots$	$\ddots$	$\vdots$	$\ddots$	$\vdots$	$\vdots$	$\ddots$	$\vdots$	$\ddots$	$\vdots$	$\vdots$	$\ddots$	$\vdots$	$\ddots$	$\vdots$	$\ddots$	$\vdots$	$\vdots$	$\ddots$	$\vdots$	$\ddots$	$\vdots$	$\vdots$	$\ddots$	$\vdots$	$\ddots$	$\vdots$
		t	0	$\cdots$	kV	$\cdots$	$kV-\overline{V}+\underline{C}+\epsilon$	0	$\cdots$	0	$\cdots$	0	0	$\cdots$	0	$\cdots$	0	$\cdots$	0	1	$\cdots$	1	$\cdots$	0	0	$\cdots$	0	$\cdots$	0
		$\vdots$	$\vdots$	$\ddots$	$\vdots$	$\ddots$	$\vdots$	$\vdots$	$\ddots$	$\vdots$	$\ddots$	$\vdots$	$\vdots$	$\ddots$	$\vdots$	$\ddots$	$\vdots$	$\ddots$	$\vdots$	$\vdots$	$\ddots$	$\vdots$	$\ddots$	$\vdots$	$\vdots$	$\ddots$	$\vdots$	$\ddots$	$\vdots$
		T	0	$\cdots$	0	$\cdots$	$\overline{V}-\underline{C}-\epsilon$	0	$\cdots$	0	$\cdots$	0	0	$\cdots$	0	$\cdots$	0	$\cdots$	0	0	$\cdots$	0	$\cdots$	1	0	$\cdots$	0	$\cdots$	0
$\underline{\dot{\boldsymbol{\theta}}}^{\alpha}$	(B5)	2	0	$\cdots$	0	$\cdots$	0	0	$\cdots$	0	$\cdots$	0	0	$\cdots$	0	$\cdots$	0	$\cdots$	0	0	$\cdots$	0	$\cdots$	0	1	$\cdots$	0	$\cdots$	0
		$\vdots$	$\vdots$	$\ddots$	$\vdots$	$\ddots$	$\vdots$	$\vdots$	$\ddots$	$\vdots$	$\ddots$	$\vdots$	$\vdots$	$\ddots$	$\vdots$	$\ddots$	$\vdots$	$\ddots$	$\vdots$	$\vdots$	$\ddots$	$\vdots$	$\ddots$	$\vdots$	$\vdots$	$\ddots$	$\vdots$	$\ddots$	$\vdots$
		$t-k$	0	$\cdots$	0	$\cdots$	0	0	$\cdots$	0	$\cdots$	0	0	$\cdots$	0	$\cdots$	0	$\cdots$	0	0	$\cdots$	0	$\cdots$	0	0	$\cdots$	1	$\cdots$	0
		$\vdots$	$\vdots$	$\ddots$	$\vdots$	$\ddots$	$\vdots$	$\vdots$	$\ddots$	$\vdots$	$\ddots$	$\vdots$	$\vdots$	$\ddots$	$\vdots$	$\ddots$	$\vdots$	$\ddots$	$\vdots$	$\vdots$	$\ddots$	$\vdots$	$\ddots$	$\vdots$	$\vdots$	$\ddots$	$\vdots$	$\ddots$	$\vdots$
		T	0	$\cdots$	0	$\cdots$	$\overline{V}-\underline{C}$	0	$\cdots$	0	$\cdots$	0	0	$\cdots$	0	$\cdots$	0	$\cdots$	0	0	$\cdots$	0	$\cdots$	1	0	$\cdots$	0	$\cdots$	1

(ii) For each $\alpha \in [1,T]_{\mathbb{Z}}$, the point with index α in group (B2), denoted by $\underline{\acute{\boldsymbol{\theta}}}^{\alpha}$, is obtained by setting $\underline{\acute{\boldsymbol{\theta}}}^{\alpha} = \acute{\boldsymbol{\theta}}^{\alpha} - \overline{\boldsymbol{\theta}}^{\alpha}$ for any $\alpha \in [1,T]_{\mathbb{Z}} \setminus \{t\}$ and $\underline{\acute{\boldsymbol{\theta}}}^{t} = \acute{\boldsymbol{\theta}}^{t} - \dot{\boldsymbol{\theta}}^{t}$. Here $\acute{\boldsymbol{\theta}}^{\alpha}$ is the point with index α in groups (A4)–(A5), $\overline{\boldsymbol{\theta}}^{\alpha}$ is the point with index α in groups (A10) and (A12), and $\dot{\boldsymbol{\theta}}^{t}$ is the point in group (A13).

(iii) For each $\alpha \in [1,T]_{\mathbb{Z}}$, the point with index α in group (B3), denoted by $\underline{\hat{\boldsymbol{\theta}}}^{\alpha}$, is obtained by setting $\underline{\hat{\boldsymbol{\theta}}}^{\alpha} = \hat{\boldsymbol{\theta}}^{\alpha} - \overline{\boldsymbol{\theta}}^{\alpha}$ for any $\alpha \in [1,T]_{\mathbb{Z}} \setminus \{t-k,\ t\}$, $\underline{\hat{\boldsymbol{\theta}}}^{t-k} = \hat{\boldsymbol{\theta}}^{t-k} - \overline{\boldsymbol{\theta}}^{t}$, and $\underline{\hat{\boldsymbol{\theta}}}^{t} = \hat{\boldsymbol{\theta}}^{t} - \dot{\boldsymbol{\theta}}^{t}$. Here $\hat{\boldsymbol{\theta}}^{\alpha}$ is the point with index α in groups (A6)–(A9), $\overline{\boldsymbol{\theta}}^{\alpha}$ is the point with index α in groups (A10) and (A12), and $\dot{\boldsymbol{\theta}}^{t}$ is the point in group (A13).

(iv) For each $\alpha \in [1,T]_{\mathbb{Z}}$, the point with index α in group (B4), denoted by $\underline{\overline{\boldsymbol{\theta}}}^{\alpha}$, is obtained by setting $\underline{\overline{\boldsymbol{\theta}}}^{\alpha} = \overline{\boldsymbol{\theta}}^{\alpha}$ for any $\alpha \in [1,t-1]_{\mathbb{Z}}$, $\underline{\overline{\boldsymbol{\theta}}}^{t} = \overline{\boldsymbol{\theta}}^{t} - \overline{\boldsymbol{\theta}}^{T} + \dot{\boldsymbol{\theta}}^{t}$ when $t < T$, $\underline{\overline{\boldsymbol{\theta}}}^{t} = \overline{\boldsymbol{\theta}}^{t}$ when $t = T$, and $\underline{\overline{\boldsymbol{\theta}}}^{\alpha} = \overline{\boldsymbol{\theta}}^{\alpha} - \dot{\boldsymbol{\theta}}^{t}$ for any $\alpha \in [t+1,T]_{\mathbb{Z}}$. Here $\overline{\boldsymbol{\theta}}^{\alpha}$ is the point with index α in group (A10), (A11), and (A12), and $\dot{\boldsymbol{\theta}}^{t}$ is the point in group (A13).

(v) For each $\alpha \in [2,T]_{\mathbb{Z}}$, the point with index α in group (B5), denoted by $\underline{\dot{\boldsymbol{\theta}}}^{\alpha}$, is obtained by setting $\underline{\dot{\boldsymbol{\theta}}}^{\alpha} = \dot{\boldsymbol{\theta}}^{\alpha}$. Here $\dot{\boldsymbol{\theta}}^{\alpha}$ is the point with index α in groups (A13)–(A14).

The matrices in Tables C.11–C.13 are lower triangular; that is, the position of the last nonzero component of a row of the matrix is greater than the position of the last nonzero component of the previous row. This indicates that the $5T-2$ points created above are linearly independent. Therefore, inequality (4.38) is facet-defining for $\text{conv}(\mathcal{D})$ when $L = 1$. □

C.15 Proof of Proposition 10

Proof. To prove that inequality (4.39) is valid for $\text{conv}(\mathcal{D})$ for any $k \in [1, \min\{T-2, \varsigma\}]_{\mathbb{Z}}$ and $t \in [k+2, T]_{\mathbb{Z}}$, it suffices to show that it is valid for $\mathcal{D}$ for such k and t. Consider any element $(\mathbf{p}, \mathbf{r}^{+}, \mathbf{r}^{-}, \mathbf{y}, \mathbf{u})$ of $\mathcal{D}$ and any $k \in [1, \min\{T-2, \varsigma\}]_{\mathbb{Z}}$ and $t \in [k+2, T]_{\mathbb{Z}}$. We show that $(\mathbf{p}, \mathbf{r}^{+}, \mathbf{r}^{-}, \mathbf{y}, \mathbf{u})$ satisfies (4.39). For ease of exposition, for any $n \in \mathcal{T} \setminus \{1\}$, we define $\psi(n) = y_n - \sum_{s=\max\{2,n-L+1\}}^{n} u_s$, which is nonnegative by Corollary 1. For any $n \in \mathcal{T}$, we define $t^{\circ}(n) = \max\{2,\ n-L+1\}$. By the above definitions and our problem setting, we have the right-hand side of (4.39) is nonnegative. Next, we divide the analysis into the following four possible cases.

Case 1: $y_{t-k} = 0$. By (4.35e) and (4.35h), we have $p_{t-k} = r^+_{t-k} = 0$. Thus, $p_{t-k} + r^+_{t-k} - p_t + r^-_t = r^-_t - p_t \leq 0$, where the inequality holds by (4.35d). Therefore, in this case, $(\mathbf{p}, \mathbf{r}^+, \mathbf{r}^-, \mathbf{y}, \mathbf{u})$ satisfies (4.39).

Case 2: $y_j = 1$ for any $j \in [t-k, t]_{\mathbb{Z}}$ and $u_i = 0$ for any $i \in [t^{\mathrm{o}}(t-k), t-k]_{\mathbb{Z}}$. Because $y_j = 1$ for any $j \in [t-k, t]_{\mathbb{Z}}$, by Corollary 1, we have $u_s = 0$ for any $s \in [t-k+1, \min\{t+1, T\}]_{\mathbb{Z}}$. It follows that $u_s = 0$ for any $s \in [t^{\mathrm{o}}(t-k), \min\{t+1, T\}]_{\mathbb{Z}}$. Thus, the right-hand side of (4.39) is $\overline{V} - \underline{C} + 2V + (k-1)V + \underline{C} + V - \overline{V} = (k+2)V$. Because $y_{t-k} = 1$ and $u_{t-k} = 0$, by (4.35c), we have $y_{t-k-1} = 1$. Thus,

$$
\begin{aligned}
&p_{t-k} - p_t + r^-_t + r^+_{t-k} \leq \sum_{s=1}^{k} \left(p_{t-s} - p_{t-s+1} + r^-_{t-s+1}\right) + r^+_{t-k} \\
&\leq \sum_{s=1}^{k} \left(\overline{V} + \left(\underline{C} + V - \overline{V}\right) y_{t-s+1} - \underline{C} y_{t-s}\right) + r^+_{t-k} \\
&= k\overline{V} + \sum_{s=1}^{k} \left(\underline{C} + V - \overline{V}\right) y_{t-s+1} - \sum_{s=1}^{k} \underline{C} y_{t-s} + r^+_{t-k} = k\overline{V} + k\left(\underline{C} + V - \overline{V}\right) - k\underline{C} + r^+_{t-k} \\
&= kV + r^+_{t-k} \leq kV + r^+_{t-k} + r^-_{t-k} = kV + \left(p_{t-k} + r^+_{t-k} - p_{t-k-1}\right) + \left(p_{t-k-1} - p_{t-k} + r^-_{t-k}\right) \\
&\leq kV + \left(\overline{V} + \left(\underline{C} + V - \overline{V}\right) y_{t-k-1} - \underline{C} y_{t-k}\right) + \left(\overline{V} + \left(\underline{C} + V - \overline{V}\right) y_{t-k} - \underline{C} y_{t-k-1}\right) = (k+2)V,
\end{aligned}
$$

where the first inequality holds by (4.35h), the second inequality holds by (4.35g), the third inequality holds by (4.35h), and the last inequality holds by (4.35f) and (4.35g). Therefore, in this case, $(\mathbf{p}, \mathbf{r}^+, \mathbf{r}^-, \mathbf{y}, \mathbf{u})$ satisfies (4.39).

Case 3: $y_{t-k} = 1$, $u_i = 0$ for any $i \in [t^{\mathrm{o}}(t-k), t-k]_{\mathbb{Z}}$, and $y_j = 0$ for some $j \in [t-k+1, t]_{\mathbb{Z}}$. Let $j_0 = \min\{j \in [t-k+1, t]_{\mathbb{Z}} \mid y_j = 0\}$, i.e., $y_s = 1$ for any $s \in [t-k, j_0-1]_{\mathbb{Z}}$. By Corollary 1, we then have $u_s = 0$ for any $s \in [t-k+1, j_0]_{\mathbb{Z}}$, implying that $u_s = 0$ for any $s \in [t^{\mathrm{o}}(t-k), j_0]_{\mathbb{Z}}$. For any $i \in [t-j_0+1, k-1]_{\mathbb{Z}}$, we have $t^{\mathrm{o}}(t-i) \geq t^{\mathrm{o}}(t-k+1) \geq t^{\mathrm{o}}(t-k)$ and $t-i \leq t-(t-j_0+1) = j_0-1$. Therefore, we have $[t^{\mathrm{o}}(t-i), t-i]_{\mathbb{Z}} \subseteq [t^{\mathrm{o}}(t-k), j_0-1]_{\mathbb{Z}} \subseteq [t^{\mathrm{o}}(t-k), j_0]_{\mathbb{Z}}$ for any $i \in [t-j_0+1, k-1]_{\mathbb{Z}}$. Because $u_s = 0$ for any $s \in [t^{\mathrm{o}}(t-k), j_0]_{\mathbb{Z}}$, we then have $u_s = 0$ for any $s \in [t^{\mathrm{o}}(t-i), t-i]_{\mathbb{Z}}$ and $i \in [t-j_0+1, k-1]_{\mathbb{Z}}$. Thus, $\sum_{s=t^{\mathrm{o}}(t-i)}^{t-i} u_s = 0$ for any $i \in [t-j_0+1, k-1]_{\mathbb{Z}}$. For any $i \in [t-j_0+1, k-1]_{\mathbb{Z}}$, we also have $t-i \geq t-k+1 \geq t-k$ and $t-i \leq j_0-1$, implying that $t-i \in [t-k, j_0-1]_{\mathbb{Z}}$. Thus, $y_{t-i} = 1$ for any $i \in [t-j_0+1, k-1]_{\mathbb{Z}}$, as $y_s = 1$ for any $s \in [t-k, j_0-1]_{\mathbb{Z}}$. Therefore, we have $\psi(t-i) = y_{t-i} - \sum_{s=t^{\mathrm{o}}(t-i)}^{t-i} u_s = 1$

for any $i \in [t - j_0 + 1, k - 1]_{\mathbb{Z}}$. Then we have

$$\sum_{i=1}^{k-1} V\psi(t-i) = \sum_{i=1}^{t-j_0} V\psi(t-i) + \sum_{i=t-j_0+1}^{k-1} V\psi(t-i) = \sum_{i=1}^{t-j_0} V\psi(t-i) + (j_0 - t + k - 1)V,$$

and the right-hand side of (4.39) is

$$\overline{V} - \underline{C} + 2V + (j_0 - t + k - 1)V + \sum_{i=1}^{t-j_0} V\psi(t-i) + (\underline{C} + V - \overline{V})\psi(t) + \sum_{s=t^o(t-k)}^{t-k-1} (t-k-s)Vu_s.$$

Because $y_{j_0} = 0$, by (4.35e) and (4.35h), we have $p_{j_0} = 0$. Thus,

$$\begin{aligned}
&p_{t-k} + r^+_{t-k} - p_t + r^-_t \le p_{t-k} + r^+_{t-k} = p_{t-k} - p_{j_0} + r^+_{t-k} \le \sum_{s=t-j_0}^{k-1} \left(p_{t-s-1} + r^-_{t-s} - p_{t-s}\right) + r^+_{t-k} \\
&\le \sum_{s=t-j_0}^{k-1} \left(\overline{V} + \left(\underline{C} + V - \overline{V}\right) y_{t-s} - \underline{C} y_{t-s-1}\right) + r^+_{t-k} \\
&= (j_0 - t + k)\,\overline{V} + \sum_{s=t-j_0}^{k-1} \left(\underline{C} + V - \overline{V}\right) y_{t-s} - \sum_{s=t-j_0}^{k-1} \underline{C} y_{t-s-1} + r^+_{t-k} \\
&= (j_0 - t + k)\,\overline{V} + (j_0 - t + k - 1)\left(\underline{C} + V - \overline{V}\right) - (j_0 - t + k)\,\underline{C} + r^+_{t-k} \\
&= \overline{V} - \underline{C} + (j_0 - t + k - 1)\,V + r^+_{t-k} \le \overline{V} - \underline{C} + (j_0 - t + k - 1)\,V + r^+_{t-k} + r^-_{t-k} \\
&= \overline{V} - \underline{C} + (j_0 - t + k - 1)\,V + \left(p_{t-k} + r^+_{t-k} - p_{t-k-1}\right) + \left(p_{t-k-1} - p_{t-k} + r^-_{t-k}\right) \\
&\le \overline{V} - \underline{C} + (j_0 - t + k - 1)\,V + \left(\overline{V} + \left(\underline{C} + V - \overline{V}\right) y_{t-k-1} - \underline{C} y_{t-k}\right) \\
&\qquad\qquad + \left(\overline{V} + \left(\underline{C} + V - \overline{V}\right) y_{t-k} - \underline{C} y_{t-k-1}\right) \\
&= \overline{V} - \underline{C} + (j_0 - t + k - 1)V + 2V \le \text{the right-hand side of (4.39)},
\end{aligned}$$

where the first inequality holds by (4.35d), the second inequality holds by (4.35h), the third inequality holds by (4.35g), the fourth inequality holds by (4.35h), the fifth inequality holds by (4.35f) and (4.35g), and the last inequality holds by the assumption of $\overline{V} < \underline{C} + V$ and Corollary 1. Therefore, in this condition, $(\mathbf{p}, \mathbf{r}^+, \mathbf{r}^-, \mathbf{y}, \mathbf{u})$ satisfies (4.39).

Case 4: $y_{t-k} = 1$ and $u_{i_0} = 1$ for some $i_0 \in [t^o(t-k), t-k]_{\mathbb{Z}}$. By Lemma 2, we have $\sum_{s=t^o(t-k)}^{t-k} u_s \le 1$. Thus, we have $u_{i_0} = 1$ and $u_s = 0$ for any $s \in [t^o(t-k), t-k]_{\mathbb{Z}} \setminus \{i_0\}$. It follows that $\sum_{s=t^o(t-k)}^{t-k-1}(t-k-s)Vu_s = (t-k-i_0)V$. Thus, the right-hand side of

(4.39) is

$$\overline{V} - \underline{C} + 2V\psi(t-k) + \sum_{i=1}^{k-1} V\psi(t-i) + (\underline{C} + V - \overline{V})\psi(t) + (t-k-i_0)V.$$

For any $s \in [i_0, t-k]_{\mathbb{Z}}$, we have $t^o(s) \leq t^o(t-k) \leq i_0$, implying that $i_0 \in [t^o(s), s]_{\mathbb{Z}}$. Then, by Corollary 1, for any $s \in [i_0, t-k]_{\mathbb{Z}}$, we have $y_s \geq \sum_{i\in[t^o(s),s]_{\mathbb{Z}}} u_i = \sum_{i\in[t^o(s),s]_{\mathbb{Z}}\setminus\{i_0\}} u_i + u_{i_0} \geq 1$, implying that $y_s = 1$. Because $u_{i_0} = 1$, by Corollary 1, we have $y_{i_0-1} = 0$, which, together with (4.35e) and (4.35h), indicates $p_{i_0-1} = 0$. Thus,

$$\begin{aligned}
&p_{t-k} + r^+_{t-k} - p_t + r^-_t \leq p_{t-k} + r^+_{t-k} = p_{t-k} + r^+_{t-k} - p_{i_0-1} \leq \sum_{s=i_0}^{t-k} \left(p_s + r^+_s - p_{s-1}\right) \\
&\leq \sum_{s=i_0}^{t-k} \left(\overline{V} + \left(\underline{C} + V - \overline{V}\right) y_{s-1} - \underline{C} y_s\right) = (t-k-i_0+1)\,\overline{V} + \sum_{s=i_0}^{t-k} \left(\underline{C} + V - \overline{V}\right) y_{s-1} - \sum_{s=i_0}^{t-k} \underline{C} y_s \\
&= (t-k-i_0+1)\,\overline{V} + (t-k-i_0)\left(\underline{C} + V - \overline{V}\right) - (t-k-i_0+1)\,\underline{C} \\
&= \overline{V} - \underline{C} + (t-k-i_0)\,V \leq \text{the right-hand side of (4.39)},
\end{aligned}$$

where first inequality holds by (4.35d), the second inequality holds by (4.35h), the third inequality holds by (4.35f), and the last inequality holds by the assumption of $\overline{V} < \underline{C} + V$ and Corollary 1. Therefore, in this condition, $(\mathbf{p}, \mathbf{r}^+, \mathbf{r}^-, \mathbf{y}, \mathbf{u})$ satisfies (4.39). □

C.16 Data Summary

We consider the following ten thermal generators in NYC (see Table C.14) and set their physical parameters (see Table C.15) based on the data in Table C.14 and IEEE 6-bus system (Jiang et al. 2011).

Table C.14. Ten Thermal Generators in NYC (EIA 2023)

Location	Utility Name	Plant Name	Nameplate Capacity (MW)	# Units
Staten Island	NRG Arthur Kill Operations Inc	Arthur Kill Generating Station	536 & 342	2
Manhattan	Consolidated Edison Co-NY Inc	East River Generating Station	200 & 200	2
Bronx	New York Power Authority	Hell Gate	56 & 56	2
Brooklyn	Brooklyn Navy Yard Cogen PLP	Brooklyn Navy Yard Cogeneration	145 & 145	2
Queens	Helix Ravenswood, LLC	Ravenswood No. 3 (Big Allis)	400 & 250	2

C.17 Machine Learning Setting

First, we define several functions to compute the statistical information of any given random parameter. Consider an arbitrary random parameter $\mathbf{w} = (w_{t,j}, \forall t \in \mathcal{T}, j \in \mathcal{S})^\top$

Table C.15. Physical Parameters of The Ten Generators

Gen No.	$\underline{C}$ (MW)	$\overline{C}$ (MW)	$L\&\ell$	V (MW/h)	$\overline{V}$ (MW/h)	SU ($)	SD ($)	a ($/MW^2)	b ($/MW)	c ($)
1.1	65	540	10	250	260	2000	0	0.0033	12.11	26.96
1.2	45	340	6	150	160	1200	0	0.0063	13.55	39.36
2.1	30	200	4	100	110	800	0	0.0130	15.21	43.84
2.2	30	200	4	100	110	800	0	0.0128	15.24	43.87
3.1	10	60	1	28	28	200	0	0.0597	17.26	74.11
3.2	10	60	1	28	28	200	0	0.0593	17.31	74.15
4.1	20	145	2	70	70	500	0	0.0191	15.81	50.14
4.2	20	145	2	70	70	500	0	0.0189	15.82	50.15
5.1	50	400	8	200	210	1500	0	0.0039	13.07	30.02
5.2	35	250	4	120	120	1000	0	0.0123	14.32	42.01

with a set of data samples $\{\tilde{w}_{t,j}, \forall t \in \mathcal{T}, j \in \mathcal{S}\}$. For any $j \in \mathcal{S}$, we define $\mathbf{w}_j = (w_{t,j}, \forall t \in \mathcal{T})^\top$, $\mathbb{E}_{\mathcal{T}}[\mathbf{w}_j] = (\sum_{t\in\mathcal{T}} \tilde{w}_{t,j})/|\mathcal{T}|$, and $\sigma_{\mathcal{T}}[\mathbf{w}_j] = \sqrt{(\sum_{t\in\mathcal{T}}(w_{t,j} - \mathbb{E}_{\mathcal{T}}[\mathbf{w}_j])^2)/|\mathcal{T}|}$. We further define

$$\mathbb{E}_{\mathcal{S}}\mathbb{E}_{\mathcal{T}}[\mathbf{w}] = \frac{1}{|\mathcal{S}|}\sum_{j\in\mathcal{S}} \mathbb{E}_{\mathcal{T}}[\mathbf{w}_j], \ \sigma_{\mathcal{S}}\mathbb{E}_{\mathcal{T}}[\mathbf{w}] = \left(\frac{1}{|\mathcal{S}|}\sum_{j\in\mathcal{S}} \left(\mathbb{E}_{\mathcal{T}}[\mathbf{w}_j] - \mathbb{E}_{\mathcal{S}}\mathbb{E}_{\mathcal{T}}[\mathbf{w}]\right)^2\right)^{\frac{1}{2}},$$
$$\mathbb{E}_{\mathcal{S}}\sigma_{\mathcal{T}}[\mathbf{w}] = \frac{1}{|\mathcal{S}|}\sum_{j\in\mathcal{S}} \sigma_{\mathcal{T}}[\mathbf{w}_j], \ \sigma_{\mathcal{S}}\sigma_{\mathcal{T}}[\mathbf{w}] = \left(\frac{1}{|\mathcal{S}|}\sum_{j\in\mathcal{S}} \left(\sigma_{\mathcal{T}}[\mathbf{w}_j] - \mathbb{E}_{\mathcal{S}}\sigma_{\mathcal{T}}[\mathbf{w}]\right)^2\right)^{\frac{1}{2}}.$$

Next, for any $t \in \mathcal{T}$ and $j \in \mathcal{S}$, we let $q'_{t,j} = \sum_{b\in\mathcal{B}}(q_{b,t,j} - p^{\mathrm{w}}_{b,t,j} - p^{\mathrm{s}}_{b,t,j})$ denote the net load in period t and scenario j. With the data in Group 1, we have 616 data samples from both $\mathcal{S}^{\mathrm{G}}$ and $\mathcal{S}^{\mathrm{EV}}$. We consider a set of instances of Problem ($\mathcal{M}$) with various scenario sizes of $\mathcal{S}$. Specifically, we augment the scenario set $\mathcal{S}$ by defining $\mathcal{S} := \mathcal{S}^{\mathrm{G}} \times \mathcal{S}^{\mathrm{EV}} = \{(j^{\mathrm{G}}, j^{\mathrm{EV}}) \mid j^{\mathrm{G}} \in \mathcal{S}^{\mathrm{G}}, j^{\mathrm{EV}} \in \mathcal{S}^{\mathrm{EV}}\}$, leading to 616×616 scenarios in $\mathcal{S}$ in total. By randomly selecting samples from $\mathcal{S}^{\mathrm{G}}$ and $\mathcal{S}^{\mathrm{EV}}$ to create such an augmented set $\mathcal{S}$, we create $4,424$ instances of Problem ($\mathcal{M}$) with $\mathcal{S}^n$ ($n \in [1, 4, 424]_{\mathbb{Z}}$) and consider $|\mathcal{S}^n| \in [10, 1, 000]_{\mathbb{Z}}$. For each instance with $\mathcal{S}^n$ for some $n \in [1, 4, 424]_{\mathbb{Z}}$, we consider 12 features (i.e., $d_{\mathrm{in}} = 12$) of the scenarios in $\mathcal{S}^n$, i.e., $\mathbf{x}_{\mathrm{in}} = (x^1_{\mathrm{in}}, \ldots, x^{12}_{\mathrm{in}})^\top$. Specifically, (i) $x^1_{\mathrm{in}} = |\mathcal{S}^{\mathrm{G}}|$ (i.e., the number of scenarios in $\mathcal{S}^{\mathrm{G}}$); (ii) $x^2_{\mathrm{in}} = |\mathcal{S}^{\mathrm{EV}}|$ (i.e., the number of scenarios in $\mathcal{S}^{\mathrm{EV}}$); (iii) $x^3_{\mathrm{in}} = \mathbb{E}_{\mathcal{S}^n}\mathbb{E}_{\mathcal{T}}[\mathbf{q}']$ (i.e., net load averaged over first $\mathcal{T}$ and then $\mathcal{S}^n$); (iv) $x^4_{\mathrm{in}} = \sigma_{\mathcal{S}^n}\mathbb{E}_{\mathcal{T}}[\mathbf{q}']$ (i.e., net load averaged over $\mathcal{T}$ then the standard deviation over $\mathcal{S}^n$); (v) $x^5_{\mathrm{in}} = \mathbb{E}_{\mathcal{S}^n}\sigma_{\mathcal{T}}[\mathbf{q}']$ (i.e., net load's standard deviation over $\mathcal{T}$ then averaged over $\mathcal{S}^n$); (vi) $x^6_{\mathrm{in}} = \sigma_{\mathcal{S}^n}\sigma_{\mathcal{T}}[\mathbf{q}']$ (i.e., net load's standard deviation over $\mathcal{T}$ then the standard deviation over $\mathcal{S}^n$); (vii) $x^7_{\mathrm{in}} = \max_{j\in\mathcal{S}^n}\{\sum_{t\in\mathcal{T}} q'_{t,j}\}$ (i.e., the largest total net load in $\mathcal{S}^n$); (viii) $x^8_{\mathrm{in}} = \mathbb{E}_{\mathcal{S}^n}\mathbb{E}_{\mathcal{T}}[\mathbf{d}]$ (i.e., EV trip demand averaged over $\mathcal{T}$ then averaged over $\mathcal{S}^n$); (ix) $x^9_{\mathrm{in}} = \sigma_{\mathcal{S}^n}\mathbb{E}_{\mathcal{T}}[\mathbf{d}]$ (i.e., trip demand averaged over $\mathcal{T}$ then the standard deviation over

$\mathcal{S}^n$); (x) $x^{10}_{\text{in}} = \mathbb{E}_{\mathcal{S}^n}\sigma_{\mathcal{T}}[\mathbf{d}]$ (i.e., EV trip demand's standard deviation over $\mathcal{T}$ then averaged over $\mathcal{S}^n$); (xi) $x^{11}_{\text{in}} = \sigma_{\mathcal{S}^n}\sigma_{\mathcal{T}}[\mathbf{d}]$ (i.e., EV trip demand's standard deviation over $\mathcal{T}$ then the standard deviation over $\mathcal{S}^n$); (xii) $x^{12}_{\text{in}} = \max_{j\in\mathcal{S}^n}\{\sum_{t\in\mathcal{T}} d_{t,j}\}$ (i.e., the largest total trip demand in $\mathcal{S}^n$).

For each instance with $\mathcal{S}^n$ for some $n \in [1, 4, 424]_{\mathbb{Z}}$, we solve Problem ($\mathcal{M}$) with $\mathcal{S}^n$ and obtain an optimal first-stage solution $(\mathbf{u}^*, \mathbf{y}^*)$, by which we can identify a worst-case scenario $j^* \in \mathcal{S}^n$ with the largest cost $\Psi(\mathbf{u}^*, \mathbf{y}^*, \boldsymbol{\xi}_{j^*})$. We consider four features (i.e., $d_{\text{out}} = 4$) of this scenario j^*, i.e., $\mathbf{y}_{\text{out}} = (y^1_{\text{out}}, \ldots, y^4_{\text{out}})^\top$. Specifically, (i) $y^1_{\text{out}} = \mathbb{E}_{\mathcal{T}}[\mathbf{q}'_{j^*}]$ (i.e., net load in scenario j^* averaged over $\mathcal{T}$); (ii) $y^2_{\text{out}} = \sigma_{\mathcal{T}}[\mathbf{q}'_{j^*}]$ (i.e., the standard deviation of net load in scenario j^*); (iii) $y^3_{\text{out}} = \mathbb{E}_{\mathcal{T}}[\mathbf{d}_{j^*}]$ (i.e., EV trip demand in scenario j^* averaged over $\mathcal{T}$); (iv) $y^4_{\text{out}} = \sigma_{\mathcal{T}}[\mathbf{d}_{j^*}]$ (i.e., the standard deviation of EV trip demand in scenario j^*). After solving all the 4,424 instances of Problem ($\mathcal{M}$), we obtain a set $\{(\mathbf{x}^n_{\text{in}}, \mathbf{y}^n_{\text{out}})\}_{n=1}^{4424}$, by which we build the linear regression model $\mathbf{y}_{\text{out}} = \mathbf{c}^\top \mathbf{x}_{\text{in}}$.

C.18 Computational Performance of Solution Approaches

Table C.16 provides computational results for the CPLEX and ADMM approaches when $|\mathcal{S}| \leq 200$.

Table C.16. Computational Performance of CPLEX and ADMM When $|\mathcal{S}| \leq 200$

$\lvert\mathcal{S}\rvert$	$\lvert\mathcal{S}^{\text{G}}\rvert$	$\lvert\mathcal{S}^{\text{EV}}\rvert$	CPLEX			ADMM		
			Cost ($)	MIP Gap (%)	Time (s)	Cost ($)	ADMM Gap (%)	Time (s)
10	10	1	409,180	0.002	43.1	411,072	0.460	3.2
	5	2	409,071	0.004	101.1	411,705	0.640	6.5
	2	5	409,077	0.005	26.1	411,747	0.648	4.0
	1	10	184,798	0.004	49.7	185,875	0.579	3.2
	Average		353,032	0.004	55.0	355,100	**0.582**	**4.2**
50	50	1	447,878	0.010	122.3	450,246	0.526	22.2
	25	2	428,342	0.000	15.2	430,190	0.430	17.6
	10	5	409,907	0.007	63.0	413,281	0.816	19.1
	5	10	409,788	0.002	34.2	413,161	0.816	25.6
	2	25	412,172	0.008	80.6	412,478	0.074	51.9
	1	50	186,258	0.006	92.4	188,124	0.992	6.0
	Average		382,391	0.006	68.0	384,580	**0.609**	**23.7**
100	50	2	447,878	0.010	328.1	450,246	0.526	69.0
	20	5	426,082	0.005	268.4	428,890	0.655	57.0
	10	10	409,909	0.004	141.1	411,773	0.453	85.1
	5	20	410,447	0.002	234.5	413,067	0.634	113.8
	2	50	412,172	0.002	259.6	412,995	0.199	90.1
	Average		421,298	0.004	243.0	423,394	**0.493**	**83.0**
200	40	5	446,661	0.010	306.8	448,965	0.513	98.8
	20	10	428,342	0	317.4	430,129	0.415	54.7
	10	20	412,312	0.004	349.1	414,867	0.616	192.0
	5	40	412,173	0.003	286.7	413,860	0.408	190.6
	Average		424,872	0.004	315.0	426,955	**0.488**	**134.0**
Average	-	-	395,398	0.005	170.0	397,507	**0.543**	**61.2**

Table C.17 provides computational results for the ADMM, Random Algorithm, and

Learning Algorithm approaches when $|\mathcal{S}| \leq 200$.

Table C.17. Computational Performance of Solution Approaches When $|\mathcal{S}| \leq 200$

$\|\mathcal{S}\|$	$\|\mathcal{S}^{\mathrm{G}}\|$	$\|\mathcal{S}^{\mathrm{EV}}\|$	ADMM			Random Algorithm						Learning Algorithm					
			Cost ($)	MIP Gap (%)	Time (s)	Initial Cost ($)	Final Cost ($)	Initial Gap (%)	Final Gap (%)	Initial Time (s)	Final Time (s)	Initial Cost ($)	Final Cost ($)	Initial Gap (%)	Final Gap (%)	Initial Time (s)	Final Time (s)
10	10	1	411,072	0.460	3.2	409,063	409,180	-0.029	0	0.4	1.3	389,452	409,184	-5.066	0.001	0.4	2.7
	5	2	411,705	0.640	6.5	402,862	409,063	-1.541	-0.002	1.1	4.7	409,063	409,063	-0.002	-0.002	0.4	0.4
	2	5	411,747	0.648	4.0	409,063	409,063	-0.003	-0.003	0.4	0.4	409,063	409,063	-0.003	-0.003	0.4	0.4
	1	10	185,875	0.579	3.2	184,798	184,798	0	0	0.4	0.4	184,798	184,798	0	0	0.4	0.4
	Average		355,100	0.582	4.2	351,447	353,026	-0.393	-0.001	0.6	1.7	348,094	353,027	**-1.268**	**-0.001**	**0.4**	**1.0**
50	50	1	450,246	0.526	22.2	409,813	447,878	-9.288	0	0.4	8.5	447,730	447,878	-0.033	0	0.5	5.0
	25	2	430,190	0.430	17.6	221,631	428,342	-93.268	0	1.1	14.5	428,321	428,342	-0.005	0	0.3	1.6
	10	5	413,281	0.816	19.1	184,798	409,905	-121.814	0	0.4	14.1	409,794	409,928	-0.028	0.005	0.4	1.5
	5	10	413,161	0.816	25.6	184,798	409,811	-121.749	0.006	0.4	17.6	409,794	409,794	0.001	0.001	0.4	0.6
	2	25	412,478	0.074	51.9	184,798	412,173	-123.039	0	0.3	10.4	412,173	412,173	0	0	0.4	0.7
	1	50	188,124	0.992	6.0	184,798	186,269	-0.790	0.006	0.6	1.9	186,269	186,269	0.006	0.006	0.4	0.6
	Average		384,580	0.609	23.7	228,439	382,396	-78.325	0.002	0.5	11.2	382,347	382,397	**-0.010**	**0.002**	**0.4**	**1.7**
100	50	2	450,246	0.526	69.0	365,066	447,878	-22.684	0	0.9	37.5	447,730	447,878	-0.033	0	0.6	5.3
	20	5	428,890	0.655	57.0	374,342	426,082	-13.822	0	0.4	18.1	426,061	426,082	-0.005	0	0.4	2.5
	10	10	411,773	0.453	85.1	374,342	409,905	-9.501	-0.001	0.4	32.6	391,162	409,928	-4.793	0.005	0.8	6.7
	5	20	413,067	0.634	113.8	374,342	410,439	-9.645	-0.002	0.4	40.6	410,450	410,450	0.001	0.001	0.4	0.9
	2	50	412,995	0.199	90.1	184,798	412,173	-123.039	0	0.4	21.8	412,173	412,173	0	0	0.4	0.9
	Average		423,394	0.493	83.0	334,578	421,295	-35.738	-0.001	0.5	30.1	417,515	421,302	**-0.966**	**0.001**	**0.5**	**3.3**
200	40	5	448,965	0.513	98.8	401,588	446,661	-11.224	0	0.4	22.6	446,560	446,661	-0.023	0	0.4	5.2
	20	10	430,129	0.415	54.7	314,202	428,342	-36.327	0	0.6	44.1	428,321	428,342	-0.005	0	0.3	3.6
	10	20	414,867	0.616	192.0	389,452	412,311	-5.870	0	0.4	62.5	395,397	412,311	-4.278	0	0.4	15.7
	5	40	413,860	0.408	190.6	402,862	412,173	-2.311	0	1.3	117.3	412,173	412,173	0	0	0.4	1.7
	Average		426,955	0.488	134.0	377,026	424,872	-13.933	0	0.7	61.6	420,613	424,872	**-1.076**	**0**	**0.4**	**6.5**
Average	-	-	397,507	0.543	61.2	322,873	395,397	-32.097	0	0.6	26.2	392,142	395,400	**-0.830**	**0.001**	**0.4**	**3.1**

C.19 Impact of Service Level on The Mobility System's Profit

We study the impact of service level α on the mobility system's profit. First, we consider the following problem on EV fleet operations where V2G is not adopted:

$$\Pi_0 = \max \Big\{ \frac{1}{|\mathcal{S}|} \sum_{j \in \mathcal{S}} \sum_{t \in \mathcal{T}} c^{\mathrm{r}} x^{\mathrm{r}}_{t,j} - c^{\mathrm{pen}} \left(d_{t,j} - x^{\mathrm{r}}_{t,j} \right) - P^-_t x^-_{t,j} \;\Big|\; (4.19) - (4.23), (4.26), \quad (\mathrm{V}_0)$$
$$x^+_{t,j} = 0, \ \forall t \in \mathcal{T}, j \in \mathcal{S} \Big\},$$

where c^{r} denotes the unit revenue of serving demands and c^{pen} denotes the unit penalty for unsatisfied demands; we set their values following Zhang et al. (2021). Problem (V_0) maximizes the mobility system's expected profit. Given the data in Group 3 in Section 4.5.1, we have 60 data samples in both $\mathcal{S}^{\mathrm{G}}$ and $\mathcal{S}^{\mathrm{EV}}$. We use them to construct a scenario set $\mathcal{S} := \mathcal{S}^{\mathrm{G}} \times \mathcal{S}^{\mathrm{EV}} = \{(j^{\mathrm{G}}, j^{\mathrm{EV}}) \mid j^{\mathrm{G}} \in \mathcal{S}^{\mathrm{G}}, j^{\mathrm{EV}} \in \mathcal{S}^{\mathrm{EV}}\}$ and obtain $|\mathcal{S}| = 3,600$. We solve Problem (V_0) with this set $\mathcal{S}$ and obtain Π_0.

Second, given $\alpha \in [0, 1]$, we consider the following EV fleet problem where V2G is adopted:

$$\Pi(\alpha) = \max \ \frac{1}{|\mathcal{S}|} \sum_{j \in \mathcal{S}} \sum_{t \in \mathcal{T}} c^{\mathrm{r}} x^{\mathrm{r}}_{t,j} - c^{\mathrm{pen}} \left(d_{t,j} - x^{\mathrm{r}}_{t,j} \right) - P^-_t x^-_{t,j} + P^+_t x^+_{t,j} \quad (\mathrm{V}_1)$$
$$\text{s.t. } (4.19) - (4.23), (4.26), \ \forall j \in \mathcal{S},$$
$$x^+_{t,j} e^+ \delta = v^+_{t,j}(\alpha), \ x^-_{t,j} e^- \delta = v^-_{t,j}(\alpha), \ \forall t \in \mathcal{T}, \ j \in \mathcal{S},$$

where $v^+_{t,j}(\alpha)$ and $v^-_{t,j}(\alpha)$ are given parameters. To determine these parameters, we solve Problem ($\mathcal{M}$) with $\alpha \in [0,1]$ and the optimal solutions of $v^+_{t,j}$ and $v^-_{t,j}$ in Problem ($\mathcal{M}$) are set equal to $v^+_{t,j}(\alpha)$ and $v^-_{t,j}(\alpha)$ for any $t \in \mathcal{T}$ and $j \in \mathcal{S}$.

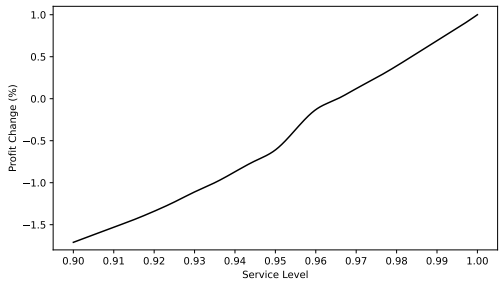

Figure C.5. Profit Changes for Different Service Levels

Given $\alpha \in [0,1]$, we define Profit Change(%) $= (\Pi(\alpha) - \Pi_0)/\Pi_0 \times 100\%$; a positive Profit Change(%) indicates that the mobility system generates a higher profit when V2G is adopted in the GVI system, compared to the case without V2G. Figure C.5 shows that when $\alpha = 0.97$, the Profit Change is slightly larger than 0, thereby ensuring the EV fleet's profitability. A further increase in α imposes greater requirements on the power grid's operation, which hurts the power grid's flexibility. Therefore, to ensure the EV fleet's profitability and the power grid's flexibility, we set service level $\alpha = 0.97$ in our numerical experiments in Section 4.5.

C.20 Costs for Various Levels of Greenness

We estimate the cost associated with various levels of greenness to offer more straightforward insights into the challenge of achieving carbon neutrality. We sum up the optimal cost of Problem ($\mathcal{M}$) (i.e., Θ), EV fleet purchase cost, and renewable generation cost. We compute the EV fleet purchase cost by multiplying the EV fleet size by the EV purchase cost averaged to a day. Note that each EV costs $\$42,645$ with an average life of 8 years (Qi et al. 2022). As a result, the EV purchase cost averaged to a day is $\$42,645/(8 \times 365) \approx \$14.6$. We estimate the renewable generation cost by multiplying the total renewable generation by the levelized cost. The levelized cost of wind energy is \$32/MWh in 2021 (U.S. DOE 2022) and that of solar is estimated at \$30-42/MWh in 2021 (Bellini 2021). Here we set the levelized cost of solar as \$32/MWh. Figure C.6 shows how the cost changes with various levels of greenness. We observe a dramatic cost increase when the greenness is high under either power load pattern. That is, achieving

carbon neutrality can be challenging for the GVI system if only increasing the renewable share and EV fleet size.

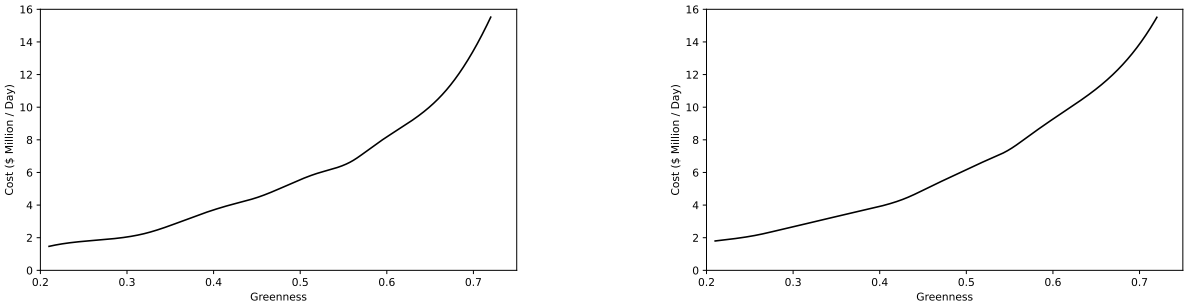

(a) Unimodal Power Load Pattern **(b)** Bimodal Power Load Pattern

Figure C.6. Costs Associated With Various Levels of Greenness

References

Abouee-Mehrizi H, Baron O, Berman O, Chen D (2021) Adoption of electric vehicles in car sharing market. *Production and Operations Management* 30(1):190–209.

American Legal Publishing (2019) *Licensing and regulating shared mobility business*. Accessed: November 7, 2023.

Anderson E, Zachary S (2023) Minimax decision rules for planning under uncertainty: Drawbacks and remedies. *European Journal of Operational Research* 311(2):789–800.

Atamtürk A, Zhang M (2007) Two-stage robust network flow and design under demand uncertainty. *Operations Research* 55(4):662–673.

Baye MR, Morgan J (2009) Brand and price advertising in online markets. *Management Science* 55(7):1139–1151.

Bellini E (2021) *Utility scale solar reaches LCOE of $0.028-$0.041/kWh in the US, Lazard finds*. Accessed: December 11, 2023.

Ben-Tal A, El Ghaoui L, Nemirovski A (2009) *Robust Optimization*, volume 28 (Princeton University Press).

Ben-Tal A, Goryashko A, Guslitzer E, Nemirovski A (2004) Adjustable robust solutions of uncertain linear programs. *Mathematical Programming* 99(2):351–376.

Ben-Tal A, Nemirovski A (1999) Robust solutions of uncertain linear programs. *Operations Research Letters* 25(1):1–13.

Benjaafar S, Wu S, Liu H, Gunnarsson EB (2022a) Dimensioning on-demand vehicle sharing systems. *Management Science* 68(2):1218–1232.

Benjaafar S, Wu S, Liu H, Gunnarsson EB (2022b) Dimensioning on-demand vehicle sharing systems. *Management Science* 68(2):1218–1232.

Bertsimas D, Brown DB, Caramanis C (2011) Theory and applications of robust optimization. *SIAM Review* 53(3):464–501.

Bertsimas D, Iancu DA, Parrilo PA (2010) Optimality of affine policies in multistage robust optimization. *Mathematics of Operations Research* 35(2):363–394.

Bertsimas D, Sim M (2004) The price of robustness. *Operations Research* 52(1):35–53.

Broneske G, Wozabal D (2017) How do contract parameters influence the economics of vehicle-to-grid? *Manufacturing & Service Operations Management* 19(1):150–164.

CAISO (2016) *Flexible Resources to Help Renewables - Fast Facts*. Accessed: December 11, 2023.

Cao G, Jin GZ, Weng X, Zhou LA (2021) Market-expanding or market-stealing? Competition with network effects in bike-sharing. *The RAND Journal of Economics* 52(4):778–814.

Carlson B, Chen Y, Hong M, et al. (2012) MISO unlocks billions in savings through the application of operations research for energy and ancillary services markets. *Interfaces* 42(1):58–73.

Carrión M, Arroyo JM (2006) A computationally efficient mixed-integer linear formulation for the thermal unit commitment problem. *IEEE Transactions on Power Systems* 21(3):1371–1378.

Chang J, Yu M, Shen S, Xu M (2017) Location design and relocation of a mixed car-sharing fleet with a CO2 emission constraint. *Service Science* 9(3):205–218.

Cheramin M, Cheng J, Jiang R, Pan K (2022) Computationally efficient approximations for distributionally robust optimization under moment and wasserstein ambiguity. *INFORMS Journal on Computing* 34(3):1768–1794.

Chevalier-Roignant B, Flath CM, Huchzermeier A, Trigeorgis L (2011) Strategic investment under uncertainty: A synthesis. *European Journal of Operational Research* 215(3):639–650.

Citi Bike (2022) *Citi Bike Homepage*. Accessed: November 7, 2023.

City of Chicago (2022) *City of Chicago scooter sharing business rules*. Accessed: November 7, 2023.

City of Philadelphia (2018) *Indego bike share announces new pass options and pricing adjustments*. Accessed: November 7, 2023.

Delage E, Ye Y (2010) Distributionally robust optimization under moment uncertainty with application to data-driven problems. *Operations Research* 58(3):595–612.

Deloitte (2018) *Super Smart City Happier Society with Higher Quality*. Accessed: January 7,

2024.

Dong Y, De Koster R, Roy D, Yu Y (2022) Dynamic vehicle allocation policies for shared autonomous electric fleets. *Transportation Science* 56(5):1238–1258.

EIA (2023) *Form EIA-860 detailed data with previous form data (EIA-860A/860B)*. Accessed: December 11, 2023.

EPA (2023) *Greenhouse Gases Equivalencies Calculator - Calculations and References*. Accessed: Dec. 11, 2023.

Erera AL, Morales JC, Savelsbergh M (2009) Robust optimization for empty repositioning problems. *Operations Research* 57(2):468–483.

Esfahani PM, Kuhn D (2017) Data-driven distributionally robust optimization using the wasserstein metric: performance guarantees and tractable reformulations. *Mathematical Programming* 171(1-2):115–166.

Evergy (2022) *Business EV Rate Plan*. Accessed: January 4, 2024.

Fan W (2014) Optimizing strategic allocation of vehicles for one-way car-sharing systems under demand uncertainty. *Journal of the Transportation Research Forum* 53(3):7–20.

Fang X, Misra S, Xue G, Yang D (2011) Smart grid—the new and improved power grid: A survey. *IEEE Communications Surveys & Tutorials* 14(4):944–980.

Fathabad AM, Cheng J, Pan K, Qiu F (2020) Data-driven planning for renewable distributed generation integration. *IEEE Transactions on Power Systems* 35(6):4357–4368.

Fishman E, Washington S, Haworth N (2013) Bike share: A synthesis of the literature. *Transport Reviews* 33(2):148–165.

Grasen (2021) *The largest V2G project for vehicle network interaction in industrial parks in China is officially put into operation*. Accessed: December 11, 2023.

Hargrove D, Ahn R (2022) *San Diego changes scooter and e-bike laws, caps amount allowed*. Accessed: November 7, 2023.

Hasija S, Shen ZJM, Teo CP (2020) Smart city operations: Modeling challenges and opportunities. *Manufacturing & Service Operations Management* 22(1):203–213.

He L, Ma G, Qi W, Wang X (2021a) Charging an electric vehicle-sharing fleet. *Manufacturing & Service Operations Management* 23(2):471–487.

He L, Mak HY, Rong Y, Shen ZJM (2017) Service region design for urban electric vehicle sharing systems. *Manufacturing & Service Operations Management* 19(2):309–327.

He P, Zheng F, Belavina E, Girotra K (2021b) Customer preference and station network in the london bike-share system. *Management Science* 67(3):1392–1412.

He QC, Nie T, Yang Y, Shen ZJ (2021c) Beyond repositioning: Crowd-sourcing and geo-fencing for shared-mobility systems. *Production and Operations Management* 30(10):3448–3466.

Huang J, Pan K, Guan Y (2021a) Cutting planes for security-constrained unit commitment with regulation reserve. *IISE Transactions* 53(4):437–452.

Huang J, Pan K, Guan Y (2021b) Multistage stochastic power generation scheduling co-optimizing energy and ancillary services. *INFORMS Journal on Computing* 33(1):352–369.

Huang Z, Zheng QP, Liu AL (2022) A nested cross decomposition algorithm for power system capacity expansion with multiscale uncertainties. *INFORMS Journal on Computing* 34(4):1919–1939.

IEA (2021a) *Global Energy Review 2021*. Accessed: December 11, 2023.

IEA (2021b) *Global EV Outlook 2021*. Accessed: December 11, 2023.

IEA (2023) *SDG7: Data and Projections*. Accessed: December 11, 2023.

Indego (2023) *2023 Expansion update*. Accessed: November 7, 2023.

Jiang R, Wang J, Guan Y (2011) Robust unit commitment with wind power and pumped storage hydro. *IEEE Transactions on Power Systems* 27(2):800–810.

Jiang S, Cheng J, Pan K, Shen ZJM (2023) Optimized dimensionality reduction for moment-based distributionally robust optimization. *arXiv preprint arXiv:2305.03996* .

Jin Z, Wang Y, Lim YF, Pan K, Shen ZJM (2023) Vehicle rebalancing in a shared micromobility system with rider crowdsourcing. *Manufacturing & Service Operations Management* 25(4):1394–1415.

Kabra A, Belavina E, Girotra K (2020) Bike-share systems: Accessibility and availability. *Management Science* 66(9):3803–3824.

Knueven B, Ostrowski J, Watson JP (2020) On mixed-integer programming formulations for the unit commitment problem. *INFORMS Journal on Computing* 32(4):857–876.

Long DZ, Sim M, Zhou M (2023) Robust satisficing. *Operations Research* 71(1):61–82.

Lorca Á, Sun XA, Litvinov E, Zheng T (2016) Multistage adaptive robust optimization for the unit commitment problem. *Operations Research* 64(1):32–51.

Lu CC (2016) Robust multi-period fleet allocation models for bike-sharing systems. *Networks*

and Spatial Economics 16(1):61–82.

Lu M, Chen Z, Shen S (2017) Optimizing the profitability and quality of service in carshare systems under demand uncertainty. *Manufacturing & Service Operations Management* 20(2):162–180.

Lu M, Chen Z, Shen S (2018) Optimizing the profitability and quality of service in carshare systems under demand uncertainty. *Manufacturing & Service Operations Management* 20(2):162–180.

Lund H, Kempton W (2008) Integration of renewable energy into the transport and electricity sectors through V2G. *Energy Policy* 36(9):3578–3587.

Ma Y, Houghton T, Cruden A, Infield D (2012) Modeling the benefits of vehicle-to-grid technology to a power system. *IEEE Transactions on Power Systems* 27(2):1012–1020.

Mahmoudi M, Zhou X (2016) Finding optimal solutions for vehicle routing problem with pickup and delivery services with time windows: A dynamic programming approach based on state–space–time network representations. *Transportation Research Part B: Methodological* 89:19–42.

Mak HY (2022) Enabling smarter cities with operations management. *Manufacturing & Service Operations Management* 24(1):24–39.

Mak HY, Tang R (2021) Collaborative vehicle-to-grid operations in frequency regulation markets. *Available at SSRN 3935760* .

Martin L, Minner S, Poças D, Schulz AS (2021) The competitive pickup and delivery orienteering problem for balancing car-sharing systems. *Transportation Science* 55(6):1232–1259.

McKinsey (2019) *Micromobility's 15,000-mile checkup*. Accessed: November 7, 2023.

McKinsey (2021) *Why micromobility is here to stay*. Accessed: November 7, 2023.

Nair R, Miller-Hooks E (2011) Fleet management for vehicle sharing operations. *Transportation Science* 45(4):524–540.

Nasdaq (2022) *PG&E to Offer Nation's First Vehicle-To-Grid Export Rate for Commercial Electric Vehicles*. Accessed: December 11, 2023.

Nikzad A (2017) Thickness and competition in ride-sharing markets. *Available at SSRN 3065672* .

NY DMV (2018) *NYS Vehicle Registrations of File - End of Year 2018*. Accessed: December 11, 2023.

NY Solar Map (2023) *NY Solar Map*. Accessed: December 11, 2023.

NYC DOT (2019) *New York City Mobility Report*. Accessed: December 11, 2023.

NYC DOT (2021) *An Electric Vehicle Vision Plan for New York City*. Accessed: January 4, 2024.

NYSERDA (2023) *Offshore Wind Projects*. Accessed: December 11, 2023.

Pan K, Zhao M, Li CL, Qiu F (2022) A polyhedral study on fuel-constrained unit commitment. *INFORMS Journal on Computing* 34(6):3309–3324.

Panwar NL, Kaushik SC, Kothari S (2011) Role of renewable energy sources in environmental protection: A review. *Renewable and Sustainable Energy Reviews* 15(3):1513–1524.

Peng X, Wu OQ, Souza G (2021) Renewable, flexible, and storage capacities: Friends or foes? *Available at SSRN 3983678* .

Qi W, Li L, Liu S, Shen ZJM (2018) Shared mobility for last-mile delivery: Design, operational prescriptions, and environmental impact. *Manufacturing & Service Operations Management* 20(4):737–751.

Qi W, Liang Y, Shen ZJM (2015) Joint planning of energy storage and transmission for wind energy generation. *Operations Research* 63(6):1280–1293.

Qi W, Sha M, Li S (2022) When shared autonomous electric vehicles meet microgrids: City-wide energy-mobility orchestration. *Manufacturing & Service Operations Management* 24(5):2389–2406.

Qi W, Shen ZJM (2019) A smart-city scope of operations management. *Production and Operations Management* 28(2):393–406.

Rahimian H, Mehrotra S (2019) Distributionally robust optimization: A review. *arXiv preprint arXiv:1908.05659* .

Rajan D, Takriti S, et al. (2005) Minimum up/down polytopes of the unit commitment problem with start-up costs. *IBM Research Report* 23628:1–14.

Reck DJ, Martin H, Axhausen KW (2022) Mode choice, substitution patterns and environmental impacts of shared and personal micro-mobility. *Transportation Research Part D* 102:103134.

Saber AY, Venayagamoorthy GK (2010) Plug-in vehicles and renewable energy sources for cost and emission reductions. *IEEE Transactions on Industrial Electronics* 58(4):1229–1238.

Sago DV (2020) *Bike sharing in China — From bicycle graveyards to a regulated industry*.

Accessed: November 7, 2023.

Salas DF, Powell WB (2018) Benchmarking a scalable approximate dynamic programming algorithm for stochastic control of grid-level energy storage. *INFORMS J. on Computing* 30(1):106–123.

Scarf H (1958) A min-max solution of an inventory problem. *Studies in the Mathematical Theory of Inventory and Production* .

Schellong D, Sadek P, Schaetzberger C, Barrack T (2019) *The promise and pitfalls of e-scooter sharing*. Accessed: November 7, 2023.

Schuijbroek J, Hampshire RC, Van Hoeve WJ (2017) Inventory rebalancing and vehicle routing in bike sharing systems. *European Journal of Operational Research* 257(3):992–1004.

Shapiro A, Dentcheva D, Ruszczynski A (2021) *Lectures on Stochastic Programming: Modeling and Theory* (SIAM).

Shu J, Chou MC, Liu Q, Teo CP, Wang IL (2013) Models for effective deployment and redistribution of bicycles within public bicycle-sharing systems. *Operations Research* 61(6):1346–1359.

Soppert M, Steinhardt C, Müller C, Gönsch J (2022) Differentiated pricing of shared mobility systems considering network effects. *Transportation Science* 56(5):1279–1303.

Sovacool BK, Hirsh RF (2009) Beyond batteries: An examination of the benefits and barriers to plug-in hybrid EVs (PHEVs) and a vehicle-to-grid (V2G) transition. *Energy Policy* 37(3):1095–1103.

Tesla (2024a) *Wall Connector*. Accessed: January 4, 2024.

Tesla (2024b) *Supercharger Support*. Accessed: January 4, 2024.

The Guardian (2021) *Car firms agree at Cop26 to end sale of fossil fuel vehicles by 2040*. Accessed: Dec. 11, 2023.

The World Bank (2023) *Urban Development*. Accessed: January 7, 2024.

TLC (2024) *TLC Trip Record Data*. Accessed: January 4, 2024.

Tomić J, Kempton W (2007) Using fleets of electric-drive vehicles for grid support. *Journal of Power Sources* 168(2):459–468.

US DOE (2022) *Land-Based Wind Market Report: 2022 Edition*. Accessed: December 11, 2023.

Valdivia AG (2020) *Barcelona's moped-sharing new licenses to challenge leading companies*.

Accessed: November 7, 2023.

Van Mieghem JA (2003) Commissioned paper: Capacity management, investment, and hedging: Review and recent developments. *Manufacturing & Service Operations Management* 5(4):269–302.

Wang J, Lindsey G (2019) Do new bike share stations increase member use: A quasi-experimental study. *Transportation Research Part A: Policy and Practice* 121:1–11.

Widrick RS, Nurre SG, Robbins MJ (2018) Optimal policies for the management of an electric vehicle battery swap station. *Transportation Science* 52(1):59–79.

Wikipedia (2023) *Plug-in electric vehicles in Norway*. Accessed: December 11, 2023.

Wikipedia (2023) *Smart City*. Accessed: January 7, 2024.

Wolsey LA, Nemhauser GL (1999) *Integer and Combinatorial Optimization*, volume 55.

Yang H, Morton DP, Bandi C, Dvijotham K (2021) Robust optimization for electricity generation. *INFORMS Journal on Computing* 33(1):336–351.

Yu M, Shen S (2020) An integrated car-and-ride sharing system for mobilizing heterogeneous travelers with application in underserved communities. *IISE Transactions* 52(2):151–165.

Zapmap (2020) *Nissan and E.On V2G charging project to expand*. Accessed: December 11, 2023.

Zeng B, Zhao L (2013) Solving two-stage robust optimization problems using a column-and-constraint generation method. *Operations Research Letters* 41(5):457–461.

Zhang C, Chen J, Raghunathan S (2022a) Two-sided platform competition in a sharing economy. *Management Science* 68(12):8909–8932.

Zhang D, Yu C, Desai J, Lau H, Srivathsan S (2017) A time-space network flow approach to dynamic repositioning in bicycle sharing systems. *Transportation Research Part B: Methodological* 103:188–207.

Zhang X, Brandt M, Tong X, Ciais P, Yue Y, Xiao X, Zhang W, Wang K, Fensholt R (2022b) A large but transient carbon sink from urbanization and rural depopulation in china. *Nature Sustainability* 1–8.

Zhang Y, Lu M, Shen S (2021) On the values of vehicle-to-grid electricity selling in electric vehicle sharing. *Manufacturing & Service Operations Management* 23(2):488–507.

Zipcar (2024) *Electric car hire with Zipcar*. Accessed: January 4, 2024.

Zolan AJ, Scioletti MS, Morton DP, Newman AM (2021) Decomposing loosely coupled mixed-integer programs for optimal microgrid design. *INFORMS Journal on Computing* 33(4):1300–1319.